Canadian Journal of Fisheries and Aquatic Sciences (Supplement)

Journal canadien des sciences halieutiques et aquatiques (Supplément)

Volume 40, Supplement No. 1, 1983

Volume 40, Supplément n° 1, 1983

Proceedings of the Symposium on the Dynamics of Turbid Coastal Environments

Canadian Journal of Fisheries and Aquatic Sciences (Supplement)

Journal canadien des sciences halieutiques et aquatiques (Supplément)

Government of Canada
Fisheries and Oceans

Scientific Information and Publications Branch
Ottawa K1A 0E6

Gouvernement du Canada
Pêches et Océans

Direction de l'information et des publications scientifiques
Ottawa K1A 0E6

Volume 40, Supplement No. 1, 1983

Volume 40, Supplément n° 1, 1983

The *Canadian Journal of Fisheries and Aquatic Sciences* has been published continuously since 1901, previously as *Contributions to Canadian Biology* 1901–25, *Contributions to Canadian Biology and Fisheries* 1926–34, *Journal of the Biological Board of Canada* 1934–37, and *Journal of the Fisheries Research Board of Canada* 1938–79.

Editorial policy — The *Journal* publishes original research articles and notes, critical reviews, essays of opinion or hypothesis, letters, and book reviews in the broad fields of fisheries science and management, marine and freshwater ecosystems, and aquatic biota relevant to Canada. Submissions in English or French are accepted without limitations as to origin, but must not have been published or copyrighted and must not be published elsewhere except in abstract form or by written consent of the Editor. The *Journal* accepts no responsibility for statements made by contributors. The use of proprietary names does not imply endorsement of the product or company.

A charge of $44 per page is made for manuscripts published. When submitting a manuscript, an author must state that the charge will be accepted.

Guide for authors — Guides for authors and typists appear in the first issue of each volume and are available free from the *Journal*.

Subscriptions — The *Journal* is issued monthly to form annual volumes of twelve numbers. Subscription rates are: Canada, $63.50 per year; other countries, $76.20. Single issues are $5.80 and $6.95, respectively. Supplements are $12.00 and $14.40, respectively. Orders must be sent directly to Supply and Services Canada, Hull, Que., Canada, K1A 0S9, and payment made in Canadian funds to "The Receiver General for Canada."

Microfilm — Issues from 1934 through the current volume can be purchased on 16 or 35 mm microfilm. Photocopies of individual articles or issues can be purchased. Address orders to Xerox University Microfilms, 300 North Zeeb Road, Ann Arbor, Michigan 48106, USA.

Publié depuis 1901, le *Journal canadien des sciences halieutiques et aquatiques* a paru sous plusieurs titres: *Contributions to Canadian Biology* 1901–25, *Contributions to Canadian Biology and Fisheries* 1926–34, *Journal of the Biological Board of Canada* 1934–37, et *Journal de l'office des recherches sur les pêcheries du Canada* 1938–79.

Politique de rédaction — Le *Journal* publie des articles et des notes fondés sur une recherche originale, des critiques, des essais portant sur une opinion ou une hypothèse, des lettres et des comptes rendus de livres dans le vaste domaine des sciences halieutiques et de la gestion des pêches, des écosystèmes marins et d'eau douce, et des biocoenoses aquatiques pertinents au Canada. Toutes contributions en français ou en anglais sont acceptées sans restriction quant à la provenance, mais elles ne doivent pas avoir été produites ni avoir fait l'objet d'un copyright et ne doivent pas être publiées nulle part ailleurs sauf sous forme abrégée ou avec le consentement écrit du directeur. Le *Journal* décline toute responsabilité pour ce qui est des affirmations des collaborateurs. L'utilisation de noms de marque de commerce ne signifie aucunement une sanction du produit en question ou de la compagnie qui le fabrique.

Les frais de publication sont de 44 $ la page. Quant un auteur présente un texte, il doit préciser que ces frais seront acceptés.

Guide des auteurs — Les guides des auteurs et le guide des dactylos paraissent dans le premier numéro de chaque volume et sont disponibles gratuitement du *Journal*.

Abonnement — Le *Journal* paraît tous les mois, formant ainsi un volume de 12 numéros par année. Les frais d'abonnement annuel sont de 63.50 $ pour le Canada et de 76.20 $ pour les autres pays. Chaque numéro coûte 5.80 $ au Canada et 6.95 $ à l'étranger. Les suppléments coûtent 12 $ au Canada et 14.40 $ à l'étranger. Prière d'adresser directement les commandes à Approvisionnements et Services Canada, Hull (Qué.), Canada K1A 0S9; les paiements doivent être faits en devises canadiennes, à l'ordre du Receveur général du Canada.

Microfilms — On peut acheter sur microfilms 16 ou 35 mm tous les numéros publiés depuis 1934. Des photocopies d'articles ou de numéros individuels sont aussi en vente. Prière d'adresser les commandes à Xerox University Microfilms, 300 North Zeeb Road, Ann Arbor, Michigan 48106, E.-U.

Director and Editor-in-Chief of Scientific Information/ Directeur et rédacteur en chef de l'Information scientifique
J. WATSON, PH.D.

Special Editors/Rédacteurs spécials
D. C. GORDON JR., PH.D./A. S. HOURSTON, PH.D.

Deputy Director and Editor/Sous-directrice et rédactrice
JOHANNA M. REINHART, M.SC.

Assistant Editors/Rédacteurs adjoints
D. G. COOK, PH.D./LORRAINE C. SMITH, PH.D.

Publication Production/Production des publications
J. CAMP/G. J. NEVILLE

French Abstracts/Résumés français
Y. JEAN, PH.D.

EDITORIAL BOARD/CONSEIL DE RÉDACTION

W. J. CHRISTIE	*Ontario Ministry of Natural Resources*
R. H. GREEN	*University of Western Ontario*
H. H. HARVEY	*University of Toronto*
S. R. KERR	*Dep. of Fisheries & Oceans, Dartmouth*
P. H. LEBLOND	*University of British Columbia*
L. LEGENDRE	*Université Laval*
W. C. LEGGETT	*McGill University*
T. C. PLATT	*Dep. of Fisheries & Oceans, Dartmouth*
P. W. WEBB	*University of Michigan*

Canadian Journal of Fisheries and Aquatic Sciences (Supplement)

Journal canadien des sciences halieutiques et aquatiques (Supplément)

Volume 40, Supplement No. 1, 1983

Volume 40, Supplément n° 1, 1983

Correct citation for this publication:

GORDON, D. C., JR., AND A. S. HOURSTON [ED.]. 1983. Proceedings of the Symposium on the Dynamics of Turbid Coastal Environments. Can. J. Fish. Aquat. Sci. 40(Suppl. 1): 1–365.

Introduction to the Symposium on the Dynamics of Turbid Coastal Environments
D. C. Gordon Jr. 3–7

Modeling tidal stress, circulation, and mixing in the Bristol Channel as a prerequisite for ecosystem studies **R. J. Uncles** 8–19

Suspended sediment transport and deposition modeling in the Bay of Fundy, Nova Scotia — a region of potential tidal power development **D. A. Greenberg and C. L. Amos** 20–34

Factors affecting the supply and distribution of sediment in the turbid coastal environment
M. P. Kendrick and B. V. Derbyshire 35–43

Supply, distribution, and transport of suspended sediment in a macrotidal environment: Bristol Channel, U.K. **M. Collins** 44–59

River-dominated suspended-sediment deposition in a new Mississippi delta
I. Ll. van Heerden, J. T. Wells, and H. H. Roberts 60–71

Transfer of water and sediment from the Yangtze River to the East China Sea, June 1980
Z.-S. Yang, J. D. Milliman, and M. G. Fitzgerald 72–82

Distribution and behavior of fine sediment in the Severn Estuary and Inner Bristol Channel, U.K. **R. Kirby and W. R. Parker** 83–95

Characteristics of suspended cohesive sediment of the Severn Estuary, U.K.
R. Bryant and D. J. A. Williams 96–101

Size of flocs suspended in Delaware Bay **R. J. Gibbs, L. Konwar, and A. Terchunian** 102–104

Modeling suspended sediment dynamics of the Miramichi Estuary, New Brunswick, Canada
G. V. Winters 105–116

Turbidity maximum migration and harbor siltation in the Tay Estuary
C. Dobereiner and J. McManus 117–129

Dynamics of coastal fluid muds in low-, moderate-, and high-tide-range environments
J. T. Wells 130–142

The northern muddy intertidal: a seasonally changing source of suspended sediments to estuarine waters — a review **F. E. Anderson** 143–159

The mudflat coast of China **Y. Wang** 160–171

Optical properties, suspended sediments, and chemistry associated with the turbidity maxima of the Delaware Estuary
R. B. Biggs, J. H. Sharp, T. M. Church, and J. M. Tramontano 172–179
Les flux de sels nutritifs dans l'estuaire de la Seine (France); rôle et importance du bouchon vaseux au cours du mélange estuarien **J.-F. Guillaud** 180–187
Behavior of nitrogen nutrients and silica in the Ems-Dollard Estuary
W. Helder, R. T. P. de Vries, and M. M. Rutgers van der Loeff 188–200
Chemical composition of suspended particles in an estuarine turbidity maximum zone
D. H. Loring, R. T. T. Rantala, A. W. Morris, A. J. Blake, and R. J. M. Howland 201–206
Sediments and metal pollutants in a turbid estuary **M. F. C. Thorn and T. N. Burt** 207–215
Heterotrophic bacterial biomasses, activities, and productivities within the Fraser River plume **L. J. Albright** 216–220
Vertical mixing and its effects on phytoplankton growth in a turbid estuary
R. J. Uncles and I. R. Joint 221–228
Primary production and respiration in pelagic and benthic communities at two intertidal sites in the upper Bay of Fundy
B. T. Hargrave, N. J. Prouse, G. A. Phillips, and P. A. Neame 229–243
Spatial and temporal variability of dinoflagellate cyst abundance in a tidal estuary
W. M. Balch, P. C. Reid, and S. C. Surrey-Gent 244–261
Stable carbon isotope studies on the Pecks Cove mudflat ecosystem in the Cumberland Basin, Bay of Fundy **P. Schwinghamer, F. C. Tan, and D. C. Gordon Jr.** 262–272
Suspended particulate loading on the macrobenthos in a highly turbid fjord: Knight Inlet, British Columbia **G. E. Farrow, J. P. M. Syvitski, and V. Tunnicliffe** 273–288
Relations between annual dredging activities, suspended matter concentrations, and the development of the tidal regime in the Ems Estuary **V. N. de Jonge** 289–300
Particle resuspension in the benthic boundary layer induced by flow around polychaete tubes
D. A. Carey 301–308
Tidal current speed and production of benthic macrofauna in the lower Bay of Fundy
D. J. Wildish and D. Peer 309–321
Effect of turbidity on the temporal and spatial utilization of the inner Bay of Fundy by American shad (*Alosa sapidissima*) (Pisces: Clupeidae) and its relationship to local fisheries
M. J. Dadswell, G. D. Melvin, and P. J. Williams 322–330
Sediment mobility in the Severn Estuary and its influence upon the distribution of shorebirds
P. N. Ferns 331–340
Development of an ecosystem model of a turbid estuary **I. R. Joint** 341–348
Concluding remarks of session chairmen at the Dynamics of Turbid Coastal Environments Symposium, I **A. J. Bowen** 349–350
Concluding remarks of session chairmen at the Dynamics of Turbid Coastal Environments Symposium, II **D. C. Rhoads** 351–352
Concluding remarks of session chairmen at the Dynamics of Turbid Coastal Environments Symposium, III **G. Evans** 353–354
Concluding remarks of session chairmen at the Dynamics of Turbid Coastal Environments Symposium, IV **P. J. Wangersky** 355–356
Concluding remarks of session chairmen at the Dynamics of Turbid Coastal Environments Symposium, V **H. Postma** 357–358
Concluding remarks of session chairmen at the Dynamics of Turbid Coastal Environments Symposium, VI **A. R. Longhurst** 359–360
Papers presented at the Symposium 361–362
Poster papers presented at the Symposium 363
List of participants 364–365

Introduction to the Symposium on the Dynamics of Turbid Coastal Environments

DONALD C. GORDON JR.

Department of Fisheries and Oceans, Marine Ecology Laboratory, Bedford Institute of Oceanography, P.O. Box 1006, Dartmouth, N.S. B2Y 4A2

The coastal zone, the interface between land and sea, has played a leading role in human history. Because of the many resources it offers such as food, minerals, energy, transportation, and recreation it has been a preferred site for settlement over the centuries. It is not by chance that most of the world's major cities are located in the coastal zone. As well as providing essential resources, coastal waters have also been used to assimilate the wastes of civilization, especially in recent years.

Many coastal regions contain excessively turbid water due to very high concentrations of suspended sediment. Such turbid coastal environments are commonly found all around the world and possess a wide range of properties. The source of suspended sediment can vary considerably. In some regions, the suspended sediment is supplied by rivers. In others, various mechanisms of resuspension are important, involving tidal currents, waves, and ice. Where biological activity is great, bioturbation can be an important source of turbidity, as can be dredging activities in seaports. The grain size of suspended sediment can also vary considerably, from fine clay up to sand-sized particles. Concentrations can commonly exceed 1 $g \cdot L^{-1}$, while concentrations as great as 10 $g \cdot L^{-1}$ are not rare. In some regions it can be difficult to determine exactly where the water column ends and the sediment begins and the vertical distribution of suspended sediment can range from uniform to highly stratified. Some turbid coastal environments are turbid all the time while others are turbid only periodically. In either case, turbidity can vary temporally at frequencies related to waves, tidal cycles, storms (both normal and catastrophic), and seasonal cycles,such as runoff, light, and temperature. Turbid coastal environments are found in all climates ranging from tropical to arctic, in all tidal conditions (micro-, meso-, and macro-tidal), and in a variety of geomorphic settings including fjords, estuaries, coastal straits and bays, and the inner continental shelf. Some are found in very remote and pristine areas while others are polluted to various degrees. Needless to say, high concentrations of suspended sediment play a very important role in determining the properties and dynamics of such turbid coastal environments.

Rapid population growth and industrialization in the coastal zone during recent years have given rise to a host of important environmental problems that affect a large segment of today's society and require immediate attention. Considerable effort is now being expended, especially in developed countries where the problems are more pressing and who possess the means to solve them, to develop coastal zone management plans that resolve conflicting uses and preserve the abundant resources for future generations. Such management plans are critically dependent upon a thorough scientific understanding of coastal zone properties and processes, and it is therefore not surprising that the coastal zone is probably the best studied part of the ocean.

Despite the scientific attention it has received, our scientific understanding of the coastal zone, including the turbid regions, is far from adequate to meet the worthy goal of sound environmental management. Turbid coastal environments are exceedingly complex to study because of the wide variety of interacting and variable factors; terrestrial, marine, and atmospheric. Conditions such as shallow depths, strong currents, poor underwater visibility, and gelatinous sediments make field work difficult and often dangerous. Much of the research done to date has been descriptive in nature with little or no consideration given to dynamic aspects. Also, few studies have been multidisciplinary. Most of the classical work on turbid coastal environments has been done on temperate estuaries in developed countries, especially in northern Europe, Great Britain, and the United States.

Printed in Canada (J6981)
Imprimé au Canada (J6981)

Fortunately, scientific interest in turbid coastal environments in other parts of the world is increasing, including Third World countries, and research is currently being conducted at numerous diverse locations around the globe.

Despite the wide variety of possible properties, all turbid coastal environments, regardless of location, have several factors in common. In addition to their turbidity, shallowness, and complexity already referred to above, they are very unstable and display spatial and temporal variability of various scales. All are profoundly influenced by hydrodynamic conditions and the processes of erosion, sediment transport, flocculation, and deposition.

With its vast coastline, it is not surprising that Canada possesses a wide variety of turbid coastal environments on all three coasts: Pacific, Arctic, and Atlantic. These were little studied until the past decade and now there are active research programs underway studying turbid regions such as west coast fjords, arctic bays, and east coast estuaries. Canada's most famous turbid coastal environment is probably the upper reaches of the Bay of Fundy which have been studied intensely in recent years because of the possibility of large-scale tidal power development (Gordon and Longhurst 1979).

Because of the present high level of interest in Canada and abroad, an international symposium entitled the *Dynamics of Turbid Coastal Environments* was held during the fall of 1981 at the Bedford Institute of Oceanography in Dartmouth, N.S. This event marked the first time that this rather specific theme was the subject of an entire scientific conference. The purpose was to bring together as many scientists as possible who are currently studying the dynamics of turbid coastal environments around the world to discuss their data, experiences, ideas, and hypotheses in a casual yet stimulating setting. The Symposium was built around the common features of turbid coastal environments and all papers considered either directly or indirectly the importance of suspended sediment. This theme was approached from a variety of disciplines including engineering, physics, chemistry, and biology, and most papers were of a multidisciplinary nature.

The Symposium was organized by the Fundy Environmental Studies Committee of the Atlantic Provinces Council on the Sciences, a regional organization of universities and government laboratories that promotes coordination and cooperation in scientific activities of particular interest to the Atlantic region of Canada. The Committee is composed of over 100 regional scientists who are actively involved in conducting or managing environmental research in the Bay of Fundy region. It decided to organize the Symposium so that members could present the results of their own research recently conducted in the Bay of Fundy and learn first hand about related research currently being conducted in similar turbid environments elsewhere in the world.

Two earlier conferences were influential in the organization of this Symposium. The first was a workshop entitled *Fundy Tidal Power and the Environment* held at Acadia University in November 1976 (see Daborn 1977) which reviewed the existing scientific knowledge of the Bay of Fundy and examined possible environmental impacts resulting from proposed large-scale tidal power developments in the upper reaches. This workshop made the regional scientific community aware of how little was known about environmental processes in the Bay of Fundy and the essential nature of this information for impact prediction. As a result, interest in Fundy environmental research was stimulated and subsequently existing university and government projects were expanded and many new ones created. The workshop also led to the formation of the Fundy Environmental Studies Committee.

The second influential conference was a symposium on *Tidal Power and Estuary Management* held at the University of Bristol in April, 1978 (see Severn et al. 1979). This symposium brought Canadian and British scientists together to discuss common environmental problems and provided the opportunity to make comparisons between the Bay of Fundy and Bristol Channel/Severn Estuary in respect to both tidal power development and the state of environmental knowledge. It was at this meeting that the idea was first raised of having a major international scientific symposium devoted to turbid estuaries such as the Severn and upper reaches of the Bay of Fundy.

The first announcement of the Symposium was made in July 1980. In response to the call for papers issued in October 1980, approximately 70 titles were submitted. These were reviewed by the Symposium Steering Committee and Session Chairmen in March 1981 and over 60 papers were accepted. Selection was based on relevance to the Symposium theme and those papers not accepted either dealt primarily with continental shelf environments, considered regions of relatively low turbidity, or did not relate to the role and importance of suspended sediment.

Fifty-one papers were presented at the Symposium, 33 verbally and 18 in poster form, over a 3-day period. To stimulate discussion between the various scientific disciplines, all sessions were plenary and papers were presented in a sequence related to geographic location. On the first day, papers describing research in Asia, South America, and North America were presented. Papers from Europe and Great Britain were given on the second day. Papers on the third and final day focused specifically upon the Bay of Fundy and the Bristol Channel/Severn Estuary. Therefore, the topics jumped from one discipline to another as the program evolved. Approximately 20 papers focused upon physical processes, 10 upon chemical processes, and 20 upon biological processes. Some papers were based upon recently collected field data, including some new methods of measurement, while others were based upon laboratory or theoretical studies. Environments considered ranged from tropical to boreal. There were no papers dealing with arctic environments, but several did touch upon the importance of ice during the winter months. The Symposium was attended by approximately 150 scientists from Canada, United States, United Kingdom, Netherlands, West Germany, France, China, Denmark, Portugal, and South Africa. Many additional overseas scientists wanted to attend and participate, some even had papers accepted, but were unable to obtain travel funds.

The climax of the Symposium came at the conclusion when the six invited Session Chairmen reviewed the content of all the papers and extracted what they individually thought were the major findings and conclusions. The Session Chairmen were selected on the basis of their multidisciplinary scientific background, ability to summarize and review, and experience in turbid coastal environments and their cogent concluding remarks gave the entire Symposium meaningful perspective which will undoubtedly influence the direction of future research. On the day following the Symposium, approximately 50 participants, mostly from overseas, took part in a field trip to the Bay of Fundy to examine firsthand many interesting natural features along the shoreline of the Minas Basin and the tidal power pilot project currently under construction at Annapolis Royal, N.S.

Judging from the enthusiasm of the participants, the number of questions after each paper, and the almost continuous discussion in and outside the auditorium, the Symposium was most successful. By hearing and seeing all the papers together, engineers and scientists were able to look at common problems and processes from quite different points of view and considerable new insight resulted. On the one hand, the Symposium clearly demonstrated the factors that all turbid coastal environments have in common, while on the other hand it emphasized how all are different. However, it was obvious that scientists have much to learn from each other no matter what turbid coastal environment they are studying. Another important result of the Symposium were the new personal contacts that were made among the participants. All in all, it is expected that the Symposium will have a very significant impact upon the development of research in turbid coastal environments during the years ahead. It will also play an important role in helping the Canadian scientific community predict the likely environmental impacts of tidal power development in the Bay of Fundy (Gordon and Longhurst 1979).

All authors presenting papers, either verbal or poster, were invited to submit a scientific manuscript. Although much of the research was very recent and some had only been interpreted in a preliminary fashion, over 35 manuscripts were submitted. This volume contains those submitted papers which passed the standard peer review and editing procedures of the *Journal* and the concluding remarks of the six Session Chairmen. In contrast to the Symposium, papers are sequenced according to discipline. The Session Chairmen's remarks are based upon all 51 papers presented at the Symposium and not merely the

limited number of papers included in this volume. For this reason, a complete list of presented papers is included.

Financial support for the Symposium was provided by Ocean Science and Surveys of the Department of Fisheries and Oceans, the Atlantic Provinces Council on the Sciences, the Institute of Resource and Environmental Studies of Dalhousie University, the Atlantic Regional Laboratory of the National Research Council of Canada, and the Atlantic Geoscience Centre of the Department of Energy, Mines and Resources. Many organizations and people, too many to mention, contributed time and materials which insured the success of the Symposium.

DABORN, G. R. [ed.]. 1977. Fundy tidal power and the environment. Proceedings of a workshop on the environmental implications of Fundy tidal power held at Acadia University, November 1976. Acadia University Inst. Rep. 28: 304 p.

GORDON, D. C. JR., AND A. R. LONGHURST. 1979. The environmental aspects of a tidal power project in the upper reaches of the Bay of Fundy. Mar. Pollut. Bull. 10: 38–45.

SEVERN, R. T., D. L. DINELEY, AND L. E. HAWKER [ed.]. 1979. Tidal power and estuary management. Proceedings of the thirtieth symposium of the Colston Research Society held at the University of Bristol, April 1978. Scientechnica, 296 p.

Steering Committee

Dr Carl L. Amos (Bedford Institute of Oceanography)
Dr Graham R. Daborn (Acadia University)
Ms Jacqueline Dale (Bedford Institute of Oceanography)
Dr David A. Greenberg (Bedford Institute of Oceanography)
Dr Donald C. Gordon Jr. (Bedford Institute of Oceanography) (Chairman)
Dr Arthur J. Hansen (Dalhousie University)
Dr Barry T. Hargrave (Bedford Institute of Oceanography)
Dr W. David Jamieson (Atlantic Regional Laboratory)
Dr Alan Logan (University of New Brunswick)
Dr David J. Scarratt (St. Andrews Biological Station)
Dr James P. M. Syvitski (Bedford Institute of Oceanography)

Session Chairmen

Dr Anthony J. Bowen (Dalhousie University)
Dr Graham Evans (Imperial College of Science and Technology)
Dr Alan R. Longhurst (Bedford Institute of Oceanography)
Dr Henk Postma (Netherlands Institute for Sea Research)
Dr Donald C. Rhoads (Yale University)
Dr Peter J. Wangersky (Dalhousie University)

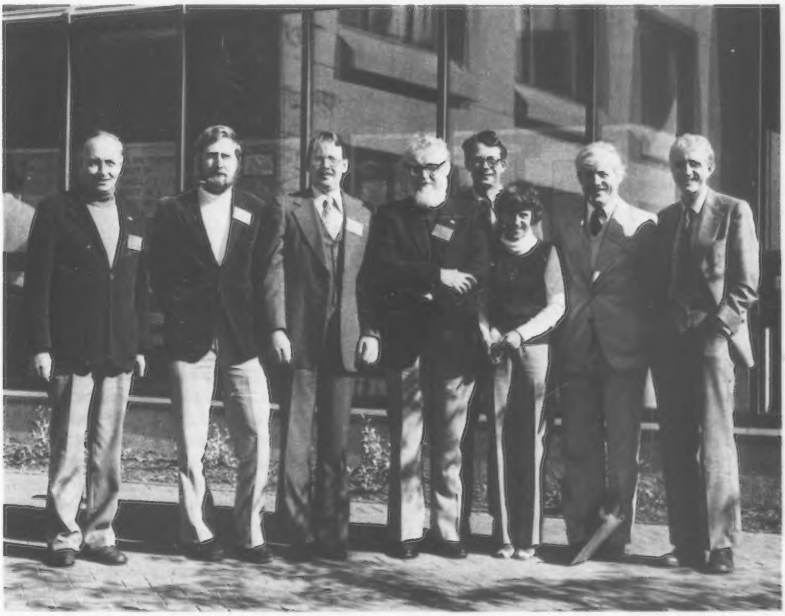

Key people involved in organizing and running the Symposium were (*left to right*): Dr Henk Postma, Dr Tony Bowen, Dr Donald Rhoads, Dr Peter Wangersky, Dr Donald Gordon Jr., Ms Jacqueline Dale, Dr Graham Evans, and Dr Alan Longhurst.

Modeling Tidal Stress, Circulation, and Mixing in the Bristol Channel as a Prerequisite for Ecosystem Studies[1]

R. J. UNCLES

Natural Environment Research Council, Institute for Marine Environmental Research, Prospect Place, The Hoe, Plymouth PL1 3DH, England

UNCLES, R. J. 1983. Modeling tidal stress, circulation, and mixing in the Bristol Channel as a prerequisite for ecosystem studies. Can. J. Fish. Aquat. Sci. 40(Suppl. 1): 8–19.

A depth-averaged hydrodynamical numerical model is used to evaluate tidal stresses, currents, and mixing in the Bristol Channel and Severn Estuary. Benthic macrofaunal associations and sediment bed types are shown to depend on the magnitude of the tidal stress, and the direction of sediment transport (as bed-load) in the central parts of the Channel is shown to be a consequence of ebb dominated stress. This asymmetry in the tidal stress is mainly caused by M_4 currents, and computed M_4 elevations and currents are compared with observed values at a number of stations. Residual flows and horizontal mixing are deduced from the hydrodynamical model, and used to construct transport relationships for an ecosystem model. Agreement between observed salinity over a number of years and that computed by the ecosystem model is generally good.

Key words: Bristol Channel, hydrodynamical model, salinity model, tidal stress, M_4 tides, sediment movement

UNCLES, R. J. 1983. Modeling tidal stress, circulation, and mixing in the Bristol Channel as a prerequisite for ecosystem studies. Can. J. Fish. Aquat. Sci. 40(Suppl. 1): 8–19.

Un modèle numérique hydrodynamique à profondeur moyenne a servi à évaluer la pression des marées, les courants et le mélange dans le chenal de Bristol et l'estuaire de la Severn. On constate que les associations macrofauniques benthiques et les types de lits de sédiment dépendent de la pression des marées. On démontre aussi que la direction du transport des sédiments (comme charge de lit) dans les parties centrales du chenal résulte de la pression exercée surtout par le jusant. Cette asymétrie de pression exercée par la marée est causée en grande partie par des courants M_4, et nous comparons les élévations et courants M_4 avec les valeurs observées à un certain nombre de stations. Les flux résiduaires et le mélange horizontal sont déduits du modèle hydrodynamique et sont utilisés dans l'élaboration de relations de transport en vue d'un modèle d'écosystème. Il y a généralement bon accord entre la salinité observée pendant plusieurs années et celle calculée à l'aide du modèle d'écosystème.

Received October 14, 1981
Accepted August 31, 1982

Reçu le 14 octobre 1981
Accepté le 31 août 1982

TIDAL streams have a profound influence on the ecology of the Bristol Channel and Severn Estuary. Because of this, hydrodynamical numerical models of tidal flow have an important role to play in quantifying ecological processes in the region. The purpose of this paper is to use currents computed from such a model, in conjunction with field observations, to investigate the frictional drag on the seabed due to current flow (tidal stress), together with long-term, large-scale circulation of sediment (as bed-load), and water in the area. The relevance of these physical processes to estuarine ecology is emphasized. The philosophy behind this work is that fundamental studies of physical processes can profitably run in parallel with, and make important contributions to, research into estuarine and coastal marine ecology. Although current meter observations alone could provide the necessary background to some ecological studies, for many it is impossible to achieve the requisite geographical and temporal coverage of observational data. Under these circumstances the application of hydrodynamical models is essential.

Using a hydrodynamical model, it is shown that tidal stresses at the seabed not only govern sediment bed types and distributions of benthic macrofaunal associations (Warwick and Uncles 1980), but are also able to explain sediment transport paths for bed-load in the central part of the Bristol Channel (Belderson and Stride 1966). The work of Pingree and

[1]This paper forms part of the Proceedings of the Dynamics of Turbid Coastal Environments Symposium convened at the Bedford Institute of Oceanography, Dartmouth, N.S., Canada, September 29–October 1, 1981.

Printed in Canada (J6673)
Imprimé au Canada (J6673)

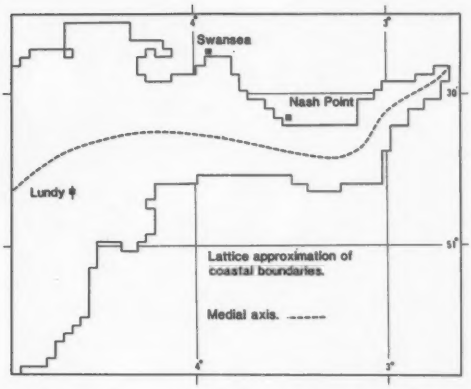

FIG. 1. Lattice approximation of coastal boundaries in the Bristol Channel and Severn Estuary (west and east, respectively, of Nash Point). The medial axis of the Channel (– – –).

Griffiths (1979) is extended to incorporate residual (tidally averaged) currents in the frictional drag law, as well as employing a much higher spatial resolution in the numerical model.

Applications of physical data to holistic ecosystem simulations entail a coarser description of the physical processes (both in time and space) than is obtained using hydrodynamical models. Here, the role of physical models is to advect and disperse biological and chemical components of the ecosystem through the region of interest and over the course of, perhaps, several years (Kremer and Nixon 1978). The long-term advection and dispersion of dissolved materials is influenced by tidally induced residual flows (Uncles 1982), which can be derived from hydrodynamical models. However, an empirical approach must generally be used to quantify the transport for ecosystem studies. Such an approach is outlined for the Bristol Channel and, as illustration of its capabilities, is used to compute distributions of salinity over the region. Comparisons of computed with observed distributions of salinity over a number of years are presented.

The hydrodynamical model uses finite-difference methods to solve the well-known depth-averaged equations of continuity and momentum in their standard nonlinear forms (Tee 1976; Pingree and Maddock 1977). The effect of buoyancy due to horizontal density gradients is taken into account; the coefficient of horizontal eddy viscosity is taken to be 10^6 cm$^2 \cdot$s^{-1} (Tee 1976), and the drag coefficient, k, in the quadratic friction law is 2.5×10^{-3}. A (53×43) lattice of points is used with a uniform spacing of 3.1 km (see Fig. 1). The Bristol Channel and Severn Estuary are arbitrarily defined here as the regions west and east of Nash Point in Fig. 1. Although not shown in Fig. 1, the upper reaches of the model Severn are extended further towards the head by 15 km, using a one-dimensional approximation of the estuary. The conditions on water level specified at the seaward boundary are the residual (tidally averaged) surface elevation relative to Ordnance Datum (Newlyn), and the amplitudes and phases of the M_2 and M_4 tides (the principal lunar semidiurnal and quarter-diurnal tidal heights). The M_2 elevations and currents derived from the model are in good agreement with observations (Uncles 1981a).

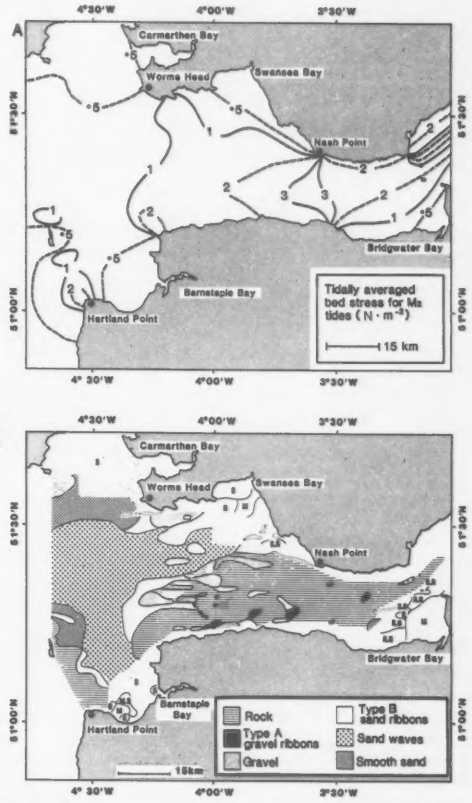

FIG. 2. Tidally averaged magnitude of seabed stress for M_2 tides, and sediment bed types: A, stress (N$\cdot$m^{-2}); B, Bed types, R(rock), G(gravel), S(sand), M(mud). Linear sand banks are drawn in.

Tidal Stress

Using the quadratic formulation, the tidal stress on the seabed due to frictional drag of water flowing over it may be written:

$$\tau = \rho k \mathbf{v}|\mathbf{v}|, \quad (1)$$

where ρ is the density of seawater, k is the drag coefficient and $\mathbf{v}$ is the depth-averaged current; its magnitude is:

$$|\tau| = \rho k |\mathbf{v}|^2. \quad (2)$$

Both equations can be easily evaluated from the hydrodynamical model of the Channel. Averaging equation (2) over a tidal cycle yields the tidally averaged magnitude of the stress, $\langle|\tau|\rangle$, which is contoured in Fig. 2A for the case of M_2

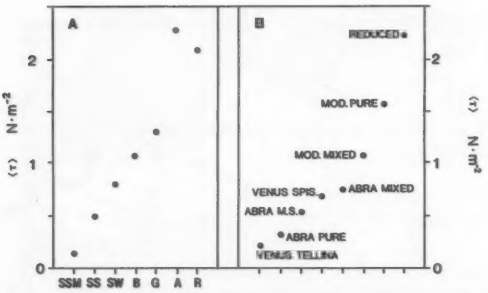

FIG. 3. Bed types and benthic macrofaunal associations against tidally averaged magnitude of bed stress for M_2 tides: A, Bed types, R(rock), A(type A gravel ribbons), G(smooth gravel), B(type B sand ribbons), SW(sand waves), SS(smooth sand), SSM(smooth sand and mud); B, Benthic macrofaunal associations.

tidal streams. Peak tidal stresses occur during maximum flood and ebb tidal streams, and these are approximately twice the values shown in Fig. 2A owing to the fact that the tidal currents at each point are essentially rectilinear, and approximately sinusoidal with time (Uncles 1981a).

The effect of tidal stress on the substrate is evident from Fig. 2B, which shows the distribution of sediment bed types in the Bristol Channel and western Severn Estuary. The region of high stress in the eastern Bristol Channel is a zone of erosion with a rock bed; gravel accumulates in the lower stress region seaward of the zone, and may form gravel ribbons (Type A of Kenyon 1970). The western part of the Channel is a region of large sand waves, which adjoins areas of smooth sand to the south and north, and which is separated from the gravel and rock areas to the east by thin sand ribbons (Type B of Kenyon 1970). In Bridgwater Bay (Fig. 2B), and further up the estuary, sediment bed types are governed by the dense suspensions of particulate material maintained in the water column by the strong currents.

Data from Fig. 2(A, B) have been synthesized in Fig. 3A, which shows each bed type as a function of the mean residual (tidally-averaged) tidal stress for which it occurs. There is a fairly smooth progression from high tidal stresses associated with the rock bed and gravel ribbons, through the intermediate stress values producing movement of sand waves, to the low stresses resulting in permanent deposition of sediment to form beds of smooth sand and muddy sand. A similar correlation is illustrated in Fig. 3B for tidal stress and benthic faunal types in the Bristol Channel, and this correlation has been considered in detail by Warwick and Uncles (1980).

According to Belderson and Stride (1966), the direction of sand transport in the Channel (as bed-load) is from the zone of erosion to the Celtic Sea. Generally, the instantaneous rate of sand transport varies as the current speed raised to some power, which is typically about four. This means that most of the transport occurs near peak flood or ebb currents (ignoring wind–wave effects). Any significant difference in the magnitudes of the peak flood and ebb currents (the asymmetry) will therefore largely determine the residual transport of sand. Tidal asymmetry in the currents has been investigated in detail for the Severn Estuary (Uncles 1981b). If infinitely repeating

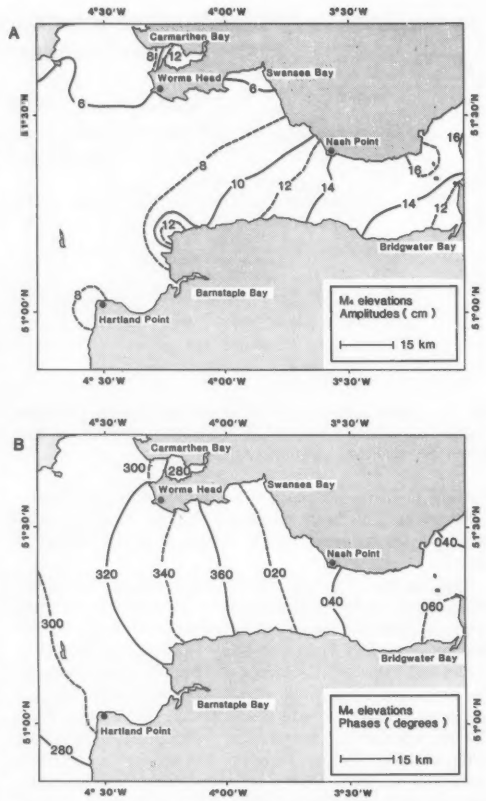

FIG. 4. M_4 elevations: A, Amplitudes (cm); B, Phases (degrees).

M_2 tides are considered as being representative of average tidal conditions in the Channel, then tidal asymmetry is produced mainly by residual (tidally averaged) currents, and by M_4 tides. The effects of higher overtides (M_6, M_8, ...) are irrelevant or small. Therefore, the hydrodynamical model has been used to investigate M_4 tides in the Channel from a fundamental viewpoint, as well as to identify possible transport paths for sediment bed-load directly from the computed tidal currents.

M_4 TIDES

Seaward boundary conditions for the M_4 elevations were derived from a coarse grid model of the southwest shelf (Miles 1979). The amplitudes and phases of the M_4 tide, according to the hydrodynamical model, are contoured in Fig. 4A and B, respectively. These values were derived by running the model over a number of tidal cycles until periodic solutions were obtained. Fourier analysis of the computed water elevations and velocities then gave the M_2, M_4, and residual properties. For velocity:

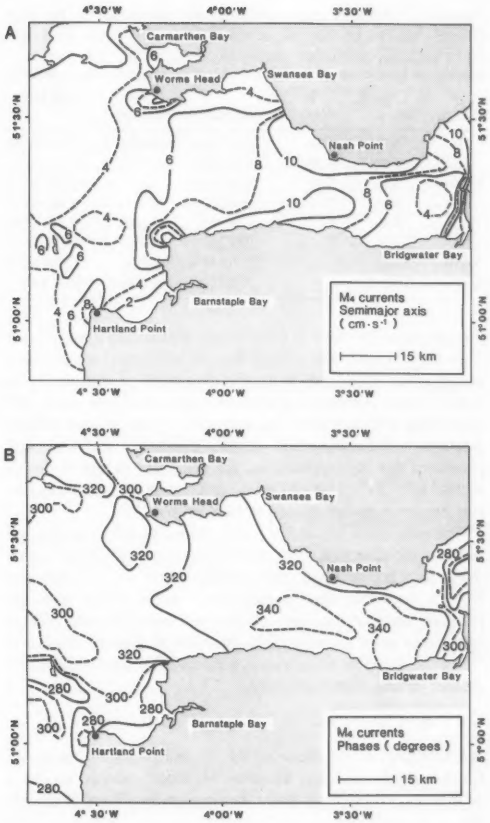

FIG. 5. M_4 currents: A, Maximum currents (semimajor axis), $cm \cdot s^{-1}$; B, Phases (degrees).

$$\mathbf{v} = \langle \mathbf{v} \rangle + \mathbf{v}_2 + \mathbf{v}_4 + \ldots$$

where $\mathbf{v}_2$ is the M_2 current, and $\langle \mathbf{v} \rangle$ and $\mathbf{v}_4$ are the much smaller residual and M_4 currents. The amplitudes of the M_4 elevations increase from about 6 cm in the west to 14 cm in the mouth of the Severn (located at Nash Point, Fig. 4A). The increase in elevation continues towards the head of the Severn. Enhanced elevations occur near headlands due to centrifugal effects (see also Pingree and Maddock 1978). The computed M_4 tide is the sum of contributions due to local nonlinear generation (Pingree and Maddock 1978; Uncles 1981b), and the presence of an M_4 wave propagating into the Channel from the Celtic Sea, where it is amplified by funnelling. The phases of the M_4 elevations in Fig. 4B are proportional to the time of maximum elevation for the M_4 tide. These show propagation into the Channel until Bridgwater Bay; thereafter the propagation is down-estuary, indicating large local generation in the upper reaches of the Severn.

The head of the depth averaged M_4 current vector describes an ellipse during the course of an M_4 tidal period of 6.2 h. The maximum currents have magnitude a_4, and define the semimajor axis of the ellipse. The orientation of the ellipse, δ_4, is the direction of the maximum current (a_4) in an up-channel sense. The maximum up-channel current is reached at a time $t = e_4/\omega_4$, where e_4 is the phase of the current, and ω_4 the angular frequency of the M_4 tide ($57.97°h^{-1}$). The M_4 currents reach minimum values one quarter of a period after they reach maximum values. The minimum currents have magnitude b_4, and define the semiminor axis of the ellipse. The semiminor axis is positive if the head of the current vector is moving cyclonically around the ellipse, and is negative if it is moving anticyclonically.

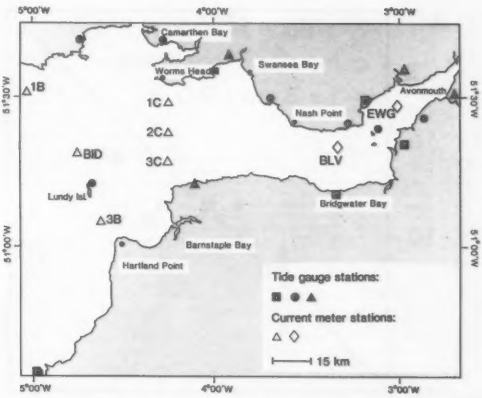

FIG. 6. Tide-gauge stations at which measurements have been made for 15 d, 1 mo, and 1 yr are shown as ■, ●, and ▲, respectively. Stations at which two or three recording current meters were deployed on a mooring for 1 mo are shown (△). Near-surface current measurements extending over 1 mo are shown (◇). Data at station BID courtesy of M. J. Howarth (personal communication).

The maximum M_4 currents (a_4, the semimajor axes of the M_4 tidal current ellipses) are shown in Fig. 5A. Large values occur near headlands, which is again due to centrifugal effects, and currents increase progressing up-channel due to funnelling and local nonlinear generation. The region of low currents near Bridgwater Bay results from opposing phases of the up-estuary travelling, and locally generated M_4 tides. Phases of the M_4 currents (e_4) are contoured in Fig. 5B, which has been drawn to show less detail in the bays than is evident from the model. Propagation is again shown to be up-channel seawards of Bridgwater Bay, and down-channel further into the Severn.

COMPARISON WITH OBSERVATIONS

Some of the results for M_4 tides can be compared with observations. Positions at which tidal heights and currents have been measured are drawn in Fig. 6.

The comparisons between observed and computed M_4 elevation amplitudes and phases are given, respectively, in Fig. 7A and 7B. The agreement is reasonable at the lower amplitudes (<15 cm, relative accuracy 16%) and phases (<20°, relative accuracy 13%) of the Bristol Channel, but

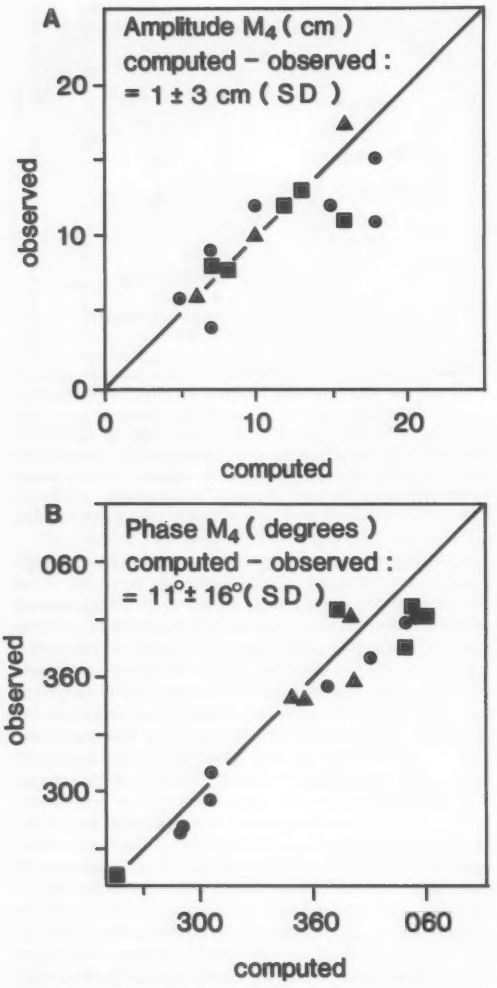

FIG. 7. Observed against computed M_4 elevations: A, Amplitudes (cm); B, Phases (degrees).

both the computed amplitudes and phases are too large in the Severn. Although not shown in Fig. 7A, the computed amplitude at Avonmouth (see Fig. 6 for location) is 45 cm, while the observed value is only 34 cm. Thus, the two-dimensional simulation of M_4 tides becomes inaccurate in the upper Severn, presumably because of its poor resolution of topography (especially depth) in the upper reaches, where local generation of M_4 tides is important. Prandle (1980) found similar excessive generation of M_4 tide at the head of both the Severn and Thames, and attributed this to inaccuracies in the computed frictional effects in shallow water.

Observed and computed properties of the M_4 tidal currents are compared in Table 1. One-month stations are used (△ and ◇ in Fig. 6), and tidal ellipse data for all current meters on a mooring are averaged. With the exception of station 2C in Table 1, the computed semimajor and semiminor axes (the maximum and minimum M_4 currents, a_4 and b_4) are within 1 cm·s^{-1} of the observed values. Computed and observed phases of the M_4 currents, e_4, are generally in agreement to within 10°–20° (~10–20 min), and a similar agreement exists for the orientations of the tidal ellipses, δ_4.

TABLE 1. Observed and computed, (•), properties of M_4 tidal ellipses. Semimajor axis, a_4, semiminor axis, b_4, phase relative to Greenwich, e_4, orientation relative to north, δ_4. $\phi = 2e_2 - e_4$.

Station	a_4 cm·s^{-1}	b_4 cm·s^{-1}	e_4 degrees	δ_4 degrees	cos (ϕ)
1B	3(3)	−1(0)	273(276)	40(60)	−0.7(−0.6)
3B	3(4)	1(1)	303(297)	41(42)	−0.1(−0.4)
1C	5(6)	1(0)	323(317)	84(102)	−0.8(−0.7)
2C	3(6)	0(−1)	334(321)	60(81)	−1.0(−0.7)
3C	5(6)	−1(−2)	328(313)	71(80)	−0.8(−0.6)
BID	2(3)	0(−1)	289(297)	53(66)	−0.5(−0.7)
BLV	5(5)	—	367(341)	92(92)	−0.9(−0.6)
EWG	11(12)	—	262(250)	57(56)	0.9(1.0)

The maximum M_2 and M_4 tidal currents tend to be aligned in the same direction with their respective tidal ellipse semimajor axes pointing along the medial axis of the Channel (see Fig. 1). Assuming that the maximum M_4 and M_2 currents are parallel, and that the cross-channel currents (the tidal ellipse semiminor axes) are negligible, then the M_4 currents reinforce either the flood or ebb streams according to whether cosϕ is greater or less than zero, where:

$$\phi = 2e_2 - e_4, \tag{3}$$

and where e_2 is the phase of the M_2 currents. The peak M_4 flood current, a_4, leads the peak M_2 flood current, a_2, by a time ϕ/ω_4, where ω_4 is twice the angular frequency of the M_2 tide.

In Table 1, cosϕ is compared for computed and observed currents. The agreement is reasonable, and shows that the summation of M_2 and M_4 currents produces ebb dominated flows ($\cos\phi < 0$) at all stations except EWG (see Fig. 6), which is some considerable distance into the Severn (see also Uncles 1981b).

RESIDUAL AND MAXIMUM TIDAL STRESSES

As a first approximation the Bristol Channel can be treated as a one-dimensional system, with currents and spatial gradients occurring only along its medial axis (see Fig. 1), so that $b_2 = 0 = b_4$. In this case the residual tidal stress on the seabed due to the sum of M_2 and M_4 currents is approximately (see equation (1) and Uncles 1981b):

$$\langle\tau\rangle' = \rho k\langle(\mathbf{v}_2 + \mathbf{v}_4)|\mathbf{v}_2 + \mathbf{v}_4|\rangle \simeq \frac{4}{3\pi}\hat{\mathbf{x}}\rho k a_2 a_4 \cos\phi. \tag{4}$$

Here, $\hat{\mathbf{x}}$ is a unit vector directed up-channel along the medial axis in Fig. 1, and ϕ is given by equation (3). In one dimension, the residual tidal stress due to the sum of M_2 and residual currents is approximately (Uncles 1981b):

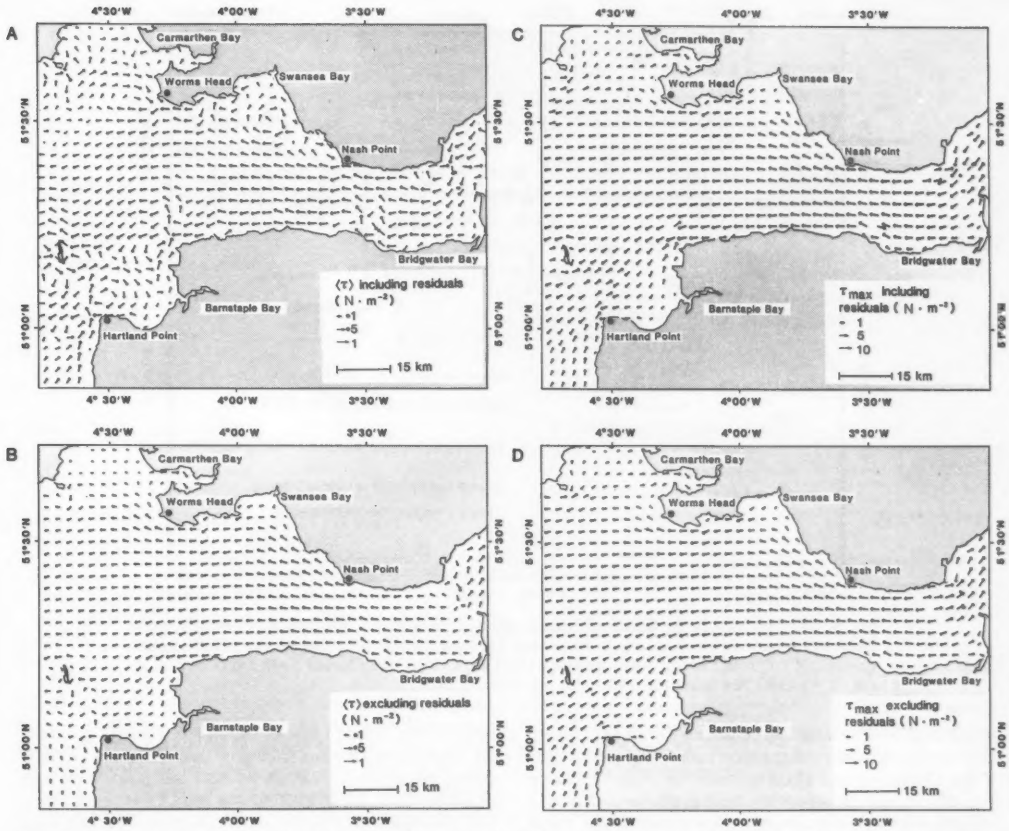

FIG. 8. Residual and maximum seabed tidal stresses $\langle\tau\rangle$ and τ_{max} ($N \cdot m^{-2}$): A, Residual stress, $\langle\tau\rangle$, including residual currents; B, Residual stress, $\langle\tau\rangle$, excluding residual currents; C, Maximum tidal stress, τ_{max}, including residual currents; D, Maximum tidal stress, τ_{max}, excluding residual currents.

$$(5) \quad \langle\tau\rangle'' = \rho k\langle(\mathbf{v}_2 + \langle\mathbf{v}\rangle)|\mathbf{v}_2 + \langle\mathbf{v}\rangle|\rangle \simeq \frac{4}{\pi}\rho k a_2 \langle\mathbf{v}\rangle.$$

From equations (1), (4) and (5) the total residual tidal stress is:

$$\langle\tau\rangle = \rho k\langle\mathbf{v}|\mathbf{v}|\rangle \simeq \langle\tau\rangle' + \langle\tau\rangle''.$$

In two dimensions, the total residual tidal stress due to overtides and residual currents, $\langle\tau\rangle$, can be computed directly from the hydrodynamical model using equation (1). The distribution of $\langle\tau\rangle$ is shown in Fig. 8A. Outside of the bays, in the deeper, central parts of the Channel, the residual tidal stress is directed from east to west. If the residual transport of sand as bed-load were determined by the residual tidal stress, then the expected sediment transport paths would be from the zone of erosion (shown in Fig. 2B), across the sand wave field to the Celtic Sea. This is in agreement with the results of Belderson and Stride (1966).

Residual currents which have been computed here using a depth averaged model may be different from those which flow near the seabed in nature (Uncles 1982), and which are able to affect sediment movement. Therefore, it is important to investigate the sensitivity of the computed distribution of residual tidal stress to the residual current flow. If the computed residual currents, $\langle\mathbf{v}\rangle$, are subtracted from the computed total currents, $\mathbf{v}$, before the stress is evaluated in equation (1), then the residual tidal stress is solely the result of M_2, M_4, and higher overtide interactions, and is given approximately by $\langle\tau\rangle'$ in equation (4). Actual values of $\langle\tau\rangle'$ from the model are drawn in Fig. 8B. Except in the bays and in the upper Severn, the exclusion of residual current flow has no qualitative effect on the residual tidal stress.

Maximum tidal stress, τ_{max}, occurs at the time of maximum water velocity, $|\mathbf{v}|_{max}$, and is given by equation (1) with $|\mathbf{v}| = |\mathbf{v}|_{max}$. The magnitude and direction of maximum stresses computed from the model are shown in Fig. 8C. The maximum stress depends primarily on the summation of the M_2, M_4, and residual currents. If the residual transport of sand

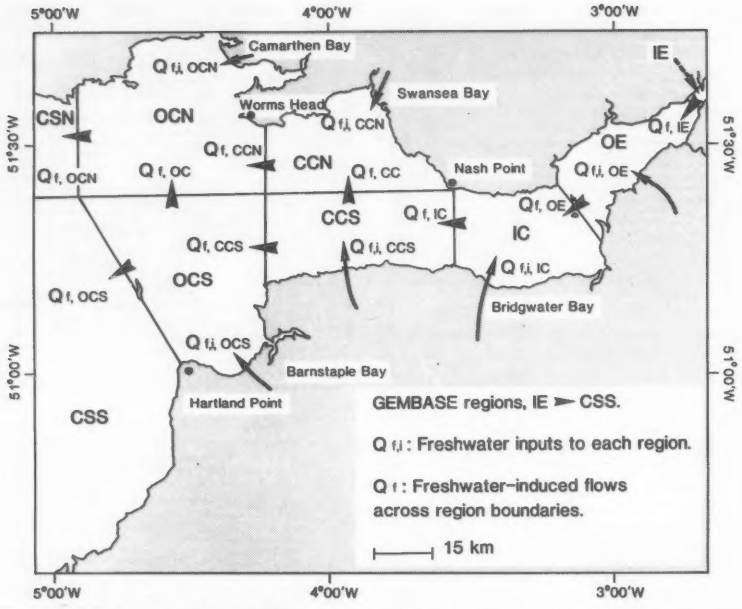

FIG. 9. Regions used in the GEMBASE model, showing freshwater inputs to each region, $Q_{f,i}$, and freshwater-induced flows across region boundaries, Q_f. Inner Estuary (*IE*); Outer Estuary (*OE*); Inner Channel (*IC*); Central Channel South and North (*CCS* and *CCN*); Outer Channel South and North (*OCS* and *OCN*); Celtic Sea South and North (*CSS* and *CSN*).

as bed-load were determined by the maximum tidal stress, then the expected sediment transport paths in the central parts of the Channel would again be from the zone of erosion (Fig. 2B), across the sand wave field to the Celtic Sea.

Figure 8D shows the maximum tidal stresses, τ_{max}, calculated in the model when computed residual currents are subtracted from the computed total currents before τ_{max} is evaluated from equation (1). In this case, maximum stresses depend primarily on the summation of M_2 and M_4 currents. The results of calculating τ_{max} including and excluding residual currents in equation (1) (Fig. 8C and 8D) are qualitatively the same in the region of bed-load sediment transport.

Similar results on the direction of sediment transport as bed-load can be inferred from work by Pingree and Griffiths (1979), who computed tidally averaged and peak stresses due solely to M_2 and M_4 interactions, using a coarse lattice model of the U.K. shelf. The present work has extended this to include the effects of residual flows, and to compute the stresses over a much finer lattice for the Bristol Channel. The problems of suspended sediment transport, both tidal and wind–wave induced, and sediment supply, have not been addressed.

Transport Equations for Ecological Modeling

The numerical model GEMBASE (general ecosystem model of the Bristol Channel and Severn Estuary) computes the interactions between biological and chemical variables during mixing and advection by tidal and residual currents (Radford 1979, 1981; Radford and Joint 1980; Joint 1983). The nine regions used in the GEMBASE model are named and depicted schematically in Fig. 9. Freshwater inputs to each GEMBASE region, denoted by $Q_{f,i}$, are also shown in Fig. 9; on average, the river inputs from the Severn Estuary contribute about 60% of the total flow of freshwater to the Bristol Channel, while inputs from the northern and southern coastlines of the Bristol Channel amount to about 30 and 10%, respectively. Additional inputs of freshwater, due to the excess of precipitation over evaporation, are small compared with river inputs, and have been neglected.

Boundary conditions for GEMBASE are applied at the Inner Estuary (*IE*), and at the Celtic Sea North (*CSN*) and Celtic Sea South (*CSS*) regions (see Fig. 9). The boundary between the Celtic Sea North (*CSN*) and Outer Channel North (*OCN*) is 6 km up-channel from the seaward boundary of the hydrodynamical model (see Fig. 1). The remaining six modelled regions were chosen as a minimum set to describe the spatially differing ecological and physical properties of the Channel; a larger number of regions would have required excessive computer time to run the model through several years of simulated time for the many numerical experiments of interest.

The problem considered here is the determination of mixing

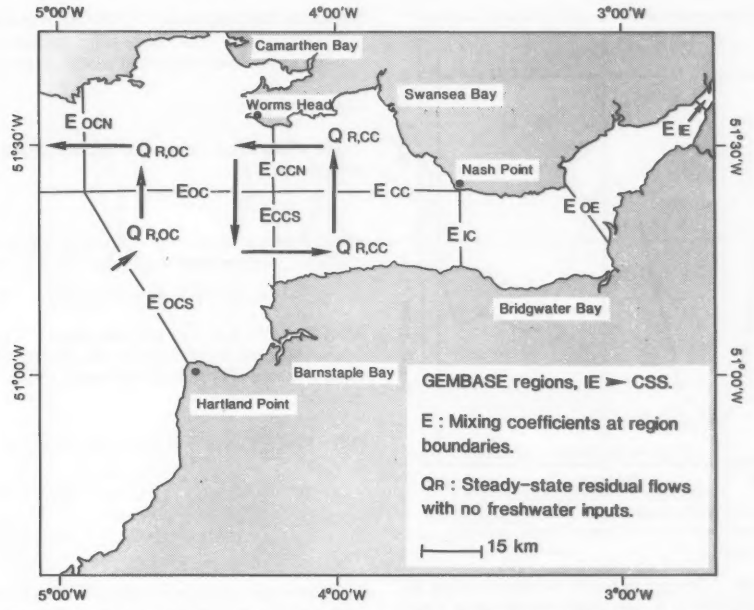

FIG. 10. Mixing coefficients at region boundaries, E, and steady-state residual flows with no freshwater inputs, Q_R.

and advection of water and dissolved materials between, and through, the large GEMBASE regions shown in Fig. 9, for periods of time of the order of several years. Both the spatial and temporal scales are much larger than those associated with the hydrodynamical numerical model of the Bristol Channel, so that some form of interfacing must be devised between the two types of models. The method devised for GEMBASE is not ideal because it relies, in part, on the calculation of residual flows and dispersion, neither of which are fully understood in estuaries subjected to strong tidal currents. However, the method has the advantages of being conceptually simple, rapid to run, and capable of generating realistic rates of transport between regions, as judged from the comparison of computed and observed distributions of freshwater in the Channel. Use is also made of the long-term salt balance, which, while being insufficient to define transport over the two-dimensional Bristol Channel regions shown in Fig. 9, is able to do so in the one-dimensional regions which represent the Severn Estuary (Uncles and Radford 1980; Radford et al. 1981).

ADVECTION AND MIXING

The transport of salt and water across any boundary between two GEMBASE regions in Fig. 9 is considered. The instantaneous rate of transport of water, Q, across the boundary is:

$$Q = A\bar{u} \tag{6}$$

where the overbar denotes an average over the boundary's area, A, and where u is the component of depth averaged velocity, v, perpendicular to A.

The associated transport of salt is:

$$F = A\overline{us} = A\bar{u}\bar{s} + A\overline{u's'} \tag{7}$$

Here, the prime denotes a deviation from the cross-sectional average; for example, $s = \bar{s} + s'$. The residual rate of transport across A follows from equations (6) and (7):

$$\langle F\rangle = \langle Q\rangle\langle\bar{s}\rangle + \{\langle\tilde{Q}\tilde{s}\rangle + \langle A\overline{u's'}\rangle\}, \tag{8}$$

where $Q = \langle Q\rangle + \tilde{Q}$ and $\bar{s} = \langle\bar{s}\rangle + \tilde{s}$ — the tildes denoting cross-sectionally averaged tidal fluctuations.

The residual transport of water can be separated into two parts: one (Q_f) is due to freshwater inputs to the Channel (for example, $Q_{f,CC}$ is shown as flowing from the Central Channel South (CCS) to the Central Channel North (CCN) in Fig. 9), and the other results from all other mechanisms, Q_R:

$$\langle Q\rangle = Q_f + Q_R,$$

so that the residual transport of salt across A is:

$$\langle F\rangle = Q_f S + Q_R S + \{\langle\tilde{Q}\tilde{s}\rangle + \langle A\overline{u's'}\rangle\}, \tag{9}$$

where $S = \langle\bar{s}\rangle$.
An empirical mixing coefficient, E, is defined by:

$$E = -\{\langle\tilde{Q}\tilde{s}\rangle + \langle A\overline{u's'}\rangle\}/\delta S, \tag{10}$$

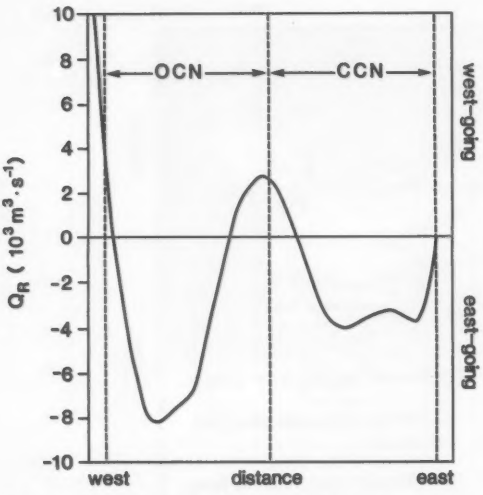

FIG. 11. Total west-going residual flow of water, Q_R, through the Outer Channel North and Central Channel North, according to the hydrodynamical model.

in which δS is the difference in tidally averaged salinity between the two GEMBASE regions under consideration. Equation (9) becomes:

$$\langle F \rangle = Q_f S + Q_R S - E\delta S. \quad (11)$$

RESIDUAL FLOWS

The freshwater flows across region boundaries in Fig. 9 can be determined from the hydrodynamical model. As the freshwater from each source enters a region it produces a head of water which drives currents out of the Channel. These currents are extremely small compared with the tidal flows, so that flow patterns can be investigated for each input of freshwater, and then summed to take into account all inputs according to:

$$\mathbf{Q}_f = \mathbf{B} \cdot \mathbf{Q}_{f,i}, \quad (12)$$

where $\mathbf{B}$ is a constant (9 × 9) matrix, $\mathbf{Q}_f$ are the flows $Q_{f,IE}$ to $Q_{f,OCS}$, and $\mathbf{Q}_{f,i}$ are the inputs $Q_{f,IE}$ to $Q_{f,OCS}$ (see Fig. 9).

Residual flows, Q_R, are shown in Fig. 10, together with mixing coefficients, E, which are defined at region boundaries. The residual flow from the Central Channel South to North is $Q_{R,CC}$, and that from the Outer Channel South to North is $(Q_{R,OC} - Q_{R,CC})$. Q_R was computed from the hydrodynamical model, and is the residual flow due to M_2 tidal nonlinearities and density currents (Uncles 1982). Wind-driven currents have not yet been incorporated in GEMBASE, and the extent to which they contribute to the seasonal variability of the ecosystem is not known.

The residual flow of water through the Outer Channel North and the Central Channel North, according to the hydrodynamical model, is drawn in Fig. 11. The spatial variability of Q_R is large, and $Q_{R,CC}$ and $Q_{R,OC}$ are, unfortunately, sensitive to the locations of the GEMBASE region boundaries. A schematic picture of the large-scale residual circulation, according to the hydrodynamical model, is drawn in Fig. 12.

MASS BALANCE

The tidally averaged mass of salt in a GEMBASE region of volume v is:

$$M_s = \langle v\bar{\bar{s}} \rangle$$

where $\bar{\bar{s}}$ is an average over v. If a tilde is now used to denote a volume averaged tidal fluctuation, then M_s may be written:

$$M_s = \langle v \rangle \langle \bar{\bar{s}} \rangle \cdot [1 + \langle \tilde{v}\tilde{s} \rangle / \langle v \rangle \langle \bar{\bar{s}} \rangle] \simeq VS,$$

using $V = \langle v \rangle$, $S = \langle \bar{\bar{s}} \rangle$ and estimating $\langle \tilde{v}\tilde{s} \rangle / VS \sim 10^{-3}$.

The mass balance for salt in the Central Channel South, using equation (11) and with reference to Fig. 9 and 10 may therefore be written:

$$\begin{aligned} V_{CCS}\frac{d}{dt}(S_{CCS}) = &+ [Q_{f,IC}(S_{IC} + S_{CCS})/2 \\ &- E_{IC}(S_{CCS} - S_{IC})] \\ &- [(Q_{f,CCS} - Q_{R,CC})(S_{OCS} + S_{CCS})/2 \\ &- E_{CCS}(S_{OCS} - S_{CCS})] \\ &- [(Q_{f,CC} + Q_{R,CC})(S_{CCN} + S_{CCS})/2 \\ &- E_{CC}(S_{CCN} - S_{CCS})] \end{aligned} \quad (13)$$

A similar equation holds for each GEMBASE region, and for each variable subjected to advection and mixing — source terms being added to equation (13) to account for possible growth or decay.

ESTIMATES FOR MIXING

Q_f and Q_R have been determined for use in equation (13); the mixing coefficients, E, are more difficult to compute. The method used to estimate E is based on the satisfaction of equation (13). If equation (13) is averaged over a number of years, then S will represent the long-term average salinity for each GEMBASE region, with $dS/dt = 0$, and Q_R and Q_f will represent the long-term flows. Thus, all of the extensive salinity data for each region in Fig. 9 were averaged to yield long-term values. For the Outer Estuary and Inner Channel the balance is given by equation (11) with $Q_R = 0$ and $\langle F \rangle = 0$ (see also Uncles and Radford 1980), so that:

$$E = Q_f S/\delta S \quad (14)$$

yielding E_{IE}, E_{OE}, and E_{IC}. In the two-dimensional region there are six mixing coefficients, E_{CC} to E_{OCS} (see Fig. 10), and only four equations of the form of equation (13) — one for each region. Therefore, two values of E must be estimated directly from the hydrodynamical model, using equation (10) in conjunction with the long-term averaged salinity data. The flux in equation (10) consists of a part due to tidal pumping, $\langle \tilde{Q}\tilde{s} \rangle$, and a part due to transverse shear in the tidal and residual currents. Following Fischer et al. (1979), the effect of tidal shear can be shown to be negligible. The flux due to shear in the residual currents is:

$$\langle A\overline{u's'} \rangle \simeq \langle A \rangle \langle \overline{u'} \rangle \langle \overline{s'} \rangle, \quad (15)$$

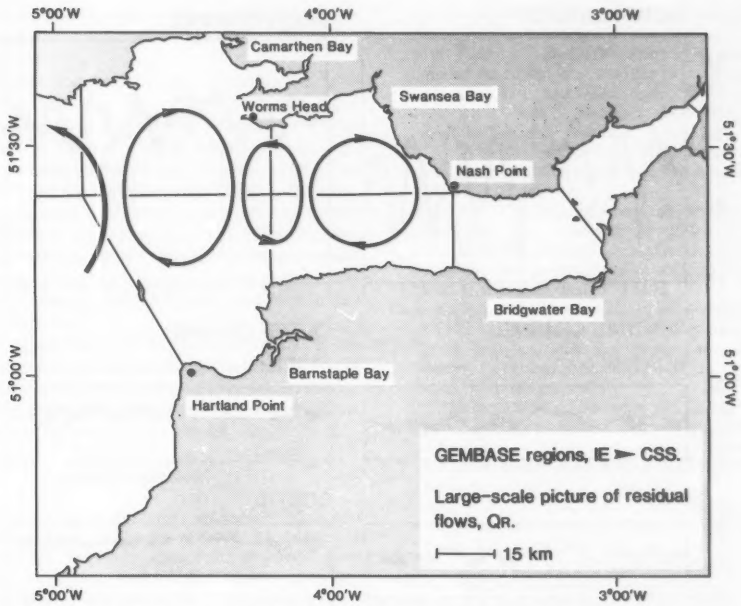

FIG. 12. Large-scale residual circulation, Q_R, in the Bristol Channel.

where, to take into account the Stokes drift (Uncles and Jordan 1979), $\langle u' \rangle$ must be computed as:

$$\langle u' \rangle = \{\langle Hu \rangle - \langle \overline{Hu} \rangle\} / \langle H \rangle,$$

and where the cross-sectional average is over $\langle A \rangle$, H being the instantaneous depth. The effects of tidal pumping cannot be estimated with any certainty, and are ignored; therefore, equations (10) and (15) give:

$$(16) \quad E = -\langle A \rangle \langle \overline{u'} \rangle \langle s' \rangle / \delta S,$$

which can be computed using $\langle u' \rangle$ from the hydrodynamical model, and using $\langle s' \rangle$ and δS from the long-term averaged salinity data.

In principle, E could be derived from equation (16) for each boundary between GEMBASE regions. However, the current shear along those boundaries which terminate on headlands are dominated by the small intense circulation patterns near the headlands (for example, boundaries with mixing coefficients E_{CCS} and E_{OCS} in Fig. 10); because the observed salinity is determined on a lattice which has only one third the resolution of the hydrodynamical model (9 km as opposed to 3 km), the shear flux of salt in these headland circulations cannot be computed with accuracy. Also, the boundary between the Outer Channel North (*OCN*) and the Celtic Sea North (*CSN*) in Fig. 9 is very close to the seaward boundary of the hydrodynamical model, and may be subject to possible spurious boundary circulation patterns (Prandle 1978) and their associated shear. Finally, in view of the very small salinity difference ($\delta S = 0.22$‰) between the Central Channel North (*CCN*) and the Central Channel South (*CCS*), it was decided to compute E_{CC} from the observed salt balance. Therefore, E_{CCN} and E_{OC} were computed directly from equation (16); the method yields a shear flux of salt into the Central Channel North (*CCN*) from the Outer Channel North (*OCN*) in Fig. 9 of 517‰ $m^3 \cdot s^{-1}$, which with $\delta S = 0.98$‰ gives:

$$E_{CCN} = 5 \times 10^2 \text{ m}^3 \cdot \text{s}^{-1}.$$

The computed shear flux from the Outer Channel South (*OCS*) to the Outer Channel North (*OCN*) in Fig. 9 is 2310‰ $m^3 \cdot s^{-1}$, which with $\delta S = 0.72$‰ gives:

$$E_{OC} = 3 \times 10^3 \text{ m}^3 \cdot \text{s}^{-1}.$$

Using these values, the remaining coefficients can be derived from the long-term salt balance for each region (equations of the form of equation (13) for S_{CCS}, S_{CCN}, S_{OCS}, and S_{OCN} with $dS/dt = 0$).

SIMULATION OF SALINITY

The results of a simulation of the salt balance using the preceding model are shown in Fig. 13. The agreement between observed and computed data is generally good, not only for the mean values of salinity for each region, but also for the seasonal variations. To achieve this measure of agreement it was necessary to increase E_{CCS} by 50% over the value computed using the long-term salt balance, and to increase E_{IC} by 25%. Such trial and error adjustment is justified in view of the neglect of tidal pumping in the application of equation (10), and, more importantly, the neglect of correlations between Q_f and S in taking the long-term average of equation (13). The

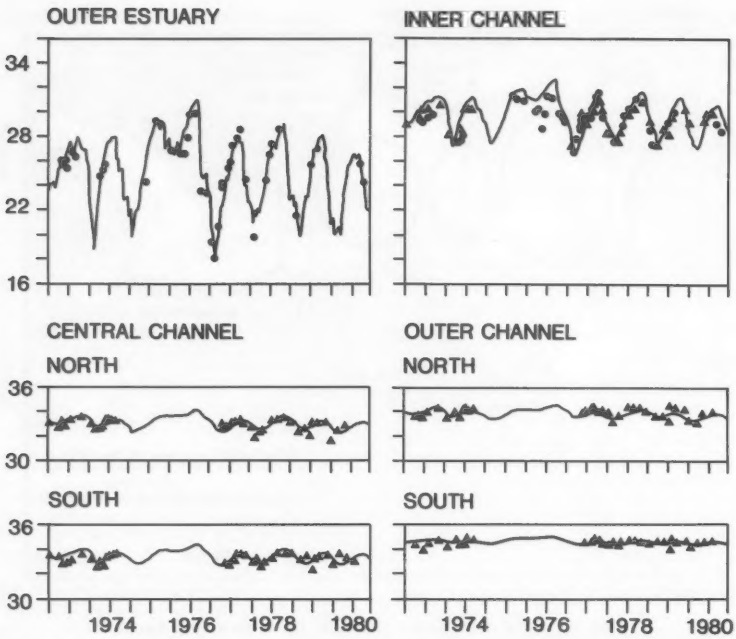

FIG. 13. Computed and observed salinities for the GEMBASE regions as functions of time. IMER data (▲), other sources (●).

agreement between observed and computed mean values of salinity for each region might be expected in view of the fact that these data were used in the process of defining mixing coefficients for the model. Nevertheless, the fact that seasonal variations are also reproduced with reasonable accuracy implies that the model has a substantial, although much simplified, physical basis.

Improvements between computed and observed data could possibly be achieved by incorporating wind-driven currents, or by further trial and error adjustment of the mixing coefficients.

Discussion

This paper has demonstrated the value of a hydrodynamical model of the Bristol Channel for two problems in marine ecology. In the first of these, the model has been used to investigate the relationships between tidal stress and sediment bed-types, and between tidal stress and benthic macrofaunal associations. The model has also been used to infer the direction of sediment transport as bed-load (neglecting wind–wave effects), and to investigate the basic mechanism producing this transport, which is the result of asymmetry in the flood and ebb currents due to M_4 and residual currents.

The second problem concerns the definition of long-term transport for use in a coarse-lattice, ecosystem model of the Bristol Channel. The approach taken here is somewhat different from that taken by Kremer and Nixon (1978) in their ecosystem model of Narragansett Bay. In that work, fine-lattice hydrodynamical and water quality models were used together, in order to determine the transport (during the course of a day) between the eight large regions used to define their ecological model of the Bay. The daily exchanges between regions were tabulated as functions of tidal range on that day, and used to express the transport between regions during the course of an ecosystem simulation. The relevance of the tidal range can be seen from the flushing time of Narragansett Bay, which is about 30 d (two spring–neap cycles). The individual flushing times of each of the eight ecosystem regions will be much less than this. Therefore, the exchanges between regions will have a strong spring–neap tidal dependence. In contrast, the flushing time for the Severn Estuary is in the range 100–200 d (Uncles and Radford 1980), and the flushing times for the whole of the Channel will be much greater. Thus, variations over a spring–neap cycle will be rather small, and the dominant variations will be seasonal. For this reason, mixing coefficients and tidally induced residual flows for the Bristol Channel have been modeled as depending on average (M_2) tidal conditions. Freshwater-induced flows are highly seasonal in character, and are therefore treated as time-dependent. The method used by Kremer and Nixon (1978) suffers from difficulties at the open (seaward) boundaries of their fine-lattice hydrodynamical and water quality models. As with all such models of limited extent, conditions are not known exactly at the open boundaries, so that dispersive transport (mixing) across them is to some degree uncertain.

This has not been a difficulty with the Bristol Channel model, in which observed salinity data have been used to define the mixing.

The present ecological model does suffer from the limitation that mixing cannot be defined immediately in those situations where major alterations have occurred to the tidal currents, as would be the case with the introduction of, say, a tidal barrage. In these circumstances, residual currents can again be derived from the hydrodynamical model, but long-term, large-scale mixing coefficients would need to be defined from theoretical considerations. The most straightforward way of generating salinity data for the method would be through the application of a fine-lattice salinity model, the open boundaries of which extended some considerable distance into the Celtic Sea.

Although not reported here, the hydrodynamical model has also been used to investigate time-scales for vertical mixing in the Channel. These data have contributed to an understanding of phytoplankton dynamics in the highly turbid waters of the Severn Estuary and eastern Bristol Channel.

Acknowledgments

I am grateful to Mr M. B. Jordan for his assistance with the field observations, and to Mr M. J. Howarth of the NERC Institute of Oceanographic Sciences, for permission to publish data from current meter station BID. Salinity data from GEMBASE simulations were kindly supplied by Mr P. J. Radford.

This work, which forms part of the estuarine ecology program of the Institute for Marine Environmental Research, a component of the Natural Environment Research Council (NERC), was partly supported by the Department of the Environment on Contract No DGR 480/48.

BELDERSON, R. H., AND A. H. STRIDE. 1966. Tidal current fashioning of a Basal Bed. Mar. Geol. 4: 237–257.

FISCHER, H. B., E. J. LIST, R. C. Y. KOH, J. IMBERGER, AND N. H. BROOKS. 1979. Mixing in inland and coastal waters. Academic Press, New York, NY. 484 p.

JOINT, I. R. 1983. The development of an ecosystem model of a turbid estuary. Can. J. Fish. Aquat. Sci. 40(Suppl. 1). (This issue)

KENYON, N. H. 1970. Sand ribbons of European tidal seas. Mar. Geol. 9: 25–39.

KREMER, J., AND S. W. NIXON. 1978. A coastal marine ecosystem. Ecol. Stud. 24: 250 p.

MILES, G. V. 1979. Estuarine modelling — Bristol Channel, p. 76–84. *In* R. T. Severn et al. [ed.] Tidal power and estuary management. Scientechnica.

PINGREE, R. D., AND D. K. GRIFFITHS. 1979. Sand transport paths around the British Isles resulting from M_2 and M_4 tidal interactions. J. Mar. Biol. Assoc. U.K. 59: 497–513.

PINGREE, R. D., AND L. MADDOCK. 1977. Tidal residuals in the English Channel. J. Mar. Biol. Assoc. U.K. 57: 339–354.

1978. The M_4 tide in the English Channel derived from a non-linear numerical model of the M_2 tide. Deep Sea Res. 25: 53–63.

PRANDLE, D. 1978. Residual flows and elevations in the southern North Sea. Proc. R. Soc. (A) 359: 189–228.

1980. Modelling of tidal barrier schemes: an analysis of the open-boundary problem by reference to AC circuit theory. Estuarine Coastal Mar. Sci. 11: 53–71.

RADFORD, P. J. 1979. Some aspects of an estuarine ecosystem model-GEMBASE, p. 301–322. *In* S. E. Jorgensen [ed.] State of the art in ecological modelling. Proceedings of the International Society for Ecological Modelling conference on ecological modelling, Copenhagen, 1978.

1981. Modelling the impact of a tidal power scheme on the Severn Estuary ecosystem. Paper presented at the International Symposium — Energy and Ecological Modelling, sponsored by the International Society for Ecological Modelling (Louisville, Kentucky, April 20–23, 1981). 13 p.

RADFORD, P. J., AND I. R. JOINT. 1980. The application of an ecosystem model to the Bristol Channel and Severn Estuary. Water Pollut. Control 79: 244–250.

RADFORD, P. J., R. J. UNCLES, AND A. W. MORRIS. 1981. Simulating the impact of technological change on dissolved cadmium distribution in the Severn Estuary. Water Res. 15: 1045–1052.

TEE, K. T. 1976. Tide-induced residual current, a 2-d non-linear numerical tidal model. J. Mar. Res. 34: 603–628.

UNCLES, R. J. 1981a. A numerical simulation of the vertical and horizontal M_2 tide in the Bristol Channel and comparisons with observed data. Limnol. Oceanogr. 26: 571–577.

1981b. A note on tidal asymmetry in the Severn Estuary. Estuarine Coastal Shelf Sci. 13: 419–432.

1982. Computed and observed residual currents in the Bristol Channel. Oceanol. Acta 5: 11–20.

UNCLES, R. J., AND M. B. JORDAN. 1979. Residual fluxes of water and salt at two stations in the Severn Estuary. Estuarine Coastal Mar. Sci. 9: 287–302.

UNCLES, R. J., AND P. J. RADFORD. 1980. Seasonal and spring–neap tidal dependence of axial dispersion coefficients in the Severn — a wide, vertically mixed estuary. J. Fluid Mech. 98: 703–726.

WARWICK, R. M., AND R. J. UNCLES. 1980. Distribution of benthic macrofauna associations in the Bristol Channel in relation to tidal stress. Mar. Ecol. Prog. Ser. 3: 97–103.

Suspended Sediment Transport and Deposition Modeling in the Bay of Fundy, Nova Scotia — a Region of Potential Tidal Power Development[1]

D. A. GREENBERG

Department of Fisheries and Oceans, Atlantic Oceanographic Laboratory, Bedford Institute of Oceanography, P.O. Box 1006, Dartmouth, N.S. B2Y 4A2

AND C. L. AMOS

Department of Energy, Mines and Resources, Atlantic Geoscience Centre, Geological Survey of Canada, Bedford Institute of Oceanography, P.O. Box 1006, Dartmouth, N.S. B2Y 4A2

GREENBERG, D. A., AND C. L. AMOS. 1983. Suspended sediment transport and deposition modeling in the Bay of Fundy, Nova Scotia — a region of potential tidal power development. Can. J. Fish. Aquat. Sci. 40(Suppl. 1): 20–34.

Two recent independent studies of the Minas Basin have been combined to produce a numerical simulation of suspended sediments. One study devised a numerical, barotropic tidal model of the Bay of Fundy and Gulf of Maine, which produced a good simulation of the tides and currents in the Minas Basin. The second, an extensive program of sediment sampling and monitoring addressed the nature of suspended sediments, bottom sediments, their various sediment sources and the postglacial evolution of the system. The only significant source of suspended sediment was from the open boundary to the Minas Basin and was of relatively uniform concentration through the water column. Consequently, the barotropic tidal model was well suited to modeling this material. Sediment laws describing sediment settling, resuspension, and the critical stress for entrainment were obtained from the literature and evaluated. The settling velocity of the suspended sediment was obtained by experimentation using actual water/sediment samples. Because the various parameters and critical stresses show a considerable variation among experimenters, runs were planned to examine a range of parameters. A close fit to existing conditions was obtained with the model generating mudflats in those regions where indeed they exist. Using the various parameters and critical stresses reflecting maximum sedimentation, the model was run to include the effects of a tidal power barrage off Economy Point. It is concluded that suspended sediment would not inhibit the operation of such a barrage through siltation directly in front of or behind the barrier. Increased siltation can be expected in the intertidal areas behind the barrage. Sediment budget considerations further limit the degree of post barrier siltation, insofar as the resident volume of suspended material (30×10^6 m^3) is not enough to significantly reduce the headpond area.

Key words: suspended sediment, sediment transport, numerical model, tide

GREENBERG, D. A., AND C. L. AMOS. 1983. Suspended sediment transport and deposition modeling in the Bay of Fundy, Nova Scotia — a region of potential tidal power development. Can. J. Fish. Aquat. Sci. 40(Suppl. 1): 20–34.

Une simulation numérique de sédiments en suspension a été obtenue en combinant deux études indépendantes récentes du bassin des Mines. La première a conduit à un modèle de marée barotropique numérique de la baie de Fundy et du golfe du Maine, produisant une bonne simulation des marées et des courants dans le bassin des Mines. La seconde, un programme intensif d'échantillonnage et de surveillance des sédiments, a porté sur la nature des sédiments en suspension, des sédiments du fond, de leurs sources et de l'évolution postglaciaire du système. L'unique source de quelque importance de sédiments en suspension est la frontière s'ouvrant sur le bassin des Mines, et la concentration est relativement uniforme dans toute la colonne d'eau. C'est dire que le modèle de marée barotropique convient bien à la modélisation de ce matériel. Nous avons extrait de la littérature et évalué les lois régissant la sédimentation, la resuspension et le stress critique nécessaire à l'entraînement. Des échantillons d'eau/sédiments réels ont permis d'obtenir par expérimentation la vitesse de déposition

[1]This paper forms part of the Proceedings of the Dynamics of Turbid Coastal Environments Symposium convened at the Bedford Institute of Oceanography, Dartmouth, N.S., Canada, September 29–October 1, 1981.

Printed in Canada (J6707)
Imprimé au Canada (J6707)

des sédiments en suspension. Comme les divers paramètres et stress critique varient considérablement d'un expérimentateur à l'autre, nous avons préparé un passage machine afin d'étudier une gamme de paramètres. Le modèle engendant des vasières dans les régions où elles existent en réalité s'accorde bien avec les conditions existantes. Un passage machine incluant les effets d'un barrage marémoteur au large de la pointe Economy a été effectué en utilisant les divers paramètres et stress critique d'un maximum de sédimentation. Nous concluons que les sédiments en suspension n'entraveraient pas le fonctionnement d'un tel barrage, que l'envasement se produise directement devant ou derrière la barrière. On peut s'attendre à un envasement accru dans les zones intertidales derrière le barrage. Les considérations de budget sédimentaire limitent encore davantage le degré d'envasement derrière la barrière, en autant que le volume résidant de matière en suspension (30×10^6 m^3) n'est pas assez grand pour réduire de façon significative la superficie du réservoir.

Received October 30, 1981
Accepted August 30, 1982

Reçu le 30 octobre 1981
Accepté le 30 août 1982

THE Bay of Fundy, situated between the Nova Scotian peninsula and New Brunswick (Fig. 1), has been the subject of study for potential tidal power development since 1919. Engineering surveys were conducted by Canada in 1945 (Anon.), 1969 (ATPPB, Atlantic Tidal Power Programming Board), and 1977 (TPRB, Tidal Power Review Board) to verify this potential. Only during the last survey was tidal power demonstrated feasible and then only for the Cumberland Basin and Minas Basin sites shown in Fig. 1. Based on economic projections, the two schemes, if built, would yield a profit of 20% in an operating lifetime of 65 yr (TPRB 1977).

The schemes proposed for the two economic sites are single-basin, single-effect types (one way ebb-flow power generation). Power generation would take place for 5–6 h during the ebbing portion of the tide only. Refilling of the basin would take place during the flooding tide with associated pumping at high and low tide. The resulting tidal range in the headpond region of the Minas Basin barrier would be reduced by 50%, though there would be both local increases in current speed (28 m·s^{-1} at the turbines), and elsewhere local decreases in current speed. The overall impact of the scheme would be a reduction in the local tidal energy available for sediment transport, but an increase in tidal energy further afield (Greenberg 1979) in the Gulf of Maine.

The Minas Basin is subject to high tidal ranges and strong tidal currents, which have been well documented (Tee 1977; Godin 1968). The consequence of these strong currents is a high mobility of sediment both in suspension and as traction load (Dalrymple 1977; Lambiase 1977). Several engineering schemes, such as solid fill causeways and reclamation dykes, have been built around the Bay of Fundy. The response of the environment to these constructions has been a dramatic increase in local siltation (Amos and Long 1980): summertime sedimentation rates reaching 5 cm·mo^{-1} near the Windsor Causeway. The question remains, however, "what effect would a tidal barrage have on the balance of sediment deposition and transport in the course of normal day-to-day operation of the scheme?"

We proposed to resolve the question by using predictive simulations of the fluid dynamic behavior after barrage construction. A well-defined set of boundary conditions to the model was used, such as source of material, initial distribution of material and presently existing deposition sites. The model employed the appropriate equations relating fluid motion to sediment response, and used properties of the suspended particulate matter found in the study region. The model was verified through a number of calibration checks of presently existing conditions prior to its use predictively.

On many occasions, the questions have been asked, "To what extent can presently existing structures be used as analogies to a potential tidal power scheme?" and, "How valid are the existing laws governing sedimentation of cohesive material?" In this paper we have attempted to address these questions by the combination of a numerical model and a sediment budget analysis. The first is a predictive numerical tidal model of the M_2 tidal excursion in the Bay of Fundy (Greenberg 1979) and the second, an analysis of the budget and character of sediment in the Minas Basin System (Amos and Joice 1977). The combination of the studies, describing the transport, settling, and resuspension of the sediment is referred to as the sediment model.

The Tidal and Sediment Models

The tidal model is a two-dimensional, depth averaged, simulation of the Bay of Fundy and Gulf of Maine tides solving the equations of continuity and motion in standard, nonlinear form. The equation of continuity is as follows:

$$(1) \qquad \frac{d[(h+\xi)u]}{dx} + \frac{d[(h+\xi)v]}{dy} + \frac{d\xi}{dt} = 0$$

The nonlinear equations of motion incorporating the effects of friction and Coriolis force are:

$$(2) \qquad \frac{du}{dt} + \frac{udu}{dx} + \frac{vdu}{dy} - \gamma v = -g\frac{d\xi}{dx} - ku\frac{(u^2+v^2)^{1/2}}{h+\xi}$$

and

$$(3) \qquad \frac{dv}{dt} + \frac{udv}{dx} + \frac{vdv}{dy} + \gamma u = -g\frac{d\xi}{dy} - kv\frac{(u^2+v^2)^{1/2}}{h+\xi}$$

where

t — time
ξ — water elevation
γ — the Coriolis parameter
k — a friction coefficient
h — depth of water from mean level
u, v — currents in x and y direction, respectively
g — acceleration due to gravity

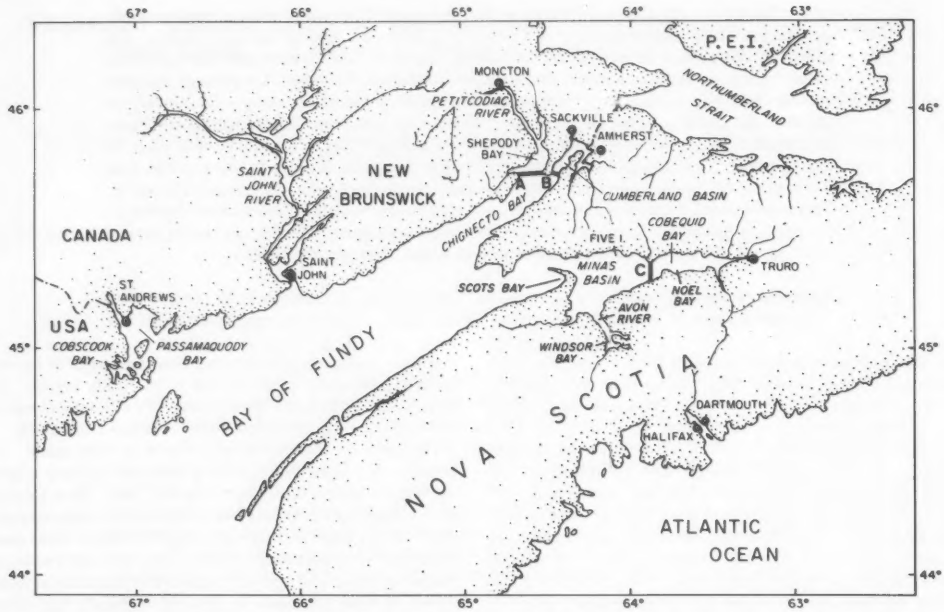

FIG. 1. Bay of Fundy showing preferred sites for tidal power development. A, B, and C refer to prime sites for tidal power development. Site C is considered in this paper.

These equations are discretised on a Richardson Lattice (Fig. 2) which represents the entire Bay of Fundy and Gulf of Maine, to the edge of the continental shelf. The grid size is 22.14 km in the Gulf of Maine and progressively decreases in size to 1.661 km in the Minas Basin (Fig. 3). The equations of motion are solved in an explicit, finite difference scheme (Greenberg 1976). The model simulates the M_2 component of tidal motion, the period of this lunar tidal constituent being 12.42 h. This is the dominant tidal constituent in the region and can be considered to be representative of mean conditions.

The model has been verified by detailed tidal elevation measurements throughout the Bay of Fundy (TPRB 1977) and the resulting barotropic currents are representative of field conditions both in magnitude and direction (Tee 1977; Godin 1968).

The Richardson Lattice (Fig. 2) is well suited to the simulation of suspended sediment transport. Current speed is defined across the margins of each cell of the model and the central point of each cell is the reference elevation point. In modeling suspended sediment transport, concentration of sediment (SSC) is defined at the central point and the advection of sediment is calculated across each of the cell boundaries. The net change in concentration of sediment at any time is computed from the difference between the transport volume into and out of the cell over a finite time step.

Numerical transport algorithms can lead to artificial diffusion in low order schemes, as the concentration in any cell is considered constant throughout that cell. In our calculation this was reduced by using an algorithm put forward by Book et al. (1975) and later improved by Zalisak (1979). This method, known as the Flux Corrected Transport method (FCT), is a two step process involving a low order calculation of transports and concentrations and a subsequent higher order calculation. The diffusion represented in the tidal model was calculated using Zimmerman's (1976) method applied to the model residual flow field and the tidal current magnitudes (Greenberg et al., unpublished data). The value of the eddy diffusion coefficient was found to be in the order of 1.4×10^3 m$^2 \cdot$s^{-1}, slightly higher than the range determined by Holloway (1981) for this region. Thus any further addition of eddy diffusion to the sediment model formulation would have been superfluous.

A routine was included to simulate the intertidal regions of the model, which become exposed at lower tidal elevations. The routine prevented the water level in the model falling below ground level in the cells in question.

The transport equations used in the sediment model are simply:

$$\frac{\partial(h+\xi)\rho}{\partial t} + \frac{\partial(h+\xi)u\rho}{\partial x} + \frac{\partial(h+\xi)v\rho}{\partial y} = S$$

Where the notation is as before, with ρ the concentration and S accounting for sources and sinks through the boundaries of the model. The initial regime (ρ) is specified using the observations described later. The motions of the water (ξ, u, v) through a tidal cycle are specified from results of the tidal

model. Details of the numerical procedure for the transport of suspended sediment are given in the appendix.

The model does not take into consideration the effect of ice or storms and therefore best represents the dynamics of mean summer conditions. To complete the definition of the sediment model, we need to know the conditions of boundary flow together with certain properties of the sediment. Suspended sediment concentration and bedload are adjusted each time step after the transport calculation. Deposition and resuspension rates which are central to the problem depend on the instantaneous bottom stress. This stress is derived directly from the tidal model using the model's quadratic friction law where $k = 2.3 \times 10^{-3}$. The nature of this dependence and critical stress is discussed later. Values are subject to much interpretation and a wide range of relationships and values are documented.

Sediment Model Assumptions

A number of assumptions have been made in implementing the model:

1) The model assumes an even distribution of suspended sediment through each cell of the model. In reality a 30% variation has been observed due to patchinesses caused by turbulence.
2) The model uses a depth averaged current value. The bottom stress based on these currents, obtained in calibrating the tidal model, is used in the appropriate sedimentation laws. In some circumstances the current profile can be more complicated than can be represented by a depth averaged current.
3) The distribution of suspended particulate matter (SPM) is considered constant throughout the water column. This was generally true except at times of high water when some gravity settling was observed.
4) No phase lag in sedimentary response to the applied stress was considered.
5) The settling rate (v_o) did not vary as a function of initial sediment concentration.

The Properties of Suspended Sediments

Size and Composition

The size, shape, and composition of suspended particulate matter in Minas Basin were determined by the analysis of 48 samples using a Cambridge Stereo Scan 180 scanning electron microscope and by Coulter Counter analysis. In the first instance results showed that the majority of the material was made up of composite sedimentary particles. These particles varied considerably in shape and composition. A variety of typical examples is shown in Fig. 4A–D. The larger particles appear to have four origins: (1) pelletization (4A), (2) flocculation (4B), (3) pelletization and flocculation (4C), and (4) single particles resuspended from the bed (4D). The sizes ranged from 5 to 100 μm, with the modal diameter at 30 μm. Particle counts from micrographs of samples taken at a variety of depths and locations yield results which are very similar in both composition and size. The Coulter Counter analyses verify the size at 30 μm with minor secondary modes at 80 and 3 μm.

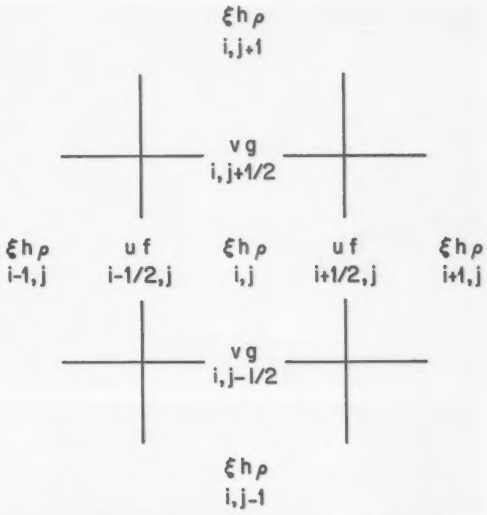

FIG. 2. Richardson Lattice, showing spatial distribution of ξ, u, v, and density elements used in sediment model.

Krone (1978) suggested that material becomes fully flocculated above salinities of 15‰ and that equilibrium of particle sizes is achieved within approximately 12 h. The theoretical equilibrium floc size can be determined using the following formula:

$$(4) \qquad r = \frac{16\Delta r}{3\pi} \cdot \frac{\tau_{max}}{\tau}$$

where $\tau = \eta \cdot \frac{du}{dz}$

and η = 0.01 poises
r = grain radius
Δr = grain roughness
τ_{max} = 0.07 dynes·cm^{-2}
$\frac{du}{dz}$ = instantaneous current slope

τ_{max} is the critical stress for floc disintegration. Herein we use the values determined by Krone.

The instantaneous shear on a suspended grain was determined for maximum current speeds (1.6 m·s^{-1}). The Karman–Prandtl velocity structure was shown to be valid for the system (Dalrymple 1977) and the boundary layer extends to the surface. The slope of the current velocity $\frac{du}{dz}$, is a function of the reciprocal of the height above the bed $\frac{1}{(h-z)}$. The implication of this is that larger particles form by flocculation higher in the water column and upon settling to the lower part of the boundary layer, break down into smaller flocs. However, this was not observed in nature. This may result from turbulent mixing which occurs on a much higher frequency than the 12-h phase lag in floc size readjustments. In view of this, the depth averaged stress at maximum flows was used to determine the equilibrium floc radius and was

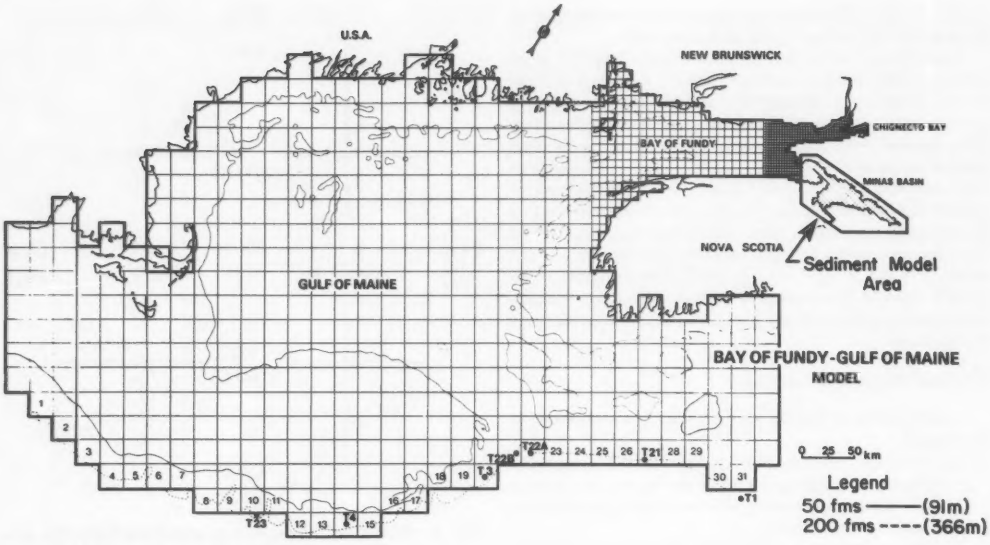

FIG. 3. Outline of numerical tidal model.

0.01 dynes·cm^{-2}, corresponding to an equilibrium grain size of 38 μm. This is close to the measured modal size of the Minas Basin suspended material and suggests that the flocs are in equilibrium with the maximum mid-flood and mid-ebb flows which constitute periods of maximum agitation.

SETTLING RATE

In view of the diversity in shape, composition and no doubt, density of the SPM, settling experiments were conducted to measure directly the settling velocity of the particles. A modified bottom withdrawal tube (Federal Interagency Sub-Committee on Sedimentation 1953) was used. Results showed that within a still water environment, settling of grains "en masse" occurs and is described (above concentrations of approximately 60 mg·L^{-1}, which is typically exceeded in much of Minas Basin) by Bradley (1965). For lower concentrations of sediment, the settling occurs as individual particles and the suspended concentration decreases in an exponentially decaying fashion.

The results of eight settling experiments, conducted along the shores of Minas Basin using actual seawater samples showed that the half-life of the surface suspended concentration was in the order of 6 min. The curve of the concentration versus time is defined by:

$$(5) \qquad C(t) = C_0 \exp^{-kt}$$

The half-life becomes significantly longer at lower concentrations which may result from upwelling effects within the tube. The coefficient k was evaluated to be 0.053 (for t measured in minutes). Krone (1978) presents the following modification to equation (5) for moving flows:

$$(6) \qquad C = C_0 e^{-[\frac{PtV_0}{y}]}$$

where

C = SSC at time (t)
C_0 = SSC at time ($t = 0$)
V_0 = particle settling rate (in still water)
y = water depth
P = probability of grain resuspension
$= \left(1 - \frac{\tau}{1.2}\right)$.

and

τ = bottom shear stress (in dynes·cm^{-2}). We have used a value of 1.2 dynes·cm^{-2} as the critical shear stress for deposition rather than the value of 0.6 dynes·cm^{-2} used by Krone (1962). This modification yielded a more realistic deposition rate upon running the model when compared to observations near Windsor Causeway.

From equation 6, a representative particle settling rate (V_0) was determined for the average size and density range of the particles. The modal size settling rate (30 μm) was determined to be 1.1×10^{-3} m·s^{-1} and this latter value was adopted as it was deemed more appropriate to the specific size of sediment being modeled.

By application of Stokes Law to the settling rate, the particle density was determined. The modal size particles have a density of 1510 kg·m^{-3}.

CRITICAL STRESS FOR PARTICLE SETTLING

The mass settling of particles through a moving water column is generally defined by the following formula:

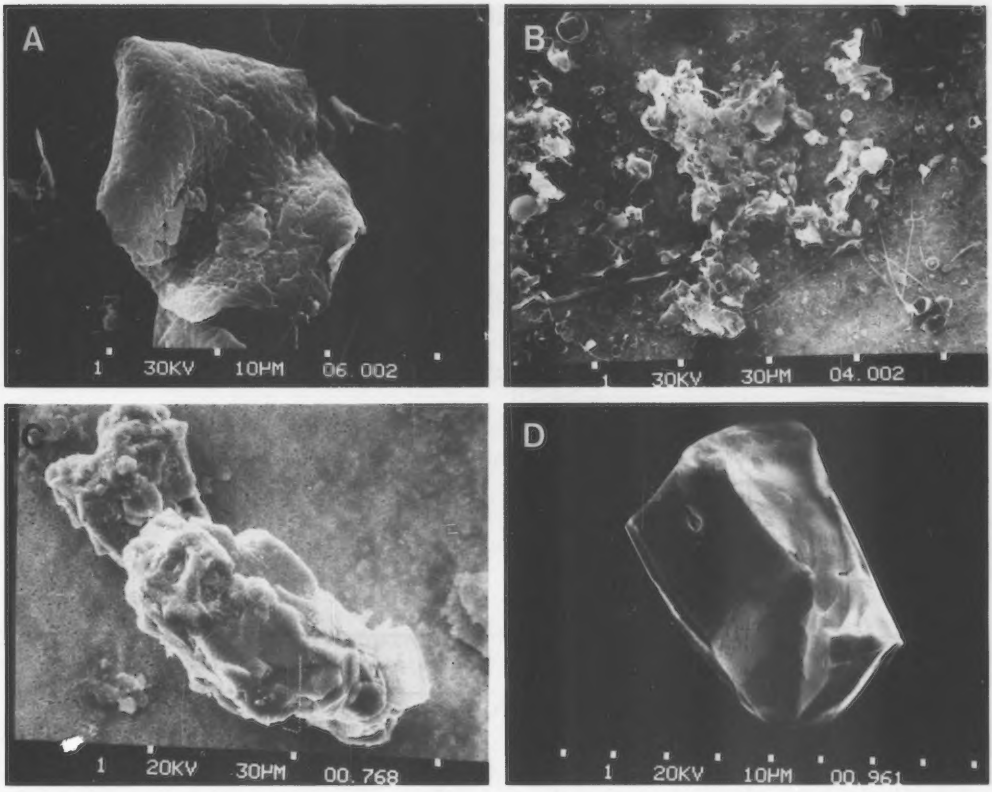

FIG. 4. Scanning electron micrographs: (A) pelletization, (B) flocculation, (C) pelletization and flocculation, and (D) single particle resuspended.

$$(7) \qquad M = C_0 \cdot V_0 \left(1 - \frac{\tau}{\tau_d}\right) P$$

Krone (1962) suggests a value for the critical stress for settling (τ_d) of 0.6 dynes·cm^{-2} whereas Parthenaides and Mehta (1971) give a value of 1.60 dynes·cm^{-2}. We chose, however, to use the intermediate results of Parthenaides (1971) who showed τ_d for flocculated material in a saline solution, to be 0.84 dynes·cm^{-2}. The length of time the stress is less than the critical value in Minas Basin is approximately 1 h over the high and low tide slack water periods.

The probability term (P) for grain deposition was not evaluated in this method and arbitrarily set to 1.0. However, the effects of ice, bioturbation, wave stirring, etc. contribute to reduce P from unity, which implies a reduction in the rate of mass settling. The equation, therefore expresses the highest deposition rates.

Critical Stress for Particle Erosion

Various studies show that the critical shear stress for sediment erosion is a time dependent function, increasing in proportion with time after deposition. This may explain, in part, the variation in critical stresses for materials quoted in the literature. These values vary from 0.11 to 4.5 dynes·cm^{-2}. Initially an intermediate critical stress value of 1.28 dynes·cm^{-2} was used in the model, however the effects of the higher value to 2.56 dynes·cm^{-2} were also examined. This value is 2−10 times larger than values quoted for the erosion of newly deposited muds (Southard et al. 1971). A list of a variety of values determined in the laboratory and in the field is given in Amos and Greenberg (1980). It is clear that the stress for erosion or deposition of a cohesive sediment should be related to the geotechnical properties of that sediment rather than to a loose verbal description of the material. In this manner, examples cited in the literature could be more confidently used in the modeling process.

To simplify the problems of erosion and deposition of cohesive mud, two critical stresses were used in the sediment model. The first stress of 0.84 dynes·cm^{-2} specified the upper limits of deposition, and the second of 1.28−2.56 dynes·cm^{-2} defined the lower limits for erosion.

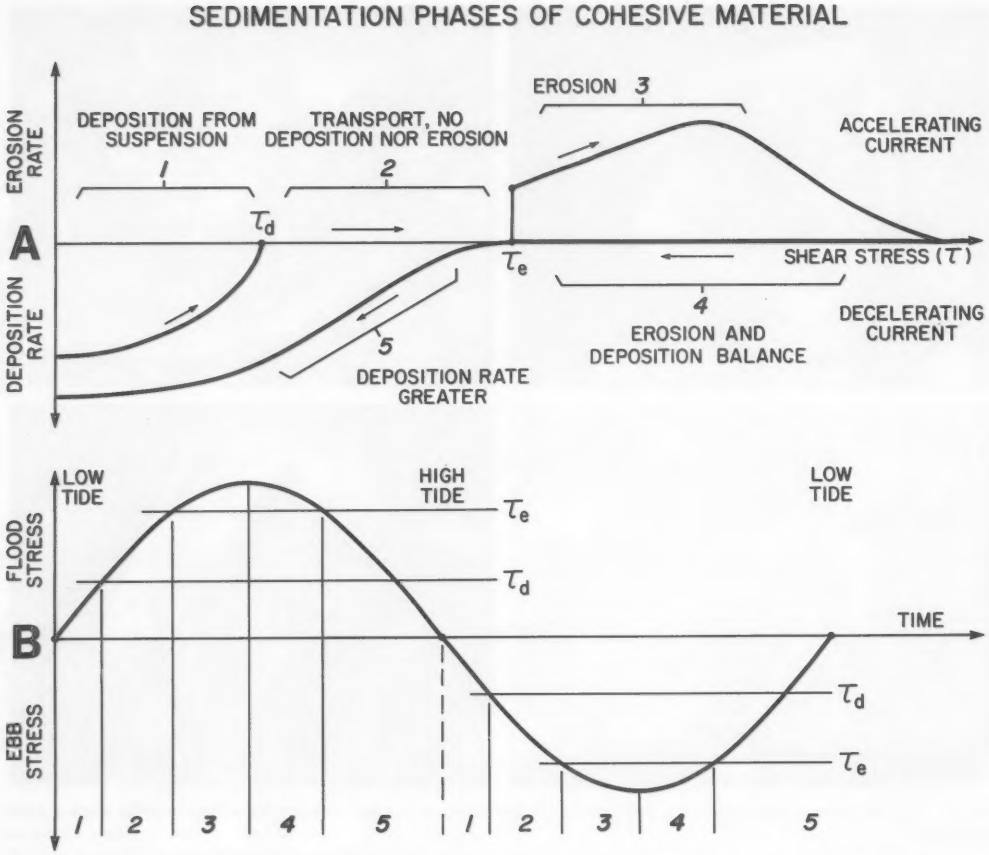

FIG. 5. (A) Erosion and deposition versus shear stress. The relationship illustrated includes the effect of saturation of suspended sediment with increased stress and resulting hysteresis on deposition in a decelerating flow. It was not necessary to include these effects in the model. (B) Erosion and deposition over a sample tidal cycle.

Between these two values, no erosion or deposition takes place.

RATE OF PARTICLE EROSION

Parthenaides (1971) stated ... "The term 'critical shear stress' ... has little meaning unless accompanied by the corresponding erosion rates." His experiments show that, within the velocity limits of the tidal model, the erosion rate is a linear function of the shear stress (τ_0) above the critical stress for erosion. On the other hand Kuo et al. (1978) observed that "... clouds of bed sediment "burst" off the bottom when currents exceed about 0.18 $m \cdot s^{-1}$", and that the erosion rate is not constant. The degree of complexity of the boundary shear stress has been shown by Nece and Smith (1970) and Heathershaw (1974).

Krone (1962, 1974) and Stow and Bowen (1978) felt that the rate of erosion is defined as the balance between upward and downward particle advection and that settling of grains continues to take place at all velocities. For unconsolidated muds, the critical erosion velocity and the critical deposition velocity should be the same. Indeed, using the results of Kuo et al. (1978), this would appear to be the case.

The erosion rate (E) used in the model was:

$E(g \cdot cm^{-2} \cdot s^{-1}) = 1.9 \times 10^{-3} \cdot \tau_0$, $\tau_0 \geq \tau_e$, τ_0 and τ_e in units of dynes $\cdot cm^{-2}$.

This erosion rate is linear for low τ_0 and $\tau_e < \tau_0$. Parthenaides' (1971) results indicate that erosion takes place at all shear stresses and therefore we could have $\tau_e = 0$; however at low stresses the erosion is balanced or reversed by settling ($C_z \cdot V_0$). The critical shear stress is that point where settling is balanced by erosion, therefore:

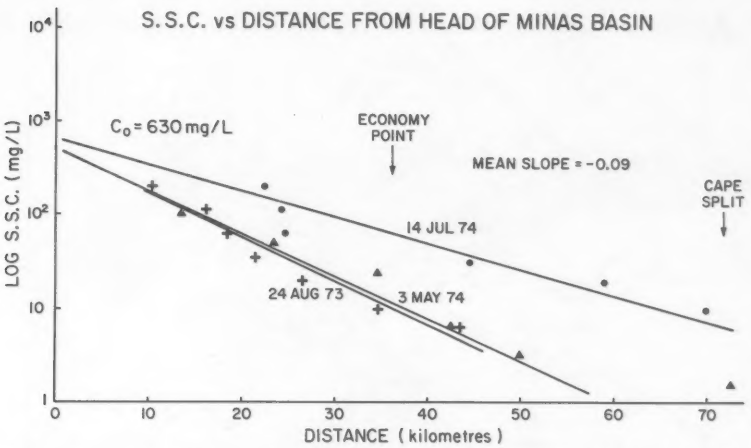

FIG. 6. Suspended sediment concentration in the Minas Basin from LANDSAT observations showing the logarithmic relationship along the basin axis.

(6) $$\frac{C_s \cdot V_0}{E} = 1$$

Krone (1962) hypothesized sediment deposition to be a function of grain settling rate and the probability of the grains sticking to the bed. He defines the limiting shear stress to be 0.6 dynes·cm^{-2}. Krone (1962) believes that erosion rates of sediment are independent of the shear strength and do not take place below a bottom stress of 0.6 dynes·cm^{-2}.

Over a typical tidal cycle, erosion will take place over the mid-stage peak velocities and deposition over the still stands. The model accounts for the hysteresis effect associated with an increase in SSC over the erosive phases of a tidal cycle, which induces greater deposition on the subsequent depositional phases. The critical stress for deposition is, however, maintained constant (see Fig. 5A).

Observed Distribution of Cohesive Sediments

SUSPENDED

The distribution of suspended sediments shows a logarithmic decrease seawards from the head of Minas Basin. The slope of the gradient is -0.09 mg·L^{-1}·km^{-1} and is relatively constant through time (Fig. 6), despite order of magnitude variations in the absolute concentration seasonally. This slope is equivalent to that observed in Chignecto Bay and presented in Amos and Asprey (1981). This gradient is thought to represent a balance in horizontal eddy diffusion and the onshore tidal transport of sediment. Concentrations range from a mean summertime concentration of 1–200 mg·L^{-1} throughout the bay, to 60–2300 mg·L^{-1} immediately after ice breakup (Amos and Long 1980).

The vertical distribution in SSC was determined by occupying 17 anchor stations throughout Minas Basin and taking samples at hourly intervals at 5 equal depth intervals. The results are given in Amos and Joice (1977). Under most circumstances, SSC was constant throughout the water column.

The highest concentrations occur in the early spring and are lowest during the summer months.

Figure 7A shows a Landsat derived map of SSC accurate to ±18% at 12 mg·L^{-1}. The image is representative of summertime conditions for which the model is most applicable. This image was used to assess the reliability of the model (Fig. 7B) to predict the distribution of the lines of equal sediment concentration. It can be seen that the SSC distribution follows closely the pattern obtained from satellite observation. The variation in absolute values results from comparison with a summertime image of lower concentration.

BOTTOM SEDIMENTS

Muds accumulate predominantly in sheltered embayments and within the upper intertidal zone surrounding Minas Basin (Fig. 8). The short term accumulation on these mudflats varies considerably seasonally, but over the long term the net accumulation is smaller than our sampling method could detect. There is however, accumulation in the summer, balanced by erosion during the winter. Field results of mud accumulation were too low to evaluate the settling rate term shown in equation (7). The various settling terms were therefore evaluated by a detailed study of the Windsor Causeway mudflat (see Fig. 9A), where the summertime accumulation rate was 5 cm·mo^{-1} (average).

During 1980, measurements were made of the parameters used in the model to calculate sedimentation (i.e. current speed, tidal inundation, SSC, and settling rate) and the actual accumulation rate measuring the depth of buried plates on Windsor Causeway. The net accumulation was 0.067 m (Fig. 9B). The mean concentration of suspended sediment over the mudflat was 30–100 mg·L^{-1} and the mean depth of inundation was 2 m. The time of inundation was approximately 3 h per tidal cycle and the mean current speed and

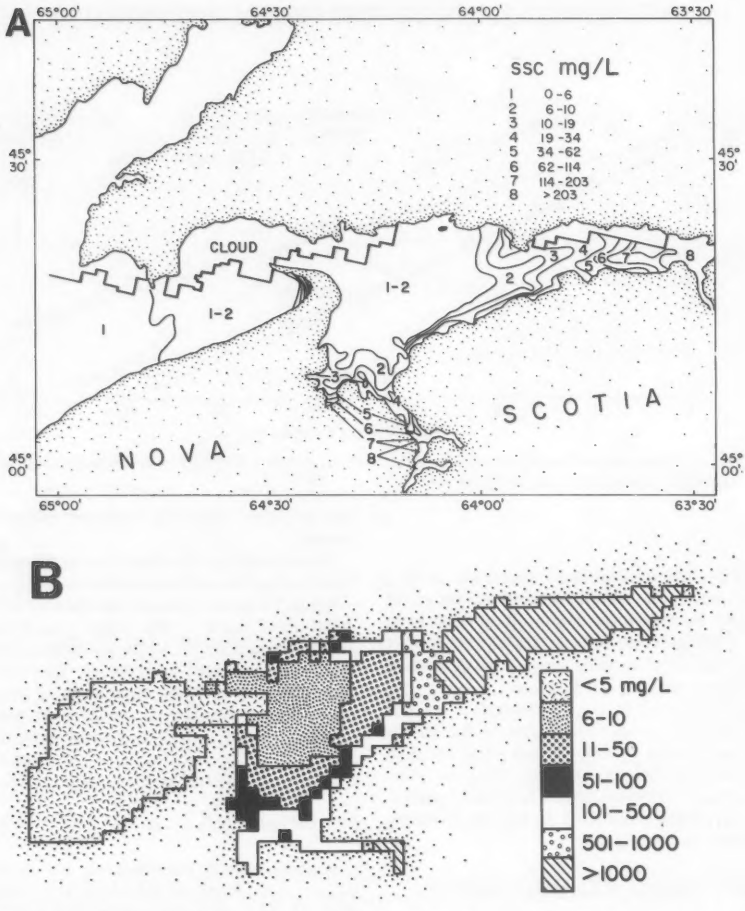

FIG. 7. (A) Suspended sediment concentration from LANDSAT August 1974. (B) Suspended sediment concentration from the model showing similar logarithmic gradient to observed SSC.

settling rate of sediment was 0.6 $m \cdot s^{-1}$ and 1.12×10^{-3} $m \cdot s^{-1}$, respectively. The theoretical accumulated volume determined by a calculation using model parameters was 0.068 m, which indicates an error of 1.5% when compared to the observed accumulation rates.

The model was initialized and bounded with conditions based on existing information on the budget of sediments. The only significant source of SPM was from the Bay of Fundy open boundary (Amos and Joice 1977) as river input was negligible (49 m^3/tidal cycle) and the eroding cliffs bordering the system tended to breakdown into sand size material.

As the prevailing concentrations in the Bay of Fundy tend to be around 1–2 $mg \cdot L^{-1}$, all concentrations seaward of Cape D'or were set to this value. Advection into the system resulted from the mean circulation derived from the nonlinearities in the tidal model.

Results

Model Calibration Without a Barrage

Using various stress values, test runs (Table 1) were carried out in order to calibrate the software and print out characteristics. Runs 1 to 7 were made to assess the various critical stress parameters and the rates of sediment erosion. Runs 8 and 9 were made with a simulation of tidal barrage operation.

Two sets of sedimentation parameters were envisaged. The higher set was used to predict the worst possible condition of sedimentation and the second set to simulate the least amount of sedimentation.

The model was run initially with $\tau_d = 0.84$ dynes $\cdot$ cm^{-2} and $\tau_e = 1.28$ dynes $\cdot$ cm^{-2} (run 1). The model was initialized with no sediment on the bed at $t = 0$. The initial concen-

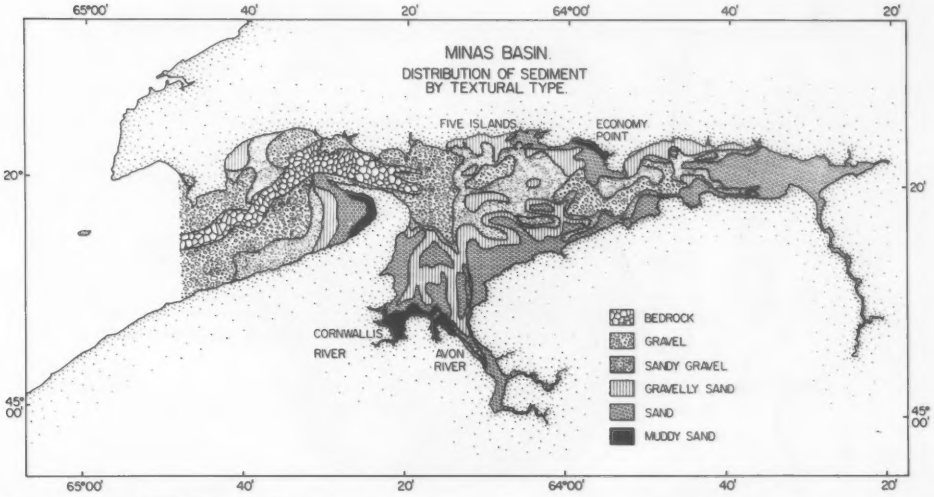

FIG. 8. Observed distribution of bottom sediment.

tration distribution used was set to that concentration which occurs during the spring thaw and is the highest concentration of any season. The values chosen were digitized from a Landsat thematic SSC map of the area taken during May 4, 1974. The concentration levels were increased 30 fold in order to represent early spring maximum conditions of SSC. Water advected into the model across the open boundary had a default sediment concentration of 2 $mg \cdot L^{-1}$ irrespective of the outgoing water mass concentration.

The result of the model run with low values of critical erosion and deposition induced very little deposition even in those regions where sediments were known to accumulate. The concentration of sediment did decrease with time and showed similarities to the LANDSAT map. However, decreases in concentration were more the result of tidal flushing into the outer Bay of Fundy, rather than by deposition.

Test run 7 used critical stress values of 0.84 dynes $\cdot cm^{-2}$ and 2.56 dynes $\cdot cm^{-2}$ for deposition and erosion. The model was run for 1920 interactions on a 3 lunar minute time step, corresponding to 8 tidal cycles. The concentration levels in the model after the run are shown in Fig. 7B. The lines of equal sediment concentration reflect those of the summer time conditions and clearly reproduce the residual transport directions demonstrated by deflections in the lines of equal sediment concentration observed from the LANDSAT map.

The distribution of seabed accumulation predicted by the model using the higher sedimentation values appeared to be a closer representation of reality than using the lower critical stress values of runs 1 to 6. It is difficult to know if the requirement for higher stress values in the model is a function of the size of the model grid (1.6 km), which is not small enough to simulate the relatively narrow zone of mud accumulation which occurs in reality, or whether it reflects sediments which are older and hence more compacted than those quoted in the literature. The higher stress values were considered more appropriate to the application, as it is this case of maximum possible sedimentation that is of interest to biologists and engineers.

The ability of the model to simulate the distribution of SSC was tested by setting the concentration across the entire grid to 75 $mg \cdot L^{-1}$. This was done in runs 1 and 2 and the output after 2 cycles began to produce contours similar to those demonstrated in the Landsat map of Fig. 6. As previously discussed, the best approximation to reality was achieved using a critical stress for deposition (τ_d) of 0.84 dynes $\cdot cm^{-2}$ (corresponding to a depth-averaged current of 0.198 $m \cdot s^{-1}$) a critical stress for erosion (τ_e) of 2.56 dynes $\cdot cm^{-2}$ (0.34 $m \cdot s^{-1}$), a settling rate of 1.1×10^{-3} $m \cdot s^{-1}$ and an erosion rate of 1.9×10^{-3} $g \cdot cm^{-2} \cdot s^{-1}$. Subject to these conditions, net accumulation occurred in Windsor Bay, Scots Bay, Five Islands, and Noel Bay. The rate of accumulation was equivalent to 0.01 m every 3 yr, which reflects the results reported in Amos and Joice (1977), and to all intents, the profiles of the intertidal area were stable.

Using the highest SSC levels did not produce a significantly larger accumulation rate, nor did deposition take place over a larger area. Due to the high water mass exchange with the upper Bay of Fundy, turbid water was lost from the system during the later stage of the ebb and substituted with clearer water inflowing along the south shore. Losses were still taking place after 4 d, and probably would continue for a further 8 cycles based on the rate of SSC decreases indicated by the model (60 $mg \cdot L^{-1}$ after 1 cycle; 30 $mg \cdot L^{-1}$ after 4 cycles; 10 $mg \cdot L^{-1}$ after 8 cycles). The concentration half-life on Minas Basin was approximately 2 d. The observed tidal flushing of sediment is thought to be most significant during the spring thaw and to take place to a lesser extent after storms.

At concentrations of 1−2 $mg \cdot L^{-1}$, a net influx of sediment took place at a measured rate of 1.6×10^6 $m^3 \cdot yr^{-1}$. This occurs, no doubt, during periods of quiescence between storms and principally during the summer.

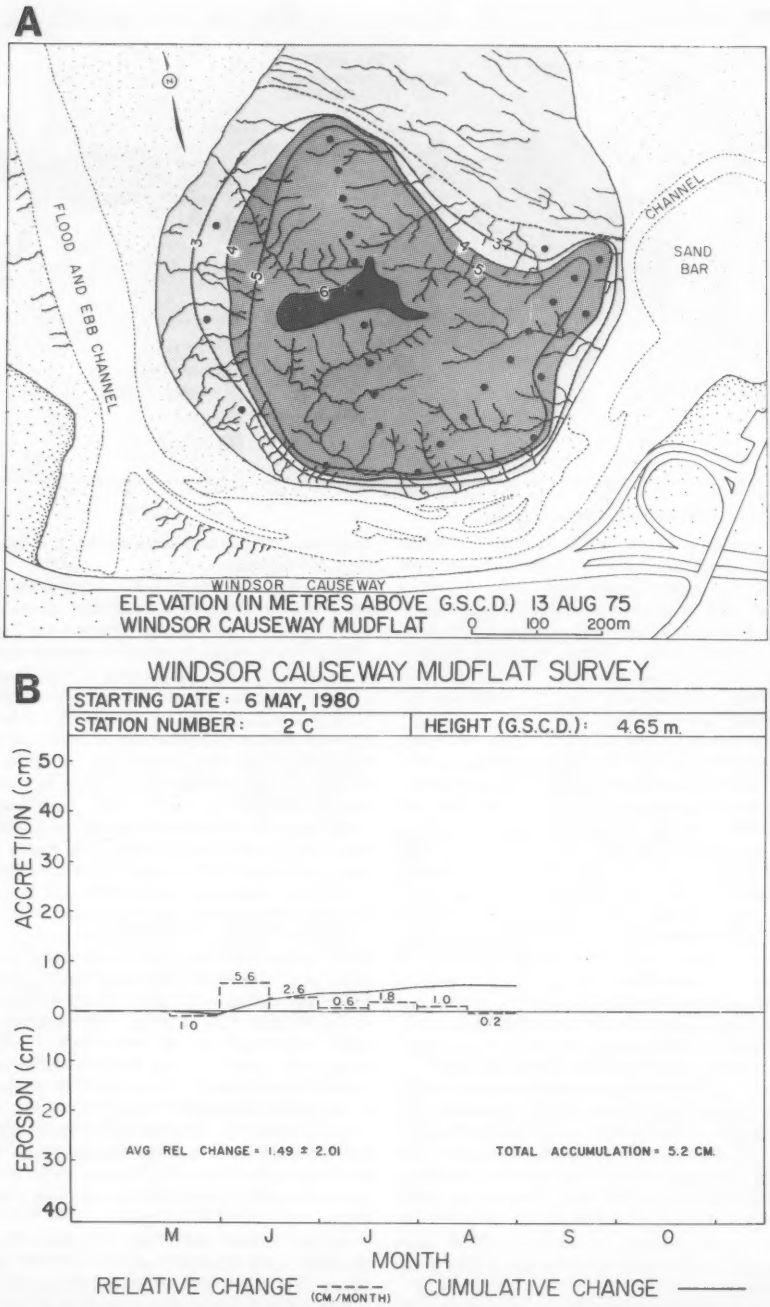

FIG. 9. (A) Windsor mudflat from aerial survey. Dots indicate reference sites. (B) Mud accumulation at one of the reference sites.

TABLE 1. Parameters used in model runs.

Run no.	Erosion rate $g \cdot cm^{-2} \cdot s^{-1}$	Deposition stress (τ_d)	Erosion stress (τ_e)	Settling velocity (V_0) $cm \cdot s^{-1}$	Tidal cycles (no.)	SSC starting condition
1	4.29	0.84	1.28	0.9079	2	constant 75 mg/L
2	4.29	0.0128	0.20	0.11167	2	constant 75 mg/L
3	4.29	0.84	1.28	0.9079	2	summer
4	4.29	0.84	1.28	0.11167	4	summer
5	4.29	0.84	1.28	0.11167	8	spring
6	2.15	0.84	1.28	0.11167	8	spring
7	2.15	0.84	2.56	0.11167	8	spring
8[a]	2.15	0.84	1.28	0.11167	8	spring
9[a]	2.15	0.84	2.56	0.11167	8	spring

[a]Runs with barrage simulation.

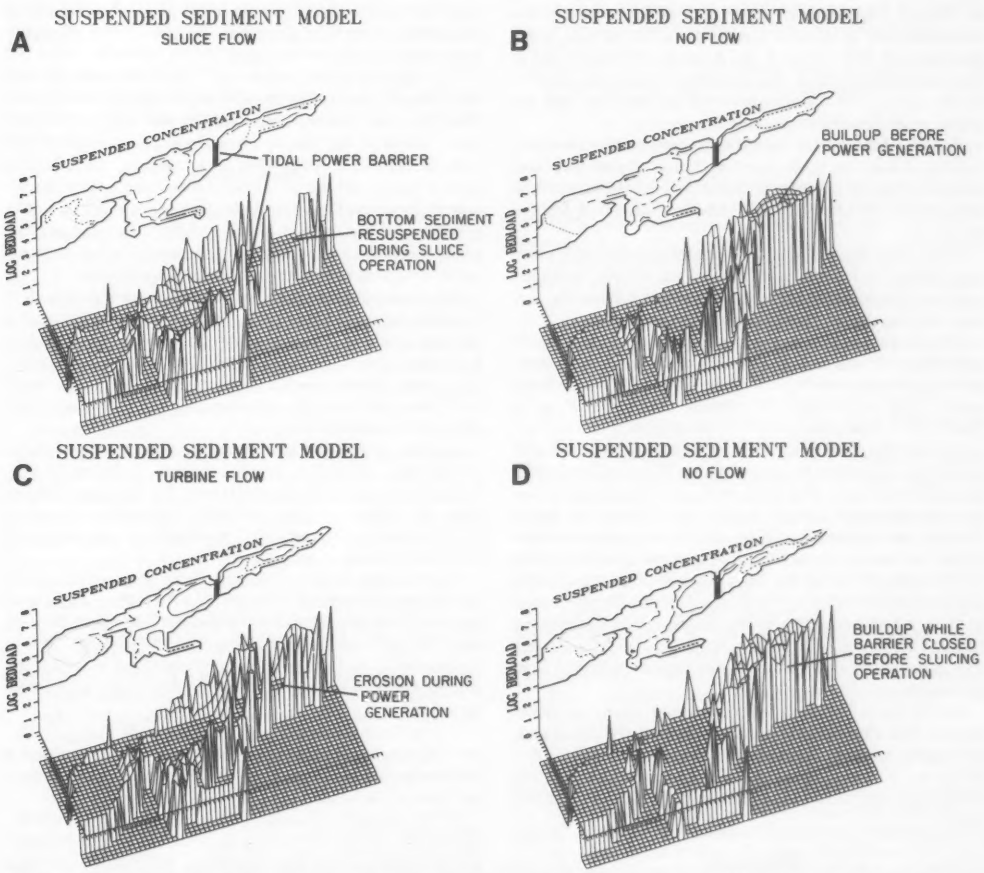

FIG. 10. Model predictions of sedimentation at different stages of the tide, with a tidal power barrier in place. Contour lines show the patterns of SSC. To illustrate a wider range of the deposited sediment, $\log_{10}$ (1 + deposited mass) is shown on the three dimensional plots.

Model Run with Barrage

The barrage simulations (runs 8 and 9) were made using two values for the critical erosion stress (1.28 and 2.56 dynes·cm^{-2}). The results using the higher value are shown in Fig. 10 for high tide, mid-ebb, low tide and mid-flood. The results were not significantly different using either stress value, and indicated that the mid-tide peak velocity (which produces a stress that is significantly larger than either value and is 1.2 m·s^{-1}) is the predominant factor controlling erosion.

Comparing the results of run 9 to those of run 7, for the high tide situation of the 8th cycle, there appeared to be only slight differences in the deposition patterns. The greatest effects were exhibited in the embayments adjacent to and behind the barrage. In Noel Bay, the deposition rate showed an increase by a factor of 10 over the present day situation. Adjacent to the barrage, there was evidence of a 60% increase in the deposition rate. In Windsor Bay there was an increase in net deposition of 10%, while in the Avon River Estuary and at Windsor Causeway there was an order of magnitude increase in deposition. The accumulation rate in Scots Bay did not appear to be significantly altered.

The area of the sites of deposition appeared only to increase slightly. Along the north shore of Minas Basin, both seawards and behind the barrage, some subtidal deposition was taking place. Windsor Bay also showed evidence of subtidal deposition.

Intermittent deposition and resuspension would take place over a tidal cycle. The post barrage intermittent deposited mass was significantly greater than occurred without the barrage and was deposited over a much larger region.

Without the barrage, intermittent deposition of between 50 and 500 g·m^{-2} was seen at each high and low tide still stand, and took place in those regions where net accretion was taking place. With the barrage, intermittent deposition of up to 2000 g·m^{-2} took place (i.e. 0.01 m accumulation) and occurred over the entire headpond area, immediately seaward of the barrage and within the greater part of Windsor Bay and the Avon River Estuary. The greatest deposition took place over the high tide period and into the mid-ebb. During this period of time, the turbines would be closed and the water mass behind the barrage would be still. Also at this time, deposition to the seaward side of the barrage takes place though to a lesser extent (i.e. 50 g·m^{-2}). At low tide, the central portion of the headpond would be totally eroded due to fast flowing currents associated with power generation, but is associated with concomitant deposition in those regions protected from the turbine jet streams.

During the period from low tide to mid-flood, the model showed that deposition occurs throughout the headpond, although to a lesser degree than during the mid-ebb (200–500 g·m^{-2}). This deposition occurs while erosion of the newly deposited sediments seaward of the barrage is taking place.

Discussion

The implications for the construction of a tidal power scheme in Minas Basin on the distribution of fine-grained sediment are not as significant as were initially thought. Analogies to the Windsor Causeway have been made and predictions that siltation would be as dramatic have been issued. Clearly this is not the case, although some interesting responses have been identified. We feel confident that the relative change in deposition patterns and rate are valid, in view of the well established boundary conditions used, even though the absolute values may be subject to error.

The intermittent deposition behind the barrier, though not accumulating on the long term, certainly constitutes the greatest response and environmental change. The accumulation of 0.01 m of sediment and subsequent removal within 3 h may well have an impact on the benthic communities.

The maximum net accumulation rates behind the barrier are likely to be no greater than 0.01–0.03 m·mo^{-1} in quiet areas which is comparable to rates of accretion presently observed in the Avon River Estuary. Present deposition rates behind the proposed barrage site vary up to 0.003 m·mo^{-1} and occur in the intertidal zone. Net accretion will diminish with respect to time due to limitations in supply.

The main parameter which will control the post barrage depositional pattern is the strength and duration of peak flows. There is a maximum particle settling rate (V_0) which will occur, however the rate of erosion increases in proportion with current speed. Away from the jet streams, the reduction in these peak flows due to barrage construction is only significant in those regions where the peak flow is close to the critical value for erosion, e.g. Noel Bay. In those regions where the critical value is greatly exceeded, no net accumulation would take place regardless of concentration.

The conditions specified in the model were designed to represent the conditions of extreme sedimentation. There is a problem resulting from the model grid size, which averages the quieter marginal depositional regions with the more energetic areas further seaward. As a consequence areas which could have post barrage deposition might not be recognized due to their unresolved size.

In terms of the lifetime expectancy of the headpond at the present rate of influx of fine-grained sediment (1.6×10^6 m^3·yr^{-1}), it would take 3000 yr to fill the basin. Considering the effects of local sea-level rise which amount to 0.15 m·century^{-1} (Grant 1970), no significant decrease in the headpond volume is anticipated.

The presently existing resident volume in suspension under maximum conditions of turbidity is 30×10^6 m^3, which, if deposited evenly over half the Cobequid Bay intertidal zone area (93 km^2) would form a layer 0.32 m thick. This is considered to be the worst possible condition to which the system can respond, and as shown in the model, will not be the case.

The following points should also be noted:

1) A "drying function" was devised, which provided a solution in intertidal regions where the water level fell below the level of the seabed locally.

2) The settling of sediment (from supporting settling experiments) appeared to be time and concentration dependent. Results indicated that mass settling (as opposed to individual grain settling) takes place initially, and with a concentration half life of 6 min. This concentration dependence was not modeled.

3) The equilibrium floc size (30 μm) corresponds to the maximum flow conditions occurring in the Minas Basin and would suggest that larger floccules tend not to be generated during quieter still stand periods. The size of the flocs is constant throughout the water column, suggesting that turbulent mixing causes exchanges which are faster than the response in the flocs to stress changes with depth.

4) The critical stress values used in the model runs were as high or higher than the highest values published. The deposition rates resulting from these stress values appeared in reality, to represent an average rather than an overestimated value. However, the results from Windsor Causeway mudflat, used as a site for the calibration of the stress and settling terms, showed that the predicted deposition and the actual were within 1.5%.

5) The model predicted well the distribution of the lines of equal suspended sediment concentration when compared with LANDSAT maps. Results show that in calm conditions during the spring thaw and after storms (cases comparable to the high suspended sediment loads simulated), sediment is flushed from Minas Basin, and that during periods of quiescence sediment is slowly advected back into the bay. The prediction of the long-term sediment budget would therefore be complex.

Conclusions

We recognize that further work is needed particularly on the nature and rates of deposition and resuspension, but within this limitation and those mentioned earlier we feel we can make the following statements:

1) The post barrage sedimentation patterns were surprising in that the deposition rates were lower than intuitively expected. Comparisons or extrapolations from existing impermeable structures such as the Windsor and Moncton causeways which showed a dramatic increase in sedimentation, would therefore appear to be erroneous.

2) Both intermittent and net accumulation of sediment would take place. In the former case, 0.01 m would deposit each tide still stand, but would be quickly eroded during power generation. Net accumulation would take place in some headpond, intertidal regions. Rates of deposition in these regions could be $0.01-0.03\ m \cdot mo^{-1}$. Further afield, the response would be less.

AMOS, C. L., AND K. W. ASPREY. 1981. Geophysical and sedimentary studies in the Chignecto Bay system, Bay of Fundy — A progress report. *In* Current Research, Part B, Geol. Surv. Can. Pap. 79-1B: 245–252.

AMOS, C. L., AND D. A. GREENBERG. 1980. The simulation of suspended particle matter in the Minas Basin, Bay of Fundy — A region of potential tidal power development. *In* Proc. Can. Coastal Conf., p. 2–20.

AMOS, C. L., AND G. H. E. JOICE. 1977. The sediment budget of the Minas Basin, Bay of Fundy, N.S. Bedford Inst. Oceanogr. Data Ser. BI-D-77-3: 411 p.

AMOS, C. L., AND B. F. H. LONG. 1980. The sedimentary character of the Minas Basin, Bay of Fundy. *In* S. B. McCann [ed.] The coastline of Canada, Geol. Surv. Can. Pap. 80-10: 153–180.

ANON. 1945. Report of tidal power, Petitcodiac and Memramcook estuaries. Department of Mines and Resources Canada, Ottawa, Ont.

ATLANTIC TIDAL POWER PROGRAMMING BOARD. (ATPPB). 1969. Feasibility of Tidal Power Development in the Bay of Fundy. Board Report and Committee Report, Halifax, Nova Scotia, October 1969.

BOOK, D. L., J. P. BORIS, AND K. HAIN. 1975. Flux-corrected transport II: generalisations of the method. J. Comput. Phys. 18: 248–283.

BRADLEY, W. H. 1965. Vertical density currents. Science 150: 1423–1428.

DALRYMPLE, R. W. 1977. Sediment dynamics of macrotidal sand bars, Bay of Fundy. Ph.D. thesis, McMaster University, Hamilton, Ont. 634 p.

FEDERAL INTERAGENCY SUB-COMMITTEE ON SEDIMENTATION. 1953. Accuracy of sediment size analyses made by the bottom withdrawal tube method. Rep. No. 10 to Federal Inter-Agency River Basin Committee. 115 p.

GODIN, G. 1968. The 1965 current survey of the Bay of Fundy — A new analysis of the data and an interpretation of the results. Mar. Sci. Br. Dep. Energy, Mines Resources, MS Rep. Ser. 8: 97 p.

GRANT, D. R. 1970. Recent coastal submergence of the maritime provinces, Canada. Thesis, Cornell University, Ithaca, NY. 109 p.

GREENBERG, D. A. 1979. A numerical model investigation of tidal phenomena in the Bay of Fundy and Gulf of Maine. Mar. Geod. 2(2): 161–187.

1976. Mathematical description of the Bay of Fundy — Gulf of Maine numerical model. Mar. Environ. Data Serv. Tech. Note 16.

HEATHERSHAW, A. D. 1974. Measurements of turbulence in the Irish Sea benthic boundary layer, p. 11–32. *In* I. N. McCave [ed.] The benthic boundary layer. Plenum Press, New York, NY.

HOLLOWAY, P. E. 1981. Longitudinal mixing in the upper reaches of the Bay of Fundy. Estuarine Coastal Shelf Sci. 13: 495–515.

KRONE, R. B. 1978. Aggregation of suspended particles in estuaries, p. 177–190. *In* B. Kjerfve [ed.] Estuarine transport processes. University of South Carolina Press, Columbia, SC.

1974. Engineering interest in the benthic boundary layer, p. 143–156. *In* I. N. McCave [ed.] The benthic boundary layer. Plenum Press, New York, NY.

1962. Flume studies of the transport of sediment in estuarial shoaling processes. Final report to U.S. Army Corps of Engineers, Contract No. Da-04-203: 110 p.

KUO, A., M. NICHOLS, AND J. LEWIS. 1978. Modelling sediment movement in the turbidity maximum of an estuary. Publ. Office of Water Research and Technology, 80 p.

LAMBIASE, J. J. 1977. Sediment dynamics in the macrotidal Avon River estuary, Nova Scotia. Ph.D. thesis, McMaster University, Hamilton, Ont. 415 p.

NECE, R. E., AND J. DUNCAN SMITH. 1970. Boundary shear stress in rivers and estuaries. J. Waterways Harbours Div. ASCE 96(WW2) Pap. 7280: 335–358.

PARTHENAIDES, E. 1971. Erosion and deposition of cohesive materials, p. 25.1–25.9. *In* H. W. Shera [ed.] River mechanics 2.

PARTHENAIDES, E., AND A. J. MEHTA. 1971. Deposition of fine sediments in turbulent flows. Report for Environmental Protection Agency Project 16050 ERS: 41 p.

SOUTHARD, J. B., R. A. YOUNG, AND C. D. HOLLISTER. 1971. Experimental erosion of calcareous ooze. J. Geophys. Res. 76(24): 5903–5909.

STOW, D. A. V., AND A. J. BOWEN. 1978. The origin of lamination in deep-sea fine-grained sediments. Nature 274: 324–328.

TEE, K. T. 1977. Tide-induced residual current — verification of a numerical model. J. Phys. Oceanogr. 7(3): 396–402.

TIDAL POWER REVIEW BOARD (TPRB). 1977. Reassessment of Fundy Tidal Power. Reports of the Bay of Fundy Tidal Power Review Board and Management Committee, November 1977, 516 p.

ZALISAK, S. T. 1979. Fully multidimensional flux-corrected transport algorithms for fluids. J. Comput. Phys. 31: 335–362.

ZIMMERMAN, J. T. F. 1976. Mixing and flushing of a tidal embayment in the western Dutch Wadden Sea, Part II: Analysis of mixing processes. Neth. J. Sea Res. 10(4): 397–439.

Appendix

The Numerical Procedure for Transport Simulation

The notation used in the sediment transport method using the Richardson Lattice is illustrated in Fig. 2. The first order scheme used herein is based on the donor cell or upwind differencing scheme. For positive values of u and v and where $\Delta x = \Delta y \equiv \Delta s$, the transport equations are approximated as follows:

$$\rho^{td}_{i,j}(t+\Delta t) = \rho_{i,j}(t) - \frac{\Delta t}{\Delta s H_{i,j}(t+\Delta t)}[f_{i+1/2,j} - f_{i-1/2,j} + g_{i,j+1/2} - g_{i,j-1/2}] \tag{9}$$

where

ρ = density
ρ^{td} = first order approximation (transported and diffused) density
f, g = transportive fluxes
$H_{i,j}$ = total depth = $h_{i,j} + \xi_{i,j}$

$$f_{i+1/2,j} = \rho_{i,j}(t)\, u_{i+1/2,j}(t)\, \bar{H}_{i+1/2,j}(t) \tag{10}$$

$$\bar{H}_{i+1/2,j}(t) = \frac{1}{2}(h_{i+1,j} + \xi_{i+1,j}(t) + h_{i,j} + \xi_{i,j}(t)) \tag{11}$$

$$g_{i,j+1/2} = \rho_{i,j}(t)\, v_{i,j+1/2}(t)\, \bar{H}_{i,j+1/2}(t) \tag{12}$$

$$\bar{H}_{i,j+1/2}(t) = \frac{1}{2}(h_{i,j} + \xi_{i,j}(t) + h_{i,j+1} + \xi_{i,j+1}(t)) \tag{13}$$

When u and v are negative, $\rho_{i+1,j}$ and $\rho_{i,j+1}$, respectively, are substituted in the above equations.

To refine these calculations to a central difference scheme (second order) the flux expressions are modified as follows:

$$A_{i+1/2,j} = |u_{i+1/2,j}(t)|\bar{\bar{H}}^{i+1,j}_{i+1/2,j}(t)\left(\frac{\rho_{i,j}(t) - \rho(t)}{2}\right) \tag{14}$$

$$A_{i,j+1/2} = |v_{i,j+1/2}(t)|\bar{H}_{i,j+1/2}(t)\left(\frac{\rho_{i,j+1}(t) - \rho_{i,j}(t)}{2}\right) \tag{15}$$

The above factors are limited in the FCT algorithm such that:

$$A^c_{i+1/2,j} = A_{i+1/2,j} C_{i+1/2,j} \qquad 0 \le C_{i+1/2,j} \le 1 \tag{16}$$

$$A^c_{i,j+1/2} = A_{i,j+1/2} C_{i,j+1/2} \qquad 0 \le C_{i,j+1/2} \le 1 \tag{17}$$

The limiter, C, is specified as in Zalesak (1979). It is this step that permits the refinement to a second order scheme, by restricting the fluxes to within physically realistic bounds. Applying the above, we get:

$$\rho_{i,j}(t+\Delta t) = \rho^{td}_{i,j}(t) - \frac{\Delta t}{\Delta s \bar{H}_{i,j}(t+\Delta t)} \cdot (A^c_{i+1/2,j} - A^c_{i-1/2,j} + A^c_{i,j+1/2} - A^c_{i,j-1/2}) \tag{18}$$

The notation of the above equations follow, in general, that of Zalesak (1979), but is not exactly the same, due to differences involving spatially varying depth and the time dependent surface elevation.

Factors Affecting the Supply and Distribution of Sediment in Some Tropical Ports[1]

MARY P. KENDRICK AND B. V. DERBYSHIRE

Hydraulics Research Station, Wallingford, Oxfordshire, England

KENDRICK, M. P., AND B. V. DERBYSHIRE. 1983. Factors affecting the supply and distribution of sediment in some tropical ports. Can. J. Fish. Aquat. Sci. 40(Suppl. 1): 35–43.

A brief review has been made of five hydraulic investigations of port siltation carried out by various international laboratories. The ports studied are distributed throughout the tropics from South America to Indonesia and the factors affecting sediment supply and distribution either directly or indirectly have been summarized. In spite of local variations, the similarity of many features suggests the existence of a common mechanism of sediment transport.

Twenty months of field measurements at one of the ports demonstrated that turbidity in the water column is low from surface to 0.15 m above the bed. These measurements, together with those from flume tests on the behavior of local mud in currents, indicated that siltation is not solely due to deposition of silt suspended in the main body of flow. Further wave flume tests showed that under certain conditions, a shallow, highly turbid layer forms on the bed, capable of being transported by weak tidal currents without significant vertical mixing. Supplementation of field measurements of water movement with more detailed hydraulic model measurements permitted the formulation of a siltation mechanism.

Appraisal of results suggests the most important immediate source of the silt to be the shallow coastal mud banks. Waves produce the turbid, near-bed layer which is transported by littoral currents into port approach channels for redistribution by the prevailing residual current, itself a function of fluvial/tidal interaction.

Key words: siltation, dredging, silt movement, flocculation, waves, tides, river flow, residual currents

KENDRICK, M. P., AND B. V. DERBYSHIRE. 1983. Factors affecting the supply and distribution of sediment in some tropical ports. Can. J. Fish. Aquat. Sci. 40(Suppl. 1): 35–43.

Nous passons brièvement en revue cinq études hydrauliques d'envasement de ports menées par divers laboratoires internationaux. Les ports étudiés sont répartis à la grandeur des tropiques, depuis l'Amérique du Sud jusqu'en Indonésie, et nous avons résumé les facteurs influençant, soit directement soit indirectement, les apports et la distribution des sédiments. En dépit de variations locales, la similitude de plusieurs caractéristiques donne à penser qu'il existe un mécanisme commun de transport des sédiments.

Des mesures effectuées sur le terrain pendant 20 mois à l'un des ports montrent que la turbidité dans la colonne d'eau est faible de la surface à 0,15 m au-dessus du lit. Ces mesures, couplées à celle d'expériences avec flumes sur le comportement de la vase locale dans des courants, indiquent que l'envasement n'est pas dû seulement à la déposition de vase en suspension dans le corps principal de l'écoulement. Des essais plus poussés avec flumes à vagues démontrent que, dans certaines conditions, il se forme sur le lit une couche de forte turbidité, qui peut être transportée par de faibles courants de marée sans qu'il y ait important mélange vertical. Il a été possible de formuler un mécanisme d'envasement en ajoutant aux mesures de mouvement de l'eau sur le terrain des mesures plus détaillées de modèles hydrauliques.

À en juger par les résultats, les bancs de vase d'eaux peu profondes de la côte seraient la source immédiate de vase la plus importante. Les vagues produisent la couche turbide située près du lit et qui est transportée par les courants littoraux dans les chenaux d'approche

[1]This paper forms part of the Proceedings of the Dynamics of Turbid Coastal Environments Symposium convened at the Bedford Institute of Oceanography, Dartmouth, N.S., Canada, September 29–October 1, 1981.

Printed in Canada (J6678)
Imprimé au Canada (J6678)

des ports, pour être redistribuée par le courant résiduaire dominant, lui-même fonction de l'interaction entre régime fluvial et marée.

Received October 14, 1981
Accepted August 31, 1982

Reçu le 14 octobre 1981
Accepté le 31 août 1982

THE expansion in international trade during the 20th century and the consequent increase in vessel size and minimum navigation depth resulted in large-scale port development involving extensive capital dredging. Where this development has taken place in the highly turbid environment, the axiom — "the deeper the dredging, the greater the siltation" — has tended to apply, and the maintenance of the required depths for navigation has often posed major problems for port authorities, leading them to seek the assistance of hydraulics laboratories in their search for causes and solutions. Five such investigations have been reviewed and similarities in certain characteristics of water and sediment movement have suggested the possible existence of a common siltation mechanism.

The ports, which are all in the tropics (Fig. 1), are Georgetown on the Demerara River, Guyana; Cochin on the Cochin Gut, southwest India; Bangkok on the Chao Phya River, Thailand; Banjarmasin on the River Barito, Kalimantan, Indonesia and Belawan on the Belawan River, Sumatra — also Indonesia. Port approach conditions (Fig. 2) have certain common features — a navigation channel through an offshore bar and shallow mud banks with bed contours indicating the main littoral currents to be either normal or oblique to the line of the channel.

Other common characteristics include a tidal range not exceeding 3 m; generally low (usually below 100 mg/L) river turbidities; frequent, though modest wave activity with wave heights rarely exceeding 1.5 m; seasonal variation in river discharge; seaward movement of silt during the wet season and landward transport (under the influence of salinity/density currents) and storage of silt in the river during the dry season; a seasonally fluctuating siltation rate, a general longshore movement of muddy sediments and the presence of fluid mud (known in Guyana as sling mud) in the navigation channel.

In an earlier examination of the dynamics of silty estuaries (Kendrick and Derbyshire 1976), certain factors had considerably more significance than others. These included "natural" agents such as saline tidal discharge, fresh river flow, and the erosional and depositional properties of the silt under the range of salinities encountered. Because of short local fetches, winds were disregarded, as were waves of whatever origin; similarly no assessment was made of the effect of living organisms on the behavior of the silt.

The relative significance of "non-natural" factors was more difficult to determine. Large-scale civil engineering works such as a tide-control barrier or extensive reclamation clearly had a noticeable impact on the dynamics of a turbid estuary, whereas the effects of a small water temperature increase due to power station operation were less obvious.

Extending the review to the turbid coastal zone introduces new significant factors, both natural (winds, waves, littoral currents) and non-natural (sea channel dredging, offshore dumping, harbor construction, and other civil engineering works).

Fundamental research into the behavior of sediments in flow is basic to hydraulic engineering: advances are, however, also made during studies of specific port projects. The following discusses the respective influence of the main factors affecting the supply and distribution of silt to the five named ports, drawing on examples of field and laboratory measurements made during the studies.

Rainfall/River Flow

All five of the ports experience significant variation in rainfall and river flow throughout the year.

Georgetown on the Demerara River has two rainy seasons (Delft Hydraulics Laboratory 1962) — May to July and December to February — and two intervening dry periods (Fig. 3). During the 1950s, the average rainfall was 2500 mm, the range extending from 3700 mm in 1954 to 1500 mm in 1957. River flow varied from a maximum monthly value of 600 m^3/s in the wet season to 50 m^3/s in the dry season, although the neighboring Essequibo River which outfalls about 20 km further along the coast to the west, has a much greater discharge range (10 000−1200 m^3/s) and so has a significant influence on water and sediment movements off the entrance to the Demerara River.

Cochin (Gole and Vaidyaraman 1969) and Bangkok (Allersma et al. 1966) have wet seasons in the months of June to September and July to December, respectively, with intervening dry seasons. The maximum river flow through Cochin Gut is about 200 m^3/s, and down the Chao Phya it is about 4000 m^3/s, falling very low in the dry season at both places (to between 25 and 250 m^3/s at Bangkok). The heaviest sea channel siltation of the year occurs soon after the onset of the freshet in the Chao Phya.

Both Banjarmasin (Pacific Consultants International 1975) and Belawan (Hydraulics Research Station 1980) experience wet seasons, though that at Belawan only lasts from September to December whereas Banjarmasin's period of higher rainfall continues from November to April (Fig. 3). An indication of the annual variation in the intensity of siltation at Belawan has been added to the upper graph, and the correlation with rainfall and river flow appears to be quite strong.

Given this seasonal variation in river flow at all the ports and the coincidence of high flows with channel siltation in the case of at least two of them, the next logical step is to examine the relationship between river discharge and turbidity to estimate whether sufficient silt is transported to make a significant contribution to annual port siltation.

The concentration of suspended silt and the river discharge at Belawan were monitored continuously for 20 mo at permanent stations installed above the limit of tidal penetration and Fig. 4 indicates how concentrations 0.5 m above the bed

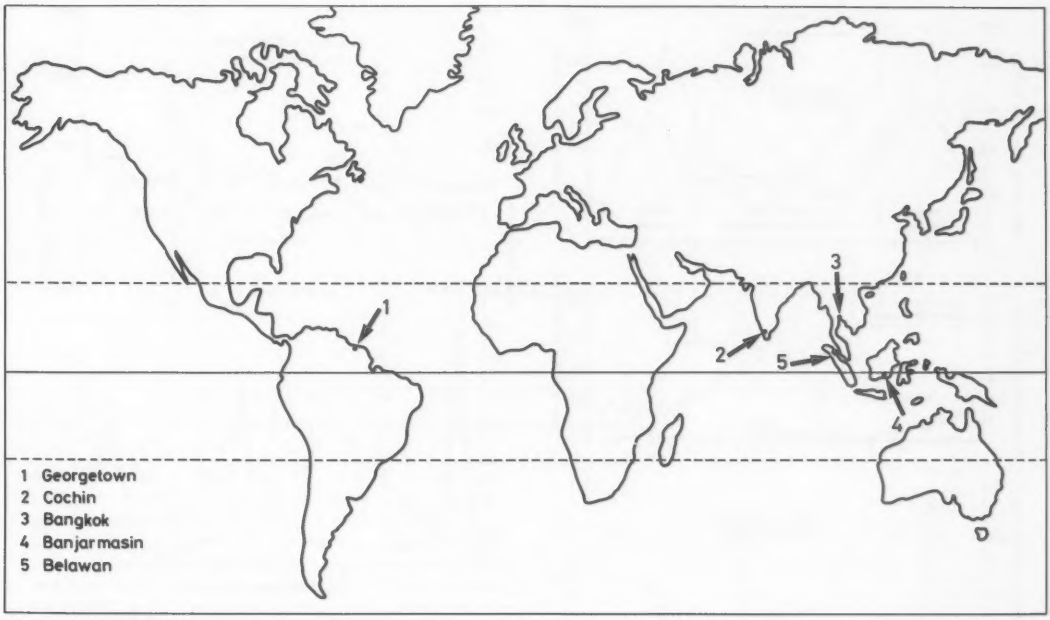

FIG. 1. Location of ports.

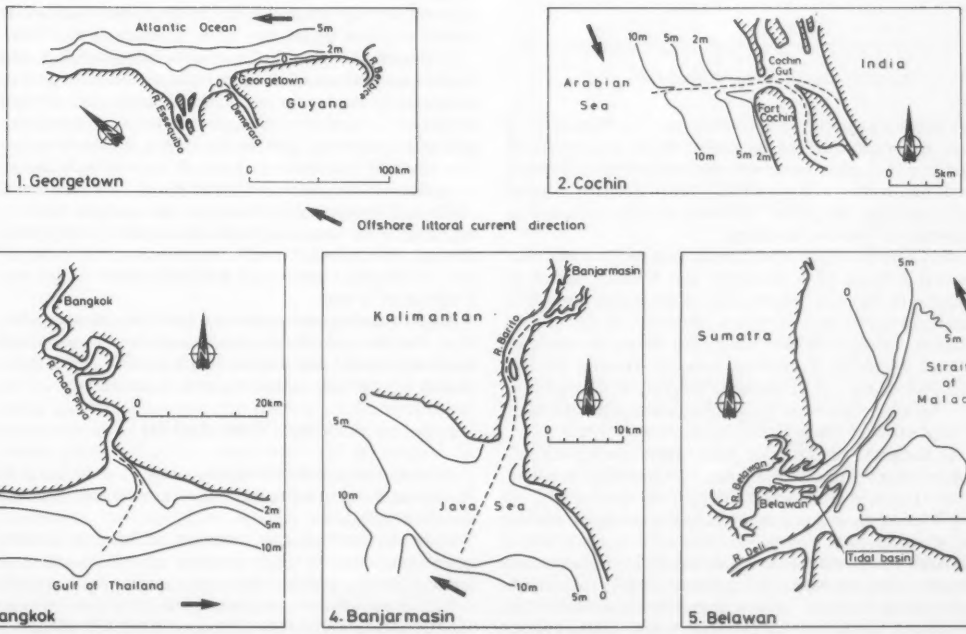

FIG. 2. Detail of ports.

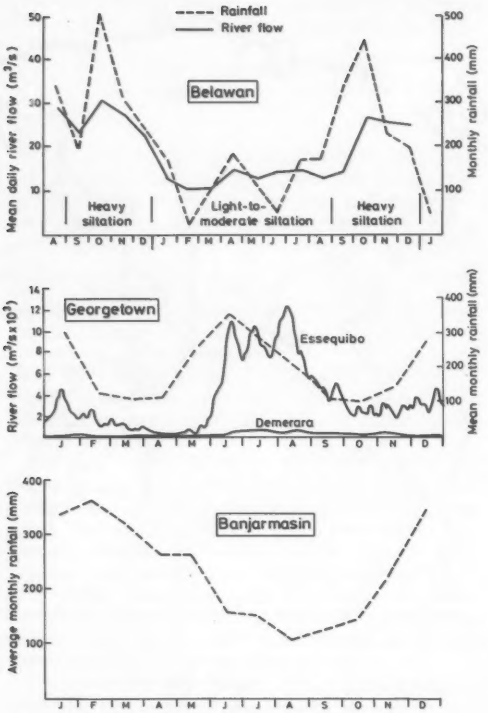
Rainfall
River flow
Belawan
Mean daily river flow (m³/s)
Monthly rainfall (mm)
Heavy siltation
Light-to-moderate siltation
Heavy siltation
A S O N D J F M A M J J A S O N D J
Georgetown
Essequibo
Demerara
River flow (m³/s x 10³)
Mean monthly rainfall (mm)
J F M A M J J A S O N D
Banjarmasin
Average monthly rainfall (mm)
J F M A M J J A S O N D

FIG. 3. Seasonal variation in rainfall/river flow.

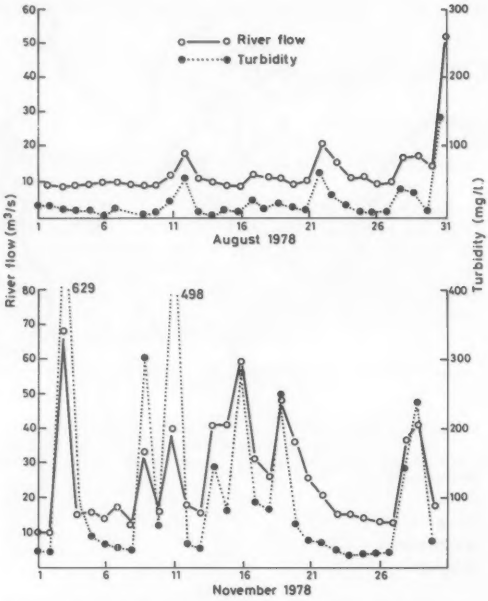

FIG. 4. Mean daily river discharge and turbidity at Belawan.

vary with river flow in the wet and dry seasons. With the flow range experienced during November 1978, an increase in discharge by a given factor was accompanied by an increase in silt transport by a factor about 3½ times greater — a value often exceeded. In general, however, turbidity increased as the square of the river discharge.

Measurements at the other ports also support a close relationship between river discharge and turbidity and it is tempting to conclude that the bulk of the silting material is directly provided by this means. However, in the case of Belawan, calculations have shown that during the course of a year, fluvial silt transported seawards accounts for less than 20% of the annual siltation. Similarly at Georgetown, "... the local rivers at present discharge very small quantities of solid matter." (Delft Hydraulics Laboratory 1962).

At Bangkok, on the other hand, approximately 12 million m^3 of silt is transported down the Chao Phya in a year, about 11 million m^3 of which arrives at the mouth during the first 3 mo of the wet season. Most of this is carried offshore and along the coast over the coastal mud flats as a plume of silt-laden water extending for more than 20 km from the river entrance. Although silt forms a temporary deposit in the channel, it is subsequently scoured during the remainder of the wet season by the now clearer river water, although some dredging is necessary to maintain navigation depths. However, the bulk of the 5 million m^3 of material which is dredged annually from the channel is in fact the result of deposition which occurs during the dry season (Allersma et al. 1966).

At Banjarmasin, Pacific Consultants International quote a highly questionable annual fluvial load of 250 million m^3 as estimated by the Indonesian Navy. However, annual river discharge and turbidity values given in the same report suggest that the annual load in the Barito should be nearer 2.5 million m^3, while dredging in river and approach channel amounts to about 5 million m^3 a year. Finally, at Cochin much of the silt transported seawards by the southern rivers is deposited in the Vembanad Lake before entering the Cochin channel, so suspended solids concentrations are relatively low. Maintenance dredging at this port amounts to just over 2 million m^3 a year.

Notwithstanding the seasonal relationship between river flow, turbidity and siltation which clearly applies at some of the ports, at least one additional factor would appear to be playing a significant role in the siltation mechanism.

Wind/Wave Activity

All five ports experience wave activity on a modest scale throughout the year with a tendency for some intensification at certain periods.

Under the conditions of water depth and fetch encountered at Belawan, onshore winds having a strength in excess of Force 3 on the Beaufort scale are capable of stirring the surface of the offshore mud banks. The occurrence of these winds increases slightly from between 10 and 15% of the day during the period May to October, to over 20% of the day

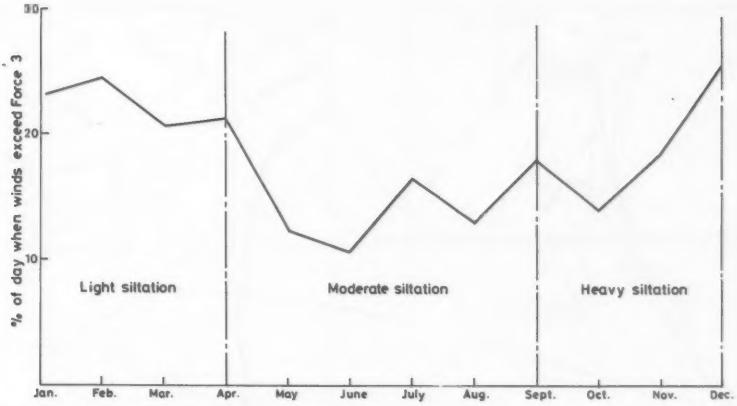

FIG. 5. Occurrence of onshore winds exceeding Force 3 at Belawan.

from December to April (Fig. 5). A fairly constant daily pattern is maintained, conditions remaining calm at night and onshore winds having the ability to generate waves 0.6 m high blowing for just over 4 h a day between 10:00 and 18:00. Allowing for the delay between the application of wind stress and water wave generation, wind in excess of Force 3 blowing for about 4 h will create mud-stirring waves at Belawan for just under 2 h, an effect demonstrated on Fig. 6 which typifies the variation in offshore turbidity measured 1 m above the bed on numerous occasions during the daylight hours.

Although the Belawan wind information on Fig. 5 and 6 exhibits both a daily occurrence and a seasonal variation, the latter bears no relationship to the seasonal siltation pattern (Fig. 5). At the other extreme, 75% of the annual siltation at Cochin occurs during the months of the SW monsoon, from June to September, when wave activity is at a maximum. The remainder of the ports lie somewhere between Belawan and Cochin, wind/waves playing an important role in the siltation cycle but varying in the extent to which they influence the time and place of maximum silt deposition.

Offshore Currents

A third factor which affects silt movements in the turbid coastal region is offshore currents of whatever origin.

At Cochin, Bangkok, and Banjarmasin, maximum wave activity tends to occur during monsoon periods, the littoral current also becoming more marked at these times. At Cochin the net movement is from north to south across the entrance channel (Gole and Vaidyaraman 1969). Off the entrance to the Chao Phya Estuary, the easterly flowing offshore current is almost normal to the approach channel. Similarly at Banjarmasin, the tidal currents entering and leaving the Barito River are deflected by the littoral current — to the northwest on the flood and to the southeast on the ebb, the seaward half of the port approach channel being virtually perpendicular to current direction (Pacific Consultants International 1975).

Conditions at Belawan and Georgetown are shown respectively on the left and right hand sketch maps on Fig. 7. The

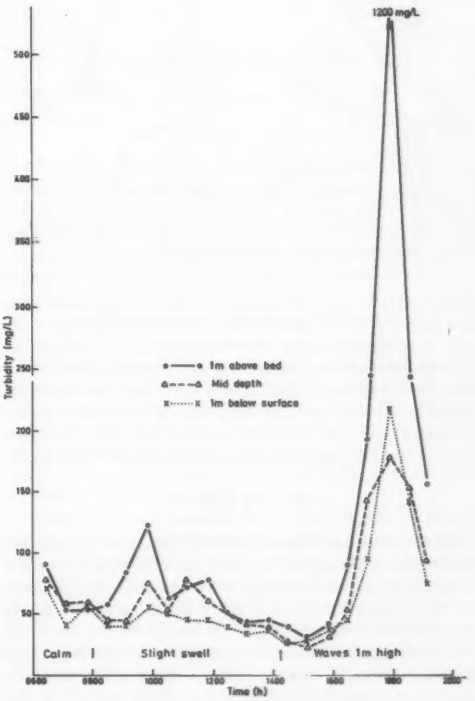

FIG. 6. Offshore turbidity and sea state at Belawan.

current pattern off the entrance to the Demerara River is complicated by the proximity of the Essequibo River mouth, the offshore equatorial current being modified by the tidal discharge into, and the combined fluvial and tidal discharges out of that much larger river (Delft Hydraulics Laboratory

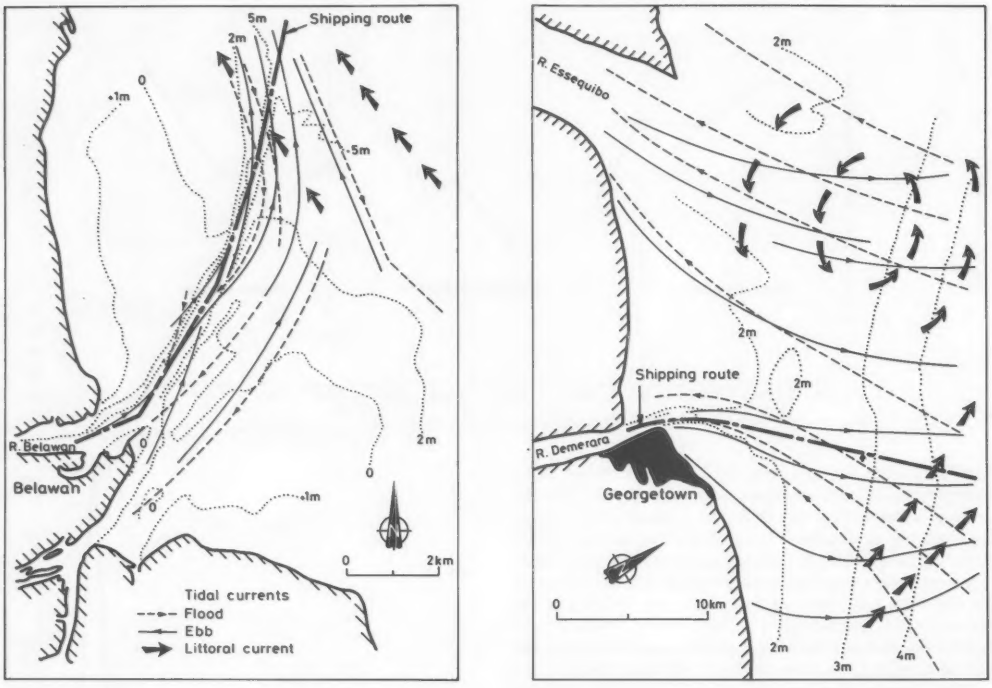

FIG. 7. Offshore currents at Belawan and Georgetown.

1962). Nevertheless, like both Belawan and the three ports just considered, the current still crosses the shipping route and, as in the other cases, the velocity of flow, although low (less than 0.5 m/s), is capable of transporting turbid suspensions over the shallow coastal mud banks into the navigation channel. The fluid mud, or sling mud, at the entrance to the Demerara River is, however, so soft that ships can pass through it and no dredging is undertaken as at the other ports.

Salinity Effects

Of the remaining factors which influence the supply and distribution of silt to the five ports, the most significant is the salinity distribution prevailing in the approach channel. Both the longitudinal and vertical distributions vary daily during the course of a particular tide (as shown by the results on Fig. 8 of measurements at Cochin) and bimonthly as the tidal amplitude changes with the spring-to-neap cycle: they also respond to changes in the fresh river flow, and where this is markedly seasonal, a modified hydraulic regime will be created soon after the onset of the rainy season.

Changes in salinity affect a system in two ways — by affecting current velocity residuals in the channel and by influencing the ability of silt particles to flocculate and deflocculate.

In a sinusoidally varying tidal flow, the current velocity residual can be obtained by integrating the area beneath the velocity-time curve at a station for each half-tidal period and calculating the mean flood and mean ebb current speeds. The difference between the two gives the net, or residual, velocity in a landward (flood) or seaward (ebb) direction. In a two-density system where tidal range is low and river discharge relatively high, tidal water enters the estuary near the bed while river water is being evacuated at the surface. At channel sections experiencing a sinusoidal rise and fall of the tide, flood flow at the bed may last for considerably longer than the half-tidal period and flood flow at the surface for considerably less, while the converse holds true for the ebb tide. These salinity/density currents, which result from imperfect mixing of salt and fresh water, produce a net landward movement of silt-laden bed water during a tide.

Current velocity residuals for Belawan, calculated from both field and hydraulic model measurements under conditions of high and low fresh river flow (Fig. 9), demonstrate that during high river flows the point in the channel where the net landward movement at the bed changes to a net seaward movement is further offshore than in the low-flow situation (km $4\frac{1}{2}$ cf. km 6). Of the silt being transported into the channel by waves and/or currents, a greater proportion will thus remain in the sea channel/river system in the wet season than in the dry season, less being carried seawards near the bed to join the general coastal drift.

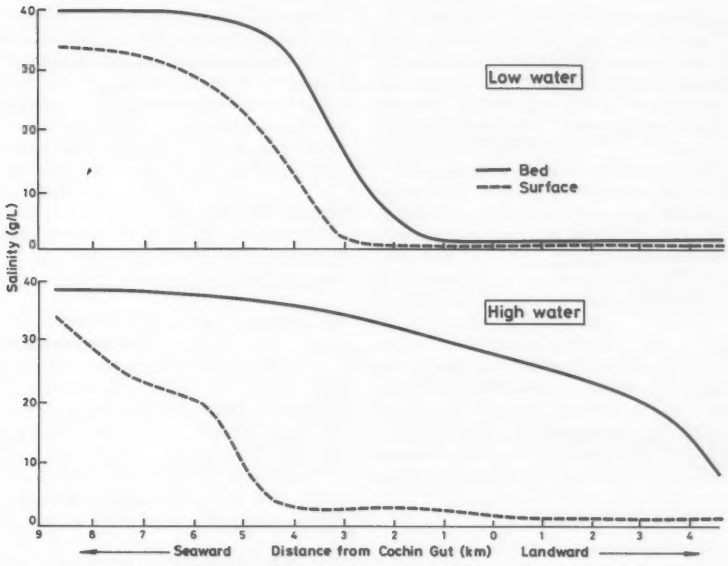

FIG. 8. Longitudinal salinity distribution — Cochin.

The way in which salinity affects the system through its effect on the flocculating ability of particles is that during times of high river flow, silt deposited in areas which are normally saline may find itself in an environment of freshwater which weakens the electrochemical bonding of particles and so allows relatively well consolidated deposits to be deflocculated and eroded at a lower bed shear velocity than usual. The accumulations of mud which build up gradually during the dry season are flushed from the river system suspended in the upper layers of flow, and pass into the sea channel to reflocculate and deposit in areas where sufficiently high salinity values are again encountered.

Dredging

Clearly many factors other than river flow, wind and waves, offshore currents and salinity variations play some part in determining the supply and distribution of silt in the coastal zone. Of these, local dredging practice probably has more significance than anything else, representing man's continued effort to modify the existing environment to his own advantage.

Silt can either be removed completely from the system by pumping ashore; prevented from consolidating by regular and frequent agitation dredging; or recirculated on a longer term basis by periodic bursts of heavy dredging, accompanied by spoil disposal at a site which, although often a considerable distance away, does not always preclude the possibility of silt being returned to the system by one or more of the factors already described. Examples of each of these methods can be found at the five ports, all three being employed at Belawan.

In the preceding paragraphs, the respective roles of the main factors affecting the movements of water and sediment in the turbid coastal environment have been summarized. In the final part of the paper, a mechanism of siltation is proposed for the port of Belawan in which field data have been used to explain how the factors interact to produce the seasonal siltation pattern experienced by many ports.

Siltation Mechanism at Belawan

Port dredging at Belawan amounts to some 4 million m^3/yr of which 3.2 million m^3 is removed from the sea channel, 0.6 million m^3 from the tidal basin (Fig. 2) and the remainder from riverside berths. The rivers outfalling into the Belawan coastal zone provide an equivalent in situ volume of 0.65 million m^3/yr, the balance of 3.35 million m^3/ yr being of marine origin.

During the early stages of the hydraulic investigation, sea channel siltation was an enigma since field measurements showed that suspended solids concentrations were low and even during wave activity, the turbidity 0.15 m above the bed rarely exceeded 100 mg/L. Laboratory flume tests on Belawan mud and in situ fall velocity measurements respectively indicated the critical shear for erosion and the settling velocity of suspended silt to be too low for substantial deposition to occur during slack water periods.

Siltation in the tidal basin was also puzzling, as demonstrated by the field observations which were obtained in October 1978 when heavy siltation was experienced (Fig. 10). The records show suspended solids concentrations to be low, the daily value varying with tidal range. However, there is no clear relationship with river discharge, which governs the rate of fluvial sediment supply, or with wind speed and

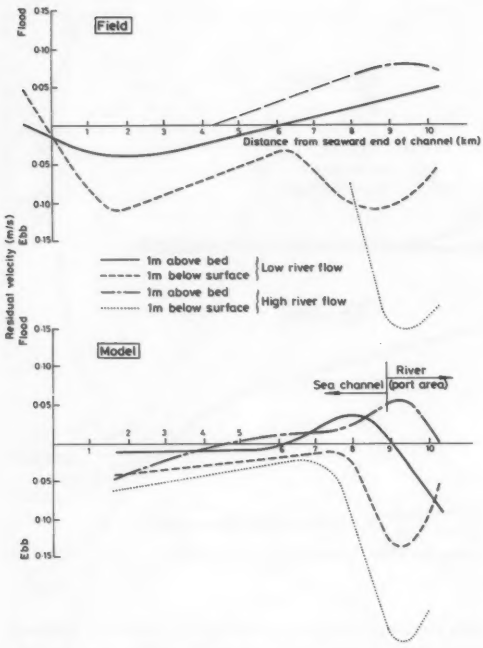

FIG. 9. Current-velocity residuals at Belawan.

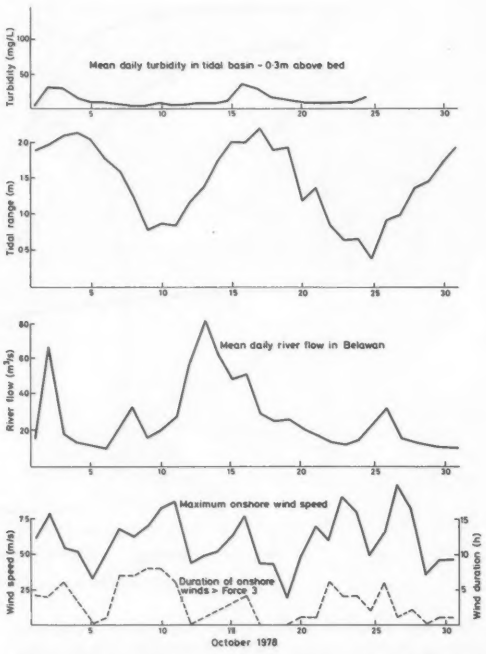
Mean daily turbidity in tidal basin - 0·3m above bed
Turbidity (mg/L)
Tidal range (m)
Mean daily river flow in Belawan
River flow (m³/s)
Maximum onshore wind speed
Wind speed (m/s)
Duration of onshore winds > Force 3
Wind duration (h)
October 1978

FIG. 10. Wind, water, and turbidity records from Belawan — October 1978.

duration which gave an indication of wave activity in stirring bed sediments.

Observations from anchored vessels under varying conditions of tidal range, river discharge, and sea state show that in the tidal basin, the vertical turbidity gradient is almost zero from surface to 1 m above the bed and a slight increase is usual in the layer 0.5−1 m above the bed. Limitations imposed by the equipment installed on the survey vessel prevented any measurements from being made nearer the bed. Results from the silt monitor installed 0.3 m above the bed would probably therefore slightly overestimate the mean turbidity of the water column above. Calculations based on tidal basin silt monitor records and settling properties of suspended sediments showed that accretion from suspension could account for only 1% of the known siltation volume.

From the data emerging from the sea channel and tidal basin, it seemed likely that siltation on the scale experienced in the port could only be due to the transport and behavior of silts in the lowest unmonitored layer, i.e. within 0.15 m of the seabed and 0.3 m of the bed of the tidal basin. This is presumably why the variations in river flow and wind activity on Fig. 10 were not reflected in monitored turbidity levels.

Because most of the sediment supplied to the port and sea channel was of marine origin, a flume study was made of the behavior of Belawan mud under wave action. The tests were made in 0.5 m of water with a wave period of 2 s. The wave height was gradually increased until at 15 cm, a turbid layer having a concentration of between 10 000 and 15 000 mg/L and a thickness of about 5 cm formed on the surface of the bed and oscillated to and fro with the water movement. A modest unidirectional current superimposed on the wave action transported the turbid layer along the flume with a well defined interface and little or no mixing with the water above.

The wave flume tests established that waves producing an orbital velocity at the bed of 0.26 m/s stir Belawan mud into a turbid layer; however, the thickness of the layer was probably limited by the area of the mud bed under test (0.75 m × 0.75 m). In the field, where the mud supply is extensive, it might be reasonable to expect an increase in both layer thickness and concentration.

At Belawan, locally generated waves have periods in the range of 2−4 s. Water depths between 2 and 4 m are typical along the side of the sea channel and adjacent mud banks and winds exceeding Force 3 on the Beaufort scale are a daily occurrence. These winds generate waves of between 0.3 and 0.7 m in height and from the wave period/water depth/wave height combinations experienced, mud-stirring orbital velocities are generated at the bed. During periods of very rough weather, when the wave orbital velocity at the bed is considerably in excess of the critical velocity for erosion, eroded mud would become dispersed throughout the water depth and no near-bed turbid layer would be formed. Such occasions are, however, rare.

Given the regular, moderate wave activity throughout the year and the currents which cross the sea channel at various

points as indicated on Fig. 7, the near-bed turbid layer would be transported across the shallow water zone and enter the sea channel to be redistributed according to the near-bed flow. Not all of the silt entering the channel would be retained; a small part would be entrained into the upper layers (Fig. 6) during the flow down the side slope and would pass over the channel. At the seaward end, material entering on the ebb tide would be transported into deeper water to join the general drift of sediment along the Malacca Straits.

Of the material retained in the channel, part would deposit during the slack water periods and not be re-entrained on the following half-tide, the remainder would be redistributed along the sea channel/river system to be stored in areas prone to siltation.

The transport process within the channel is governed by near-bed residual currents (described earlier), themselves a function of freshwater flow and saline tidal penetration.

Figure 9 demonstrated that during high river flow the supply of marine sediment to the port is increased. Similarly saltwater penetration into the river is reduced and silts, trapped in deposits in areas which were formerly saline, are deflocculated and transported seawards in the upper layers of flow towards the port and its approaches where flocculation and deposition occur again when sufficiently saline water is encountered.

The ability of a near-bed turbid layer to behave in the way described was examined on a physical model on which the natural salinity distribution throughout a tide was reproduced. The turbid layer was modeled by a dyed, enriched, saline solution which was injected over the shallow water mudbanks and allowed to flow under the action of tidal currents. The tests confirmed the ability of the denser layer to flow into the channel and eventually become redistributed within the channel/port system.

In further experiments to explore flow in the tidal basin, the dyed, enriched, saline solution was released into the lower water layer near the entrance while the surface of the basin was seeded with small polystyrene balls. The motion of the dyed liquid and polystyrene balls was monitored and recorded by a closed-circuit video system.

The results demonstrated that while surface water flowed into and out of the basin during the flood and ebb of a tide, the dyed bed water continued to flow into the basin and accumulated there. Areas of accumulation on the model compared favorably with field observations of fluid mud encountered during echo-sounding operations.

Assuming a turbid layer thickness of 0.1 m and a concentration of 20 000 mg/L, calculations were made of annual siltation volumes in the sea channel, tidal basin and riverside berths. The results compared favorably with those known to occur at Belawan. It was therefore possible to use the same procedure to predict annual siltation rates for port development schemes.

The formation under moderate wave action of a near-bed turbid layer only a few centimetres thick, cited as the main agency for generating siltation at Belawan, has not been confirmed in the field due to the lack of suitable instrumentation. So far the evidence is largely circumstantial, but the Hydraulics Research Station has now developed an instrument for field use with a vertical resolution of 0.03 m, capable of detecting a turbid layer and monitoring density flow strength and direction within it, and flow strength and direction of the water immediately above. It is hoped that an opportunity will arise to use the instrument at Belawan to confirm or refute the existence of such a layer.

It is possible that similar near-bed suspensions are formed by wave activity at the four other ports considered, but it would be rewarding to establish this by direct measurement.

Acknowledgments

This paper is published by permission of the Director of Hydraulics Research, Wallingford, England. The authors are indebted to the originators of the papers referenced for the information contained therein and also to the Indonesian Government and their consultants for the Belawan studies, Sir William Halcrow & Partners. They gratefully acknowledge the co-operation of the Station's drawing office, photographic section, and typists in preparing the paper.

ALLERSMA, E., A. J. HOEKSTRA, AND E. W. BIJKER. 1966. Transport patterns in the Chao Phya Estuary. Proc. 10th Engineering Conference, Tokyo, Japan.

DELFT HYDRAULICS LABORATORY. 1962. Report on Demerara Coastal Investigation. The Netherlands.

GOLE, C. V., AND P. P. VAIDYARAMAN. 1969. Deepening the approach channel to the Port of Cochin. Proc. 13th Congress of IAHR, Kyoto, Japan.

HYDRAULICS RESEARCH STATION. 1980. Port of Belawan, Indonesia. Third report on hydraulic studies, EX 879. Wallingford, U.K.

KENDRICK, M. P., AND B. V. DERBYSHIRE. 1976. Factors influencing estuary sediment distribution. Proc. 15th Coastal Engineering Conference, Honolulu, Hawaii.

PACIFIC CONSULTANTS INTERNATIONAL. 1975. Survey and design report for the construction of the approach channel at the mouth of Barito River. Tokyo, Japan.

Supply, Distribution, and Transport of Suspended Sediment in a Macrotidal Environment: Bristol Channel, U.K.[1]

MICHAEL COLLINS

Department of Oceanography, University College, Singleton Park, Swansea SA2 8PP, Wales, U.K.

COLLINS, M. 1983. Supply, distribution, and transport of suspended sediment in a macrotidal environment: Bristol Channel, U.K. Can. J. Fish. Aquat. Sci. 40(Suppl. 1): 44 – 59.

Various independent sets of data are used to investigate near-surface suspended sediment concentrations. The data include satellite (LANDSAT) imagery, field verification and near-synoptic surveys of specific areas and integrated, longer-term, surveys of the Channel. The information is used to identify areas of high turbidity, which relate to tidal and wave resuspension of the mobile sediments within the Estuary and Channel system. Thematic maps produced from the satellite imagery are comparable directly with the survey results and are combined with them, through a radiance/log$_e$ concentration relationship. Derived estimates of material present within the waters of the Channel range from 4.5×10^6 t to 13.4×10^6 t. Fluvial contributions are estimated to be of the order of 1.6×10^6 t/yr. Other evidence is available for the supply of material from the Celtic Sea. Isopleths of suspended sediment concentration are used to infer residual water and fine-grained sediment transport directions; these are compared with a more general model, which includes observed and predicted near-bed sand transport directions.

Key words: Bristol Channel, Severn Estuary, suspended sediment, satellite imagery, sediment budget, sediment transport, residual water movement

COLLINS, M. 1983. Supply, distribution, and transport of suspended sediment in a macrotidal environment: Bristol Channel, U.K. Can. J. Fish. Aquat. Sci. 40(Suppl. 1): 44 – 59.

On a utilisé diverses séries indépendantes de données dans l'étude des concentrations du sédiment en suspension près de la surface. Ces données comprennent la prospection par satellite (LANDSAT), la vérification sur le terrain et relevés presque synoptiques d'aires spécifiques, et des relevés intégrés, à plus long terme, du chenal. Les données ainsi recueillies ont servi à identifier les aires de forte turbidité, reliée à la resuspension sous l'action des marées et des vagues des sédiments meubles dans le système de l'estuaire et du chenal. Les cartes thématiques résultant de la prospection par satellite sont directement comparables avec les résultats des relevés et ont été combinés avec ces derniers, en une relation radiance/log$_e$ de la concentration. Les estimations du matériel présent dans les eaux du chanal sont comprises entre $4{,}5 \times 10^6$ t et $13{,}4 \times 10^6$ t. On estime que les contributions fluviales sont de l'ordre de $1{,}6 \times 10^6$ t/an. On possède d'autres données sur les apports de matériel en provenance de la mer Celtique. A l'aide des isoplèthes de concentration de sédiment en suspension, on a pu déduire les directions du mouvement de l'eau résiduaire et du sédiment à fines particules; nous les comparons avec un modèle plus général, incluant les directions observées et prédites du transport de sable près du lit.

Received October 14, 1981
Accepted July 17, 1982

Reçu le 14 octobre 1981
Accepté le 17 juillet 1982

INTERACTION between water and sediment in the Bristol Channel has produced a natural sedimentation laboratory, in which complex sediment transport processes occur. These processes relate to the supply, transport and deposition of fine-grained material under the influence of tides, waves, and wind.

Transport of material as bed load within the Channel and Severn Estuary (Fig. 1) has been the subject of a number of investigations (Stride 1963; Belderson and Stride 1966; Kenyon and Stride 1970; Collins et al. 1979; Pingree and Griffiths 1979; Murray et al. 1980; Heathershaw 1981; and G. Ferentinos and M. B. Collins, unpublished data); these

[1]This paper forms part of the Proceedings of the Dynamics of Turbid Coastal Environments Symposium convened at the Bedford Institute of Oceanography, Dartmouth, N.S., Canada, September 29–October 1, 1981.

Printed in Canada (J6674)
Imprimé au Canada (J6674)

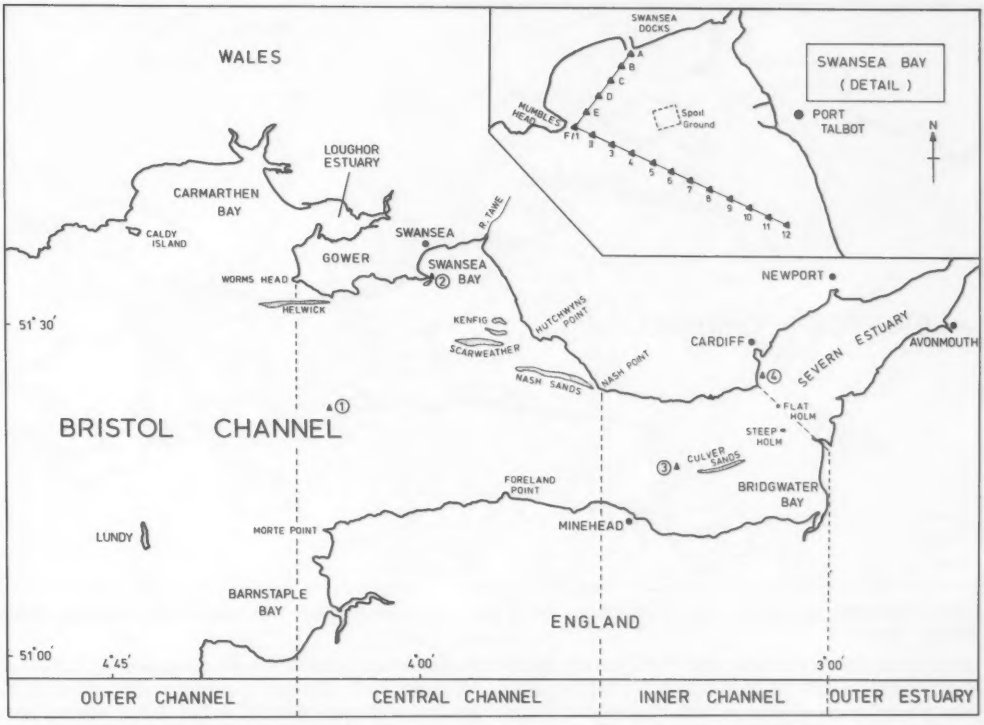

FIG. 1. Bristol Channel, showing locations referred to in text. Outer, Central, and Inner Channel and Outer Estuary sections based upon scheme adopted by IMER (Plymouth, U.K.). Locations 1 to 4 represent supplementary monitoring positions (see text). Inset shows locations of collection of surface concentration data, for "sea-truth" calibration in Swansea Bay.

provide a reasonably comprehensive interpretation of near-bed sediment movement. In contrast, transport of material in suspension has been the subject of only a few detailed studies, such as those in Swansea Bay (Davies 1974, 1980) and the Inner Channel and Severn Estuary (Parker and Kirby 1981). In the latter area, a suspended sediment "front" has been reported recently (Kirby and Parker 1982). For the Channel as a whole, only a few summary figures have been presented (e.g. Murray et al. 1980, fig. 4) and transport paths for fine-grained material in suspension have been inferred from foraminiferal evidence (Murray and Hawkins 1976; Culver and Banner 1978; Culver 1980).

The present study is concerned with the source and transport paths of near-surface suspended sediment concentrations in the Bristol Channel. Analyses are based upon LANDSAT imagery of the Bristol Channel, field verification surveys, and longer-term survey data made available to the author. All the clear satellite overpasses in the U.K., as of May 1982, are described; these amount to 12 occasions between 1975 and 1982. Comparable imagery is not available for the occasions of the field verification surveys, due to excessive cloud cover (see also Robinson and Srisaengthong 1981, concerning the Solent, southern England). Instead, the available imagery is compared with the results of the verification surveys, 21 near-synoptic (over approx. 2 h) surveys of surface turbidity in Swansea Bay (by the Tidal Waters Unit, Welsh Water Authority (WWA)) and 27 longer-term (over 3–29 tidal cycles) surveys of the Bristol Channel (by the Institute for Marine Environmental Research (IMER)).

The inherent difficulties in studying the distribution and transport of suspended sediment in a macrotidal environment have been summarized elsewhere, in relation to the application of remote sensing to the determination of circulation patterns, sources, and volumes of material present in the Bay of Fundy (Amos 1976; Amos and Alföldi 1978). Similar objectives are the aim of the present investigation in the Bristol Channel, by combining thematic maps generated by the LANDSAT imagery with turbidity data made available for this investigation by the various Authorities. All the information presented and discussed here is previously unpublished.

Area Under Investigation

General water circulation in the Channel is controlled by a branch of the North Atlantic Drift moving in along the

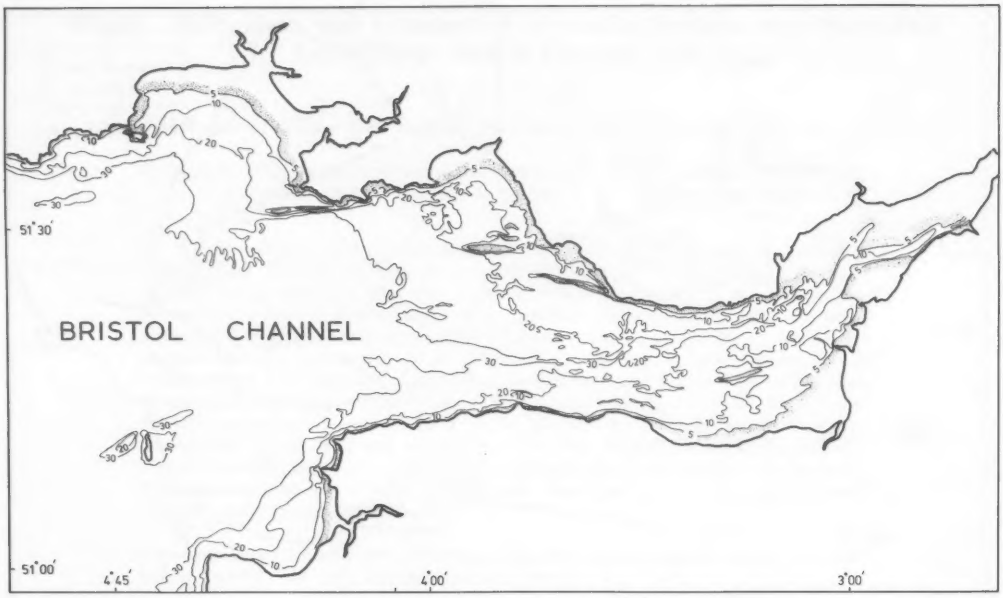

FIG. 2. Bathymetry (in metres) of the Bristol Channel, based upon U.K. Admiralty Chart 1179. Stippled areas represent offshore depths < 5 m.

southern coastline (Banner and Collins 1975) and low salinity waters flowing to seaward along the northern coastline. This pattern is enhanced at times of high freshwater discharge (fig. 3, Hamilton et al. 1979), when it is possible that reinforcement of a supposed anticlockwise density circulation pattern takes place at the mouth of the Channel (Hamilton 1973).

Tides in the Bristol Channel are the response of co-oscillations with those of the Celtic Sea (Defant 1951). Channel constrictions (Fig. 2) create some of the largest tidal ranges in the world (8.6, 11.1, and 12.3 m spring ranges at Swansea, Cardiff, and Avonmouth, respectively) and tidal power generation schemes are being considered (Shaw 1975; Owen and Heaps 1979; and Severn et al. 1979).

Tidal currents are essentially rectilinear and directed along the main axis of the Channel. Maximum surface speeds are of the order of 1.5 and 0.9 $m \cdot s^{-1}$ in the Inner Channel and Outer Channel, respectively (Stations L and A, Admiralty Chart 1179). This system is modified by the headlands and embayments of the northern coastline, where tidal current eddies are formed (Ferentinos and Collins 1979, 1980). Depth-averaged tidal current patterns have been modelled recently, predicting the eddies (Owen 1980), and an interesting attempt made to differentiate between the various components of the residual water circulation (Uncles 1982).

Parts of the Channel are exposed to swell wave approach from the southwest, with a fetch of over 6000 km. At Swansea, on the northern coastline (Fig. 1), observed wave heights are occasionally in excess of 7 m and wave heights of 5–6 m are not uncommon (Jackson and Norman 1980). There is close correspondence between the general distribution of wind and wave directions (Ferentinos and Collins 1978, fig. 36), with swell recorded at Port Talbot arriving from directions between 220° and 250° for about 40% of the time (Heathershaw et al. 1980).

In other areas of the Channel, wave heights are limited by the available fetch for waves generated by local winds (see, for example, Tyler and Shackley 1980).

Major rivers discharge into the upper reaches of the Channel. The bulk of the runoff is supplied by the Severn, Avon, Usk, and Wye (Fig. 3), supplying large quantities of land-derived material and industrial waste (Abdullah et al. 1973). Freshwater discharges are seasonal, with the minimum during the summer months. Short-term variability in discharge takes place in response to rainfall (HMSO, 1978, fig. H, p.165), creating a distinctive pattern of cross-channel stratification in the surface waters. At such times, the normal north–south orientation of the isohalines is changed to a northwest–southeast direction, with the low salinity waters present over the longitudinal axis and extending along the northern section of the Channel (fig. 3, Hamilton et al. 1979).

The residence time for waters in the Channel is long and a flushing time of between 150 and 400 d, dependent upon freshwater discharge, has been estimated (Abdullah et al. 1973; Hamilton et al. 1979).

Methods

The field verification surveys were carried out along two sampling lines in Swansea Bay (inset to Fig. 1). Surface water

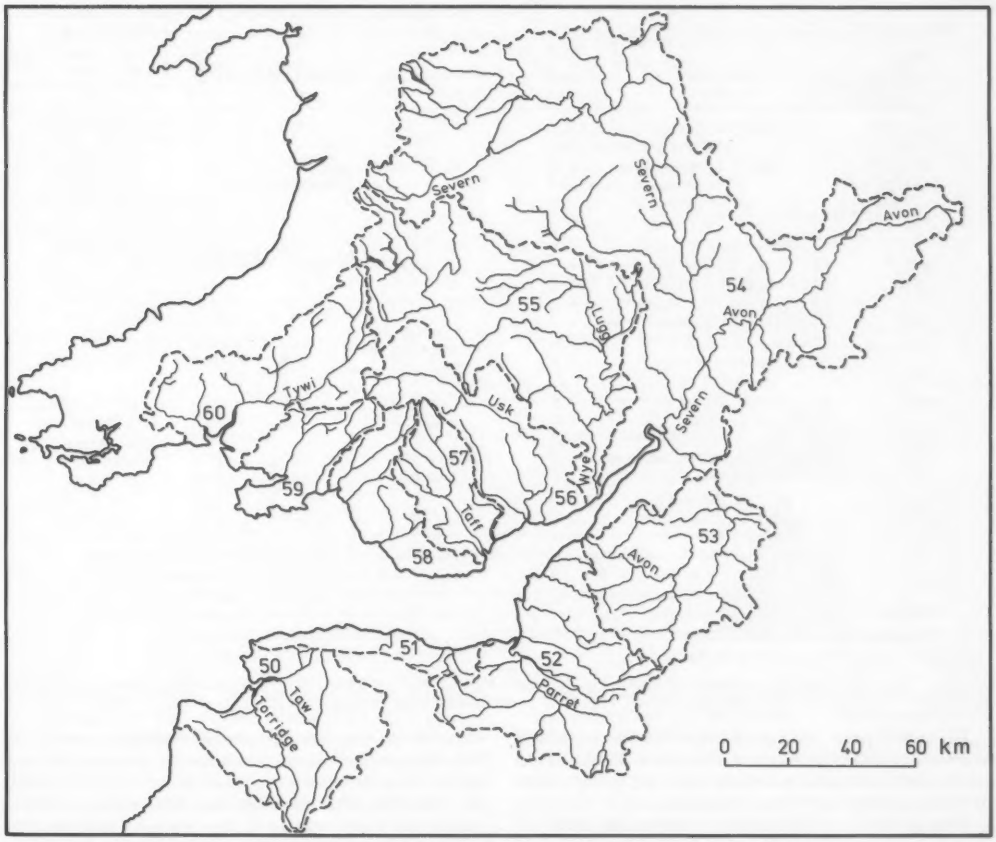

FIG. 3. Catchment areas of rivers draining into the Bristol Channel, abstracted from HMSO Publication: *Surface Water — United Kingdom* 1971–73. Hydrometric Area 50 monitored by the South West Water Authority (WA); similarly, Areas 51 to 53 by the Wessex WA, Area 54 by the Severn Trent WA, Areas 55 to 60 by the Welsh (National) Water (Development) Authority.

sampling was carried out, around 10:34 to 10:44 GMT (Farmer 1979) on eight occasions (Fig. 4) using M. V. *Nicola*. In a busy shipping lane, sample location was based on fixed time intervals of 4 min; this resulted in an overall sampling period of 50 min, in comparison with an ideal "window time" of 20 min. Samples of the water–sediment mixture were filtered in the laboratory through either nuclipore 0.4 μm (Dixon 1980) or membrane 0.47 μm filters (Buncle 1981).

Although no attempt is made in this investigation to correct for different color saturation conditions, chromaticity determinations were carried out on two sets of samples from 13/11/79 and 9/3/80. These analyses showed remarkable consistency between the two data sets, with the trichromatic coefficient X ranging from 0.310 to 0.317 and 0.309 to 0.317, respectively; comparable values for Y were 0.312 to 0.321 on both occasions (Dixon 1980).

Supplementary turbidity data to which reference is made (Locations 1 to 4, Fig. 1) were collected using turbidity meters, with gravimetric calibration from field samples (Murray et al. 1980; Moore 1975; Matthews 1975; and Glydon-Jones 1976).

LANDSAT imagery for the Bristol Channel was analyzed at the Space Department, Royal Aircraft Establishment, Farnborough. The total U.K. holding of the computer compatible tapes from LANDSAT 1 and 2 (Table 1) have been analyzed using an Image Analysis System, IDP 3000. Contrast enhancement, density slicing with an 8 bit intensity resolution and representation using false color imagery was applied to all the tapes. MSS Band 5 (600–700 nm; red) was selected, as spectral reflectivity within this band has been shown to usefully represent near-surface suspended sediment concentration (SSC) in such coastal waters. The majority of the solar energy penetration (70%), and hence backscatter and reflectance, is contained within the upper 2 m of the water (Charnell and Maul 1973).

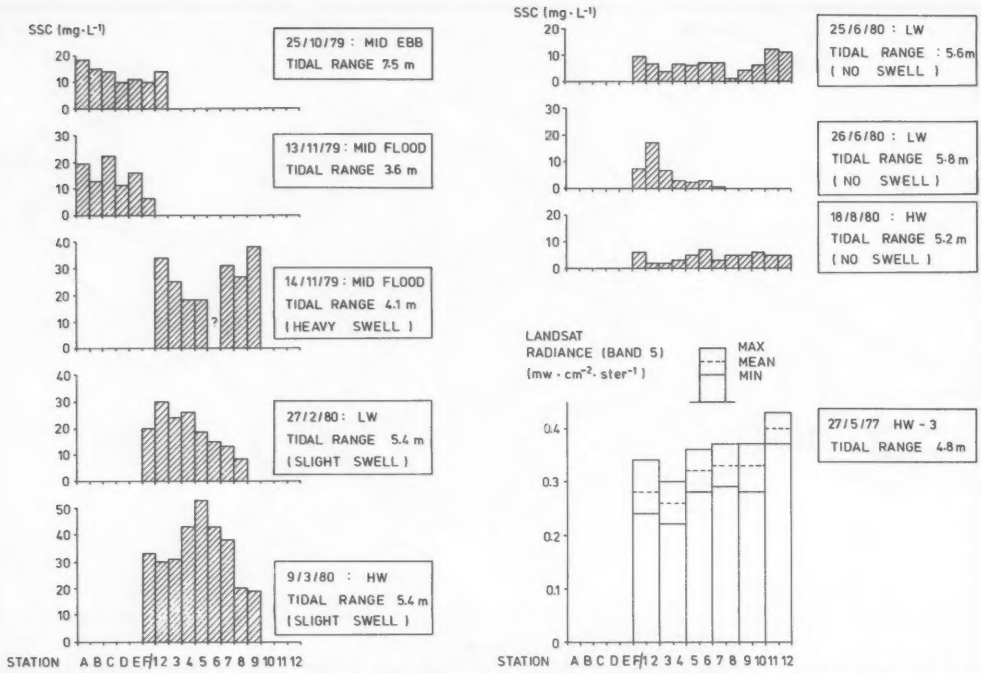
SSC (mg·L⁻¹)
25/10/79 : MID EBB
TIDAL RANGE 7.5 m
13/11/79 : MID FLOOD
TIDAL RANGE 3.6 m
14/11/79 : MID FLOOD
TIDAL RANGE 4.1 m
(HEAVY SWELL)
27/2/80 : LW
TIDAL RANGE 5.4 m
(SLIGHT SWELL)
9/3/80 : HW
TIDAL RANGE 5.4 m
(SLIGHT SWELL)
STATION A B C D E F 1 2 3 4 5 6 7 8 9 10 11 12
SSC (mg·L⁻¹)
25/6/80 : LW
TIDAL RANGE : 5.6m
(NO SWELL)
26/6/80 : LW
TIDAL RANGE 5.8 m
(NO SWELL)
18/8/80 : HW
TIDAL RANGE 5.2 m
(NO SWELL)
LANDSAT
RADIANCE (BAND 5)
(mw · cm⁻², ster⁻¹)
MAX
MEAN
MIN
27/5/77 HW - 3
TIDAL RANGE 4.8 m
STATION A B C D E F 1 2 3 4 5 6 7 8 9 10 11 12

FIG. 4. "Sea-truth" data (Station location on inset to Fig. 1). Results from 25/10/79 to 09/03/80 from Dixon (1980); those from 25/06/80 to 18/08/80 from Buncle (1981). Radiance values, MSS band 5, are shown for the overpass of 27/05/77 (see also Fig. 6A).

The satellite passes analyzed, together with concurrent tidal and wave conditions at Swansea are listed in Table 1. Tidal ranges can be compared with mean neaps and springs ranges at Swansea of 4.1 and 8.6 m, respectively.

In the absence of direct comparison between the field verification surveys and the analysis of tapes, reflectivity along the sampling line (1 to 12, inset, Fig. 1) was examined in the tape for 27/05/77. Radiance values for subscenes of 50 pixels (picture elements, each 56 m × 79 m) of the image were analysed; these are compared with field verification data (Fig. 4).

Turbidity data collected in Swansea Bay by the WWA are based on water samples collected from a helicopter. Seventy stations were sampled on Surveys 1 to 3 and 94 stations on Surveys 4 to 21 (for locations, see fig. 27.1, Humphrey et al. 1980). Filtration took place through GF/C filters with a pore size about 2 μm. These data were supplied to the author in terms of contoured charts with concentration isopleths of < 20, 20 to 40, 40 to 60, 60 to 80, and > 80 mg·L^{-1} (C. Pattinson, personal communication). Tidal and wave conditions during sampling are summarized in Table 2.

The IMER surveys in the Bristol Channel are listed in Table 3 in which, due to the length of time taken for each of the surveys, wave conditions have been omitted. Surface turbidity during these cruises was monitored using a Partech suspended solids monitor, calibrated by means of gravimetric determinations (IMER 1974). The data were supplied to the author (I. R. Joint, personal communication) in terms of either contoured individual observations or computerized contoured charts; the latter with contours at 5, 10, 15, 20, 30, 50, 80, 100, 200, 300, 500, 800, and 1000 mg·L^{-1}. Observations had been corrected to their positions corresponding with either HW or LW at Swansea (fig. 3, Hamilton et al. 1979); this results in displacement of the stations along the Channel.

Meteorological data referred to in the text have been obtained from the Coastguard Station at Mumbles Head (inset to Fig. 1) or from the Daily Charts of the Meteorological Office, Bracknell, U.K.

In the quantitative calibration of the thematic satellite imagery, reference is made to all the available survey data outlined above. Use is made of a relationship between the natural logarithm of the suspended sediment concentration (log$_e$SSC) and the band 5 radiances, established for environments comparable to that of the Bristol Channel (Williamson and Grabau 1973; Bowker et al. 1975). For example, a correlation coefficient of 0.95 was found for comparable data from the Bay of Fundy (Amos and Alföldi 1979).

Results

SEA-TRUTH DATA

The results presented in Fig. 4 relate to concentrations

TABLE 1. Details of LANDSAT imagery analyzed.

Date	Path	Row	Overpass, relative to HW, Swansea	Tidal range (m)	Meteorological[a,d] conditions	Wind[a] speed (knots)
24/04/75	220	024	LW − ½ h	8.5	High west of Ireland, winds NE	13 to 17
04/07/75[d]	219	024	LW + 3h	4.4	Low over N. France, winds N	2 to 3
14/02/76[b]	—	—	LW − ½h	7.5	Low over N. Italy, winds NE	1 to 2
08/04/76	219	024	HW − 1½h	4.1	High over mid-Atlantic, winds E	8 to 12
26/02/77[d]	219	024	HW − 1h	4.3	High over N. England	Calm
27/05/77	219	024	HW − 2½h	4.8	High over N. Sea, winds S	3 to 7
28/05/77[c]	220	024	LW + 3h	4.4	See note	
02/07/77	219	024	HW + 3h	8.8	High over Germany, winds S/SW	3 to 7
03/07/77	220	024	HW + 2½h	8.6	High over N. Germany	Calm
13/09/77	220	024	LW + 1½h	8.2	High over Irish Sea, winds NE	8 to 12
27/08/80	219	024	HW + 3½h	9.5	Low over English Channel	Calm
02/10/80	219	024	HW − 2h	4.1	High over Scillies, winds NE	8 to 12
13/01/82	219	024	HW + 1½h	8.4	High over N. Germany	8 to 12

[a]Abstracted from the Daily Weather Charts produced by the Meteorological Office, Bracknell, U.K.
[b]Individual print made available to the author.
[c]Hazy image, analyzed only for the Loughor Estuary and eastern Carmarthen Bay.
[d]Comparable freshwater inputs from the River Severn (Fig. 3) are all $< 10 \times 10^9$ L·d^{-1}, except for a maximum on 26.02.77 (53×10^9 L·d^{-1}) and a minimum on 04.07.75 (1.4×10^9 L·d^{-1}); based on information supplied by the Severn Trent Water Authority.

between 1 and 53 mg·L^{-1} and appear to indicate that levels in Swansea Bay are independent of tidal range, but dependent upon wave conditions. For example, there is reasonable compatibility between measured concentrations on the 25/10/79 and 13/11/79, corresponding with tidal ranges of 7.5 and 3.6 m, respectively. In contrast, levels are higher in the presence of swell waves.

Other comparable studies in Swansea Bay have recognized the importance of waves in increasing suspended sediment concentrations, particularly in the shallow water areas (Moore 1975; Glydon-Jones 1976). Indeed, at Mumbles Pier (Location 2, Fig. 1), a distinct plume of highly concentrated water is discharged into the main channel on the ebb (Plate 1, Collins et al. 1979). This plume is thought to result from wave reworking of the intertidal zone and subsequent transport of material by tidal currents (Moran and Collins 1980). Wave action could also explain the observed higher concentrations within the embayment, at the same tidal state, on neaps than on springs (Davies 1974).

SATELLITE IMAGERY

Two methods of analysis have been applied to hard copy color and black and white images obtained from the IDP 3000 Image Analyser. Firstly, patterns of concentration and inferred transport directions have been identified from the complete set of images (Fig. 5). Secondly, thematic maps from specific overpasses have been produced (Fig. 6); these are used later (see Discussion), in association with calibration data derived from all the available turbidity information, to derive estimates of the total quantity of material present in the Channel at different tidal states.

The satellite overpasses summarized in Fig. 5 represent the early ebb to LW phases of spring tides and middle to late phases on neaps, with mainly low wind speeds (Table 1). Turbidity patterns are represented in the Figure by areas of low, medium, and high concentration.

The surface distribution of suspended sediment remains consistent between the images, with the main area of high concentration being located up-channel. The location of the boundaries between zones of high and medium concentrations and medium and low concentrations are located farther up-channel on neaps, at low freshwater discharge, than on springs. These boundaries run generally north to south or northwest to southeast across the Channel, but also include a series of tongues which extend offshore.

A persistent feature of the boundaries is their extension along the northern coastline towards, and then away from, the headland-associated linear sandbanks in eastern Swansea Bay. Other tongues of higher concentration waters develop midway across the Channel (Fig. 5A(i) to (v) and 5B(v)). These tongues then move out across the Channel in a southwesterly direction, inferring movement from the northern coastline into Barnstaple Bay (Fig. 1). This pattern might be enhanced at times of strong (13−17 knot) northeasterly winds (Fig. 5A(vi)). Inferred movement of material along the southern coastline is less pronounced or persistent and waters are generally clearer here. The orientation of some of the

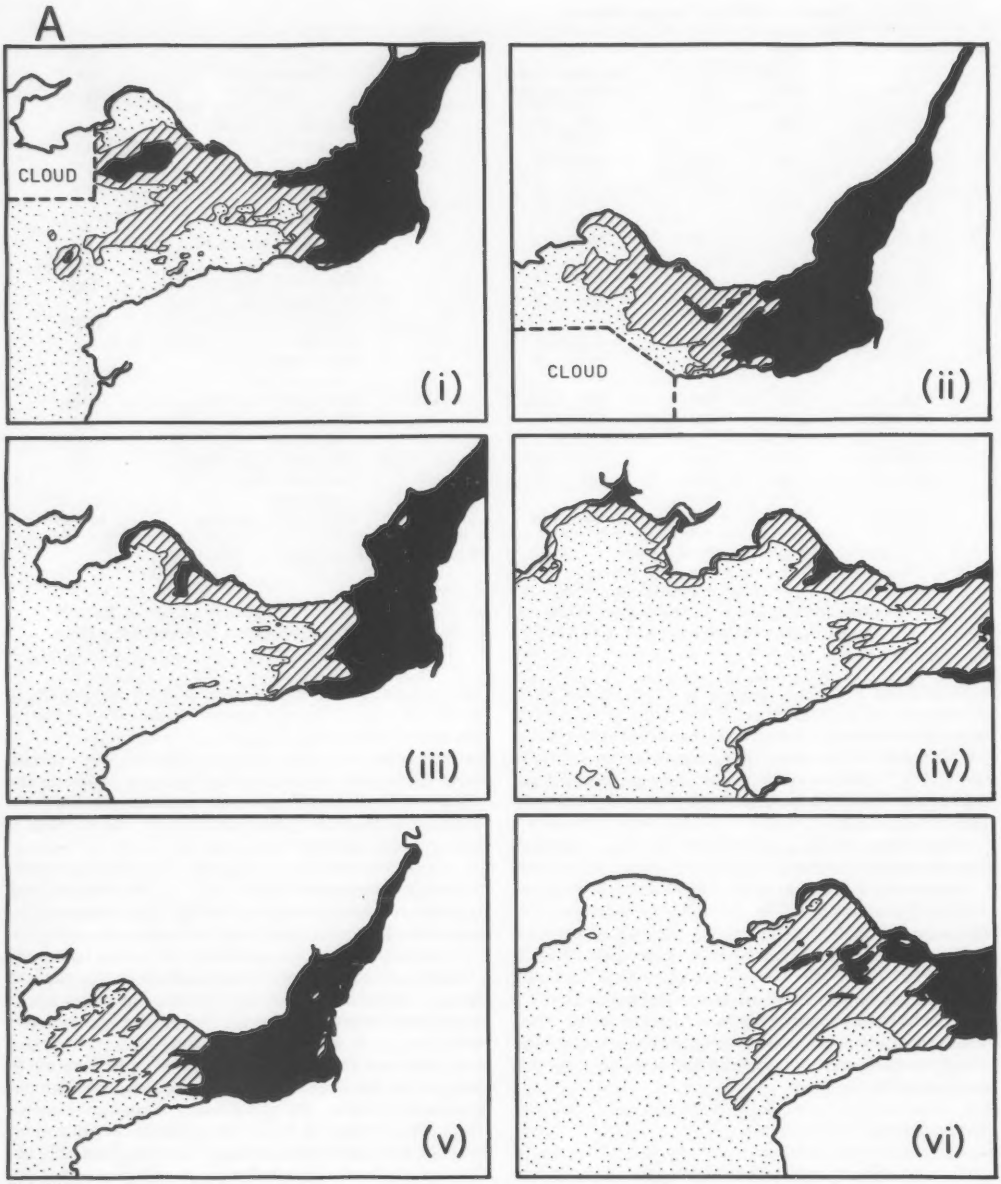

FIG. 5A.

concentration isopleths in the satellite imagery (e.g. 5A(i), (ii), (vi) and 5B(i) and (v)) are remarkably similar to the pattern of isohalines at times of high freshwater discharge, with the lower salinity waters moving out along the northern coastline (e.g. Hamilton et al. 1979, fig. 3).

The geometry of the boundaries in the offshore areas infers lateral shearing within the tidal waters, with flow in parallel ribbons moving at different speeds (Munday et al. 1979; fig. 16(B)). This type of flow often creates a distinctive linear surface suspended sediment "front," such as that resulting in

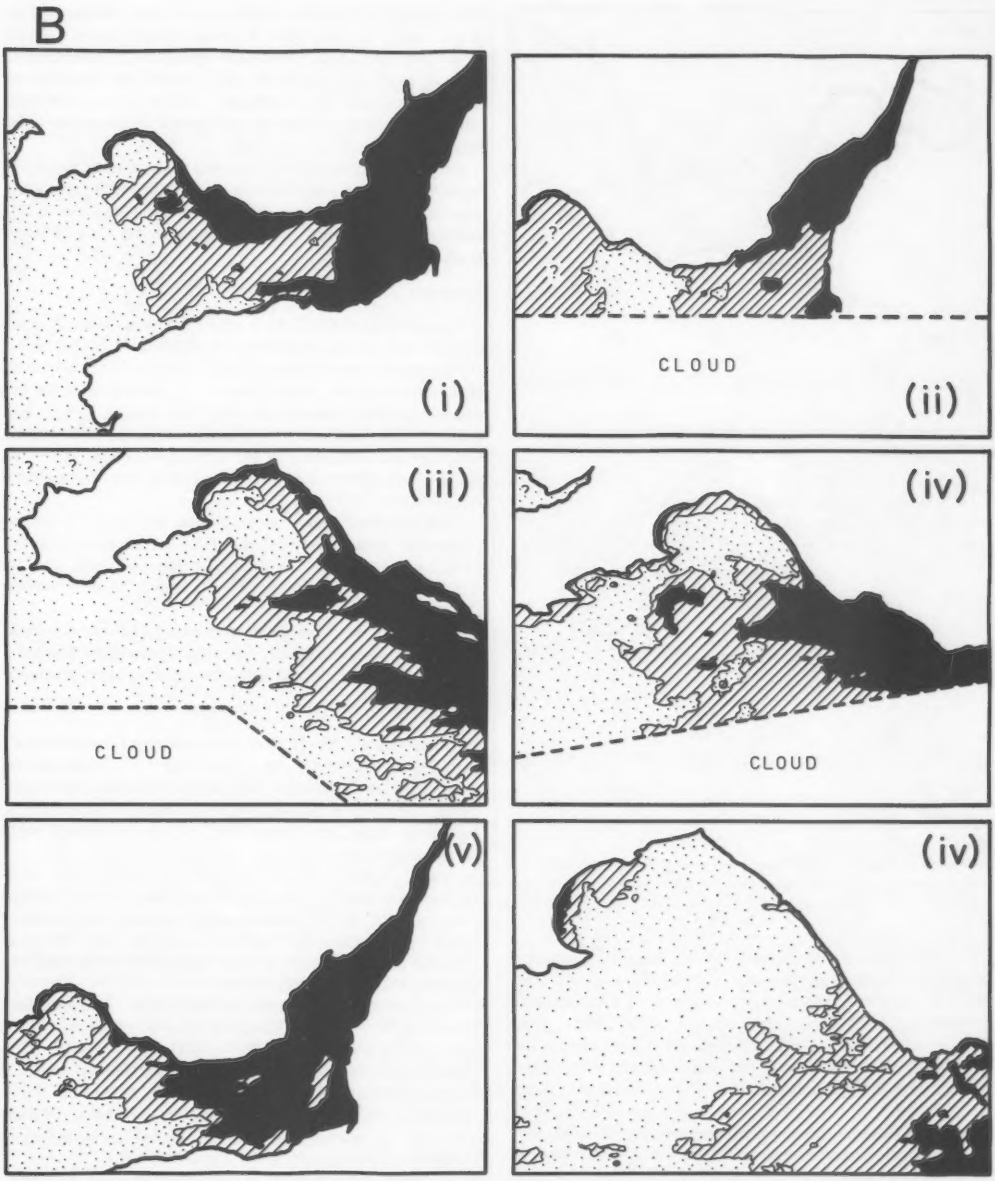

FIG. 5. High, medium and low turbidity areas identified from the satellite imagery. Overpasses as follows: 5(A): nominally Springs (range > 7.5 m) — (i) Mid-ebb on 27/08/80 (see also Fig. 6C); (ii) Mid-ebb on 13/09/77; (iii) Mid-ebb on 02/07/77; (iv) Mid-ebb on 03/07/77 (see also Fig. 6B); (v) Late-ebb on 14/02/77; (vi) Low Water on 24/04/75.
5(B): nominally Neaps (range < 4.8 m), except 5B(vi) — (i) Mid-flood on 27/05/77 (see also Fig. 6A); (ii) Mid-flood on 04/07/75; (iii) Late-flood on 02/10/80; (iv) Late-flood on 26/02/77; (v) Late-flood on 08/04/76; (vi) Early Ebb on 13/01/82 (Spring). See Table I for synoptic meteorological conditions.
Key to turbidity levels: High — black; Medium — cross hatched; Low — stippled.

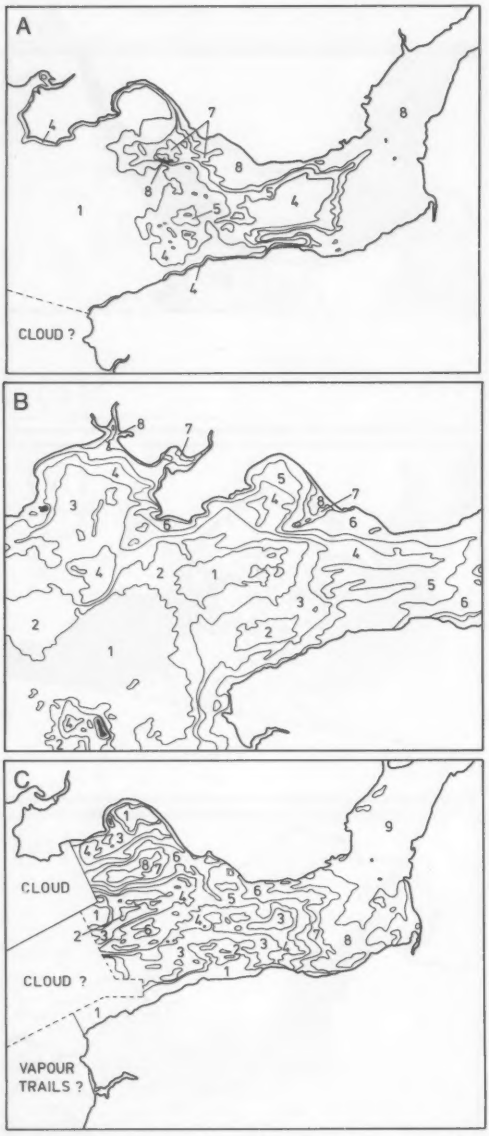

FIG. 6. Thematic representations of MSS band 5 overpasses. Concentrations (in $mg \cdot L^{-1}$) are given for the middle of the range of the density slice setting. (A) 27/05/77 (Orbit 219, Row 024): Mid-flood of a Neap Tide (4.8 m range). (1) — 5; (4) — 20; (5) — 36; (7) — 60; (8) — 250; (B) 03/07/77 (Orbit 220, Row 024): Mid-ebb on a Spring Tide (8.6 m range). (1) — 5; (2) — 8; (3) — 13; (4) — 20; (5) — 30; (6) — 47; (7) — 63; and (8) — 148; (C) 27/08/80 (Orbit 219, Row 024): Mid-ebb on a Spring Tide (9.6 m range). (1) — 8; (2) — 12; (3) — 16; (4) — 22; (5) — 33; (6) — 52; (7) — 63; (8) — 148; and (9) — 500.

the isolation of clearer waters in western Swansea Bay (Figs. 5A(i), (v) and (vi)). A similar linear feature extends westwards from Nash Point and appears to be enhanced at times of winds from the south, which restrict the dispersion of material towards the southwest. Under strong northerly winds, the tongues of highly concentrated waters appear to be broadened (Fig. 5A(ii) and (vi)).

Irregular sections of the contoured boundaries between the higher and lower concentration waters, in Fig.5, appear to represent patterns which could be associated with either accelerating or "dwindling" tidal currents (cf. fig. 16, Munday et al. 1979).

SWANSEA BAY (WWA) SURVEYS

Typical results (Fig.7) from the survey data (Table 2) demonstrate that in the progression from Neap to Spring tides: (i) the overall concentration levels increase; (ii) a tongue of high concentration waters developed, extending from the eastern coastline towards the west; (iii) relative to (ii), low concentration waters are constrained within the embayment; and, (iv) the orientation of the turbidity isopleths infers residual water and sediment movement away from the northern coastline.

Concentration levels (up to approx. 80 $mg \cdot L^{-1}$) can be compared with those of the field verification surveys ($1-52\ mg \cdot L^{-1}$) and to supplementary offshore (up to $5\ mg \cdot L^{-1}$) and nearshore ($32-90\ mg \cdot L^{-1}$) observations (Moore 1975).

The results described here, in contrast to those described previously as sea-truth data, appear to represent the influence of tidal range and current speeds on concentration levels.

BRISTOL CHANNEL (IMER) SURVEYS

These data (Table 3) show that maximum concentrations varied from 80 $mg \cdot L^{-1}$ to $> 1000\ mg \cdot L^{-1}$. There was no direct correlation between concentrations and the mean tidal range, due to the averaging procedure adopted. Nevertheless, increasing mean tidal range (Fig. 8) was associated with: (a) corresponding increases in high turbidity (i.e. $> 30\ mg \cdot L^{-1}$) areas; (b) the extension of turbid waters along the southern coastline, past Bridgwater Bay as far as Foreland Point in the Central Channel; and (c) inferred movement of turbid waters along the northern coastline from the Inner Channel into Swansea Bay, with transport then towards the southwest (Fig. 8, Cruise 3/79).

These levels can be compared with surface concentrations of: 40 $mg \cdot L^{-1}$ for the Central Channel (Location 1, Fig. 1; Murray et al. 1980); 50 $mg \cdot L^{-1}$ to 800 $mg \cdot L^{-1}$ for the Inner Channel (Location 3, Fig. 1; I. R. Joint (IMER) personal communication); 163 $mg \cdot L^{-1}$ (Matthews 1975) and 200 to $> 1000\ mg \cdot L^{-1}$ (Parker and Kirby 1981; Kirby and Parker 1982) for the northern and southern coastlines of the Inner Channel/Outer Estuary, respectively.

Discussion

OVERALL TURBIDITY PATTERNS

Areas of high turbidity and inferred sediment transport paths remain consistent throughout the various data sets, obtained using a variety of collection and analytical techniques.

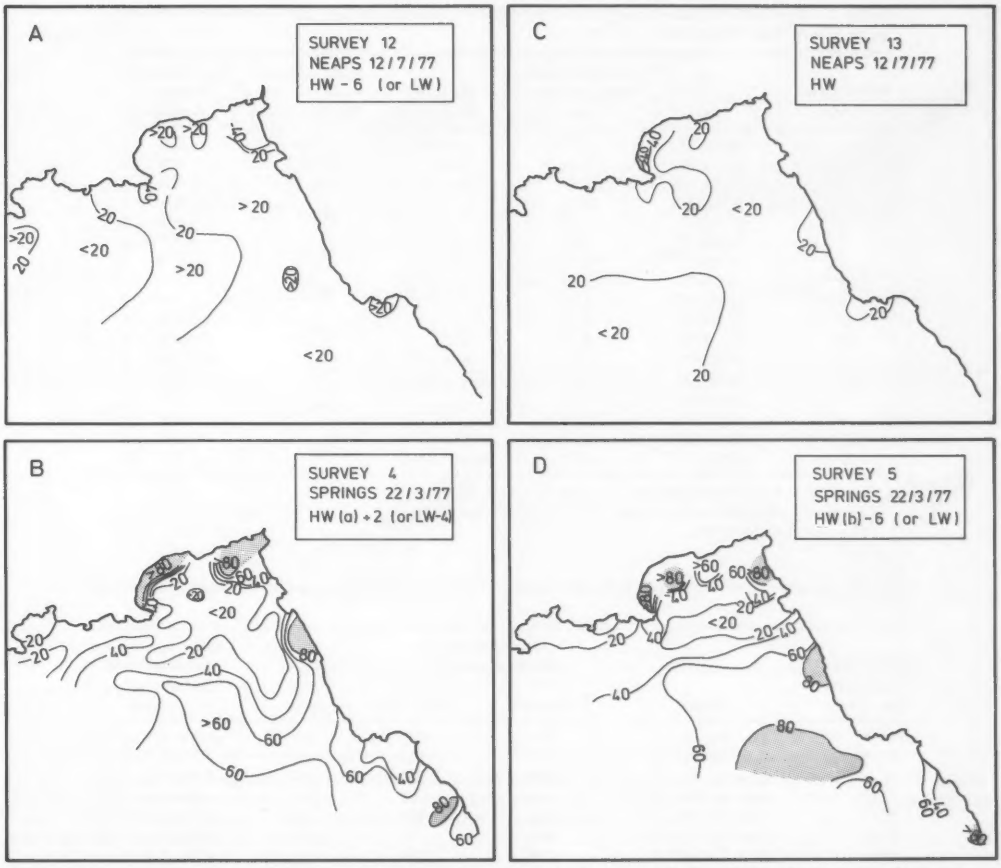

FIG. 7. Typical results of near-synoptic surveys of surface concentration (Welsh Water Authority). Predicted tidal ranges (Swansea) are: Survey 4 — 8.3 m; Survey 5 — 8.2 m; Survey 12 — 5.0 m; and Survey 13 — 5.0 m. See Table 2 for overall availability of similar data. Key to turbidity level: Stippled = >80 mg·L^{-1}.

High concentration waters are present within the Inner Channel and Outer Estuary, in water depths < 30 m. Seaward movement of the boundary of these waters, on spring tides, infers local resuspension of material and dependence upon tidal current speeds. Such an interpretation is consistent with the conclusions reached by other investigators of the Channel (IMER 1974, p. 26; 1975) and other large estuaries of the British Isles (Inglis and Allen 1957; Halliwell and O'Connor 1965; and BTDB 1970).

The high turbidity surface waters described above move out along the northern coastline, at all states and phases of the tide. Lower turbidity waters are present along corresponding sections of the southern coastline. To the west of Nash Point, concentration levels are sometimes enhanced by wave-reworking of the linear sandbanks. Indeed, throughout the Outer and Central Channel, wave reworking of the shallow water areas produces a supplementary mechanism for the generation of high suspended sediment concentrations, in an area where sediment transport is controlled by a variety of combinations of tidally and wave-induced currents (Collins et al. 1979, 1980). For example, based upon data from a wave-rider buoy in Swansea Bay, the threshold wave-induced velocity for fine/medium sand is exceeded some 20% of the year in 20 m and $> 40\%$ in 10 m water depth (Ferentinos and Collins 1978, fig. 60).

Finally, the observed turbidity patterns infer offshore transport of material from the Central Channel, in a westerly/southwesterly direction, at all states of the tide (see Fig. 5B(i) and (v) and Fig. 8). (Cruises 2/79 and 3/79).

THE SEDIMENT BUDGET OF THE CHANNEL

Even though there is evidence of fine-grained sediment supply from the Celtic Sea (Culver 1980), it is of interest to

TABLE 2. Availability of Near-surface Suspended Sediment Concentration[a] Data from Swansea Bay (Provided by the WWA: Tidal Waters Unit).

WWA survey reference	Date	Predicted tidal range, Swansea (m)	Sea state[b] (ft)/Swell	Wind direction[c] and strength (Beaufort Scale)	Tidal state relative to Swansea (h)
1	28/10/76	7.3	1 to 4	NE,2	HW
2	03/11/76	5.7	2 to 4	NNE,1	HW
3	09/11/76	7.4	4 to 13	SW,5	HW + 3
4	22/03/77	8.3	2 to 4	NE,3	HW + 2
5	22/03/77	8.2			HW − 6
6	24/03/77	7.4	0 to 1	SE,2	HW − 1
7	24/03/77	7.3			HW + 3
8	10/05/77	5.3	1 to 2	SW,3	HW − 3
9	10/05/77	4.8			HW + 3
10	12/05/77	4.7	2 to 8	NW,3	HW − 5
11	12/05/77	4.7			HW − 1
12	12/07/77	5.0	8 to 13 (Heavy Swell)	SW,6	HW − 6
13	12/07/77	5.0			HW
18	15/09/77	9.2	1 to 2	NW,2	HW
19	15/09/77	9.2			HW − 6
20	08/11/77	6.6	4 to 8 (Heavy Swell)	SW,7	HW − 6
21	08/11/77	6.6			HW − 1

[a]Concentration range throughout is < 20 mg·L^{-1} to > 80 mg·L^{-1}.
[b]Based on visual observations at Mumbles Coastguard Station.
[c]10.00 GMT at Mumbles.

TABLE 3. Availability of Near-surface Suspended Sediment Concentration Data from the Bristol Channel (as provided by IMER).

IMER cruise reference (No./Year)	Dates	Suspended sediment concentrations (mg·L^{-1})		No. of tidal cycles	Range and mean of predicted[a] tides (m) over cruise period
		Minimum	Maximum		
1/74	Jan. 16–Jan. 22	17	215	13	5.8 to 8.9 (7.9)
2/74	Feb. 20–Feb. 22	9.5	155	6	7.7 to 8.8 (8.3)
8/74	May 13–May 17	zero	250	9	5.3 to 7.2 (6.4)
2/77	Feb. 8–Feb. 19	<5	179	23	4.6 to 8.9 (6.9)
5/77	May 19–May 23	<2	900	10	6.1 to 7.4 (6.8)
6/77	June 16–June 20	zero	150	9	6.8 to 7.1 (6.9)
8/77	Sept. 2–Sept. 6	<10	1000	9	4.0 to 7.8 (6.0)
9/77	Oct. 25–Nov. 6	<3	100	25	3.6 to 8.0 (6.4)
2(A)/78	Feb. 24–Mar. 3	<10	1000	16	4.9 to 8.6 (7.5)
3/78	Apr. 13–Apr. 17	<6	300	9	3.4 to 6.3 (4.5)
4(A)/78	May 31–June 4	<3	800	10	5.1 to 7.3 (6.3)
5/78	July 19–July 25	<5	900	13	7.3 to 9.6 (8.7)
6/78	Sept. 7–Sept. 11	<5	500	9	4.6 to 7.8 (6.3)
8/78	Nov. 9–Nov. 12	<5	800	8	4.6 to 7.9 (6.1)
1/79	Jan. 11–Jan. 23	<5	400	25	4.5 to 7.5 (6.4)
2/79	Mar. 20–Apr. 3	<10	800	29	4.3 to 10.0 (7.7)
3/79	May 17–May 21	<5	1000	9	5.1 to 6.9 (5.8)
4/79	July 16–July 17	0.1	500	3	5.7 to 6.6 (6.1)
5/79	Aug. 7–Aug. 16	<1	1000	19	4.5 to 9.9 (8.0)
6/79	Sept. 11–Sept. 12	<3	500	4	6.2 to 8.2 (7.2)
7/79	Nov. 2–Nov. 5	<3	800	7	7.8 to 9.6 (9.0)
1/80	Jan. 14–Jan. 18	15	80	9	5.0 to 8.8 (6.9)
2/80	Mar. 14–Mar. 24	<1	500	20	4.4 to 10.4 (8.3)
4/80	May 19–May 29	<1	300	21	3.9 to 7.4 (5.5)
5/80	June 19–June 21	75	600	5	4.3 to 5.4 (4.9)
6/80	Aug. 11–Aug. 21	<5	1000	21	3.8 to 7.8 (6.2)
7/80	Oct. 6–Oct. 17	190	1000	23	4.5 to 8.0 (6.8)

[a]At Swansea.

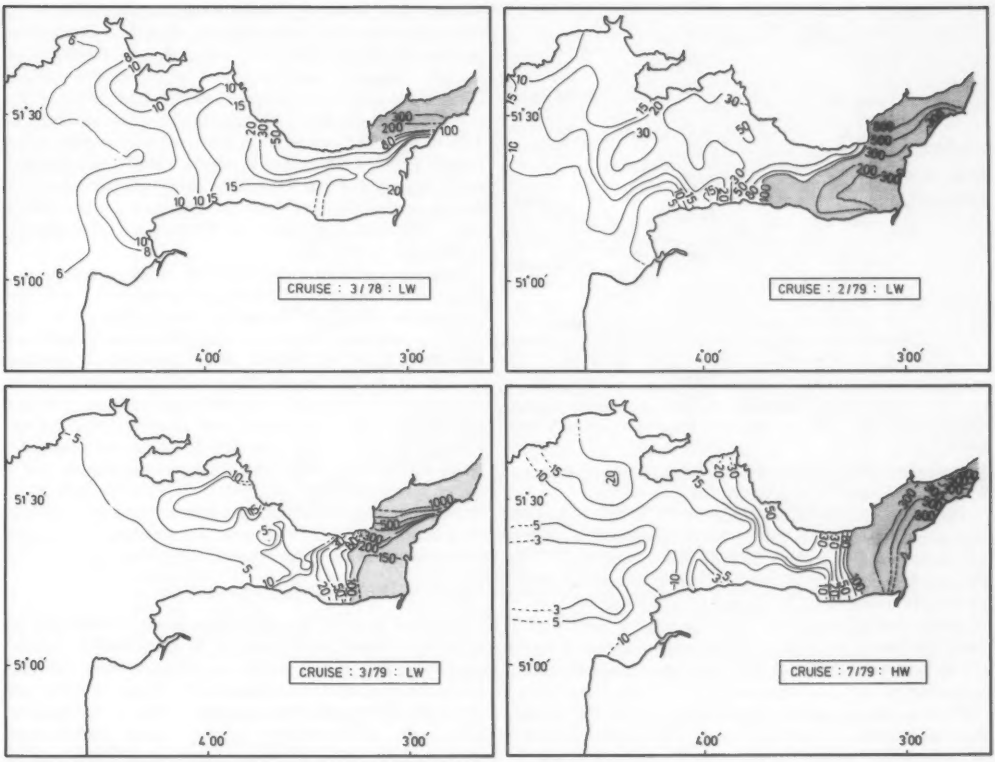

FIG. 8. Typical results of integrated surveys of surface concentration in the Bristol Channel (Institute for Marine Environmental Research). Number of tides and average range are: Cruise 3/78 — 9 tides (4.5 m); Cruise 2/79 — 29 tides (7.7 m); Cruise 3/79 — 9 tides (5.8 m); and Cruise 7/79 — 7 tides (9.0 m). See Table 3 for overall availability of similar data.
Key to turbidity level: Stippled = > 100 mg·L^{-1}.

examine the potential contribution of the rivers to the quantity of material contained within the system.

An example of the application of a natural logarithmic "rating curve" to the LANDSAT data, to examine the whole of the Channel, is shown as Fig. 9; this represents the overpass of 27/05/77 (Fig. 6A). The upper and lower limits of the calibration were set from data provided by IMER cruises 3/78 and 3/79 (Fig. 8). Confirmation of intermediate points on the graph was provided by the WWA Surveys, with the sea-truth and supplementary data. This approach was applied to the remainder of the thematic data from overpasses (Fig. 6B and C), with concentrations ranging from 5 to 148 mg·L^{-1} and 8 to 500 mg·L^{-1}, respectively. An iterative procedure was used to accommodate the various field observations.

Using the calibration curves, in conjunction with bathymetric data (Fig. 2) and tidal levels (table 5, Admiralty Manual of Tides, 1981), computations for the total amount of suspended sediment present within the system have been carried out, for MHWN and MHWS tidal heights. The area considered in the load computations is that between the northern and southern coastlines and between 4°40′W and 2°40′W.

On a MHWN tide (based on the results of Fig.6A) and assuming initially that concentrations are uniform throughout the water column, it is estimated that some 4.5×10^6 t of material are in suspension; this increases to 6.7×10^6 t at MHWS (based on the combination of Fig. 6A and C). In both cases, the majority of the material is contained within the Inner Channel and Central Channel sections of the System.

Much of the information available on the vertical distribution of suspended sediment at various locations in the Bristol Channel (Murray et al. 1980; Moore 1975; Matthews 1975; Parker and Kirby 1981; Kirby and Parker 1982) shows that near-bed concentrations are considerably higher than those at the water surface. In this respect, the Bristol Channel is not similar to the Bay of Fundy, where surface concentrations of sediment are typical of those throughout the water column (Amos and Alföldi 1979). Surface/bed concentration ratios in the Bristol Channel vary from 1:3 to 1:10, with an average around 1:4, even when ignoring localized fluid mud patches. If the values derived above are doubled, therefore, to take into

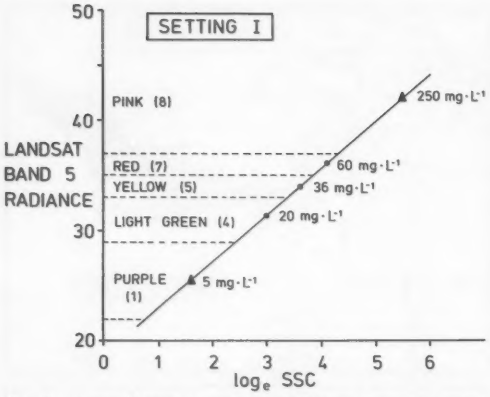

FIG. 9. Linear/Natural Logarithmic Calibration Curve for Landsat overpass of 27/05/77 (see also Fig. 6A), based on all available field data.

account vertical inhomogeneity, the revised estimates become 9×10^6 t on MHWN and 13.4×10^6 t on MHWS.

These estimates can be compared with: 5×10^6 t of mobile fine sediment, which is considered to be "potentially available for resuspension, especially during storm conditions, ... for the area between Swansea Bay and just above Avonmouth" (p. 142, Hamilton et al. 1979); and 10×10^6 and 30×10^6 t of mobile fine sediment being available in the Estuary section from The Shoots, just upstream from Avonmouth, to 3°30′W (Kirby and Parker 1975 and table 3 in Parker and Kirby 1982, respectively).

These sediment loads are now compared with the annual suspended sediment input from rivers. The areas of catchments draining into the Channel (Fig. 3), above their lowest monitoring station, have been abstracted (HMSO 1978). These areas were increased by 20%, to allow for the catchment downstream of the tidal limits. Modified areas (x) were then used to calculate annual suspended sediment loads (y), based upon the regression equation, $y = 12.9x^{1.21}$, derived empirically from catchment investigations in the British Isles and areas up to 2000 km^2 (Collins 1981).

The overall drainage area into the Channel is 25 000 km^2 and the annual predicted suspended sediment load is 1.63×10^6 t. The Wye, Avon, and Severn rivers contribute 1.25×10^6 t, or 77% of the annual input. Contributions to the various embayments are as follows: Carmarthen — 0.10×10^6 t (7% of the annual total); Swansea — 0.28×10^6 t (2%); Bridgwater — 0.29×10^6 t (2%); and Barnstaple — 0.96×10^6 t (6%).

The prediction for Swansea Bay can be compared with a value of 0.75×10^6 t/yr (Stoner, WWA, personal communication), presented elsewhere (Collins et al. 1979). Loads for the Rivers Wye, Avon, and Severn compare with an alternative overall prediction of 0.70×10^6 t/yr (table 1, Kirby and Parker 1975; based on data from Brookes 1974), $0.7-0.96 \times 10^6$ t/yr (table 2, Parker and Kirby 1981) and 0.83×10^6 t/yr (Owens 1982).

In addition to fine-grained sediment supply from the rivers, plankton, and sewage might be present in suspension. Within Swansea Bay, however, turbidity was considered to be "a contributory factor to, rather than the result of phytoplankton production" (Joint 1980). Similarly, approx. 400 000 t of sewage sludge and small quantities of industrial waste are dumped annually in the Central Channel (Location 1, Fig. 1). It is suggested that this is of local significance, amounting to 51% of the direct inputs of organics and trace metals to the Central Channel (Murray et al. 1980). Finally, sea dumping of dredge spoil is not thought to be an original source of fine-grained material, as it only recycles a small proportion of the mobile population of the Inner Channel and Outer Estuary (Parker and Kirby 1981).

Sediment load data derived from the present investigation, both for the Channel as a whole and for the river inputs, are comparable with those derived by other investigators. The mobile population of fine-grained material in the Channel, of between 4.5 and 13.4×10^6 t, is equivalent to between 3–8 yr of river sediment supply. This assessment can be compared with one of 20 yr, for the Estuary, made by Parker and Kirby (1981). However, with flushing times for the Channel of the order of 150–400 d, fluvial sediment input could still influence long-term sedimentation patterns and it has been suggested (IMER, 1974, p. 26) that "the bulk of the sedimentary material is retained within the system for periods of at least tens of years" and that "resuspension is the major source of particulate load observed at any one time."

Sediment Transport Paths

Near-bed sediment transport paths in the Bristol Channel have been inferred on the basis of the interpretation of: side-scan sonar data (Stride 1963); modeling of interaction between the M_2 and M_4 tidal current constituents (Pingree and Griffiths 1979); and bedload transport formulae, in conjunction with self-recording current meter observations (Heathershaw 1981). These investigations define a zone of bed load parting around the Inner/Central Channel (Fig. 1). Bed-load transport is to seaward to the west of this zone and to landward to the east, in the Inner Channel. Sand circulation patterns within the Inner Channel/Outer Estuary themselves are complicated by the presence of sandbanks and intertidal areas; they appear to be represented by landward transport along the northern coastline and seaward along the southern (Parker and Kirby 1982; Fig. 4).

In order to explain the landward transport of stenohaline marine foraminifera into Swansea Bay (Culver and Banner 1978) and the Severn Estuary (Murray and Hawkins 1976), in the presence of the well-established westerly near-bed seaward transport path, Culver (1980) has proposed a vertical differential two-way transport model for the Channel. The model represents the upstream transport of fine-grained material by surface wind drift. This hypothesis can be considered within the context of the results of the present investigation.

Residual surface water movement in the Channel is shown in Fig. 10. Survey data and satellite imagery indicate net movement in an offshore direction along zones adjacent to the northern coastline, the longitudinal axis of the main Channel and the southern coastline. The orientation of the boundaries between high and medium turbidity waters indicate that movement is stronger to the north. To seaward, there is some evidence of movement out along the northern coastline, but

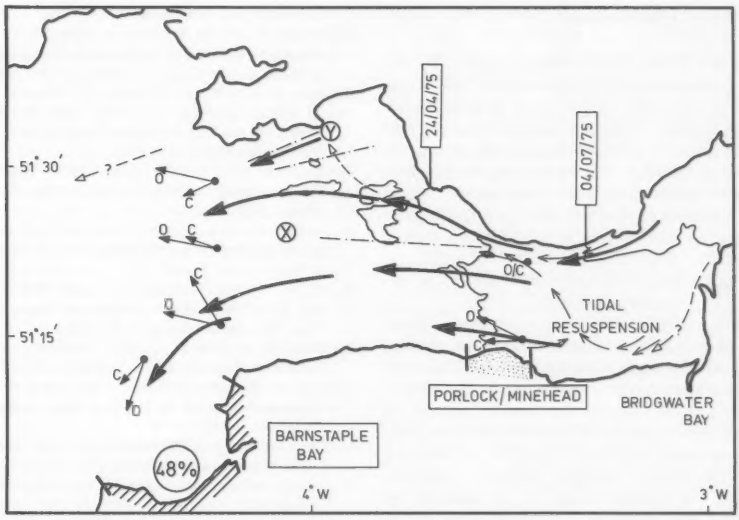

FIG. 10. Summary of inferred residual surface water and suspended sediment movement in the Bristol Channel, based on data from a variety of sources. ⟵ Transport directions, based upon satellite imagery and survey data (⟵ – – – Possible Directions); – · – · – Suspended sediment "front," identified from satellite imagery; [04/07/75] Upper Boundary of zone of High Turbidity (abstracted from Fig. 5); [24/04/75] as above, but Lower Boundary; O, C ⟵● Observed (O) and computed (C) surface residual currents, based upon density and nonlinear tidal effects (Uncles 1982); ⟵ Schematized residual surface water circulation (from Parker and Kirby 1982; Fig. 2); ⊗ Release position for surface (Woodhead) drifters, with 48% recovery in Barnstaple Bay (within hatched area of coastline) (Norton (MAFF), personal communication); Ⓨ Release position for drift cards, some of which were recovered from Porlock/Minehead (from stippled area of coastline).

also into Barnstaple Bay, to the south. These directions of movement correspond with the orientation of the surface tidal streams (Admiralty 1973) and with both observed and computed near-surface (Eulerian) residual currents (Uncles 1982).

Residual water movement in the Central/Outer Channel is confirmed by the surface drifter recovery patterns from Station X (Fig. 10), where 48% of those released were recovered from Barnstaple Bay within the first 75 d (Norton, MAFF, personal communication). For the Inner Channel, the results of the present investigation are comparable with those presented by Parker and Kirby (1982, Fig. 2), except for the area just to the west of Bridgwater Bay.

The residual water movement described above is dominated by the tidal excursion of water particles, which can be of the order of 16–24 km (Fig. 3, IMER, 1974). Wind drift is superimposed upon this pattern. For example, drift cards released at Station Y (Fig. 10) moved initially in response to the tidal currents; subsequent recovery was dominated by wind direction. Under northwesterly winds, some drift cards reached the Porlock/Minehead area of the southern coastline, within 2–6 d (Borthwick and Collins 1976). Hence, wind drift causes movement oblique to the tidally dominated residual current directions; it appears to act as a secondary mechanism for cross-channel dispersion of suspended material.

Outflow of surface waters occurs throughout the width of the Channel, but is enhanced along the northern coastline. This pattern is indicative of a large-scale estuarine system, under the influence of Coriolis effect; it corresponds with results obtained from physical oceanographic investigations (Lee 1960; Cooper 1967; and IMER 1974; Banner and Collins 1975).

Net seaward movement of fine-grained material in suspension in the surface waters, in the presence of wind drift, provides a mechanism of supply to offshore mud deposits (Stride 1963), but is somewhat contradictory to the model proposed by Culver (1980). In order to explain both the landward transport of foraminifera and the presence of fine-grained material in the Severn Estuary considered to originate from the Celtic Sea (Hamilton et al. 1980), movement must take place upstream. Based upon seabed drifter recovery patterns, Ferentinos and Collins (unpublished data) suggest that such upstream transport takes place along coastal boundary zones of the northern and southern coastlines. Such movement is confirmed by the upstream near-shore transport of heavy mineral grains along the southern coastline (Barrie 1980). A similar model of lateral variation in transport paths was proposed by Robinson (1973), to explain the marine origin of fine-grained sediment deposits in the Humber Estuary.

Conclusions

1) Turbidity in the Channel is caused primarily by resuspension of bottom material by tidal current and waves.
2) Between 4.5×10^6 t and 13.4×10^6 t of material are present within the Bristol Channel/Severn Estuary system at any instant; these compare with a predicted annual fluvial input of 1.63×10^6 t. These estimates are in agreement with those produced by other investigators demonstrating, in the short term, that the mobile population in the Channel is equivalent to between 3–8 yr of river sediment supply. In relation to the time of retention of water and sediment particles, long-term fluvial input may be an important source of fine-grained material.
3) Outflow of material in the surface waters represents movement in response to tidally induced residual circulation, which is typical of a large estuarine system. Wind drift provides a secondary mechanism for cross-channel dispersion of suspended material. Seaward movement of fines is directly opposed to the "differential two-way transport model," described elsewhere to explain the landward transport of fine-grained material. Near-bed upstream transport along the coastal boundaries, as indicated by seabed drifter studies, might provide the necessary mechanism for this transfer.

Acknowledgments

The author wishes to acknowledge warmly the following: Mrs A. Kirton and Mr E. ("Chippy") Jones of the Remote Sensing Unit, R. A. E. Farnborough, U.K., for their exceedingly helpful organisation and practical assistance with the CCT's, respectively; Dr I. Joint (IMER) and Dr C. Pattinson (WWA) for providing SSC data from their Institutions, with a refreshingly open attitude towards the provision of such information; Dr C. L. Amos (Bedford Institute of Oceanography), for his encouragement in the project and constructive review of the first draft; Ms J. Greengo and Miss Tracey Brewer for typing various drafts of the manuscript and Dr S. Shackley and Professor F. T. Banner for reading it through; Mr A. Cramp for assistance in the abstraction of meteorological information and, finally, Mr K. Naylor, Mrs A. Carr, and Mr A. Holbrook for excellent draughting of the Figures, reprographic, and photographic work, respectively. Financial support from the Natural Environment Research Council, for the use of satellite imagery facilities, is acknowledged.

ABDULLAH, M. I., H. M. DUNLOP, AND D. GARDNER. 1973. Chemical and hydrographic observations in the Bristol Channel during April and June, 1971. J. Mar. Biol. Assoc. U.K. 53: 299–319.

ADMIRALTY. 1973. Tidal Stream Atlas: The English and Bristol Channels. Hydrographic Office, Taunton, U.K. 16 p.

1981. Tide Tables, Vol. I., European Waters. Hydrographic Office, Taunton, U.K. 384 p.

AMOS, C. L. 1976. Suspended sediment analysis of seawater using LANDSAT Imagery, Minas Basin, Nova Scotia. Geol. Survey Can. Pap. 76-1C: 55–60.

AMOS, C. L., AND T. T. ALFÖLDI. 1979. The determination of suspended sediment concentration in a macrotidal system using LANDSAT Data. J. Sediment. Petrol. 49(1): 0159–0174.

BANNER, F. T., AND M. B. COLLINS. 1975. Field Meeting: 'Introduction to Oceanography' at University College of Swansea. Proc. Geol. Assoc. 86(1): 87–93.

BELDERSON, R. H., AND A. H. STRIDE. 1966. Tidal current fashioning of a basal bed. Mar. Geol. 4: 237–257.

BORTHWICK, I., AND M. B. COLLINS. 1976. Tidal movements around Mumbles Head and along the south Gower Coast. Final Report to Swansea City Council, Swansea, U.K. 31 p.

BOWKER, D. E., W. G. WHITEE, P. FLEISHER, T. A. GOSINK, W. J. HANNA, AND J. C. LUDWICK. 1975. An investigation of the waters of the Lower Chesapeake Bay area. 10th Int. Symp. Remote Sensing 1: 411–420.

BRITISH TRANSPORT DOCKS BOARD. 1970. Silt movement in the Humber Estuary. BTDB Res. Station Rep. No. R221, Southall, Midx., U.K. 8 p.

BROOKS, R. E. 1974. Suspended sediment and solute transport for rivers entering the Severn Estuary. Ph.D. thesis, Univ. Bristol, U.K.

BUNCLE, K. I. 1981. Calibration of LANDSAT multispectral imagery. Final year. B.Sc. dissertation, Dep. of Oceanography, Univ. College, Swansea, U.K. 67 p.

CHARNELL, R. L., AND G. A. MAUL. 1973. Oceanic observation of New York Bight by ERTS-1. Nature 242: 451–456.

COLLINS, M. B. 1981. Sediment yield studies of headwater catchments in Sussex, S. E. England. Earth Surface Processes and Landforms 6: 517–539.

COLLINS, M. B., G. FERENTINOS, AND F. T. BANNER. 1979. The hydrodynamics and sedimentology of a high (tidal and wave) energy embayment (Swansea Bay, northern Bristol Channel). Estuarine Coastal Mar. Sci. 8: 49–74.

COLLINS, M. B., C. B. PATTIARATCHI, F. T. BANNER, AND G. FERENTINOS. 1980. The supply of sand to Swansea Bay, p. 193–213. *In* M. B. Collins et al. [ed.] Industrialised embayments and their environmental problems: a case study of Swansea Bay, Pergamon Press, Oxford.

COOPER, L. H. N. 1967. The physical oceanography of the Celtic Sea. Oceanogr. Mar. Biol. Ann. Rev. 5: 99–110.

CULVER, S. J. 1980. Differential two-way sediment transport in the Bristol Channel and Severn Estuary, U.K. Mar. Geol. 34: M39–M43.

CULVER, S. J., AND F. T. BANNER. 1978. Foraminiferal assemblages as Flandrian palaeoenvironmental indicators. Palaeogeogr. Palaeoclim. Palaeoecol. 24: 53–72.

DAVIES, C. M. 1974. Variability of suspended sediment in rotatory currents, Swansea Bay. Mar. Geol. 16: M31–M38.

1980. Suspended sediment distributions in northern Swansea Bay, p. 289–302. *In* M. B. Collins et al. [ed.] Industrialised embayments and their environmental problems: a case study of Swansea Bay, Pergamon Press, Oxford.

DEFANT, A. 1951. Physical oceanography, Vol. I. Pergamon Press, Oxford, 729 p.

DIXON, G. 1980. The calibration of LANDSAT satellite photographs using ground truth data. B.Sc. dissertation, Dep. of Oceanography, Univ. College, Swansea, U.K. 60 p.

FARMER, G. H. 1979. The use of satellite imagery to measure suspended sediment concentration. Int. Rep., Dep. of Oceanography, Univ. College, Swansea, U.K. 22 p.

FERENTINOS, G., AND M. B. COLLINS. 1978. Sediment transport through the area south of eastern Gower, as related to the sediment budget of Swansea Bay. Final Rep. to IOS Taunton, Dep. of Oceanography, Univ. College, Swansea, U.K. 120 p.

1980. Effects of shoreline irregularities on a rectilinear tidal current and their significance in sedimentation processes. J. Sediment. Petrol. 50(4): 1081–1094.

GLYDON-JONES, C. 1976. Aspects of suspended sediment in Swansea Bay with particular reference to varying synoptic weather situations. B.Sc. dissertation, Dep. of Oceanography, Univ. College, Swansea, U.K. 106 p.

HALLIWELL, A. R., AND B. A. O'CONNOR. 1965. Flow and siltation measurements in the Mersey Estuary. J. Liverpool Eng. Soc.

11(3): 21–45.

HAMILTON, D., J. J. SOMMERVILLE, AND P. N. STANFORD. 1980. Bottom currents and shelf sediments, southwest of Britain. Sediment. Geol. 26: 115–138.

HAMILTON, E. I., P. G. WATSON, J. J. CLEARY, AND R. J. CLIFTON. 1979. The geochemistry of Recent sediments of the Bristol Channel – Severn Estuary system. Mar. Geol. 31: 139–182.

HAMILTON, J. 1973. The circulation of the Bristol Channel. Geophys. J. R. Astron. Soc. 32: 409–422.

HEATHERSHAW, A. D. 1981. Comparison of measured and predicted sediment transport rates in tidal currents. Mar. Geol. 42: 75–104.

HEATHERSHAW, A. D., M. W. L. BLACKLEY, AND P. J. HARDCASTLE. 1980. Wave direction estimates in coastal waters using radar. Coast. Eng. 3: 249–267.

H.M.S.O. 1978. Surface water: United Kingdom 1971–73. Dep. of the Environ., Water data unit. H.M.S.O. Lond., 192 p.

HUMPHREY, N. C., C. PATTINSON, AND J. H. STONER. 1980. Water quality studies in Swansea Bay, p. 409–437. *In* M. B. Collins et al. [ed.] Industrialised embayments and their environmental problems: a case study of Swansea Bay, Pergamon Press, Oxford.

I.M.E.R. 1974. Institute for Marine Environmental Research (N.E.R.C.) Rep. 1973–74. IMER, Plymouth, Devon, 71 p.

1975. Institute for Marine Environmental Research (N.E.R.C.) Rep. 1974–75. IMER, Plymouth, Devon, 85 p.

INGLIS, SIR C. C., AND F. H. ALLEN. 1957. The regimen of the Thames Estuary as affected by currents, salinities and river flow. Inst. Civ. Eng., Maritime Pap. 38, Maritime and waterways engineering division meeting 30th May, Preprint, 30 p.

JACKSON, W. H., AND D. R. NORMAN. 1980. Port Talbot — accretion and dredging in the harbour and entrance channel, p. 573–582. *In* M. B. Collins et al. [ed.] Industrialised embayments and their environmental problems: a case study of Swansea Bay, Pergamon Press, Oxford.

JOINT, I. R. 1980. Phytoplankton production in Swansea Bay, p. 469–479. *In* M. B. Collins et al. [ed.] Industrialised embayments and their environmental problems: a case study of Swansea Bay, Pergamon Press, Oxford.

KENYON, N. H., AND A. H. STRIDE. 1970. The tide-swept continental shelf sediment between the Shetland Isles and France. Sedimentology 14: 159–173.

KIRBY, R., AND W. R. PARKER. 1975. Sediment dynamics in the Severn Estuary: a background for studies of the effects of a barrage, p. 35–46. *In* L. T. Shaw [ed.] An environmental appraisal of the Severn Barrage, Univ. Bristol, U.K.

1982. A suspended sediment front in the Severn Estuary. Nature 295: 396–399.

LEE, A. 1960. Hydrographic observations in the Irish Sea, Jan.–March, 1953. M.A.F.F. Fish. Invest. Ser. II, Vol. XXIII(2), H.M.S.O. Lond.: 1–25.

MATTHEWS, C. L. 1975. A study of suspended sediment in the Upper Bristol Channel (Penarth Pier). B.Sc. dissertation, Dep. of Oceanography, Univ. College, Swansea, U.K. 101 p.

MOORE, N.H. 1975. Some aspects of the suspended sediment concentrations in Swansea Bay. B.Sc. dissertation, Dep. of Oceanography, Univ. College, Swansea, U.K. 47 p.

MORAN, A. D., AND M. B. COLLINS. 1980. Sediment transport in the vicinity of Knab Rock, western Swansea Bay. Final Rep. to Swansea City Council, Dep. of Oceanography, Univ. College, Swansea, U.K.

MUNDAY, J. C., T. T. ALFÖLDI, AND C. L. AMOS. 1979. Bay of Fundy verification of a system for multidate LANDSAT measurement of suspended sediment. Satellite Hydrol. Am. Wat. Res. Assoc. 622–640.

MURRAY, J. W., AND A. B. HAWKINS. 1976. Sediment transport in the Severn Estuary during the past 8000–9000 years. J. Geol. Soc. Lond. 132: 385–398.

MURRAY, L. A., M. G. NORTON, R. S. NOWRY, AND M. S. ROLFE. 1980. The field assessment of effects of dumping wastes at sea: 7. Sewage sludge and industrial waste disposal in the Bristol Channel. Fish. Res. Tech. Rep. 59, M.A.F.F., Lowestoft, 40 p.

OWEN, A. 1980. The tidal regime of the Bristol Channel: a numerical modelling approach. Geophys. J. Roy. Astr. Soc. 62: 59–75.

OWEN, A., AND N. S. HEAPS. 1979. Some recent model results for tidal barrages in the Bristol Channel, p. 85–92. *In* Severn et al. [ed.] Tidal power and estuary management, Scientechnica, Bristol, U.K.

OWENS, M. 1982. Discussion on Papers 18–20. *In* Severn Barrage, Thomas Telford, London, 213–214.

PARKER, W. R., AND R. KIRBY. 1981. The behaviour of cohesive sediment in the Inner Bristol Channel and Severn Estuary. IOS Rep. 117, Taunton, U.K. 54 p.

1982. Sources and transport patterns of sediment in the Inner Bristol Channel and Severn Estuary. Chapt. 18. *In* Severn Barrage, Thomas Telford, London, 181–194.

ROBINSON, A. H. W. 1973. The use of the sea bed drifter in coastal studies with particular reference to the Humber. Zeitsch. für Geomorph. 7: 1–23.

ROBINSON, I. S., AND D. SRISAENGTHONG. 1981. The use of LANDSAT MSS imagery to measure sediment movement in estuaries. Int. Rep., Dep. of Oceanography, Univ. Southampton, U.K. 74 p.

PINGREE, R. D., AND D. K. GRIFFITHS. 1979. Sand transport paths around the British Isles resulting from M_2 and M_4 tidal interactions. J. Mar. Biol. Assoc. U.K. 49: 497–513.

SEVERN, R. T., D. DINELEY, AND L. E. HAWKER [ed.]. 1979. Tidal power and estuary management, Scientechnica, Bristol, U.K. 296 p.

SHAW, T. L. 1975. Tides, currents and waves, p. 1–34. *In* T. L. Shaw [ed.] An environmental appraisal of the Severn Barrage, Univ. Bristol, U.K.

STRIDE, A. H. 1963. Current-swept sea floors near the southern half of Great Britain. Q. J. Geol. Soc. Lond. 119: 175–199.

TYLER, P. A., AND S. E. SHACKLEY. 1980. The benthic ecology of linear sandbanks: a modified *Spisula* sub-community, p. 539–551. *In* M. B. Collins et al. [ed.] Industrialised embayments and their environmental problems: a case study of Swansea Bay. Pergamon Press, Oxford.

UNCLES, R. J. 1982. Computed and observed residual currents in the Bristol Channel. Oceanol. Acta 5(1): 11–20.

WILLIAMSON, A. N., AND W. E. GRABAU. 1973. Sediment concentration mapping in tidal estuaries. 3rd Earth Res. Tech. Sat-1 Symp. 11: 1347–1386.

River-Dominated Suspended-Sediment Deposition in a New Mississippi Delta[1]

IVOR LL. VAN HEERDEN, JOHN T. WELLS, AND HARRY H. ROBERTS

Department of Marine Sciences and Coastal Studies Institute, Louisiana State University, Baton Rouge, LA 70803, USA

VAN HEERDEN, I. LL., J. T. WELLS, AND H. H. ROBERTS. 1983. River-dominated suspended-sediment deposition in a new Mississippi delta. Can. J. Fish. Aquat. Sci. 40(Suppl. 1): 60–71.

Progradation of Atchafalaya Delta, one of the most dynamic geological events in historical times within the Mississippi Delta complex, has produced a 230 km^2 new sediment body on the Louisiana coast of which 28 km^2 is subaerial. Sedimentation in Atchafalaya Bay was initiated in the early 1950s, and by 1973 a complex subaerial feature had evolved. Between 1972 and 1980 the area of Atchafalaya Delta dominated by coarse sedimentation increased. The greatest increase occurred along the delta's western flank as a result of introduction of dredge spoil from a navigation channel, as well as greater discharges in this area. Detailed field studies in the natural (spoil-free) eastern Atchafalaya Delta show that discharge and suspended load vary greatly between flood and nonflood conditions. Recognition of sedimentary environments, each characterized by sedimentary structures and grain size, indicates rates and modes of deposition. Processes of deposition in this fluvially dominated environment are characterized by rapid settling of suspended loads generally under waning flood conditions.

Key words: new Mississippi delta, Atchafalaya River, suspended sediment, river-dominated deposition

VAN HEERDEN, I. LL., J. T. WELLS, AND H. H. ROBERTS. 1983. River-dominated suspended-sediment deposition in a new Mississippi delta. Can. J. Fish. Aquat. Sci. 40(Suppl. 1): 60–71.

L'engraissement du delta d'Atchafalaya, un des événements géologiques les plus dynamiques de l'histoire dans le complexe du delta du Mississippi, a donné naissance à 230 km^2 de nouveau sédiment sur la côte de la Louisiane, dont 28 km^2 sont à l'air. La sédimentation dans la baie d'Atchafalaya a commencé au début des années 1950, et dès 1973 s'était développé un caractère subaérien complexe. Entre 1972 et 1980, la superficie du delta d'Atchafalaya, dominé par un sédiment grossier, a augmenté. La plus forte augmentation se produisit sur le flanc occidental du delta, par suite du déversement de déblais de dragage d'un chenal de navigation, ainsi que d'un plus grand débit dans cette région. Des études détaillées sur le terrain dans la partie est du delta d'Atchafalaya dans son état naturel (libre de déblais) démontre que le débit et la charge en suspension sont très différents dans des conditions de crue et de non-crue. L'identification d'environnements sédimentaires, caractérisé chacun par la structure du sédiment et la taille des particules, indique le taux et le mode de déposition. Les processus de déposition dans cet environnement à caractère surtout fluvial comportent une précipitation rapide de la matière en suspension ordinairement en périodes de décroît des crues.

Received January 12, 1982
Accepted August 13, 1982

Reçu le 12 janvier 1982
Accepté le 13 août 1982

THE development of two marine deltas in Atchafalaya Bay, Louisiana, provides the first opportunity to document, from inception, the evolution of new Mississippi delta lobes in a setting dominated by fine-grained sediments (Fig. 1). As a result of this unique opportunity, numerous studies have been conducted which provide a solid foundation for future research in Atchafalaya Bay (e.g. Shlemon 1972; Cratsley 1975; Rouse et al. 1978; Roberts et al. 1980; van Heerden 1980; van Heerden and Roberts 1980a, b; van Heerden et al. 1981).

Atchafalaya Bay is a broad (20 × 20 km), shallow (<2 m) complex with a submerged oyster-reef barrier forming the seaward margin (Fig. 1). The essentially fresh bay waters are mixed and unstratified (U.S. Fisheries and Wildlife Service

[1]This paper forms part of the Proceedings of the Dynamics of Turbid Coastal Environments Symposium convened at the Bedford Institute of Oceanography, Dartmouth, N.S., Canada, September 29–October 1, 1981.

Printed in Canada (J6776)
Imprimé au Canada (J6776)

FIG. 1. Regional setting, Atchafalaya Bay, Louisiana.

1976). This setting is in contrast to that of the modern Mississippi birdfoot delta, which has been spreading sediment in the form of a true marine delta on the continental shelf of Louisiana for nearly 800 yr.

The purpose of this paper is to discuss recent research that extends our present understanding of the processes of sedimentation in the extremely turbid Atchafalaya Bay by providing (1) details of discharge and sediment distribution through the eastern delta area and (2) interpretation of sedimentary processes and response features associated with major deltaic environments in the eastern half of the delta.

Methodology

The data presented in this paper were compiled from:

1) Interpretation of unpublished monthly discharge data collected since May, 1979, by the U.S. Geological Survey, Baton Rouge office, in seven major distributaries of the Atchafalaya Delta.

2) Collection of 250 bottom grab samples between June and September 1980. Sample sites were equally spaced throughout the bay. Grain size was determined by sieve and hydrometer analysis. The data were compared to a map of median grain size prepared by Cratsley (1975).

3) Continuous mid-depth current measurements of an average span of 1 mo using Bendix Corporation Q15 and Endeco 174 meters at 12 locations in Atchafalaya Bay. Preliminary results of the measurements taken between January 1979 and July 1981 are used in this paper. In addition, two distributary channels were selected for channel cross section discharge and suspended load determinations during May (high water) and October (low water) of 1980. Total suspended load volume was calculated using a mass to volume conversion suggested by Wells and Roberts (1981).

4) Collection of 55 shallow sediment cores from Atchafalaya Delta. The cores were taken in both subaqueous (using scuba) and subaerial environments to depths of 7 m. Each core was split parallel to the inferred predominant direction of flow

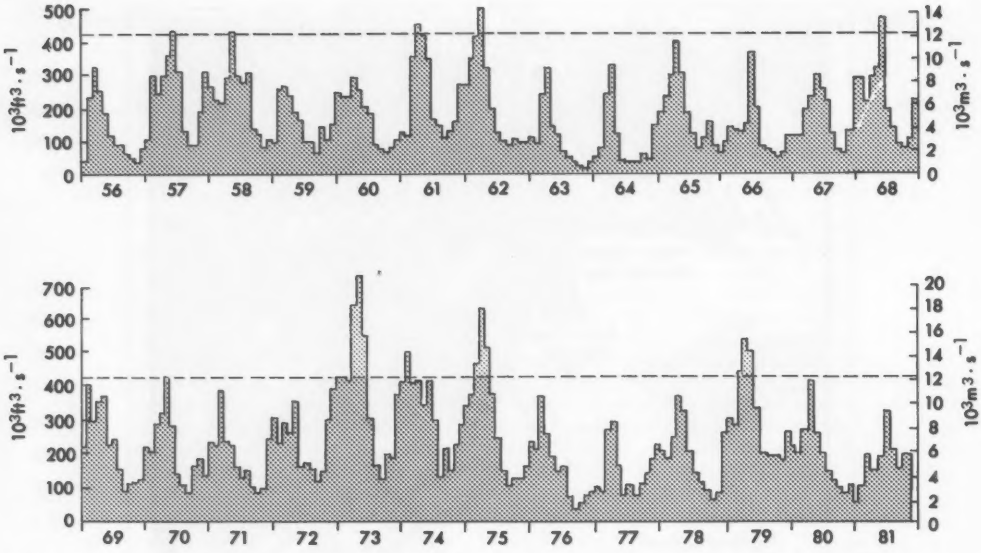

FIG. 2. Average monthly discharge of the Atchafalaya River. Modified from van Heerden and Roberts (1980b). The dotted line represents average annual peak flow.

and then examined by X-ray radiography using the techniques described by Roberts et al. (1976).

Hydrologic Regime

Since the early 1500s, Mississippi River flow through the Atchafalaya River system has been sporadic and periodically has been aided by dredging (Shlemon 1975). By the mid-1900s, a natural channel had become established, and volume of flow to Atchafalaya River began to increase steadily. Fisk (1952) predicted abandonment of the main Mississippi River in favor of the Atchafalaya River by 1975. A control structure that was authorized by an act of Congress was completed at Old River, north of Baton Rouge, in 1963. Diversion of Mississippi River flow was limited by the control structure to 30% of the 1950 combined Mississippi River and Red River flow regimes.

Annual Atchafalaya River flow averaged from 1938 to 1972 at Simmesport, near the diversion point in the upper Atchafalaya basin, was 5 126 $m^3 \cdot s^{-1}$. Highest discharge flow occurred between January and May, with average annual peak flow of 11 326 $m^3 \cdot s^{-1}$. Approximately 70% of the flow at Simmesport now passes through the lower Atchafalaya River outlet into eastern Atchafalaya Bay, whereas the remainder passes into the western part of the bay via Wax Lake Outlet (U.S. Army Corps of Engineers 1974) (Fig. 1).

A comparison of the relative magnitudes of yearly Atchafalaya River floods for the past 25 yr (U.S. Army Corps of Engineers 1974, plus unpublished data) is given in Fig. 2. From 1956 to 1972 peak flood discharge was close to the long-term average. However, in the flood of 1973 the average annual peak flow was exceeded for 6 mo of the year (Fig. 2). This pattern was repeated during the following 2 yr, 1974 and 1975. The years 1976 through 1978 were again average with respect to Atchafalaya River flood discharges. Another major flood in 1979 made the decade 1970–80 one of anomalous high water and sediment discharge. Discharge during 1980, the period of data collection for this study, can be considered average.

The percentage of flow from the Lower Atchafalaya River that enters the eastern half of the delta (Fig. 3) varies with overall river flow. Monthly discharge measurements between May 1979 and May 1981 (U.S. Geological Survey unpublished data) indicated that an average of 27% of the river flow entered East Pass (Fig. 3). During low flow months (June–November) East Pass may carry more than 36% of the Lower Atchafalaya River flow, while only about 23% is carried during high flow months (December–May). A greater percentage of the discharge enters East Pass during low flow periods as a result of either diminished effects of flood tides in the eastern half of the bay during high discharge or topographic/bathymetric controls exerted during low flow conditions.

Sediment Flux

Sediment reaching Atchafalaya Bay has changed from a dominance of silt and clay to silt and fine sand since 1960. Sediment coarser than fine sand is generally not carried down the Atchafalaya River as the control structure at Old River prevents a proportional share of Mississippi bedload from entering the system. However, scouring and suspended load transport of sand-sized bed material in the lower basin and lower Atchafalaya River occurs during intense pulses of high water (Roberts et al. 1980).

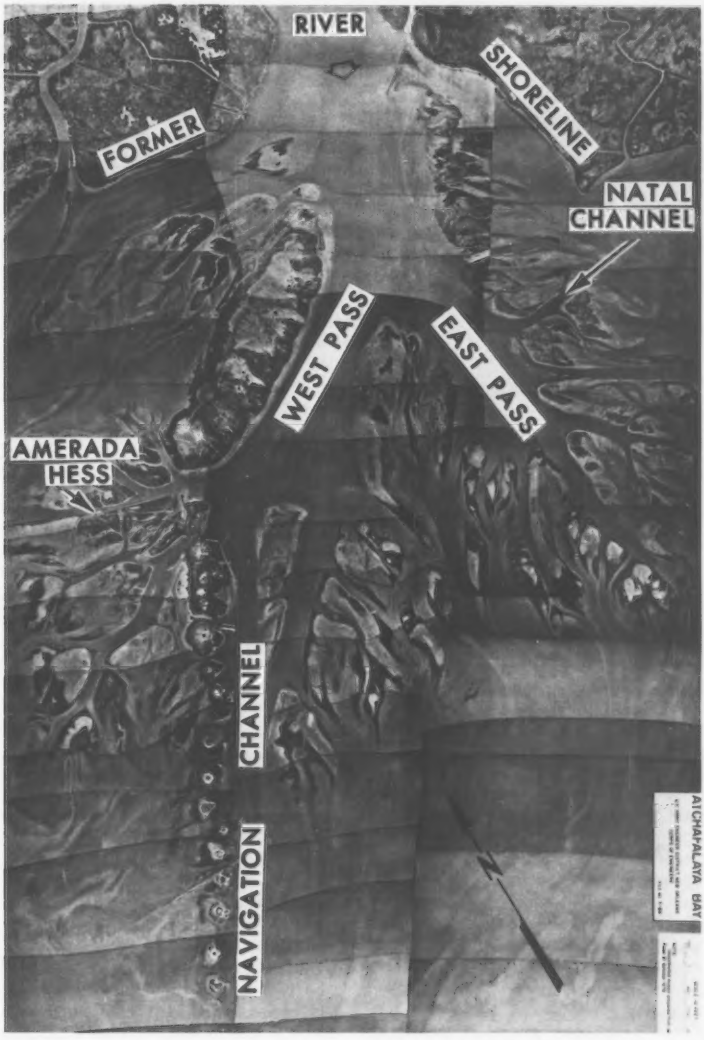

FIG. 3. Aerial photomosaic of Atchafalaya Delta, October 21, 1976. Water level MSL — 0.22 m.

Roberts et al. (1980) show that between 1965 and 1971 the annual average sediment load was 42.6×10^6 t. During the high water years of 1973, 1974, and 1975, the average annual load nearly doubled (88.9×10^6 t) reflecting both scour in the lower reaches of the Atchafalaya River system and effects of above average river discharge.

Before the early 1950s, most of the sediment carried by Atchafalaya River was deposited in river-basin lakes and swamps. Shlemon (1975) showed the development (between 1952 and 1972) of a subaqueous delta-shaped lobe of sediments emanating from the Lower Atchafalaya River mouth. Initial subaerial exposures appeared in 1972. These small shoals were composed of spoil from the dredging of a navigation channel. By 1973, however, well-developed natural subaerial lobes were apparent in Atchafalaya Bay. The unusual hydrologic conditions during the first 3 yr of subaerial exposure played an important role in the rapid development of this latest dynamic phase of Atchafalaya Delta growth.

Through analysis of LANDSAT imagery, Rouse et al. (1978) showed that by early 1976, 32.5 km^2 of new land

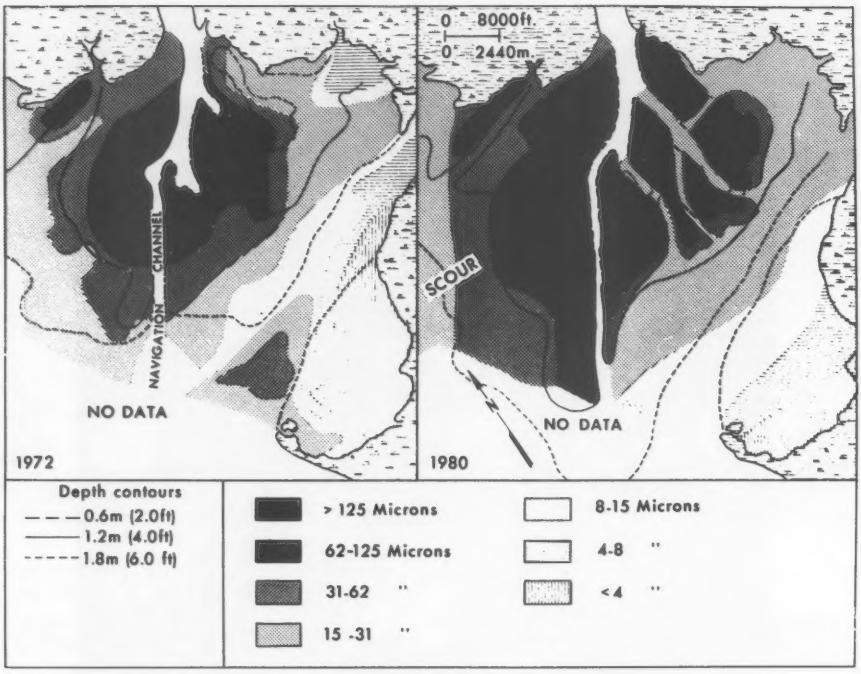

FIG. 4. Median grain size, Atchafalaya Bay, 1972–80.

TABLE 1. Average monthly discharge and suspended sediment characteristics.

Date	Mouth ($m^3 \cdot s^{-1}$)	East pass ($m^3 \cdot s^{-1}$)	Delta channel ($m^3 \cdot s^{-1}$)	Suspended load ($m^3 \cdot s^{-1}$)	Mean size (μm)	Concentration ($mg \cdot L^{-1}$)	Location
May 9, 1979	8300	1937	—	—	—	—	
May 7, 1980	5409	1294	107.40	0.057	8.69	224	Natal Channel
			11.63	0.006	8.27	220	S. Natal Channel
Oct. 23, 1980	1007	300	38.00	0.005	5.79	52	Natal Channel
			4.64	0.0007	6.40	59	S. Natal Channel

NOTE: All data averaged over one rising and one falling tide.

(above mean low water) had formed, corresponding to an average growth rate of 6.5 $km^2 \cdot yr^{-1}$. By using aerial photographs of the eastern half of the delta, van Heerden (1980) confirmed the dramatic growth rate in the high flood years of 1973, 1974, and 1975 and the major flood in 1979. Average-sized floods were found to produce at most a moderate growth rate (van Heerden 1980).

Between 1972 and 1980, median grain size of sediments in the eastern half of Atchafalaya Bay increased (Fig. 4). These changes reflect delta progradation as well as the increased input of sand-sized particles, particularly during the major floods of the 1970s. The greatest seaward migration of coarse facies was west of the navigation channel because of its greater discharge capacity and redistribution of dredge spoil. The presence in 1980 of sediments with median diameters greater than 125 μm indicates gradual coarsening with bar aggradation as the delta progrades.

Discharge and Suspended Load Measurements

Data collected regarding discharge and suspended load give an indication of the energy and sediments available to the delta system. Two different-sized but connected channels were monitored during periods of high and low river discharge (Fig. 5). During high flows in May 1980, 57×10^{-3} $m^3 \cdot s^{-1}$ of suspended sediment was passing through cross section 1 (Table 1). Of this, only 6×10^{-3} $m^3 \cdot s^{-1}$ was entering cross section 2, which opens into the back

bar environment. Associated peak flows were on the order of 120 $cm \cdot s^{-1}$.

During the major flood in 1979, peak velocities were greater than 180 $cm \cdot s^{-1}$. Unfortunately, suspended load data were unavailable for this period, but the assumption can be made that the suspended load would have been higher and coarser grained.

During high flows, continuous discharge measurements at cross section 1 revealed minor velocity fluctuations, the peaks of which were correlated with rising tide conditions (Fig. 6). During low flow periods, discharges varied considerably in the distributary channels. Overall velocities were lower and the large velocity fluctuations had a positive relationship to tidal conditions (Fig. 6). In October 1980, mean sediment discharge through cross section 1 in Natal Channel (Table 1) was 5×10^{-3} $m^3 \cdot s^{-1}$. This value is one-tenth the sediment discharge during May of the same year. Suspended load concentrations were also lower and mean grain size smaller (Table 1). These data indicate that the fluvial regime varies considerably within a single hydrologic year.

Depositional Environments

Continuous discharge and suspended sediment data were not available for the eastern delta during the major flood in 1979, when aggradation and progradation of sedimentary environments were more marked than in 1980 or 1981. However, sediment cores taken in conjunction with topographical surveys revealed thicknesses of depositional units, grain size, and primary sedimentary structures associated with major and minor flood deposits. For the purpose of discussion, the environments of deposition have been divided into two groups on the basis of whether the environment is predominantly submerged (subaqueous) or exposed (subaerial).

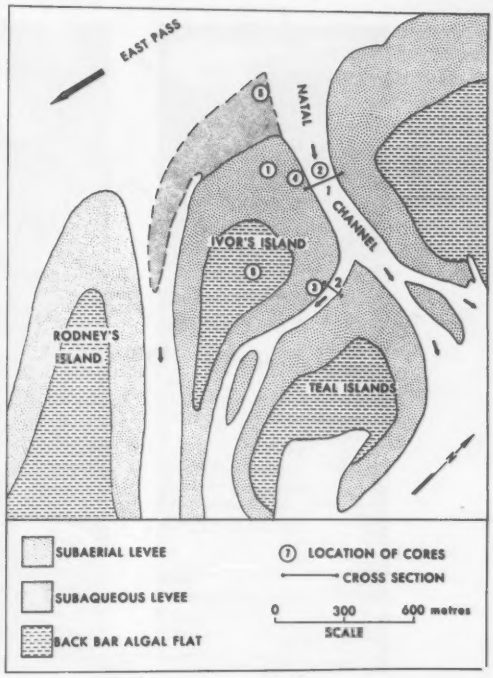

FIG. 5. Location of discharge cross sections and sediment cores, eastern delta.

SUBAQUEOUS DEPOSITIONAL ENVIRONMENTS

Prodelta — Figure 7a is representative of prodelta sediments taken from a depth of 2.5 m below mean sea level (MSL). The prodelta sequence was made up of cycles (2−10 cm thick) of parallel laminated silty clays and clays that were separated by thin (2−3 mm) silt lenses. Some of the silt lenses contained clam shell fragments and were the origin of small polychaete worm burrows. The prodelta facies consisted of a blanket of clays deposited from suspension, having high lateral continuity and low lithologic variation (Table 2). Because deposition was almost entirely from suspension, parallel laminations were by far the most common primary structure. However, the thin silt lenses were deposited in response to basinal reworking processes during periods of low fluvial input.

Distributary-mouth bar — In the eastern half of Atchafalaya Delta, the prodelta sediments coarsened upward into sediments of the distributary-mouth bar. Although the distributary-mouth bar deposits also coarsened upward, they consisted of upward-fining cycles of cross-laminated and parallel-laminated clayey silts which passed into parallel-laminated silty clays (Fig. 7b). The distributary-bar cycles varied in thickness from 5 to 8 cm and represented flood-related depositional events. Upward fining of each cycle was a result of suspended-sediment deposition under waning flood conditions. Some upper horizons of distributary-mouth bar deposits contained up to 10-cm-thick layers of parallel-laminated silts and clays with numerous erosional surfaces. These deposits resemble lenticular bedding (Reineck and Wunderlick 1968) and indicate tidal and storm-related reworking of the higher elevated surfaces of distributary-mouth bars during periods of low river discharge.

Channel fill — Distributary channels in the eastern delta are undergoing reduction in cross-sectional area by aggradation of channel flanks and general shallowing of the channel (van Heerden 1980). Channel-fill material (Fig. 7c) consisted of parallel-laminated silts and clays (Table 2). Erosional surfaces were present, as were polychaete worm burrows. Occasionally, thin lenses of cross-laminated silts that represented starved ripples were noted. Deposition of fine-grained suspended sediment in Natal Channel occurs during periods of low water discharge. During low-flow months, the channel bottom could be covered with a maximum of 10 cm of fluid mud (water content up to 80%). By the onset of the following flood, this material, by means of dewatering, contained only 50% water and consequently must have undergone a dramatic increase in cohesive strength (Postma 1968, Fig. 1). This

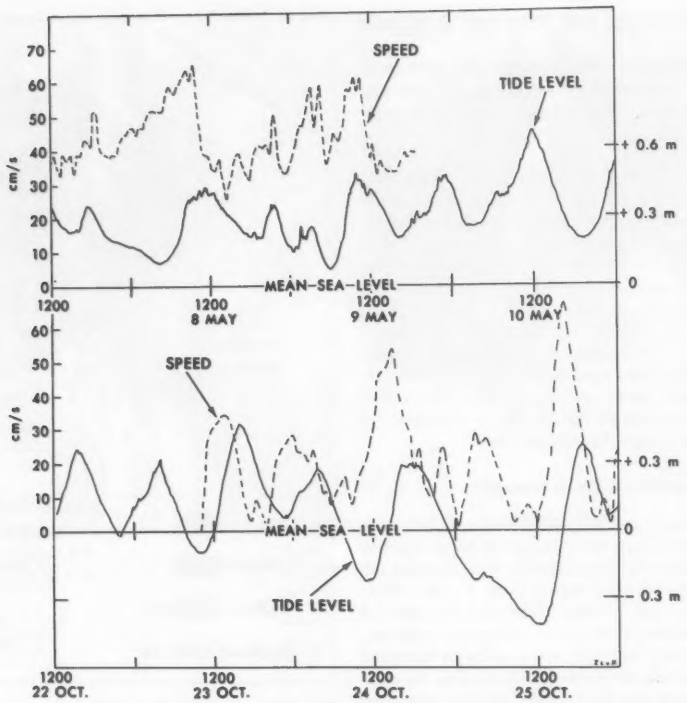

FIG. 6. Continuous mid-depth flow velocity and tidal curves for Natal Channel during high (May) and low (October) river stage, 1980. See Fig. 5 for location of current meter.

strength, improved by algal growth, resulted in greater resistance to erosion during the following flood. During floods, the extreme turbulence prohibited any deposition in confined channels except on the flanks, where friction effects became important.

SUBAERIAL DEPOSITIONAL ENVIRONMENTS

Levee — Subaqueous and subaerial levee deposits were similar and gradational. For the purpose of discussion they were considered as one environment. Levee deposits had a number of forms, depending on the amount of flood-related sedimentation, which was dependent on elevation and location.

High sedimentation rate deposits (>0.3 m/annual flood) — Figure 8a shows a channel flank core taken in the eastern delta, where 1.5 m of deposition had occurred in the 1979 flood (van Heerden 1980, Fig. 2a). These sediments were characterized by trough and climbing ripple cross laminations, weak to strong festoon-shaped cross-bed sets, and tangential to concave foreset laminae. Such features indicated migration of undulatory, linguoid, and climbing ripples. Deposition from predominantly suspended loads occurred under moderately high flow strengths with high bed shear stress (Reineck and Singh 1973; Jopling 1965).

Medium sedimentation rate deposits (0.15 to 0.30 m/annual flood) — Levee material of this type (Fig. 8b) commonly exhibited simple cross laminations and occasional trough cross laminations. The former bedform results from the migration of straight-crested, small current ripples at low flow strengths, just capable of initiating and maintaining ripple migration (Reineck and Singh 1973; Harms et al. 1975). Trough cross laminations are probably formed by undulatory small ripples, which represent a transition form between low-energy, straight-crested ripples and higher energy, linguoid, small ripples (Reineck and Singh 1973). A combination of these laminations and low-angle tangential foreset laminae indicates deposition of suspended and bedload material at low flow strengths and medium bed shear stresses (Jopling 1965).

Low sedimentation rate deposits (<0.15 m/annual flood) — Levees deposited under low sedimentation rates displayed features indicating the dominance of local basinal process effects, unlike the previously mentioned levee subenvironments. Because floods of 1976, 1977, and 1978 were well below normal (van Heerden and Roberts 1980b), sedimentation rate was low and basinal processes were dominant in the

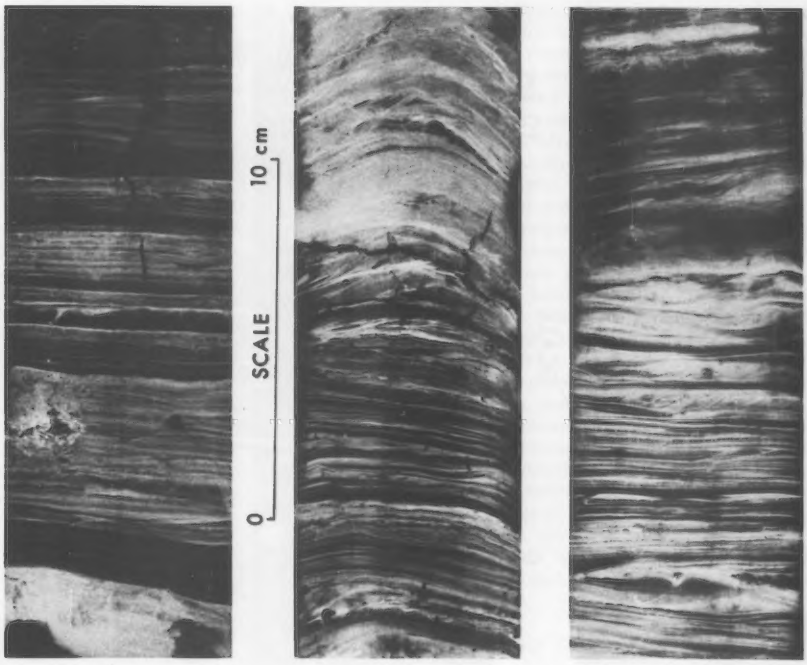

FIG. 7. X-ray radiographs of (a) prodelta (core 1), (b) distributary-mouth bar (core 1), and (c) channel fill (core 2) deposits.

TABLE 2. Characteristics of sedimentary environments.

Core no.	Environment	Primary sedimentary structures	Mean grain size (μm)	Deposition record
1	Prodelta	Parallel laminations	10	Settling suspended river sediments.
2	Distributary-mouth bar	Simple and trough cross-laminated silts, parallel laminated clays	30	Deposited fluvial suspended sediments — some tidal reworking.
3	Channel fill	Parallel laminated clays	20	Deposited fluvial suspended sediments at low water. Scour during floods.
4	High deposition rate levee	Trough and climbing ripple laminated silts. Festoon shaped cross-bed units. Foreset laminae concave	65	Rapid deposition (>0.3 m/annual flood) from mainly suspended loads. High flow strengths.
5	Medium deposition rate levee	Simple and trough cross-laminated silts, weakly festoon shaped cross-bed units. Tangential foreset laminae	50	Fairly rapid deposition (0.15−0.3 m/flood). Suspended and bedload material. Medium flow strengths.
6	Low deposition rate levee	Parallel-laminated silts and clays. Algal mats	34	Slow deposition of suspended load. Low flow strength. Tidal reworking.
7	Back-bar algal flat	Parallel-laminated silts and clays. Some cross-laminated silts. Algal mats	25	Slow deposition of suspended load. Low flow strengths. Tidal reworking.

area of the delta where the core was taken (Fig. 8c). Response features in this subaqueous levee environment were parallel laminations with minor scour surfaces. Parallel laminations suggested tidal reworking as well as deposition of

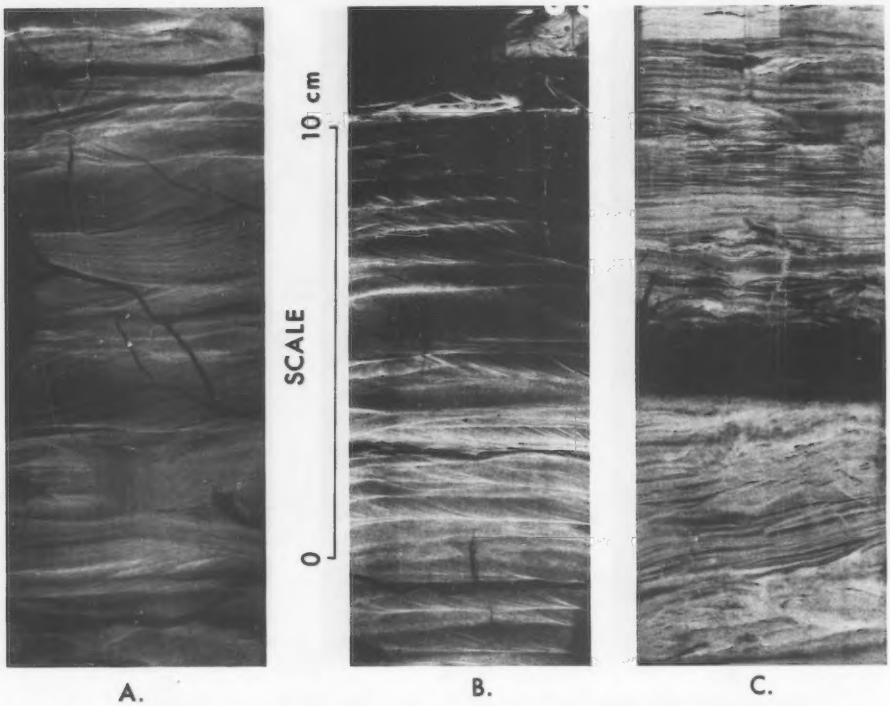

FIG. 8. Radiographs of levee deposits. (a) High sedimentation rate — core 3; (b) medium sedimentation rate — core 4; (c) low sedimentation rate — core 5.

fine-grained sediment brought in by weak tidal currents. Organic-rich layers indicated very low sedimentation rates when algal mats would have become established.

Back-bar algal flats — This environment occurred between subaerial levees and usually forms the central parts of lobes (Fig. 5). Generally the sediments were highly organic and consisted of parallel laminated silts and clays interbedded with thin reduced organic layers (Fig. 9a). Sediments entered these environments by four pathways: levee overtopping, tidal pumping, flood feeder channels, and winter levee erosion. Parallel laminated silts were deposited through levee overtopping, which is an important mechanism during river floods. Weak tidal currents deposited thin clay veneers during periods of low river water.

Coarse sediments may also enter the algal flat via feeder channels or through the erosion and redistribution of levee material during storms. Small feeder channels activated during floods resulted in the formation of thin cross-laminated algal flat sand lobes (Fig. 9b). These lobes occurred in the vicinity of feeder channel mouths and covered small areas. Algal flat sand sheets were formed when a veneer of eroded levee material was deposited over the algal flat as a result of levee erosion and overtopping during the passage of cold fronts (van Heerden 1980). Although these sheets covered large areas of the backbar, they were only a few centimetres thick (van Heerden et al. 1981).

Sedimentation Model

As the fluvial effluent passes from the confined distributary channel to the shallower unconfined bay, it rapidly experiences a reduction in velocity. Associated with the frictional deceleration of the flow is a reduction in turbulence and the coarsest part of the suspended load is deposited, initiating a mid-channel bar (Fig. 10). Once initiated, shoaling bayward of the mouth causes an increase in the friction-induced deceleration and effluent spreading, which in turn increases the shoaling rate (Bates 1953; Wright 1977).

The overall effect of these bar-forming processes is channel bifurcation into two distributaries (Fig. 10). Because frictional resistance per unit volume of flow increases with decreasing channel size, other factors being equal, the channel appears to lose efficiency upon bifurcating (Axelsson 1967; Welder 1959). This phenomenon is interesting, as it appears that the channel bifurcates because river mouth dynamics are controlled by bathymetry and there is a resulting loss in efficiency. Velocities also decrease away from the center line of

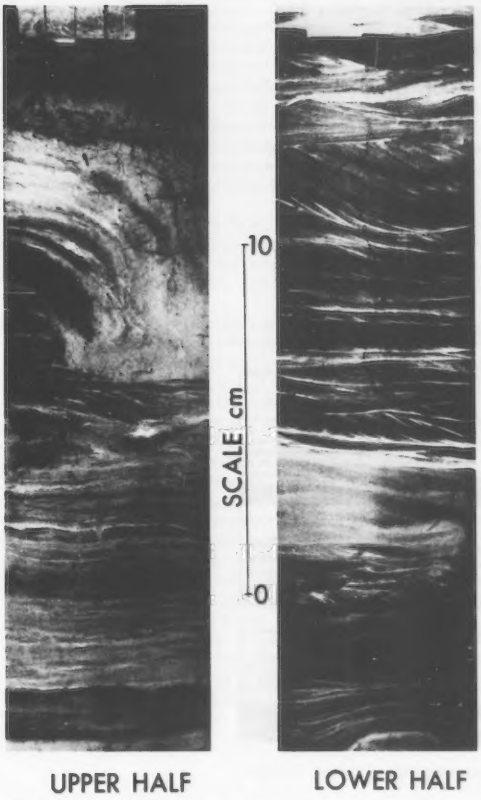

FIG. 9. X-ray radiograph of back-bar algal flat deposits (core 6).

the divergent current field. Deposition occurs at the outer edges of the effluent plume, giving rise to subaqueous levees. The levee ridges flare away from the mouth, reflecting the divergent current field that results from the abrupt transition to unconfined flow.

Each sedimentary environment associated with a bifurcating distributary channel has characteristics that reflect deposition during both high and low fluvial discharges.

HIGH-DISCHARGE DEPOSITION

During major floods sediment load (mainly suspended) is large. Flow is strongly turbulent (Reynolds number >7000) and suspended-load concentrations are nearly vertically homogeneous throughout the channel. The high turbulence prevents sedimentation along the channel bottom. Along channel flanks and tops of levees, where frictional forces are most important, current velocities and turbulence are lower. Here the coarsest part of the suspended load is deposited, resulting in the various cross-laminated bedforms displayed by levees (Fig. 8). Rate of deposition is highest during major floods and on the inner flanks of bends in distributary channels. Primary sedimentary structures reflect the deposition rate. Because of the turbulent nature of the flow, sediment is continuously available to the levee environment; thus, as portions of the load are deposited, so turbulence resupplies sediment.

During high water, levee overtopping is important in building the backbar algal flat. Here turbulence and current velocities are generally low, a phenomenon reflected by the parallel-laminated primary sedimentary structures. Occasionally, small channels feed more turbulent waters into the algal flat, creating algal flat sand lobes characterized by cross-laminated deposits.

The maximum grain size of transported sediments decreases as the flood wanes. The deposition cycles displayed by distributary-mouth bars reflect this waning phenomenon. During the peak flow the areas bayward of confined distributary channels are the sites of coarse sediment deposition because of frictional reduction in flow velocity. As flood levels fall, the grain size of available sediments decreases, and net accumulation after a flood is a single upward-fining cycle. Parts of the suspended load that bypass the distributary-mouth bar environment are deposited in the prodelta environment. Here sedimentation results from settling of suspended sediments through salt flocculation and/or the aggradation effects of large numbers of benthic filter feeders. However, a large portion of the suspended load moves entirely out of the bay and is then subjected to marine processes (Wells and Roberts 1981).

LOW-DISCHARGE DEPOSITION

Sedimentation rates are slow when fluvial regime is low. During these periods basinal processes (tides and storms) influence the form of the primary sedimentary structures. In shallow areas tidally induced reworking or sedimentation generally results in the formation of parallel-laminated deposits. Storms, especially during the passage of winter cold fronts, rework the outer exposed parts of interdistributary lobes and are responsible for redistributing originally flood-derived sediments.

Deposition in distributary channels occurs during low flow periods. Fluid muds deposited in the channels dewater and may attain enough cohesive strength to resist the following high river discharge velocities.

Conclusions

Progradation of the Atchafalaya Delta has produced a 230 km^2 sediment body on the Louisiana coast. Similar types of "bayhead deltas" are present in lakes (e.g. Atchafalaya Basin) and elsewhere along the northern coast of the Gulf of Mexico. These features are thus presently far more common although smaller, than the Mississippi Birdfoot delta.

The Atchafalaya Delta is evolving in such a manner that the environments of deposition are similar to those described for subdeltas of the modern Mississippi River and other shallow water deltas. Presently the mass and areal extent of the Atchafalaya delta are comparable to that of the Mississippi River's Baptiste Collette subdelta (Roberts et al. 1980). Deltas of the Colorado, Trinity, and Guadalupe rivers of

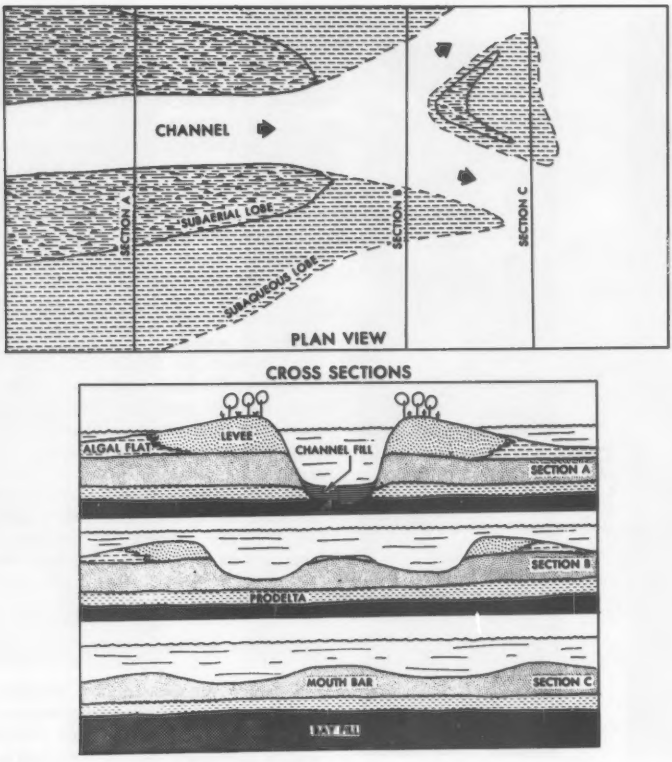

FIG. 10. Plan view and stratigraphic facies relationships for a channel bifurcation.

eastern Texas, which are building into shallow bays behind barrier islands, are somewhat analogous to the Atchafalaya setting, with its seaward oyster reef barrier. A study by Donaldson et al. (1970) of the depositional environments and sediment characteristics of the Guadalupe Delta show a close resemblance to those of the Atchafalaya Delta (Roberts et al. 1980).

Research in the extremely turbid Atchafalaya has resulted in the following conclusions.

1) Since initiation of the subaerial phase (1972) coarse sedimentation has spread throughout Atchafalaya Bay, forming a classical coarsening-upward sequence of prodelta clays through distributary-mouth bar deposits. Higher rates of deposition are occurring on the west side of the delta as a result of redistribution of dredge spoil and higher discharges associated with the dredged navigation channel.

2) During high river discharge, tidal currents do not greatly affect flow velocities in the eastern delta. However, the opposite holds true during periods of low river flow. Suspended-sediment concentration and grain size are independent of water depth, but both increase during floods.

3) The coarsest fraction of the sediment load (predominantly suspended material) is deposited on channel flanks and distributary-mouth bars. The finer parts of the load may end up as channel fill, algal flat material, or prodelta deposits, or may bypass the system completely. Sedimentary environments may display two suites of primary sedimentary structures, one that correlates with high fluvial regime, the other, with low fluvial regimes.

4) Deposition is river dominated. Sedimentation occurs from predominantly suspended loads under waning but fluctuating flood conditions. The Atchafalaya Delta should continue to prograde and will eventually cover most of Atchafalaya Bay. In contrast to the modern Mississippi Delta, the Atchafalaya should prograde more rapidly and form thinner sand bodies. The ultimate rates of growth and geometry depend on the degree of man's intervention in the delta-building process.

Acknowledgments

This research was supported by the Army Corps of Engineers, Contract No. DACW 29-77-C-0163, and the Coastal Sciences Program, Office of Naval Research, Arlington, VA 22217. Part of the research was also supported by the Louisiana Sea Grant Program, a part of the National Sea Grant Program, maintained by the National Oceanic and Atmospheric Administration, U.S. Department of Commerce.

AXELSSON, V. 1967. The Laitaure Delta, a study of deltaic morphology and processes. Geografiska Annaler 49: 3–27.

BATES, C. C. 1953. Rational theory of delta formation. Bull. Am. Assoc. Petrol. Geol. 37: 2119–2161.

CRATSLEY, D. W. 1975. Recent deltaic sedimentation, Atchafalaya Bay, Louisiana. M.S. thesis, Dep. of Marine Sciences, Louisiana State Univ., Baton Rouge, LA. 142 p.

FISK, H. N. 1952. Geological investigation of the Atchafalaya Basin and the problem of Mississippi River diversion. U.S. Army Corps of Engineers, Mississippi River Commission, Vicksburg, MS. 1: 145 p.

HARMS, J. C., J. B. SOUTHARD, D. R. SPEARING, AND R. G. WALKER. 1975. Depositional environments as determined from primary sedimentary structures and stratification sequences. Lecture Notes, Soc. Econ. Paleon. and Mineral. Short Course No. 2, Dallas, TX. 161 p.

JOPLING, W. A. 1965. Hydraulic factors and the shape of laminae. J. Sediment. Petrol. 35: 777–791.

POSTMA, H. 1967. Sediment transport and sedimentation in the estuarine environment, p. 158–179. *In* G. H. Lauff et al. [ed.] Estuaries. Am. Assoc. Adv. Sci. Pub. 83: 757 p.

REINECK, H. E., AND I. B. SINGH. 1973. Depositional sedimentary environments. Springer-Verlag, New York, NY. 439 p.

REINECK, H. E., AND F. WUNDERLICK. 1968. Classification and origin of flaser and lenticular bedding. Sedimentology 11: 99–104.

ROBERTS, H. H., R. D. ADAMS, AND R. H. W. CUNNINGHAM. 1980. Evolution of the sand-dominant subaerial phase, Atchafalaya Delta, Louisiana. Bull. Am. Assoc. Petrol. Geol. 64: 264–279.

ROBERTS, H. H., D. W. CRATSLEY, AND T. WHELAN, III. 1976. Stability of Mississippi Delta sediments as evaluated by analysis of structural features in sediment borings. 8th Offshore Tech. Conf., Houston, TX. p. 9–28.

ROUSE, L. J., H. H. ROBERTS, AND R. H. W. CUNNINGHAM. 1978. Satellite observations of the subaerial growth of the Atchafalaya Delta, Louisiana. Geology 6: 405–408.

SHLEMON, R. H. 1975. Subaqueous delta formation — Atchafalaya Bay, Louisiana, p. 209–221. *In* M. L. Broussard [ed.] Deltas. Houston Geol. Soc., Houston, TX.

SHLEMON, R. J. 1972. Development of the Atchafalaya Delta: hydrologic and geologic studies of coastal Louisiana. Rept. No. 8, Center for Wetland Resources, Louisiana State Univ. Baton Rouge, LA. 51 p.

U.S. ARMY CORPS OF ENGINEERS. 1974. Preliminary draft environmental impact statement, Atchafalaya Basin floodway. New Orleans, LA.

U.S. FISHERIES AND WILDLIFE SERVICE. 1976. A progress report — fish, wildlife and related resources, Atchafalaya Rim basin, Louisiana. U.S. Dep. of Interior. 347 p.

VAN HEERDEN, I. LL. 1980. Sedimentary responses during flood and non-flood conditions, new Atchafalaya Delta, Louisiana. Master's thesis, Dep. of Marine Sciences, Louisiana State Univ., Baton Rouge, LA. 76 p.

VAN HEERDEN, I. LL., AND H. H. ROBERTS. 1980a. The Atchafalaya Delta: rapid progradation along a traditionally retreating coast (south–central Louisiana). Zeit. Geomorph. N.F. 34: 188–201.

1980b. The Atchafalaya Delta — Louisiana's new prograding coast. Trans. Gulf Coast Assoc. Geol. Soc. 30: 497–506.

VAN HEERDEN, I. LL., J. T. WELLS, AND H. H. ROBERTS. 1981. Evolution and morphology of sedimentary environments, Atchafalaya Delta, Louisiana. Trans. Gulf Coast Assoc. Geol. Soc. 31: 399–408.

WELDER, F. A. 1959. Processes of deltaic sedimentation in the Lower Mississippi River. Coastal Studies Inst., Louisiana State Univ. Tech. Rep. 12: 90 p.

WELLS, J. T., AND H. H. ROBERTS. 1981. Fluid mud dynamics and shoreline stabilization. Proc., 17th Conf. Coastal Engr., Sydney, Australia: 1382–1401.

WRIGHT, L. D. 1977. Sediment transport and deposition at river mouths: a synthesis. Bull. Geol. Soc. Am. 88: 857–868.

Transfer of Water and Sediment from the Yangtze River to the East China Sea, June 1980[1,2]

YANG ZUO-SHENG

Shandong College of Oceanography, Qingdao, China

JOHN D. MILLIMAN AND MICHAEL G. FITZGERALD[3]

Woods Hole Oceanographic Institution, Woods Hole, MA 02543, USA

YANG, Z.-S., J. D. MILLIMAN, AND M. G. FITZGERALD. 1983. Transfer of water and sediment from the Yangtze River to the East China Sea, June 1980. Can. J. Fish. Aquat. Sci. 40(Suppl. 1): 72–82.

The Yangtze River, fourth largest in the world in terms of sediment discharge, contributes about 500×10^6 t annually to the East China Sea. A disproportionate part of the load is carried after peak summer discharge, presumably the result of draining the rice fields. During a week-long study of the estuary, greatest water discharge was observed in the North Passage. Suspended sediment concentrations were highest in the South Channel of the South Passage, although in contrast to the North Passage little of the suspended sediment was coarse. The high sediment concentrations in the South Channel appear to be the result of oscillatory (net transport upstream) movement of material, in contrast to the marked seaward transport measured in the North Passage.

Key words: Yangtze River, sedimentation, discharge, transport, estuary

YANG, Z.-S., J. D. MILLIMAN, AND M. G. FITZGERALD. 1983. Transfer of water and sediment from the Yangtze River to the East China Sea, June 1980. Can. J. Fish. Aquat. Sci. 40(Suppl. 1): 72–82.

Le fleuve Yang-Tseu, le quatrième en importance dans le monde en terme de transport de sédiment, contribue environ 500×10^6 t annuellement à la mer de Chine orientale. Une partie disproportionnée de la charge est transportée après le maximum estival de débit, résultant probablement du drainage des rizières. Au cours d'une étude d'une semaine de l'estuaire, le débit d'eau le plus important a été observé dans le passage Nord. Les concentrations de sédiment en suspension étaient les plus élevées dans le chenal Sud du passage Sud, bien que, contrairement à ce que l'on a observé dans le passage Nord, il y avait très peu de particules grossières en suspension. Les hautes concentrations de sédiment dans le chenal Sud semblent résulter du mouvement oscillatoire (transport net vers l'amont) du matériel, contrairement au transport nettement vers la mer observé dans le passage Nord.

Received October 14, 1981
Accepted August 19, 1982

Reçu le 14 octobre 1981
Accepté le 19 août 1982

IN terms of sediment discharge, the large rivers of the world drain Asia and, to a lesser extent, South America (Table 1). Combined, the rivers of southern and eastern Asia and neighboring oceanic islands contribute nearly 70% of the estimated 13.5×10^9 t of suspended fluvial sediment reaching the ocean annually, while South America rivers account for an additional 13% (Milliman and Meade 1982). With the exception of the Chinese rivers, however, none of the great Asian rivers have been studied in detail. The largest river, the Ganges/Brahmaputra, for example, has not been measured during flood conditions, and the estimated 1.1×10^9 t annual figure could be in error by 50%. Even more extreme is the Irrawaddy, whose reported sediment discharge (265×10^6 t·yr^{-1}) is based on 19th century data. The lack of gauging data from these big rivers is matched by our ignorance concerning the transfer of their solid and dissolved loads to the ocean. The best estuarine studies come from North America and Europe, which generally have small rivers.

To help rectify this problem, we are studying the sediment

[1]This paper forms part of the Proceedings of the Dynamics of Turbid Coastal Environments Symposium convened at the Bedford Institute of Oceanography, Dartmouth, N.S., Canada, September 29–October 1, 1981.

[2]Contribution No. 5216 from the Woods Hole Oceanographic Institution.

[3]Present address (M.G.F.): Exxon Oil Company, Houston, TX 77001, USA.

Printed in Canada (J6680)
Imprimé au Canada (J6680)

TABLE 1. Ranking of the largest world rivers, with particular reference to the Yangtze River. Data compiled by Milliman and Meade (1982).

Drainage area ($\times 10^6$ km^2)		Water discharge (km$^3 \cdot$yr^{-1})		Sediment load ($\times 10^6$ t$\cdot$yr^{-1})	
Amazon	6.15	Amazon	5519	Ganges/Brahmaputra	1170
Zaire	3.82	Zaire	1250	Huangho	1140
Mississippi	3.27	Orinoco	1007	Amazon	900
Nile	2.96	Ganges/Brahmaputra	971	YANGTZE	500
La Plata	2.83	YANGTZE	900	Irrawaddy	265
Yenisei	2.58				
Lena	2.50				
Ob	2.50				
YANGTZE	1.94				

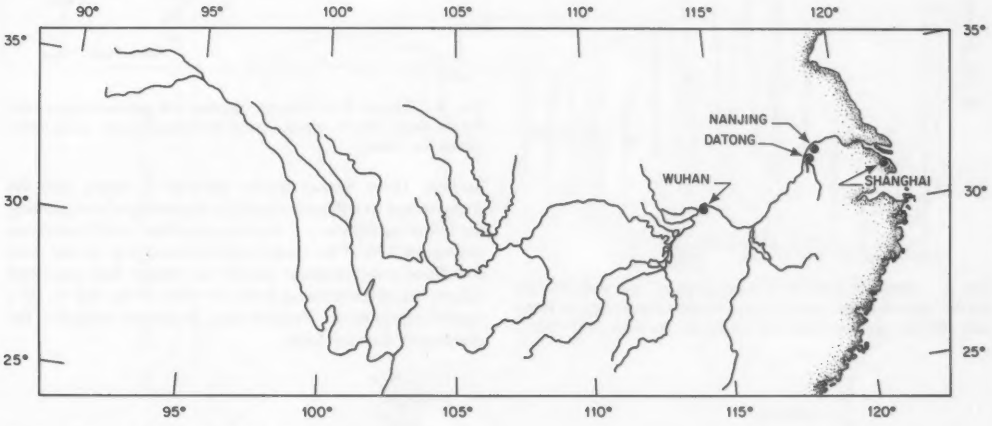

FIG. 1. Drainage Basin of Yangtze River.

transfer from the Yangtze River (Chang Jiang) to the East China Sea. This river is ranked fourth in terms of sediment discharge (500×10^6 t$\cdot$yr^{-1}) and, together with the Huangho (ranked second in the world), has been studied carefully by the Chinese since 1951. These rivers are unquestionably the best documented in Asia, with a fluvial data base that allows a more efficient and thorough study of their estuaries.

The Yangtze River and Estuary

The Yangtze is more than 6000 km long, and its 1.94 million km^2 drainage basin is the home for nearly half of China's billion inhabitants. The river is the major source of irrigation for agriculture (particularly rice), serves as a principal means of transportation to the interior, and yet also is a frequent source of disaster during devastating floods. The large basin area contains a wide diversity of terrain, geology, and climate; its headwaters are located in the Tibetan high plateaus, while its southern tributaries are subtropical and its northern tributaries are temperate (Fig. 1). The river discharges an average of 23 000 m^3 of water per second, with relatively little year-to-year variation (generally less than 30%). The period of main runoff occurs from late June through early August, when rainfall is highest (Hayami 1938), but the diversity of the terrain and climate within the basin modulates the runoff so that no one month averages more than 15% of the runoff (Fig. 2).

The annual suspended load, averaging about 500×10^6 t at the head of the estuary (Huang et al. 1980), shows relatively little fluctuation from year to year. At Hangkow, 400 km upstream from the mouth, for instance, sediment discharge between 1954 and 1972 ranged from 267 and 579×10^6 t; 15 of the 19 yearly values fall between 372 and 515×10^6 t. Suspended matter concentrations generally range from 100 to 1000 mg/L with only about 30% or less being coarser than 10 μm (Hayami 1938). Peak sediment loads occur during and just after peak discharge (Fig. 2), nearly 60% of the annual load being carried in July, August, and September. Concentrations of suspended solids during the 6 mo after peak discharge are about twice as high as those during the months preceding or during the peak, resulting in a hysteresis loop running counter to that for most other rivers (Fig. 3). In most rivers, early season flow removes the easily entrained material, resulting in higher sediment concentrations during these months but lower values later (e.g. Milliman 1979). The higher concentrations in the Yangtze *after* peak runoff may be related to the draining of the rice fields in August, prior to

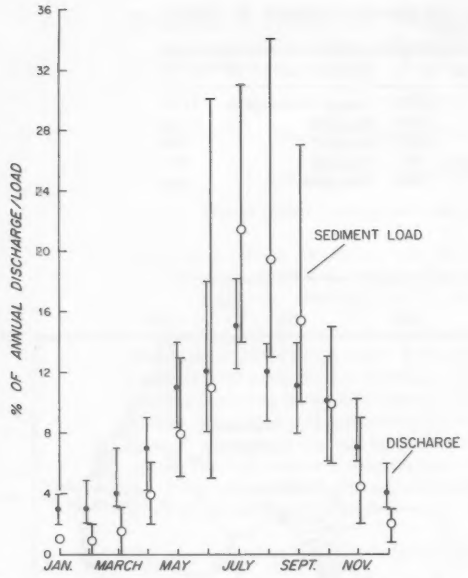

FIG. 2. Annual distribution of water discharge and sediment load for the Yangtze River, based on unpublished Chinese data (at Hangkow, 400 km upstream from the mouth) for the years 1958–72.

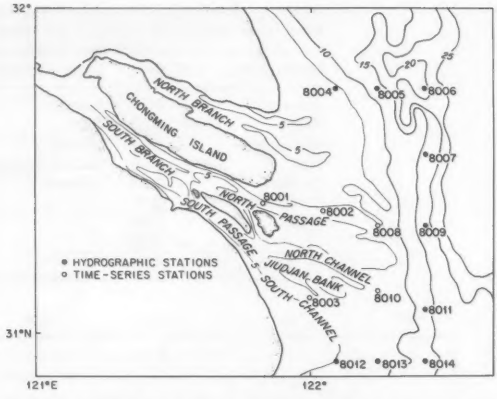

FIG. 4. Yangtze River Estuary, together with stations occupied during this study. Depth contours, based on Chinese charts, are in metres (mean low water).

harvest. These muddy waters continue to empty into the Yangtze and its tributaries until the beginning of rice planting the following February. Since the post-flood runoff carries an average of 53% of the annual sediment load (Fig. 2) and since post-flood concentrations should be smaller than pre-flood values, we suspect that at least 20–30% of the 500×10^6 t carried yearly by the Yangtze must be directly related to the draining of the rice fields.

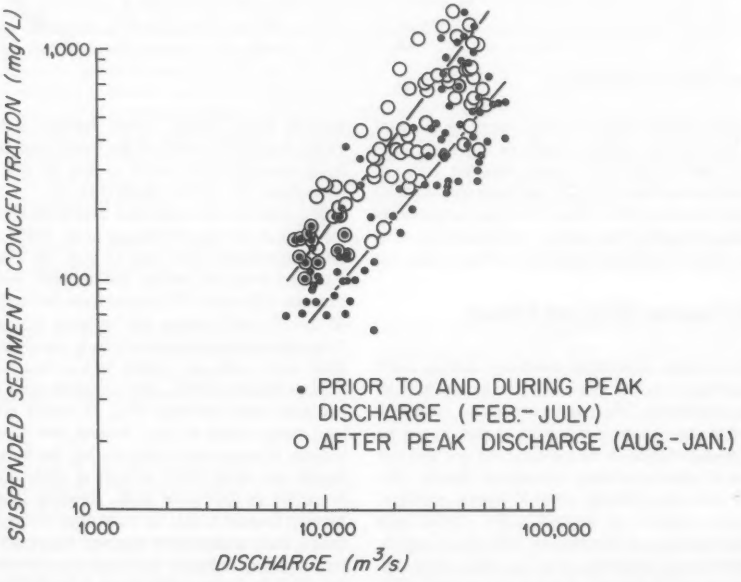
SUSPENDED SEDIMENT CONCENTRATION (mg/L)
DISCHARGE (m³/s)
• PRIOR TO AND DURING PEAK DISCHARGE (FEB.–JULY)
○ AFTER PEAK DISCHARGE (AUG.–JAN.)

FIG. 3. Rating curve for the Yangtze, showing the comparison of pre- and post-flood sediment concentrations. Based on monthly averages of sediment data from the Hangkow station, 1958–72.

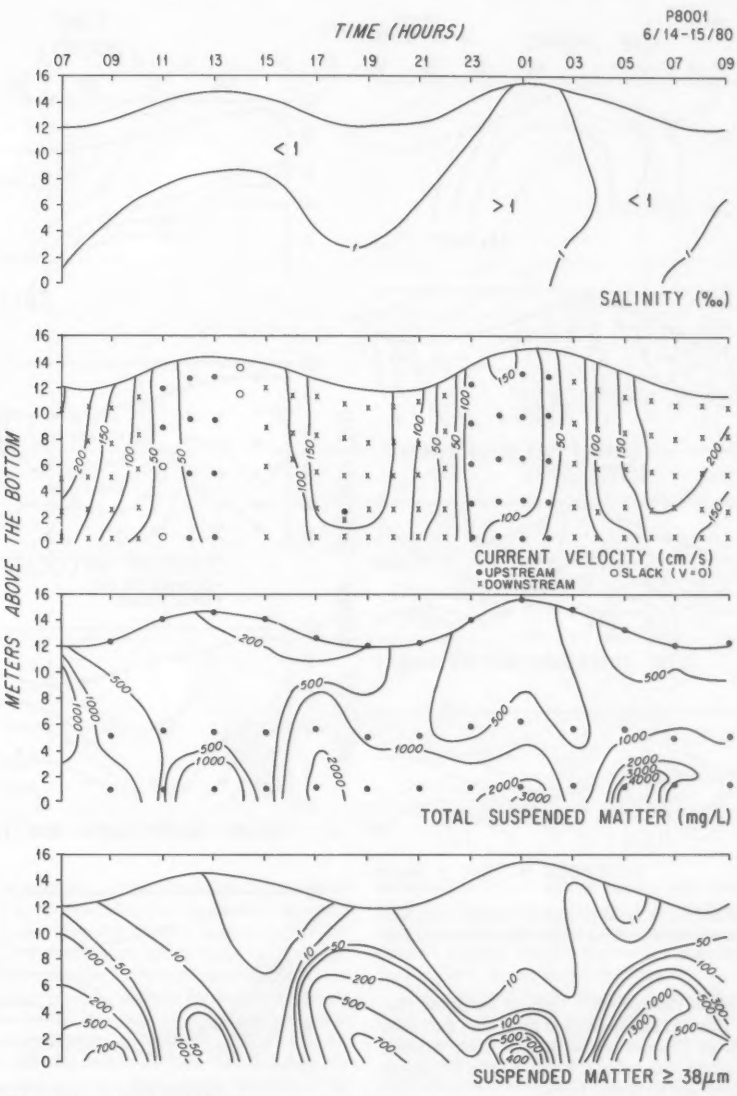

FIG. 5. Time-series plot of salinity, current velocity, total suspended matter, and suspended material coarser than 38 μm at station 8001, June 14–15, 1980.

The Yangtze Estuary bifurcates into North and South branches around Chongming Island (Fig. 4). In turn, the South Branch divides into the North and South passages at Changxin Island, and the South Passage is split into North and South channels by Jiudjan Bank. At present, the North Branch of the river has no net discharge of freshwater; in fact, according to our Chinese colleagues, it experiences a net landward influx of salt water, resulting in slightly saline river water (0.5–1‰) in the South Branch (Huang et al. 1980). It is a mark of the rapid evolution of this estuary that less than 1000 years ago, the North Branch was the major distributary of the Yangtze, and within the past 3000 years, the mouth was considerably to the north (Ren and Tseng 1980). At present, best estimates are that the North Passage has discharged more

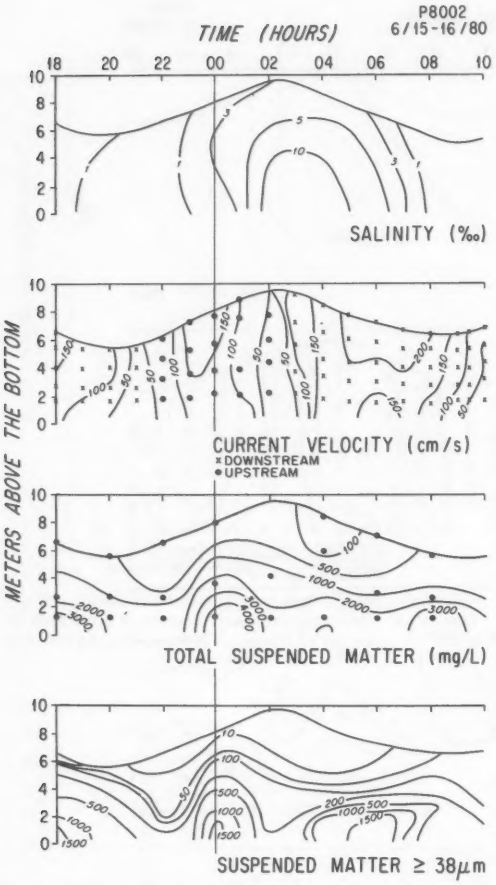

FIG. 6. Time-series plot of salinity, current velocity, total suspended matter, and suspended material coarser than 38 μm at station 8002, June 15–16, 1980.

water than the South Passage since 1966; in the South Passage, the South Channel has discharged more than the North Channel. The South Channel around Jiudjan Bank, exhibits considerable shoaling (Huang et al. 1980), a point of concern for ship navigation into Shanghai Harbor.

Another important feature of the Yangtze is the great range of tides (mixed with a strong semidiurnal component). In the North Passage, tidal range can exceed 4.5 m (Huang et al. 1980), and the tidal component of the current locally can exceed 2 $m \cdot s^{-1}$ (Shen et al. 1980). Even during peak runoff, tidal reversals in the current occur during flooding tide. Results presented in this paper plus preliminary data from 1981 cruises suggest, in fact, that the tidal range (spring versus neap) may play as important a role in sediment discharge as the river stage.

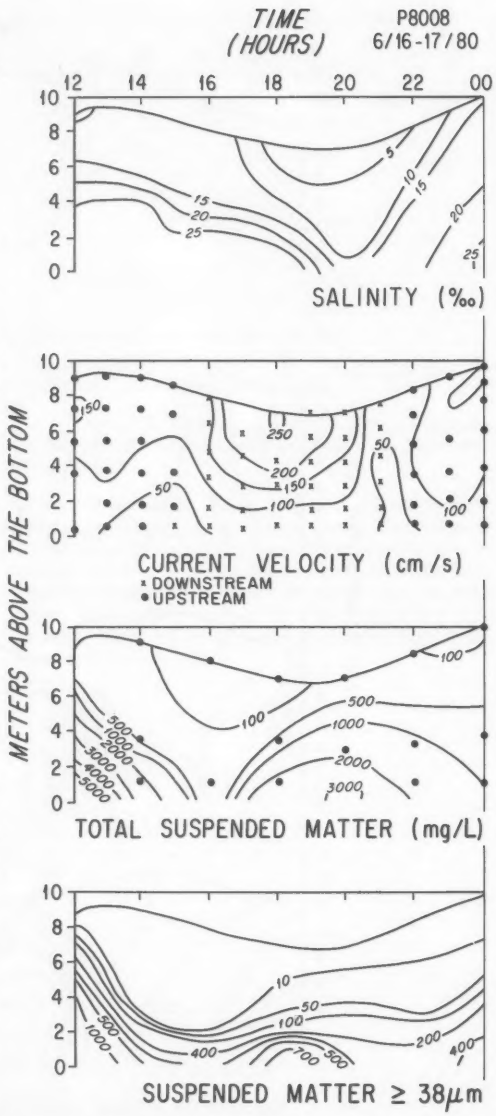

FIG. 7. Time-series plot of salinity, current velocity, total suspended matter, and suspended material coarser than 38 μm at station 8008, June 16–17, 1980.

Methods

Data were collected from the Chinese oceanographic vessel Shuguong No. 6 during mid-June 1980 at five anchor stations within the estuary and nine hydrographic/suspended matter

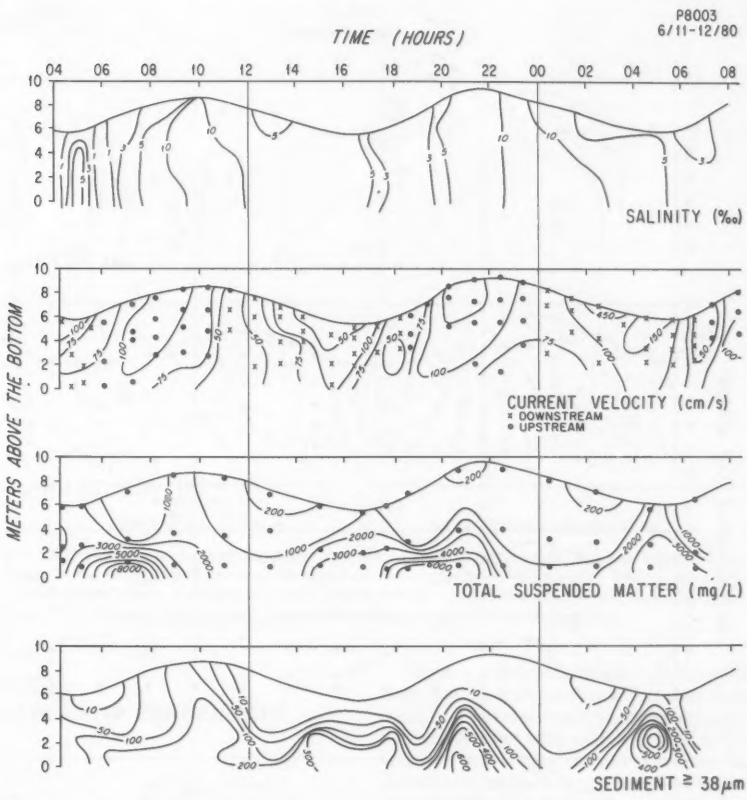

FIG. 8. Time-series plot of salinity, current velocity, total suspended matter, and suspended material coarser than 38 μm at station 8003, June 11–12, 1980.

stations around the northern, southern and eastern boundaries of the estuary (Fig. 4). Each anchor station was occupied for at least 13 h and three for the full tidal cycle (25 h). Hydrographic stations were taken before (June 10) and after (June 17) the anchor stations. Although daily data are not available for the study period, discharge for the month of June averaged 32 000 m^3/s, about normal for that month and about 80% the value of normally high discharge in July–August. Predicted spring tides occurred on June 14, inferring increased discharge and upstream flow during the time of the anchor stations. Measured tidal range at station 8002 (North Passage) was 4 m.

At each of the time-series stations (three in the North Passage and two in the South Passage), temperature, salinity, suspended solids, and current speed and direction were measured, as well as dissolved solids (J. Edmond et al., Earth and Planetary Science, Massachusetts Institute of Technology, Cambridge, MA, unpublished data). Current measurements were made hourly using a Chinese-made meter at the surface and bottom as well as 0.8, 0.6, 0.4, and 0.2 the water depth; measured velocities agreed closely with those made by an Endeco current meter used by U.S. scientists, although at high velocities, the latter meters tended to be erroneously low (G. Cannon, Pacific Marine Environmental Laboratory, Seattle, WA, personal communication).

The suspended matter samples were collected every other hour in 1-L horizontal water bottles (to prevent the loss of sand when sampling) at three levels within the water column — surface, mid-depth, and 1 m above the bottom. Salinities were measured from the water samples using an optical refractometer. The samples were emptied through two sieves (62 and 38 μm) to remove the coarse fraction, and the filtrate passed through micro-filters, either Millipore or Gelman filters, with nominal pore diameters of 0.45 μm. No control filters were needed, since the weight change of the filters was small compared to the quantity of material collected on the filters. Both the filters and the coarse fraction were rinsed with distilled water and stored until return to the laboratory, where they were air dried and weighed. The concentrations of both the coarse and fine fraction were computed subsequently.

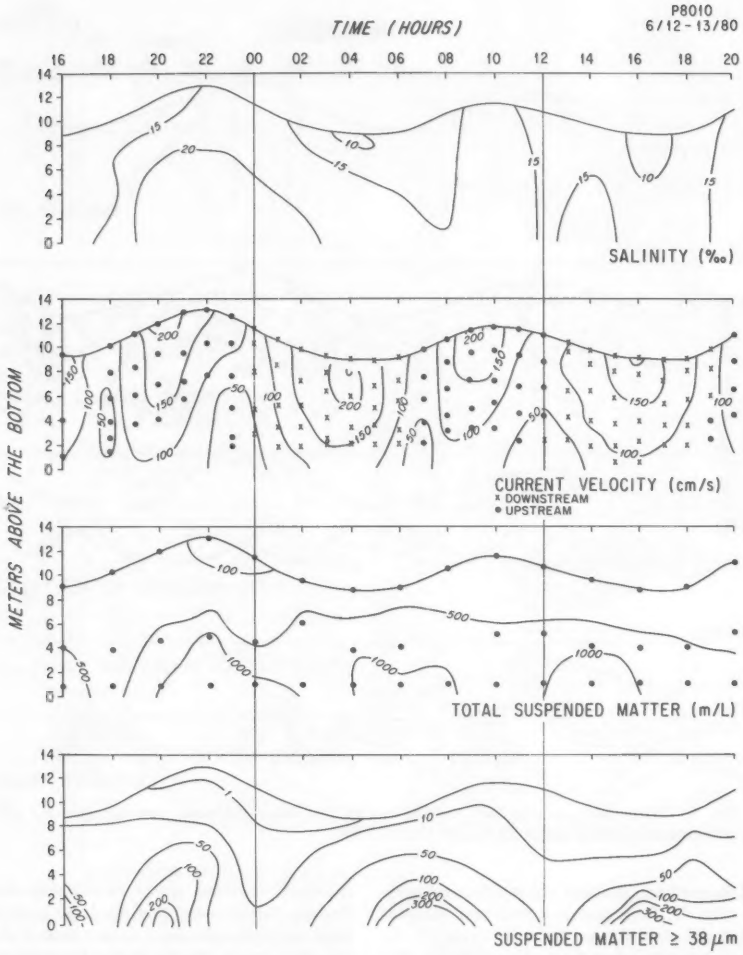

FIG. 9. Time-series plot of salinity, current velocity, total suspended matter, and suspended material coarser than 38 μm at station 8010, June 12–13, 1980.

Some filters were ashed (at 500°C) to determine the organic content. Most filters were mounted on glass slides with optical oils for visual inspection under transmitted light. Those samples that proved particularly interesting were then examined under the scanning electron microscope.

Results

Because of the great tidal range in the Yangtze, both hydrographic and suspended material character changed markedly with time. In the North Passage, the innermost station (8001) experienced essentially fresh water during the entire 26 h of measurement (Fig. 5), while downstream at station 8002, subsurface values exceeded 10‰ during high tide (Fig. 6). At both North Channel stations currents were predominantly offshore (peak velocity exceeding 200 cm/s), but landward during part of the flood tide (generally 50–100 cm/s). Surface and mid-depth suspended matter concentrations at both stations ranged from 200 to 500 mg/L, values consistent with predicted river concentrations during this season (Fig. 3). Near-bottom values, in contrast, generally exceeded 1000 mg/L (occasionally greater than 4000 mg/L), of which more than 40% was coarse (≥ 38 μm) (Fig. 5, 6).

Salinities in the south channel of South Passage (just south of Jiudjan Bank) generally were less than 5‰ except during

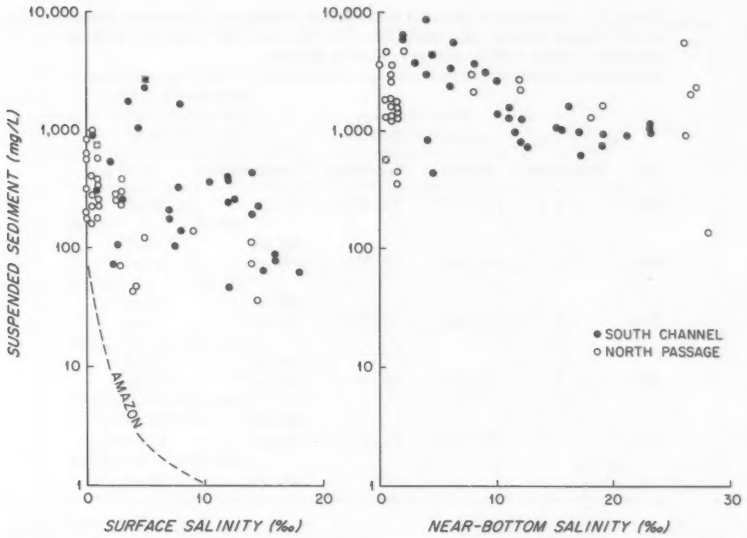

FIG. 10. Variation of suspended sediment and water salinity in surface (left) and near-bottom waters (right) of the Yangtze Estuary. Note the higher relative concentration of suspended solids in the south channel surface waters. Comparison with the trend for surface waters in the Amazon River (after Milliman et al. 1975) illustrates the turbulent (resuspended sediment) nature of the water column.

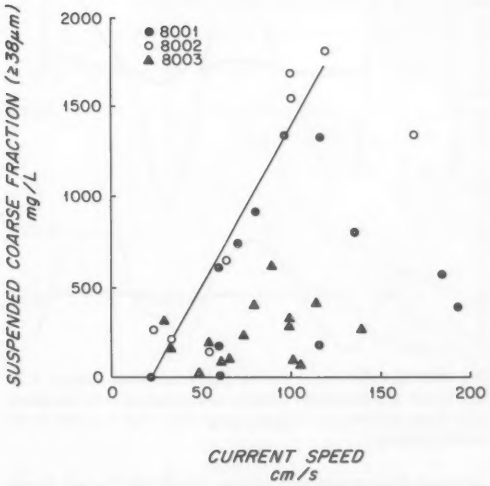

FIG. 11. Comparison of the coarse fraction in suspension and the current speed 1 m above the bottom at stations 8001, 8002, and 8003.

high tides (Fig. 7). Ebb currents exceeded 150 cm/s, but bottom currents during rising tides reached 100 cm/s (upstream). Near-bottom suspended solid concentrations were much higher (6000–8000 mg/L) than in the North Passage, but sand and coarse silt contents were small (Fig. 8).

Salinities at stations 8008 and 8010, the seaward ends of the North and South Passages, were far more marine, with near-bottom values exceeding 20‰ during high tide (Fig. 8 and 9). Surface velocities were as high as those at the landward stations but near-bottom currents never exceeded 100 cm/s, probably the result of density stratification. In contrast to the shoreward stations, peak currents were during high and low tides, not at flood and ebb, and thus were out of phase with tidal stage. Highest concentrations of suspended matter occurred during flooding tide (Fig. 8 and 9).

The high concentrations of suspended sediment at various salinities (as compared to a drastic decrease with increased salinity in the Amazon) (Fig. 10) indicates that a large portion of the surface water sediment was resuspended or maintained in suspension by turbulence. Although peak velocities in the South Channel (station 8003) were lower than in the North Passage, the concentration of suspended matter was higher (compare Fig. 5, 6, and 7). Interestingly, the amount of suspended coarse material in the South Channel was far lower than in the North Passage, the concentrations apparently unrelated to current speed (Fig. 11).

Time-averaged surface currents at all five time-series stations flowed offshore, but the average speeds were greater in the north than the south (Table 2). This agrees with Chinese observations, and explains the lower average salinities in the North Passage. Current speed decreased with water depth at all stations, but net water transport generally remained offshore.

Integrating the sediment concentration and current speed over one or more tidal cycles allows calculation of the

TABLE 2. Calculation of net water and sediment discharge for five anchor stations in the Yangtze Estuary. Mid-June 1980. The "On" and "Off" after the sediment discharge numbers refer to onshore or offshore transport.

		Water discharge (cm/s) (direction)		Sediment discharge (t/m of river width) (on or off shore)	
Sta.	Tidal cycles	Surface	Near-bottom	Total sediment	≥ 38 μm
8001	1	110 (110°)	75 (115°)	180 on	30 on
				480 off	190 off
				660 off	220 off
8002	<1	105 (70°)	70 (72°)	190 on	40 on
				250 off	120 off
				440 off	160 off
8008	<1	55 (60°)	35 (275°)	112 on	30 on
				3 off	20 on
				115 off	10 off
8003	1	30 (68°)	35 (95°)	660 on	50 on
				180 on	0
				480 off	50 off
8010	1	45 (132°)	35 (112°)	220 on	10 on
				170 off	10 off
				390 off	20 off

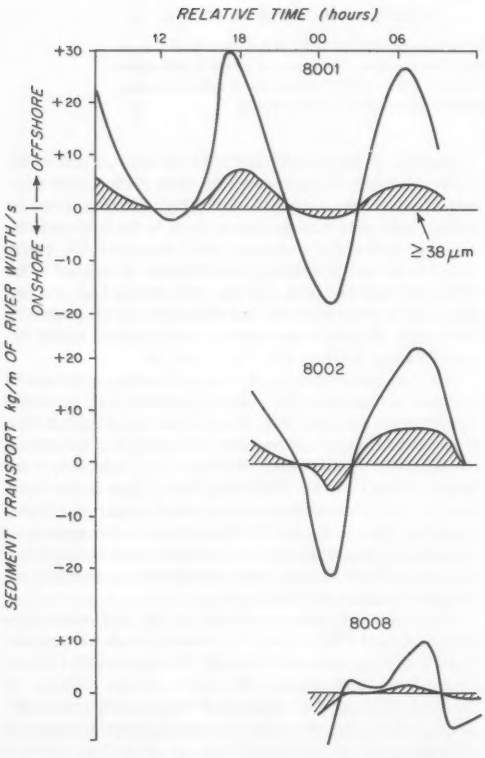

FIG. 12. Calculated sediment transport in the North Passage. Current speeds and suspended sediment concentrations were integrated over depth and time to yield this curve. Sand flux is shown hatched pattern.

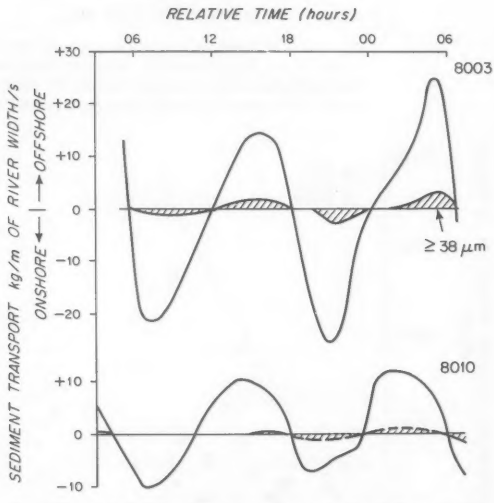

FIG. 13. Calculated sediment transport in the South Passage. Current speeds and suspended sediment concentrations were integrated over depth and time to yield this curve. Sand flux is shown in the hatched pattern.

sediment discharge at each station. The North Passage during the study period displayed a marked offshore transport; landward transport at station 8001 occurred only during low low-tide (LLT). Although station 8002 was not occupied for a full 25-h tidal cycle, the measured flux was similar (Fig. 12). Sand transport accounted for 40% of the net sediment flux at 8001 and nearly 50% at 8002, with little landward transport during flooding tide (Fig. 12; Table 2).

In contrast, calculations for the south channel of the South

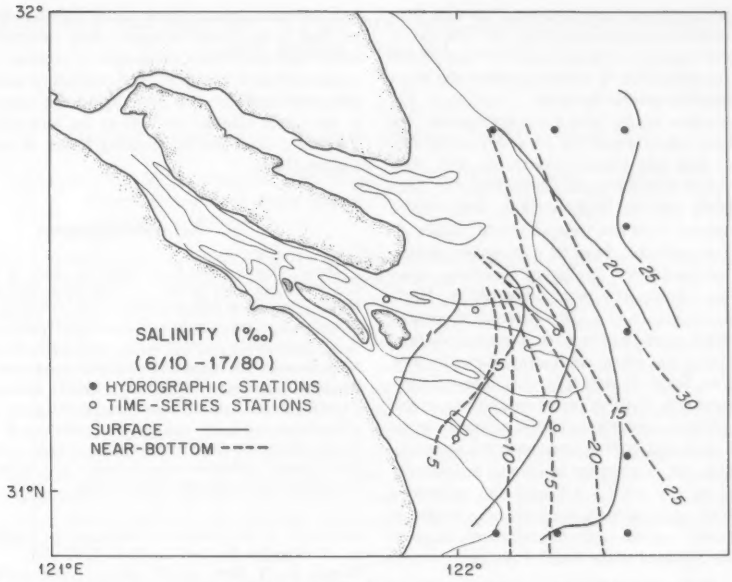

FIG. 14. Average salinity distribution in the surface waters of the Yangtze Estuary during the period June 10–17, 1980. The values for the time-series stations represent tidally averaged values, while the hydrographic stations were measured at the beginning and end of the survey period.

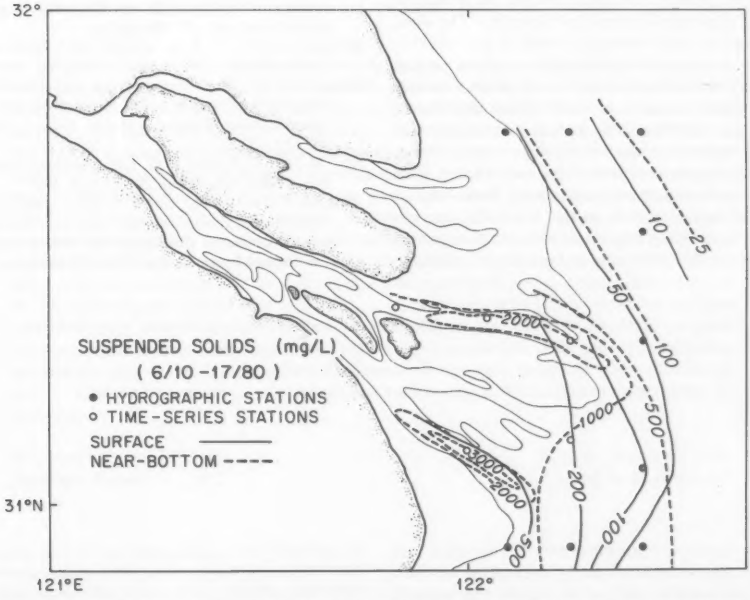

FIG. 15. Distribution of suspended solids in the surface waters of the Yangtze Estuary, June 10–17, 1980.

Passage showed landward sediment transport, but with large upstream and downstream components (Fig. 13). The strong oscillatory nature of transport with net landward flux would explain the high concentrations of sediment within the water column and the shoaling around the bank.

While the time-series results give transport vectors, the hydrographic stations taken around the periphery of the area do not take into account tidal variations or fluxes. Still, plotting these latter values with the mean values from the time-series stations shows that the fresh/brackish water plume escaped to the southeast from the Yangtze mouth; values off the North Branch, as predicted, were far more saline, indicative of the lack of freshwater discharge. Similarly, near-bottom waters were significantly more saline off the North Branch than the South Branch (Fig. 14). In terms of concentration, the suspended solids in both surface and near-bottom waters were greatest in the south, decreasing markedly both north and east of the South Branch (Fig. 15). These hydrographic data represent only distributions of concentrations and not fluxes, since offshore transport occurred primarily in the North Passage. Highest near-bottom concentrations were confined to the channels, but much of the study area had concentrations in excess of 100 mg/L. Although the suspended coarse fraction on the outer parts of the study area tended to be greater in the south, highest sand concentrations, as mentioned above, were confined to the North Passage.

Discussion

The Yangtze River, carrying 500×10^6 t of suspended sediment annually, is one of the major rivers of the world and the biggest river emptying into the East China Sea. Our data, based on observations taken during the week of June 10–17, 1980, describe a complete hydrographic regime: waters within the estuary are well mixed with nearly vertical salinity gradients. In contrast, waters seaward of the distributary channels are more stratified both in terms of salinity and suspended solid concentrations. Tidal variations play an important role in the discharge of both water and sediment from the river, upstream transport occurring during flood tides.

Calculated net current speeds in the North Passage exceeded 100 cm/s, resulting in a major offshore transport of suspended sediment, 40–50% sand and coarse silt. Although sediment concentrations are much higher in the South Channel than in the North Passage, tidally integrated calculations show large oscillatory excursions of material, with a net upstream sediment transport. The oscillatory sediment transport with a net upstream flux may explain the highly turbid waters in the South Channel as well as the relatively low concentrations of sand and the shoaling nature of the channel near Jiudjan Bank.

Acknowledgments

These studies have been made as part of the cooperative U.S.–Chinese study of the sediment dynamics, sponsored by the National Bureau of Oceanography (NBO) of China and the National Oceanic and Atmospheric Administration (NOAA) of the USA. Acquisition of the data was funded by a NOAA contract to WHOI. Preparation of this report was funded in part by the Office of Naval Research (contract no. N00014-81-C-0009). We thank Jeffrey Ellis (WHOI) for his help with the preparation of the materials for the 1980 cruise and I. N. McCave, K. O. Emery, R. H. Meade, and D. G. Aubrey for their constructive comments on this manuscript. Our Chinese colleagues assisted greatly in collecting and analyzing the samples and collecting velocity data.

HAYAMI, S. 1938. Hydrological studies on the Yangtze River, China: J. Shanghai Sci. Inst., Sect. 1, 1: 97–162.

HUANG, S., N. HAN, AND X. ZHANG. 1980. Analysis of siltation at mouth bar of the Yangtze River estuary. Chinese Soc. Hydraulic Eng., International Symposium on River Sedimentation, Beijing, 10 p.

MILLIMAN, J. D. 1980. Sedimentation in the Fraser River and its estuary, southwestern British Columbia (Canada). Estuarine Coastal Mar. Sci. 10: 609–633.

MILLIMAN, J. D., AND R. H. MEADE. 1982. World-wide delivery of river sediment to the oceans. J. Geol. 00: 000–000.

MILLIMAN, J. D., C. P. SUMMERHAYES, AND H. T. BARRETTO. 1975. Oceanography and suspended matter in the surface waters off the Amazon River, February–March, 1973. J. Sediment. Petrol. 45: 189–206.

REN, M., AND C. TSENG. 1980. Late Quaternary continental shelf of East China. Acta Ocean. Sinica 2(2): 1–9.

SHEN, H. T., W.-F. ZHU, AND Z-C. MAO. 1980. The Chang Jiang estuarine circulation and their effect on the transport of suspended sediments. (translated from Chinese) Institute Estuarine and Coastal Research, East China Normal Univ. Publ., 12 p.

Distribution and Behavior of Fine Sediment in the Severn Estuary and Inner Bristol Channel, U.K.[1]

R. KIRBY AND W. R. PARKER

Institute of Oceanographic Sciences, Crossway, Tauton, Somerset, U.K.

KIRBY, R., AND W. R. PARKER. 1983. Distribution and behavior of fine sediment in the Severn Estuary and Inner Bristol Channel, U.K. Can. J. Fish. Aquat. Sci. 40(Suppl. 1): 83–95.

During the 10 yr, 1970–80 a variety of field measurements using some new techniques have allowed the distribution of muddy sediment in the Severn Estuary and Inner Bristol Channel to be defined. Based on these measurements, a behavioral model has been adopted comprising mobile and stationary suspensions, and settled mud. The regional distribution of mobile suspensions shows a suspended solids front located along the main channel axis with the more turbid water on the southern, English, side. At maximum current velocities on spring tides, vertical suspended sediment profiles are homogeneous. As velocity decreases, a stepped structure develops due to settling, which is then remixed on the next accelerating semidiurnal tidal phase. Over the lunar timescale these steps become more stable, eventually settling to the bed. The steps are unrelated to salinity, temperature, grain-size, or mineralogy. On neap tides, layered, acoustically detectable stationary suspensions, which occasionally consolidate to form settled mud, develop from the mobile suspensions. An idealized "three-zone" model has been devised characterizing the structures developed in the mobile suspensions.

Key words: Severn Estuary, vertical profiling, siltmeter, densimeter, suspended solids, fronts, stratification

KIRBY, R., AND W. R. PARKER. 1983. Distribution and behavior of fine sediment in the Severn Estuary and Inner Bristol Channel, U.K. Can. J. Fish. Aquat. Sci. 40(Suppl. 1): 83–95.

Pendant la décennie de 1970–80, diverses mesures sur le terrain à l'aide de techniques nouvelles ont permis de définir la distribution du sédiment vaseux dans l'estuaire de la Severn et le chenal de Bristol intérieur. À partir de ces données, un modèle de comportement a été adopté, comprenant des suspensions mobiles et stationnaires, et de la vase compacte. La distribution régionale des suspensions mobiles montre un front de solides en suspension situé le long de l'axe du chenal principal, l'eau plus turbide se trouvant dans la partie sud, du côté anglais. Pendant les marées de vive eau, les profils de sédiment en suspension sont homogènes à la vitesse maximale des courants. À mesure que diminue la vitesse, il se développe une structure en paliers par suite de la sédimentation. Le sédiment se mélange de nouveau dans la phase de marée semi-diurne suivante, les courants augmentant de vitesse. À échelle temporelle lunaire, ces paliers deviennent plus stables, et se déposent éventuellement sur le lit. Ils n'ont aucune relation avec la salinité, la température, la taille des particules ou leurs caractéristiques minéralogiques. Pendant les marées de morte eau, il se développe, à partir des suspensions mobiles, des suspensions stationnaires en couches, détectables par méthodes acoustiques, qui se consolident occasionnellement en une vase compacte. On a élaboré un modèle idéal « à trois zones » caractérisant les structures qui se forment dans les suspensions mobiles.

Received October 14, 1981
Accepted August 31, 1982

Reçu le 14 octobre 1981
Accepté le 31 août 1982

[1]This paper forms part of the Proceedings of the Dynamics of Turbid Coastal Environments Symposium convened at the Bedford Institute of Oceanography, Dartmouth, N.S., Canada, September 29–October 1, 1981.

Printed in Canada (J6677)
Imprimé au Canada (J6677)

THE behavior of fine sediments is complex. Unlike noncohesive sediments, which are affected principally by hydrodynamic and inertial forces, fine cohesive sediments are also influenced by physico-chemical forces, which are important

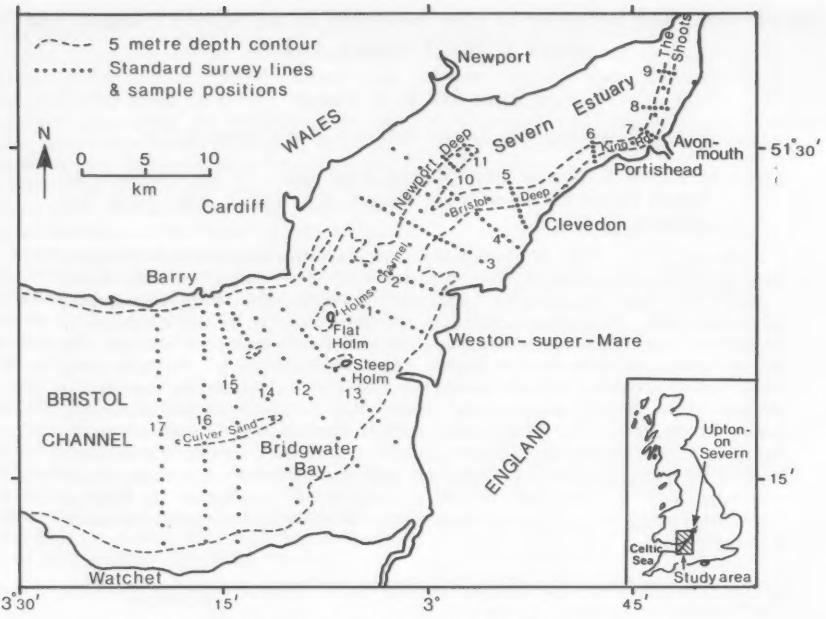

FIG. 1. Location of standard stations used in surveys of suspended solids distribution.

because of the small mass of the particles. In the past these complexities have resulted in an emphasis on laboratory studies, where some control over the many relevant variables could be achieved. Field studies of fine sediments have generally been confined to point sampling and simple observations and thus, by comparison with noncohesive sediment, the level of understanding of the behavior of fine sediment in the sea is relatively primitive.

Since 1970, the Institute of Oceanographic Sciences has undertaken 24 surveys to study the behavior of fine sediments in the Severn Estuary and Inner Bristol Channel, where natural conditions of high and variable tidal energy and large suspended load result in the various types of fine sediment phenomena being well developed. This paper reviews the essential results on the basis of a general "three-state model" of fine sediment behavior in the area. The distribution, structure, and formation of each state is considered in turn. These fine sediment phenomena are compared with those of other areas and the wider implications of the behavior are considered.

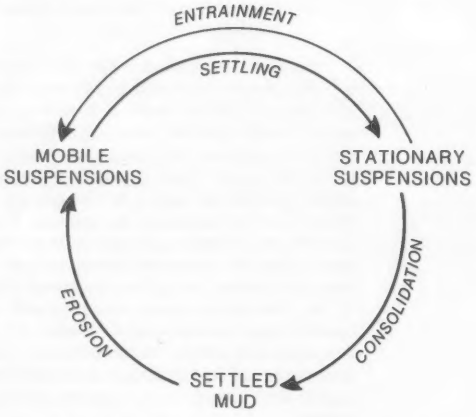

FIG. 2. Fine sediment behavioral model showing states of occurrence and linking processes.

The Study Area

The Severn Estuary extends for 150 km from Upton-on-Severn to Flat Holm and Steep Holm Islands (Fig. 1). The Bristol Channel extends westwards from these islands and opens into the Celtic Sea.

The Severn has a high and variable tidal range (14.5 m Highest Astronomical Tide, 12.3 m Mean Spring Range, and 6.5 m Mean Neap Range at Avonmouth), which leads to high and variable tidal stream velocities (2.3 $m \cdot s^{-1}$ Maximum Spring Flood, 1.2 $m \cdot s^{-1}$ Maximum Neap Flood at Avonmouth).

Owing to the large tidal volume relative to the freshwater flow, the Severn is commonly quoted as a classical vertically mixed estuary with regard to the salinity field (e.g. Stommel

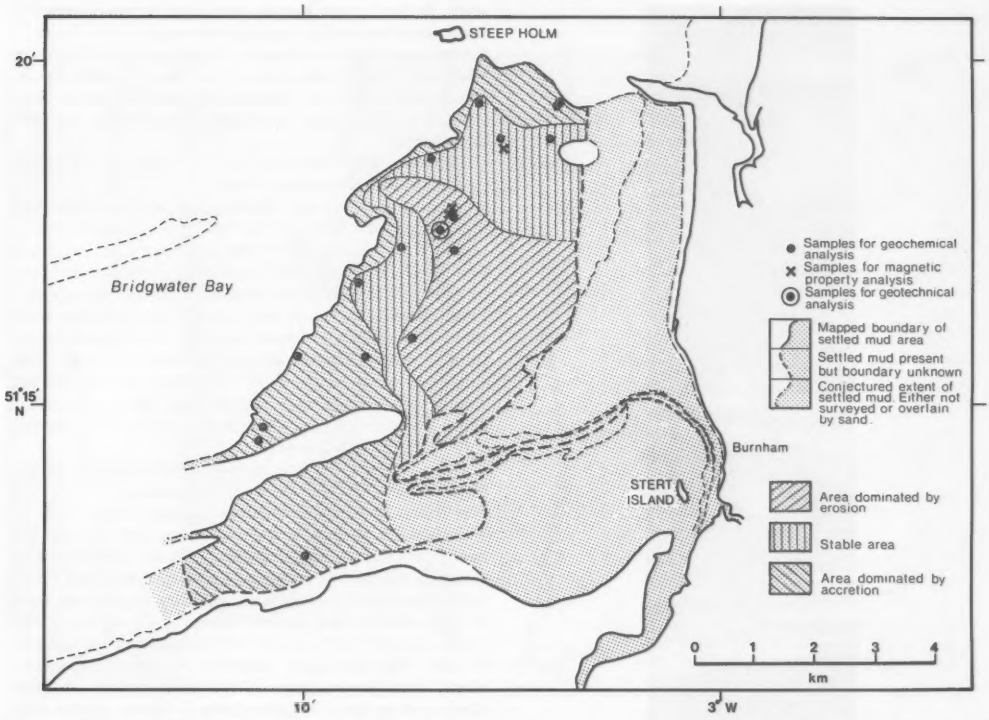

FIG. 3. The Bridgwater Bay settled mud area showing areas of erosion, stability, and accretion based on analysis of acoustic records and samples.

1953). More recent measurements generally confirm this (Welsh Water Authority 1983). Longitudinal salinity gradients are slight, while strong lateral gradients are confined to the coastal margin and no marked lateral gradients are observed along the main channel, even on neap tides. Continuous vertical conductivity profiles made by IOS (unpublished) and the Hydraulics Research Station (HRS 1980, p. 4) show only occasional and slight departures from well-mixed profiles. Maximum surface to bed gradients of 0.1‰ are typical.

The turbidity maximum extends from Watchet in the Bristol Channel to well above "The Shoots," which is the upstream limit of this study (Fig. 1). As a direct result of the energy cycles and availability of erodible fine sediment, the suspended solids concentrations are high and variable ranging from <0.1 to $>200\ g \cdot L^{-1}$. Based on IOS water volume and suspended sediment mass computations in this region, preliminary estimates (unpublished) show that on spring tides of the order of 17 million t of fine sediment is suspended in the water column whilst on neap tides $\simeq 50\%$ of this sediment settles to the bed to form dense stationary layers.

Data coverage in the Severn is restricted by difficulties in reaching the bank areas. However, the overbank waters are thought not to contain a significant fraction of the mobile fine sediment, owing to the sandy nature and short period of submergence of the banks.

Samples of suspended sediment from a variety of locations within the turbidity maximum reveal a spatial uniformity of mineralogy, with a mineral suite dominated by illite ($44 \pm 9\%$), with subsidiary amounts of quartz ($23 \pm 3\%$), chlorite ($19 \pm 6\%$), and kaolinite ($4 \pm 4\%$) (Bryant and Williams 1983). The grain size of the sediment has been investigated and also shows relatively limited variation throughout the area, 70–80% of the "primary particles" in samples being 1 μm or less in size (Williams and Bryant 1979). This material is invariably flocculated and although no in situ measurements of floc sizes have been made, shipborne settling rate measurements on freshly sampled suspensions and IOS measurements of the settling rates of suspension layers suggest that the mean Stokes size is in the region of 100 μm, with a maximum around 140–150 μm.

Fine Sediment Behavioral Model

From previous observations (Inglis and Allen 1957; Delft Hydraulic Laboratory 1962; Krone 1963; Partheniades 1964; Migniot 1968) and our own work (Kirby and Parker 1977; Parker and Kirby 1977) we have adopted a conceptual model

FIG. 4. X-radiograph of 1.0 cm thick slab of settled mud core BC283 from Bridgwater Bay showing broad zones of felty-textured massive "structureless," unbioturbated clay interbedded with narrow submillimetre laminated silt and clay and also cross-bedded silty zones. Depth 13.5–32.5 cm. Diameter 5.7 cm.

of the behavior of fine sediment in highly turbid areas. It takes into account the phenomena observed in the field and such understanding as exists of the rheological properties of suspensions and pastes of flocculated fine particles. In particular, it avoids terms which, in the past, have been tied to specific values of solids content since, although the behavioral properties of materials depends in part on the solids content, they are also strongly influenced by the mineralogy, solids volume concentration (state of flocculation), water chemistry and shear field to which the two-phase medium is subjected.

We have distinguished three basic states of occurrence on the basis of the large field data set from the Severn Estuary and Inner Bristol Channel. Figure 2 shows these three states and the processes of erosion, transport, deposition, and consolidation whereby material moves between them:

Settled mud is deposited fine sediment in which individual particles are supported by the surrounding particle framework. In the Severn Estuary and Inner Bristol Channel it occurs over the density range approximately $1.3-1.7\ t\cdot m^{-3}$. Settled muds have a residence time measured in months or years and develop over a period of days or weeks by the consolidation of those stationary suspensions which occasionally survive. Their rheological behavior has not been investigated.

Stationary suspensions are fluid-supported or partly framework supported assemblages of particles having no lateral component of movement. Stationary suspensions occur over the concentration range <0.1 to $\simeq 200\ g\cdot L^{-1}$. They evolve by settling from concentrated mobile suspensions and the period over which relatively thick layers ($\simeq 3$ m) come to halt may be extremely short (a few seconds). Following this they continue consolidation slowly and generally have a lifespan measured in hours or days. Some stationary suspensions are detectable by echo sounders and are commonly known as "fluid mud" (Inglis and Allen 1957). Stationary suspensions are thought to be pseudoplastic (Bryant et al. 1980). As consolidation proceeds, a shear strength develops which increases with depth in the suspension.

Mobile suspensions are moving, fluid-supported assemblages of particles. They have been encountered in the Severn over solids mass concentrations ranging from <1.0 to $>150\ g\cdot L^{-1}$. They arise from several sources, by sea and river input (Parker and Kirby 1982b), by the gradual erosion of settled muds over a prolonged timescale (years) and by the rapid entrainment (minutes) of stationary suspensions from the bed. Much of this material returns to the stationary suspension state by settling over intermediate timescales (hours or days). The rheological properties of mobile suspensions extend from Newtonian to, at high concentrations, pseudoplastic with no unequivocal evidence of a lower critical yield stress at high concentrations (Bryant et al. 1980).

This conceptual model provides the basis from which the examination of the distribution, structure, behavior, and interrelationships of the various states of occurrence of fine sediments in the Severn Estuary and Inner Bristol Channel has been conducted. The methodology used for making these measurements is discussed below.

Methods

SETTLED MUDS

The distribution of settled mud has been mapped using a variety of acoustic sources. It was recognised as a bed material producing a long and acoustically "turbid" signal on an echo sounder (Schubel and Schiemer 1973). The boundaries, thicknesses, and structure of the settled mud areas have been investigated in the course of five seismic surveys using a modified 30 kHz echo sounder together with 3.5 kHz boomer, 3.5–7.5 kHz pinger and 110 kHz sidescan sonar equipment. These surveys have been supported by a program of core sampling and analysis using sedimentological, radiochemical, geotechnical, and palaeomagnetic techniques (Kirby and Parker 1980), with the object of assessing the rates of accretion or erosion at the settled mud surface and their relationship to the overlying suspensions.

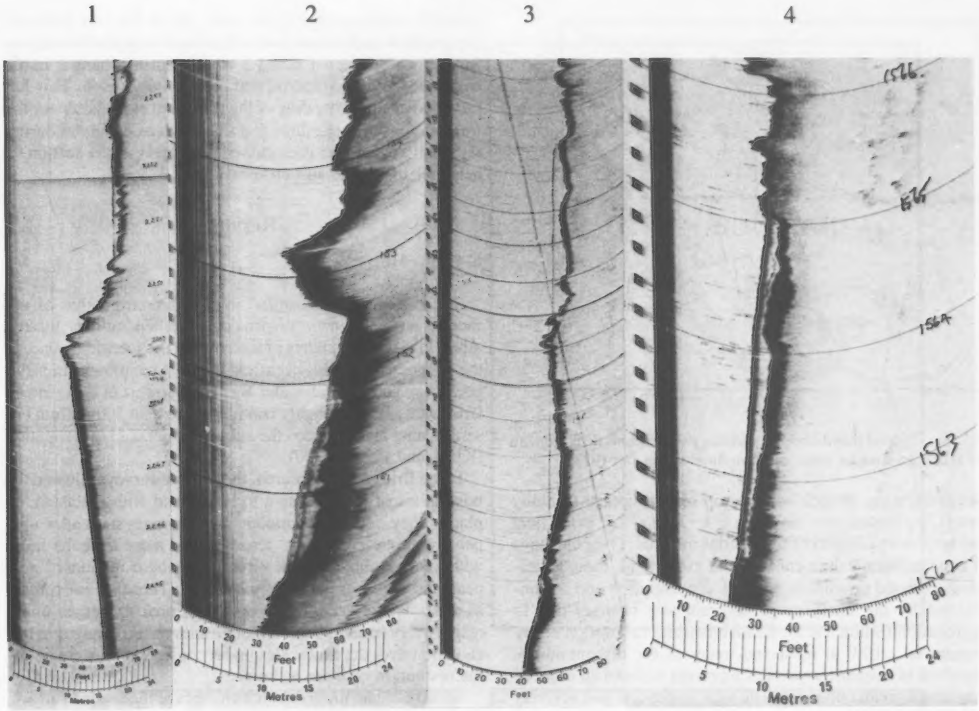

FIG. 5. Stationary suspensions seen with a 30 kHz echo sounder showing: (1) Single layer in channel floor, Fix 2250 onwards. King Road. (2) Multiple layering on slope. King Road. (3) Reflector fading at Fix 157, near Avonmouth. (4) Lower reflector aping underlying settled mud topography. Fix 1564–1565. Avonmouth.

STATIONARY SUSPENSIONS

Stationary suspensions have been detected and mapped using the modified 30 kHz echo sounder. Acoustically detectable stationary suspensions are recognised as faint, single or multiple, horizontal to subhorizontal "ghost reflectors" beneath or between which the acoustic energy returned is below the threshold of the receiver and no signal is printed. The apparatus used is incapable of detecting stationary suspensions less than ≃25 cm thick or those which have not developed a sufficiently sharp upper surface to be located by this technique (Parker and Kirby 1977, 1982a). Hence the distribution maps produced using this subjective technique are conservative.

IOS has undertaken reconnaissance studies of the distribution of acoustically detectable stationary suspensions in the Severn Estuary on eight specific surveys. Supporting information has been obtained incidentally on other surveys. More localized Port Authority records from the area have also been monitored. These represent many neap tide periods in all seasons and weather conditions over several years. Owing to the size of the survey area and the rapidly changing character of the phenomenon, comprehensive coverage on one neap tide sequence throughout the area has not proved possible. Although formation of a stationary suspension at slack water on the semidiurnal timescale is thought to occur at all sites in the estuary, the major areas of formation of acoustically detectable stationary suspensions over the neap tide cycle are more localized. These sites cannot readily be predicted because they change in response to meteorological and other factors whose influence is, as yet, insufficiently documented. Despite this slightly unpredictable character of the neap tide distributions, there is a sufficiently large body of data that the general distribution of stationary suspensions is now well known.

The echo sounder surveys of stationary suspensions provide the regional context which has been complemented by a detailed study of their internal structure. The concentration values encountered in stationary suspensions exceed the range of electro-optical turbidity meters and two gamma ray densimeters have been developed and used to make continuous vertical profiles of density versus depth into them (Parker et al. 1975).

MOBILE SUSPENSIONS

The solids concentration in the mobile suspensions is

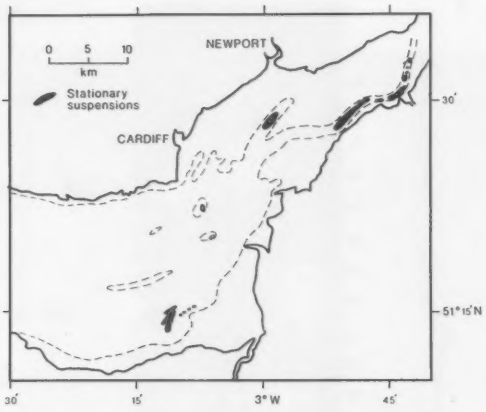

FIG. 6. Typical distribution of stationary suspensions detected with 30 kHz echo sounder made up from three surveys in 1973.

measured using Partech narrow-gap electro-optical turbidity meters, calibrated over the range $0.1-20.0\ g \cdot L^{-1}$ using field and laboratory samples of indigenous material. Over the range of concentration values encountered in the field, these instruments respond principally to mass concentration and are unaffected by the likely range of grain size changes due to aggregation (Smith 1982). Readability and calibration errors amount to $\pm 10\%$ at most and many of the discontinuities observed in suspension profiles represent features an order of magnitude greater than this. The high suspended load severely restricts daylight penetration and reduces microorganism production, while there is a regional uniformity in mineralogy. Together these factors decrease the uncertainties in the interpretation of the data.

The dynamic nature of changes in the concentration field and the large range in values led us in 1972 to devise a new system which permits rapid ($1\ m \cdot s^{-1}$) and continuous vertical profiles of solids concentration versus depth (Kirby and Parker 1977).

Using this system two types of measurements, regional suspended solids surveys and anchored experiments, have been undertaken. Some 2300 vertical profiles have been obtained on nine regional surveys covering almost all ranges of tide, most seasons and most weather conditions. During each survey, the vessel steams to and fro along one of the 17 standard cross sections of the estuary profiling the turbidity and occasionally the conductivity, versus depth, at each station for a complete semidiurnal cycle (Fig. 1). To assess the regional distributions of mobile suspensions, data from each of the 210 stations on Fig. 1 were divided in time (hourly) and tidal height (0.5 m) increments to provide a quasi-synchronous coverage spanning both the semidiurnal and lunar timescales. Data were then subdivided into spring (>9.0 m tidal range) and neap (<9.0 m tidal range) sets. For each station, the average concentration at 0.3 m below surface and 0.3 m above bed was calculated for all spring and all neap profiles irrespective of their position in the semidiurnal cycle.

The regional surveys from a moving ship do not permit velocity measurements to be made, so in the two anchored experiments undertaken to date the vessel remained on station for periods between 1 d and 3 wk measuring changes in the suspended solids, velocity, and conductivity fields. This has provided an understanding of the processes responsible for the formation of the structures and distributions observed during regional surveys and is discussed separately in the section on behavior of mobile suspensions.

Results

SETTLED MUD

The distribution of settled mud differs from that of the mobile and stationary suspensions. Settled mud is located along low-lying stretches of the coast in the intertidal zone, in the tributary estuaries, occasionally off Avonmouth, in Newport Deep and in Bridgwater Bay. The largest of these areas, Bridgwater Bay, probably contains more than 500 million t of settled mud and has been the subject of detailed investigation (Kirby and Parker 1980).

In the Bridgwater Bay area, the seismic surveys allowed the boundaries of the mud area to be defined with precision. In places they indicated smooth areas where stationary suspensions were commonly detected, and more irregular areas with outcropping internal structures where stationary suspensions were less commonly detected. These are interpreted as areas where accretionary and erosional processes might respectively be dominant, although anticipated changes in bed elevation over the timescales under consideration were below the resolution of these techniques.

To investigate these detailed changes at the seabed surface, 18 cores were analyzed for Caesium^{137} and Lead^{210} levels and showed areas of rapid deposition, up to 130 cm in 21 yr, in cores with high levels of these elements and showed other areas which were apparently erosional, since the radioisotopes were absent even in the uppermost layer. A third type of core profile showing limited isotope enrichment with depth was found. In some cases, cores of this latter group had a brittle ferromanganese crust at the surface providing supportive, unequivocal, evidence that the bed level has remained unchanged in the recent past. The radiochemical determinations were confirmed by geotechnical measurements of unloading and by palaeomagnetic measurements of variation in magnetic declination and inclination.

A map showing the distribution of accretionary, erosional, and stable zones over the settled mud area in Bridgwater Bay has been compiled, the boundaries of which coincide in general terms with those defined from the echo sounder surveys (Fig. 3).

Examination of another set of cores from Bridgwater Bay showed the sediment to consist typically of very soft, pale brown, silty clay grading down into grey, silty clay in which occasional fine quartz sand lenses and layers are intercalated. The number and thickness of the sand layers commonly increased with depth. In many circumstances, the clay and sand layers were inclined from the vertical, sometimes at angles reaching 35°. Detailed examination of the X-radiographs showed massive "structureless" clay layers up to 10 cm thick interbedded with submillimetre silt and clay layers or with the

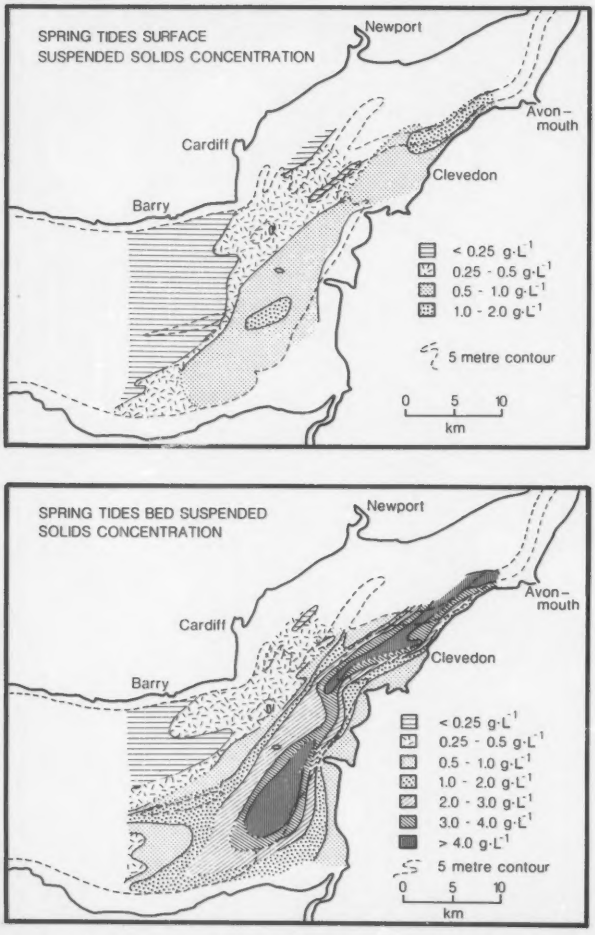

FIG. 7. Distributions of suspended solids averaged concentrations based on vertical profile

cal profile data from stations shown in Fig. 1.

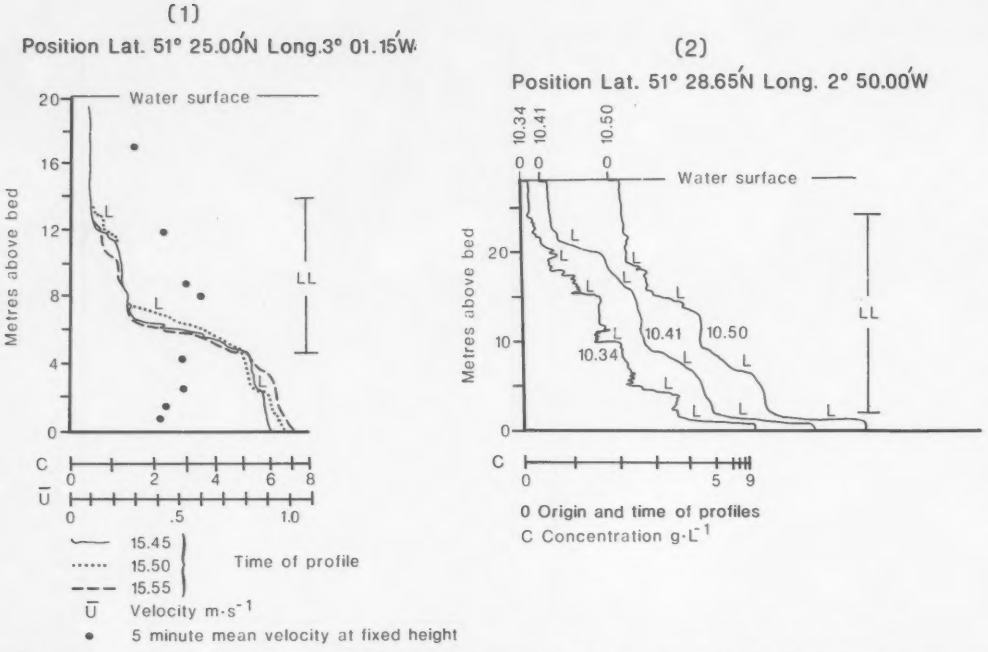

FIG. 8. Typical suspended solids concentration profiles showing "steps" and their stability over 10- and 16-min periods. Synchronous velocity data is available in (1). By analogy with stratification of salinity (halocline) (US Naval Oceanographic Office 1966) and temperature (thermocline) (Defant 1961) we have adopted the term LUTOCLINE (L) (from "Lutum," Latin = mud) to describe these discontinuities. A "lutocline" separates two layers of near constant suspended solids concentration and must have a degree of spatial and temporal continuity. Where two well-mixed layers are separated by a series of steps in the profile or by a rapid change in gradient, this comprises a "lutocline layer" (LL) (by analogy with Proudman 1953). See also Fig. 10.

sand layers (Fig. 4). The origin of the massive "structureless" clay layers is unknown, but the occasional presence of stationary suspensions in the area and the absence of mineral segregation within them indicates that the massive layers may represent single depositional events.

Kirby and Parker (1980) have suggested that deposition in this environment is likely to be of a rapid and discontinuous nature in which regularly developed dense stationary suspensions, or parts thereof, dewater and "survive" only exceptionally. Such a process still results in a deposition rate of some tens of centimetres in a few years. Bridgwater Bay is clearly a complex area involving both long-term sediment source areas, which contribute sediment to the overall fine sediment circulation system, and long-term sinks to which sediment eventually returns.

STATIONARY SUSPENSIONS

Acoustically detectable stationary suspensions generally occur in the bottom of channels as a single layer with a horizontal surface, but also show multiple layering, in which the lowermost layer has a marked relief, mirroring the underlying seabed topography (Fig. 5). The characteristics of the reflectors have been shown to depend on the state of consolidation of the stationary suspension (Parker and Kirby 1977, 1982a). These echo sounder records show stationary suspensions at various stages of consolidation towards settled mud.

The distribution of acoustically detectable stationary suspensions is shown in Fig. 6. In contrast to the mobile suspensions the distribution was confined to localized pools, which were principally located in the channels. They were common in the channel from "The Shoots," where they reached 5 m in thickness, approximately to Portishead, although they occasionally extended as far downstream as Clevedon (Fig. 1). In Newport Deep such suspensions were generally 0.5–1.5 m thick and occurred over every neap period surveyed. Stationary suspensions were less frequently observed, and reached only 0.5 m thick in Bridgwater Bay. They were occasionally found in the Holms Channel but have never been observed in the area west of Flat Holm and north of Culver Sand.

Tides with a range ≈6.5 m at Avonmouth form an approximate limit below which large scale "survival" of acoustically detectable stationary suspensions occurs throughout the estuary. Tides with these or lower ranges, and hence energy conditions, occur on up to 5 d (mean 1.5 d) in the lunar cycle. Recent Port of Bristol Authority surveys are broadly consis-

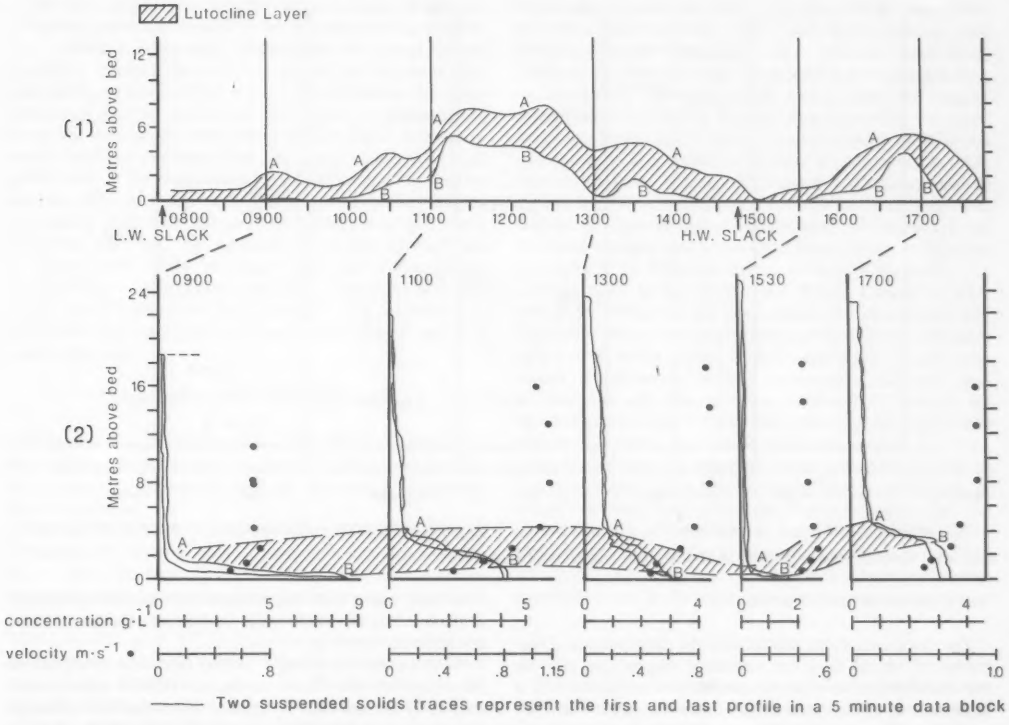

FIG. 9. (1) Variation in thickness of the lutocline layer A−B during 10 h of a neap tide with, (2), accompanying suspended solids profiles and velocity field. Position Lat. 51°25.00′N; Long. 3°01.15′W.

tent with the IOS data confirming that stationary suspensions become detectable on tides ≃7.0 m range and have a residence time of 3−4 d during neaps in the vicinity of Avonmouth (R. Pickstock personal communication). Stationary suspensions remain acoustically detectable throughout the semidiurnal cycle under these conditions, indicating that mixing of the sharp upper interface does not occur and that any lateral translations are of limited extent. In situ continuous gamma-ray transmission density profiles show that such stationary suspensions have a surface density ≃1.05 $t \cdot m^{-3}$ and a layered structure with a variable maximum basal density value (Kirby and Parker 1977).

Tides of ≃6.5 m range correspond to maximum surface tidal stream velocities in the range 1.8−2 $m \cdot s^{-1}$ in the Bristol Deep (Admiralty Chart 1176). On tides of similar height, anchored experiments off Clevedon (IOS unpublished data) revealed maximum velocities in the range 0.55−0.6 $m \cdot s^{-1}$ at 0.25 m above the bed. Fitting a logarithmic velocity profile to mean velocity data from a bed mounted rig in the lower 2 m of the flow gave maximum shear velocities of 0.06−0.1 $m \cdot s^{-1}$ with correlation coefficients which were always >0.95 and generally >0.97. However, care must be taken when interpreting these shear velocities in terms of a bed shear stress as the velocity profile can depart significantly from logarithmic in the lower 0.25 m of the flow, especially where high sediment concentrations occur.

MOBILE SUSPENSIONS

The plan distribution of average suspended solids data (Fig. 7) shows a zone of marked lateral concentration gradient along the main channel of the Severn between "The Shoots" and the Holm Islands and extending across the Inner Bristol Channel to the English coast near Watchet (Kirby and Parker 1982). This suspended solids front occupies a narrow zone at the surface and bed on spring and neap tides. The concentration on the English side of the front was consistently higher, >4.0 $g \cdot L^{-1}$ at the bed on spring and neap tides, than on the Welsh side, where it is generally <0.5 $g \cdot L^{-1}$.

Instantaneous vertical profiles and long-term time average data shows that over much of its length, the front is steeply inclined and extends to the bed of the estuary. It is not a passive feature associated with some controlling salinity or temperature structure of the estuary, although the mechanisms leading to its formation and stability are not entirely clear (Kirby and Parker 1982).

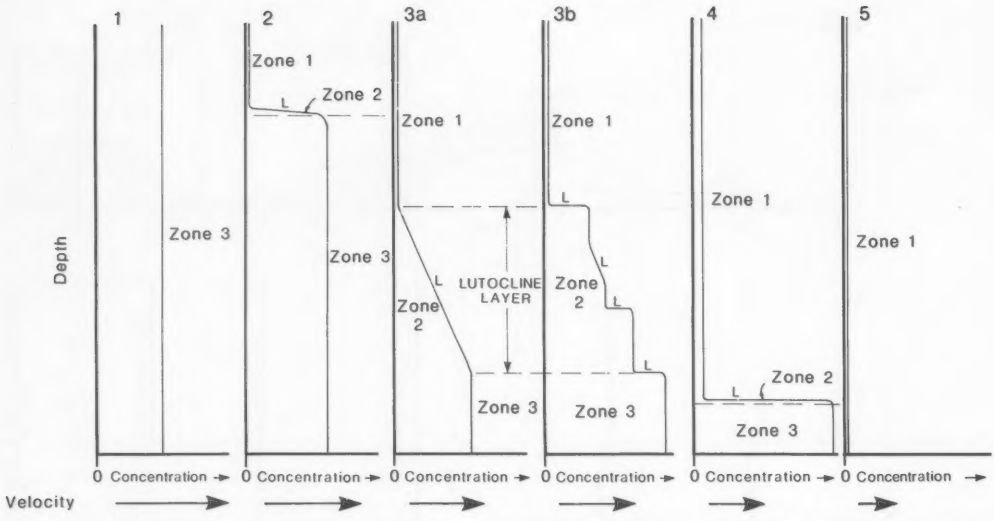

FIG. 10. Concentration profiles in ideal three zone mobile suspension model.

BEHAVIOR OF MOBILE SUSPENSIONS

The discussion above has outlined the distribution and formation of settled mud and stationary suspensions and the regional distribution of mobile suspensions on the basis of a large number and a varied range of measurements. The 2300 vertical profiles considered on a regional average basis can also be used to examine the sequence of changes in the vertical structure of mobile suspensions resulting from the controlling semidiurnal and spring-neap tidal current energy cycles. The anchored ship experiments provide velocity data to assist in interpretation of the processes involved.

On the semidiurnal timescales, an examination of the vertical structure of the suspensions during spring tides shows the following sequence of changes. At maximum flood or ebb velocities, suspended solids concentrations tend to be constant from the bed to the surface reaching 5.0 $g \cdot L^{-1}$ in the Bristol Deep. As the tide decelerates, the suspended fine sediment starts to settle while the suspension is still moving along the estuary at 0.5–1.0 $m \cdot s^{-1}$. This settling results in the creation of one or more marked "discontinuities" or "steps" in the vertical profiles. As velocity continues to decrease, the layers subside through the water column. Figure 8 shows a typical set of results. The persistence of this identifiable structure over periods of many minutes implies that the discontinuities have a length scale measured in hundreds of metres. Quasi-simultaneous measurements show the process to occur throughout the estuary, although it is particularly well developed in the turbid water mass on the English side.

Eventually, towards slack water, the layers subside to the bed forming dense mobile layers with concentrations in the range 3.0–15.0 $g \cdot L^{-1}$ and with a maximum thickness ≈3 m. Near slack water, these dense layers come to a halt and finally at slack water, the whole water column may become stationary for a short period.

After a period of perhaps 1 h this layer is re-entrained on the succeeding tide. The re-entrainment phase is again characterized by the presence of marked discontinuities, although the duration of this phase and the stability of the discontinuities is less than on the decelerating (settling) phase.

Thus, the semidiurnal timescale on spring tides is characterized by alternate mixing of fine sediment to the water surface and subsequent settling, in which all but a background population, <0.5 $g \cdot L^{-1}$, which is supported by the residual turbulence in the water column, reaches the estuary bed (Kirby and Parker 1977).

Over the longer, spring to neap cycle, the total turbulent energy in the system progressively decreases. This results, firstly, in incomplete mixing and the turbid layers persist progressively longer into the tide until they completely survive each velocity maximum. They remain as discrete layers, with a spatial continuity over several kilometres, moving with each tide and changing thickness in response to fluctuations in the energy field. A typical set of results during this phase is shown in Fig. 9.

Eventually, towards neap tides, the tidal velocities are insufficient to re-erode the dense near-bed layer after slack water and it survives throughout an entire semidiurnal cycle as a stationary suspension. After several days, the layer is re-entrained and dispersed during the early part of the next neap to spring cycle. The entrainment phase is short. Individual profiles show discontinuities similar in appearance to those observed on the settling phase although, as on the same phase of the semidiurnal cycle, the discontinuities have only a short lifespan.

The rise and fall through the water column of stepped suspension structures caused by the alternate mixing and settling, which is particularly pronounced on springs, is too dynamic a process to be coupled in any way to the temperature and salinity structure of the estuary. Field observations have confirmed that the occasional and slight departures from vertically well-mixed conductivity profiles result in gradient zones which are not coincident with those of the suspended solids field (IOS unpublished data). Although the sensors used are affected by the state of aggregation of the particles it is likely that, with the possible exception of the lower 0.5 m of the flow, the variations in output as steps are traversed relate solely to changes in mass concentration (Smith 1982). In addition, the few analyses of the different layers which have been completed do not show any significant mineralogical segregation (R. Bryant personal communication).

Comparison with other Estuaries

When the concentration values and states of occurrence of fine sediment in the Severn are placed in the context of other turbid coastal environments, they are seen to be typical rather than exceptional.

Two of the better documented, large, muddy estuaries in Europe are the Gironde and the Loire (France). The Gironde has a lower tidal range (2−6 m) but the suspended sediment field experiences similar semidiurnal and spring-neap fluctuations to those in the Severn (Glangeaud 1938; Allen et al. 1974a, b; Allen et al. 1975). The estuary possesses a regional lateral asymmetry in the suspended solids field with the turbid zone on the left bank, as in the Severn. However, in the Gironde, the asymmetry is more pronounced on neap tides and no marked suspended solids front has been reported to date.

Mobile suspensions range between 0−5 and 5−10 $g \cdot L^{-1}$ in the Gironde. These are the "dispersed suspensions" and "bouchon vaseaux" described by Bellesort (1973). Denser suspensions (100−300 $g \cdot L^{-1}$) are also detected commonly and radioactive tracer experiments have been interpreted as showing the slow creep of these dense layers (Allen et al. 1975). Such suspensions are detectable acoustically and are termed "creme de vase"; they are equivalent to the phenomena known to us as stationary suspensions. A further similarity to our findings in the Severn is that the radioactive tracer experiment showed a very low dispersion rate of the silt both on the regional scale and in the vertical (Allen et al. 1975).

In the Loire Estuary, suspended solids concentrations commonly reach 10 $g \cdot L^{-1}$ at the surface and 100−150 $g \cdot L^{-1}$ at the bed creating a turbidity field comparable with that in the Severn (Migniot 1974; Gallenne 1974).

Even though less rigorous measurement techniques have been employed, the turbidity fields of these French examples are sufficiently well documented that lutoclines and fronts might be expected to occur here too. The distribution of mobile suspensions is not well enough known in other estuaries to allow direct comparisons with Severn and Bristol Channel results. However, acoustically detectable stationary suspensions are commonly encountered in coastal waters. They are known from temperate latitudes, e.g. from the UK: Thames (Inglis and Allen 1957), Humber (BTDB 1981), Mersey (Price and Kendrick 1963), and other estuaries; from Belgium: Scheldt (Wartel 1974); from Holland: Lower Rhine (Kirby et al. 1980). In subtropical and tropical latitudes, they are distributed even more widely — e.g. along the coast of South America stretching from the Amazon past the Demerara River in Guyana (Delft Hydraulics Laboratory 1962) to the Orinoco delta in Venezuela (Eisma et al. 1978); in the USA: Savannah Estuary (Harris 1965) and the Mississippi and its approaches (Wright 1970; Wells 1983). In South East Asia they occur along the Indian coast (Kurup 1977; Kendrick and Derbyshire 1983), and in the Chao Phya estuary in Thailand (Allersma et al. 1966), as well as in many other areas.

From work in the Severn and Bristol Channel (Parker and Kirby 1982a), it has been established that acoustically detectable stationary suspensions develop from stationary suspensions which are not, initially, detectable by such techniques. Furthermore, initially undetectable stationary suspensions can only develop where the flux of sediment to the bed is too rapid to permit a normally consolidated settled mud bed to be formed. Such rapid sedimentation can only arise from the halting of a dense near-bed mobile suspension as described above for the Severn. The examples cited above, in which stationary suspensions are known to occur, span the complete range of estuary types from well-mixed to highly stratified and from micro- to macro-tidal and include open-sea situations, indicating that discontinuously stratified mobile suspensions are likely to be equally widespread in nature.

Discussion

The distribution and behavior of fine sediment in the Severn Estuary and Inner Bristol Channel based on a large field data set obtained using some new instruments and techniques has been reviewed. In the course of this work we have adopted a behavioral model, describing three distinct states of fine sediment occurrence and the processes and timescales on which they evolve, which is applicable to this and other highly turbid coastal environments. Fine sediment phenomena in the region considered are large in scale, well developed, and predictable in occurrence, making them relatively easy to document. However, the conclusions based on these observations may also be relevant to less extreme, lower turbidity environments where the phenomena are smaller in scale and less well, or only occasionally, developed.

In trying to rationalise the range of structures present in the 2300 vertical profiles through mobile suspensions it has become apparent that they may be represented by a multilayer model which, ideally, has three principal zones (Fig. 10). The basis for this division of the structure is that different processes are dominant, at least during the formation of each layer. The zones comprise:

1) An upper "well-mixed" zone of nearly constant concentration, whose base is formed by the first lutocline. The settling flux of sediment is dominant during the initial development of this layer. The concentration is generally $<0.5\ g \cdot L^{-1}$.

2) A lutocline layer in which concentration increases rapidly with depth. The lutocline layer may consist of one, two, or several distinct or identifiable lutoclines. Individual details

of this structure may be followed for periods of several minutes (hundreds of metres) while the gross structure of the lutocline layer persists, at times, over the whole tidal period (thousands of metres). The turbulent momentum flux and settling flux are implied to be more or less in balance over long periods. The layer may broaden or narrow as one process achieves a relative ascendancy, or disappear if either process becomes significantly dominant.

3) A lower "well-mixed" zone of higher concentration which is a reservoir from which mobile fine sediment is mixed up into zone 1 via the lutocline layer during accelerating phases of the tide and to which it returns by settling during decelerating phases. The processes operating in this layer are perhaps influenced by hindered settling or may, at times, be dominated by turbulent momentum fluxes which maintain the mixing.

The cycles of mixing and settling occur on the semidiurnal and lunar timescales, as outlined above, and thus at any time, one or two zones may be absent from the ideal structure depending on how much mixing has occurred.

Recognition of this generalized structure, which is provisional and the subject of further study, has a number of consequences for our approach to the study of fine sediment behavior, among which the more significant are:

1) The presence of lutoclines implies that for long periods settling dominates or balances mixing, even in this turbulent, high energy estuary.

2) Settling of material while the suspensions are still mobile leads to a much higher flux to the bed than would be possible if settling proceeded only over slack water.

3) The regular halting of thick ($\simeq$3 m) suspended sediment layers, virtually as single units, causes difficulties in deciding when "deposition" has occurred. Similarly, grain by grain attachment to the bed is not an appropriate mechanism for deposition in such environments.

4) Erosion by grain by grain detachment from the bed is not an appropriate concept in areas where stationary suspensions occur. The density structure of these suspensions varies spatially as well as increasing with depth and through time and consequently their erosion potential cannot be parameterized by a single critical shear stress value.

5) The presence of persistent vertical discontinuities in the structure of mobile suspensions may have general implications for estuarine dynamics, for sediment flux computations based on depth-average data and for environmental management. The vertical and horizontal discontinuities in suspended solids concentration are indicative of the differing behavior of sediment compared to dissolved components in the water column. The presence of stationary suspensions leads to many dredging, hydrographic surveying and environmental problems.

Acknowledgments

Thanks are due to R. Bryant (Swansea University), the Port of Bristol Authority and Welsh Water Authority for permission to use unpublished data. We appreciate the comments and advice of Dr D. J. A. Williams in the Department of Chemical Engineering at Swansea University and Dr G. C. Sills in the Marine Soils Group at Oxford University who have cooperated in this research. In IOS we are grateful for the guidance and assistance of T. J. Smith (now Swansea University), C. A. Kirk, M. A. S. Moore, K. R. Dyer, and members of the Taunton Instrumentation Group.

ALLEN, G. P., P. CASTAING, AND A. KLINGEBIEL. 1974a. Suspended sediment transport and deposition in the Gironde Estuary and adjacent shelf. International Symposium on Inter-relationships of Estuarine and Continental Shelf Sedimentation. Institut de Géologie du Bassin d'Aquitaine. 7: 27–36.

ALLEN, G. P., R. BONNEFILLE, G. COURTOIS, AND C. MIGNIOT. 1974b. Sedimentary processes of the mud in the Gironde Estuary. Contribution of a radioactive tracer to the study of mud displacements. La Houille Blanche N° 1/2: 129–136. (In French)

ALLEN, G. P., G. SAUZAY, P. CASTAING, AND J. M. JOUANNEAU. 1975. Transport and deposition of suspended sediment in the Gironde Estuary, France. Estuarine Processes II, Academic Press, New York, NY. p. 63–79.

ALLERSMA, E., A. J. HOEKSTRA, AND E. W. BIJKER. 1966. Transport patterns in the Chao Phya Estuary. Proc. Conf. Coastal Eng. 10: 632–650.

BELLESORT, B. 1973. Tracer techniques in sediment transport. The use of tracers in sedimentology. Centre d'études nucléaires de Saclay. IAEA Tech. Rep. Ser. 145: 31–40.

BRITISH TRANSPORT DOCKS BOARD. 1981. A report on density measurements and echo sounding at Humber ports. Report 286: 43 p.

BRYANT, R., A. E. JAMES, AND D. J. A. WILLIAMS. 1980. Rheology of cohesive suspensions, p. 279–287. *In* Collins et al. [ed.] Industrial embayments and their environmental problems. A case of study of Swansea Bay. Pergamon, New York, NY.

BRYANT, R., AND D. J. A. WILLIAMS. 1983. Characteristics of suspended cohesive sediment of the Severn Estuary, U.K. Can. J. Fish. Aquat. Sci. 40(Suppl. 1). (This issue)

DEFANT, A. 1961. Physical oceanography. Vol. 1: p. 120. Pergamon, New York, NY.

DELFT HYDRAULICS LABORATORY. 1962. Report on siltation of the Demerara Bar Channel and coastal erosion in British Guiana. Demerara Coastal Investigations, Delft Hydraulics Laboratory, Delft, Netherlands. 237 p.

EISMA, D., S. J. VAN DER GAAST, J. M. MARTIN, AND A. J. THOMAS. 1978. Suspended matter and bottom deposits of the Orinoco Delta. Turbidity, mineralogy and elementary composition. Neth. J. Sea Res. 12: 224–251.

GALLENNE, B. 1974. Study of fine material in suspension in the estuary of the Loire and its dynamic grading. Estuarine Coastal Mar. Sci. 2: 261–272.

GLANGEAUD, L. 1938. Transport and sedimentation in the estuary and mouth of the Gironde (petrographic character of the fluviatile, brackish coastal and neritic deposits). Bull. Soc. Geol. Fr. Paris Ser. 5: 599–631. (In French)

HARRIS, J. W. 1965. Means and methods of inducing sediment deposition and removal. *In* Proc Federal Inter-Agency Sedimentation Conference 1963. U.S. Dep. Agric. Misc. Publ. 970: 669–674.

HYDRAULICS RESEARCH STATION. 1980. The Severn Estuary. Measurements of the vertical and lateral distribution of mud suspensions. Rep. No. Ex 965. 5 p.

INGLIS, C. C., AND F. H. ALLEN. 1957. The regimen of the Thames Estuary as affected by currents, salinities and river flow. Proc. Inst. Civ. Eng. London 7: 827–868.

KENDRICK, M. P., AND B. V. DERBYSHIRE. 1983. Factors affecting the supply and distribution of sediment in the turbid coastal environment. Can. J. Fish. Aquat. Sci. 40(Suppl. 1). (This issue)

KIRBY, R., W. R. PARKER, AND W. H. A. VAN OOSTRUM. 1980. Definition of the seabed in navigation routes through mud areas.

Int. Hydrogr. Rev. LVII(1): 107–117.

KIRBY, R., AND W. R. PARKER. 1977. The physical characteristics and environmental significance of fine sediment suspensions in estuaries. National Academy of Sciences/American Association for the Advancement of Science. Symposium on Estuaries, Geophysics and the Environment. NAS. p. 110–120.

1980. Settled mud deposits in Bridgwater Bay, Bristol Channel. IOS Rep. 107: 65 p.

1982. A suspended sediment front in the Severn Estuary. Nature 295: 396–399.

KRONE, R. B. 1963. Rheologic properties of estuarial sediments. University of California, Berkeley, CA. Rep. SERL No 63-8: 91 p.

KURUP, P. G. 1977. Studies on the physical aspects of the mud banks along the Kerala Coast with special reference to the Purakad Mud Bank. Bull. Dep. Mar. Sci. Univ. Cochin VIII: 72 p.

MIGNIOT, C. 1968. A study of the physical properties of various forms of very fine sediment and their behaviour under hydrodynamic action. La Houille Blanche 7: 591–620. (In French)

1974. Comparative study of the rate of siltation in different zones of the Loire Estuary. La Houille Blanche 1/2: 137–147. (In French)

PARKER, W. R., G. C. SILLS, AND R. E. A. PASKE. 1975. In situ nuclear density measurements in dredging practice and control. B.H.R.A. Fluid Engineering. First International Symposium on Dredging Technology. Paper B3, p. 25–42.

PARKER, W. R., AND R. KIRBY. 1977. Fine sediment studies relevant to dredging practice and control. Second International Symposium on Dredging Technology. B.H.R.A./Texas A and M Pap. B2: 15–25.

1982a. Time dependent properties of cohesive sediment relevant to sedimentation management — European experience, p. 573–589. *In* V. J. Kennedy [ed.] Estuarine comparisons. Academic Press, New York, NY.

1982b. Sources and transport patterns of sediment in the inner Bristol Channel and Severn Estuary. "Severn Barrage." Proceedings of Institution of Civil Engineers Symposium. Thomas Telford. Pap. 18: 181–194.

PARTHENIADES, E. 1965. Erosion and deposition of cohesive soils. J. Hydraul. Div. Proc. Am. Soc. Civ. Eng. 91(HY1) Paper 4204: 105–139.

PRICE, W. A., AND M. P. KENDRICK. 1963. Field and model investigation into the reasons for siltation in the Mersey Estuary. Proc. Inst. Civ. Eng. London 24: 473–518.

PROUDMAN, J. 1953. Dynamical oceanography. Methuen, London, p. 196.

SCHUBEL, J. R., AND E. W. SCHIEMER. 1973. The cause of the acoustically impenetrable, or turbid, character of Chesapeake Bay sediments. Mar. Geophys. Res. 2: 61–71.

SMITH, T. J. 1982. The response of electro-optical turbidity meters to cohesive sediments. IOS Rep. 137: 22 p.

STOMMEL, H. 1953. Computation of pollution in a vertically mixed estuary. Sewage Indust. Wastes, p. 1065–1071.

US NAVAL OCEANOGRAPHIC OFFICE. 1966. Special publication glossary of oceanographic terms, p. 75.

WARTEL, S. 1974. Bed features in the estuary of the Schelde (Belgium). Professional Paper 1974/11. Ministère des Affaires Économiques. Bruxelles. 11 p.

WELLS, J. T. 1983. Dynamics of coastal fluid muds: low, moderate and high tide range environments. Can. J. Fish. Aquat. Sci. 40(Suppl. 1). (This issue)

WELSH WATER AUTHORITY. 1983. Severn Estuary Survey and Systems Panel. Severn Estuary Joint Committee. (In press)

WILLIAMS, D. J. A., AND R. BRYANT. 1979. Rheology of suspensions. Report 7 of Research Grant F60/B4/02 from Natural Environment Research Council. 15 p.

WRIGHT, L. D. 1970. Circulation, effluent diffusion and sediment transport, mouth of South Pass, Mississippi River Delta. Coastal Stud. Inst. Louisiana State Univ. Tech. Rep. 84: 56 p.

Characteristics of Suspended Cohesive Sediment of the Severn Estuary, U.K.[1]

R. BRYANT AND D. J. A. WILLIAMS

Department of Chemical Engineering, University College of Swansea, Swansea SA2 8PP, U.K.

BRYANT, R., AND D. J. A. WILLIAMS. 1983. Characteristics of suspended cohesive sediment in the Severn Estuary, U.K. Can. J. Fish. Aquat. Sci. 40(Suppl. 1): 96–101.

Characteristics of suspended cohesive sediment from the benthic boundary layer of the Bristol Channel/Severn Estuary were examined at one location (51°27.66′N, 2°53.20′W). Samples were collected in vertical profiles over the bottom 2 m of the water column at times near to, and at low and high slack water periods on spring and neap tides. Primary particle size distributions obtained using a Coulter Counter (range 1.59–50 μm) and electron microscopy (range 0.1–20 μm) reveal bimodal (volume) frequency distributions with a lower mode fixed at 1.59 μm and a higher mode variable between 6 and 30 μm. When these data are converted to number frequency distributions, the higher mode effectively vanishes, while the lower is retained. Suspended sediment mineralogy, of dispersed samples, was determined by individual and multiple particle examination using analytical electron microscopy. Average suspended sediment composition was found to be illite 44%, quartz 23%, chlorite 19%, calcium carbonate 5%, kaolinite 4%, and organic carbon 3% (by weight). Floc diameters estimated from hindered settling experiments were ≈ 140 μm possessing a sedimentation velocity in the range 1.8–2.0 $mm \cdot s^{-1}$, in good agreement with field observations of temporal changes in the vertical distribution of turbidity.

Key words: suspended cohesive sediment, flocculation, Bristol Channel.

BRYANT, R., AND D. J. A. WILLIAMS. 1983. Characteristics of suspended cohesive sediment in the Severn Estuary, U.K. Can. J. Fish. Aquat. Sci. 40(Suppl. 1): 96–101.

On a examiné à un endroit (51°27.66′N, 2°53.20′W) les caractéristiques du sédiment cohésif en suspension de la couche limite benthique du chenal Bristol/estuaire de la Severne. Des échantillons ont été prélevés en des profils verticaux au-dessus des 2 m inférieurs de la colonne d'eau à l'étale du courant, ou à peu près, de basse ou de haute mer en périodes de marées de vive eau et de morte eau. La distribution des tailles des particules primaires, obtenues par compteur Coulter (gamme de 1,59–50 μm) et microscope électronique (gamme de 0,1–20 μm), indique des fréquences bimodales (en volume), avec mode inférieur à 1,59 μm et un mode supérieur variable entre 6–30 μm. Le mode supérieur disparaît quand ces données sont converties en distributions de fréquence par nombre, alors que le mode inférieur demeure. Un examen individuel et multiple, par microscopie électronique analytique, a été utilisé pour déterminer les propriétés minéralogiques du sédiment en suspension d'échantillons dispersés. La composition moyenne en est la suivante: illite 44%, quarts 23%, chlorite 19%, carbonate de calcium 5%, kaolinite 4% et carbone organique 3% (en poids). Le diamètre des flocons, estimé dans des essai de sédimentation retenue, est ≈ 140 μm, avec vitesse de sédimentation comprise entre 1,8 et 2,0 $mm \cdot s^{-1}$, ce qui s'accorde bien avec des observations sur le terrain de changements temporels de distribution verticale de la turbidité.

Received December 9, 1981
Accepted July 16, 1982

Reçu le 9 décembre 1981
Accepté le 16 juillet 1982

THE ubiquitous nature of cohesive sediment deposits on the coastline of the Bristol Channel/Severn Estuary have been reported by Sollas (1883). Since that study these sediments received little attention until recently when the distribution of sediment types and the nature of suspended material in surface waters was investigated by Hamilton et al. (1979). The occurrence of dense suspensions of cohesive sediment was observed by Kirby and Parker (1977) and the areal distribution of a high turbidity zone of this estuarine system located by Kirby and Parker (1983). The physico-chemical properties of such suspensions are of theoretical and practical interest since their understanding is essential to the analysis of engineering and environmental problems involving cohesive sediment transport (Krone 1972; Odd and Owen 1972).

This paper describes particle size, mineralogy, and the

[1]This paper forms part of the Proceedings of the Dynamics of Turbid Coastal Environments Symposium convened at the Bedford Institute of Oceanography, Dartmouth, N.S., Canada, September 29–October 1, 1981.

Printed in Canada (J6754)
Imprimé au Canada (J6754)

distribution of solids concentrations of cohesive suspensions collected over the bottom 2 m of flow at one location (51°27.66'N, 2°53.20'W), Fig. 1. Such information is previously unreported for these dense suspensions in the Severn Estuary. This location is sited at a position in the Severn Estuary where the flow is essentially in a SW−NE direction parallel to the English coast. The tidal excursion at this position is ~ 25 km and allows the acquisition of an integrated picture of the suspended sediment in the zone of high turbidity over complete tidal cycles.

Materials and Methods

Sixty-eight samples of suspended sediment were collected during the cruise of the M. V. *Gardline Locater* (September 1978) using the vacuum sampling apparatus previously described by Bryant et al. (1980). The apparatus was allowed to rest on the seabed for a minute or two to allow the sampling nozzles to align with the current and to allow transport of any disturbed bed sediments away from the sampling nozzles.

Samples were collected synoptically in vertical profiles spaced from 0.1 to 2.0 m from the seabed. Due to weather conditions, samples were mainly collected near slack water periods when the vertical movement of suspended sediment is largely towards the bed. Sampling times and tidal ranges are shown in Table 1.

Once the samples had been brought aboard ship they were divided. One portion was refrigerated (at 40°C) and stored until return to the laboratory, the other portion was centrifuged, dried, and kept as reference material. Large aliquots of freshly collected samples were used for hindered settling tests and gravimetric analysis. After desalination and hydrogen peroxide digestion, samples were peptized with sodium pyrophosphate solution and diluted for particle size analysis and specimen preparation for analytical electron microscopy. Refrigerated (untreated) samples were diluted and prepared for electron microscopy so that the composition of individual flocs or fragments thereof could be examined. The mean density of the particulate phase determined from triplicate tests with an s.g. bottle was found to be 2500 $kg \cdot m^{-3}$.

Gravimetric Analysis

Aliquots of the freshly collected samples were drawn on to preweighed Sartorius membrane filters (0.2 μm pore diameter). The filters were then vacuum dried to constant weight. In some cases serial dilutions were necessary to dilute samples possessing high suspended solid concentrations to render them amenable to analysis.

Hindered Settling Experiments

Hindered settling experiments were performed on two samples of high suspended solids concentrations (~ 40−50 $kg \cdot m^{-3}$) (collected at 8:06 and 7:14 GMT on September 12, 1978). The concentration of suspended solids in these samples was increased by decantation of the supernatant fluid and decreased by dilution with a surface seawater sample of a salinity similar to that of the original sample (27‰ ± 0.5). The range of suspended solids concentrations

FIG. 1. The Severn Estuary/Upper Bristol Channel showing the location of the sampling site.

studied in these experiments (40−140 $kg \cdot m^{-3}$) is within the range of concentrations encountered in the field (Kirby and Parker 1983). Settling experiments were performed with suspensions held in one litre measuring cylinders illuminated from the rear and supported on a vibration free platform in the ship's laboratory. The maximum settling rate (U) of flocculated sediment/water interface was determined for each solids concentration.

Particle Size Analysis

Particle size distributions were obtained using a Model TA II Coulter Counter fitted with a 140 μm sensing orifice immersed in a sodium chloride solution (35 $kg \cdot m^{-3}$) precleaned by membrane filtration (0.45 μm pore diameter). In the absence of a Population Accessory, particle numbers were calculated from the histogram of relative volumes versus particle size assuming the particles to be spherical.

The response of the Coulter Counter is nonlinear outside the range of 10−40% of the orifice diameter (Treweek and Morgan 1977). The errors produced by such a nonlinear

TABLE 1. Sampling information.

Date	Predicted time GMT Cardiff[a]	Predicted height Cardiff[a]	Sampling times GMT	Sampling times Local tidal[b]	Local tidal range[b]	Depth Average Suspended Solids Concn $\langle C \rangle_2$ kg·m^{-3}
Sept. 12, 1978	01:29	9.3	7.14	26 min pre LW		8.7
	07:30	3.5	8.06	35 min post LW		3.9
	14:23	9.6	8.43	72 min post LW	7.5 m	0.9
	20:32	3.1	13.10	129 min pre HW	5.8 m	0.4
			13.49	72 min pre HW		0.4
			14.41	4 min post HW		0.4
			15.33	48 min post HW		0.8
Sept. 21, 1978	03:52	1.1	15.50	(Data not available)		6.1
	09:37	11.9	16.40	(Data not available)		8.4
	15:57	1.4				
	21:59	11.5				
Sept. 23, 1978	04:24	2.4	16.43	0 min pre LW	9.3 m	8.1
	10:39	10.2	17.33	50 min post LW		9.6
	16:24	2.8				
	23:05	9.7				
Sept. 24, 1978	04:44	3.1	17.18	42 min pre LW		1.6
	11:19	9.5				
	16:53	3.5				
	23:54	9.0				

[a]Data from Admiralty Tide Tables, Vol. 1, European Waters 1978. High and Low Water.
[b]From data collected on station.

response, for small particles are such that these fractions may be underestimated (Shideler 1976). Triplicate sample analyses indicated that data were reproducible to 1% maximum variation per channel.

It has been observed that floc diameters determined with a Coulter Counter are not equivalent to those determined microscopically (e.g. Ham 1967). The volume of an aggregate determined by the Coulter Counter was equivalent to the solid component of the floc, virtually no contribution being made by the pore fluid within a floc. At certain porosities the solid material of the floc may be underestimated by as much as 25% (Treweek and Morgan 1977). Although flocs may survive the sampling, stirring, and sensing procedures of the Coulter Counter, analysis of flocculated systems gives no indication of the actual physical (hydrodynamic) size of the floc in the natural environment without some independent estimate of the floc porosity. Any physical interpretation of the diagnostic value of the size of flocculated estuarine suspended sediment so determined, (e.g. as reported by Kranck (1973) or Hamilton et al. (1979)) is therefore to be treated with caution.

The present study, in contrast to that of Hamilton et al. (1979), was therefore restricted to the analysis of dispersed samples to estimate the primary particle size distribution.

Electron Microscopy

Diluted aliquots of disaggregated, peroxide digested, suspended sediment samples were drawn on to Nuclepore filters (0.2 μm pore diameter) with the assistance of vacuum. These filters were subsequently carbon-coated and then floated in chloroform whereupon the filter free, particle impregnated, carbon film could be floated on to wide aperture gold E.M. grids. Specimens were examined using a Phillips E301 Transmission electron microscope fitted with an energy dispersive X-ray analyzer, calibrated for quantitative chemical analysis after the method of Pooley (1977).

Sediment Composition

Mineralogical composition was obtained by the solution of a set of simultaneous mass balance equations incorporating bulk chemical sediment composition with mineral component chemistries (determined by analytical electron microscopy) (Bryant and Williams 1981).

The carbonate content of the samples was determined by the weight loss from sediment bearing filters after gravimetric analysis and subsequent digestion in hydrochloric acid (1 mol/L). Organic carbon was determined by chromic acid oxidation (Gaudette et al. 1974).

Results and Discussion

Suspended Solids Concentration

Gravimetric analysis of the samples possesses the advantage over in situ optical methods of suspended solids determination in that in the former, analysis is independent of particle size whereas in the case of optical methods analysis is affected by the state of flocculation of the solid. Gravimetrically determined suspended solids concentrations in the bottom 2 m of flow ranged between 0.2 and 67 kg·m^{-3} and varied with time of collection and depth (Fig. 2).

Stratification of suspended solids in this region of the Severn Estuary has been previously described (Kirby and Parker 1983). If the suspended solids concentration at 2 m above the bed (the uppermost sampling point used in the present study) is taken to be representative of that of the overlying waters (0.2–5.6 kg·m^{-3}, Fig. 2) then up to 70%

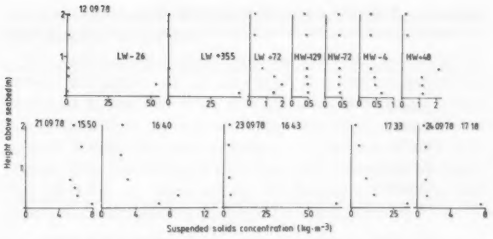

FIG. 2. Gravimetrically determined suspended solids concentrations in the bottom 2 m of flow (showing tidal time in minutes or GMT).

of the total suspended load is contained in the bottom 2 m of flow. Unless the suspended solids concentrations in the region of flow adjacent to the bed are considered in the sediment transport modelling of estuaries possessing highly turbid zones, then estimates of sediment flux and sedimentation rates may be grossly in error. For estuaries without high turbidity zones, the depth mean concentration $\langle C \rangle$ may be taken as typical of near bed values without introducing a significant error.

The data further suggest that the concentration of suspended solids in the surface waters of this high turbidity zone can be two orders of magnitude lower than that within the bottom 0.1 m of flow (i.e. 30−60 kg·m^{-3}). The sampling procedure described herein provides improved resolution of the suspended solids concentration in the benthic boundary layer over that provided by optical methods (Kirby and Parker 1983).

Particle Size Distributions

Size distributions initially obtained as histograms of the relative particle volume as a function of particle diameter (independent of time of collection or position in the water column), are bimodal. This feature is reflected in the average particle size distribution for 68 samples (Fig. 3) revealing a mode at 1.6 μm equivalent spherical diameter (esd) and a minor one at ~ 10 μm (esd). The mode at 1.6 μm can only be so defined in terms of the limited particle size range examined and may lie at smaller particle diameter. Since 1.6 μm is less than10% of the orifice diameter of the Coulter Counter sensing tube, where the instrumental response becomes nonlinear, it is probable that magnitude of this mode has been underestimated. This will, however, only reinforce some of the arguments presented herein.

Conversion of the relative volume data to cumulative volume histograms allowed median particle sizes to be determined. No dependence was found between median particle diameter and suspended solids concentration for all samples (coefficient of correlation = 0.46) suggesting no significant dependence of the particle size distribution on the concentration of suspended solids. Division of the samples into two groups, those collected on September 12, 1978 and those collected between September 21 and 24, 1978, yield corresponding correlation coefficients of 0.18 and 0.7, respectively, thereby confirming the above suggestion.

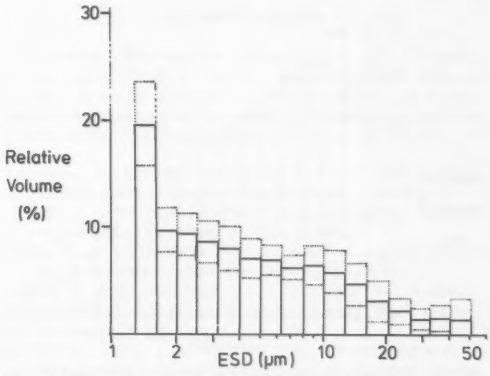

FIG. 3. The average particle size distribution (relative particle volume) for all samples collected. The standard deviation for each size division is shown by the broken lines.

The overall variation of the median particle(volume)diameter was found to be 2.5−9.2 μm.

In heterogeneous flocculating suspensions containing N_i and N_j particles per unit volume of suspension, the frequency of collision between i and j type particles is $\alpha (N_i N_j)$ (Krone 1963). Therefore, relative particle number histograms are appropriate representations of the primary particle size distribution in suspensions of cohesive sediment. Conversion of the relative volume histogram (Fig. 3) to a relative number histogram (Fig. 4) indicates that on the basis of particle number per unit volume of solid, particles < 1.6 μm diameter determine the overall magnitude of the particle population. The secondary mode present in the relative volume histogram disappears and particles < 10 μm contribute < 0.1% of the total number of particles. This suggests that in these samples there exists a stable relative number distribution of fine particles < 10 μm (maximum variation 15%) which is independent of sample position, time of collection, and suspended solids concentration. This implies homogeneous mixing of the suspended sediment at the time and place of flocculation.

The sensitivity of the Coulter Counter response to particles decreases with decreasing particle size below 10% of the orifice diameter and the instrument fails to detect many particles in the submicron range (Shideler 1976). To estimate the magnitude of this undetermined particle size fraction, one sample (collected 2 m above the bed 16:40 GMT, September 21, 1978) was subjected to electron microscope examination. Particle numbers were counted as a function of size for ~ 1000 particles. Analysis showed that 66% of the particles had diameters < 0.25 μm and ≈ 90% of the particles were less than 0.5 μm diameter, indicating that the contribution made by submicron particles to the overall particle size distribution may be quite large.

Suspended Sediment Composition and Floc Properties

The average mineralogy and composition of the suspended sediment (Table 2) indicates that the material is dominated by illitic and chloritic clay minerals with a 20−25% contribution

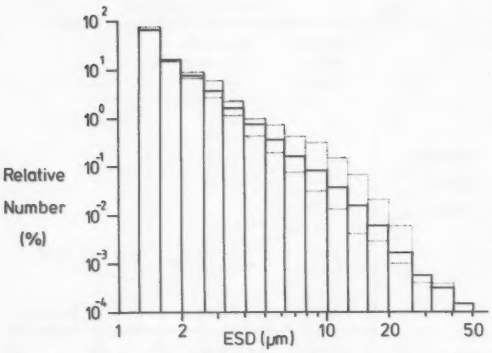

FIG. 4. The average particle size distribution (relative particle number) for all samples collected. The maximum variation for each size division is shown by the broken lines.

from quartz. Although this composition is derived from chemical analysis, it is corroborated by X-ray diffraction analysis (Bryant and Williams 1982). The range of particle sizes examined using analytical electron microscopy (transmission mode) is limited to < 8-10 μm (larger particles being lost from the specimen prior to examination in the microscope). The large particles retained in the specimen were found to be mainly quartz. The precision of bulk chemical analysis (carried out over a large section of the specimen and therefore including many particles) tends to be low, when such a wide particle size range is examined, reflecting the inhomogeneity of the small mass of material inspected. The results of individual particle analysis indicated that the occurrence of quartz particles (those most readily identified) reduced rapidly with particle size, none being found below 0.5 μm diameter. The analysis of size fractions of the suspended sediment extracted from one sample indicates that the mineralogy changed as a function of size, e.g. the minor component kaolinite being enhanced in the 0.1−2.0 μm fractions with respect to the bulk sample from 2 to ~ 10% (Bryant and Williams 1982).

Variations of the sediment composition between groups of samples, depth averaged for various times of collection and time averaged for various positions above the seabed were estimated. These average values were compared within their respective groups. The maximum probability of a significant difference (α) was found to be $0.2 < \alpha < 0.3$ for time averaged groups and $0.1 < \alpha < 0.2$ for depth averaged. The lack of significant mineral segregation throughout the boundary layer suggests an apparent common source for material in the high turbidity zone.

Although the organic carbon content is only 3% by weight of the sediment, the volume will be about 7%, assuming it possesses a specific gravity ≈ 1. The exact effect of this material is at present not known.

Samples of suspended sediment diluted with filtered seawater were filtered on to Nuclepore filters and prepared for electron microscope examination as described previously. This study revealed that the small aggregates or fragments of aggregates that had survived the preparation consisted of particles of mixed mineralogies (quartz and various alumi-

TABLE 2. Sediment composition (average of all samples).

	%
Illite	44 ± 9
Quartz	23 ± 3
Chlorite	19 ± 6
$CaCO_3$	5 ± 2
Kaolinite	4 ± 4
Organics	3 ± 0.5

TABLE 3. Floc properties from hindered settling experiments.

diameter	140−150 μm
density	1150−1160 kg·m^{-3}
floc volume/solids volume	~ 10
max. sedimentation velocity	1.8−2.0 mm·s^{-1}

nosilicates); and that small particles < 0.5 μm tend to be clustered about larger ones (2−10 μm). The arrangement of particles relative to one another in these flocs, observed in the electron microscope cannot be assumed to represent the exact structure that such a floc or aggregate would possess in the natural environment and in this respect is of no further diagnostic value.

Estimates were made of certain physical properties of characteristic flocs of these sediment suspensions using the hindered settling analysis of Michaels and Bolger (1962). Hindered settling occurs in these concentrations down to ~ 10 kg·m^{-3} (Ariathurai et al. 1977). At concentrations above 140 kg·m^{-3} the volume of the flocs is equal to the total volume of the suspension. Such a situation is equivalent to the condition of a recently settled bed prior to the onset of consolidation.

At low concentrations of particles (probably equivalent to << 10 kg·m^{-3}) floc diameter may be limited by a low rate of inter-particle collisions. As the concentration of particles is increased, floc diameter increases and continues to increase until a concentration is reached where floc diameter remains virtually constant. As the concentration further increases the tendency for floc growth is balanced by a concommitant increase in the local shear rate induced by hindered settling of the flocs. Over this concentration range, a dynamic equilibrium is achieved resulting in a floc of constant diameter.

The relationship between $U^{1/5}$ (Peirce and Williams 1966) and volumetric solids concentration ϕ was linear over the range equivalent to 40−100 kg·m^{-3}, yielding characteristic mean floc properties (Table 3). The maximum settling velocity (U_o) of 1.8−2.0 mms^{-1}, which is that of a characteristic mean size floc in an infinitely dilute fluid, approximates the temporal changes of vertical distribution occurring in the field during slack water periods (Kirby and Parker 1982). The hydrodynamic forces applied to the suspended sediment prior to the onset of settling may be different in the laboratory tests compared with the field situation. A short induction period is usually observed in the laboratory tests before the floc settling velocity increases to its maximum value. This implies that when the suspension is homogenized immediately prior to the test, floc structure is, at least, partially destroyed but on

standing, reflocculation rapidly occurs until the equilibrium floc diameter is reached.

The agreement between U_o and the observed changes in the vertical distribution of turbidity imply that characteristic flocs produced in near bed zones of high solids concentration in a hindered settling regime are being advected, without disruption, through the water column during periods of high tidal energy. The magnitude of the shear field (temporal average) that the flocs experience during this process is similar to that experienced in hindered settling experiments (i.e. $\simeq 15\ s^{-1}$).

Conclusions

Complementary analytical techniques are required for estimate of the relative particle number distribution because electronic particle counting techniques cover only a limited size range which does not extend usefully below $\sim 1\ \mu m$. Such techniques similarly return very limited information when they are used to examine flocculated systems. Analytical electron microscopy is a valuable technique for the identification of the size ranges and relative numbers of the different component minerals of the sediment, particularly in the submicron size ranges. In the transmission mode, the upper limit of particle size that can be examined is $\sim 8-10\ \mu m$.

The cohesiveness of suspended sediments in the Severn Estuary is explained by the large clay mineral fraction (especially illite at 70–80% on a particle number basis) which undergoes orthokinetic flocculation in saline environments (e.g. Edzwald et al. 1974). It is clear, however, from the microstructure of the flocs that larger quartz particles become involved in their formation. Indeed this heterogeneity is reflected in the ratio of floc volume to solid volume (~ 10; Table 3) for these suspensions, which is much lower than that for pure aluminosilicate clay suspensions (~ 100; Michaels and Bolger 1962). It is clear from a comparison of laboratory estimates of U_o with in situ observations of changes in the vertical distribution of turbidity, that floc structure generally withstands a local shear rate (temporal average) on upward advection similar to that experienced in settling.

These data indicate that when sampling high energy turbid environments such as the Severn Estuary, it is necessary to obtain information on suspended sediment distributions close to the bed (0.10 m); otherwise a major proportion of the suspended load present in the water column may be neglected in subsequent transport and sedimentation analysis. It is clear from laboratory tests that hindered settling of suspended sediment is occurring in the field when the concentration of suspended sediment C lies in the range $10\ kg \cdot m^{-3} \leq C \leq 140\ kg \cdot m^{-3}$. This is probably the case in other turbid estuaries. This mode of settling probably results in the development of dense stationary suspensions observed in the Severn and other estuaries (for examples see Kirby and Parker 1982).

Acknowledgments

The authors wish to thank the Captain and crew of M.V. *Gardline Locater*, the staff of the Institute of Oceanographic Sciences (Taunton, U.K.) for assistance with sample collection and the provision of data, and gratefully acknowledge the financial support of the Natural Environment Research Council (Contract F60/B4/02).

ARIATHURAI, R., R. C. MACARTHUR, AND R. B. KRONE. 1977. Mathematical model of esturial sediment transport. Tech. Rep. D-77-12 U.S. Army Engineer Waterways Experiment Sta. Environmental Effects Laboratory, Vicksburg, MS.

BIDDLE, P., AND J. H. MILES. 1972. The nature of contemporary silt in British Estuaries. Sediment. Geol. 1: 23–33.

BRYANT, R., A. E. JAMES, AND D. J. A. WILLIAMS. 1980. A sampler for cohesive sediment in the benthic boundary layer. Limnol. Oceanogr. 25: 572–576.

BRYANT, R., AND D. J. A. WILLIAMS. 1982. Mineralogical analysis of suspended cohesive sediment using an analytical electron microscope. J. Sediment. Petrol. 52: 299–306.

EDZWALD, J. K., J. B. UPCHURCH, AND C. R. O'MELIA. 1974. Coagulation in Estuaries. Environ. Sci. Technol. 8: 58–63.

GAUDETTE, H. E., W. R. FLIGHT, L. TONER, AND D. W. FOLGER. 1974. An inexpensive titration method for the determination of organic carbon in sediments. J. Sediment. Petrol. 44: 249–253.

HAM, R. K. 1967. A study of particle size changes during coagulation. Ph.D. thesis, University of Washington, Seattle, WA.

HAMILTON, I. E., P. G. WATSON, J. J. CLEARY, AND R. J. CLIFTON. 1979. The Geochemistry of recent sediments of the Bristol Channel/Severn Estuary system. Mar. Geol. 31: 139–182.

KIRBY, R. R., AND W. R. PARKER. 1977. The physical characteristics and environmental significance of fine-sediment suspensions in estuaries, p. 110–120. *In* Studies in sciences, Washington, DC.

1983. The distribution and behaviour of fine sediment in the Severn Estuary and Inner Bristol Channel, U.K. Can. J. Fish. Aquat. Sci. Suppl. 40. (This issue)

KRANCK, K. 1975. Deposition from flocculated suspensions. Sedimentology 22: 111–123.

KRONE, R. B. 1972. A field study of flocculation as a factor in esturial shoaling processes. U.S. Army, Corps. of Eng., Comm. Tidal Hydraul., Tech. Bull. 19.

MICHAELS, A. S., AND J. C. BOLGER. 1962. Settling rates and sediment volumes of flocculated kaolin suspensions, Ind. Chem. Eng. Fundam. 1: 24–33.

ODD, N. U. M., AND M. W. OWEN. 1972. A two layer model of mud transport in the Thames Estuary. Proc. Inst. Civ. Eng. Pap. 7517–5 p.

PEIRCE, T. J., AND D. J. A. WILLIAMS. 1966. Experiments on certain aspects of sedimentation of estuarine muds. Proc. Inst. Civ. Eng. 34: 391–402.

POOLEY, F. D. 1977. The use of an analytical electron microscope in the analysis of mineral dusts. Phil. Trans. R. Soc. Lond. A. 286: 625–638.

SHIDELER, G. L. 1976. A comparison of electronic particle counting and pipette techniques in routine mud analysis. J. Sed. Petrol. 46: 1017–1025.

SOLLAS, W. J. 1883. On the estuaries of the Severn and its tributaries; an enquiry into the nature and origin of their tidal sediment and alluvial flats. Q. J. Geol. Soc. London, 49: 611–627.

TREWEEK, G. P., AND J. J. MORGAN. 1977. Size distributions of flocculated particles: Application of electronic particle counters. Environ. Sci. Technol. 11: 707–714.

Size of Flocs Suspended in Delaware Bay[1]

RONALD J. GIBBS, LOHIT KONWAR, AND ARAM TERCHUNIAN

College of Marine Studies, University of Delaware, Newark, DE 19711, USA

GIBBS, R. J., L. KONWAR, AND A. TERCHUNIAN. 1983. Size of flocs suspended in Delaware Bay. Can. J. Fish. Aquat. Sci. 40(Suppl. 1): 102 – 104.

This study extended from the Delaware River down the Delaware Bay into the upper Delaware Bay. The suspended material concentration in the lower Delaware River and upper Delaware Bay was determined by filtration, and the size and nature of flocs were determined by optical microscope. The principal turbidity maximum, at a salinity of 1‰, was composed of the largest flocs (up to 130 μm diameter), and sizes found in the water column decreased progressively down the Bay. This maximum was probably related to the formation of flocs. A second turbidity maximum, not related to floc formation or resuspension, may have occurred at a salinity of 5‰.

Key words: flocs, turbidity maximum, Delaware Bay

GIBBS, R. J., L. KONWAR, AND A. TERCHUNIAN. 1983. Size of flocs suspended in Delaware Bay. Can. J. Fish. Aquat. Sci. 40(Suppl. 1): 102 – 104.

La présente étude couvre la partie avale du fleuve Delaware se déversant dans la Baie de Delaware jusqu'à la partie supérieure de la Baie Delaware. La concentration des matières en suspension dans le bassin inférieur du fleuve Delaware et dans le haut de la Baie de Delaware a été déterminée à l'aide d'un microscope optique. Le principal maximum de turbidité, observé à une salinité de 1‰, était caractérisé par la présence des plus gros flocons (pouvant atteindre un diamètre de 130 μm) et on a noté que la taille des flocons présents dans la colonne d'eau diminuait progressivement en descendant vers la Baie. Ce maximum était probablement lié à la formation de flocons. Il se peut qu'un deuxième maximum de turbidité, non lié à la formation de flocons ou à la remise en suspension, se soit produite à une salinité de 5‰.

Received November 9, 1981
Accepted August 30, 1982

Reçu le 9 novembre 1981
Accepté le 30 août 1982

THE existence of flocs in brackish and marine environments has been shown by Berthois (1961), Biddle and Miles (1972), Kranck (1975 and 1981), Krone (1972), Owen (1971), Schubel and Kana (1972), Sheldon (1968), and Zabawa (1978). The purpose of this paper is to document the size distribution of flocs from the Delaware River and down the estuary of Delaware Bay. This measurement is difficult because of the fragile nature of flocs. However, flocs may be the form in which the majority of the river-derived suspended sediment is transported, so it is critical to obtain reliable systematic data on them.

Procedures

The locations of stations along the upper Delaware Bay (Fig. 1) extended from the Delaware River (above saltwater influence) across the turbidity maximum and into the upper Bay. To obtain comparable data with respect to hydrodynamic properties, the samples were all obtained at high tide from stations along the major channel. The cruise was conducted on November 15, 1980 starting at the lower Bay station at high tide, progressing up the Bay with the tide. This permitted samples from all the stations to be obtained at close to high tide (± 30 min), thereby having all stations on a comparable basis. The tidal range in this area is about 1.5 m. The river discharge was low at the time of this study. Salinity and temperature profiles were obtained using an Interocean 514 STD. The samples for suspended material were obtained using 5-L Niskin bottles at three depths. Suspended material samples were taken 1 m below the surface, mid-depth (samples were taken at half the water depth) and near-bottom (samples were taken 1 m above the bottom). The samples studied for suspended material concentration and mineralogy (which will be described in a separate publication) were filtered through 0.4-μm Nuclepore filters and then rinsed with distilled water. Samples studied for size distribution of the suspended material were obtained with a 5-mm diameter glass tube through the top of the Niskin bottle. Sampling of flocs using glass tubes was shown by Gibbs and Konwar (1982) not to break flocs. Use of Niskin bottles in sampling minimizes floc breakage as long as samples are extracted through the top

[1]This paper forms part of the Proceedings of the Dynamics of Turbid Coastal Environments Symposium convened at the Bedford Institute of Oceanography, Dartmouth, N.S., Canada, September 29–October 1, 1981.

Printed in Canada (J6717)
Imprimé au Canada (J6717)

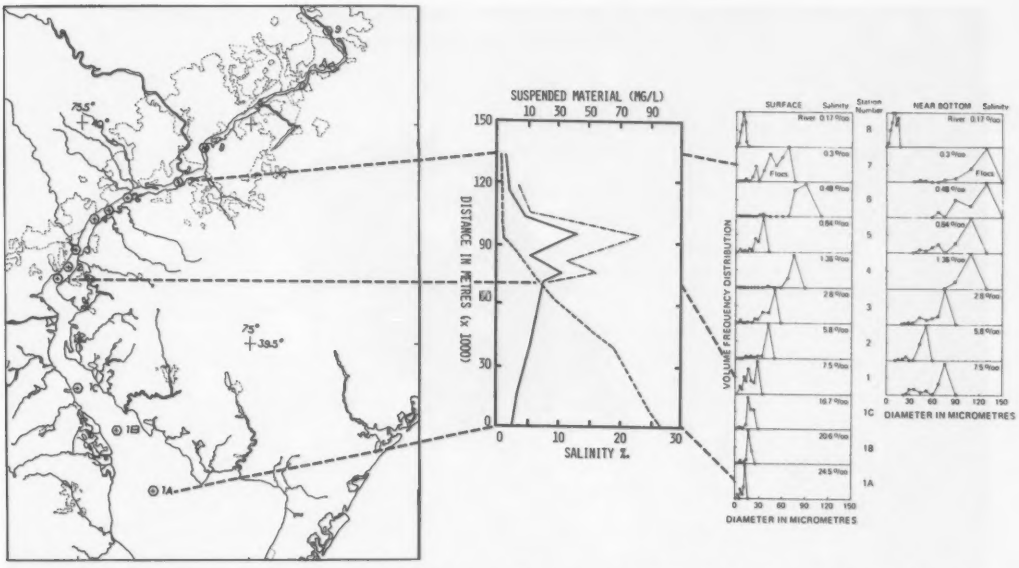

FIG. 1. Composite diagram showing location map (on left); the center diagram shows the salinity (dashed line), surface suspended material concentration (solid line) and the near-bottom suspended material (dot and dash line) and the diagrams on the right show the floc size distribution for the surface and near-bottom samples.

of the bottle (R. J. Gibbs and L. Konwar unpublished data). The suspended material particles were counted immediately using an optical microscope at 450 and 100 magnification with the sample material placed on special slides having a 400-μm deep well. A stratified counting technique was used to increase accuracy.

Results and Discussion

On the day of sampling, the suspended material concentration in the Delaware River was very low (Fig. 1). However, when sampling at low-river stage, one can expect low sediment concentrations. Toward the Bay, the suspended material concentration increased very quickly to a salinity of about 1‰. The principal turbidity maximum occurred at just under 1‰ salinity and the minor turbidity maximum occurred at about 5‰ salinity. It should be noted that the surface and near-bottom suspended material concentrations were similar, with the near-bottom concentrations in the turbidity-maximum zone higher than the surface concentrations. Oceanward from the turbidity-maximum zone, the concentration of suspended material steadily decreased.

The suspended material flowing into the Delaware Bay from the Delaware River during our period of sampling was small, having an average diameter (on a volume basis) of less than 15 μm for both the surface and near-bottom water samples (Fig. 1). These samples were not flocculated, and the majority of the material was in the form of individual inorganic particles. In the next sample taken down bay, where salinity was 0.3‰, the surface water material had formed flocs whose modal diameter was 70 μm diameter and the near-bottom material had formed flocs whose modal diameter was over 120 μm. The size of the flocs found in the near-bottom waters decreased progressively down the Bay. The flocs of suspended material in the surface water reached a maximum diameter at a salinity of 0.5‰ and then floc size decreased progressively down the Bay. A photomicrograph of a floc typical of these samples is shown in Fig. 2. Flocs such as this one are composed of about 90% water and therefore have correspondingly low densities and settling velocities.

The mechanism causing the flocs to form from the river-delivered material appears to be the effect of the sea water destabilizing the particles by compressing the double layer of ions in solution, thereby permitting particles to form flocs. Why the distribution of flocs encountered in the surface and bottom waters occurs is a complicated question. It could be (1) that the larger flocs simply settle more rapidly to the bottom, or (2) that longer exposure to turbulent environment breaks the flocs as they move down the estuary, or (3) that the larger flocs are progressively diluted down the Bay, or (4) that the flocs are concentrated by the estuarine two-layer flow, or (5) it could be some combination of these possibilities.

The mechanisms that cause the observed double turbidity maximum are likewise complex and data on the currents and turbulence that could possibly answer this question are not available. However, some conclusions can be made. The principal turbidity maximum, at 1‰ salinity, was also the position of the maximum floc diameter, so this turbidity maximum was apparently related to floc size. The second turbidity maximum, at about 5‰ salinity, was based on a single pair

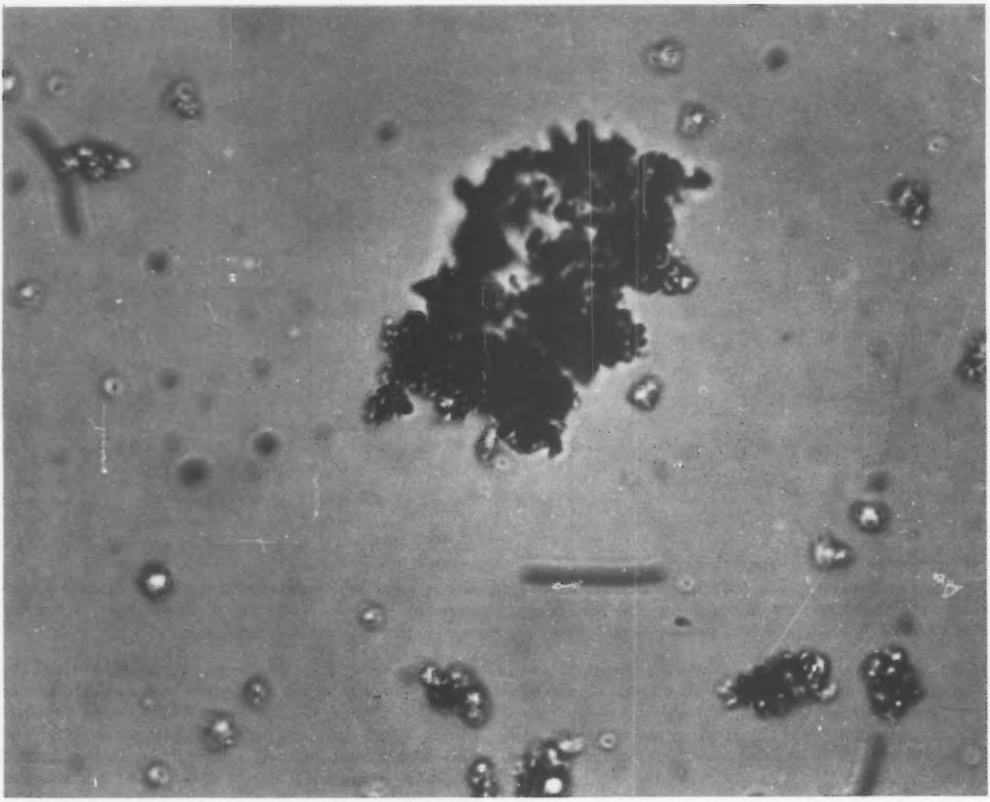

FIG. 2. Photomicrograph of a typical floc from the turbidity maximum.

of observations and could be a spurious result of sampling or analytical error and/or patchiness or discontinuity in the distribution of suspended sediments. If, on the other hand, this second maximum really existed, it would not appear to have been related to the trend in floc diameter since it was characterized by flocs that were about 60% the size of the flocs in the first turbidity maximum and floc size showed a progressive decrease from the first turbidity maximum down the Bay. Resuspension can also be ruled out as a mechanism here as this would require higher currents and turbulence. The hydrography for this region does not appear to be significantly different. Further, the higher turbulence required for resuspension would cause breakage of flocs, resulting in smaller floc size, but no decrease in floc size was observed at this location.

Acknowledgments

Appreciation is extended to other class members participating in the field cruise: Harris Martin, Wayne Mitchell, and John Scibek. Thanks are extended to the University of Delaware for ship time and to the skipper and crew of the R.V. *Wolverine*.

BERTHOIS, L. 1961. Observations directe des particules sedimentaires fins dans l'eau. Rev. Geogr. Phys. Geol. Dyn. IV, 1: 39–42.

BIDDLE, P., AND J. H. MILES. 1972. The nature of contemporary silts in British estuaries. Sediment. Geol. 7: 23–33.

GIBBS, R. J., AND L. KONWAR. 1982. Effect of pipetting on mineral flocs. Environ. Sci. Technol. 16: 119.

KRANCK, K. 1975. Sediment deposition from flocculated suspensions. Sedimentology 22: 111–123.

1981. Particulate matter grain-size characteristics and flocculation in a partially mixed estuary. Sedimentology 28: 107–114.

KRONE, R. B. 1972. A field study of flocculation as a factor in estuarial shoaling processes: US Army Corps of Engineers Committee on Tidal Hydraulics. Tech. Bull. 19: 62 p. + 3 app.

OWEN, M. W. 1971. The effect of turbulence on the settling velocities of silt flocs. International Association for Hydraulic Research Congress, 14th, Paris, 1971, Proceedings 4: 27–32.

SCHUBEL, J. R., AND T. W. KANA. 1972. Agglomeration of fine-grained suspended sediment in northern Chesapeake Bay. Powder Technol. 6: 9–16.

SHELDON, R. W. 1968. Sedimentation in the estuary of the River Crouch, Essex, England. Limnol. Oceanogr. 13: 72–83.

ZABAWA, C. 1978. Microstructures of agglomerated suspended sediments in northern Chesapeake Bay Estuary. Science 202: 49–51.

Modeling Suspended Sediment Dynamics of the Miramichi Estuary, New Brunswick, Canada[1]

G. V. WINTERS

Environmental Marine Geology, Atlantic Geoscience Centre, Geological Survey of Canada, Bedford Institute of Oceanography, Dartmouth, N.S. B2Y 4A2

WINTERS, G. V. 1983. Modeling suspended sediment dynamics of the Miramichi Estuary, New Brunswick, Canada. Can. J. Fish. Aquat. Sci. 40(Suppl. 1): 105–116.

Polynomial models were used to estimate the annual transport of suspended sediment in an estuary with a variable salt-wedge. The models are empirical, based on water flux measurements and SPM concentration, and these are shown to be a function of the tidal oscillations and river discharge.

The Miramichi River discharge varies from about 50 $m^3 \cdot s^{-1}$ in January to 1700 $m^3 \cdot s^{-1}$ in April. Diurnal inequality in the semidiurnal tides and variation in river discharge produces a continual inequality in the suspended sediment (SPM) transports for individual flood and ebb tides. Consequently, the models rely on integrating observations for each flood and ebb cycle. Empirical data indicate that semidiurnal tidal transport generally varies from 30 to 300 t in either ebb or flood direction. However, an order of magnitude increase can occur when the ebb tide couples with high runoff (i.e. 3300 t during a single ebb cycle in May 1976). A two-layer model gives a small (20%) increase in the residual sediment transport compared to a one-layer model. The 1976 net transport was calculated as −100 000 t (seaward). Sedimentation rates estimated from core samples agree with model estimates.

Key words: Modeling, suspended sediment, SPM, transport, Miramichi, estuary

WINTERS, G. V. 1983. Modeling suspended sediment dynamics of the Miramichi Estuary, New Brunswick, Canada. Can. J. Fish. Aquat. Sci. 40(Suppl. 1): 105–116.

Des modèles polynomiaux ont été utilisés pour estimer le transport annuel de sédiment en suspension dans un estuaire à poussée d'eau salée variable. Ces modèles sont empiriques, reposant sur des mesures de flux d'eau et de concentration de SPM qui, à leur tout, sont fonctions des oscillations de la marée et du débit du cours d'eau.

Le débit de la Miramichi varie, passant d'environ 50 $m^3 \cdot s^{-1}$ en janvier à 1 700 $m^3 \cdot s^{-1}$ en avril. Par suite d'une inégalité diurne des marées semi-diurnes et de la variation du débit de la rivière, il y a continuelle inégalité des transports de sédiment en suspension (SPM) entre marées individuelles de jusant et de flot. Les modèles doivent donc dépendre de l'intégration d'observations pour chaque cycle de flot et de jusant. D'après des données empiriques, le transport semi-diurne de la marée varie généralement de 30 à 300 t en direction, soit du jusant soit du flot. Cependant, il peut se produire une augmentation d'un facteur 1 quand le jusant est accompagné d'un abondant ruissellement (c.-à-d. 3 300 t pendant un seul cycle de jusant en mai 1976). Un modèle à deux couches donne une faible (20%) augmentation du transport de sédiments résiduaires comparativement à un modèle à une couche. On a calculé à −100 000 t (en direction de la mer) le transport net en 1976. Les taux de sédimentation estimés à partir de carottes s'accordent avec les estimations du modèle.

Received October 14, 1981
Accepted June 23, 1982

Reçu le 14 octobre 1981
Accepté le 23 juin 1982

THE Miramichi Estuary is situated in New Brunswick Canada on the southwestern shore of the Gulf of St. Lawrence (Fig. 1). It is a shallow funnel-shaped estuary, consisting of an inner drowned river channel and an outer shallow basin which is partially enclosed by a Holocene-age island system (Rashid and Reinson 1979). The river estuary is 55 km long, 1 km or less wide, and up to 15 m deep. The estuary is very shallow with a mean depth of approximately 6 m. A triangular basin at the mouth of the inner estuary (Inner Miramichi Bay) is 25 km in length, and fans out to a width of 25 km at the barrier islands. The Miramichi River has a drainage basin of 11 800 km^2 with discharge variation of 1700 $m^3 \cdot s^{-1}$ (April 1976) to 50 $m^3 \cdot s^{-1}$ (February 1977). Spring freshet

[1]This paper forms part of the Proceedings of the Dynamics of Turbid Coastal Environments Symposium convened at the Bedford Institute of Oceanography, Dartmouth, N.S., Canada, September 29–October 1, 1981.

Printed in Canada (J6681)
Imprimé au Canada (J6681)

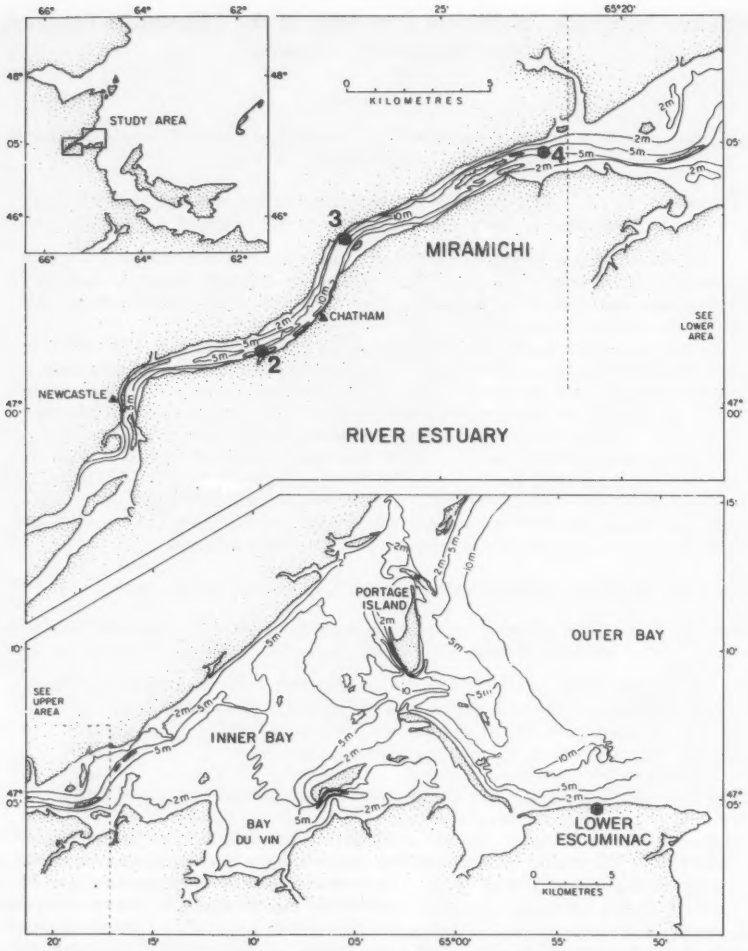

FIG. 1. Locations of monitoring stations and the bathymetry of the Miramichi Estuary. The 2, 5, and 10 m isobaths are shown.

values greater than 2640 $m^3 \cdot s^{-1}$ are exceeded less than 1% of the time (Krauel and Birch 1979). The mean freshwater discharge for 1976 was 360 $m^3 \cdot s^{-1}$, which is only slightly higher than the mean annual discharge of 305 $m^3 \cdot s^{-1}$.

The estuary is a coastal plain estuary which is normally highly stratified. Vilks and Krauel (1982) show that it is typically a variable salt-wedge estuary, with a seaward residual flow at the surface and an inward residual flow at the bottom. During high river discharge, the salinity intrusion extended less than 10 km into the river estuary (near Station 3), however, during low river discharge, it extended to the limit of tidal influence (14 km above Newcastle).

Tides in the Miramichi are a mixed type, predominantly semidiurnal, that can have a large diurnal inequality in their amplitudes (0.2 versus 1.2 m). When the moon has low declination the two semidiurnal tides are of nearly equal heights. The diurnal form can predominate at maximum lunar declination.

Most of the sediment in motion in this estuary is derived through erosion of river channel material; the river flows through sandstones, glacial outwash deposits, and volcanic rocks. Much of the sediment load is deposited in the estuary due to a trapping mechanism related to the nature of the circulation (Kranck 1974).

In situ monitoring data on the water column in the drowned river channel (Winters and Buckley 1978, 1980) indicate that bottom sediments are resuspended by tidal currents. Their observations were made over several tidal cycles at 1 m depth

intervals and 1 h time intervals during spring high river discharge (May 1976), fall low river discharge (October 1976), and winter ice cover low river discharge (February 1977), and at three locations in the channel (Fig. 1). They can be compared to concurrent oceanographic observations for salinity, temperature, and current speed. Hourly tide heights at Lower Escuminac and daily mean river discharge data were also incorporated into the model. The observed hourly tide heights for Lower Escuminac were obtained from the Marine Environmental Data Services Branch, Marine Sciences and Information Directorate, Department of Fisheries and Oceans, Ottawa, Canada. These data were corrected for each station location, according to the cotidal model discussed by Vilks and Krauel (1982). The daily mean river discharge data were obtained from the Water Survey of Canada which maintains continuous water-stage recorders at four locations in the Miramichi watershed. The time lag between observations made in the tributaries and observations made in the river–estuary was approximately 1 d in the spring and 2 d in the fall and winter (Vilks and Krauel 1982).

Suspended Particulate Matter Concentrations

A plot of sea level is superimposed on SPM contours with depth and time relative to maximum sea level during the May high river discharge period (Fig. 2). This period shows up as a primary semidiurnal tidal cycle followed by a secondary semidiurnal tide cycle of lower magnitude. There is a regular occurrence of SPM concentration maxima during the ebb cycles of the semidiurnal tides. The relative SPM magnitudes suggest a diurnal inequality for SPM which appears to parallel a diurnal inequality in the tidal cycle.

During the May freshet the SPM concentration maximum in the bottom water at Station 4 was limited to the salt-wedge dominated part of the water column during both flood and ebb tides (Fig. 3). During the ebb tide retreat of the salt-wedge, the bottom concentration maximum decreased as the current speed within the salt-wedge subsided. The maximum ebb current speeds observed were at the surface of the freshwater layer. A turbidity maximum became more pronounced at the surface near the end of the ebb tide. This occurred when the salt-wedge began moving in the flood direction along the bottom, and the SPM laden fresh water was forced to flow over its leading edge. The maximum occurred 3–4 h after the occurrence of the peak ebb-current speed. Oostdam (1977) observed lag times of up to 1 h in the response of the SPM concentrations to increasing current speed for the resuspension of bottom sediment in Delaware Bay. The implication of the 4-h lag time observed at Station 4 was that these surface water SPM concentrations were probably not the result of sediment resuspension in the immediate area. Instead, the freshwater load of SPM was probably transported to Station 4 from farther upstream. A current velocity of -100 cm·s^{-1} would have required 3.6 h to transport the SPM from Station 2 and 2.2 h to transport the SPM from Station 3.

The following flood tide was of a lesser magnitude and a lower amplitude SPM maximum occurred within the limits of the advancing salt-wedge. Maximum flood current speeds were observed at the center of the salt-wedge.

Interpretation of SPM data for Stations 2, 3, and 4 (Fig. 2a, 2b, and 3a, respectively) suggests that the source of the SPM, which was carried by the fresh water, was upstream. These observations were for similar diurnal periods. Station 2 was located 13 km upstream from Station 4 and Station 3 was 8 km upstream from Station 4. Concurrent oceanographic observations (Winters and Buckley 1978; Vilks and Krauel 1982) indicated that the influence of the salt-wedge was negligible at Stations 2 and 3 during the May observation period. Thus the effects of two-layer circulation were also negligible at stations 2 and 3 and the SPM concentration maxima at these locations were greatest at the bottom with decreased concentrations towards the surface. Comparison of Fig. 2a and 2b showed the highest SPM values at Station 2, but more homogeneous distribution at Station 3. The upstream station (2) must be closest to the primary source of SPM and that the riverborne SPM settles during times of slack tidal current. This sediment is then later eroded and resuspended by ebb currents acting concurrently with high river currents.

In the stratified column at Station 4 there appeared to be a residual seaward transport of SPM near the surface and a net landward transport near the bottom (Fig. 3a). However, during the period of high river discharge, the seaward SPM transport appears to greatly exceed the landward transport.

In October, the SPM concentration maxima, which occurred in both the bottom and surface water layers, appeared to behave in a manner similar to that observed in May. However, the concentration maxima were of a lesser magnitude and the salinity intrusion extended beyond the uppermost observation station and possibly to the limit of tidal influence.

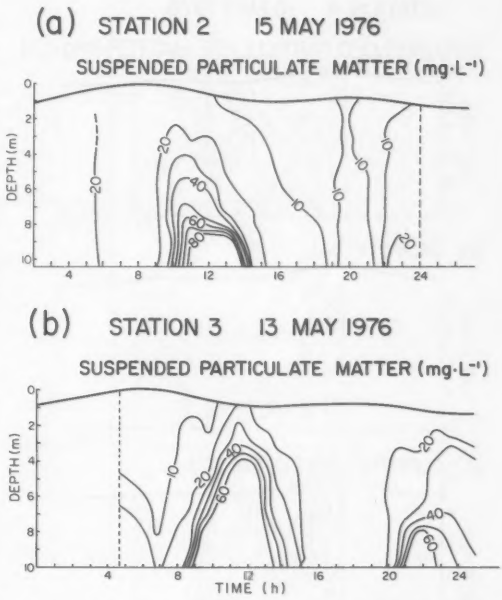

FIG. 2. SPM concentration contoured with depth and time at Stations 2 and 3 during May. The depth intervals are relative to the maximum sea level observed during the specific diurnal periods.

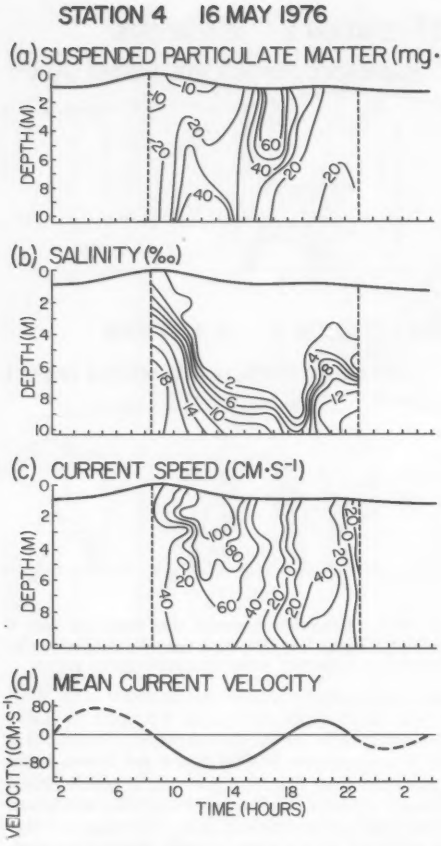

FIG. 3. SPM concentration (a), salinity (b), and current speed (c) contoured with depth and time, and the mean current velocity (d) for the vertical column at Station 4 during May. The depth intervals are relative to the maximum sea level observed during this diurnal period. Dashed lines for the mean current velocity (d) represent extrapolated values that were computed from the observed change in sea level and river discharge.

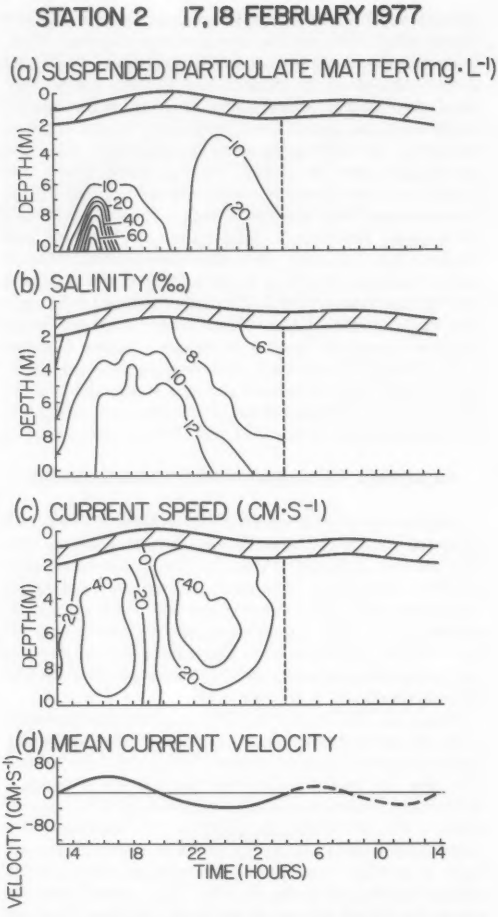

FIG. 4. SPM concentration (a), salinity (b), and current speed (c) contoured with depth and time, and the mean current velocity (d) for the vertical column at Station 2 during February. The depth intervals are relative to the maximum sea level observed during this diurnal period. Dashed lines for the mean current velocity (d) represent extrapolated values that were computed from the observed change in sea level and river discharge. The upper boundary represents ice cover which is 1 m thick.

During February, the estuary was ice covered and no surface maxima were observed for SPM concentration (Fig. 4a). The current regime was similar for both flood and ebb tides (Fig. 4c). Maximum currents occurred near the center of the water column and generally the currents were higher near the bottom compared to the surface. The surface ice cover apparently caused a reduction of the current speeds in the upper water column and thus limited its ability to support a high SPM load. The SPM concentration maxima observed at Station 2 displayed higher SPM concentrations than were observed at Station 4 during the same diurnal period. Therefore the bottom sediments must be more easily resuspended at the up-estuary location, which is nearer to the estuarine flocculation zone described by Kranck (1981). This hypothesis is supported by the salinity data given in Vilks and Krauel (1982) which suggest that during February the flocculation zone probably lies upstream of Station 2.

Transport of Water and Suspended Sediment

Long-term evaluation of the suspended sediment transport can best be modeled by integrating the hourly observations for each flood and ebb tide. The magnitude of the SPM concentration maxima varies with the diurnal inequality in amplitude

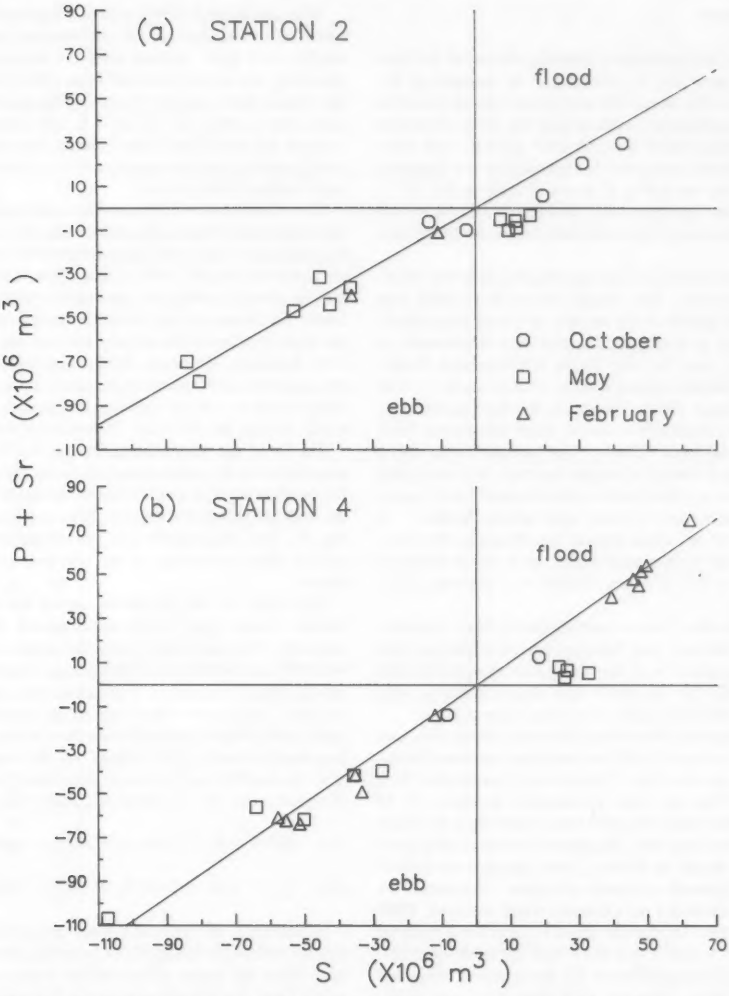

FIG. 5. Combined water transport by the tide and river versus transport computed from observed current velocities.

and time of each flood and ebb tide, and in conjunction with the river discharge.

Flux of water and suspended sediment were computed at hourly and 1 m depth intervals as the product of concentration (c) and velocity (v). The integrated flux for flood and ebb tides, F, was then computed by Equation 1.

$$(1) \quad F = \sum_{t=1}^{T} \left[\left(\sum_{i=1}^{h} c_i \cdot v_i \right) \Big/ h \right]_t$$

T is used to notate the unequal time periods of the individual flood and ebb tides and h is the height of the water surface.

The transport (S) is then described by Eq. 2 for the flood and ebb tides assuming that the observed flux in the channel is a reasonable representation of the transport through the total cross section (A).

$$(2) \quad S = A \cdot F$$

The total cross sectional areas at mean sea level were determined from the Canadian Hydrographic boat-board charts: A = 4590 m^2 at Station 2 and 5460 m^2 at Station 4.

WATER TRANSPORT

The validity of the assumption requiring the use of the total cross-sectional area (Eq. 2) was tested by computing the water transports as the sum of the tidal prism volume variation for this hypersynchronous estuary and the river discharge volume for specific flood and ebb tidal periods, and comparing them with the transports computed from the observed flux (by Eq. 2 and by setting C_i equal to unity in Eq. 1).

The river water transport (Sr), during specific flood and ebb tides, was determined from the daily means for freshwater discharge.

The tidal prism volume (P) at a specific location was determined as: $\Delta H \cdot f_L \cdot Ax_L$. The change in sea level (ΔH) was monitored at the mouth of the estuary at Lower Escuminac. Sea-level change at a specific location was determined as $\Delta H \cdot f_L$, where f_L was the tide height reinforcement factor. Values for f_L at Station 2 and 4 were: $f_2 = 1.17$ and $f_4 = 1.06$ (in Vilks and Krauel 1982). The areas, for the estuarine surface above these reference stations, were determined from Canadian Hydrographic Charts. The surface area above each station was sectioned at regular intervals and multiplied by the corresponding tide height reinforcement factor increment. The incremented surface area above Station 2 is $Ax_2 = 29.4 \times 10^6$ m^2 when Station 2 is chosen as the reference point and the incremented surface area above Station 4 is $Ax_4 = 52.6 \times 10^6$ m^2 when Station 4 is chosen as the reference point.

Except for the flood tides observed during May, observations for May, October, and February appear to indicate that the flux is representative of the transports through the total cross section (Fig. 5). The flood tides observed during May were excluded from the regression curve computations.

The transport for the May flood tides was greater than was expected when compared with the combined individual transport by the tide and the river. This anomaly occurred at both Station 4 and 2 but was more pronounced at Station 2. At Station 2 the river water transport was greater than the water transported by the flood tide. Because of the negligible presence of the salt-wedge at Station 2, the expected net overall effect was a seaward transport of water. However, the observed flux indicated a net upstream water transport. Concurrent observations for current speed (Winters and Buckley 1978; Vilks and Krauel 1982) show that the freshwater column at Station 2 was partitioned by the opposing river and tidal water transports. The ebb tidal flow gave way to the flood tidal flow earlier in the bottom half of the water column. Also, the current velocities in the bottom zone increased more rapidly when compared with current velocities in the surface. During the flood tide the river transport was confined to the surface and was not truly represented by the vertical water column mean trend. This effect in the model was enhanced because the estuarine cross section was not rectangular.

At Station 4, the two-layer density circulation was superimposed on the tidal transport of water in the stratified water column during May. Increased flood tidal transport in the bottom layer increased the flux mean trend for the vertical water column. Thus, the magnitude of the river water transport at the surface was obscured by the increased flood tidal transport in the bottom layer.

Vilks and Krauel (1982) reported that during times of high runoff in the Miramichi, the ebb currents increased in magnitude while flood currents were not noticeably suppressed. However, the current reversal from ebb to flood occurred at the bottom first, and the reversal progressed toward the surface over a period of up to 7 h. On some occasions the reversal did not occur at the surface. For this, the transport model used the time of current reversal as determined from the water column mean trend.

The discrepancies between the calculated and observed water transports during flood tides are also dependent on the fact that the water levels are extrapolated from observations made near the mouth of the estuary. These water level values include changes which are principally due to tidal influence. Under conditions of high river discharge, the water level in the upper reaches of the estuary will rise due to the increased river discharge. However, if this were the primary cause for the water transport model discrepancy during the flood tides, there would also be an opposing discrepancy of similar magnitude during the ebb tides. This was not observed.

The fit of the May observations to the regression curves improve when the water transports by the tide only are plotted for the flood cycles and the water transports by the tide plus the river are plotted for the ebb cycles (comparing Fig. 6 with Fig. 5). The observations for October and February are only slightly affected because of the low river discharge at those times.

The slopes of the regression curves are 0.90 ± 0.09 for Station 2 and 1.08 ± 0.06 for Station 4 (95% confidence intervals). The associated water transports, which are determined by two independent methods, are therefore similar and indicate that the apparent or effective cross-sectional areas at Stations 2 and 4 are within 10% of the actual cross-sectional areas, which were measured from the Canadian Hydrographic boat-board charts. The slopes of the regression curves (Fig. 6a and 6b) can be used to determine the apparent cross-sectional areas, A_L', at Stations 2 and 4 (Eq. 3a and 3b).

$$(3a) \quad A_2' = 0.90 \pm 0.09\, A_2 = 4100 \pm 400$$

$$(3b) \quad A_4' = 1.08 \pm 0.06\, A_4 = 5900 \pm 300$$

In summary, the integrated observations for the mean water column reflect the transports by both tide and river during ebb tides when the entire water column flows as a single water mass. Thus, for ebb tides the water flux can be estimated by Eq. 4 as the total volume of water transport (by the tide and river) divided by the apparent cross-sectional area.

$$(4) \quad F = (P + Sr)/A'$$

During flood tides the integrated observations for the mean water column reflect transports by the tide only and the influence of the river is obscured. This deviation from the model (Eq. 4) is attributed to the fact that the observed flux is computed from observed current data which is depth averaged for the channel. The observed flux is thus biased by the tidal transport, which is restricted to the channel, while the opposing river transport is restricted to the surface. The bias is enhanced because the estuarine cross section is not rectan-

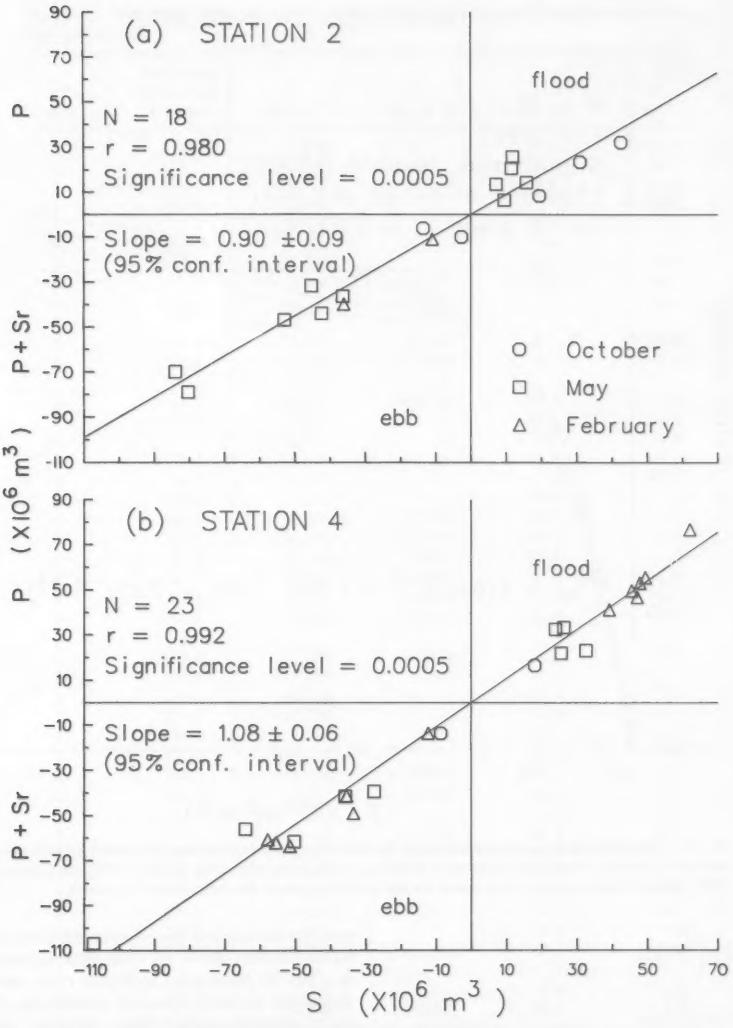

FIG. 6. Water transport by tide only, during flood tide, but combined water transports by the tide and river during ebb tide versus transport computed from observed current velocities.

gular and decreases with depth. If the opposing transports by the tide and the river remain separate during the flood tide, and if they flow through reduced cross sections, then two-layer circulation is established and increased current speeds are observed. The tidal water flux, F_t, and the river water flux, F_r, are estimated by

(4a) $F_t = P/A'$

(4b) $F_r = Sr/A'$

To estimate the transport of the nonconservative quality, suspended sediment, it is necessary to know the apparent cross-sectional areas through which this mass is transported during times when two-layer circulation is established. The fractional apparent cross-sectional areas through which the suspended sediment is transported by the tide, At', and the river, Ar', are taken as the proportion of the absolutes of the values for the water transport by the tide or the river to the sum of the absolutes of these values (Eq. 5a and 5b).

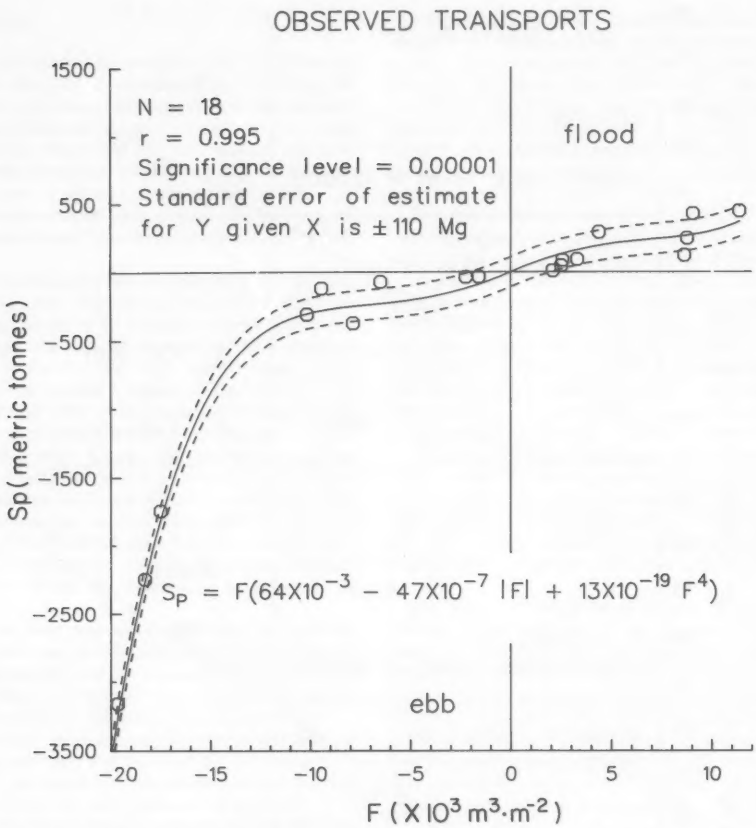

FIG. 7. Suspended sediment transports versus the water flux. Observations were integrated for each flood and ebb tidal cycle, which were observed at Stations 2 and 4 during May 1976, October 1976, and February 1977. Dashed lines represent error bands for the standard error of the estimate for Y given X.

$$\text{(5a)}\quad At' = A' \frac{|St|}{|St| + |Sr|}$$

$$\text{(5b)}\quad Ar' = A' \frac{|Sr|}{|St| + |Sr|}$$

SUSPENDED SEDIMENT TRANSPORT

The suspended sediment transports (S_p) are described as a function (Eq. 6, Fig. 7) of the observed water flux per flood or ebb tide. The water flux was used instead of the water transport so that one function could be derived which would describe the suspended sediment transport at both Stations 2 and 4.

$$\text{(6)}\quad S_p = F(64\times10^{-3} - 47\times10^{-7}|F| + 13\times10^{-19}F^4)$$

As was discussed earlier, these observed data reflect the transports by the tide and river during ebb tides and the transports by the tide only during the flood tides. Equation 6 was derived as a best fit polynomial regression curve and it describes all suspended sediment transport observations (Table 1) which were recorded during May, October, and February at Stations 2 and 4. The significance level for the correlation coefficient is $\alpha < 0.00001$ and the standard error for the estimate of Y given X is 110 t. The equation describes 99% of the variation in the observations for total suspended sediment transport.

For 15 of the 18 flood and ebb tide observations, the total suspended sediment transport can be described by a simple linear regression relationship. However, excessive quantities of suspended sediment were transported through the river estuary during the three ebb tide observations for May. These ebb tides occurred during the larger of the semidiurnal tides, during the spring tidal cycle, and during a freshet (peak fluvial discharge period). The magnitude of the river discharge

TABLE 1. Water and suspended sediment flux or transports integrated for observed flood and ebb tidal cycles.

Station	Initial time (Julian day fraction)	F ($m^3\ m^{-2}$)	F_p (Mg m^{-2})[a]	P ($\times 10^6\ m^3$)	Sr ($\times 10^6\ m^3$)
4	130.4	5,976		23.2	−17.5
4	130.6	−11,736		−32.0	−24.0
4	131.2	−9,720		−39.0	−22.6
4	131.5	4,680		22.1	−18.6
4	131.7	−6,552		−26.1	−15.3
4	135.7	4,824		33.4	−26.6
4	135.9	−5,040		−16.4	−20.9
4	136.3	−19,656	−0.5357	−77.8	−29.1
4	136.7	4,392	0.0864	32.6	−24.2
4	274.3	3,312	0.0194	16.7	−3.9
4	274.6	−1,584	−0.0058	−9.7	−3.9
4	41.5	−6,480	−0.0122	−39.4	−1.8
4	42.3	7,200		41.4	−1.6
4	42.5	−10,584		−58.9	−1.8
4	43.3	8,640	0.0216	46.9	−1.8
4	43.7	−6,120		−47.4	−1.5
4	44.4	8,352		49.7	−1.7
4	45.4	11,376	0.0770	76.8	−1.7
4	45.7	−10,150	−0.0526	−60.4	−1.7
4	46.4	8,784	0.0432	53.1	−1.5
4	47.3	−2,232	−0.0065	−12.6	−1.0
4	47.5	9,072	0.0734	55.5	−1.2
4	47.8	−9,432	−0.0202	−62.0	−1.6
2	126.8	2,088	0.0086	6.5	−16.5
2	130.4	3,455		14.4	−17.5
2	130.6	−9,216		−19.9	−23.9
2	131.2	−11,520		−24.3	−22.5
2	131.5	1,584		13.7	−18.7
2	131.7	−9,864		−16.2	−15.3
2	134.3	−18,288	−0.5443	−41.2	−28.6
2	134.7	2,592	0.0490	25.8	−34.7
2	134.8	7,920		−11.9	−24.3
2	135.3	−17,496	−0.4234	−46.2	−32.6
2	135.7	2,520	0.0259	20.2	−26.5
2	272.6	−2,952		−4.2	−1.9
2	272.7	9,288		32.3	−2.6
2	273.3	4,248		8.5	−2.7
2	273.5	−576		−5.9	−4.0
2	273.7	6,768		23.6	−3.0
2	47.3	−2,376		−9.9	−1.0
2	47.7	−7,848	−0.0907	−38.1	−1.6

[a]Megagrams or metric tonnes per m^2.

rivaled the water transported by these ebb tides of maximum magnitude. Under these conditions, the current speeds were at an annual high. Thus, both riverborne suspended sediments which settle during periods of current reversal and consolidated bottom sediments were readily eroded, resuspended, and exported from the river estuary (past Station 4).

During times of low river discharge, the current velocities in the drowned-river channel are predominantly dependent upon total water transport. The low current regime resulted in sedimentation of a large proportion of the suspended sediment, especially during neap tidal cycles. It is predicted that the net suspended sediment transport would be observed to be approximately zero during very low river discharge if continuous monitoring were conducted over several tide cycles. However, this conservative assumption is in disagreement with other researchers. For example, Groen (1967) used a model for the vertical exchange of SPM in a nonstationary current. His model hypothesizes a residual horizontal transport of suspended sediment in the flood direction which could be brought about in an alternating tidal current with zero residual water transport and equal maximum current strengths of flood and ebb tides. However, Groen (1967) assumed that

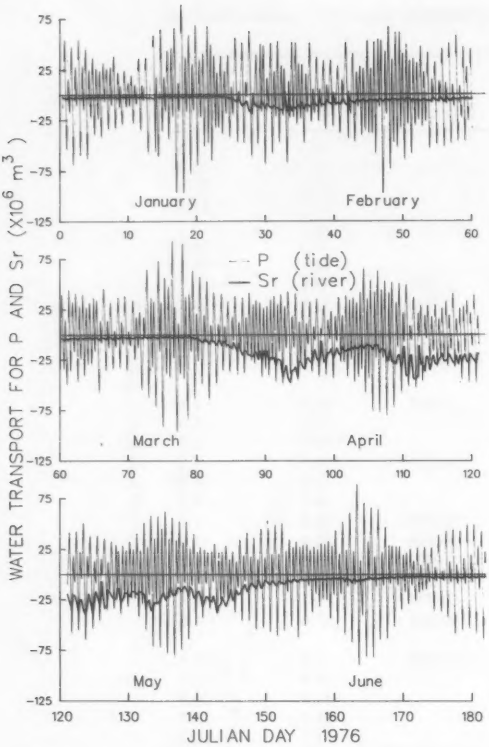

FIG. 8. Water transports for the tide and the river. Transports are integrated for each flood and ebb tidal cycle time interval.

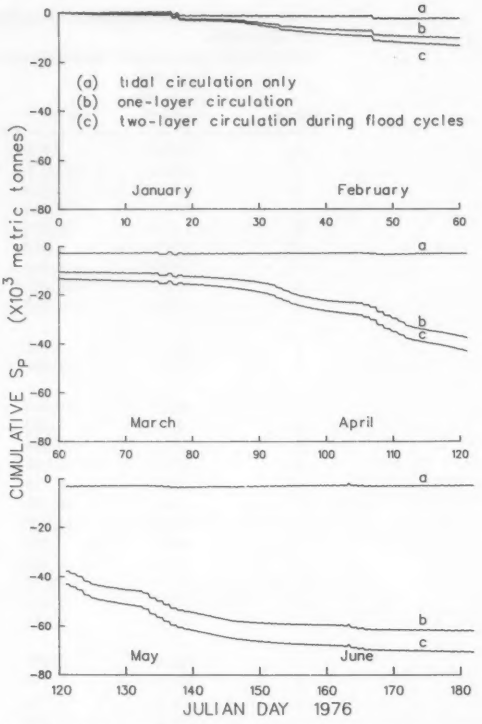

FIG. 9. Model estimates for suspended sediment cumulative transport. The transport was computed for each flood and ebb tidal cycle time interval.

there was an unlimited supply of particles from the bottom. In the Miramichi Estuary, the fine sediment supply which is available for transport in the flood direction is located in the western part of the Inner Bay. The existence of this sediment facies suggests that the area is mainly a sink for suspended sediment transported through the inner estuary. Because the cross section at this location is 4–8 times wider than the river estuary width near Station 4, it is probable that bottom currents only seldom reach the critical velocity that is required to resuspend this sediment for transport in the flood direction.

The up-estuary transport of suspended sediment, during storm conditions, is of minor importance in an annual budget. Wind driven currents can elevate suspended sediment concentrations in the inner bay and these elevated concentrations can range from 10 to 20 $mg \cdot L^{-1}$. If it is assumed (1) that a volume of water, which is equal to the tidal prism volume and which contains 20 $mg \cdot L^{-1}$ suspended sediment, enters the river estuary on a flood tide; (2) that the suspended sediment settles during slack water; and (3) that the sediment is resuspended on the subsequent ebb tide and that this seaward transport can be estimated by the model (Eq. 6); then the net transport (past Station 4) for a neap and a spring tide is up-estuary and is 0.1 and 0.9%, respectively, of the annual budget. If the flood tidal currents are channelized during a storm surge (i.e. flood currents are restricted to the drowned river channel which extends into the inner bay) additional sediment may be resuspended. The maximum net transport estimate is then, an up-estuary transport of <1.4% of the annual budget. These estimates are larger than one would expect to observe because the influence of the wind driven currents declines at the mouth of the river estuary and much of this suspended sediment will settle before entering the river–estuary.

In the Miramichi the absolute values for suspended sediment transports on both flood and ebb tides generally vary from 30 to 300 t. This difference is primarily due to the diurnal inequality in tidal cycle but is also dependent upon fluctuations in river discharge and upon whether or not two-layer circulation is established during flood cycles. The greatest unidirectional sediment transport occurs during ebb tides, when the tidal currents are enhanced by high river currents. Observations indicate that during the May freshet, 3300 t were exported from the river estuary on a single ebb tide. During the preceeding flood tide, two-layer circulation was established and the net transport was only 160 t in the flood direction. During the secondary or smaller flood and

ebb tides, which followed in the same diurnal period, only 70 t was transported in the flood direction and 220 t in the ebb direction. Thus the net transport for this diurnal period was 3290 t in the ebb direction.

Prediction Model

The suspended sediment transport model described here is designed to incorporate tide stage hourly observations and daily mean river discharge observations. Thus, the model will reflect long cyclic changes in the tide and seasonal variation in river discharges, and noncyclic changes caused by storms.

Water transported (at the mouth of the river estuary) by the river and the tide was computed from river discharge data and tides stage data during each flood and ebb tidal cycle (Fig. 8). The results show the effects of the lunar cycle by the magnitude of the diurnal inequality for the semidiurnal tides. The river water transport values (concurrent with flood and ebb tidal cycles) clearly reflect seasonal and storm-related variations. The river mean monthly discharge for January, February, March, and June was the same as that observed for the period July 1 to December 31 (230 ± 100 $m^3 \cdot s^{-1}$). High river discharge was prevalent only during April and May.

Model estimates for cumulative suspended sediment transport (for the period January 1 to June 30, 1976) are computed by Eq. 6 for three circulation hypotheses (Fig. 9): (a) tidal circulation only, where the effect of the river discharge is omitted, (b) one-layer circulation during both flood and ebb cycles, and (c) two-layer circulation during flood cycles and one-layer circulation during ebb cycles. The suspended sediment transport was estimated, for each flood and ebb tide, by substituting the values for the water flux in Eq. 6. The water flux was computed (a) for tidal circulation using Eq. 4a; (b) for one-layer circulation using Eq. 4; and (c) for two-layer circulation during flood cycles using Eq. 4a for the tidal component and using Eq. 4b for the river component. The water transports during ebb cycles were estimated by Eq. 4. During two-layer circulation, the tidal and river component suspended sediment transports were estimated by Eq. 6 before the net effect was determined by summing these latter values.

The first half-year estimates for residual suspended sediment transport were: (a) -2800 t assuming tidal circulation only, (b) $-62\,000$ t assuming one-layer estuarine circulation, and (c) $-71\,000$ t assuming two-layer estuarine circulation during flood cycles and one-layer circulation during ebb cycles. The annual transport estimates were (a) a negligible transport ± 2000 t assuming tidal circulation, (b) $-90\,000$ t assuming one-layer circulation, and (c) $-110\,000$ t assuming two-layer circulation.

The largest estimate for export of suspended sediment resulted when two-layer circulation was postulated during the flood cycles. But this estimate was only 20% greater than the estimate for one-layer circulation. Postulation of one-layer circulation during flood tides causes a reduction in the absolute value for water flux estimate. Because the sediment transport versus water flux relationship is nonlinear, a decrease and disproportionately lower sediment load is postulated. These estimates, which assume one layer and two-layer circulation during flood tide, are considered as minimum and maximum estimates, respectively, because conditions controlling SPM flux vary seasonally and spatially from that of a partially mixed to a stratified water column.

The 1976 net transport estimate is $-100\,000 \pm 10\,000$ t and one half of this suspended sediment export occurred during April and May. This model estimate is corroborated by other published studies for the Miramichi Inner Bay on the surficial sediment distribution and on sedimentation rates. At the mouth of the river estuary, a depositions zone of fine sediment (mud) has been identified (Reinson 1976, 1977; Rashid and Reinson 1979) which covers an area of about 54 km^2. C. T. Schafer et al. (unpublished data) collected sediment cores near the upstream end and in the middle of this deposit and estimated average sedimentation rates of about 0.24 $g \cdot cm^{-2} \cdot yr^{-1}$ based on Pb-210 geochronology (i.e. about 0.5 $cm \cdot yr^{-1}$) near the upstream end of this depositional zone. A sedimentation rate of 0.15 $g \cdot cm^{-2} \cdot yr^{-1}$ (about 0.3 cm yr^{-1}) occurs at about the middle of this depositional zone.

Based on these two sedimentation rates, the average annual sediment mass addition to the 54 km^2 mud deposition zone appeared to range between 80 000 and 130 000 t/yr. The latter estimates encompass the suspended sediment transport model estimate for 1976.

Conclusion

Suspended sediment transport in the Miramichi estuary is controlled by processes of sedimentation and resuspension and can be described as a function of the water flux. The water flux (and thus the suspended sediment transport) varies with the magnitude of the half tidal (ebb or flood) cycle as well as river discharge. Tidal variation in the Miramichi Estuary is subject to a large diurnal inequality in addition to the neap-spring cycle. For this reason the suspended sediment data are best modeled by integrating observations for each ebb and flood cycle.

During periods of low fluvial input the suspended sediment is primarily derived from the resuspension of unconsolidated bottom sediment. A large semidiurnal tide during the spring cycle can increase this sediment resuspension and transport by one order of magnitude relative to condition during the neap cycle. However during a period of high river discharge the transport can increase by three orders of magnitude if the freshet coincides with the spring tides.

The model shows that if two-layer circulation is established during flood cycles, then the net effect is a 20% increase in the annual export of suspended sediment from the river–estuary (as compared with conditions during one-layer circulation). At the mouth of the river–estuary the cross sectional area increases seaward allowing a reduction in current, which then permits the suspended sediment to settle and to be consolidated as part of the mud depositional zone in the inner bay.

In an estuary of similar dimensions to the Miramichi, an increase in either the tidal amplitude or the river discharge would result in increased sediment erosion and resuspension, and a subsequent increase in the net annual export of suspended sediment. The net effect would be less siltation within the confines of the river–estuary.

Acknowledgments

The collection of samples and field data required the cooperation and dedication of many colleagues at the Atlantic Geoscience Centre. I am very grateful for the efforts of D. Buckley, G. Vilks, G. Reinson, J. Willey, C. Schafer, K. Robertson, M. Gorveatt, R. Filtzgerald, R. Murphy, F. Jodrey, T. Cole, and D. Frobel, all of whom spent many uncomfortable days and nights in support of efforts to collect these data. I also thank D. Buckley, C. Schafer, G. Budgen, and J. Syvitski for reviewing earlier versions of this manuscript and making helpful suggestions for improving the text.

GROEN, P. 1967. On the residual transport of suspended matter by an alternating tidal current. Neth. J. Sea Res. 3: 564–574.

KRANCK, K. 1974. The role of flocculation in the transport of particulate pollutants in the marine environment, p. 41–46. Proceedings of the International conference on the Transport of Persistent Chemicals in Aquatic Ecosystems, Ottawa, Canada.

1981. Flocculation and particulate matter dynamics in a partially mixed estuary. Sedimentology 28: 107–114.

KRAUEL, D. P., AND J. R. BIRCH. 1979. Wind and freshwater inflow effects on the circulation of the Miramichi estuary, N.B. — a numerical model. Royal Roads Military College, FMO Victoria, B.C. Coastal Marine Science Laboratory MS Rep. 79-2: 140 p.

OOSTDAM, B. L. 1977. Suspended sediment transport in the Delaware Bay, p. 425–472. *In* I. H. Suffet [ed.] Fate of pollutants in the air and water environments, Part 1, Advances in environmental science and technology, vol. 8, Wiley-Interscience Publications, New York, NY.

RASHID, M. A., AND G. E. REINSON. 1979. Organic matter in surficial sediments of the Miramichi estuary, New Brunswick, Canada. Estuarine Coastal Mar. Sci. 8: 23–36.

REINSON, G. E. 1976. Surficial sediment distribution in the Miramichi estuary, New Brunswick. Report of Activities, Part C. Geol. Surv. Can. Pap. 76-1C: 41–44.

1977. Tidal-current control of submarine morphology at the mouth of the Miramichi estuary, New Brunswick. Can. J. Earth Sci. 14: 2524–2532.

VILKS, G., AND D. P. KRAUEL. 1982. Environmental geology of the Miramichi estuary: physical oceanography. Geol. Surv. Can. Pap. 81–24.

WINTERS, G. V., AND D. E. BUCKLEY. 1978. *In situ* monitoring data on the water column in the Miramichi estuary, New Brunswick. Bedford Inst. Oceanogr. Data Ser. BI-D-78-9: 131 p.

1980. *In situ* determination of suspended particulate matter and dissolved organic matter concentrations in an estuarine environment by means of an optical beam attenuance meter. Estuarine Coastal Mar. Sci. 10: 455–466.

Turbidity Maximum Migration and Harbor Siltation in the Tay Estuary[1]

C. DOBEREINER AND J. MCMANUS

Department of Geology, The University, Dundee, Scotland DD1 4HN

DOBEREINER, C., AND J. MCMANUS. 1983. Turbidity maximum migration and harbor siltation in the Tay Estuary. Can. J. Fish. Aquat. Sci. 40(Suppl. 1): 117–129.

Multiboat simultaneous survey along the 50 km macrotidal Tay Estuary suggested that the turbidity maximum was related to resuspension from tidal flats. New monthly analyses revealed that the turbidity maximum varies in position not only with neap/spring tidal cycles but also in response to river runoff. No relationship was found between elemental particle size and aggregate diameter. Both organic and inorganic particles were found to contribute to aggregate growth, the former exhibiting a slightly greater range of particle diameters than the latter. Aggregate diameters increased with suspension concentration and it is suggested that pH as well as salinity also contribute to aggregate formation.

Continuous siltmeter recordings at Dundee show maximum suspension concentrations on the ebb phase of neap tides and on spring flood tides. In the lower estuary suspension concentrations and salinities vary from shore to shore. The lateral differences are substantial so that a purely one-dimensional variation pattern does not provide sufficient data for thorough analysis of the processes active in this estuary. The observed behavior of the turbidity maximum and related siltation patterns suggest that concentrating maintenance dredging in late spring and early summer would be cost-effective for Dundee Harbour and similar estuarial situations.

Key words: turbidity maximum, suspended sediment, aggregation, estuary, fluvial discharge, harbor siltation

DOBEREINER, C., AND J. MCMANUS. 1983. Turbidity maximum migration and harbor siltation in the Tay Estuary. Can. J. Fish. Aquat. Sci. 40(Suppl. 1): 117–129.

Des levés simultanés réalisés par plusieurs bateaux le long des 50 km de l'estuaire macrotidal du Tay portent à croire que la turbidité maximale est associée à la resuspension des sédiments des veys. De nouvelles analyses mensuelles révèlent que la turbidité maximale varie de position non seulement en fonction des cycles de marée de morte eau et de la marée de vive eau, mais aussi en réponse à l'écoulement des rivières. Aucune relation n'a été découverte entre la taille élémentaire des particules et le diamètre des agrégats. Les particules organiques et inorganiques contribuent à la croissance des agrégats; les premières ont une variété de tailles un peu plus grande que les dernières. Le diamètre des agrégats augmente en fonction de la concentration de la suspension et l'on avance l'hypothèse que le pH ainsi que la salinité contribuent à leur formation.

Des lectures continues de la turbidité à Dundee montrent des concentrations maximales en suspension au cours de la phase descendante de la marée de morte eau et de la phase montante de la marée de vive eau. Dans l'estuaire inférieur, les concentrations des suspensions et les salinités varient d'un rivage à l'autre. Les différences latérales sont importantes; par conséquent, un modèle strictement unidimensionel de la variation ne fournit pas assez de données pour une analyse approfondie des processus en action dans cet estuaire. Le comportement observé de la turbidité maximale et les régimes d'envasement connexes portent à croire que la concentration des activités de dragage à la fin du printemps et au début de l'été serait rentable pour le port de Dundee et les autres estuaires semblables.

Received October 26, 1981
Accepted October 13, 1982

Reçu le 26 octobre 1981
Accepté le 13 octobre 1982

[1]This paper forms part of the Proceedings of the Dynamics of Turbid Coastal Environments Symposium convened at the Bedford Institute of Oceanography, Dartmouth, N.S., Canada, September 29–October 1, 1981.

Printed in Canada (J6701)
Imprimé au Canada (J6701)

IN estuaries throughout the world, normally the river and sea waters contain lower suspended sediment concentrations than the waters of the central estuarine reaches (Balay 1961; Allersma et al. 1966; d'Anglejan 1970; Gibbs 1973; Meade 1972; Urien 1972; Reinson 1977). This zone containing enhanced levels of suspension concentrations is termed the

"turbidity maximum" zone or "bouchon vaseux" (Migniot 1968; Allen and Castaing 1973). It is recognized in virtually all estuaries, but the peak suspension concentrations vary from a few hundred $mg \cdot L^{-1}$ to hundreds of $g \cdot L^{-1}$ according to locality (Inglis and Allen 1957; Einstein and Krone 1962; Biggs 1978). The waters of increased turbidity occur in the reaches where fresh and salt waters meet, in the zones with greatest salinity gradients (Schubel 1968).

Where suspension concentrations are increased, the numbers of particles present are high and there is an increased probability of interparticle collisions with the consequent growth of aggregates. The controls of collision frequency, and therefore aggregate growth rates, include the particle numbers and also their sizes. When Brownian motion alone acts in such a system (as at slack water), perikinetic flocculation is active. However, the application of velocity gradients gives rise to orthokinetic flocculation because under such conditions, the particles have a greater chance of encountering each other. As the salt content of the water rises, further flocculation may occur because increased electrolyte concentrations enhance interparticulate attractions (Owen 1971; Krone 1972; Mehta and Partheniades 1973). Although the presence or absence of flocculation determines only the state of the particles, not whether a turbidity maximum zone is present or absent, it may determine whether the aggregates will settle and cause shoaling problems.

Although Guilcher (1967) demonstrated the migration of the turbidity maximum during the tide and Allen et al. (1970) showed that tidal range also exerted an influence on its position within the estuary, the river runoff is important to the circulation and exerts a control on the nature of the turbidity maximum (Allen 1971). In the extreme case of the Vellar Estuary, Dyer and Ramamoorthy (1969) showed that runoff from monsoons swept the estuary virtually free from salt and removed the turbidity maximum. However, in most estuaries the river discharges vary over a much more limited range and the motion of the turbid zone is correspondingly more restricted. The River Tay of eastern Scotland is a normal stream, with mean daily discharges of 198 $m^3 \cdot s^{-1}$ (Pontin and Reid 1975) which fall to 15 $m^3 \cdot s^{-1}$ in drought conditions and rise to 1450 $m^3 \cdot s^{-1}$ in 40-yr floods (McManus 1968). Under all conditions the turbidity maximum zone remains within the estuary. In this paper we examine the behavior of the turbidity maximum and some variations of associated particle aggregation in the Tay Estuary under different river discharges but identical tidal ranges.

Study Area

The Tay Estuary is situated within a graben cut obliquely across the axis of the Sidlaw anticline in the east of the Midland Valley of Scotland. Prominent hills of L. Devonian lavas dip away from the estuary to north and south, while the graben floor contains Upper Old Red Sandstone and Lower Carboniferous sequences.

Into the 50-km-long tidal reach drain waters from a 6500 km^2 catchment, which is mostly situated in highland terrain on metamorphic rocks. Rainfall varies greatly within the basin, but the higher parts receive up to 3000 mm of precipitation. Much of this is retained as snow during winter to be released to the rivers in March and April. The river discharges rise and fall irregularly in response to the largely orographic rain. At the seaward end of the estuary the North Sea neap tides give ranges of 2.5 m, and 5.0 m spring tides are normal, with equinoctial springs ranging to 6.0 m.

In the upper reaches, the principal channel hugs the southern shore, and tidal flats, which increase seaward in width to 3 km, line the northern shore. In the lower estuary, a constriction caused by the outcropping of lavas between Dundee and Newport reduces the total breadth of high waters from 5 to 2 km (Fig. 1), and the single channel is replaced by three separate channels with intervening sand banks. The waters deepen from 8 m at low water at the Rail Bridge to over 25 m in the single channel between Broughty Ferry and Tayport, the seaward limit of the constriction. Further east still tidal flats again flank the northern and southern shores as far as the estuary mouth.

The stratification varies from partially to well-mixed according to locality. At any one site the salinity values are dependent upon tidal range and river flow (West and Williams 1972; Williams and West 1972, 1975). In the upper reaches the tidal depth-mean salinity is strongly influenced by fluvial discharge and less by tidal range. Although tidal averaging suggests a high degree of mixing, instantaneous profiles frequently show the presence of a well developed salt wedge and resultant stratification during part of the rising tide. During high river flows, salinities at Tayport in the lower estuary at low water on a 5.2 m spring tide vary from 13 to 20‰ in the vertical profile, whereas at high water, they vary from 25 to 30‰. During low river discharges on similar 5.2 m spring tides at the same site, low water ranges are 21−23‰ and at high water 31−32‰.

Fluvial and Marine Suspended Sediments

As in most river systems during normal and low fluvial discharges suspension concentrations in the river waters are low (Al-Ansari and McManus 1979; Al-Jabbari et al. 1980). The loads transported increase with water discharge, although the peak sediment concentrations frequently reach the head of the estuary some time after the greatest river discharges (Buller and McManus 1976). The North Sea waters generally have low suspension concentrations with 10 $mg \cdot L^{-1}$ a normal high figure (Charlton 1981; Cracknell et al. 1982). Following periods of storm activity in which waves rework the sea floor sediments, giving rise to extra entrainment, the suspension concentrations in the influent marine waters may become much greater and have been measured at 40 $mg \cdot L^{-1}$.

While suspension concentrations of around 10 $mg \cdot L^{-1}$ are normal under average conditions at each extremity of the estuary, the concentrations increase substantially within the upper and middle reaches where a turbidity maximum with concentrations exceptionally reaching over 400 $mg \cdot L^{-1}$ is developed.

The suspension concentrations determined on two separate occasions in June 1972 from seven boats moored simultaneously at stations along the estuary channel throughout complete tidal cycles (Buller et al. 1972) were not uniform through the depth of the water column. During most of the tide, concentrations in the surface were similar to those in the

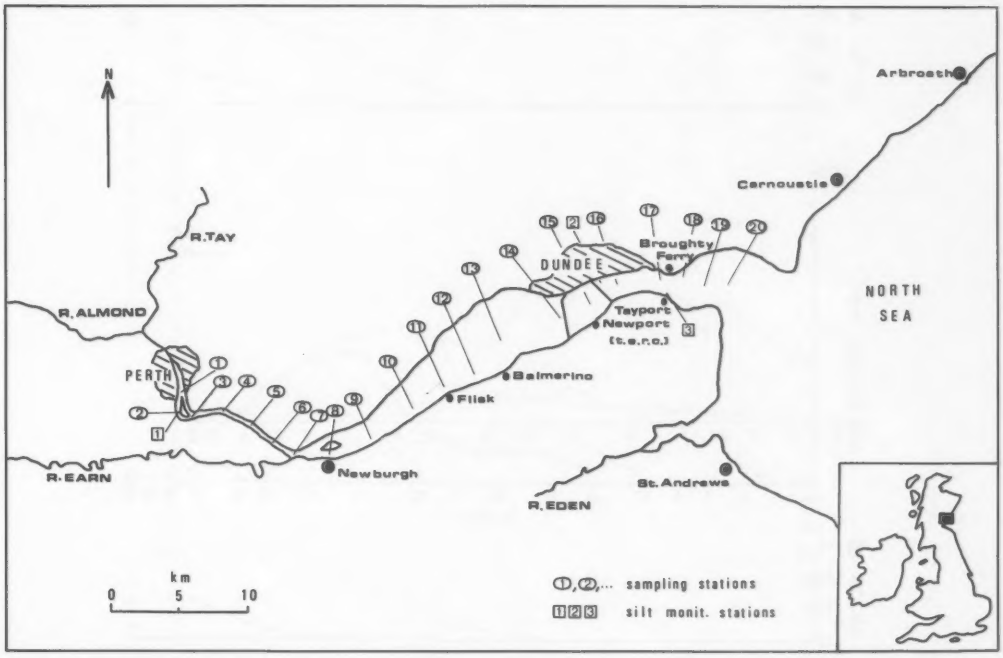

FIG. 1. Sampling sites in Tay Estuary.

middle and bottom waters, with which they varied in step and in magnitude of change. Along the channel, settling may occur at slack water and some stratification of suspension concentration was detected an hour after low water. The turbidity maximum migrated in position during the tidal cycle, was best developed at low water, and was most diffuse at high tide (Buller and McManus 1974). The multiple nature of the turbidity maximum was attributed partly to sediments entrained in ebb tidal waters draining from the extensive tidal flats (Buller 1975).

Methods

To further understand the behavior of the suspensions and their responses to river flows, monthly water samples were taken over an 18-mo period from the middle of the channel along the estuary at high and low water during tides with similar predicted range. The 5.0 m tide was selected as the most commonly occurring spring tide, for which proven numerical models of salinity (Williams and West 1975), tidal height and current speed variations (Williams and Nassehi 1980) were available. Some tides of other ranges were also measured. Near surface water samples were collected by EURASEP sampler from a fast launch which moved landwards with the peak or trough of the tide. (The tidal wave takes about 1 h to penetrate the estuary.)

After determination of temperature, salinity, and pH, up to 1 L of water was filtered through a 1.25-μm glass fibre filter and the residual weight determined after desiccation.

Tay Profile Patterns of Variaton

The suspension concentrations exhibit a regular pattern of variation through the estuary, a pattern whose location changes with river discharge and also with tide range. The winter 5.0 m spring high and low tide distributions associated with high river discharge (280 $m^3 \cdot s^{-1}$) are illustrated in Fig. 2A.

At high water, the peak of concentration of no more than 35 $mg \cdot L^{-1}$ was detected at Jock's Hole (station 9), although the turbid suspensions of over 28 $mg \cdot L^{-1}$ stretched to Birkhill (station 12), beyond which it fell gradually seawards to 10 $mg \cdot L^{-1}$ at the Rail Bridge. To landward the concentrations fell sharply to 5 $mg \cdot L^{-1}$ at the Earn confluence.

At low water, the greatest measured concentrations reached 84 $mg \cdot L^{-1}$ off Balmerino (station 13), although the zone of enhanced values (over 20 $mg \cdot L^{-1}$) stretched from Flisk to Tayport (stations 11 to 17). To seaward and landward concentrations fell to 10 $mg \cdot L^{-1}$. Reference to the salinity plot reveals that at high water the peak concentrations occurred in waters with 0–6‰ salinity, and at low water in the zone with similar salinities (0–8‰).

Similar observations were made on many occasions, demonstrating the strong association of the limit of salt

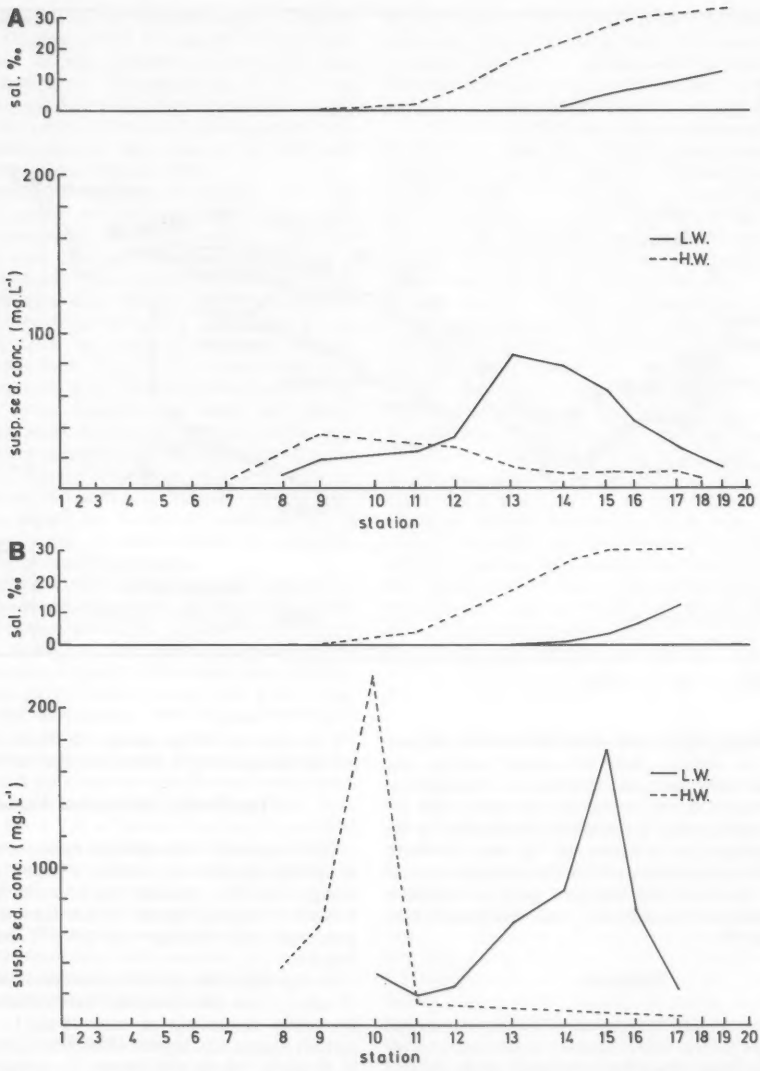

FIG. 2. Variations of surface salinity and suspended sediment concentrations at high and low water on a (A) 5 m spring tide with river discharge (Q_f) of 280 $m^3 \cdot s^{-1}$; (B) 5.8 m spring tide with river discharge (Q_f) of 210 $m^3 \cdot s^{-1}$.

penetration to the position of the turbidity maximum. Thus, the Tay waters behave like those of most other estuaries.

During equinoctal 5.8-m tides associated with river discharges of a little above average (210 $m^3 \cdot s^{-1}$), the distribution of concentrations was similar although the absolute values rose to 170 $mg \cdot L^{-1}$ at low water and 220 $mg \cdot L^{-1}$ at high water (Fig. 2B). As before, the spread of the turbidity maximum was greater at low water than at high tide. Although the peak high water concentrations occurred between Jock's Hole (station 8) and Flisk (station 11) as on a 5.0 m tide, the low water peak occurred much farther (6 km) seawards, within the Dundee Harbour area (station 15). The turbidity peak coincided with salinities in the range 0–5‰ at high water but also in the range 0–8‰ at low water. Thus, the

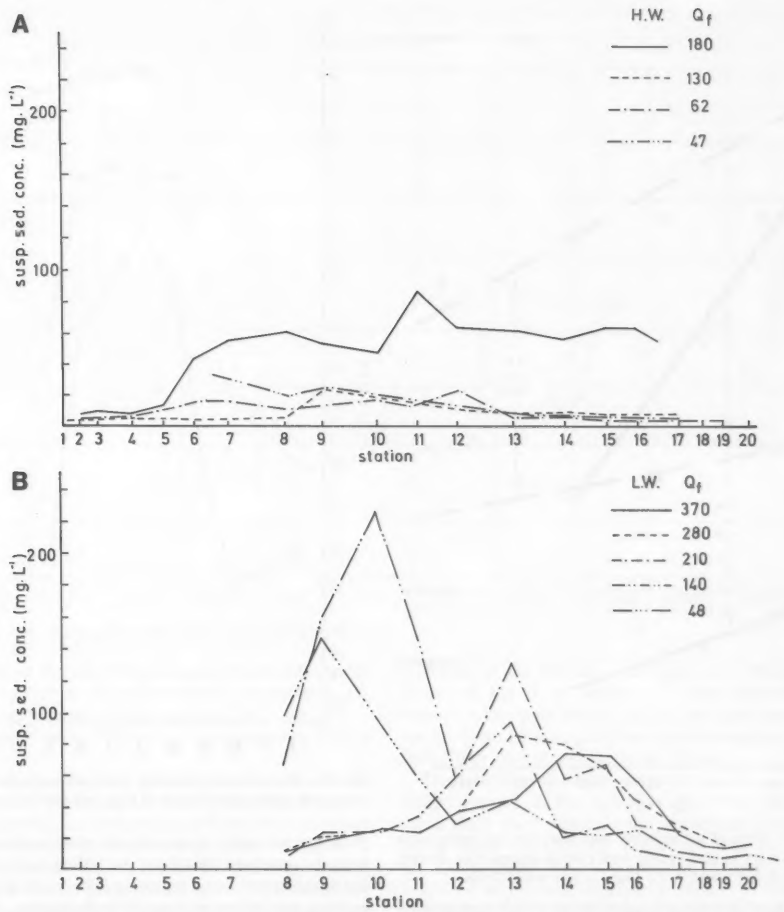

FIG. 3. Surface suspended sediment concentration variations along the Tay Estuary for (A) high water of 5 m spring tides with different river discharges (Q_f given in $m^3 \cdot s^{-1}$); (B) low water of 5 m spring tides with different river discharges (Q_f given in $m^3 \cdot s^{-1}$).

effect of tidal range is clear; the turbidity maximum moves the full length of excursion of a single water parcel during a tide.

Sampling on 5.0 m spring tides through the year has enabled us to examine the variation of concentration peaks against fluvial discharge (Fig. 3A). At low tide during high river flows (370 $m^3 \cdot s^{-1}$) the peak was situated between the Rail and Road Bridges (stations 14 and 15). As river discharge decreased, so the greatest suspension concentration moved landwards so that with flows of 280 $m^3 \cdot s^{-1}$ it lay at station 13, with 103 $m^3 \cdot s^{-1}$ at station 10, and with 48 $m^3 \cdot s^{-1}$ it was at station 9.

The peak absolute value of suspension concentration for the same tidal range increased with decreasing river discharge. In summer when river discharge is low and suspended load transport into the head of the estuary is very small, high concentrations within the upper estuary at low water probably result from increased tidally induced scour, which is directly related to the volume of the tidal prism passing a given point on the channel. During high river discharge the tidal volume passing landward of a given location in the upper estuary is much smaller than during low river discharge.

At high water of spring tides the concentrations are normally much lower than those at low water. There is a small increase of values above background concentrations to seaward and landward (20–35 $mg \cdot L^{-1}$ compared with 5–10 $mg \cdot L^{-1}$). The subdued turbidity maximum extends from a seaward limit at station 13, usually as far as the Earn mouth (station 7), but it has been observed to reach station 6 during sustained storm conditions with east–northeasterly winds blowing up estuary throughout the flood tide. This

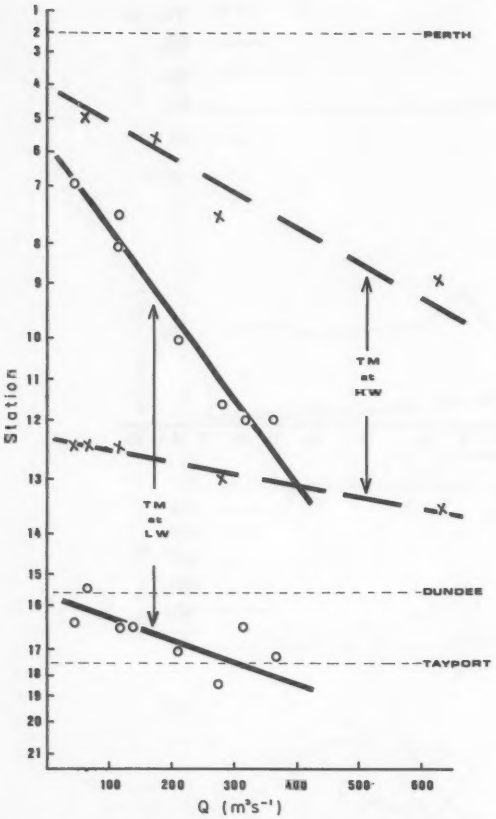

FIG. 4. The limits of the turbidity maximum on 5 m spring tides in the Tay Estuary plotted against total river discharge (Q_f). Broken lines — high water limits; Solid lines — low water limits.

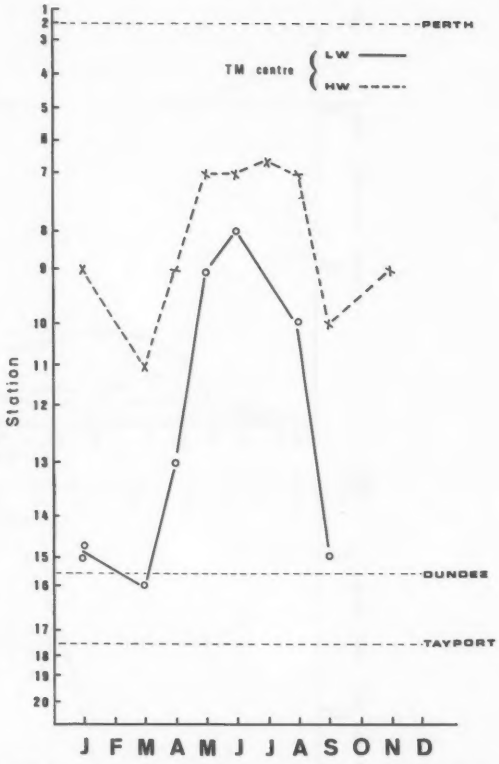

FIG. 5. The location of the peak concentration in the turbidity maximum zone in the Tay Estuary at high and low water through 1980.

substantial wind activity generated waves which resuspended fine sediments from the marginal tidal flats, so that the suspension distribution pattern was abnormal.

Multiple Concentration Maxima

The nature of the turbidity maximum zone itself varied with fluvial discharge (Fig. 3B). With discharges of 280 $m^3 \cdot s^{-1}$ and above, a single concentration peak zone was present. Multiple peaks were detected on all discharge conditions from 210 $m^3 \cdot s^{-1}$ downwards. Peak concentrations were normally detected at stations 13 and 15, but on low flows other major concentration maxima occurred further upstream.

In his early studies, Buller (1975) detected a double peak of suspension concentrations on neap tide, but only a single peak on spring tide. The river discharges during the period of his single peak measurement were 260 $m^3 \cdot s^{-1}$ which compares well with discharges showing single peaks of concentration. Buller (1975) attributed the neap tide double peak phenomenon partly to erosion and resuspension of sediment from the emergent tidal flats. According to our observations, the double peak occurs on spring tides but in association with average and below average river discharges. No clear evidence of a suspension source from the tidal flats emerged during the present study.

In the period since the observations were taken on which Buller's suggestion was based (Buller et al. 1972), there has been a change in the configuration of the margin of the tidal flats. A major channel draining southwards from the tidal flats opposite Birkhill (station 12) has become silted up so that the flow from the flats now joins the channel very near station 13, a site at which subsidiary peaks are often detected today. However, subsidiary peaks also occur further seaward during low water of other tides.

The suspension concentrations measured in the surface waters were normally similar to those occurring at depth. On one cruise, samples taken from three depths in the water column at each location on the profile revealed that surface, middle, and near bed concentrations increased and decreased at similar sites although the absolute values normally increased with depth.

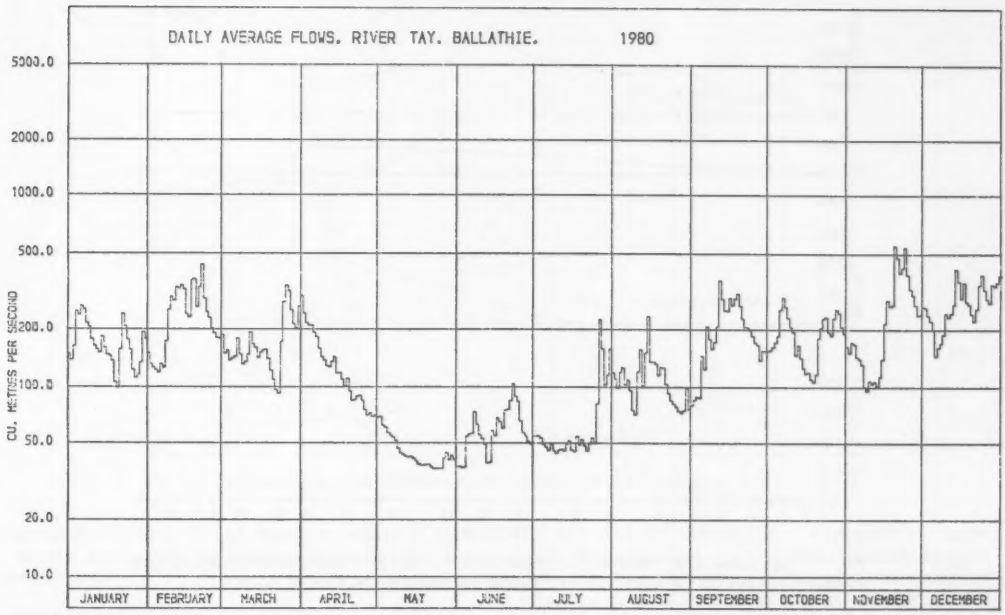

FIG. 6. Mean daily discharges of the River Tay at Ballathie in 1980.

During most of the tide vertical concentration differences from bed to surface in the main channel occasionally exceeded 15%, but during slack water of low tide, downward increases of over 30% occur at several sites (Buller et al. 1972).

We drew together the data on surface water suspension concentrations on 5 m spring tides and plotted the limits of the zones of increased concentration (defined by the presence of sharp concentration gradients usually above 10 $mg \cdot L^{-1}$) against river discharge (Fig. 4) of both Tay and Earn. During low river discharge, the geographical spread of the turbidity maximum zone at high water (broken lines) was greater than during high discharge. The seaward migration of the turbid waters at higher discharges was likewise revealed. A similar variation in the extent of the turbid waters at low tide compared with river discharge was observed (solid lines). Thus, during high river flows, the turbid waters became much more geographically restricted than during average and low discharge conditions.

At sites within the central triangle, formed between the landward low water and seaward high water limits of the high concentration zone, lies a stretch of water where the waters remained relatively turbid throughout 5 m spring tides for all river discharges of less than 400 $m^3 \cdot s^{-1}$. With greater river discharges (more than twice the mean daily average flows), clearer surface water was present for part of the tide. To landward and seaward of this sector, the waters cleared for at least part of the tide.

As the zone of enhanced concentration migrated, the location of the point of peak concentration also changed. The migration of the turbidity maximum (s.s.) through 1980 is plotted in Fig. 5. In summer the peak concentrations lay entirely in the upper estuary, as did high water peaks throughout the year. However, at low water in autumn, winter, and spring they moved into the lower estuary.

The turbidity maximum migration relative to river discharge appears in Fig. 6 which shows the annual plot of mean daily discharge past the lowermost gauging station on the River Tay (Fig. 6). The inflow from the River Earn provides a further 16% of the total freshwater discharge and follows a very similar distribution pattern. A relatively normal water year, 1980 was characterized by low river flows in May–July, with flows rising in August towards winter maxima of a little over 500 $m^3 \cdot s^{-1}$. An absence of heavy snowfall and subsequent snowmelt maintained high flows from the cyclonic-orographic rainfall throughout most of the winter, without exceptional peaks.

Comparison of Fig. 5 and 6 serves to emphasize the greater movement of the waters during high discharge, the distance of migration of the turbidity maximum being much greater in winter than in summer.

In their analyses of salinity variations in the estuary, Williams and West (1972) demonstrated a strong dependence upon river discharge and found optimal correlation with 10-d average flows into the estuary. However, we have not been able to confirm such a relationship with suspensions and there was little improvement in correlation between 1-d, 5-d, and 10-d averaged discharges and suspension concentration positional variation, and a direct single-day discharge is used here as a comparator.

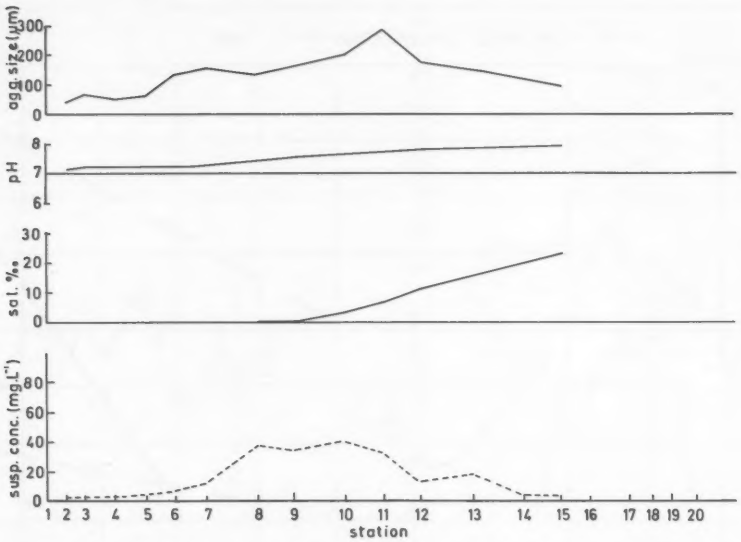

FIG. 7. High water surface variations of aggregate diameter, water pH, salinity, and suspended sediment concentration along the Tay Estuary on a 4.5 m neap tide with river discharge of 105 $m^3 \cdot s^{-1}$.

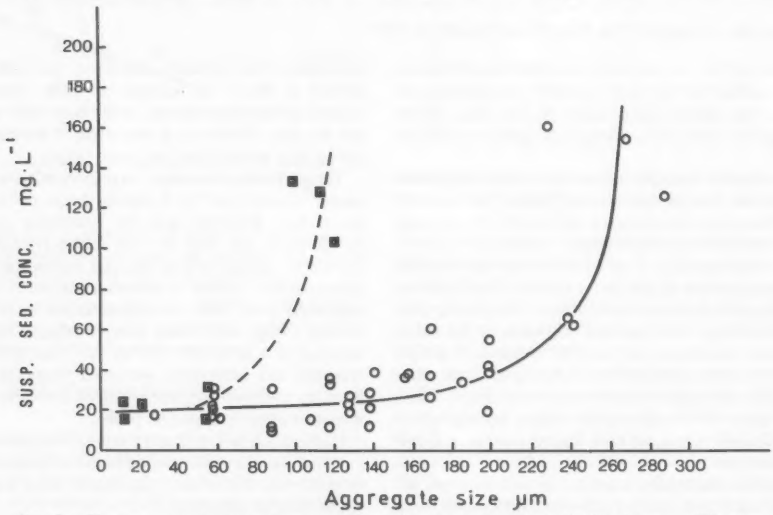

FIG. 8. Plots of aggregate size against suspended sediment concentration in the Tay Estuary, 1980–81. Curve fitted by eye. Open circles — calm conditions; Squares — storm conditions.

The Suspended Sediments

COMPOSITION

The particles in suspension in the Tay Estuary waters are of both organic and inorganic matter. X-ray diffraction studies have shown that the mineral fraction is largely of muscovite and illite, with important kaolinite and chlorite–biotite and with variable proportions of quartz and feldspar (F. H. Hubbard, Geology Dep., Univ. Dundee, Scotland, personal communication). The organic matter varies in proportion through the year, rising to 25% by weight during the

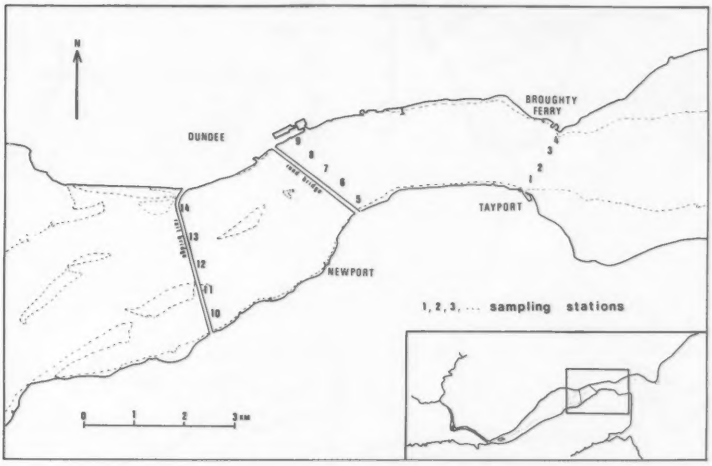

FIG. 9. Sampling locations on profiles across the middle and lower Tay Estuary.

spring algal blooms. At such times, the volume of organic material may almost completely mask the mineral matter of the sample.

PARTICLE SIZE

Disaggregation of the suspensions by ultrasonic means for 30 min prior to analysis using a Model TIIa Coulter Counter enabled the diameters of individual small particles to be determined. Analyses of suspensions without removal of organic particles suggested that the mean particle size ranged from 4 to 20 μm and that less than 5% of the material was finer than 3 μm. Resuspension after ashing (on Millipore filters at 600°C for 1 h) to remove combustible organic material provided a second sample for examination. Since ashing may also destroy clay mineral structures, the resultant reanalysis diameters must be interpreted with great caution; however, Coulter analysis indicated median sizes between 5 and 16 μm in all cases, and less than 3% of the material was finer than 3 μm.

Thus, the "organic" particles appeared to have diameters of a broader range than the "inorganic" materials in suspension. On balance the coarser "organic" particles were more abundant in the upper reaches of the estuary and fine "organics" at the seaward end. In May 1981, samples taken during the spring algal bloom along the entire estuary showed substantially finer median diameters (4−6 μm) but after removal of the "organics," reanalysis showed median diameters of 6−10 μm according to locality.

AGGREGATE SIZE

Subsamples of surface waters retrieved with minimal disturbance were examined within 2 min of sampling under the optical microscope on board a larger vessel. The aggregates varied greatly in shape, some being composed of long thin strings of particles, while others were nearly circular in profile. It is suggested that the former were partly of organic fibres, whereas the latter appeared to be principally inorganic grains with associated equant organic detritus. The nonfibrous aggregates observed were normally closely similar in diameter and only rarely was substantial size variation detected.

Aggregate diameter was defined as the diameter of the near-circular materials or was calculated as the mean of the sum of length and width of the fibrous aggregates. In all cases, at least 20 aggregate diameters were measured to determine a local mean diameter. Since aggregate growth could be observed in the sample under examination, the numbers measured were restricted and the mean recorded diameter was quoted to the nearest 5 μm to emphasize the approximate nature of the determination. The mean aggregate diameter, determined visually with a gridded mesh of known scale, varied from 40 μm in the river sections through 135 μm by the Earn confluence, to peak diameters of 260 μm off Birkhill (station 12), before decreasing seawards to less than 100 μm at the Road Bridge. An example of the aggregate size variation at high water on a 4.5 m neap tide is given in Fig. 7. Suspended sediment concentrations were low overall. The increase in aggregate diameter appeared at the landward end of the turbid zone. Greatest aggregate diameters were found towards the seaward end of the turbid waters. Both the turbid waters and the increased aggregate sizes were detected substantially landwards of the 1‰ salinity readings. The growth of aggregate size has often been linked with salinity and if this is true for the Tay, then the levels of salinity associated with initiation of growth are below 1‰. Small aggregates have been recognized in the waters at Perth with salinity values from 0.08 to 0.3‰ on different occasions. Similar aggregates are also present in freshwater lakes in the catchment, so at least some of the aggregation appears to be unrelated to salinity.

Other aspects of water chemistry may be important. In the uppermost estuarine reaches, the pH of the waters varied

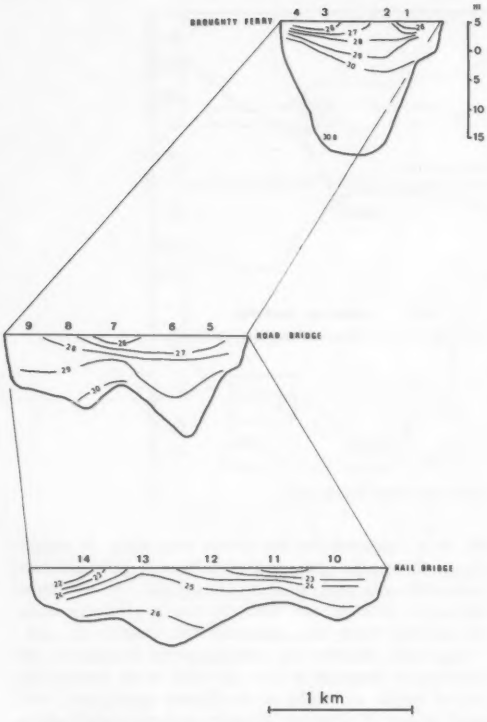

FIG. 10. High water salinity variations on profiles in the middle and lower Tay Estuary on a 5.4 m spring tide during near average river discharge (220 $m^3 \cdot s^{-1}$), but during above average 7-d mean river flow, Q_7 of 270 $m^3 \cdot s^{-1}$ (January 21, 1981).

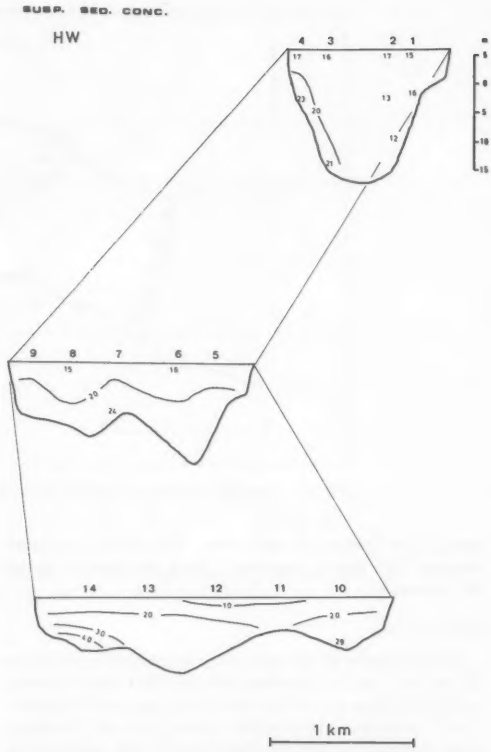

FIG. 11. High water suspended sediment concentrations ($mg \cdot L^{-1}$) on profiles across the middle and lower Tay Estuary on a 5.4 m spring tide during near average river discharge (220 $m^3 \cdot s^{-1}$) but during above average 7-d mean daily river flow, Q_7 of 270 $m^3 \cdot s^{-1}$ (January 21, 1981).

little from the 7.2 of the effluent river. However, from Seggieden (station 5) seawards, the pH values rose steadily to reach 8.0 at the Road Bridge. The increase in pH of the waters coincided with the start of the measured aggregate diameter increase in the upper estuary. Similar observations of coincidence of pH and aggregate size increase were obtained on several cruises, so that the relationship does not appear to be fortuitous. At times pH of the fluvial input was as low as 6.7 (compared with 6.4 in the lochs of the Tay system; R. W. Duck, Geology Dep., Univ. Dundee, Scotland, personal communication).

Aggregate growth also coincided with the zone of raised suspension concentrations in the estuary. Under conditions of low concentration, there was an apparent increase of aggregate size from 20 to 200 μm as concentrations increased to some 40 $mg \cdot L^{-1}$ (Fig. 8). A spread of data points in this plot reflects variability in the natural system. For samples in natural suspensions of over 60 $mg \cdot L^{-1}$, the aggregate diameters increased less rapidly but large fluffy clots of sediment 230–290 μm in diameter were obtained in calm waters with concentrations of 105–140 $mg \cdot L^{-1}$. A possible relationship curve is given in Fig. 8. Deviations were found when aggregates formed under stormy conditions. The largest diameters measured at such times were around 120 μm in waters having concentrations of 80–120 $mg \cdot L^{-1}$. This reduced maximum aggregate diameter may have resulted from the added turbulence which prevented the formation of larger stable particles or breakup of any which may have formed previously. Thus, whereas during calm conditions virtually all aggregates appeared to be of similar size, during storm conditions, although many were similarly sized, there were also smaller aggregates suggesting that breakup of larger aggregates had taken place.

Preliminary observations suggest that seaward of the concentration peak, aggregate size may be greater than landward of it for similar suspension concentrations. There was no evidence that size variation of the primary particles (determined from samples taken at the same time) exerted any influence on aggregate diameter.

Profiles Across Estuary

When salinity and suspension concentrations across the

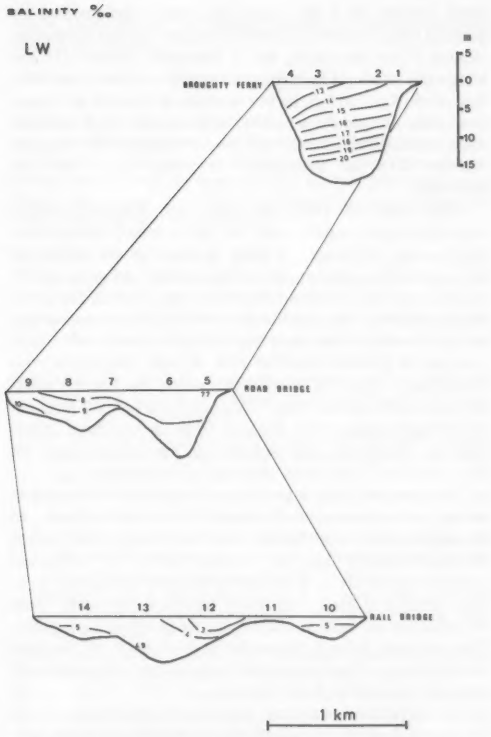

FIG. 12. Low water salinity variations on profiles across the middle and lower Tay Estuary on a 5.4 m spring tide during near average river discharge (January 21, 1981).

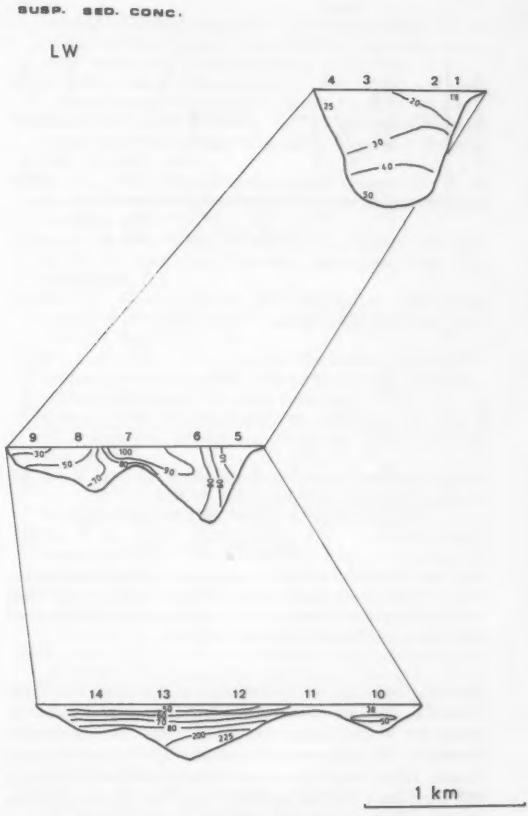

FIG. 13. Low water suspended sediment concentration ($mg \cdot L^{-1}$) on profiles across the middle and lower Tay Estuary on a 5.4 m spring tide during near average river discharge (January 21, 1981).

lower and middle reaches on three cross-sections from the Rail Bridge to Broughty Ferry (Fig. 9) at high and low water on a range of tidal conditions are examined, the motions are elucidated. The salinities and concentrations measured at high and low water on a 5.4 m spring tide (January 21, 1981) during average river discharge conditions (220 $m^3 \cdot s^{-1}$) are shown in Fig. 10–13.

At high water, stratification of salinity is seen in all three sections (22–26, 26–30, and 26–31‰ from land to sea, respectively). At this time, the suspensions varied little at Broughty Ferry and along the Road Bridge, but along the Rail Bridge the northern channel was floored with higher concentrations in a poorly layered water column.

At low water, stratification of salinity was striking at Broughty Ferry (13–30‰), but was more subdued further west. The mass of relatively fresh ebbing waters in the main channel migrated along a path approximately from stations 12 to 6 to 4 (Fig. 9). The suspensions were much higher than at high water (Fig. 13) with greatest values near the floor off Broughty Ferry, around the end of Middle Bank (station 7) at the Road Bridge, and flooring the main channel beside the Rail Bridge.

During neap tides with high river discharges (January 29, 1981), salinity stratification reached 12–27‰ off Broughty Ferry at high water and values of 10–20 and 7–14‰ were detected at the Road and Rail Bridges, respectively, at low water. On this tide there was virtually no suspension load at Broughty Ferry at either high or low water, and little at the Road Bridge. The turbid waters were present at the Rail Bridge at low water, within the main channel.

The ebbing turbid waters normally pass seawards along the main channel so that when river discharges are high, the turbid waters extend seaward of the Road Bridge. As the tide rises into the estuary in the Road–Rail Bridge reach, it moves largely along the northern shore, so that the rising tides carry turbid waters into channels which transport relatively clear waters during the ebb. This lateral transfer of sediment may permit net landward flows onto the tidal flats but net seaward fluxes in the main channel. The northward swing has encouraged the accretion of soft but cohesive fine sediments which form a substantial bank on the inter-bridge foreshore of

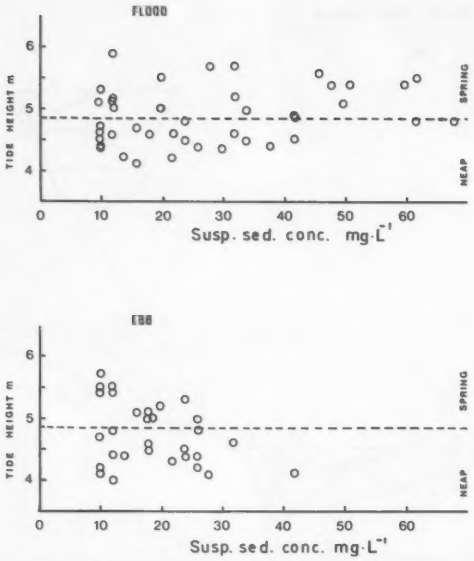

FIG. 14. Variation of peak suspended sediment concentration ($mg \cdot L^{-1}$) on flood and ebb tides of differing predicted high water levels at Dundee Harbour (July 15 – December 10, 1980). Flood tides based on 41 points; ebb tides, 30 points.

Dundee. It also led to rapid siltation of the Craig Pier Ferry Terminal Harbour after regular services were terminated when the Road Bridge opened in 1966. The equivalent harbor on the southern shore, at the Tay Estuary Research Centre, suffers much less acute siltation problems. Although this site comes into the turbidity zone, the high suspensions are present for much shorter time periods and have less opportunity to settle.

The installation of frequently calibrated recording silt meters in Dundee Harbour has revealed that during 1980–81, whereas the mid-ebbing tidal waters rarely carried suspension concentrations above 30 $mg \cdot L^{-1}$ (and those only on neap tides), the mid-rising tide frequently carried waters with greater turbidity, with concentrations of more than 60 $mg \cdot L^{-1}$ recorded on several occasions (Fig. 14). Such patterns support the suggestion of a northward lateral swing of the waters after low tide. Moreover, the scattered distribution demonstrates that suspension concentrations at midtide are independent of tidal range.

Implications for Harbor Siltation

Within the upper estuary, the single channel flanked by tidal flats formed an important waterway for transport of agricultural produce during the 18th and 19th centuries. The principal ports of Dundee and Perth served to concentrate importing and exporting commerce, with smaller, feeder harbors established for low tonnage craft in the intervening areas. The small harbors from Newburgh (station 8) and Port Allen (station 9) in the upper area were supplemented by quays at Flisk (station 11), Birkhill (station 12) and Balmerino (station 13) to the south, and at Powgavie (station 11) and Kingoodie (station 13) on the margin of the northern marshes. East of the Rail Bridge, harbor facilities at Dundee are extensive with on-estuary wharves, tidal basins, and nontidal docks; small harbors exist at Newport (station 15), Tayport (station 17), and Broughty Ferry (see Fig. 1 for site locations).

While trade was brisk, the small upper estuarine harbors were kept open, usually with the aid of minor maintenance excavations. However, as trade declined in the middle of the nineteenth century, the small harbors became rapidly silted up and this process continues today, even in the lower estuary harbors. The sites which have filled most consistently are those within the upper and middle estuary and which coincide in position with the zone of high suspension concentrations. Only the Newburgh harbor on-channel wharf survives in this sector today. Extensive areas of low strength fluffy muds characterize the area north of Mugdrum Island opposite Newburgh, but deposits of "fluid mud" have not been detected in the main channels of the estuary.

The transport and deposition of suspended sediment is strongly dependent upon the patterns of the tidal currents. In the upper estuary, the flowing waters are largely confined to the main channel along the southern shore. Off Balmerino (station 13) the channel swings northwards and lateral channels develop to north and south, separated physically from the principal navigation channel by large linear sand banks. The southern channel rejoins the main channel off Newport but the other, a flood-dominated water course, hugs the north shore to beyond the Road Bridge.

The suspension sampling analyses discussed above have been related entirely to samples taken along the main channel. The discussion of these results in a one-dimensional sense may be partly misleading in that it assumes that the motion, and hence change, takes place entirely in the direction of the main channel. However, our own float tracking, current measurement and multiple simultaneous water monitoring sessions from four or more boats across several reaches all serve to confirm that there is substantial lateral motion of the waters, at least in the middle reaches.

While the harbors of the "fluvial" reaches of the estuary suffer little from siltation, those of the seaward end likewise experience relatively slight sedimentation. Harbors in intervening locations silt up rapidly once they fall into disuse. Siltation may occur largely on one side of a reach rather than on the other, and it is suggested that the lateral motion of waters soon after low tide may be important. Analysis using one-dimensional variations would not predict such apparent imbalances.

Since the period of high siltation potential in the Dundee Harbour area is directly linked to high river discharges, when the turbidity maximum zone is in the lower estuary, it is sensible to recommend that maintenance dredging be concentrated into the late spring–early summer period. After excavation at such a time, river discharges decrease, siltation potential is low and a period of several months elapses before siltation is likely to recommence in the following winter. It is anticipated that where similar behavior of the turbidity maxi-

mum is recognized elsewhere, similar dredging strategies would be cost-effective.

Acknowledgments

The work has been carried out with a grant from Conselho Nacional de Desenvolviment Cientifico e Tecnologico (CNPQ), Brazil whose assistance is gratefully acknowledged. Access to gauging records and harbor installations have been given by the Tay River Purification Board and Dundee Port Authority without whose cooperation the work could not have been completed.

AL-ANSARI, N. A., AND J. MCMANUS. 1979. Fluvial sediments entering the Tay Estuary: sediment discharge from the River Earn. Scott. J. Geol. 15: 203–216.

AL-JABBARI, M. H., J. MCMANUS, AND N. A. AL-ANSARI. 1980. Sediment and solute discharge into the Tay estuary from its river system. Proc. R. Soc. Edinb. (B) 78: 15–32.

ALLEN, G. P. 1971. Déplacements saisonniers de la lentille de 'crême de vase' dans l'estuaire de la Gironde. C. R. Acad. Sc., Paris 273: 2429–2431.

ALLEN, G. P., AND P. CASTAING. 1973. Suspended sediment transport from the Gironde estuary (France) onto the adjacent continental shelf. Mar. Geol. 14: M47–53.

ALLEN, G. P., P. CASTAING, A. FERAL, A. KLINGBIEL, AND M. VIGNEAUX. 1970. Contribution à l'étude des facies de comblement et interprétation paléogéographique de l'évolution des milieux sédimentaires et actuels de l'estuaire de la Gironde. Bull. Inst. Géol. Bassin Aquitaine 8: 99–155.

ALLERSMA, E., A. J. HOEKSTRA, AND E. W. BIJKER. 1966. Transport patterns in the Chao Phya estuary. Proc. 10th Conf. Est. Eng. Tokyo, Japan. 1: 632–650.

BALAY, M. A. 1961. El Rio de la Plata entre la atmosfera y el mar. Servicio de Hidrografia Naval, Buenos Aires, Publ. 621.

BIGGS, R. B. 1978. Coastal bays, 69–92. *In* R. A. Davis Jr. [ed.] Coastal sedimentary environments. Springer-Verlag, New York, Heidelberg, and Berlin.

BULLER, A. T. 1975. Sediments of the Tay Estuary II. Formation of ephemeral zones of high suspended sediment concentrations. Proc. R. Soc. Edinb. (B) 75: 65–89.

BULLER, A. T., J. A. CHARLTON, AND J. MCMANUS. 1972. Data from physical and chemical measurements in the Tay estuary for neap and spring tides, June 1972. Tay Estuary Research Centre Rep. 2: 53 p.

BULLER, A. T., AND J. MCMANUS. 1974. Factors influencing the formation of turbidity maxima with examples from the Tay Estuary, Scotland. Bull. Inst. Géol. Bassin Aquitaine. 7: 37–44.

1976. Fluctuations of suspended sediment in estuaries: a descriptive review. Tay Estuary Research Centre Rep. 3: 39 p.

CHARLTON, J. A. 1981. EURASEP site GB.3. Outer Tay Estuary Sea-Truth Cruise Data, 1979–80. Tay Estuary Research Centre Rep. 6: 21 p.

CRACKNELL, A. P., N. MACFARLANE, K. MCMILLAN, J. A. CHARLTON, J. MCMANUS, AND K. A. ULBRICHT. 1982. Remote sensing in Scotland using data received from satellites: A study of the Tay Estuary region using LANDSAT multispectral scanning imagery. Int. J. Remote Sensing 3: 113–137.

DYER, K. R., AND K. RAMAMOORTHY. 1969. Salinity and water circulation in the Vellar estuary. Limnol. Oceanogr. 14: 4–15.

EINSTEIN, H. A., AND R. B. KRONE. 1962. Experiments to determine modes of cohesive sediment transport in salt water. J. Geophys. Res. 67: 1451–1461.

GIBBS, R. J. 1973. Amazon river estuarine system, 85–88. *In* B. W. Nelson [ed.] Environmental framework of coastal plain estuaries. Mem. Geol. Soc. Am. 133.

GUILCHER, A. 1967. Origin of sediments in estuaries, 149–157. *In* G. H. Lauff [ed.] Estuaries. Am. Assoc. Adv. Sci. Washington, D.C.

INGLIS, C. C., AND F. H. ALLEN. 1957. The regimen of the Thames estuary as affected by currents, salinities and river flow. Proc. Inst. Civ. Eng. 9: 193–216.

KRONE, R. B. 1972. A field study of flocculation as a factor in estuarial shoaling processes. Committee on Tidal Hydraulics, Corps of Engineers, U.S. Army Tech. Bull. 19: 62 p.

MCMANUS, J. 1968. The Hydrology of the Tay Basin, 107–124. *In* S. J. Jones [ed.] Dundee and District. Br. Assoc. Adv. Sci. Dundee.

MEADE, R. H. 1972. Transport and deposition of sediments in estuaries. 91–120. *In* B. W. Nelson [ed.] Environmental framework of coastal plain estuaries. Mem. Geol. Soc. Am. 133.

MEHTA, A. J., AND E. PARTHENIADES. 1973. Effect of physicochemical properties of fine suspended sediment on the degree of deposition. Proc. Int. Symp. River Mech. IAHR, Bangkok.

MIGNIOT, C. 1968. Étude de propriétés physiques de différents sédiments très fins et de leur comportement sous des actions hydrodynamiques. La Houille Blanche 7: 591–620.

OWEN, M. W. 1971. The effect of turbulence on the settling velocities of silt flocs. Proc. 14th Cong. IAHR, Paris, Paper D-4, 27–32.

PONTIN, R. A., AND J. A. REID. 1975. The freshwater input to the Tay Estuary. Proc. R. Soc. Edinb. (B). 75: 1–9.

REINSON, G. E. 1977. Hydrology and sediments of a temperate estuary — Mallacoota Inlet, Victoria. Bur. Min. Res. Geol. Geophys. Bull. 178: 91 p.

SCHUBEL, J. R. 1968. Suspended sediment of the northern Chesapeake Bay. Chesapeake Bay Institute, Johns Hopkins University, Tech. Rep. 35: 264 p.

URIEN, C. M. 1972. Rio de la Plata Estuary environments, p. 213–234. *In* B. W. Nelson [ed.] Environmental framework of coastal plain estuaries. Mem. Geol. Soc. Am. 133.

WEST, J. R., AND D. J. A. WILLIAMS. 1972. An evaluation of mixing in the Tay Estuary. Proc. 13th Coastal Eng. Conf. Ch. 123.

WILLIAMS, D. J. A., AND V. NASSEHI. 1980. Mathematical tidal model of the Tay Estuary. Proc. R. Soc. Edinb. (B) 78: 171–182.

WILLIAMS, D. J. A., AND J. R. WEST. 1973. A one-dimensional representation of mixing in the Tay Estuary. Tech. Pap. Wat. Pollut. Res. London. HMSO 13: 117–125.

1975. Salinity distribution in the Tay Estuary. Proc. R. Soc. Edinb. (B) 75: 29–39.

Dynamics of Coastal Fluid Muds in Low-, Moderate-, and High-Tide-Range Environments[1]

JOHN T. WELLS

Coastal Studies Institute, Louisiana State University, Baton Rouge, LA 70803-7527, USA

WELLS, J. T. 1983. Dynamics of coastal fluid muds in low-, moderate-, and high-tide-range environments. Can. J. Fish. Aquat. Sci. 40(Suppl. 1): 130–142.

Field studies of intertidal and subtidal fluid muds in low-, moderate-, and high-tide-range environments have revealed several similarities in process-response behavior despite the wide range in tidal energy. Using data from Louisiana (tide range 0.5 m), Surinam (tide range 2.0 m), and South Korea (tide range 5–9 m), examples are given for the unifying characteristics of (1) extreme wave attenuation, (2) high suspended-sediment concentration, and (3) rapid migration and "shifting" of soft muds. The loss of incoming wave energy results in natural protection to shorelines that are fronted by fluid muds. The opportunity thus exists to predict areas of future progradation and erosion from knowledge of fluid mud behavior. Fluid muds can be easily resuspended by small waves, and the high concentrations of suspended sediments in regions of mudshoals suggest that net transport rates can be enormous even under relatively weak currents. In addition to serving as temporary and transitory storehouses for littoral sediments, intertidal mudflats and subtidal mudshoals can become "welded" to the shoreline and colonized by vegetation in a single season.

Key words: fluid mud, fine-grained sediments, wave attenuation

WELLS, J. T. 1983. Dynamics of coastal fluid muds in low-, moderate-, and high-tide-range environments. Can. J. Fish. Aquat. Sci. 40(Suppl. 1): 130–142.

Des études sur le terrain des vases fluides intertidales et subtidales dans des environnements d'amplitudes de marées faibles, modérées et élevées ont démontré plusieurs points de similitude dans leur comportement, en dépit de la gamme étendue d'énergie des marées. Faisant appel à des données de la Louisiane (amplitude de marée de 0,5 m), du Surinam (amplitude de marée de 2,0 m) et de la Corée du Sud (amplitude de marée de 5–9 m), nous donnons des exemples des caractéristiques unificatrices de (1) l'atténuation extrême des vagues, (2) la concentration élevée de sédiments en suspension et (3) la migration et le « glissement » rapides des vases molles. Par suite de la perte d'énergie par les vagues, les rivages auxquels font face des vases fluides sont dotés d'une protection naturelle. Connaissant le comportement des vases fluides, on pourra donc prédire les aires où il y aura accumulation et érosion. Les vases fluides peuvent être facilement resuspendues sous l'action de petites vagues, et les fortes concentrations de sédiments en suspension dans les régions de hauts-fonds de vase laissent supposer que les taux de transport net peuvent être énormes, même avec courants relativement faibles. En plus de servir comme entrepôt temporaire des sédiments du littoral, les vasières intertidales et les bancs de vase subtidaux peuvent se « souder » au rivage et être colonisés par la végétation en une seule saison.

Received January 6, 1982
Accepted July 15, 1982

Reçu le 6 janvier 1982
Accepté le 15 juillet 1982

ACCUMULATIONS of gel-like fluid mud, referred to variously as soft silt, sling mud, fluff mud, and creme de vase, front many coastlines of the world, from the humid tropics of the equatorial latitudes to the frozen "deserts" of the Arctic. Most coastal fluid muds occur as intertidal and subtidal mudshoals near major rivers, and the source of mudshoal sediments can be traced directly to these rivers. For example, the Mississippi River supplies muds to the coast of Louisiana, the Amazon River supplies muds to the shorelines of French Guiana, Surinam, and Guyana, and the mudflats of the Yellow Sea and Gulf of Po Hai are derived from both the Yangtze and Hwangho rivers in China. Inasmuch as nearly 30% of the world's fluvial sediment is derived from rivers in Asia (Holeman 1968), the greatest concentrations of fine-grained sediment are found in Asian countries such as India, Malaysia, Thailand, China, and Korea.

Defined by Krone (1962) as sediment–water mixtures in

[1]This paper forms part of the Proceedings of the Dynamics of Turbid Coastal Environments Symposium convened at the Bedford Institute of Oceanography, Dartmouth, N.S., Canada, September 29–October 1, 1981.

Printed in Canada (J6770)
Imprimé au Canada (J6770)

TABLE 1. Climatic and oceanographic setting for the muddy coast environments of Louisiana, Surinam, and Korea.

	Louisiana (U.S.)	Surinam (S.Am.)	Korea (W. Coast)
Latitude	29°30′N	6°00′N	34°31′–38°00′N
Climate	Subtropical	Tropical	Temperate
Tide range	0.5 m	2 m	5–9 m
Wind effects	Mid-latitude fronts	Northeast trade winds	Mid-latitude monsoonal
Wave energy	Low-moderate	Moderate	High

which sediment concentration exceeds 10^4 mg·L^{-1}, fluid muds are often described as thixotropic substances that possess the rheological properties of pseudoplastics and Bingham plastics. Bulk density ranges from 1.03 g·cm^{-3}, slightly greater than that of seawater, to a yogurt-like consistency with density greater than 1.30 g·cm^{-3}. Water contents are high, shear strengths are low, and behavior may be complex and contradictory to intuitive expectations. Widespread flocculation by inorganic salts and organic compounds and the agglomeration by marine and nonmarine organisms complicate the behavior of fluid muds in the natural environment (Krone 1972; Meade 1972).

Shoals composed of fluid mud range in size from a few hundred metres wide (Louisiana) to gigantic shore-attached banks of soft mud that are exposed 25 km or more at low tide (Korea). Thickness varies from a few centimetres to at least 2 m (Wells and Coleman 1981a, b). Most soft muds are backed by coastal wetlands, either salt marsh or mangrove swamp, and nearly all mudshoals are tenacious yet ephemeral features. Despite suggestions to the contrary, fluid muds can form and survive in coastal environments that receive at least moderate levels of wave energy from the outer continental shelf (Wells and Coleman 1981a).

Mechanisms that lead to the accumulation of fluid muds are poorly understood. Some scientists report that fluid mud is a natural state in all pelite deposition (Augustinus 1978) and that processes such as waves and coastal currents simply concentrate and trap muds to form large shoals (Delft Hydraulics Laboratory 1962; NEDECO 1965, 1968). Specific processes often cited for trapping muds near the coast (McCave 1972) are settling lag-scour lag (Postma 1967), estuarine-type inner-shelf circulation (Eisma 1967; Gibbs 1976), and onshore transport by solitary waves (Wells and Coleman 1981a). The general lack of understanding stems from the paucity of field studies, a result of major obstacles from the standpoint of logistics, instrumentation, and complexity of the problem. The purpose of this paper is to provide a summary of data and ideas generated as part of a long-term program at the Coastal Studies Institute to address the dynamics of muddy coastal environments.

Data Acquisition

Field studies have been conducted in southwest Louisiana (tide range 0.5 m), Surinam, South America (tide range 2.0 m), and the west coast of South Korea (tide range 5–9 m) (Table 1). Quantity and quality of field data from these three environments varied considerably as a result of duration and success of individual field efforts. Data collection was oriented primarily toward coastal processes, with the basic field program consisting of simultaneous measurements of wave height and period, current speed and direction, tide elevation, bathymetry, and collection of water and bottom samples. At the time of this writing the most complete data sets are from Louisiana and Surinam; the most extensive aerial photography and LANDSAT coverage are from South Korea. Details of field methods are given only for the acquisition of data that are discussed in this paper.

LOUISIANA

The primary purpose of field studies in Louisiana, initiated in 1979, was to examine the processes responsible for a new pulse of mudflat growth along the chenier plain of western Louisiana (Fig. 1). Examination of existing maps, charts, and aerial photos was first conducted in order to determine shoreline changes since the early 1900s, when discharge from the Atchafalaya River to the east began increasing (Wells and Roberts 1981). In 1980, nine survey stations were established to monitor beach face and surf zone variations along both prograding and eroding segments of coast. Resurveys have been conducted every two months to chart movement of transitory fluid muds.

Simultaneous measurements of waves, currents, tides, and suspended sediment were collected in July 1981. Waves and tides were measured with a pressure-sensing system designed and fabricated at Coastal Studies Institute. Currents were measured with Endeco 174 ducted-impeller current meters. Water samples were collected simultaneously in 1-L Van Dorn bottles that were mounted on a rigid spar in a vertical array for instantaneous triggering. Further details of methods are provided in Wells and Roberts (1981) and Wells and Kemp (1981).

SURINAM

Field studies in Surinam (Fig. 2) were conducted during August–October 1975 and 1977, when rainfall was low and winds were moderate (<3 m·s^{-1}). Objectives of this research were to examine the mechanism of mudflat migration, particularly the behavior of fluid muds and the interaction between shallow-water waves and soft muds. Ten field stations were occupied over migrating mudshoals for durations of several hours to several days. Waves, currents, and tide elevation were measured simultaneously at many of these stations. A pressure-sensing device consisting of two amplibridge pressure transducers was used to monitor in situ variations in mud density that resulted from suspension, deposition, and

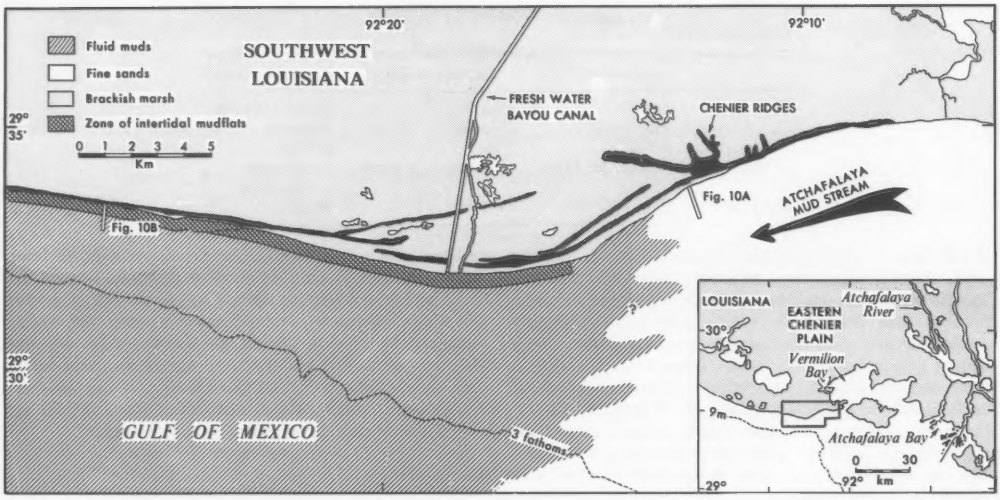

FIG. 1. Louisiana chenier plain showing fluid muds derived from Atchafalaya Bay, to the east.

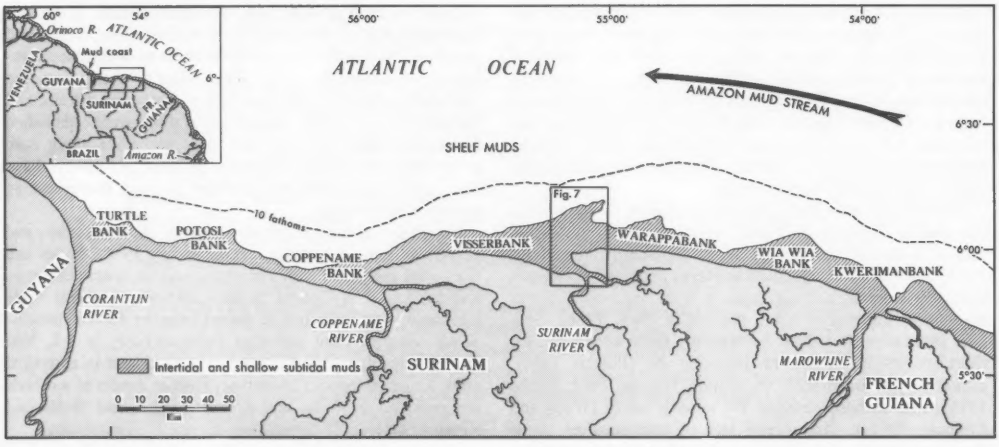

FIG. 2. Northeastern South America showing location of mudbanks from Amazon-derived sediments.

advection of sediment (for details see Wells et al. 1979; Wells and Coleman 1981a).

Sixteen wave attenuation experiments were conducted over a fluid-mud bottom at various stages of tide along the central Surinam coast. Three wave stations were established to record wave height and period simultaneously at 22, 11, and 4 km from the high-tide shoreline. Instrumentation included a Datawell wave-rider buoy at the outer station in 8 m of water and Statham pressure transducers at the intermediate and inner stations in 5 and 1.5 m of water, respectively. All data were recorded as analog signals on Gould Brush strip-chart recorders.

KOREA

Field research in Korea (Fig. 3) began with a reconnaissance of tidal mudflats in 1979. The overall objectives were to provide a better understanding of (1) how muds respond to storm events and to seasonal meteorological forcing, (2) the fate of coastal water and sediment which moves south into the Korea Strait, and (3) the role of tidal flats as a storage facility for fine-grained sediments. Low-cloud-cover LANDSAT imagery (Bands 4 and 7) since 1972 and selected high-altitude aerial photography since 1950 were acquired for comparing coastal changes. Water samples and salinity

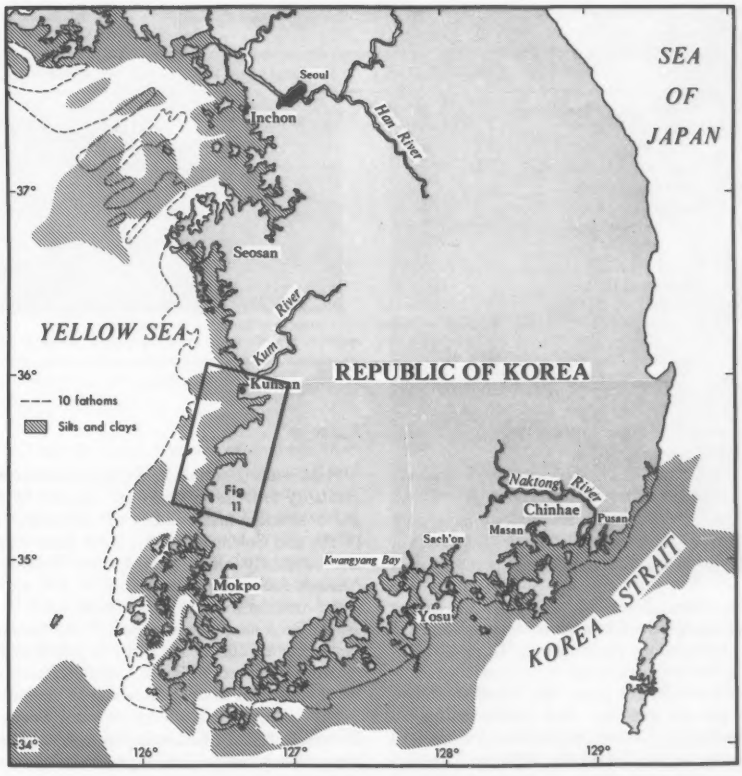

FIG. 3. South Korea showing generalized distribution of fine-grained sediments, compiled from Niino and Emery (1961), Lee (1970), Park and Song (1971), Choi and Hahn (1975), Kim et al. (1975), Kim and Chang (1979), and Wells and Huh (1979).

and temperature hydrocasts were collected on two cruises (November 1980, 1981) in the Korea Strait and southeastern Yellow Sea. Data from the coastal areas of Korea are scarce, and studies are continuing. Further details are given in Wells and Huh (1979).

Morphology and Sedimentology

LOUISIANA

The eastern margin of the Louisiana chenier plain is characterized by localized accumulations of fluid mud, backed by salt marsh and sand/shell chenier ridges. The origin of the fluid muds is the Atchafalaya River to the east (Fig. 1), from which they are transported west in a band of highly turbid water ($10-100\ mg \cdot L^{-1}$) referred to as the Atchafalaya mud stream (Wells and Kemp 1981). Figure 1 shows that muds first begin to accumulate as interfingerings with fine sands east of Freshwater Bayou Canal. They extend west in a semi-continuous fashion for approximately 20 km. Seaward of

FIG. 4. Intertidal mudflat, southwest Louisiana coast west of Freshwater Bayou Canal. Colonization of mud surface by marsh grass in a single season will aid in stabilizing the mudflat.

TABLE 2. Summary of morphology and sedimentology of coastal fluid muds in Louisiana, Surinam, and Korea.

	Louisiana (U.S.)	Surinam (S.Am.)	Korea (W. Coast)
Dimensions of mudshoals			
Alongshore	1–5 km	10–20 km	1–30 km
Offshore	0.5–3 km	10–20 km	5–50 km
Width of intertidal zone	100–300 m	2–5 km	5–30 km
Fluid mud thickness	0.2–1.5 m	0.5–2 m	0.1–3 m
Bulk density	1.15–1.30	1.03–1.30	1.20–1.30
Surface features	Generally absent	Small drainage channels	Extensive drainage channels; scour depressions
Mean particle size	3–5 μm	0.5–1 μm	6–11 μm
Mineralogy	Montmorillonite: illite:kaolinite (3:1:1)	Kaolinite:illite: montmorillonite (2:2:1)	Illite:chlorite: kaolinite (3:1:1)

the zone of soft muds (5–8 km offshore), shelf sediments become alternating sands and muds.

The pattern of muds, marsh, and chenier ridges that we see today has been persistent in western Louisiana for at least 5000 yr (Gould and McFarlan 1959). During the final stage of postglacial rise in sea level, some 3000 yr ago, the chenier plain began to prograde rapidly, and eventually a wedge of recent sediments 6–8 m thick was deposited over a cross-shelf distance of 24 km. Pulses of sediment from former mouths of the Mississippi River, transported by longshore and coastal currents, produced the progradational stage of development. At times when river sediments were introduced in the vicinity of the present chenier plain, the shoreline shifted seaward; during periods when the river mouth discharged farther east, sediment influx to the chenier plain was low and wave attack was able to slow or halt the advance. Cheniers formed during these latter periods and now stand as "islands" on the marsh–mudflat substrate.

Because of the low tide range, mudflats in Louisiana are exposed intertidally (normal to the shoreline) for only a few hundred metres (Fig. 4) but extend subtidally as mudshoals for several kilometres. Probes and shallow cores indicate that thicknesses of fluid muds range from several centimetres to perhaps as much as 1.5 m. A sharp density gradient forms the transition between the layer of fluid mud (bulk density < 1.3 g·cm^{-3}) and the underlying firm clay base (bulk density 1.60–1.80 g·cm^{-3}). In plan view, intertidal exposures of fluid mud are linear- to arcuate-shaped, with surface slopes of 0.001. Muds often fill in small embayments along the crenulated and previously eroded marsh shoreline.

Fluid muds are composed of predominantly montmorillonitic clays with median grain sizes of 3–5 μm (Table 2). Except for miniscule drainage channels and occasionally blocky textures in the denser muds, surface features are generally absent. Patches of fine sand and shell hash occur over muds as isolated veneers that were deposited from longshore drift material during storms. On the trailing edges of migrating mudflats, fluid muds exposed above the mean high-water mark dewater to form mudcracks, which are later eroded and transported as armored mudballs.

SURINAM

Fluid muds in northeastern South America bear remarkable similarity to those in Louisiana. Backed by extensive mangrove swamps and bundles of subparallel chenier ridges (Wells and Coleman 1981b), these muds extend intertidally and subtidally along 1600 km of coastline between the Amazon and Orinoco rivers (Fig. 2). The source of sediment is the Amazon River to the southeast, and transport is within the Amazon mud stream as part of the Guiana Current. The first accumulation of mud can be noted in Brazil near the Amazon River mouth; muds to the northwest of the Amazon River are spread from the shoreline to the mid-shelf position.

The chenier plain of northeastern South America (the Guianas) formed simultaneously with the Louisiana chenier plain. Over a period of 6000 yr a Holocene mud wedge up to 50 km wide and 24 m thick was deposited in Surinam from an annual sediment input of roughly 2.5×10^8 m^3 (NEDECO 1968). The overall pattern of mud deposition was interrupted at times by erosional processes which formed sand/shell beaches by wave action (Vann 1969). These beaches became isolated as chenier ridges by subsequent periods of mud accretion. Today the Guianas experience in proximal locations simultaneous accretion and erosion, which are controlled largely by the presence or absence of accumulations of fluid mud.

Intertidal mudflats and their subtidal mudshoal extensions front the coast of the Guianas every 30–60 km (NEDECO 1968). A typical mudflat–mudshoal system is 10–20 km wide, extends 20 km offshore, and may contain on the order of 10^9 m^3 of sediment. Intertidal exposures are 2–5 km wide measured normal to the shoreline (Fig. 5); slopes are approximately 0.0005. Thixotropic fluid muds that make up the western flanks of mudflats and mudshoals provide shelter from wave attack and allow temporary periods of coastal accretion. Fluid muds are up to 2 m thick. In interbank areas between mudshoals waves impinge directly on the shoreline and produce an abrasion platform of clay as the shoreline is rapidly eroded.

The particles of kaolinite- and illite-rich muds of Surinam are among the finest in the world; median particle diameters

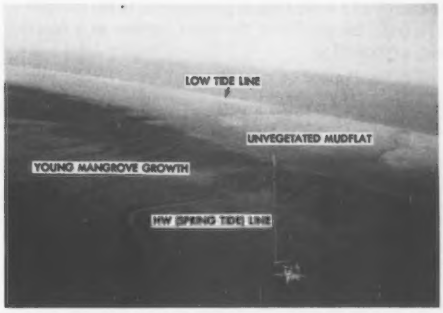

FIG. 5. Intertidal mudflat, central Surinam coast. Width of intertidal zone is approximately 3 km. Colonization of mud surfaces by mangrove vegetation results in the annual addition of new sediment wedges to the Surinam coast.

are 0.5−1.0 μm (Table 2). Small amounts of sand and shell are spread locally across the beach face and incorporated into muds as thin laminations. Fluid muds with bulk density less than 1.22 $g \cdot cm^{-3}$ begin to dewater rapidly when exposed at low tide, thus producing a layer of clear water several centimetres thick that overlies the mud surface. Numerous fractures, contortions, and flow lines, each evidence of mass movement, can be observed through this layer of water. Small drainage channels, 0.3 m deep by 1 m wide, may carry tidal waters across muds that have bulk density greater than 1.25 $g \cdot cm^{-3}$.

KOREA

Backed by rugged headlands, conical hills, and occasional salt marshes, and fronted by extensive tidal mudflats and subtidal sand bodies, the west coast of South Korea is both complicated and bizarre. High-tide range (5−9 m) and severe winter storms create current and wave conditions of sufficient intensity to place the eastern shelf of the Yellow Sea and the west coast of Korea in a category of high energy. However, despite these severe conditions, muds and fine sands persist intertidally, subtidally, and on some parts of the inner shelf from Mokpo to Inchon (Fig. 3).

The fact that the west coast of South Korea is an area of geological submergence accounts for the many peninsulas and embayments and the hundreds of islands, which represent the tops of submerged hills. According to Park (1969), sea level has been rising in the eastern Yellow Sea at relative rates of 0.5−1.5 $mm \cdot yr^{-1}$ for the past 7000 years. It was during this transgression that many embayments were filled with mud and that broad tidal flats developed from locally derived sediments. At low tide 2850 km^2 of "oozing" mudflats are exposed on the west coast alone (Bartz 1972) as a result of high tide range and gentle offshore slope.

Whereas sand predominates in the eastern Yellow Sea and on the outer continental shelf (Niino and Emery 1961), closer inshore, within the coastal boundary layer of the west coast, a band of mud 10−100 km wide exists, complicated by patches of sand, shell, and gravel. In contrast to the single major point source of muds in Louisiana and Surinam, sediments along the west coast of Korea are derived from the Yalu, Han, Kum, and Yeongsan rivers. Although chenier ridges are absent, some beaches are composed entirely of sand or shell (Park and Park 1977).

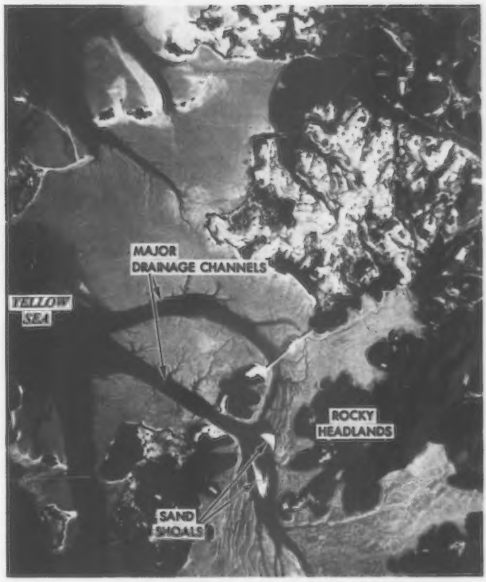

FIG. 6. Intertidal mudflat, west coast of South Korea, showing dendritic drainage channels and parabolic sand shoals. Scale approximately 1:50 000.

Mudflats are perhaps best developed at the entrance to the Kum River, where most of the sediment discharge is silt and clay sized (Fig. 6). Overlying a basement of deeply weathered granitic rocks, mudflat sediments are 3−4 m thick (Park 1969). Intertidal exposures are 10−15 km wide; farther north, in the Inchon Bight, mixed intertidal flats of mud, sand, and gravel are at least 30 km wide (Wells and Huh 1979). Dendritic drainage channels cut through muds to depths of 2−3 m. Dish-shaped scour depressions several meters across and small burrows from crabs and bivalves provide additional relief on muds where bulk densities exceed 1.25 $g \cdot cm^{-3}$.

Wave Attenuation

Aside from the coffee-colored waters so characteristic of muddy shorelines, the single most obvious feature of the nearshore zone is the lack of large waves. As noted since at least the early 1800s in southwest India and northeastern South America, incoming waves are damped by soft muds, often to such a degree that they never reach the shoreline (Bristow 1938; Delft Hydraulics Laboratory 1962). In southwest India, boundaries of the fluid mud accumulations that serve as safe anchorage during southwest monsoons are mapped visually from the calming effect on incident waves (Nair 1976). In northeastern South America, areas of wave

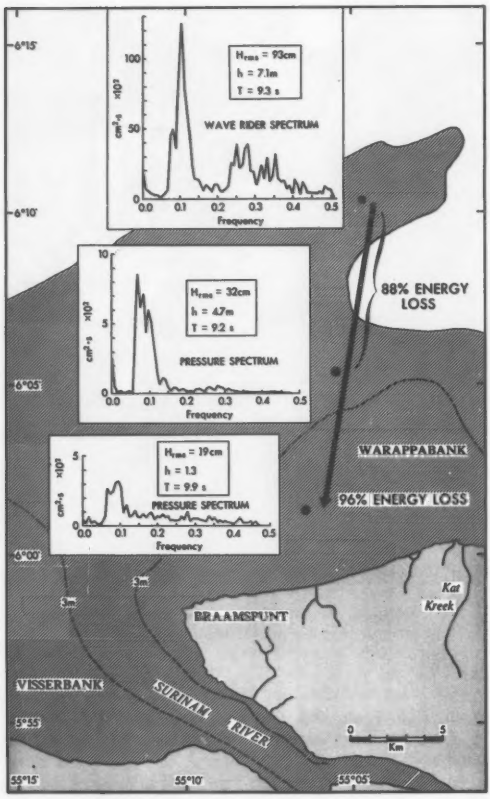

FIG. 7. Wave spectra from simultaneous wave stations at 22, 11, and 4 km offshore, showing loss of wave energy over a fluid-mud bottom. See Fig. 2 for location.

attenuation and coastal progradation follow migrating mudshoals, whereas in intertidal areas between mudshoals breaking waves cause severe coastal erosion (NEDECO 1968). In southwestern Louisiana, shrimpers often take refuge during stormweather in waters over localized accumulations of fluid mud, such as the "mud hole" (Morgan et al. 1953).

Experiments that sought to quantify the rate of wave energy loss over a fluid mud boundary were conducted at three wave stations in Surinam during August 1977 (Wells and Coleman 1981a). Determination of wave energy loss was made from wave spectra constructed from time series records of wave height and period. Given total wave energy per unit surface area in the linearized case

$$(1) \quad \bar{E} = \rho g \frac{H^2}{8}$$

where ρ = density of seawater, g = acceleration of gravity, and H = wave height, it is possible to compute energy loss from wave height. Kinsman (1965) has shown that the average energy of a wave train is proportional to the average value of $[\eta\ (t)]^2$, the profile of the water surface as a function of time, expressed as

$$(2) \quad \eta = \left(\frac{H}{2}\right) \cos\ (kx - \sigma t)$$

where $k = 2\pi/L$, $\sigma = 2\pi/T$, and L and T are wave length and period, respectively. The average value of $[\eta\ (t)]^2$ is identical to σ^2, the variance of the wave record, given by

$$(3) \quad \sigma^2 = \int_o^\infty E(\omega)\, d\omega$$

where ω is frequency. Thus from analog wave records, total energy is determined by constructing a wave spectrum in which total variance of the energy spectrum is equal to total area under all spectral peaks. The standard deviation of the wave record is proportional to the root-mean-square wave height, H_{rms}, usually given as

$$(4) \quad H_{rms} = 2\sqrt{2}\,\sigma.$$

Because data at two of the wave stations were acquired using pressure sensors below the surface of the water, a pressure correction was applied to restore loss of high-frequency waves. Pressure under a wave less atmospheric pressure, is given by

$$(5) \quad P = \rho g\ (\eta K_z - z)$$

where the pressure response factor, K_z, is given by

$$(6) \quad K_z = \frac{\cosh\ [2\pi\,(z + h)/L]}{\cosh\ (2\pi h/L)}.$$

In equations (5) and (6), z = distance below the still-water level, h = water depth, and η is to be determined. Harris (1972) has expressed equation (5) in the form

$$(7) \quad \eta(x,t) = \frac{\cosh\ (2\pi h/L)}{\cosh\ [2\pi\,(z+h)/L]} \frac{P\,(x,z,t)}{\rho g}$$

where z is the depth at which the pressure is to be evaluated. Since $[\eta\ (t)]^2$ is proportional to wave energy, equation (7) can be written to compensate for each frequency band of the spectrum

$$(8) \quad E_{sfc} = \left[\frac{\cosh\ (2\pi h/L)}{\cosh\ [2\pi\,(z + h)/L]}\right]^2 \frac{P^2}{(\rho g)^2}$$

Figure 7 shows an example of wave energy attenuation after correction of the pressure spectra using equation (8). Wave energy loss between the outer and intermediate stations, a distance of 11 km, was 88%; between the intermediate and inner stations, an additional 7 km, energy loss increased to a total of 96%. Although water depth at the inner station was less than 1.5 m, waves did not break, nor did they undergo the typical shoaling transformation that leads to a height

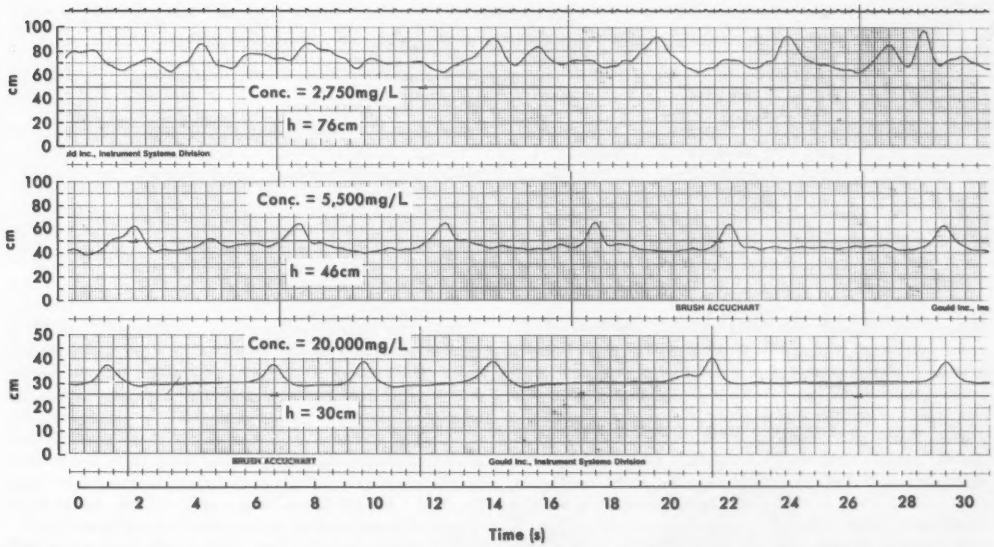

FIG. 8. Wave records taken over Warappabank, central Surinam coast, on a falling tide. Note increase in suspended-sediment concentration with decreasing water depth, h.

increase just prior to the time of breaking. Winds were from the northeast at 7 $m \cdot s^{-1}$ during data collection. Wave spectra at the outer station show a combination of swell waves (T = 9–10 s) and sea waves (T = 3–5 s).

Total wave energy losses ranged from 93 to 96% during the course of five experiments conducted at the stations shown in Fig. 7. Relocation of the inner station to a distance of 1 km offshore resulted in a recorded rate of energy loss of 97–99%. Between the inner stations and the shoreline, waves did not break but were completely attenuated. Along the line of wave travel, the bottom was composed of fluid muds 0.1–1.0 m thick. Bulk density of the fluid mud layer was less than 1.25 $g \cdot cm^{-3}$ (an average bulk density of firm clay is 1.6–1.8 $g \cdot cm^{-3}$).

Concurrent with the rapid loss of wave energy, wave profile is transformed into a form that is very close to that given by solitary wave theory. Steep, symmetrical wave crests are separated by flat troughs that appear to be at still-water level. The solitary-like wave form has been noted 5–10 km offshore of the high-tide shoreline; however, it becomes more pronounced closer inshore or, at a given location, as tide falls and turbidity increases (Fig. 8).

The solitary-like wave form affects the shape of the inner-station wave spectra. Because the construction of wave spectra involves "fitting" sinusoids to the analog wave records, spectral peaks at harmonic frequencies arise when the analog wave signal is strongly nonsinusoidal. Thus the apparent increase in wave energy at frequencies of 0.15–0.45 cps between the intermediate and inner stations (Fig. 7) probably does not represent a true energy increase.

Computation of H_{rms} using equation (4) for fifty 20-min wave records taken over Warappabank (for locations see

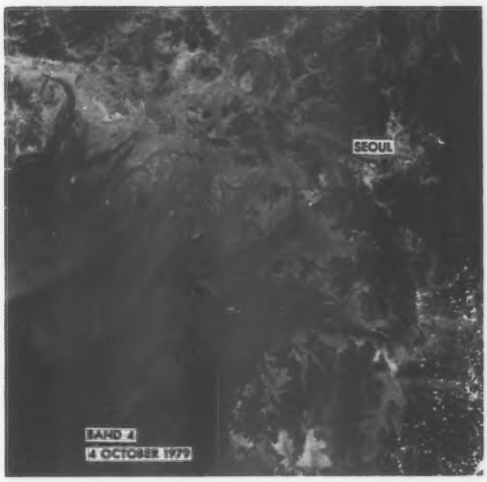

FIG. 9. LANDSAT Band 4 image of the Inchon Bight, west coast of South Korea. Note boundary between high suspended-sediment concentration (white) and 10-fath line on Fig. 3.

Wells and Coleman 1981a) shows that the wave height/water depth ratio for solitary-like waves remains nearly constant at 0.19. The implications of this observation are that (1) the low ratio, 0.19 versus 0.78 for theoretical solitary waves, is another manifestation of severe wave attenuation and (2) in

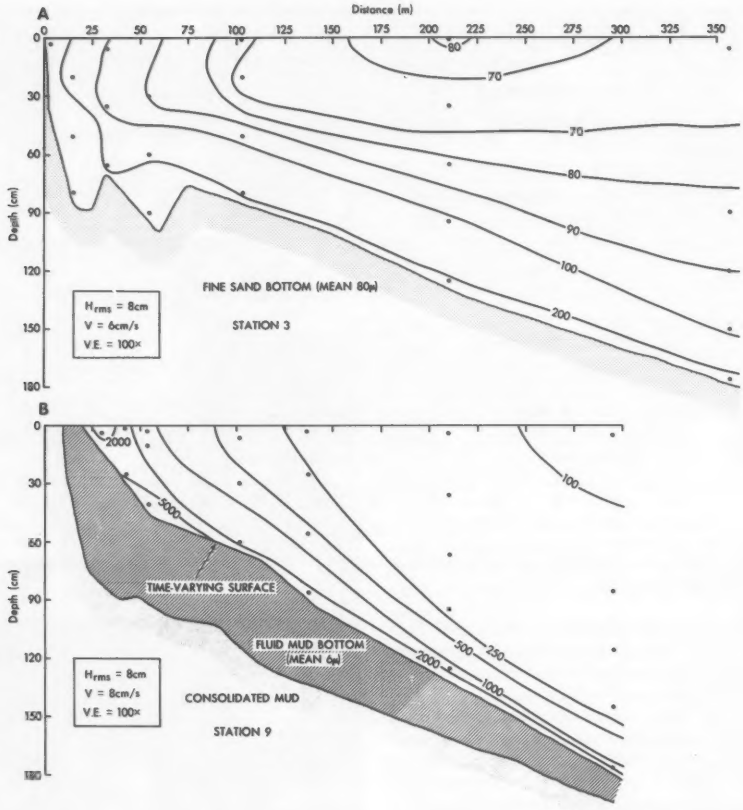

FIG. 10. Suspended-sediment concentration on August 4, 1981 over a fine sand and a fluid mud bottom. See Fig. 1 for location of stations.

order to maintain this ratio on days in which waves are higher, more of the fluid mud bottom must be suspended.

Several reasons can be given for the rapid loss of wave energy over a fluid-mud bottom: internal friction in highly turbid waters; bottom or boundary-layer friction; and dissipation into a fluid bottom by generation of a mudwave. Wells (1977) determined that internal friction from sediment-laden waters (kinematic viscosity $0.1-1.0$ stoke) could be important in attenuating waves up to 3 s. Further, it was found by applying an equation derived by Keulegan (1948) for energy loss from viscous shear beneath solitary waves that viscosities of $0.1-1.0$ stoke were sufficient to reduce wave heights at the seaward edge of Warappabank ($H/h = 0.78$) to those observed in the wave records ($H/h = 0.19$). Hsiao and Shemdin (1978) showed that attenuation from bottom friction was highly dependent on bottom sediment characteristics and that the common practice of selecting a friction coefficient of 10^{-2} was not universally acceptable. Tubman and Suhayda (1976), following theoretical work by Gade (1958, 1959), showed from field measurements that waves over a muddy bottom could be attenuated by generation of a mudwave. Dissipation of wave energy occurred at one or more orders of magnitude greater than that from percolation or bottom friction.

From a practical standpoint, the most important implication of wave attenuation is that it offers protection to the shoreline; offshore fluid muds, such as those of the Louisiana mud hole, will prevent wave attack at the shoreline itself, thus creating conditions favorable for further sedimentation. The fact that fine-grained sediments exist in wave-dominated environments (based on deepwater wave statistics) may be largely a result of the attenuation from fluid muds on the inner shelf. An understanding of why and how these fluid muds accumulate and move subaqueously may provide us with the ability to predict areas of future erosion and accretion.

Suspended Sediments

Along the coastlines of Louisiana, Surinam, and Korea a band of turbid water extends seaward to a distance of

TABLE 3. Characteristics of mud transport in the coastal zone.

	Louisiana (U.S.)	Surinam (S.Am.)	Korea (W. Coast)
Mud source	Atchafalaya River	Amazon River	Yalu, Han, Kum, Yeongsan rivers
Transport direction	West	Northwest	South
Migration rates	1–3 km·yr^{-1}	1–2 km·yr^{-1}	Unknown
Transport mode	Continuous and discrete	Continuous	Discrete
References	Wells and Kemp (1981) Wells and Roberts (1981)	NEDECO (1968)	Chough and Kim (1981)

NOTE: Muds on the west coast of South Korea may also be derived from the Yangtze and Hwangho rivers. The direction of mud transport is inferred from water movement and sediment dispersal patterns. Shifting of individual mudshoals seasonally suggests a discrete mode of movement.

1–50 km. This sediment-laden water is visible from aircraft and shows up well in LANDSAT imagery as partially saturated returns in Bands 4 and 5 (Fig. 9). Visual observations and surface water samples indicate that the most turbid waters are over shoals of fluid mud. In fact, suspended-sediment concentration can faithfully provide information on the locations of soft muds on the bottom. The high concentrations can be attributed to resuspension of muds by waves and advection of sediments in coastal mud streams and plumes.

Concentrations of sediments that are maintained in suspension range from 100 to 1000 mg·L^{-1} over shoals of fluid mud. This is in contrast to the lower values of 10–100 mg·L^{-1} for muddy coasts in general and 1–10 mg·L^{-1} for inner-shelf waters over a sandy bottom (Wells and Coleman 1977). Ambient turbidity levels in nearshore and inner-shelf waters are 10–100 mg·L^{-1} in Louisiana, 100–500 mg·L^{-1} in Surinam, and 10–50 mg·L^{-1} in Korea. The actual values of suspended sediment at a given location are highly dependent on wave height, strength of tidal currents, and stage of tide. Regionally, shoalest waters are the most turbid. Exponential increase in turbidity of near-bottom waters is common, as a sharp gradient usually exists between the overlying water and the fluid-mud surface.

Figure 10 shows examples from Louisiana of suspended-sediment concentration over a fine sand and a fluid-mud bottom on the same day at the same stage of tide. Distance between stations, shown in Fig. 3, is approximately 25 km. In both cases suspended-sediment contours are nearly parallel and follow the contour of the bottom. At a distance of 250 m offshore, surface water values are not markedly different: 70 mg·L^{-1} for the sand bottom and 100 mg·L^{-1} for the fluid-mud bottom. However, large differences occur closer inshore and with depth. Near-bottom values are an order of magnitude higher, 2000 mg·L^{-1} versus 200 mg·L^{-1}, for the same water depth, and up to an order of magnitude greater in surface waters landward of 100 m.

Coastal conditions were calm during collection of data in Fig. 10. H_{rms} was 8 cm, and nearshore currents, directed west, were 8 cm·s^{-1} or less. Certainly during storm conditions the fluid-mud surface, which should be considered as a time-varying surface, adjusts itself to the intensity of incoming waves. Severe storms and hurricanes can strip an entire layer of fluid mud from the bottom, putting it into suspension.

In coastal areas where the tide range is substantial (Surinam and Korea), suspended sediment concentrations may undergo at tidal frequency a cyclic variation of several orders of magnitude (Wells and Coleman 1977). For example, the variation in wave form in Fig. 8, partly a result of the falling water level, can also be attributed to higher suspended-sediment concentration near the time of low tide. As incoming waves propagate over shoals of fluid mud on a falling or rising tide, sediments of the softest muds are resuspended. Redeposition can occur near time of high tide (Wells and Coleman 1981a). Thus fluid muds are continually engaged in an exchange process with overlying water.

One method for determining the adjustment of the fluid-mud bottom to incoming waves is to monitor pressure variations within the fluid-mud layer, then convert to density variations using a hydrostatic pressure concept (Wells et al. 1979). Using equation (5) under conditions of shallow-water waves such as the tide ($h/L \ll 0.05$), K_z approaches unity and equation (5) reduces to

$$(9) \quad P = \rho g (\eta - z) = \rho g z'$$

where z' can be considered a depth below the time-varying fluid-mud surface. If pressure is measured simultaneously at two depths below the mud surface, z_A' and z_B', then

$$(10) \quad P_B - P_A = \rho g (z_B' - z_A')$$

and, provided $z_B' - z_A'$ is constant with time, any variation in $P_B - P_A$ is directly proportional to a density variation. For higher frequency gravity waves K_z becomes significant and density can be obtained from equation (10) only if K_z is known at depths z_A' and z_B'.

Applying the above concepts in the field, simultaneous measurements of pressure variations, suspended-sediment concentration, and wave height have verified the suggestion of rapid dispersion of fluid mud into overlying waters (Wells and Coleman 1981a). Waves less than 50 cm high can disperse 80 cm of low-density fluid mud in 3 h, thus effectively lowering the bottom by that amount. Examination of differential pressure records from muds in the bulk density range 1.1–1.3 g·cm^{-3} during different wave and tide conditions revealed that sediments are not periodically resuspended if bulk density exceeds 1.22 g·cm^{-3}.

The possibility exists that denser fluid muds (> 1.22 g·cm^{-3}) along the coast of Korea are dispersed and replenished at a seasonal time scale. Examination of LANDSAT images shows wide bands of turbid water during winter months (December–March), when strong cold-air

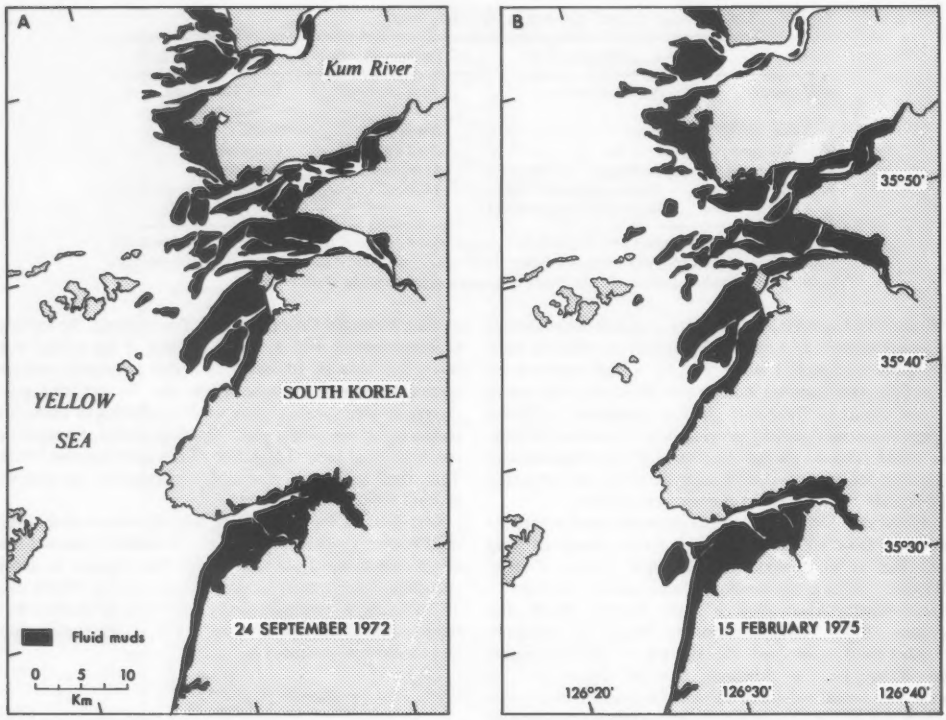

FIG. 11. Intertidal muds south of the Kum River entrance on the west coast of Korea, September 24, 1971 and February 15, 1975, mapped from enlarged (1:50 000) LANDSAT Band 7 images. See Fig. 3 for location.

outbreaks move to the south down the axis of the Yellow Sea. Coastal muds are believed to be eroded in winter by large waves, then carried south into the Korea Strait by the South Korea Coastal Current. In summer, coastal muds are replenished during high river discharge and reform the band of soft sediments near the coast. Examination of suspended-sediment data from the southwest coast of Korea near Mokpo (Fig. 3) at the onset of winter monsoons in November shows characteristic values in 50 m of water of 25 $mg \cdot L^{-1}$ at the surface and 2000 $mg \cdot L^{-1}$ near the bottom.

The significance of high suspended-sediment concentration is that rate of sediment transport can be large, even under relatively weak currents. Transport of suspended sediment through a cross-sectional area normal to the shoreline can be calculated by

$$(11) \quad T = \iint_A C(x, z) \cdot v(x, z)\, dxdz$$

where C is sediment concentration and v is velocity. Limitations in field data usually require use of the more pragmatic relationship:

$$(12) \quad T = \bar{C} \cdot \bar{v} \cdot A$$

where A is cross-sectional area. Using equation (12) to obtain order of magnitude estimates of mud transport, 50×10^6 $m^3 \cdot yr^{-1}$ are transported in the Atchafalaya Mud Stream (Wells and Kemp 1981), 150×10^6 $m^3 \cdot yr^{-1}$ in the Amazon Mud Stream (NEDECO 1968), and 75×10^6 $m^3 \cdot yr^{-1}$ in the South Korea Coastal Current.

Mud Migration

Intertidal and subtidal fluid muds change rapidly in time and space (Table 3). In addition to the resuspended sediments that are carried by coastal mud streams, the entire locus of deposition of mudflats and mudshoals is unstable. Beach-face and nearshore profiles of migratory muds in Louisiana show a shift to the west with both continuous and discrete movement. Seasonal migration is likely, since variations in wave climate affect nearshore circulation. Over the 12-yr period from 1969 to 1981, photo and ground comparisons show the following recognizable patterns: (1) simultaneous erosion and accretion at different locations along the shoreline, (2) increasing length of shoreline fronted by mudflats, and (3) shift in the locus of sedimentation to the west.

Migration of mudshoals to the northwest in Surinam has been noted since the 1600s. Areas of coastal erosion and

accretion follow migration patterns because of the buffer produced by the mudshoals. From maps, charts, and aerial photographs, the average rate of movement has been established as $1-2\ km \cdot yr^{-1}$ (NEDECO 1968). Fluid muds appear to move continuously, barring the as yet unexplained stabilization that results in mudshoals being "welded" to the shoreline.

Figure 11 shows the relocation of fluid muds along the coast of Korea between September 1972 and February 1975. Intertidal exposures of muds were taken at the same tide level from LANDSAT Band 7 images enlarged to a scale of 1:50 000. Patterns of movement do not appear to be continuous and unidirectional, but random and unpredictable. A seasonal cycle of winter cut–summer fill conditions is consistent with the discrete pattern of movement.

Migrating mudshoals are unique in that they provide both benefits and liabilities to man's coastal habitat. The primary benefit of offering protection from wave attack is in itself unique because the buffering mechanism shifts alongshore at rates up to $3\ km \cdot yr^{-1}$. On the other hand, the primary liability is that soft masses of transitory mud can cause severe shoaling in unwanted places, particularly in harbors, turning basins, and shipping channels.

Conclusions

1) In addition to the more common macro-tide-range occurrences, tidal mudflats can also occur in micro- and meso-tide-range environments. The major requirement is a large source of fine-grained sediments.

2) The distribution of nearshore wave energy along muddy coasts is controlled largely by fluid muds because of their attenuating effect on waves. Intertidal mudflats and subtidal mudshoals form a protective buffer that fronts the shoreline.

3) Wave attenuation creates conditions favorable for further sedimentation. An understanding of why and how fluid muds accumulate and move subaqueously may provide us with the ability to predict areas of future erosion and accretion.

4) Because of the high concentration of suspended sediments over accumulations of fluid mud, longshore transport rates may be enormous even under relatively weak currents.

5) Fluid muds form a temporary and transitory storehouse of littoral sediments that, upon stabilization, lead to extensive coastal progradation.

Acknowledgments

This research was supported by the Coastal Sciences Program, Office of Naval Research, Arlington, VA 22217. Additional support for data collection in Louisiana was provided by the Louisiana Sea Grant Program, a part of the National Sea Grant University Program maintained by the National Oceanics and Atmospheric Administration of the U.S. Department of Commerce. Field data were collected jointly with Jim Coleman in South America, Oscar Huh in South Korea, and Paul Kemp in Louisiana. Discussions with these individuals led to many of the ideas presented here.

AUGUSTINAS, P. G. E. F. 1978. The changing shoreline of Surinam (South America). Ph.D. dissertation, Univ. of Utrecht, The Netherlands. 232 p.

BARTZ, P. M. 1972. South Korea. Clarendon Press, Oxford. 203 p.

BRISTOW, R. C. 1938. Cochin harbour development: history of mud banks, vol. I. Cochin Government Press, Ernakulam, India. 175 p.

CHOI, H. I., AND S. D. HAHN. 1975. Marine geological study of the Kum River Estuary. Geol. Mineral. Inst. Korea 3: 79–105.

CHOUGH, S. K., AND D. C. KIM. 1981. Dispersal of fine-grained sediments in the southeastern Yellow Sea: a steady-state model. J. Sediment. Petrol. 51: 721–728.

DELFT HYDRAULICS LABORATORY. 1962. Demerara coastal investigation. Delft, The Netherlands. 240 p.

EISMA, D. 1967. Oceanographic observations on the Surinam shelf. Hydrogr. Newsl. Spec. Publ. 5: 21–53.

GADE, H. G. 1958. Effects of a nonrigid, impermeable bottom on plane surface waves in shallow water. J. Mar. Res. 16: 61–82.

1959. Notes on the effect of elasticity of bottom sediments to the energy dissipation of surface waves in shallow water. Arch. Math. Natur. Oslo 55: 69–80.

GIBBS, R. J. 1976. Amazon River sediment transport in the Atlantic Ocean. Geology 4: 45–48.

GOULD, H. R., AND E. MCFARLAN JR. 1959. Geologic history of the chenier plain, southwestern Louisiana. Gulf Coast Assoc. Geol. Soc. Trans. 9: 1–10.

HARRIS, D. L. 1972. Wave estimates for coastal regions, p. 99–125. *In* D. J. P. Swift, D. B. Duane, and O. H. Pilkey [ed.] Shelf sediment transport: process and pattern. Dowden, Hutchinson and Ross, Stroudsburg, PA.

HOLEMAN, J. N. 1968. The sediment yield of major rivers of the world. Water Resour. Res. 4: 737–747.

HSIAO, S. V., AND O. H. SHEMDIN. 1979. Bottom dissipation in finite-depth water waves. Proc. Conf. Coastal Eng. Hamburg, p. 434–446.

KEULEGAN, G. H. 1948. Gradual damping of solitary waves. J. Res. NBS 40: 487.

KIM, S. W., AND J. H. CHANG. 1979. Sedimentological properties of the bottom sediment between Mokpo and Cheongsan Island off the southern coast of Korea. Rep. Geosci. Mineral Resour. KIGAM, 5: 5–44.

KIM, C. G., S. W. KIM, M. Y. YANG, AND C. H. CHANG. 1975. Study on the bottom sediments in the middle part of the Yellow Sea (Part V). Geol. Mineral. Inst. Korea 3: 1–53.

KINSMAN, B. 1965. Wind waves. Prentice-Hall, Englewood Cliffs, NJ. 676 p.

KRONE, R. B. 1962. Flume studies of the transport of sediment in estuarial shoaling processes. Final Rep. Hydraulic Engr. Lab Sanitary Eng. Res. Lab., Univ. California, Berkeley, CA. 110 p.

1972. A field study of flocculation as a factor in estuarial shoaling processes. Tech. Bull. 19, Committee on Tidal Hydraulics, Corps of Eng., U.S. Army, 62 p.

LEE, S. W. 1970. Inchon outer harbor stabilization study, phase I, current survey. Oceanographic Inst., Seoul, Korea. 69 p.

MCCAVE, I. N. 1972. Transport and escape of fine-grained sediment from shelf areas, p. 225–248. *In* D. J. P. Swift, D. B. Duane, and O. H. Pilkey [ed.] Shelf sediment transport: process and pattern. Dowden, Hutchinson and Ross, Stroudsburg, PA.

MEADE, R. H. 1972. Transport and deposition of sediments in estuaries, p. 91–120. *In* B. W. Nelson [ed.] Environmental Framework of Coastal Plain Estuaries. Geol. Soc. Am. Mem. 133.

MORGAN, J. P., J. R. VAN LOPIK, AND L. G. NICHOLS. 1953. Occurrence and development of mudflats along the western Louisiana coast. Coastal Studies Inst., Louisiana State Univ. Tech. Rep. 2: 34 p.

NAIR, R. R. 1976. Unique mud banks, Kerala, Southwest India. Bull. Am. Assoc. Petrol. Geol. 60: 616–621.

NEDECO. 1965. A study on the siltation of the Bangkok port channel, v. II. Netherlands Eng. Consultants, The Hague. 474 p.

1968. Surinam transportation study. Netherlands Eng.

Consultants, The Hague, The Netherlands. 293 p.

NIINO, H., AND K. O. EMERY. 1961. Sediments of shallow portions of East China Sea and South China Sea. Bull. Geol. Soc. Am. 72: 731–762.

PARK, Y. A. 1969. Submergence of the Yellow Sea coast of Korea and stratigraphy of the Sinpyeongcheon Marsh, Kimje, Korea. J. Geol. Soc. Korea 5: 57–67.

PARK, Y. A., AND S. C. PARK. 1977. Sedimentologic natures of the Daechon beach carbonate sediments. J. Geol. Soc. Korea 13: 41–46.

PARK, Y. A., AND M. Y. SONG. 1971. Sediments of the continental shelf off the southern coast of Korea. J. Oceanol. Soc. Korea 6: 16–24.

TUBMAN, M. W., AND J. N. SUHAYDA. 1976. Wave action and bottom movements in fine sediments. Proc. 15th Conf. Coastal Eng. Honolulu 2: 1168–1183.

VANN, J. H. 1969. Landforms, vegetation and sea level change along the Guiana coast of South America. State Univ. College, Buffalo, N.Y. Tech. Rep. 3: 128 p.

WELLS, J. T. 1977. Shallow-water waves and fluid-mud dynamics, coast of Surinam, South America. Ph.D. dissertation, Louisiana State Univ., Baton Rouge, LA. 99 p.

WELLS, J. T., AND J. M. COLEMAN. 1977. Nearshore suspended sediment variations, central Surinam coast. Mar. Geol. 24: M47–M54.

1981a. Physical processes and fine-grained sediment dynamics, coast of Surinam, South America. J. Sediment. Petrol. 51: 1053–1068.

1981b. Periodic mudflat progradation, northeastern coast of South America: a hypothesis. J. Sediment. Petrol. 51: 1069–1075.

WELLS, J. T., J. M. COLEMAN, AND W. J. WISEMAN JR. 1979. Suspension and transportation of fluid mud by solitary-like waves. Proc. Conf. Coastal Eng. Hamburg, Germany 16: 1937–1952.

WELLS, J. T., AND O. K. HUH. 1979. Tidal flat muds in the Republic of Korea: Chinhae to Inchon. Sci. Bull. Off. Naval Res. Tokyo 4: 21–30.

WELLS, J. T., AND G. P. KEMP. 1981. Atchafalaya mud stream and recent mudflat progradation: Louisiana Chenier Plain. Trans. Gulf Coast Assoc. Geol. Soc. p. 409–416.

WELLS, J. T., AND H. H. ROBERTS. 1981. Fluid mud dynamics and shoreline stabilization. Proc. Conf. Coastal Eng. Sydney 17: 1382–1401.

The Northern Muddy Intertidal: Seasonal Factors Controlling Erosion and Deposition — A Review[1]

FRANZ E. ANDERSON

Department of Earth Sciences

and

Jackson Estuarine Laboratory, University of New Hampshire, Durham, NH 03824, USA

ANDERSON, F. E. 1983. The northern muddy intertidal: seasonal factors controlling erosion and deposition — a review. Can. J. Fish. Aquat. Sci. 40(Suppl. 1): 143–159.

This review summarizes the seasonal physical and biological processes which take place on and in the muddy intertidal zone during the year and affect the erosion or deposition of sediment. The main physical processes that are considered are the effects of ice, waves, sediment dewatering, rain, and mud and water temperatures. The biological processes include the growth of benthic diatoms, algal mats, and higher plants as well as the effects of bioturbation, pellet formation, biodeposition, and changes in the intertidal microrelief.

In the early spring in northern temperate estuaries, ice break-up is the most significant factor affecting muddy intertidal sedimentation. The ice-roughened intertidal has not yet been affected significantly by either plant or animal activity, and is particularly susceptible to sediment resuspension by waves. During the summer, organic processes dominate the intertidal as organisms feed on, pelletize, and bioturbate the sediments. Plant growth, especially benthic diatoms and algal mats, may stabilize the sediment. The few storms during this season combined with lower rainfall insure that the muddy intertidal only rarely undergoes erosion. In fall, seasonal storms increase while both plant and animal activity begin to slow down. Lower rates of bioturbation make the muddy intertidal more resistant to erosion, but the intensity of the fall storms, and higher rainfall, cause significant sediment scouring. With the onset of winter, ice forms over and on the muddy intertidal, reducing resuspension and erosion. However, significant sediment erosion and transportation occurs during winter thaws, when temporary ice break up occurs. But the effect of ice "armoring" all but eliminates sediment resuspension by waves over the muddy intertidal for most of the coldest winter months.

Key words: intertidal zone, erosion, deposition

ANDERSON, F. E. 1983. The northern muddy intertidal: seasonal factors controlling erosion and deposition — a review. Can. J. Fish. Aquat. Sci. 40(Suppl. 1): 143–159.

Le présent rapport consiste en une révision sommaire des processus biologiques et physiques qui ont lieu dans et sur la zone vaseuse intertidale pendant l'année et qui influent sur l'érosion ou le dépôt des sédiments. Les principaux processus physiques étudiés sont les suivants: l'incidence de la glace, des vagues, de l'assèchement des sédiments, de la vase et de la pluie, et la température de l'eau. Les processus biologiques comprennent la croissance des diatomées benthiques, des tapis d'algues et des plantes vasculaires ainsi que l'incidence du remuement et de la formation des grains, du dépôt de matières organiques, et les changements du microrelief intertidal.

Au début du printemps dans les estuaires septentrionaux tempérés, la débâcle des glaces constitue le facteur le plus important qui influe sur la sédimentation dans la zone vaseuse intertidale. La zone intertidale perturbée par les glaces n'a pas encore été modifiée de façon significative par l'activité animale ou végétale et elle est particulièrement réceptive à la suspension des sédiments par les vagues. Pendant l'été, les processus organiques dominent dans la zone intertidale alors que les organismes se nourrissent de sédiments, les mettent en boulettes et les remuent. Les plantes en croissance, surtout les diatomées benthiques et les tapis d'algues, peuvent stabiliser les sédiments. La zone vaseuse intertidale subit une érosion

[1]This paper forms part of the Proceedings of the Dynamics of Turbid Coastal Environments Symposium convened at the Bedford Institute of Oceanography, Dartmouth, N.S., Canada, September 29–October 1, 1981.

Printed in Canada (J6700)
Imprimé au Canada (J6700)

minimale au cours de cette saison car il y a peu de tempêtes et de chutes de pluie. À l'automne, les tempêtes saisonnières augmentent tandis que l'activité végétale et animale diminue. Des taux moins élevés de remuement rendent cette zone plus résistante à l'érosion, mais les tempêtes de remuement rendent cette zone plus résistante à l'érosion, mais les tempêtes plus intenses et les chutes de pluie plus abondantes érodent les sédiments. À l'approche de l'hiver, la glace se forme dans et sur la zone, entraînant une diminution de l'érosion et de la suspension des sédiments. Toutefois, une érosion et un déplacement importants des sédiments ont lieu au cours de la fonte hivernale, quand il se produit une débâcle temporaire. Mais le "blindage" des glaces élimine pratiquement la suspension des sédiments par les vagues sur la zone vaseuse intertidale pendant presque tous les mois les plus froids de l'hiver.

Received October 25, 1981
Accepted September 20, 1982

Reçu le 25 octobre 1981
Accepté le 20 septembre 1982

As in any review, a comprehensive literature survey forms the basis for the presented material. In addition, since my own research interest has been focused on muddy intertidal environments for the past 20 yr, I have drawn heavily from previous work both from readily accessible journals as well as from less accessible "gray" literature (technical reports, in-house reports, etc.). Numerous undergraduate projects and unpublished graduate theses provide additional sources of data that pertain to muddy intertidal sedimentation but normally remain "inaccessible" to the scientific community.

When one considers the many sources of suspended sediment to an estuarine system, usually the rivers and offshore waters receive most of the attention (Mead 1969, 1972). On the other hand, carefully calculated sedimentary budgets of estuaries indicate that internal sources such as shore and bottom erosion may spatially or seasonally be more dominant (Schubel 1968; Schubel and Biggs 1969; Biggs 1970; d'Anglejan et al. 1981). The purpose of this review paper is to describe the seasonal processes that control intertidal deposition and erosion. A review of these processes should help the estuarine ecologist evaluate the seasonal role of mudflats in the estuarine ecosystem.

This review is divided into the physical and biological processes occurring on and in the muddy intertidal sediment that affect deposition and erosion. A number of physical and biological factors are discussed in detail, first developing a literature review, and then where possible, field and/or laboratory evidence is presented to document the sedimentological effect. Finally, in the conclusion section, each season is considered independently, and the important factors pertaining to erosion and deposition are summarized.

Physical Factors

Ice

In northern temperate regions, one of the most important seasonal factors affecting the muddy intertidal is ice. The effects of ice on the intertidal can be considered from at least three viewpoints: the scarring or microtopographic changes; the armoring or protection of the intertidal; and the erosion, deposition, and transportation of intertidal sediments adhering to ice blocks or incorporated in the ice structure.

The microtopographic changes caused by ice in intertidal can be dramatic. Dionne's extensive investigations in the St. Lawrence Estuary (1969a, b, 1971, 1972, 1973, 1974a, b) have documented the size and form of the gouges, grooves, pans, "skip marks," mud ridges, etc. caused by ice dragging, pushing, and squeezing in the muddy intertidal. In addition to the negative scour features, positive microrelief can occur when clumps of *Spartina* marsh are dragged seaward by ice and deposited lower in the intertidal (Sasseville and Anderson 1976). Redfield (1972) considered this one of the main mechanisms for colonizing mudflats; however, most clumps appear to die out in the early spring and are subject to erosion by waves and tidal currents (personal observation).

Intertidal ice can also "smooth out" the tidal flat surface. Dionne (1974a) noticed in a few cases that ice pressures resulted in a partial compaction and dewatering of muddy intertidal, resulting in a "polished" smooth mud surface. In areas artificially roughened by clam and baitworm digging, intertidal ice may be the only factor that can rapidly smooth out the "artificial" microtopography (Anderson et al. 1979).

In general, however, the surface of the mudflat is initially "rough" after the ice leaves in the early spring. This makes the tidal flat particularly susceptible to erosion, since under similar flow conditions "rough" sediment surfaces will be scoured more readily than smooth (Middleton and Southard 1977; Nowell and Church 1979).

Besides increasing the relief of the muddy intertidal surface, floating tidal ice may protect it from wind wave erosion. Anderson (1970) suggested that low quantities of suspended sediments in estuarine waters in the winter months are at least partially related to "ice-armored" intertidal zones. To test this Sasseville and Anderson (1976) conducted an experiment to compare wave resuspended sediment concentrations in front of an intertidal ice pack vs. those underneath the ice. Samples were collected simultaneously from the pack ice front and 75 m landward under 10 cm of ice cover. At the beginning of the flood tide in 20 cm water depth, small wavelets (3 cm wave height) were breaking and resuspending sediments with concentrations up to 1800 mg/L. In contrast, the suspended sediment concentrations under the ice were only 90 mg/L (Fig. 1). As the tide continued to flood, concentrations under the ice decreased, even though wavelets continued to break at the pack edge throughout the sampling period.

The ice itself can incorporate sediment in three ways; either by nucleation of ice crystals around sediment particles, freezing to the bottom, or pore water freezing. Studies of sediment incorporated into the estuarine ice structure have shown concentrations ranging from 0.14 to 27 g/L (Sasseville and Anderson 1976; Thompson 1977). Sediment also gets

frozen to the bottom of the ice while it lies on the tidal flat at low tide (Fig. 2). Thompson (1977) showed that this method of incorporating sediment is most effective in the early stages of ice formation before the ice thickness has increased its insulation ability. Finally, the pore water of the mud can freeze on exposure to extreme low temperatures, forming extensive mud/ice crusts (Knight and Dalrymple 1976) (Fig. 3).

Studies of sediment accretion have been conducted over the winter in the muddy intertidal zones to monitor ice effects. Sasseville and Anderson (1976), using buried tiles, determined there was net sediment loss of a few centimetres over the winter months. In a similar study in the same area, using buried metal plates, marker cores, and precise leveling, Thompson (1977) determined that the middle and upper intertidal zone were areas of winter erosion ranging up to 35 cm (Fig. 4). More detailed studies by Rust (1980) on the same tidal flat showed both erosion and deposition occurred simultaneously. Finally, Richard (1978) and Anderson et al. (1981b) have made year-long studies of intertidal erosion and deposition on New England tidal flats and both concluded that ice effects were primarily erosional.

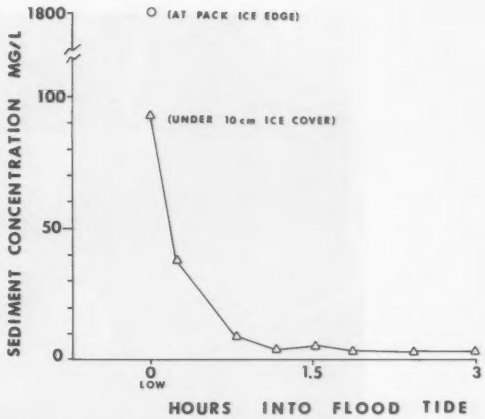

FIG. 1. Suspended sediment concentration measured under the ice during a flood tide at Adams Cove, New Hampshire. Note the high concentrations at the ice-shelf edge in contrast to those taken 50 m further landward under a 10 cm ice cover (after Sasseville and Anderson 1976).

WAVES

Waves themselves are not a seasonal phenomenon, but the cause of local waves, the wind stress, can be highly seasonal. Anderson (1970) and Bohlen (1975) consider seasonal wind activity a major factor in contributing sediment from the margins of the estuary to the suspended sediment pool. Biggs (1970) determined that shoreline erosion was a major source of particulate matter, accounting for some 13% of the suspended sediment in the upper Chesapeake Bay, and 52% in the lower bay area.

There is little doubt that small amplitude wind waves can resuspend high quantities of sediment over shallow intertidal areas. Krone (1966) measured concentrations of suspended sediment exceeding 1 g/L from shallow areas of San Francisco Bay and inferred wind waves were the causitive factor. Laboratory experiments by Alishahi and Krone (1964) verified that these same bottom sediments could be easily resuspended by low amplitude wind-generated waves, even though the sediments were "cohesive clays." Schubel (1968), working in the Chesapeake Bay area, observed that high winds and rough seas temporarily increased suspended sediment concentrations; however, the effects disappeared within a few days. European investigators have also suggested that wind waves can be responsible for temporary high increases in estuarine suspended sediment concentrations (Postma 1967; Buller and McManus 1974; Buller 1975; Carling 1982).

Unfortunately, because of sampling difficulties there have been few investigations of in situ wave erosion and resuspension over shallow muddy intertidal environments. Anderson (1972) showed that small amplitude waves (less than 5 cm) are capable of resuspending fine-grained sediments in shallow water and can increase the suspended sediment concentration by a factor of three over calm conditions (Fig. 5).

Other experiments using artificially generated waves have measured the in situ, wave-induced bottom orbital velocities and drag forces necessary to resuspend muddy intertidal bottom sediment (Anderson 1974, 1975, 1976; Anderson and Mayer 1982). These "critical erosion" type experiments, however, are only significant for a given sediment and its particular physical and biological attributes at that instant in time. However, all the experiments indicated that once sediment was resuspended, it appeared to settle very rapidly! Figure 6 shows the results of seven in situ experiments measuring suspended sediment concentrations following the passage of boat waves (Anderson 1976). The sediment concentrations increased significantly over the base concentrations shortly after the wave passed; however, all resuspended sediment had resettled within a few minutes. Additional nearby sampling also ruled out advection as a possible cause. Apparently the resuspended sediments are much coarser than indicated by bottom sediment analysis, and probably represent resuspended bioaggregates or fecal pellets (Haven and Morales-Alamo 1968; Rhoads 1974; McCall and Fisher 1980).

Finally, the muddy intertidal is subject to decreasing wave-energy gradient extending from the low to high tide mark. The coarser sediments often observed in the lower intertidal reflect not only the higher wave energy in this region, but also the longer period the waves have had to rework the surficial sediment (Evans 1965; Reineck 1967; Anderson 1976).

DEWATERING

In considering the muddy intertidal, the term "dewatering" rather than desiccation is used because to many sedimentologists, desiccation implies a process where sediments are taken to a "dried" state, whereas "dewatering" should imply just a lessening of the water content. The water content of sediments is a major factor in determining the critical velocity necessary for erosion, as shown by laboratory studies

FIG. 2. Bottom side of block of ice excavated from the muddy intertidal at Adams Cove, New Hampshire. The mud layer (approximately 1 cm thick) is frozen in place.

(Partheniades 1965; Rees 1966; Young 1970; Rhoads et al. 1977; Mantz 1977, 1978; Gularte et al. 1980; and Rhoads and Boyer 1982).

In the muddy intertidal, two temporal factors should affect the amount of dewatering that occurs in the surface sediment; exposure time and insolation. In this case we are not considering long-term sediment compaction relative to the tidal time scale. If all other factors are equal, upper intertidal sediments should dewater more than lower intertidal sediments because of longer exposure times. This implies that these upper intertidal sediments might be more difficult to erode (Anderson 1973, 1976, 1979, and Buller and McManus 1974). Welsh (1980), in a seasonal study of nutrient resuspension, concluded that the dewatered upper intertidal sediments were inhibiting both sediment and nutrient resuspension.

Insolation, coupled with low relative humidity and high evaporation, should also affect the surficial water contents. Warm sunny days with moderate breezes should maximize evaporation and decrease water contents.

To determine if dewatering is a significant factor in effecting in situ intertidal erosion, a complex field experiment would have to be designed to examine diurnal dewatering at different intertidal exposure zones during different seasons (Aller 1977; Boyer 1980). The study would be further complicated by changes in sediment texture as well as seasonally changing biota. To the author's knowledge, there have been no comprehensive intertidal dewatering investigations; however, some limited field data do suggest there are temporal changes in surface water contents that appear to be insolation dependent.

Figure 7 shows the results of an experiment which measured surficial water contents over two different August days at two different exposure sites on the same muddy intertidal (unpublished data). Station one had over 5 h of exposure time, while station two had slightly less than 4 h. During the "sunny" day, surficial water content decreased by approximately 8% at both exposure sites. However, there was no indication that a dewatering gradient was established across the tidal flat, and in fact, the higher exposure zone had higher water contents! Unfortunately, there was no control on sediment texture which also strongly affects the water content.

RAIN

Many sedimentologists have linked rainfall to river discharge and the amount of sediment carried into an estuarine system. Studies by Meade (1969, 1972), Anderson (1970), Biggs (1970), Conomos and Gross (1972), and Al-Jabbari et al. (1980) all indicated or implied the importance of the rivers in supplying particulate matter to the estuary. However, the muddy intertidal is also exposed to rainfall and may contribute eroded sediments directly to the estuarine offshore waters.

Raindrops falling during typical storms range between 2.2 and 5.5 mm (Laws and Parsons 1943), and each drop will have reached terminal velocity after falling a minimum of 14 m (Green and Houk 1980). The effect of the rain on the muddy intertidal would be twofold; firstly, the microtopography of the sediment surface will be increased due to the raindrop imprints (Fig. 8, upper) and secondly, the water content of the surface sediment will substantially increase because the rain water's low density will cause it to float above the salt water in the pore space of the muddy sediments. Thus, rainfall should enhance wave and tidal current resuspension by increasing the roughness of the bottom, as well as by increasing the water content of the sediment.

Even when the muddy intertidal is covered by shallow water, the rainfall impact may be important. Laboratory studies of raindrops falling into tanks of still water with sediment

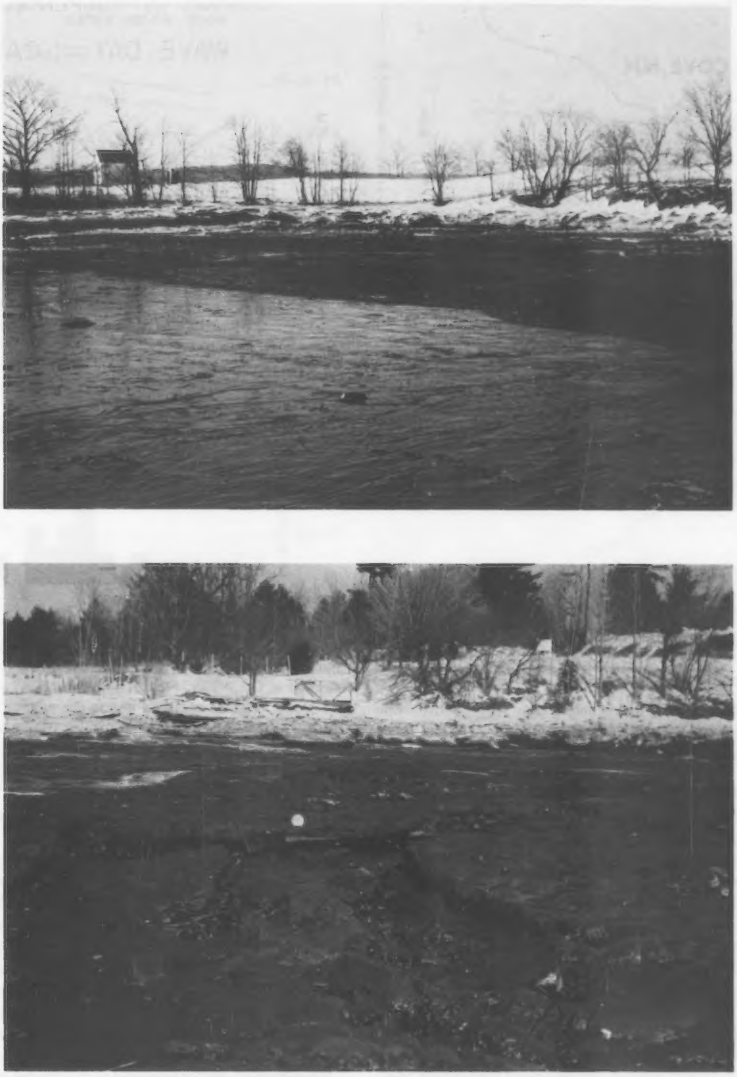

FIG. 3. *Upper:* Adams Cove, New Hampshire, following a severe freeze (−10°C Feb. 28, 1979). Note the line separating the unfrozen lower muddy intertidal from the frozen crust of the upper intertidal; *Lower:* Closeup of the frozen mud crust in the upper intertidal taken the same day.

on the bottom have shown increased bottom sediment resuspension as a function of raindrop size and intensity (Green and Houk 1980). In addition to the turbulent water motions induced by raindrop impact, the larger drops form vortex rings (Chapman and Critchlow 1967) that can penetrate up to 1 m water depth and transfer kinetic energy to the sediment (Fig. 8 lower). Finally, in shallow water under low mixing conditions, the rainwater may form a thin buoyant halocline over the salt water. Green and Houk (1979) showed that internal waves formed at such a boundary could aid in loosening and resuspending bottom sediments.

Again, to the author's knowledge, there hasn't been a study

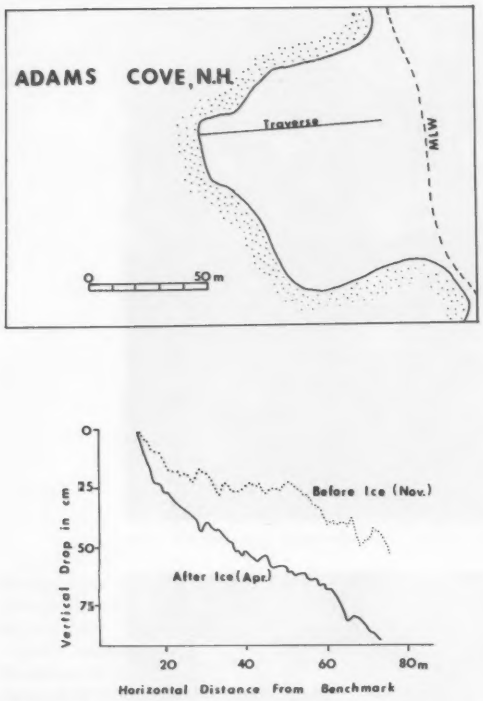

FIG. 4. Topographic profiles of the intertidal of Adams Cove, New Hampshire, before and after ice during the winter 1976–77 (after Thompson 1977).

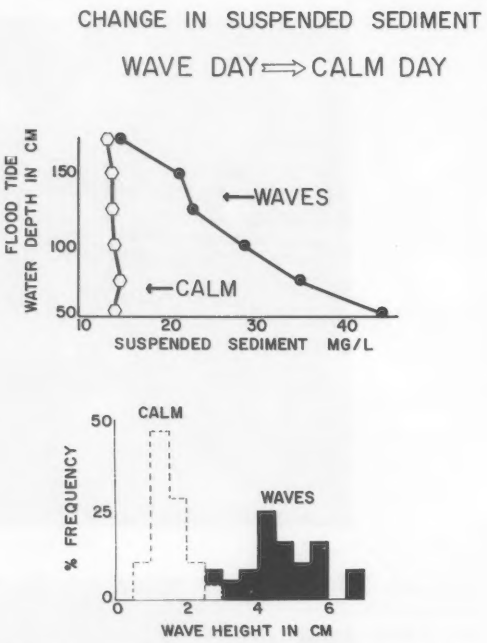

FIG. 5. *Upper:* Near-bottom (+15 cm) suspended sediment concentrations measured on two successive flood tides over a muddy intertidal in Great Bay, New Hampshire. The high suspended sediment concentrations occurred during the windy flood period, when small amplitude waves of height 3–6 cm were passing over the tidal flat; *Lower:* Frequency distribution of the wave heights observed during the two flood tide periods (after Anderson 1972).

designed to specifically examine the effects of rain on the intertidal resuspension. However, during a field study set up to examine the change in particulate concentrations over a tidal cycle (Anderson 1973), a severe summer rainstorm developed midway through a flood sampling period. Figure 9 shows the salinities and particulate matter concentrations that were observed before and during the storm. Although the water depth was 90 cm, the storm samples (15 cm off the bottom) were lower in salinity and higher in suspended sediment concentration, opposite to what would normally occur on a flooding tide. Although mechanisms other than rainfall could be invoked to cause the observed changes, this author and others have noted other instances where there is almost an immediate link between rainfall and intertidal particulate concentrations (Ward 1980; Anderson 1981a). Direct rainfall as a first-order resuspending agent certainly warrants further research.

MUD AND WATER TEMPERATURE

There are strong diurnal and seasonal changes in the temperature of the bottom sediment in the intertidal zone (Johnson 1965; Spencer 1970; Anderson 1977). The mud temperature affects biological activity (bioturbation, feeding, defecation, microbial growth, etc.) and also may have a physical influence on sediment transport (Jackson 1964; Buller and McManus 1976).

Boon (1974, 1975) measured lower quantities of suspended solids flushing from tidal creeks during colder periods. He attributed the lower sediment concentrations to reduced turbulent mixing in the colder water caused by a well-formed laminar sublayer at the flow boundary. Anderson (1970) also observed lower quantities of suspended estuarine sediment during the winter months, but attributed this to a lack of wave resuspension over the tidal flats which were protected by intertidal ice (see section on Ice).

Rhoads et al. (1974) noticed that subtidal marine sediments eroded at a higher critical velocity in the winter, but attributed this to lower water contents within the sediments caused by decreased bioturbation and lower numbers of micro and macrofauna. Boyer (1980) and Grant et al. (1982) also observed a seasonal cyclicity to critical erosion velocities of marine sediments and attributed it in part to the relationship between temperature and biological activity.

Anderson (1979) examined the diurnal changes in the mud and water temperatures from a fixed station in the muddy intertidal. Figure 10 shows the temperatures of the first flood

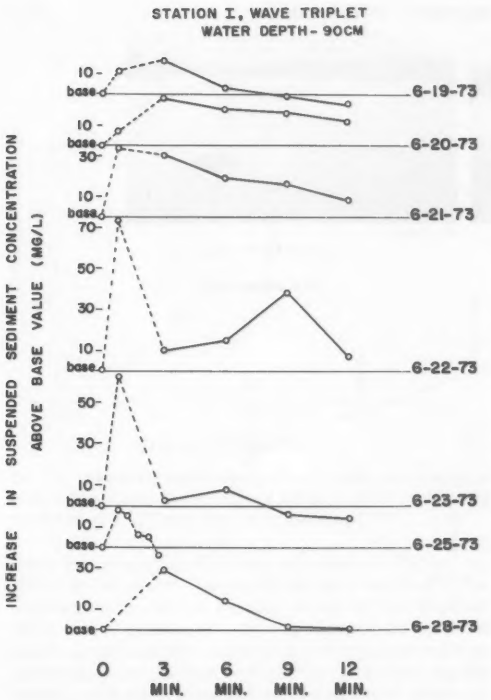

FIG. 6. Increase in near-bottom (+15 cm) suspended sediment concentrations over the background concentration (base ranged between 15–20 mg/L) following resuspension by boat waves. Note the apparent rapid settling of the particulates (after Anderson 1975).

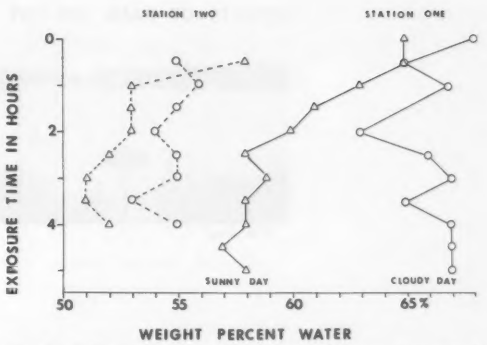

FIG. 7. The temporal variation in percent water as a function of climatic conditions in the surface sediments of the muddy intertidal at Adams Cove, New Hampshire. Data were taken on a sunny day (triangles) (August 18, 1973) with mean air temperatures of 33°C and a cloudy day (circles) (August 14, 1973) with mean air temperatures of 18°C.

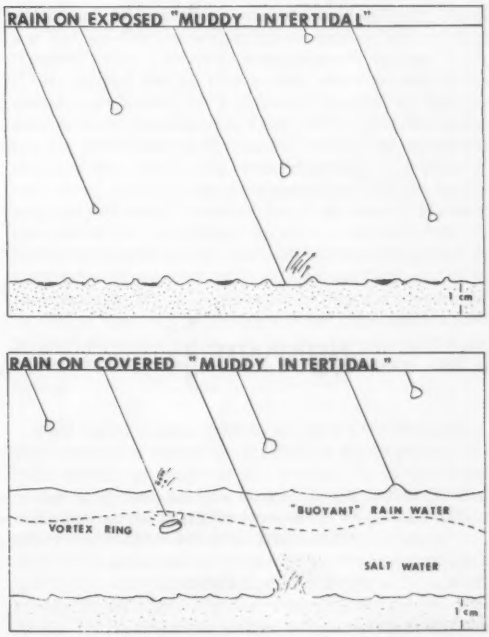

FIG. 8. *Upper:* Raindrops impacting the exposed muddy intertidal. The drops create a microtopography as well as loosen the surface sediments making them more susceptible to erosion; *Lower:* Here the rain is impacting shallow water over the muddy intertidal. The more buoyant freshwater forms a halocline, while the raindrop's energy is transferred to the bottom via "vortex rings," aiding in the resuspension and erosion process.

water relative to the mud on 19 summer sampling days. It is apparent from the graph that sampling time (i.e. insolation) directly affects both the mud and water temperatures. During warm sunny days, shallow water temperatures approach 35°C, approximately double those observed during early morning or late evening flooding. These low viscosity, warm waters should enhance both particle resuspension as well as settling, and may partially explain why flood-tide resuspension processes seem more effective than those observed on the ebb (Anderson 1973, 1974, 1975, 1976, 1977, and 1979), and why resuspension processes in general seem more effective during the summer months than the winter.

Anderson (1980) also looked at the change in shallow water temperatures as the flood-front moved across the tidal flat. Figure 11 shows an increase in water temperatures with flooding during a sunny period vs. a decrease during an evening sampling. Theoretically, these tidal flat temperature gradients should also affect the erodability and subsequent settling of particles, in different intertidal zones. With a seasonal change from summer to winter, we would expect onshore/offshore intertidal water temperature gradients to reverse prior to the onset of ice formation. In this case, warmer water would be flooding over cooler mudflats. To date, no one has documented the effect of these changes on intertidal sedimentation.

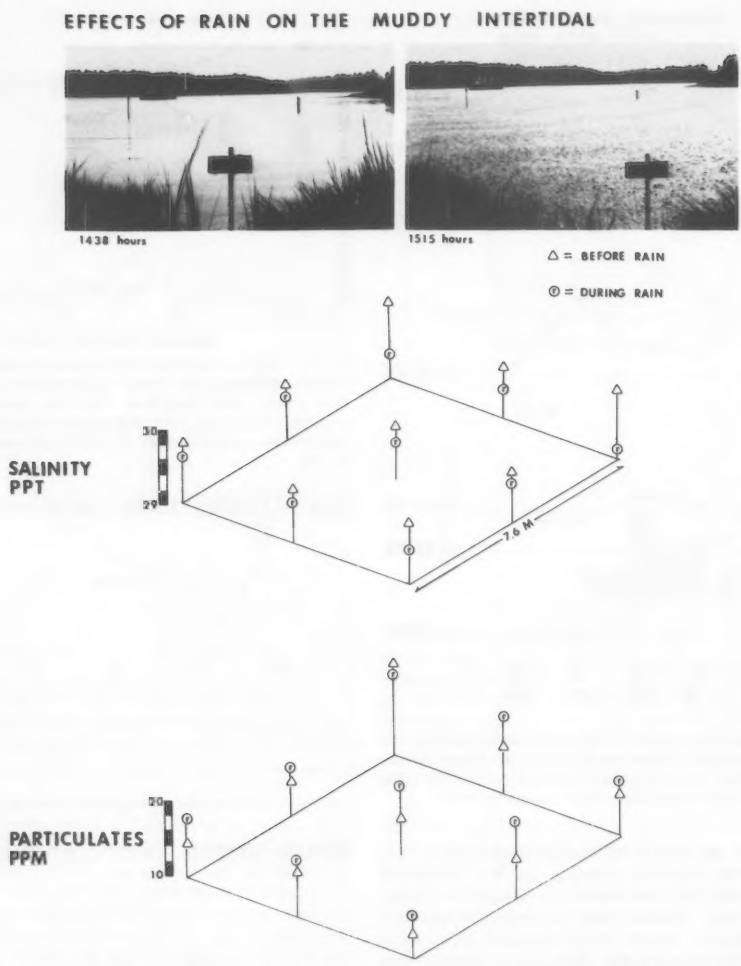

FIG. 9. *Upper:* Intertidal water surface before and during rainstorm; *Middle:* Salinities of near bottom (+15 cm) water samples before and during rain storm; *Lower:* Sediment concentrations of near bottom water samples before and during rainstorm (after Anderson 1973).

Biological Factors

MICROBIOLOGY

In very simplistic terms, the growth rates of microbiological populations in the muddy intertidal are seasonally controlled by temperature changes. In reality however, there are complex animal–plant–microbial interactions that complicate the picture. There is no doubt that microbial populations provide a food source for deposit feeding organisms (Yingst 1976; Lopez et al. 1978; Tenore 1977). The deposit feeding macrofauna themselves may enhance microbial production by providing mucus-coated pellets or tube linings for growth (Hylleberg 1975; Yingst and Rhoads 1976; Rhoads et al. 1977, 1978a). The reworking activities of the benthic fauna, including feeding, burrowing, and irrigation have a strong control on microbial standing crop as well as their production (Yingst and Rhoads 1980).

Accepting that microbial–faunal interactions are complex, there still should be greater microbial productivity in the warmer months (Nedwell and Floodgate 1972; Aller and Yingst 1980). What might be their effect on intertidal sediment processes? Rhoads et al. (1978b) showed that the critical rolling velocities from a glass bead bed study in a seawater

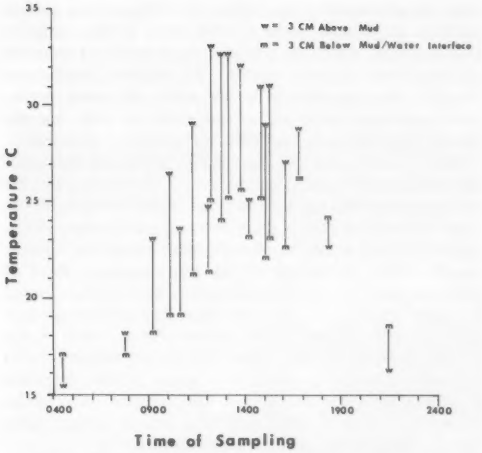

FIG. 10. Water and mud temperatures at a single muddy intertidal station. Temperatures were collected just as the flood-front reached the station on 19 different days (after Anderson 1979).

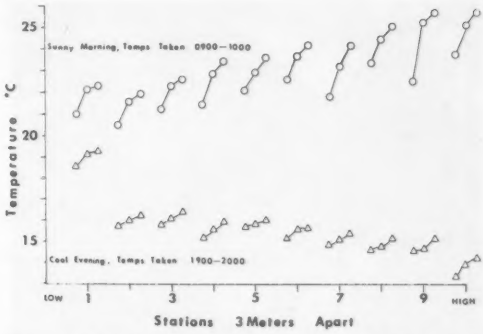

FIG. 11. Water temperature (+3 cm) of the flood-front at 10 successive tidal flat stations across the intertidal, at the same water depth on a sunny day (August 13, 1977) and a cloudy day (August 18, 1977). The three points for each station represent first the air temperature, then the initial water temperature, and finally the water temperature 2 min after flooding.

flume increased up to 60% after microbial growth had stabilized the bed surface. Apparently the mucus secreted by the microorganisms reduced the drag on the bottom (Landahl 1972) and/or increased the binding between the sediment grains. At the same time, surficial microbial growth might be accompanied by an increased number of surface deposit feeders. Both the feeding and the defecation of pellets by these organisms could destabilize the sediment and make it more susceptible to erosion.

FLORA

Unicellular, motile algae — There are strong seasonal and diurnal controls on the populations of benthic diatoms in intertidal estuarine sediments. Pomeroy (1959) and Leach (1970) found maximum chlorophyll levels in benthic intertidal sediments during the summer months and minimums in the winter (Fig. 12). Leach (1970) determined that both productivity and vertical migration within the sediments was strongly controlled by solar radiation and temperature, with night surface populations decreasing to less than one half their daytime equivalent.

The productivity of benthic diatoms can be very high. Pamatmat (1977, 1978) showed the chlorophyll content of surface intertidal benthic sediments was 2–4 times that of the overlying water column. Baille and Welsh (1980) in a 15-mo study of a New England tidal flat found that the microalgal biomass in a square metre of surface sediment was one to two orders of magnitude greater than that in a cubic metre of the overlying water. They also determined that benthic diatoms were resuspended in the flood tide waters and transported landward as a potential flood source for upper intertidal bivalves.

Epipelic diatoms migrate vertically to reach insolation (Hopkins 1963; Round and Palmer 1966). As the diatoms move, they produce mucus which can bind sediment (Drum and Webber 1966) as well as reduce surface frictional drag (Landahl 1972). Laboratory experiments by Holland et al. (1974) showed that the critical shear stress for erosion increases significantly for a sediment inhabited by epipelic diatoms. Field experiments by Coles (1977), where the motile diatoms were removed by scraping or killed by chemicals, indicated that considerable sediment erosion took place in these areas, again implying the diatoms act to stabilize muddy intertidal sediments. Recent studies by de Boer (1981) have also shown that microalgae can prevent the movement of bedforms (ripples) in the intertidal. Field investigations of intertidal sediment accretion by Frostick and McCave (1979) showed maximum sediment deposition occurred between the months of April and September and were attributable to the presence of microalgae; in contrast, erosion took place in the winter months, when the algal populations were dead or absent.

Algal mats — Other species of algae form filamentous mats. In tropical waters, the presence of algal mats can stabilize bottom sediments so that it takes two to five times greater critical erosion velocity to scour the bottom (Scoffin 1970; Newmann et al. 1970). On northern temperature muddy intertidals, *Enteromorpha*, a filamentous green algae, can also form a dense mat up to 1 cm thick. The growth of these mats is also seasonal, with maximum coverage in the summer months in the upper intertidal where conditions are drier (Coles 1977). However, precise measurements of surface elevations of *Enteromorpha* mats on muddy intertidal areas indicate that their main function is to stabilize the sediment rather than cause accretion (F. E. Anderson, unpublished data).

Other plants — Welsh (1980), in a study of the nutrient dynamics of a mudflat ecosystem, noticed that the presence of *Ulva* enhanced bottom sediment resuspension by keeping the surface moist, as well as by mechanical abrasion as the fronds

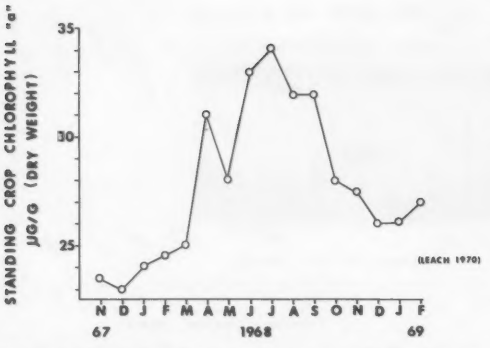

FIG. 12. Mean seasonal standing crop of chlorophyll *a* in the sediments measured on a muddy intertidal from the Ythan Estuary, Scotland (after Leach 1970).

rose during flood tide. This would be especially important during summer months when *Ulva* populations are maximum. Although *Fucus* sp. are not commonly found living in place in the muddy intertidal, they are found attached to rocks or fixed objects and can mechanically abrade the sediment as the plants float off the intertidal surface on the rising tide. In addition, algal air bladders often have sufficient buoyancy to drift stones, sometimes of considerable size (30–40 cm, in diameter), across the intertidal causing scarring and changes in the microrelief (Rasmussen 1973).

Marshall and Lukas (1970) and Rasmussen (1973) examined the effect of eelgrass (*Zostera marina*) and its role in intertidal sediment modification. Eelgrass is a seasonal intertidal plant which reaches maximum growth in the summer months, while in the winter experiences a considerable loss of leaves. The plant, which grows well in the muddy intertidal, acts as both a sediment trap and buffer against waves and currents (Fig. 13). In the 1930s, there was mass destruction of the plant on both sides of the Atlantic caused by either fungus, slime mold, or environmental changes (McRoy 1966). Following the death of the *Zostera* beds, bottom sediments became coarser and the benthic communities changed from primarily being deposit feeders to suspension feeders (Rasmussen 1973). To the author's knowledge, there were no comparative intertidal sediment studies carried out before and after the *Zostera* decline; however, it is likely that the newly unprotected bottom was eroded by waves and tidal currents. Fishermen, who worked in the Great Bay Estuary of New Hampshire at the time of the *Zostera* loss, recall an apparent shrinkage of the intertidal and an infilling of the estuarine channels.

In the upper reaches of some estuaries, the reed *Phragmites* plays an important role in estuarine sedimentary processes. In some estuaries, the reed has even been introduced to encourage sediment deposition for future land reclamation (McManus 1968). As waves and currents are baffled moving through reed beds, sediments are deposited at a fairly high rate as shown by Harrison and Bloom (1977), who measured annual accumulations of 17 mm in New England. Sediment deposition should be maximized during the summer months when the reed densities are highest. In addition to the current baffling, the broken stems of *Phragmites* act as miniature sediment traps, which can collect as much as 16 g of sediment per stem over a year's period. This trapping mechanism would be most important in the late winter and spring months when suspended sediment concentrations are high, and the broken, dead stems are available for sediment collection.

Some of the most common plants occupying the upper intertidal are the *Spartina* species. Again, the theory is that the sedimentation rates are high in areas of *Spartina* growth because of baffling effects (Van Stratten and Kuenen 1957). Again, baffling would be most important during the summer months when *Spartina* growth was at a maximum. Rates of sediment accretion of *Spartina* marshes have been measured by many investigators, and range from 2 to 100 mm per year (Ranwell 1964; Keene 1970; Anderson et al. 1981). Other studies by Bloom (1967), Coles (1977), and Richard (1978) suggest that sediment accretion in some *Spartina* intertidal areas may be slower than in open mudflat areas, and that the main effect of the *Spartina* may be to prevent erosion rather than to substantially increase deposition.

FAUNA

Bioturbation — Bioturbation, the reworking of the surface and near surface sediments of the intertidal area, is also an important seasonal process in tidal flat sedimentation. Seasonally, bioturbation is highest in the summer and fall months, occurring somewhat later than the temperature maximum (Aller and Cochran 1976). Several investigators have examined the relationship between bioturbation and the erodability of the sediment (Rhoads and Young 1970; Rhoads 1973; Southard et al. 1975; Young 1977; Boyer 1980; Nowell et al. 1981; Grant et al. 1982). An increase in bioturbation is usually accompanied by higher water content, and most investigators have found an inverse relationship between water content and the threshold erosion velocity (Partheniades 1965; Postma 1967; Gularte et al. 1980). The relationship between temperature, bioturbation and sediment erosion is not simple; for example Boyer (1980) found that surface intertidal sediment from Barnstable Harbor was more stable with respect to erosion in the late summer and fall. Other studies from subtidal waters, indicate a positive relationship between the amount of bioturbation and the turbidity of the overlying waters, implying that the bioturbated sediments are more easily eroded and resuspended (Rhoads and Young 1970; Rhoads 1973; Rhoads 1974; Rhoads and Boyer 1982). Settlemyre and Gardner (1975) concluded that bioturbation and destabilization of the intertidal surface was the primary reason for the observed export of suspended matter from a salt marsh environment during the summer months.

Summer bioturbation rates can be very high in intertidal areas. A study by Winston and Anderson in the spring and summer (1971) showed that 6 cm of artificially structured fine-grained intertidal estuarine sediments were bioturbated within 1–3 mo after implacement depending on the estuarine location and the type of fauna. Cadee's study (1979) of a polychaete (*Heteromastus filiformis*) in the Wadden Sea showed that it reworked an annual amount of sediment corresponding to a sediment layer 4 cm thick. Similar studies in the

FIG. 13. Muddy intertidal of the Dutch Wadden Sea showing eelgrass (*Zostera marina*) "islands." The "islands" are approximately 3 m in diameter and protrude slightly above the normal tidal flat surface.

FIG. 14. Muddy intertidal in Maine showing a biopelletized surface. Coin is 19 mm in diameter.

same area on the lugworm *Arenicola marina* (Cadee 1976; Beukema 1976) have shown mean sediment reworking rates corresponding to 6–33 cm/yr depending on the animal density, with summer reworking about an order of magnitude greater than winter. Thus the temporal variation in bioturbation should be an important factor in affecting the seasonal erosion of sediment from an intertidal mudflat.

Pelletization — Many marine invertebrates in the intertidal produce fecal pellets or pseudofecal material, and much of the estuarine particulate matter may be of this origin. Haven and Morales-Alamo (1968), in a study of the James River Estuary, determined that up to 27% of the coarser material in suspension was actually pelletized sediments.

The organisms themselves change the size distribution of the particulate matter. In the case of suspension feeders such as barnacles, the size of particles ingested may be on the order of 3–4 μm, while the fecal pellets ejected have a nominal diameter of 200–1500 μm (Haven and Morales-Alamo 1968). Laboratory studies of the surface deposit feeder *Macoma balthica* (Risk and Moffat 1977; Black 1980) have shown that it produces sand-sized pellets from fine-grained clayey-silt bottom sediments. The rapid settling rate of these sand-sized fecal particles may be enhanced by drag reduction from the muco-polysaccharide coatings on the pellets (Chase 1979). Anderson (1975, 1976, 1980) measured the in situ settling rate of resuspended intertidal sediments and found it to be much higher than predicted from size analysis of the clayey-silt bottom; he attributed the rapid settling to bioaggregated particles. Even in sandy intertidal bottoms, filter feeding organisms can produce pellets that are predominately clay, yet hydraulically settle at the same velocity as sand grains.

The quantity of fecal pellets on the intertidal surface may also vary seasonally. Anderson et al. (1981a) found that surficial pellet concentrations (all species) in an intertidal area in Maine ranged from 4 to 20% by weight, with maximums in the late summer. The disintegration of the pellets is a complex process, in part depending on mechanical abrasion as well as bacterial degradation of the muco-polysaccharide sheath (Risk and Moffat 1977; Black 1980; Jumars et al. 1981). Field and laboratory studies of *Macoma balthica* have shown the pellets to be more durable than expected, with complete breakdown taking from 1 to 2 wk in simulated intertidal environments (Black and Anderson 1978).

FIG. 15. *Arenicola marina* zone, taken of the muddy intertidal in the Firth of Forth, Scotland. Lugworm densities are approximately $20/m^2$.

The production of pellets and pseudofecal material should affect the seasonal mobility of the interface sediments. In general, the fecal pellets are large (sand size) but low density (less than 2.0 g/cm^2) (Fig. 14). When present in large numbers, they tend to pack loosely, resulting in high surface water contents (greater than 60%). Because of their size and density, these bioaggregates are more easily resuspended and transported than the normal cohesive clayey-silts of the muddy intertidal (Banner 1979); however once resuspended, many settle very rapidly after water motion ceases (Anderson 1980).

Biodeposition by suspension feeders — Deposit feeders ingest sediment and associated organic matter that is already on the bottom. In contrast, suspension feeders remove particulates from the water column, repackage the material, and deposit it on the bottom. In some cases, the amount of suspended sediment "deposited" by these organisms can be quite substantial. Rhoads (1974), in a very complete review paper on organisms on the muddy sea floor, lists some typical suspension feeder species and the amount of sediments they can process (see table II, page 275). Benthic organisms such as the soft-shelled clam (*Mya arenaria*) and the oyster (*Crassostrea virginica*) can repackage and deposit between 0.03–2.0 g of dry sediment per individual per day (Haven and Morales-Alamo 1966). Anderson et al. (1981a) determined that three bivalves alone accounted for approximately 40% of the annual net deposition that had taken place in the intertidal on a Maine tidal flat. In the Dutch Wadden Sea, Verwey (1952) calculated that, between the cockles and mussels, over 125 million kg of fecal matter were deposited annually. In the Minas Basin of Canada, one bivalve species alone (*Macoma balthica*) can pelletize up to 2.2 billion kg of sediment over a year's period (Risk and Moffat 1977). Again, since feeding rates are in part temperature dependent, one would expect higher biodeposition rates during the spring and summer seasons.

Microrelief — Tidal flats are not smooth, gently sloping surfaces as pictured as textbook drawings. On closer examination, the surface is covered with invertebrate and vertebrate tracks, feeding depressions, fecal mounds, and surface feeding organisms.

Fecal mounds are one of the most obvious changes in microrelief. The subtidal holothurian (*Molpadia oolitica*) produces mounds 10–30 cm in diameter with elevations 2–3 cm above the sea floor (Rhoads and Young 1971). High turbidity above these mounds was attributed to increased turbulent stress from tidal currents acting on a "rough" easily erodable bottom. This same mechanism also occurs on the intertidal. Figure 15 is a photograph of a tidal flat, pocked with *Arenicola marina* mounds. These mounds are about 10 cm in diameter and protrude 5 cm above the intertidal, with typical densities of 20 per square metre. The mounds enhance surface sediment mobility and aid in the resuspension and erosion processes. (Cadee 1976; Anderson and McLusky 1981).

Surface roughness can also be caused by the presence of organisms. In the summer on northern temperate tidal flats, snails such as *Nassarius obsoletus* and *Hydrobia minuta* are present in very large numbers (10's to 100's per m^2). The presence of the shells increase the roughness of the bottom causing increasing turbulent stress and scour on the surrounding sediment.

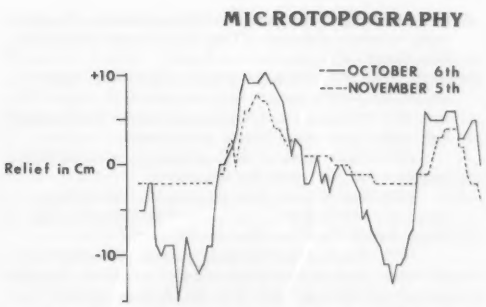

FIG. 16. Topographic recovery of two mounds and basins that were dug in 1980 on the muddy intertidal of the Firth of Forth, Scotland. The horizontal scale is 160 cm.

Animal tubes or burrows (polychaetes, amphipods, etc.) may protrude out of the intertidal surface, especially where minor erosion has taken place, also increasing the roughness of the bottom (Nowell and Church 1979). On the other hand, a dense network of tubes may act as a sediment stabilizer and inhibit tidal current resuspension (Rhoads and Young 1971; Eckman 1979, 1981; Eckman et al. 1979).

Tracks of organisms and those made by sampling equipment on the deepsea bottom are quite persistent, as observed by submarine investigations off the New England continental slope (MacIlvaine and Ross 1979). In the absence of strong currents, most of the smoothing of these trails appears to be done by the meiobenthos (Cullen 1973). In contrast to the deep sea, one might expect stronger physical factors in the muddy intertidal (waves, currents, exposure etc.) would erase trails in a tidal cycle or two (Boyer 1980). However, tracks and scars caused during sampling have often persisted for a number of months (F. E. Anderson, personal observations). The number of tracks and trails seem to be maximized during the spring and summer months, when the surface deposit feeders are most active. The rate of disappearance is in part related to storm events, which are less common during the warmer months.

Probably one of the greatest microrelief changes that occurs in the intertidal is caused by the harvesting of clams and baitworms. The physical recovery of dug intertidal zones, as well as the resuspension of sediments over these areas, has been examined in detail (Anderson et al. 1979; Anderson and McClusky 1981). Depending on the type of bottom sediment, the topography created in the digging process can be quite persistent. Figure 16 shows a series of dug mounds and basins that were microtopographically measured over a number of weeks on an intertidal zone in the Firth of Forth, Scotland. Although the basins filled relatively fast, the mounds were quite persistent, with measurable relief present months after the initial digging. Again, the amount of baitworm and clam digging is in part controlled by the demand, which often peaks during the warmer tourist season.

Conclusions

The relative seasonal importance of each physical and biological factor affecting mudflat erosion or deposition is summarized in Fig. 17.

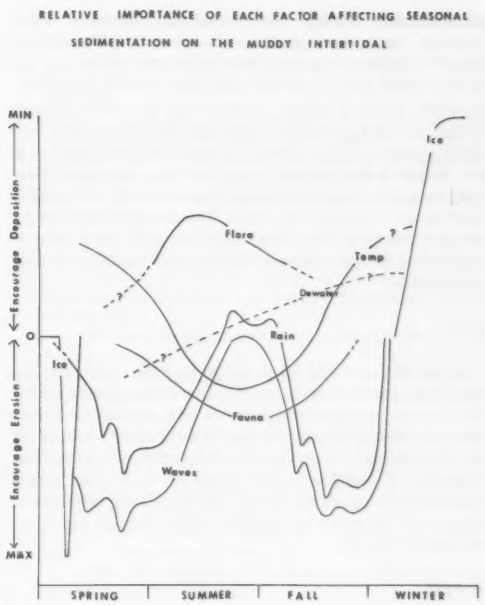

FIG. 17. Relative importance of the major physical and biological factors affecting intertidal sedimentation during each season.

SPRING

Early in the spring, intertidal ice begins to break up, drag across the bottom, and partially leave the intertidal zone. Sediments frozen into and on the ice blocks are taken seaward out of the intertidal zone, shifted to another mudflat, or get rafted high onto *Spartina* marshes during spring tides. The drifting ice scars the intertidal, leaving a rough mudflat surface that is highly susceptible to wave and tidal current scour.

Storms, which are common in the spring, cause erosion, especially since the mudflat has not yet been stabilized by significant plant growth. The bottom, however, is still resistant to scouring, as benthic organisms have only just begun to burrow and pelletize the intertidal sediment. Because water and mud temperatures are cold, bottom sediments may be initially more difficult to erode, but will remain in suspension for a longer period.

SUMMER

In the summer, maximum insolation encourages plant growth (benthic diatoms, algal mats, *Spartina*, etc.), which tend to stabilize intertidal sediments. Microbial production, however, is also high, encouraging both epifaunal and infaunal organisms to feed, pelletize, and bioturbate the muddy sediment, thereby increasing the water content and

paradoxically making the sediments potentially more erodable. The macro-organisms besides tracking the surface, create "roughness" elements with their shells which may aid in the erosion process. At the same time, warmer water temperatures make it easier to erode and resuspend bottom sediments under given flow conditions. The bioturbated, high water content, surface sediment is easily put in suspension in the shallow waters; however, such sediment suspensions are quite temporary, and the bioaggregated deposit will quickly settle to the bottom in the warm, low viscosity water of the summer intertidal. However, since summers are a time of relatively few major storms, depositional processes usually predominate.

FALL

In the fall, rain and wind storms increase again, causing significant sediment resuspension over the muddy intertidal. As the mud and water temperatures cool, resuspended sediment settles more slowly and may be more readily flushed off the intertidal with the ebbing tide. As insolation decreases and temperatures continue to fall, plants die back, and animal processes slow as winter sets in. The decreasing bioturbation allows the sediments to become more compact and more resistant to erosion.

WINTER

In the early winter, before ice forms on the tidal flat, biological processes have nearly stopped. The reduction of bioturbation, feeding etc. allows the tidal flat to become temporarily "smooth." In northern temperate latitudes, ice cover begins in late December and usually reaches a maximum by early February. Although severe storms occur during this period, the precipitation generally falls as snow, and the waves impact on the ice front at the edge of the tidal flat, rather than on the flat itself. Although sediments may freeze to the bottom of the tidal ice during this period, there is little other physical erosion that can take place during these coldest months. Extreme cold water temperatures, coupled with a near complete shut down of biological processes, keeps tidal flat erosion in check until the spring ice thaw occurs, again exposing a scarred intertidal surface susceptible to wave and tidal current erosion.

AL-JABBARI, M. H., J. MCMANUS, AND N. A. AL-ANSARI. 1980. Sediment and solute discharge into the Tay Estuary from the river system. Proc. R. Soc. Edin. 78B: S15–S32.

ALISHAHI, M. R., AND R. B. KRONE. 1964. Suspension of cohesive sediment by wind-generated waves. Univ. Calif. Inst. Eng. Tech. Rep. HEL-2-9: 1–24.

ALIZAI, S. A. K., AND J. MCMANUS. 1980. The significance of reed beds on siltation in the Tay Estuary. Proc. R. Soc. Edin. 78B: S1–S13.

ALLER, R. C. 1977. The influence of macrobenthos on chemical diagenesis of marine sediment. Ph.D. dissertation, Department of Geology and Geophysics, Yale University, New Haven, CN.

ALLER, R. C., AND J. K. COCHRAN. 1976. $^{234}Th/^{238}U$ disequilibrium in nearshore sediment: particle reworking and diagenetic time scales. Earth Planet. Sci. Lett. 29: 37–50.

ALLER, R. C., AND J. Y. YINGST. 1980. Relationships between microbial distributions and anaerobic decompositions of organic matter in surface sediments of Long Island Sound, U.S.A. Mar. Biol. 56: 29–42.

ANDERSON, F. E. 1970. The periodic cycle of particulate matter in a shallow temperate estuary. J. Sediment. Petrol. 40: 1128–1135.

1972. Resuspension of estuarine sediments by small amplitude waves. J. Sediment. Petrol. 42: 602–607.

1973. Observations of some sedimentary processes acting on a tidal flat: Mar. Geol. 14: 101–116.

1974. The effect of boat waves on the sedimentary processes of a New England tidal flat: O.N.R. Tech. Rep. No. 1, Geog. Branch. Task No. NR 388-107: 38 p.

1975. The short term variation in suspended sediment concentration caused by the passage of a boat wave over a tidal flat environment. O.N.R. Tech. Rep. No. 2, Geog. Branch. Task No. NR 388-107: 45 p.

1976. Rapid settling rates observed in sediments resuspended by boat waves over a tidal flat. Neth. J. Sea. Res. 10: 44–58.

1977. Diurnal changes in sediment temperatures of tidal flats and their possible role in sedimentation. Geol. Soc. Am. (ABST). 9: 235.

1979. How sedimentation pattern may be affected by extreme water temperatures on a northeastern coastal intertidal zone. Northeastern Geol. 1: 122–132.

1980. The variation in suspended sediment and water properties in the flood-water front traversing the tidal flat. Estuaries 3: 28–37.

ANDERSON, F. E., L. BLACK, L. M. MAYER, AND L. E. WATLING. 1981a. A temporal and spatial study of mudflat texture. *In* J. Leonard and E. Maurmeyer [ed.] Coastal and nearshore processes of the western Altantic. Northeastern Geol. 3: 184: 191.

ANDERSON, F. E., L. BLACK, L. WATLING, AND L. MAYER. 1979. Can clam-diggers affect estuarine sedimentation patterns? Geol. Soc. Am. (ABST) 11: 1–2.

ANDERSON, F. E., L. BLACK, L. E. WATLING, W. MOOK, AND L. M. MAYER. 1981. A temporal and spatial study of mudflat erosion and deposition. J. Sediment. Petrol. 51: 726–736.

ANDERSON, F. E., AND D. S. MCLUSKY. 1981. Physical recovery of an intertidal area disturbed by baitworm harvesting. Final report to Natural Environment Research Council Ref. GR3/4061. United Kingdom. 47 p.

ANDERSON, F. E., AND L. M. MAYER. 1982. The action of wave induced currents on a disturbed intertidal bottom. (in preparation)

ANDERSON, R. S., C. D. RACE, H. W. BORNS, AND D. C. SMITH. 1981. A rising sea-level in Maine as determined from salt marsh data. Geol. Soc. Am. (ABST) 13: 121.

BAILLE, P. W., AND B. L. WELSH. 1980. The effect of tidal resuspension on the distribution of intertidal epipelic algae in an estuary. Estuarine Coastal Mar. Sci. 10: 165–180.

BANNER, F. T. 1979. Sediments of the north European Shelf, p. 271–299. *In* F. T. Banner, M. B. Collins, and K. S. Massie [ed.] The north-west European shelf seas: the sea bed and the sea in motion. Elsevier, Netherlands.

BEUKEMA, J. J. 1976. Biomass and species richness of the macrobenthic animals living in the tidal flats of the Dutch Wadden Sea. Neth. J. Sea Res. 10: 236–261.

BIGGS, R. B. 1970. Sources and distribution of suspended sediment in northern Chesapeake Bay. Mar. Geol. 9: 187–201.

BLACK, L. F. 1980. The biodeposition cycle of a surface deposit-feeding bivalve, *Macoma balthica*, p. 389–402. *In* V. S. Kennedy [ed.] Estuarine perspectives. Academic Press, New York, NY.

BLACK, L. F., AND F. E. ANDERSON. 1978. What is the role of pellet

producers in estuarine tidal flat sedimentation? Geol. Soc. Am. (ABST) 10: 367.

BLOOM, A. L. 1967. Coastal geomorphology of Connecticut. Final Report. O.N.R. Contract NONR-401 (45) Task No. 388-U65: 72 p.

BOHLEN, W. F. 1975. An investigation of suspended material concentrations in eastern Long Island Sound. J. Geophys. Res. 80: 5089–5100.

BOON, J. D. 1974. Optimized measurement of discharge and suspended sediment transport in a salt marsh drainage system. Mem. Ins. Geol. Basin d'Aquitaine. 7: 67–73.

1975. Tidal discharge asymmetry in a salt marsh drainage system. Limnol. Oceanogr. 20: 71–80.

BOYER, L. F. 1980. Production and preservation of surface traces in the intertidal zone. Ph.D. dissertation, Dep. of Geophysical Sciences. The University of Chicago, Chicago, IL.

BULLER, A. T. 1975. Sediments of the Tay estuary. Part II. Formation of ephemeral zones of high suspended sediment concentrations. Proc. R. Soc. Edin. 75: 65–89.

BULLER, A. T., AND J. MCMANUS. 1974. Factors influencing the formation of 'turbidity maxima' with examples from the Tay estuary, Scotland. Mem. Inst. Geol. Basin d'Aquitaine 7: 37–44.

1976. Fluctuations of suspended sediment in estuaries: a descriptive review. Rep. #3. Tay Estuary Research Center. 39 p.

CADEE, G. C. 1976. Sediment reworking by *Arenicola marina* on tidal flats in the Dutch Wadden Sea. Neth. J. Sea Res. 10: 440–460.

1979. Sediment reworking by the polychaete *Heteromastus filiformis* on a tidal flat in the Dutch Wadden Sea. Neth. J. Sea. Res. 13: 441–456.

CARLING, P. A. 1982. Temporal and spatial variations in intertidal sedimentation rates. Sedimentology 29: 17–24.

CHAPMAN, D. S., AND P. R. CRITCHLOW. 1967. Formation of vortex rings from falling drops. J. Fluid. Mech. 29: 177–185.

CHASE, R. R. P. 1979. Settling behavior of natural aquatic particulates. Limnol Oceanogr. 24: 417–426.

COLES, S. M. 1977. Benthic microalgal populations on intertidal sediments and their role as precursors to salt marsh development, p. 25–42. *In* R. L. Jefferies and A. J. Davy [ed.] Ecological processes in coastal environments. Blackwell Scientific Publications, Oxford.

CONOMOS, T. J., AND M. G. GROSS. 1972. River-ocean suspended particulate matter relations in summer, p. 176–202. *In* A. T. Pruter and D. L. Alverson [ed.] Columbia River Estuary and adjacent ocean waters. University Washington Press, Seattle, WA.

CULLEN, D. J. 1973. Bioturbation of superficial marine sediments by interstitial meiobenthos. Nature 242: 323–324.

D'ANGLEJAN, B. G. INGRAM, AND J. P. SAVARD. 1981. Suspended-sediment exchanges between the St. Lawrence estuary and a coastal embayment. Mar. Geol. 40: 85–100.

DEBOER, P. L. 1981. Mechanical effect of micro-organisms on inter tidal bedform migration. Sedimentology 28: 129–132.

DIONNE, J. C. 1969a. Tidal flat erosion of ice at LaPocatière, St. Lawrence Estuary. J. Sediment. Petrol. 39: 1174–1181.

1969b. Erosion glacielle littorale, Estuaire du St. Laurent. Rev. Geogr. Montr. 23: 5–22.

1971. Polygonal patterns in muddy tidal flats. J. Sediment. Petrol. 41: 838–839.

1972. Ribbed grooves and tracks in mud tidal flats of cold regions. J. Sediment. Petrol. 42: 848–856.

1973. Monroes: a type of so-called mud volcanoes in tidal flats. J. Sediment. Petrol. 43: 848–856.

1974a. Polished and striated mud surfaces in the St. Lawrence tidal flats, Quebec. Can. J. Earth Sci. 11: 860–865.

1974b. Mud cracks and polygons on ice push ridges in tidal flats of the St. Lawrence Estuary. Can. J. Earth Sci. 11: 480–494.

DOLAN, R., B. HAYDEN, G. BORNGERGER, J. ZIEMAN, AND M. VINCENT. 1972. Classification of the coastal environments of the world: Part I. The American Department of Environmental Science, University of Virginia, Tech. Rep. 1: 1–193.

DRUM, R. W., AND E. WEBBER. 1966. Diatoms from a Massachusetts salt marsh. Bot. Mar. 9: 70–77.

ECKMAN, J. E. 1979. Small-scale patterns and processes in a soft substratum intertidal community. J. Mar. Res. 37: 437–457.

ECKMAN, J. E., A. R. NOWELL, AND P. A. JUMARS. 1979. The influence of animal motility on sediment entrainment. E.O.S. 60: 847 (abst.).

1981. Sediment de stabilization by animal tubes. J. Mar. Res. (in press)

EVANS, G. 1965. Intertidal flat sediments and their environments of deposition in the Wash. Q. J. Geol. Soc. Lon. 121: 209–241.

FROSTICK, L. E., AND I. N. MCCAVE. 1979. Seasonal shifts of sediment within an estuary mediated by algal growth. Estuarine Coastal Mar. Sci. 9: 569–576.

GRANT, W. D., L. F. BOYER, AND L. P. SANFORD. 1982. The effect of biological processes on the initiation of sediment motion in non-cohesive sediment. (in press)

GREEN, T., AND D. HOUK. 1979. The mixing of rain with near-surface water. J. Fluid. Mech. 90: 569–588.

1980. The resuspension of underwater sediment by rain. Sedimentology 27: 607–610.

GULARTE, R. C., W. E. KELLY, AND V. A. NACCI. 1980. Erosion of cohesive sediments as a rate process. Ocean Eng. 7: 539–551.

HARRISON, E. Z., AND A. L. BLOOM. 1977. Sedimentation rates on tidal salt marshes in Connecticut. J. Sediment. Petrol. 47: 1484–1490.

HAVEN, D. S., AND R. MORALES-ALAMO. 1966. Aspects of biodeposition of oysters and other invertebrate filter feeders. Limnol. Oceanogr. 11: 487–498.

1968. Occurrence and transport of fecal pellets in suspension in a tidal estuary. Sediment. Geol. 2: 141–151.

HOLLAND, A. F., R. G. ZINGMARK, AND J. M. DEAN. 1974. Quantitative evidence concerning the stabilization of sediments by marine benthic diatoms. Mar. Biol. 27: 191–196.

HOPKINS, J. T. 1963. A study of the diatoms of the Ouse Estuary, Sussex. I. The movement of the mudflat diatoms in response to some chemical and physical changes. J. Mar. Biol. Assoc. U.K. 43: 653–663.

HYLLEBERG, J. 1975. Selective feeding by *Abarenicola pacifica* with notes on *Abarenicola vagabunda* and a concept of gardening in lugworms. Ophelia 14: 113–137.

JACKSON, W. H. 1964. The effect of tidal range, temperature, and fresh water on the amount of silt in suspension in an estuary. Nature 201: 1017.

JOHNSON, R. G. 1965. Temperature variation in the infaunal environment of a sand flat. Limnol. Oceanogr. 10: 114–120.

JUMARS, P. A., A. R. NOWELL, AND R. L. SELF. 1981. A simple model of flow-sediment-organism interactions. Mar. Geol. (in press)

KEENE, H. W. 1970. Salt marsh evolution and post-glacial submergence in New Hampshire. Thesis, Univ. New Hampshire, Durham, N.H.

KNIGHT, R. J., AND R. W. DALRYMPLE. 1976. Winter conditions in a macrotidal environment, Cobequid Bay, Nova Scotia. Rev. Geogr. Montreal 30: 65–85.

KRONE, R. B. 1966. Predicted suspended sediment inflows to the San Francisco Bay System: Rep. Central Pacific River Basins

Comprehensive Water Pollution Project, F.W.P.C.A., Southwest Region: 33 p.

LANDAHL, M. T. 1972. Drag reduction by polymer addition. Air Force Office of Scientific Research, Interim Scientific Rep. AFOSR-TR-73-1200: 59 p.

LAWS, J. O., AND D. A. PARSONS. 1943. The relationship of raindrop size to intensity. Trans. Am. Geophys. Union 24: 452–460.

LEACH, J. H. 1970. Epibenthic algal production in an intertidal mudflat. Limnol. Oceanogr. 15: 514–521.

LEVINTON, J. S., AND G. R. LOPEZ. 1977. A model of renewable resources and limitation of deposit-feeding benthic population. Oecologia 31: 177–190.

LOPEZ, G. R., AND J. S. LEVINTON. 1978. The availability of microorganisms attached to sediment particles on food for *Hydrobia ventrosa* Montagu. Oecologia 32: 263–275.

MACILVAINE, J. L., AND D. A. ROSS. 1979. Sedimentary processes on the continental slope of New England. J. Sediment. Petrol. 49: 563–574.

MANTZ, P. A. 1977. Incipient transport of fine grains and flakes by fluids — an extended Shields diagram. Am. Soc. Civil. Eng., J. Hydraul. Div. 103 (Hy6): 601–615.

1978. Bedforms produced by fine cohesionless, granular and flakey sediments under subcritical water flows. Sedimentology 25: 83–103.

MARSHALL, N. K., AND K. LUCAS. 1970. Preliminary observations on the properties of bottom sediments with and without eelgrass, *Zostera marina*. Proc. Nat. Shell Fish. Assoc. 60: 107–111.

MCCALL, P. L., AND J. B. FISHER. 1980. Effects of tubificid oligochaetes on physical and chemical properties of Lake Erie sediments, p. 253–317. *In* R. O. Brinkhurst and D. G. Cook [ed.] Aquatic oligochaete biology. Plenum Press, New York, NY.

MCMANUS, J. 1968. The hydrology of the Tay Basin, p. 107–124. *In* S. J. Jones [ed.] Dundee and District. Br. Assoc. Adv. Sci., Dundee, U.K.

MCROY, C. P. 1966. The standing stock and ecology of eelgrass (*Zostera marina* L.) in Izembek. Lagoon, Alaska. M.Sc. thesis, University Washington, Seattle, WA. 138 p.

MEADE, R. H. 1969. Landward transport of bottom sediments in estuaries of the Atlantic Coastal Plain. J. Sediment. Petrol. 39: 222–234.

1972. Transport and deposition of sediments in estuaries. Geol. Soc. Am. Mem. 133: 91–120.

MIDDLETON, G. V., AND J. B. SOUTHARD. 1977. The mechanics of sediment movement. S.E.P.M. short course #3 notes: 1.1–10.1.

NEDWELL, D. B., AND G. D. FLOODGATE. 1972. The effect of microbial activity upon the sedimentary sulphur cycle. Mar. Biol. 16: 192–200.

NEUMANN, A. C., C. D. GEBELEIN, AND T. P. SCOFFIN. 1970. The composition structure and erodability of subtidal mats, Abaco, Bahamas. J. Sediment. Petrol. 40: 274–297.

NOWELL, A. R. M., AND M. CHURCH. 1979. Turbulent flow in a depth-limited boundary layer. J. Geophys. Res. 84: 4816–4824.

NOWELL, A. R. M., P. A. JUMARS, AND J. E. ECKMAN. 1981. Effects of biological activity on the entrainment of marine sediments. Mar. Geol. 42: 133–154.

PAMATMAT, M. M. 1977. Benthic community metabolism: a review and assessment of present status and outlook, p. 89–111. *In* B. C. Coull [ed.] Ecology of marine benthos, v.6, University of South Carolina Press, Columbia, SC.

1978. Oxygen uptake and heat production in a metabolic conformer (*Littorina irrorata*) and a metabolic regulator (*Uca pugnax*). Mar. Biol. 48: 317–325.

PARTHENIADES, E. 1965. Erosion and deposition of cohesive soils. Proc. Am. Soc. Civil. Eng., J. Hydraul. Div. 91: 105–139.

POMEROY, L. R. 1959. Algal productivity in salt marshes in Georgia. Limnol. Oceanogr. 4: 386–397.

POSTMA, H. 1967. Sediment transport and sedimentation in the estuarine environment, p. 158–179. *In* G. H. Lauff [ed.] Estuaries. Publ. No. 83, Am. Assoc. Adv. Sci., Washington, D.C. 757 p.

RANWELL, D. S. 1964. *Spartina* salt marshes in Southern England. II. Rate of seasonal pattern of sediment accretion. J. Ecol. 52: 79–94.

RASMUSSEN, E. 1973. Systematics and ecology of the Isefjord marine fauna (Denmark). Ophelia 11: 1–507.

REDFIELD, A. C. 1972. Development of a New England salt marsh. Ecol. Monogr. 42: 201–237.

REES, A. I. 1966. Some flume experiments with a fine silt. Sedimentology 6: 209–240.

REINECK, H. E. 1967. Layered sediments of tidal flats, beaches, and shelf bottoms of the North Sea, p. 191–206. *In* G. H. Lauff [ed.] Estuaries. Publ. No. 83, Am. Assoc. Adv. Sci. Washington, D.C. 757 p.

RHOADS, D. C. 1963. Rates of sediment reworking by *Yoldia limatula* in Buzzards Bay, Massachusetts and Long Island Sound. J. Sediment. Petrol. 33: 723–727.

1970. Mass properties, stability and ecology of marine muds related to burrowing activity, p. 391–406. *In* T. P. Crimes and J. C. Harper [ed.] Trace fossils. J. Geol. Spec. Issue No. 3.

1973. The influence of deposit feeding benthos on water turbidity and nutrient recycling. Am. J. Sci. 273: 1–22.

1974. Organism–sediment relations on the muddy sea floor. Oceangr. Mar. Biol. Ann. Rev. 12: 263–300.

RHOADS, D. C., R. C. ALLER, AND M. GOLDHUBER. 1977. The influence of colonizing benthos on physical properties and chemical diagenesis of the estuarine seafloor, p. 113–138. *In* B. C. Coull [ed.] Ecology of marine benthos. v. 6. University South Carolina Press, Columbia, SC.

RHOADS, D. C., AND L. F. BOYER. 1982. The effects of marine benthos on physical properties of sediments. *In* Plenum Geobiology Series. v. 2. (in press)

RHOADS, D. C., P. L. MCCALL, AND J. Y. YINGST. 1978a. Disturbance and production on the estuarine seafloor. Am. Sci. 66: 577–586.

RHOADS, D. C., J. Y. YINGST, AND W. ULLMAN. 1978b. Seafloor stability in central Long Island Sound. Pt. I. Seasonal changes in erodibility of fine-grained sediments, p. 221–244. *In* M. Wiley [ed.] Estuarine interactions. Academic Press, New York, NY.

RHOADS, D. C., AND D. K. YOUNG. 1970. The influence of deposit-feeding organisms on sediment stability and community trophic structure. J. Mar. Res. 28: 150–178.

1971. Animal–sediment relations in Cape Cod Bay, Massachusetts II. Reworking by *Molpadia oolitica*. Mar. Biol. 11: 255–261.

RICHARD, G. A. 1978. Seasonal and environmental variations in sediment accretion in a Long Island marsh. Estuaries 1: 29–35.

RISK, M. J., AND J. S. MOFFAT. 1977. Sedimentological significance of fecal pellets of *Macoma balthica* in the Minas Basin, Bay of Fundy. J. Sediment. Petrol. 47: 1425–1436.

ROUND, F. E., AND J. D. PALMER. 1966. Persistent vertical-migration rhythms in benthic microflora. II. Field and laboratory studies on diatoms from the banks of the river Avon. J. Mar. Biol. Assoc. U.K. 46: 191–214.

RUST, L. D. 1980. Temporal and spatial variations in topography and surface texture on a tidal flat in the Great Bay Estuary, New Hampshire. M.Sc. thesis, University of New Hampshire, Durham, NH. 75 p.

SASSEVILLE, D. R., AND F. E. ANDERSON. 1976. Sedimentological consequences of winter ice cover on a tidal flat environment, Great Bay, New Hampshire. Rev. Geogr. Montr. 30: 87–93.

SCHUBEL, J. R. 1968. Suspended sediment of the northern Chesapeake Bay. Chesapeake Bay Inst. Rep. 35: 1–264.

SCHUBEL, J. R., AND R. B. BIGGS. 1969. Distribution of seston in upper Chesapeake Bay. Chesapeake. Sci. 10: 18–23.

SCOFFIN, T. P. 1970. The trapping and binding of a subtidal carbonate sediments by marine vegetation in Bimini Lagoon, Bahamas. J. Sediment. Petrol. 40: 249–273.

SETTLEMYRE, J. L., AND L. R. GARDNER. 1975. Low-tide storm erosion in a salt marsh. South. Geol. 16: 205–212.

SOUTHARD, J. B., C. D. HOLLISTER, R. A. YOUNG, AND P. F. LONSDALE. 1975. Dynamics of small-scale interaction between marine bottom currents and mud substrate (ABST) EOS. 75: 372.

SPENCER, J. F. 1970. Diurnal and seasonal-temperature changes in the littoral soil on Pwllcrochan Flats, Milford Haven in relation to Pembroke Power Station, p. 11–27. *In* E. B. Cowell [ed.] Effects of industry in the environment. Field Studies Council, U.K.

TENORE, K. R. 1977. Food chain pathways in detrital feeding benthic communities: a review, with new observations in sediment resuspension and detrital recycling, p. 37–53. *In* B. C. Coull [ed.] Ecology of marine benthos. v. 6. University South Carolina, Columbia, SC.

THOMPSON, C. I. 1977. The role of ice as an agent of erosion and deposition of an estuarine tidal flat. M.Sc. thesis, University of New Hampshire, Durham, NH. 64 p.

VAN STRAATEN, L. M. J. U., AND PH. H. KUENNEN. 1968. Accumulation of fine grained sediments in the Dutch Wadden Sea. Geol. Mijnbouwk 19: 329–354.

VERWEY, J. 1952. On the ecology of distribution of cockle and mussel in the Dutch Wadden Sea, their role in sedimentation and the source of their food supply. Arch. Neerland Zool. 10: 171–239.

WARD, L. G. 1980. Suspended-material transport in marsh tidal channels, Kiawah Island, South Carolina. Mar. Geol. 40: 139–154.

WELSH, B. L. 1980. Comparative nutrient dynamics of a marsh-mudflat ecosystem. Estuarine Coastal Mar. Sci. 10: 143–164.

WINSTON, J. E., AND F. E. ANDERSON. 1971. Bioturbation of sediments in a northern temperate estuary. Mar. Geol. 10: 39–50.

YINGST, J. Y. 1976. The utilization of organic matter in shallow marine sediments by an epibenthic deposit-feeding holothurian. J. Exp. Mar. Biol. Ecol. 23: 55–69.

YINGST, J. Y., AND D. C. RHOADS. 1976. The role of bioturbation in the enhancement of bacterial growth rates in marine sediments, p. 407–421. *In* K. R. Tenore and B. C. Coull [ed.] Marine benthic dynamics. Univ. South Carolina Press, Columbia, SC.

YOUNG, R. A. 1977. Seaflume: a device for in-situ studies of threshold erosion velocity and erosional behavior of undisturbed marine muds. Mar. Geol. 23: M11–M18.

The Mudflat System of China[1]

YING WANG[2]

Department of Energy, Mines and Resources, Atlantic Geoscience Centre, Bedford Institute of Oceanography, Dartmouth, N.S. B2Y 4A2

WANG, Y. 1983. The mudflat system of China. Can. J. Fish. Aquat. Sci. 40(Suppl. 1): 160–171.

Most of the 2000 km of intertidal mudflat on the Chinese coastline is developed in the mesotidal Bohai Sea, where the Yellow River now discharges, and on its pre-1855 delta 600 km to the south on the Yellow Sea coast. The Yellow River has the largest sediment suspended load of any river in the world, with an average of 24.7 kg of sediment per cubic metre of water at its mouth. Four hundred million tons of sediment are deposited annually in the lower reaches of the river, and 1200 million tons are transported to sea in the surface mud plume. This accumulates either in the deeper waters of Bohai Bay or on the intertidal mudflats. These mudflats are typically 3 km wide, but are up to 18 km wide at the delta. They are divided into four zones: the polygonal zone with mud cracks and sparse vegetation above normal HTL; the inner depositional zone of mud on the higher part of the flat; a central erosional zone; and an outer depositional zone of silt on the lower intertidal flat. Landwards a salt marsh is developed. Seawards the sediment passes from sandy silt at LTL to fine mud (silt and clay) in water depths of 10 m. The historical changes in the course of the Yellow River are well known, and the formation of cheniers on the Bohai Bay coast can be correlated with times when there was little or no fluvial sediment supply. For almost 700 yr prior to 1855, the Yellow River discharged to the Yellow Sea in North Jiangsu. Submarine sand bars reworked by tidal currents from the submerging former delta mouth protect about 200 km of coastline from erosion, and intertidal flats are prograding. Elsewhere in North Jiangsu, coastal retreat is rapid, and in places a modern chenier-like shell beach is developing. The history of development of this entire coastal system is dominated by the Yellow River and anthropogenic modifications of its basin.

Key words: sediment, mudflats, Yellow River, Bohai Bay, China

WANG, Y. 1983. The mudflat system of China. Can. J. Fish. Aquat. Sci. 40(Suppl. 1): 160–171.

Le vey intertidal de 2 000 km le long de la côte de la Chine se manifeste surtout dans la partie mésotidale de la mer de Bohai, où le fleuve Jaune se déverse, et sur son delta formé avant 1855 à 600 km au sud, le long de la côte de la mer Jaune. De tous les cours d'eau du globe, le fleuve Jaune a la charge la plus élevée de sédiments en suspension: en moyenne, 24,7 kg de sédiments par mètre cube d'eau sont présents à l'embouchure. Quatre cent millions de tonnes de sédiments sont déposées chaque année dans la partie inférieure du fleuve et 1 200 millions de tonnes sont transportées en mer dans le panache vaseux de surface. Ces sédiments s'accumulent soit dans les eaux plus profondes de la baie de Bohai ou sur les veys intertidaux, qui ont typiquement 3 km de largeur mais qui peuvent atteindre 18 km au niveau du delta. Les veys se divisent en quatre zones, soit la zone polygonale de craquelures et de végétation clairsemée au-dessus de la laisse de haute mer, la zone intérieure de dépôts de vase sur la partie supérieure du vey, une zone centrale d'érosion et une zone extérieure de dépôts de limon sur le vey intertidal inférieur. Du côté de la terre se forme un marais salé. Vers la mer, les sédiments passent de vase sablonneuse, à la laisse de basse mer, à une vase fine (limon et glaise), à une profondeur de 10 m. Les changements qui ont marqué le cours du fleuve Jaune sont bien connus et la formation de cheniers sur la côte de la baie de Bohai peut être mise en corrélation avec les périodes où il y avait peu ou pas d'apport fluvial de sédiments. Pendant près de 700 ans avant 1855, le fleuve Jaune s'est déversé dans la mer

[1]This paper forms part of the Proceedings of the Dynamics of Turbid Coastal Environments Symposium convened at the Bedford Institute of Oceanography, Dartmouth, N.S., Canada, September 29–October 1, 1981.

[2]Present address: Department of Geography, University of Nanking, Nanking, People's Republic of China.

Printed in Canada (J6679)
Imprimé au Canada (J6679)

Jaune, dans le Jiangsu nord. Des barres de sable sous-marines à l'ancienne embouchure du delta ont été remodelées par les courants de marée et protègent de l'érosion environ 200 km de côte. Les veys intertidaux tendent à avancer vers la mer. Ailleurs dans le Jiangsu nord, le retrait de la côte est rapide et à certains endroits une plage de coquilles semblable à un chenier est en formation. La genèse de la formation de tout ce système côtier est dominée par le fleuve Jaune et les modifications anthropogéniques de son bassin.

Received October 14, 1981
Accepted October 6, 1982

Reçu le 14 octobre 1981
Accepté le 6 octobre 1982

MUCH of the coast of China consists of mudflats that extend along ~200 km of the coastline. This coastal type is most prominent along the Yellow Sea coast to the north of Hangzhou Bay and along the Bohai Sea coast of the Great Plain of North China (Fig. 1). This paper describes the turbid water environment of the mudflat coast. This entire coastal area has subsided over 300 m since the beginning of the Cenozoic, and has been built by the huge volumes of sediment brought down by several large rivers, notably the Huanghe (Yellow River) and Chang Jiang (Yangtze River). The great plain built by these sediments extended onto the continental shelf at times of low sea level and was partly submerged during postglacial transgression. At present, the Yellow River and the Yangtze River continue to deliver sediment to the coast and continental shelf of North China, forming extensive coastal mudflats in Bohai Bay and to the north of the Yangtze River.

The intertidal flat is the major constituent of the mudflat coast and is also the active zone of the coast. Two contrasting types of intertidal mudflats have been studied by a coastal dynamic research group from the University of Nanking. Between 1963 and 1965, sediment dynamics were monitored on the mudflats along the west coast of Bohai Bay, including topographic and hydrological measurements during different seasons and tidal periods, together with observations on changes in morphology, sediment, and material movement along several fixed profiles (sediment size nomenclature is shown in Table 1). Since 1980, similar systematic work has been started on the north Jiangsu coast.

Physical Environment

In Bohai Bay the water is less than 20 m deep and the coastal slopes are gentle. Tidal currents are the major agents of sediment transport and, with plenty of sediment supplied by the Yellow River, they develop the typical intertidal mudflats. Along the north Jiangsu plain the coast is exposed to the large waves of the Yellow Sea, and as a result waves are important in addition to the currents in sediment movement. The coastal sediment here is also coarser than in Bohai Bay. The extensive mudflats along the coastline of the north Jiangsu plain develop because of the protection that is provided by the offshore bars of the former Yellow River delta.

BOHAI BAY

The Yellow River delta has been located to the south of Bohai Bay since 1855, the eighth major recorded change in its course since 2278 B.C. (Fig. 1). The apex of the fan-shaped delta is at Lijin. The coastline of the delta is 170 km long and the total area of the delta is 5860 km^2 (Pang and Si 1980). The annual water discharge of the Yellow River is 43% of the total water discharge to the Bohai Sea, and its annual sediment discharge is the largest in the world. The mean suspended sediment concentration near the mouth is approx. 24.7 kg/m^3.

The coarser sediments are deposited close to the river mouth to form the river-mouth bars, and the finer fraction (mean diameter = 0.006 mm) is always moved by longshore currents as a distinct sediment plume in longshore drift, often called "fluid mud."

Nearly 400 million t of sediment per year is deposited in the lower reaches of the river. As a result, the river bed becomes progressively higher and its course longer, as it progrades seaward (Table 2). Every 6–8 yr the prograding river breaks the banks and changes to a new course because of siltation (Wang 1980). As a rule, the course changes from north to northeast, to east and southeast, and then to the north again. This process of clockwise migration has an approximate 50-yr cycle (Pang and Si 1979).

The tides in Bohai Bay are mainly semidiurnal. The average tidal range is about 3 m with a minimum (0.8 m) around the mouth of the Yellow River. Along the coast the currents are rectilinear. Flood currents dominate towards the west (210°–310°), and ebb currents towards the east (60°–95° or 135°), except at the Yellow River mouth. Here tidal periods are unequal; the ebb tide lasts 7 h and the flood 4 h. As a result, the velocity of the flood is higher than the ebb, especially on the intertidal flat. The highest concentrations of suspended particulate matter (SPM) (Table 3) are found at the beginning of the flood tide when the water is shallow and turbulent. The SPM concentrations decrease to a minimum at high tide as the water becomes less turbulent. During the ebb tide, the suspended sediment concentration is low because of the long-lasting ebb period with lower current speeds. As a result, the principal transport of sediment is by the flood tide

TABLE 1. Sediment classification used during the 1960s and 1970s by Chinese marine geologists.

	Mean diameter (mm)
Gravel	>1
Coarse sand	1–0.5
Medium sand	0.5–0.25
Fine sand	0.25–0.1
Coarse silt	0.1–0.05
Fine silt	0.05–0.01
Clay	<0.01

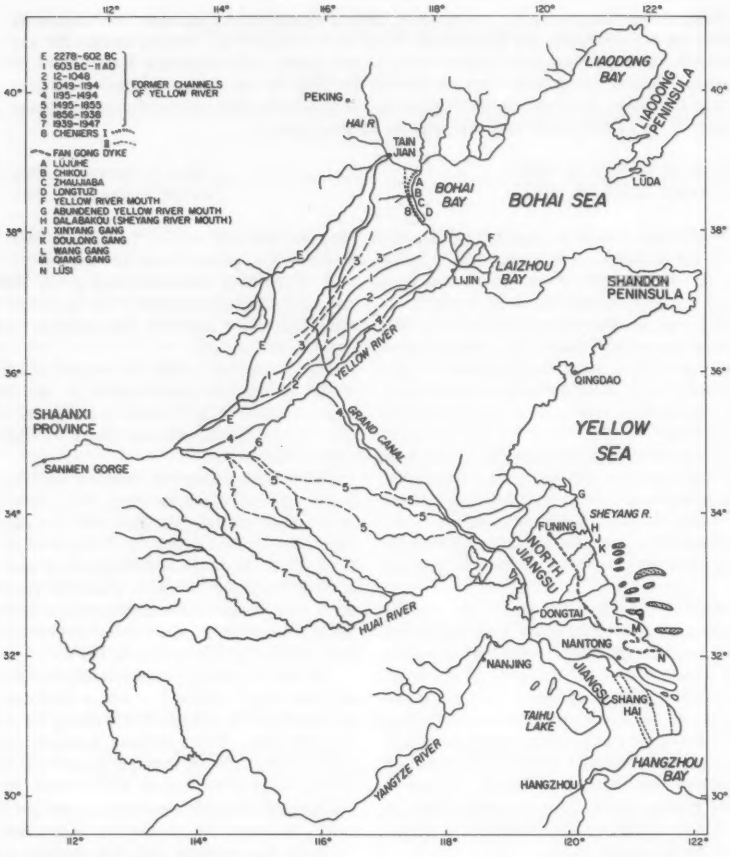

FIG. 1. Major part of mudflat coast of China.

TABLE 2. The rate of progradation of the Yellow River delta.

Time period	Area of delta	Progradation rate	
		River	Delta
1855–1980	5860 km^2	1.5 km/yr	50 km^2/yr
1964–1971	400	1.97–3.45 km/yr	57 km^2/yr

in a landward direction. Very fine sand and coarse silt (mean diameter = 0.077 mm) are transported mainly as traction load. Fine silt (mean diameter = 0.0026 mm) is transported in suspension in the bottom 20 cm of the water column, and clay (mean diameter = 0.006–0.008 mm) in the upper layer of water.

In Bohai Bay the waves are mainly wind-induced with very little swell. The wave climate reflects the direction and speed of the wind. There are strong waves during winter and spring, when northeast winds predominate. Extreme wave height is over 4 m and average maximum wave height is 1.9 m. During the summer and autumn, southeast and east waves predominate with the average height in the order of 0.4–0.5 m. The effect of wave action on the mudflat is weak, because the water is shallow during the period of flood tide. The waves stir up the sediment which is then transported by tidal currents along the intertidal flat. In addition to tidal currents, there also are wind-induced currents with velocities between 10 and 30 cm/s. These currents are important in carrying suspended sediment as a longshore drift, but not in transverse movement on the flat.

NORTH JIANGSU COAST

Much of the North Jiangsu coast is developed on the pre-1855 delta of the Yellow River (Fig. 1), and lies immediately north of the Yangtze River.

The annual sediment discharge of the Yangtze River is only about one-third of that of the Yellow River (Table 4), and at the present time most is deposited in the channels at the river

TABLE 3. Hydrographic measurement along the middle part profile of Bohai Bay, July 5–6, 1965.

Station (on profile)		+2.0 m	±0 m	−2 m	−4 m
Water depth (m)		0.2–1.8	0.2–3.8	1.5–5.4	3.5–6.8
Flood	Velocity (m/s)	0.3	0.3–0.25	0.34–0.52	0.2–0.57
	Direction	265°		55°–40°	60°–70°
Ebb	Velocity (m/s)	0.2	0.2–0.3	0.3–0.45	0.2–0.4
	Direction	35°		250°–260°	280°
Wave	λ (m)	0.1	0.2	0.2–0.45	0.29–0.4
	T (s)	1–2.2	2.8–4.0	1.6–3.0	3.0–4.0
Sediment concentration ‰		165.4[a] 5.2 3.7	4–6	2–3	

[a]NOTE: The maximum sediment concentration (164.5‰) appears at the first hour of the flood. It decreases by one-half during the second hour, by one-tenth at the third hour, and only one-thirtieth, i.e., 5.2‰, at the fourth hour, then all between 5.2 and 3.7‰.

TABLE 4. Hydrographic data for the Yellow and Yangtze rivers.

	Yellow River	Yangtze River
Total drainage area (km^2)	752 443	1 807 199
Total length of river (km)	5 464	6 380
Average water discharge (m^3/s)	1 480	29 200
Maximum water discharge (m^3/s)	10 400	
Minimum water discharge (m^3/s)	5.2	
Average sediment concentration (kg/m^3)	24.7	0.616
Maximum sediment concentration (kg/m^3)	184.0	
Average annual sediment discharge (10^8 t)	12.0	4.78
Maximum annual sediment discharge (10^8 t)	21.0	
Minimum annual sediment discharge (10^8 t)	9.0	
Percent of suspended sediment with size <0.025 mm	1950–59 60.7% 1974–77[a] 40.6%	
Percent of suspended sediment with size >0.025 mm	1950–59 39.3% 1974–77[a] 59.4%	

[a]After completion of Sanmen dam.

mouth. Sediment deposited outside these channels is remobilized as longshore drift towards the south, where it forms the mudflats in the bays of Zhejing and Fujing Provinces to the south. Longshore drift towards the north from the Yangtze River mouth contributes very little to the development of the North Jiangsu coast.

Along the coast of the Yellow Sea semidiurnal tides are predominant with different tidal ranges (Table 5). The average tidal range is 1.5–1.7 m around the abandoned Yellow River mouth; and 2.6–3.7 m at the Yangtze River mouth and Dongtai. The maximum tidal range at the Yangtze River is 6.02–6.8 m. To the north of this area, average tide is 3.0–3.4 m, and maximum is 4.5–6.44 m. Off Jiangsu Province there are rotary currents along the sea shore and tidal current speeds range between 50 and 100 cm/s. Flood currents are faster than ebb currents, which last nearly 8–10 h. The wave heights are smaller (0.6–1.2 m) because the coast is protected by offshore sandy ridges. Outside of the sand ridges, wave height can reach 4 m. Along the North Jiangsu coast, waves are also controlled by the wind. There are northeast/north–northeast waves during winter with maximum heights of 2.9–4.1 m, and southeast waves predominantly during summer, with maximum heights in the range 1.7–3.2 m. In autumn, easterly swell prevails.

SEDIMENTS OF THE NORTH CHINA MUDFLAT COAST

The coastal mudflats of the North China plain consist of three zones. From land to sea these are the salt marsh plain, intertidal mudflats, and submarine coastal slope (Fig. 2).

Salt marsh plain — The marsh plains are located above the maximum high tidal level, are normally flat, and may contain several lagoonal depressions. The vegetation is sparse.

TABLE 5. Some topographic and hydrographic data of the North Jiangsu coast.

Location	Altitude (m)	Rate of coastline retreat (−) or progress (+)(m/yr)	Average tidal range (m)	Flood period (h)	Ebb period (h)	Width of tidal flat (km)	Slope of tidal flat (‰)
Abundant Yellow River mouth	1.40	−230	1.58	4:00	8:25	3.3	1.26
Sheyang River mouth	1.70	+330	2.12	3:17	8:17	7.7	0.30
Xinyang Gang	2.0	+300	2.08	3:42	8:38	13.0	0.23
Dou-Long Gang	2.3	+500	2.01	3:09	9:16	18.5	0.21
Wang Gang	4.6	+400		2:17	10:08	18.0	
Qiang Gang	3.0	+500	2.01	3:13	9:12	14.5	0.91
Lüsi	4.1		1.90	3:08	9:17	3.7	1.0

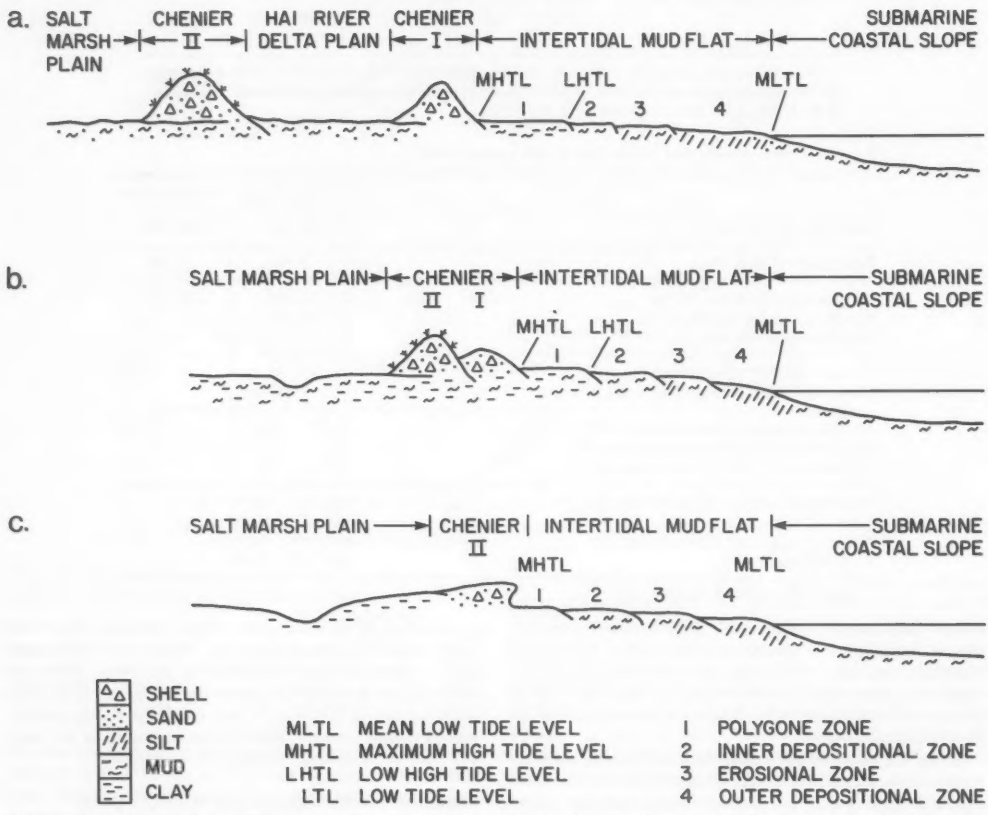

FIG. 2. Coastal profile of (a) prograding part of west coast of Bohai Bay, (b) stable part of west coast of Bohai Bay, and (c) slightly eroded part of west coast of Bohai Bay.

Along the northwest coast of Bohai Bay, salt marsh plains are the main marine depositional features. These salt marsh plains contain shell ridges (cheniers) (Fig. 1 and Table 6) (Wang 1964). The shell ridges were formed by breaking waves as the principal shore-forming agent. The sediment was mainly silt or sandy silt and the coastal slope in the range of 1−2 m/km (Wang 1964; Ren and Cheakai 1980). At present the shore of Bohai Bay consists of mud with tidal currents as the major shore-forming processes, and under the present condition, the shell ridges are not formed.

TABLE 6. Shell beach ridges of the west coast of Bohai Bay.

Name of chenier	Position	Relative height (m)	Width (m)	Form	Sediment	Note	Age (yr)
I	Along shoreline above maximum high tide	0.5–1.0 (northward of Hai River) 2.0 (southward of Hai River)	20–30	Discontinuous arc beaches and branching ridges along advanced river mouth area. Continuous ridges along advanced and stable coast	Shells and shell fragments mainly *Arca* (*Anadara*) *subcrenata* Lischkei, with several silt layers. Also there are a few china fragments. All in the natural deposited limilations. Unconsolidated.	Almost bare vegetation	300–600
II	On land, distance from coast range from 40 km at Hai River mouth to zero at Chikou and ZhauJiabo.	5	100–200	Basically continuous ridge along the coast except in the southern eroded coast.	Shells and shell sand. *Arca* (*Anadara*) *subcrenata* Lischkei, *Meretrix* Linné, *Umbonium townsi* (Croose), *Tympanotomus cingulatus* (Gmelin), *Rapana rhomasian* Crosse and Papna, *Pechilionsis* Graban and King, *Dosinia japonica* Reeve, etc., with little silt and net weight all in natural deposit state and little consolidated.	With grass, bushes, and freshwater	1300–1900

FIG. 3. Dynamic geomorphological map of west coast of Bohai Bay.

Along the coast of North Jiangsu, there is an extensive alluvial plain containing at least one old shell ridge, with a C^{14} date of 4800 ± 150 yr B.P. (Zhu 1980). At the seaward margin of the plain is a salt marsh, termed the grass flat zone by Zhu (1980, Fig. 3). It is about 2–5 km wide, with a slope between 0.1 and 0.2 m/km. This zone is only occasionally flooded with water. The flat consists of silty clay, which was carried in suspension by extreme flood tides. The sediment is about 2–3 m thick with micro laminations. The salt content of the sediment is less than 0.3‰ and organic matter is 1–2%. The zone is covered with a thick growth of various grasses, mainly *Seluropus liuttoralis* var. *sinensis*, *Suaeda salsa*, *Phragmites ausfralis*, and *Imperate cylindrica* var. *major*.

TABLE 7. The intertidal zones of the west coast of Bohai Bay.

Zone	Outer depositional zone	Erosional zone	Inner depositional zone	Polygon zone
Location	Immediately shoreward of the low tide level	Around mid-tide level	Immediately below the lower high tide level	Between lower high and maximum tide level
Morphology	Wave or current ripple	Overlapping fish scales structure or tidal channels	Mudflat of mud pools	Polygon fields or marsh (near river mouth)
Sediment	Very fine sand or coarse silt	Alternating laminae of fine silt and mud	Mud	Clay or clayey-mud
Dynamics	Tidal currents and microwaves	Tidal currents, mainly ebb currents	Tidal currents, mainly flood currents	Tidal currents and evaporation due to solar heating
Processes	Deposition of thin layers over large area	Deposition during flood, erosion during ebb current	Extensive deposition	Stable (during maximum tide deposition, erosion during storm)

Intertidal mudflat — In Bohai Bay, the width of the intertidal mudflat is generally 3−7 km, increasing toward the south to 16−18 km at the Yellow River delta. The intertidal flat can be divided into four geomorphological and sedimentary zones (Wang et al. 1964), which, from land to sea, are the polygon zone, inner depositional zone, erosional zone, and outer depositional zone (Table 7, Fig. 4).

The *polygon zone* is located between lower and maximum high tides, with its landward limit marked by a chenier. The zone is 70−870 m wide with slopes of 0.5−0.6 m/km. Sediment is greyish-yellow clay, with gray silty mud 1.5 m below the surface. Only during spring high tide is this zone covered by water. Normally, high water does not cover the polygon zone and under the dry conditions polygonal desiccation cracks develop in the clay. These average 10−50 cm in diameter with 1−2-cm-wide cracks. Where there is freshwater influence some vegetation may grow, including several grass species such as *Suaeda glance* Bunge, *Limonium bicolor* Kuntie, and *Phragmites communis* Irin.

The *inner depositional zone* consists of soft mud in the form of pools from 500 to 1000 m in diameter with an average slope of 0.67 m/km. Mud and clayey mud is deposited here during the flood tide. The soft sediment makes walking through this area difficult.

The *erosional zone* occurs around the midtide level. In northern Bohai Bay, the zone is 500 m wide with a slope of 0.57 m/km, and exhibits alternating laminae of fine silt and clay. The surface is eroded into an overlapping series of scours called fish-scale structures, 3−18 m long and 0.5 m wide which dip seaward. Scarps between each layer of scales are 2 to 10 cm high and face the coast. These are erosional forms produced by ebb flow.

In the middle part of Bohai Bay, the erosional zone is about 1000 m wide, with a slope of 0.42 m/km, and consists of mud. Small tidal channels may be eroded in the mud. This zone is eroded mainly by the ebb tide. The sediments are carried to margins of the zone, mainly toward the sea where the silt settles in the outer depositional zone.

The *outer depositional zone* is present between the erosional zone and the low tide level. It is approximately 1000 m wide and has a 0.5 m/km slope. The zone consists of coarse silt with current ripple marks on the surface. The ripples have a wavelength of 3−7 cm, with the steep slope facing seawards along the outer part of this zone and shorewards along the inner part. In the middle part of the zone they are symmetrical. At the low tide level, the ripples are overlapped by micro wave marks. Wave action always influences the zone of low tide level, where coarser material (coarse silt and very fine sand) is deposited. The sediments become finer both offshore and onshore.

On the North Jiangsu coast, only three zones are recognized (Zhu 1980).

The *Suaeda salsa flat zone* corresponds approximately to the polygon zone and partly to the inner depositional zone. It is 4−5 km wide with a slope of 0.1−0.2 m/km, and extends from maximum high tide level to mean high tide level. Tidal channels extending to this zone are parallel or branched, normally 10 m wide, and 0.2−0.5 m deep. Between channels, the sediment is laminated silty clay. There are occasional polygons, impregnated with extensive burrows of invertebrates such as *Arenicola* and *Iiyoplax dentinierosa*. Over one-third of the zone is covered by *Suaeda salsa*.

The *mud flat zone* extends between mean high tide level and lower high tide level. The slope of the zone increases to 2−3 m/km. It consists of alternating laminae of clay and silt. Tidal channels are concentrated in this zone. Silt is deposited mainly in the channels, but a thin layer of the silt may also be deposited on the flat during extreme high tides. Mainly clay is deposited on the flat. This zone may compare with the outer part of the inner depositional zone and the erosional zone of Bohai Bay. Big rice grass (*Spartina anglica*) is being planted on the inner part of this zone. This grass traps mud and is thus 10 cm higher than the surface of the surrounding mudflat.

The *silt zone* between mean high tide level (or low high tide) and mean low tide level occupies nearly half the width of the whole flat. The slope here is between 0.3−0.4 m/km; the sediment is 60−70% silt (0.1−0.01 mm) and 24−30% fine sand (>0.1 mm). The sediment is transported mainly as traction load and ripple marks are common on the flat.

Two sediment units are distinguished in vertical section through the mudflats of North Jiangsu. The upper unit is principally well-laminated clay and occurs mainly above

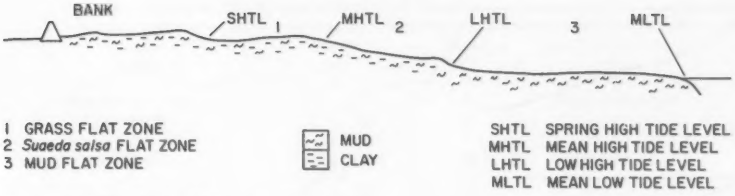

FIG. 4. Mudflat profile of North Jiangsu coast.

TABLE 8. Submarine coastal slope data of Bohai Bay.

Locality	Range (m)	Slope (‰)	Notes
LüJüHe	0 to −16	0.26	Deposited and advanced part (a)
Chiko	0 to −12	0.21	Stable part (b)
Zhau Jia Bo	0 to −14	0.23	
Longtuzi	0 to −12.5	0.24	Slightly eroded part (c)
Diaoko (Yellow River mouth)	0 to −14	0.51	Along sand bars of 1965 river mouth

mean high tide level, i.e. in the high flat. It is 2−3 m thick, but its total thickness is not over half of the maximum tidal range. The lower unit is sand or silt. It is found mainly along a zone from the mean tide level to the bottom of the submarine coastal slopes at a water depth of 25 m. The sandy unit is 20 m thick along much of the North Jiangsu coast.

Submarine coastal slope — In Bohai Bay the submarine coastal slope is very gentle. The sediment becomes finer offshore, from sandy silt at the low tidal level to very fine mud in depths of more than 10 m (Table 8, Fig. 5, profile of 5a, b, c, d).

The submarine coastal slope of North Jiangsu also shows gentle slopes and concave profiles in the inner part of the offshore (Table 9 and Fig. 5e, f, g). However, the slopes are steeper here than in the Bohai Bay and the profiles are complex toward the sea (Fig. 5h) because of submarine sand ridges developed at the former Yellow River mouth. The sediment of the submarine coastal slope of North Jiangsu is mainly fine sand.

CONTEMPORARY COASTAL DYNAMICS

In Bohai Bay, the principal source of sediment is the Yellow River, which plays a predominant role in the development of the mudflat coast of west Bohai Bay. The plume of suspended river sediment is the major source of coastal sediment. The "fluid mud" is deposited only in the upper part of the tidal flats or in deep water.

Three years of monitoring indicate that the flats are areas of rapid sediment deposition. The net depositional rate varies from 0.2 to 0.6 m annually and is concentrated in the outer and inner depositional zones. The higher rates of deposition are in the southern part of the Bay, closer to the Yellow River, where mainly mud is deposited. More silty sediment is deposited in the northern part of the Bay.

The tidal flat zonation is the result of the varying importance of different tidal processes acting on the flat, and is summarized in Table 7. Sediment type on the flat is controlled by the velocity of the tides. On the very low gradient, frictional drag is of major importance. The deposition of very fine sand and coarse silt on the lower flat, alternating laminae of fine silt and mud on the middle flat, and clay on the upper flat is a result of settling lag (discussed by Postma 1967; Wang et al. 1964) and the decrease in current velocity landwards as water depth decreases. Although the ebb current is slower than the flood current, gravitational acceleration on the steeper middle flat leads to slight erosion. The alternating mud and silt laminae of this zone accentuate the erosional features.

Seasonal changes in depositional processes are also important. In Bohai Bay, freezing starts in late November. Coastal ice to a thickness of 0.5 m accumulates mainly between high and middle tide level. Normally there are alternating layers of ice and mud. During March, ice melts and leaves patches of mud on the flat. During May and June the wind is predominantly northeasterly. The mud flat suffers from erosion by the strong wind waves, but sediment is redeposited during the summer. With southeasterly and easterly winds, the flat is covered with yellowish mud that was carried from offshore and originated in the Yellow River.

Tidal currents are the major agents of transport along the North Jiangsu coast, but wave action is also important. The tidal flat here is wider than along the west coast of Bohai Bay. The Sheyang River separates two different coastal sedimentary regimes. To the north the coast is retreating, especially around the former mouth of the Yellow River, with the development of shelly beach ridges (cheniers) (Fig. 6). To the south a 200 km length of coastline is prograding, protected by a field of submarine sand ridges (Ren and Cheakai 1980). These sand ridges are about 5−10 m high and extend for about 200 km from north to south, and 90 km from west to

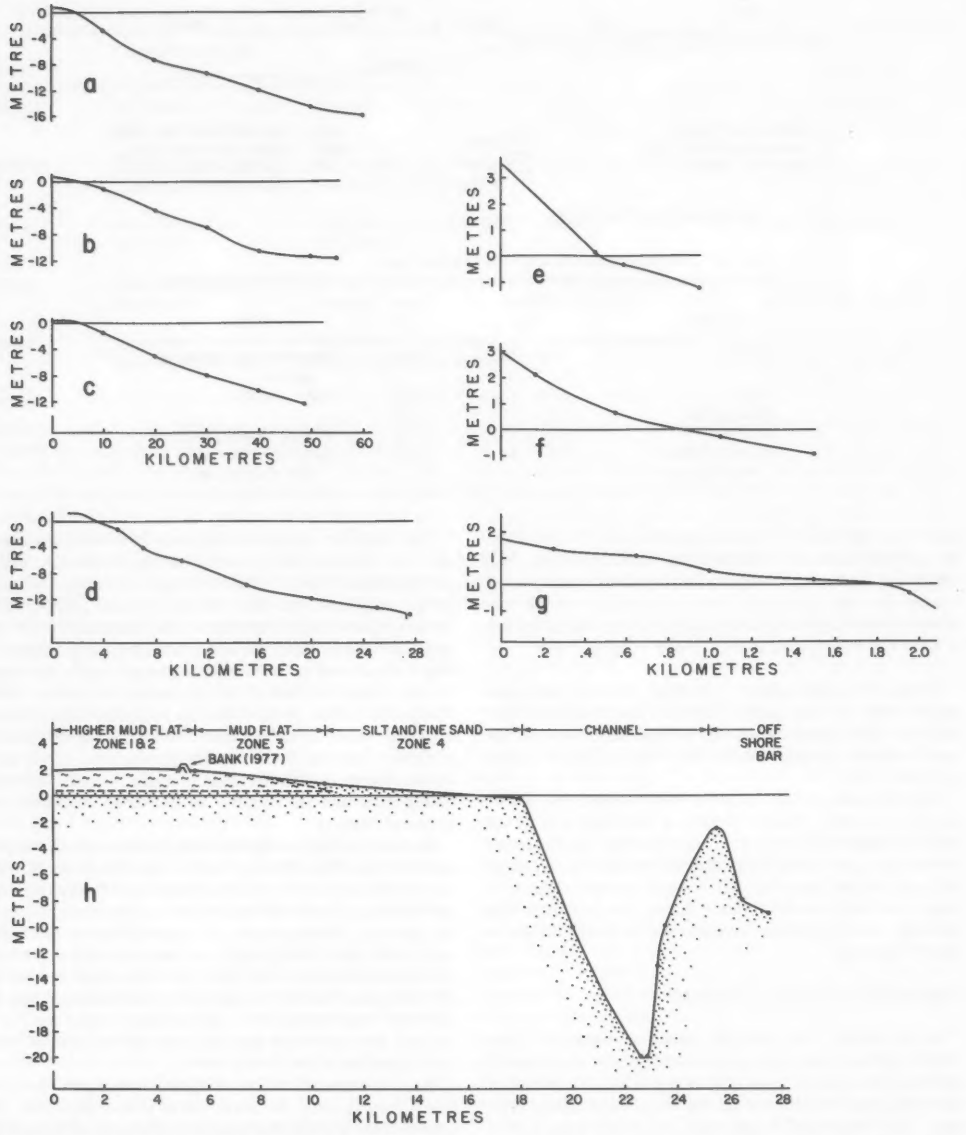

FIG. 5. Submarine coastal slope profile of (a) Lüjühe, (b) Chikou, (c) Longtuzi, (d) Diaokou (1965 river mouth of Yellow River), (e) northern part of abundant Yellow River mouth (Location G, Fig. 1.), (f) southern part of abundant Yellow River mouth, (g) DalaBakou (river mouth of Sheyang River), and (h) Wang gang profile.

east. The ridges represent an old Yellow River delta formed between 1194 and 1855 A.D. Since the return of the Yellow River to Bohai Bay, strong tidal currents have reshaped the deltaic features to the field of sandy shoals. Further to the south, from Qiangang southwards, the coast is retreating behind a narrow tidal flat (Table 5).

TABLE 9. Submarine coastal slope data of North Jiangsu.

Locality	Range (m)	Slope (‰)	Notes
Abandoned Yellow River mouth	0 – −5	1.66	Rapid eroded part
	−5 – −10	1.25	
Dala Ba Kou	0 – −10	1.66	Stable part
Xinyang Gang	0 – −10	2.27	Deposited part
Wang Gang	0 – −20	4.39	
Chuang Dong Gang	0 – −10	3.9	Rapid deposit part

FIG. 6. Modern cheniers on coast of Jiangsu Province.

HISTORICAL EVOLUTION

During historic times, there have been eight major shifts in the course of the Yellow River (Wang 1964; Pang and Si 1979; Shen 1979), which at times flowed into Bohai Bay and at other times to the North Jiangsu coast of the Yellow Sea. The Yellow Sea is named after the turbid mud plume from the former Yellow River delta in North Jiangsu in historic times.

Coastal progradation occurs in the vicinity of the active delta of the Yellow River, as illustrated by the Bohai Sea coast at present. In contrast, erosion occurs along abandoned deltaic coasts (Fig. 7).

The Yellow River changed its course from the Yellow Sea back to Bohai Sea in 1855. Since then, the North Jiangsu coastline has retreated by as much as 30 m per year. The most rapidly eroding sections are along 150 km of the coast where the Yellow River mouth used to be (Wang 1961). In this area nearly 1400 km^2 of land area has been lost since 1855. During the last 50 yr the coast has retreated 230 m (Zhu 1980), and the 1957 coastline is now located under 1 m of water. No retreat has occurred where the coastline is protected by offshore bars, such as the middle part of the North Jiangsu coast.

The coarse and shelly sediment of the cheniers that occur in the salt marsh plain of both the Bohai and North Jiangsu coasts must have been formed under erosional and wave-dominated conditions, rather than under a depositional tidal current regime.

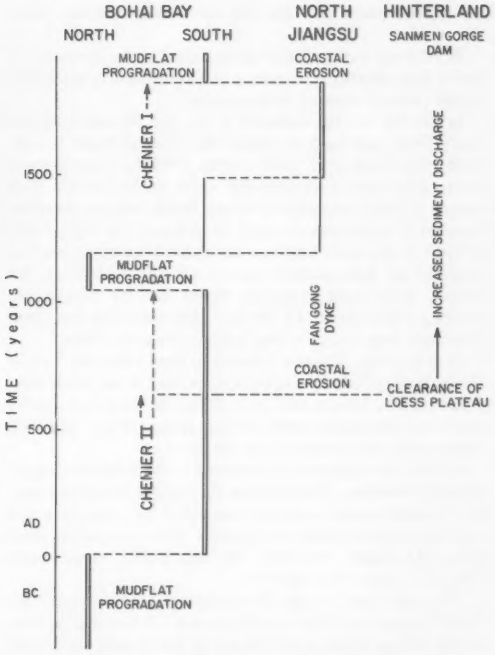

FIG. 7. Summary of changes in the course of the lower Yellow River in the last 2000 yr and their effects on coastal development.

In early historical times (prior to 11 A.D.) the Yellow River entered northwestern Bohai Bay near the present Hai River. In 12 A.D., the river shifted to close to its present course, entering southwestern Bohai Bay. Erosional retreat of the former delta formed Chenier II, which began to take its shape at the time of the Eastern Han Dynasty (70 A.D.), after Wang Ching had successfully put the Yellow River under control.

The sediment of the Yellow River is derived mainly from the Loess Plateau in the middle reach of the river. The total load is 16 × 10^8 tons after the river passes through the Loess Plateau. Each year 4 × 10^8 tons of sediment are deposited in

the lower reach plain, and 12×10^8 tons are discharged to the sea. During historical times the sediment load of the Yellow River has fluctuated. Before the Tang Dynasty the population was lower on the northwest plateau, which was used mainly as pasture. There were plenty of forests and grass to retain the runoff. The loess was more stable, and during that time the Yellow River was cleaner, with little sediment load. For nearly 500 yr after 71 A.D., the Yellow River entered the southwest Bohai Sea without any major course shifting or floods, and Chenier II developed on the northwest coast. During the Tang Dynasty (618–906 A.D.), people migrated to the west. The settlers cut the forests and cultivated the pastures. As a result the bare loess was eroded by runoff and wind, increasing the sediment load of the river. This caused the formation of a large Yellow River delta, changing the characteristics of Bohai Bay by forming mudflats along the coast.

In 1049 the Yellow River again shifted to the northwest of Bohai Bay, thereby terminating the accumulation of Chenier II and causing renewed progradation.

In the 9th to 11th centuries A.D., the 580-km-long Fan Gong Dyke was built to protect the coast of North Jiangsu from tidal flooding (Ji 1980). After 1194 the Yellow River changed its course from the Bohai Sea to the Yellow Sea. This caused a rapid progradation of the North Jiangsu shoreline because of the increased supply of sediment. By 1453 a strip of land 15 km wide had been deposited seaward of the Fan Gong Dyke. Subsequently, during the next 7 centuries, the Yellow River delta prograded 90 km into the Yellow Sea creating a new area of 15 700 km^2. Since then the Fan Gong Dyke has been a road a long distance from the shore.

In Bohai Bay, Chenier I started to form when the Yellow River changed its course to the Yellow Sea (Wang 1964; Zhau et al. 1979). During this time Bohai Bay did not receive sediment, the mudflat suffered from wave erosion, and shell ridges were also formed along the coast.

In 1855 the Yellow River returned to the Bohai Sea again, forming mudflats adjacent to the shell ridges along the coast. It is possible to trace the development of the coast since that time by using the chenier as a marker. Thus, prograding areas (Fig. 2A), stable areas (Fig. 2B), and slightly eroded coast (Fig. 2C) can be distinguished.

This shift in the Yellow River also caused the retreat of the North Jiangsu coast due to wave erosion. The submarine delta of the Yellow River was reshaped by strong tidal currents to a system of submarine sandy ridges and channels.

The dynamic processes of the natural environment are in a precarious equilibrium. Human activities such as cutting forests, cultivating grassland, and building dams may suddenly change this equilibrium and cause serious results. In China there are good examples of this kind of human interference. The historical examples of the control of the Yellow River by Wang Ching and the erosion of the Loess Plateau started during the Tang Dynasty have already been discussed.

There are also more recent examples of environmental modifications. In the early 1950s a series of dams was built in the estuaries of the North Jiangsu plain. The purpose of the project was to harness the tidal currents, and to use fresh river water for irrigation. However, the results were disastrous. All the river channels in front of the dams were silted up because of the reduced tidal circulation. Eventually, the dams had to be opened to wash away the silt and to maintain the depth of the river channel (Wang 1961).

At Sanmen Gorge a dam was built to separate the middle and lower reaches of the Yellow River. The Sanmen Reservoir rapidly accumulated silt, and changed the base level of the Wei River, which is a tributary to the Yellow River upstream of Sanmen Gorge and very important for irrigation of Shaanxi Province. As a result, the fertile soil of the Wei River plain and the lower reach plain of the Yellow River became salty. The water quality at the mouth of the Yellow River was also changed, influencing the migration route of prawns. Difficulties such as siltation and erosion were also encountered when a harbor was built on a mudflat (Wang 1980).

There are also examples of successful environmental modification such as the planting of the big rice grass on mudflats to enhance the deposition of sediment. It is therefore very important to understand the nature of the environment before starting any construction along the coast. Human activity should not interfere with the natural processes.

Acknowledgments

I am indebted to Drs D. J. M. Piper and G. Vilks who critically reviewed the original manuscript and contributed many useful suggestions incorporated in the revised version. I wish particularly to thank Prof. Meie Ren and Da-Kuei Zhu for their encouragement and continual support of this study. Thanks are extended to my other Chinese colleagues for their contribution in field and laboratory work. I am grateful to Dr D. Forbes for critical comments on the manuscript.

JI, C. 1980. The building of the Fangong Embankment and its uses. Fudan J. (Social Science) Suppl. Ed., August 1980: 56–61. (In Chinese with English abstract)

POSTMA, H. 1967. Sediment transport and sedimentation in the environment, *In* Lauff [ed.], Estuaries. AAAS Publication 83: 158–179.

PANG, J., AND SI. SHUHENG. 1979. The estuary changes of Huanghe River I. Changes in modern time. Oceanol. Limnol. Sinica 10(2): 136–141. (In Chinese with English abstract)

1980. Fluvial process of the Huanghe River Estuary. Oceanol. Limnol. Sinica 10(4): 295–305. (In Chinese with English abstract)

REN, M., AND C. ZSNG. 1980. Late Quaternary continental shelf of East China Sea. Acta Oceanol. Sinica 2(2): 106–111.

SHEN, H. W. 1979. Some notes on the Yellow River. EOS 60: 545–546.

WANG, Y. 1961. The properties of China's silted plain coast and problems of seaport's construction. Postgraduate thesis, 1961: 2. Department of Geology and Geography, Peking University. (In Chinese)

1964. The Shell coast and ridges and the old coastlines of the west coast of the Bohai Bay. Acta Scientiarum Naturalium universitati Nankinesis 8(3): 424–442. (In Chinese with English abstract)

1980. The coast of China. Geosci. Can. 7(3): 109–113.

WANG, Y., D.-K. ZHU, X.-H. GU, AND C.-C. CHUEI. 1964. The characteristics of mudflat of the west coast of Bohai Bay. Abstracts of theses in the Annual Symposium of Oceanographical and Limnological Society of China in 1963, Wahan,

Science Press. The Research on Siltation of Newport, No. 2: 49–63. (In Chinese)

ZHU, D.-K. 1980. The problems concerning the development and utilization of Jiangsu coast. Science Symposium of Nanking University, Nanking, May 20, 1980. (In Chinese)

ZHAU, X., S.-S. GUANG, AND J.-W. ZHANG. 1979. The sea level fluctuation during last 20,000 years in East China. Acta Oceanol. Sinica 1(2): 269–280. (In Chinese)

Optical Properties, Suspended Sediments, and Chemistry Associated with the Turbidity Maxima of the Delaware Estuary[1]

ROBERT B. BIGGS, JONATHAN H. SHARP, THOMAS M. CHURCH, AND JOHN M. TRAMONTANO

College of Marine Studies, University of Delaware, Newark and Lewes, DE 19711, USA

BIGGS, R. B., J. H. SHARP, T. M. CHURCH, AND J. M. TRAMONTANO. 1983. Optical properties, suspended sediments, and chemistry associated with the turbidity maxima of the Delaware Estuary. Can. J. Fish. Aquat. Sci. 40(Suppl. 1): 172–179.

Two turbidity maxima were found in the Delaware Estuary and were distinct both in terms of optical properties of the water and in quantity of suspended material. The upstream maximum occurred at about 1‰ salinity. Both the diffuse attenuation coefficient (K_D) and the beam attenuation coefficient (α) responded to the double turbidity maxima. The upstream maximum contains a larger number of individual mineral grains with a mean diameter of about 3 μm; the downstream maximum, which occurred at salinities of 7.5–10‰, was dominated by composite particles with a mean size of 12 μm; at salinities >10‰, the suspended sediment population was dominated by large (10–20 μm) individual particles with few composite particles.

Nutrients, productivity, particulate organic matter, and dissolved and particulate metals all showed relationships to the turbidity maxima when viewed on salinity and on geographic axes. An excess of dissolved inorganic nitrogen in relation to dissolved inorganic phosphorus was mirrored by exceptionally low particulate C/P ratios in the region of the turbidity maxima. Primary productivity appeared to be greatly reduced in the region of the downstream turbidity maximum.

The trace metals Fe, Mn, Cd, Cu, Co, and Ni showed a general association with particulate phases at lowest salinities, at the upstream turbidity maximum. The more particle reactive metals (Fe, Mn, and Co) reflected this as enrichment relative to particulate aluminum. At the downstream turbidity maximum, in the mid-salinity range, the trace metals showed a minimum relative to Al, probably due to dilution by resuspended bottom sediments. In the lower estuary, the trace metals exhibited the highest enrichment (relative to aluminum) and an association with high concentrations of particulate carbon.

Key words: Delaware Estuary, turbidity maxima, optical properties, suspended sediments, chemistry

BIGGS, R. B., J. H. SHARP, T. M. CHURCH, AND J. M. TRAMONTANO. 1983. Optical properties, suspended sediments, and chemistry associated with the turbidity maxima of the Delaware Estuary. Can. J. Fish. Aquat. Sci. 40(Suppl. 1): 172–179.

Deux extrêmes de turbidité sont présentes dans l'estuaire du Delaware et diffèrent pour ce qui est des propriétés optiques de l'eau et de la quantité de matières en suspension. En amont, ce maximum se produit à une salinité d'environ 1‰. Les coefficients de l'affaiblissement linéique de la diffusion (K_D) et du faisceau (α) réagissent aux deux extrêmes de turbidité. Le maximum d'amont est caractérisé par un grand nombre de granules minérales individuelles d'un diamètre moyen d'environ 3 μm; en aval, le maximum, qui a lieu à des salinités variant de 7,5 à 10‰, est dû principalement à des particules complexes de taille moyenne de 12 μm. À des salinités supérieures à 10‰, les sédiments en suspension sont surtout composés de grosses particules individuelles (10 à 20 μm) et de quelques particules complexes.

Les bioéléments, la productivité, les particules de matière organique et les métaux dissous ou en particules ont tous un rapport avec les extrêmes de turbidité en fonction de la salinité et de la position géographique. Un excédent d'azote inorganique dissous par rapport au phosphore inorganique dissous se reflète dans des rapports de particules C/P peu élevés

[1]This paper forms part of the Proceedings of the Dynamics of Turbid Coastal Environments Symposium convened at the Bedford Institute of Oceanography, Dartmouth, N.S., Canada, September 29–October 1, 1981.

Printed in Canada (J6728)
Imprimé au Canada (J6728)

dans la région de turbidité maximale. La productivité primaire semble être nettement réduite dans la région de turbidité.

Dans la zone de turbidité maximale en amont, les oligo-éléments Fe, Mn, Cd, Cu, Co et Ni s'associent généralement aux particules aux plus basses salinités. Les métaux qui réagissent le plus avec les particules (Fe, Mn, Co) manifestent ceci comme un enrichissement relatif à l'aluminium en particule. En aval, les concentrations d'oligo-éléments relatifs à l'aluminium sont minimales dans la zone de turbidité maximale à salinité moyenne, probablement à cause de la dilution entraînée par la remise en suspension des sédiments. Les oligo-éléments présentent le meilleur enrichissement (par rapport à l'aluminium) dans l'estuaire inférieur et s'associent avec les concentrations élevées de carbone en particule.

Received November 13, 1981
Accepted September 15, 1982

Reçu le 13 novembre 1981
Accepté le 15 septembre 1982

NATURAL weathering and erosion processes lead to river turbidity in the form of suspended sediment load. Man's use of the earth's surface for agriculture, industry, and high density housing can increase the susceptibility of land to erosion. Additionally, man contributes to the suspended sediment load of rivers by direct introduction of particulates from industrial and sewage effluents and atmospheric fallout.

Several small, mature, and unpolluted rivers in the northeastern United States contain suspended sediments in concentrations from 1 to 25 $mg \cdot L^{-1}$. In the mainstream of the Delaware River at the New York–New Jersey boundary, average annual suspended sediment loadings are 10 $mg \cdot L^{-1}$ with maximum values of 150–250 $mg \cdot L^{-1}$ during a short (2–10 d) spring freshet (United States Geological Survey 1975). At the head of the tide at Trenton, NJ, the average concentration of suspended sediment doubles to 22 $mg \cdot L^{-1}$.

Modification of upland agriculture practices and modification of industrial and sewage effluents might result in a reduction of 50% of the headwaters, tributaries, industrial, and utilities inputs of particulates. If such reductions were achieved, what would be the effect on phytoplankton primary production, benthic organisms, and the quantity and quality of particulate associated pollutants?

We are presently engaged in a comprehensive study of the Delaware Estuary with emphasis on natural and man-induced chemical inputs and biological and geochemical reactivities. A first paper on the chemistry of the Delaware Estuary (Sharp et al. 1982) and a data report are available (Culberson et al. 1982), and information on salinity has been published (Sharp and Culberson 1982). The purpose of the present paper is a multifaceted examination of the role of suspended sediments in the estuary, especially in relation to the turbidity maxima.

Background

The Delaware Bay is the drowned river valley of the Delaware River (Weil 1977) and, during mean flow conditions, behaves as a vertically homogeneous estuary in its lower reaches (Biggs 1978). During both high and low discharge events, a pronounced halocline can develop and persist, shifting the middle reaches of Delaware Bay to a partially mixed estuary. The Delaware River at Trenton, NJ has a mean discharge of 332 $m^3 \cdot s^{-1}$: the Schuylkill River adds 77 $m^3 \cdot s^{-1}$, and its point of discharge into the Delaware is almost always above the limit of saltwater intrusion. Ketchum (1952) has calculated an 80-d cumulative flushing time for the Delaware Estuary.

The cross-sectional area of the estuary decreases logarithmically and maximum salinity penetration is 125 km from the bay mouth. Mean tidal range is 1.8 m through most of the estuary. A null area, where there is neither strong upstream nor downstream net flow predominance, occurs in the region from 75 to 90 km from the estuary mouth.

Bottom sediments in the upper bay are generally muds or sandy muds, the middle bay sediments are sands in the central portion, muddy sands in the eastern portion, and sandy muds along the Delaware (western) margin. The lower bay bottom is dominated by sands with trace concentrations of muds, except along the extreme western margin (Weil 1977).

Neilheisel (1973) studied the suites of heavy minerals present in Delaware Bay bottom sediments and developed a model for sand-sized sediment sources and dispersal. He found that the eastern (New Jersey) side of the estuary was dominated by a continental shelf sand source while the western (Delaware) side was dominated by mixed fluvial and coastal plain sources. He also found a distinctive boundary between fluvial sediments and mixed fluvial–coastal plain sediments at 80 km above the mouth of the bay, almost exactly at the seaward end of the null zone. Weil (1977) mapped the bottom sediment texture for Delaware Bay and identified an estuarine submarine delta extending from 120 to 60 km above the mouth of the bay, essentially extending from the upstream limit of salt intrusion to just seaward of the downstream end of the null zone. Bopp and Biggs (1981) studied cations in the bottom sediments of the estuary and identified a suite of metals (Mg, Fe, Al, K) associated with the fluvial environment and found in the upper and western side of the bay. They also identified a seawater suite (Na, Ca, Sr) found in the lower and eastern side of the bay and a trace metal suite (Zn, Cd, Cr, Ni, Pb) associated with particulate organic matter and found just seaward of the downstream end of the null zone, at 50–60 km from the bay mouth.

SAMPLING AND METHODS

Thirteen research cruises traversed the Delaware Estuary during the period May, 1978 through July, 1981 (Table 1). On each cruise, sampling sites in the estuary were located on the basis of salinity, usually at 0, 1, 2.5, 5, 7.5, 10, 12.5, 15, 17.5, 20, 25, and 30‰. The station locations were

TABLE 1. Research Cruises on the Delaware Estuary and number of surface samples taken along the salinity gradient (numbers in parentheses are total number of samples taken on the cruise for extensive chemical analyses-over depth, overtime, laterally in the lower estuary, and outside the mouth of the estuary). Monthly discharge observed at Trenton, New Jersey (the head of the estuary) is shown in $m^3 \cdot s^{-1}$ for the month nearest to the sampling data.

Cruise no.	Date	Samples	Monthly discharge prior to sampling period
Salsx 1	May 24–26, 1978	7 (25)	583 (May)
Salsx 2	July 10–12, 1978	6 (30)	274 (June)
Salsx 3	Nov. 27–30, 1978	11 (17)	120 (Nov.)
Salsx 4	July 8–13, 1979	10 (102)	318 (June)
Salsx 5	Dec. 7–8, 1979	10 (43)	404 (Nov.)
Salsx 6	July 21–25, 1980	12 (52)	114 (July)
Salt 1	Oct. 1–3, 1980	12 (49)	84 (Sept.)
Salt 2	Nov. 17–20, 1980	20 (41)	112 (Nov.)
Salt 3	Jan. 28, 1981	12 (12)	69 (Jan.)
Salt 4	Mar. 1–3, 1981	18 (22)	632 (Feb.)
Salt 5	Mar. 23–25, 1981	19 (29)	211 (Mar.)
Salt 6	May 4–7, 1981	16 (29)	222 (Apr.)
Salt 7	June 29–July 1, 1981	18 (33)	195 (June)

determined by salinity as monitored with a flow-through salinity–temperature–depth (STD) system. On several cruises, sampling was also conducted in the greater Philadelphia municipal area, at subsurface depths, at single stations over time, in lateral transects in the lower estuary, and beyond the mouth of the estuary in coastal waters. This paper deals primarily with surface samples taken down the salinity gradient; sufficient sampling was done to assure that these samples were representative of the seasonal and annual distribution of measured properties.

Samples were taken in Niskin bottles equipped with reversing thermometers. Analytical methods were the same as reported in Sharp et al. (1982). In addition, total suspended seston was determined by passing a known volume (400–600 mL) of sample, immediately after collection, through a standard Millipore® filtration apparatus mounted with an acid rinsed, dried, preweighed Nuclepore® filter (47 mm diameter, 0.4 μm pore size). After filtration, each filter was rinsed with 50-100 mL quartz sub-boiled water to remove salts, stored in plastic petri dishes, and frozen until analysis in the laboratory. In the laboratory, the filters were dried at 70°C and reweighed to determine, by weight, the total suspended seston present in the sample. The seston was then carefully washed and lifted in mass from the filter with 5–10 mL spectographic grade acetone into tared acid-washed Teflon® beakers. The acetone was gently evaporated on a hot plate under a clean hood. The Teflon® beakers were cooled and reweighed to determine the amount of particulate material removed from the filter. A precise amount (5.0 mL) of 0.1 N quartz sub-boiled HCl was then added to the beakers and the sediments leached, covered, for 18 h at room temperature. Three to 4 mL of the resulting solute were carefully pipetted from each of the beakers in such a way as to not resuspend the sediments, and were analyzed directly by flameless atomic absorption for Fe, Mn, Al, Cu, Co, Cd, and Ni.

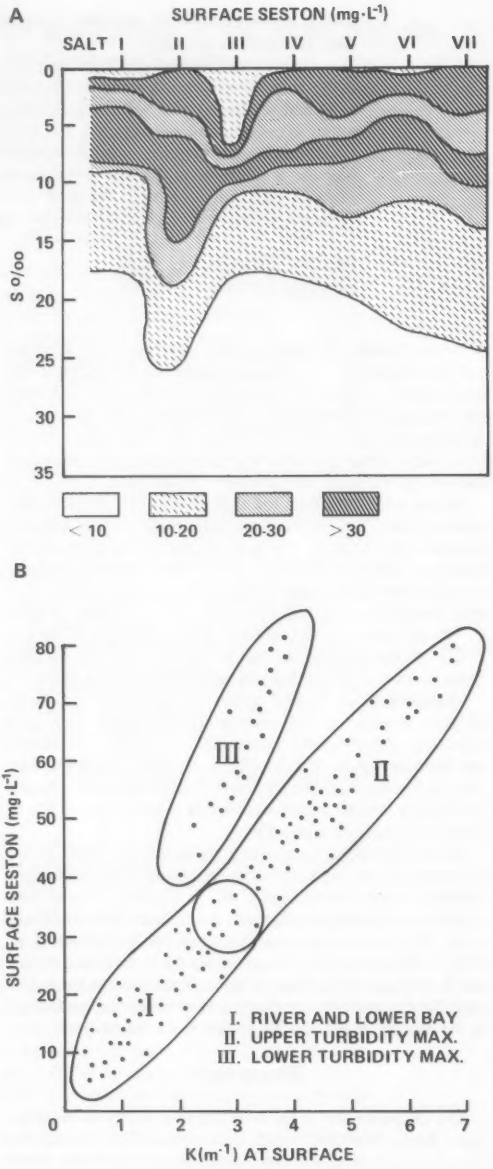

FIG. 1. Total suspended matter and optical characteristics of the Delaware. (A) Mass of surface seston ($mg \cdot L^{-1}$) along estuarine salinity gradient for all cruises; (B) Extinction (K_D) values for various estuarine regions; I. River and lower bay, II. Upper turbidity maximum, III. Lower turbidity maximum.

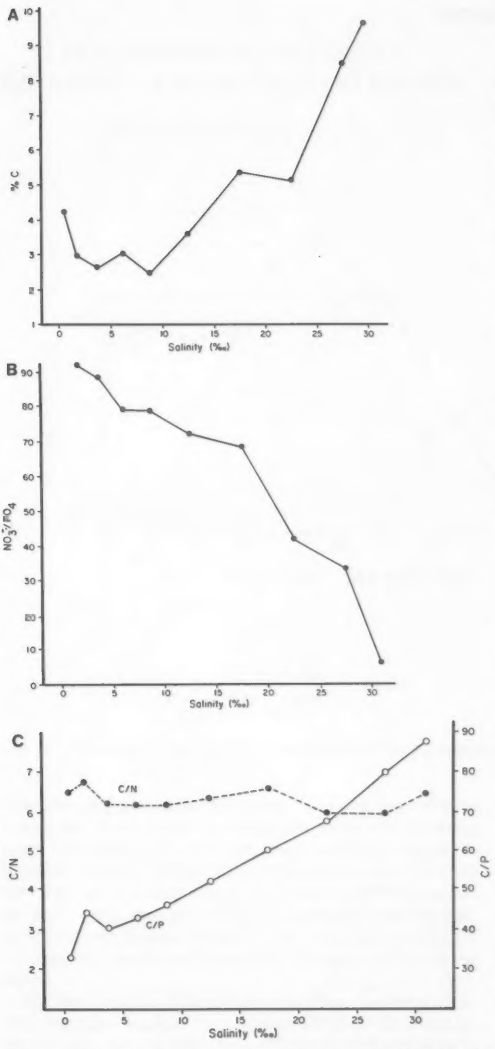

FIG. 2. Nutrient concentrations in surface waters of the Delaware Estuary. (A) Percent carbon in surface seston; (B) Nitrate−phosphate concentrations ratios for all cruises; (C) C/N and C/P average ratios. All values plotted as a function of estuarine salinity.

Light was measured with a Biospherical Instruments QSP-200 underwater scalar irradiance meter. The diffuse attenuation coefficient, K_D, was calculated from a regression of light measurements versus depth for each station. Water samples were collected and absorption spectra measured in a Pye-Unicam model 8-150 recording spectrophotometer with 10 cm path length. From the spectrophotometer data scanned from 400 to 900 nm, the beam attenuation coefficient, α, was calculated for each 25 nm interval.

TABLE 2. Average carbon to nitrogen and carbon to phosphorus ratios of the particulate matter. Sampling periods are grouped so that cruises Salsx 4 and 6 are considered summer, Salsx 3 and 5 and Salt 2 and 3 as winter, and Salt 1, 4, 5, and 6 as other (October, March, and May). The C/P data are split for upper estuary (salinity between 0−16‰) and lower estuary (16−32‰). The number of samples averaged is given in parentheses.

Season	C/N	C/P (upper estuary)	C/P (lower estuary)
Summer	5.59 (19)	52.0 (14)	104.8 (7)
Other	6.16 (59)	41.3 (36)	70.3 (23)
Winter	6.80 (51)	45.0 (28)	70.9 (19)

Primary productivity was estimated using the C-14 method with sample handling as given in Eppley and Sharp (1975). Surface samples were put into a series of bottles with attenuator bags representing 1−100% light transmission; these were incubated for 24 h in a deck incubator with flowing surface seawater. Productivity was integrated over the depth of the photic zone using data from the attenuation series and light attenuation depths from quantum meter profiles.

Results and Discussion

Surface seston concentrations are plotted for all cruises in Fig. 1A. Although one value exceeded 100 mg·L^{-1} (at 9‰ on Salt 2), typical high values ranged from 40 to 70 mg·L^{-1}. The most striking observation regarding the seston concentration was the presence of two turbidity maxima, one centered near 1−3‰ and one centered around 7.5−10‰. Both the river water (0‰) and high salinity (>20‰) water contained low seston concentrations, generally <20 mg·L^{-1} and frequently <10 mg·L^{-1}. Suspended sediment particle number size distributions were estimated on surface samples from Salt 3 and Salt 6 cruises by photographing, on shipboard, suspended particles in plankton counting chambers which had been spiked with artificial 10-μm spheres. The results of these two sets of measurements indicate that the upstream turbidity maximum was dominated by particles with a mean diameter of 3 μm and that the particles, by number, were principally (>60%) individual or primary particles; some composite particles up to 100 μm were present. The downstream turbidity maximum had a suspended sediment population dominated by composite particles bound together in a weakly birefringent (organic?) matrix. The particles in this downstream maximum had a mean particle diameter of 12 μm, with a maximum diameter of 125 μm. Downestuary from the turbidity maxima, the suspended sediment population consisted of large (10−20 μm) individual grains, with few composite particles and a significant phytoplankton assemblage.

The diffuse attenuation coefficient for natural waters, K_D, is largely determined by the concentration and size of suspended particulate matter (DiToro 1978). In Delaware Bay, the spatial variations in suspended particulate matter, and in extinction coefficients, were large. Figure 1B illustrates a plot of all values for K_D (surface to 1 m depth) and suspended sediment concentration in surface waters for all Salt cruises.

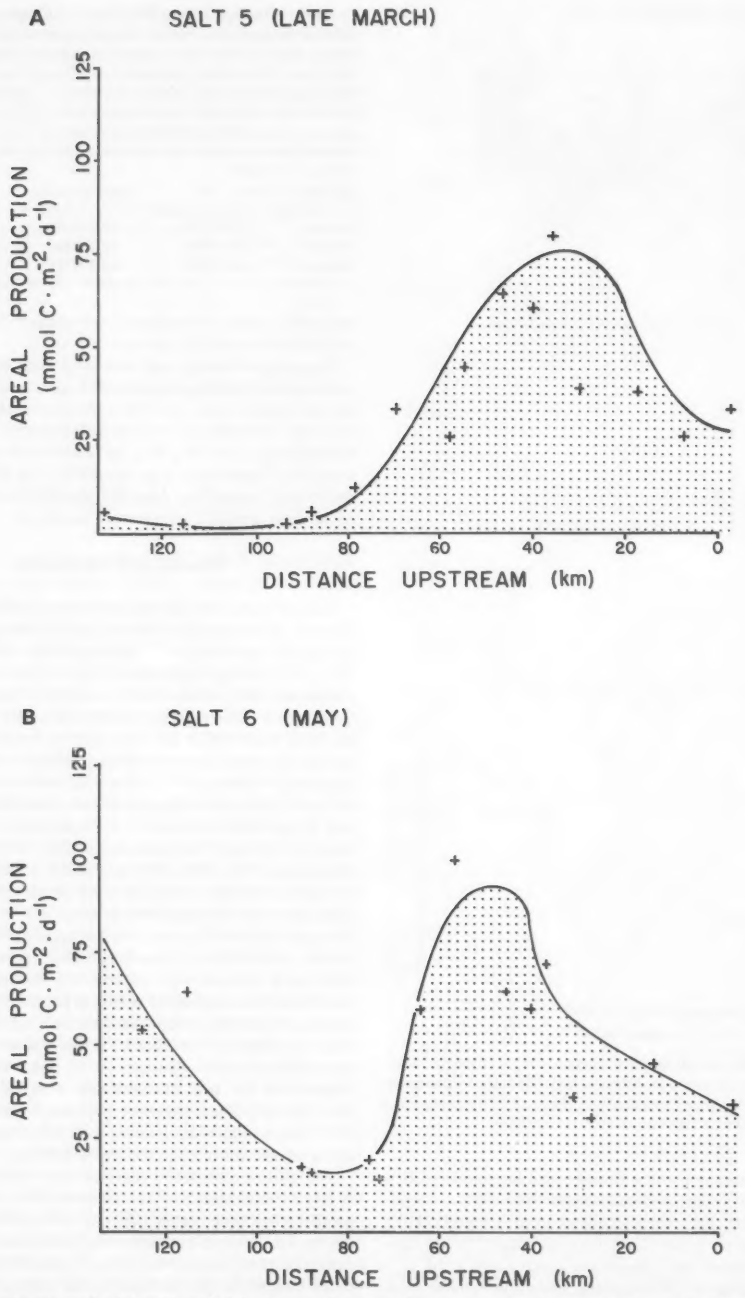

FIG. 3. Areal primary productivity ($C \cdot m^{-2} \cdot d^{-1}$) for two Delaware Estuary cruises. (A) March data, 1981; (B) May data, 1981 (mmol $C \cdot m^{-2} \cdot d^{-1}$).

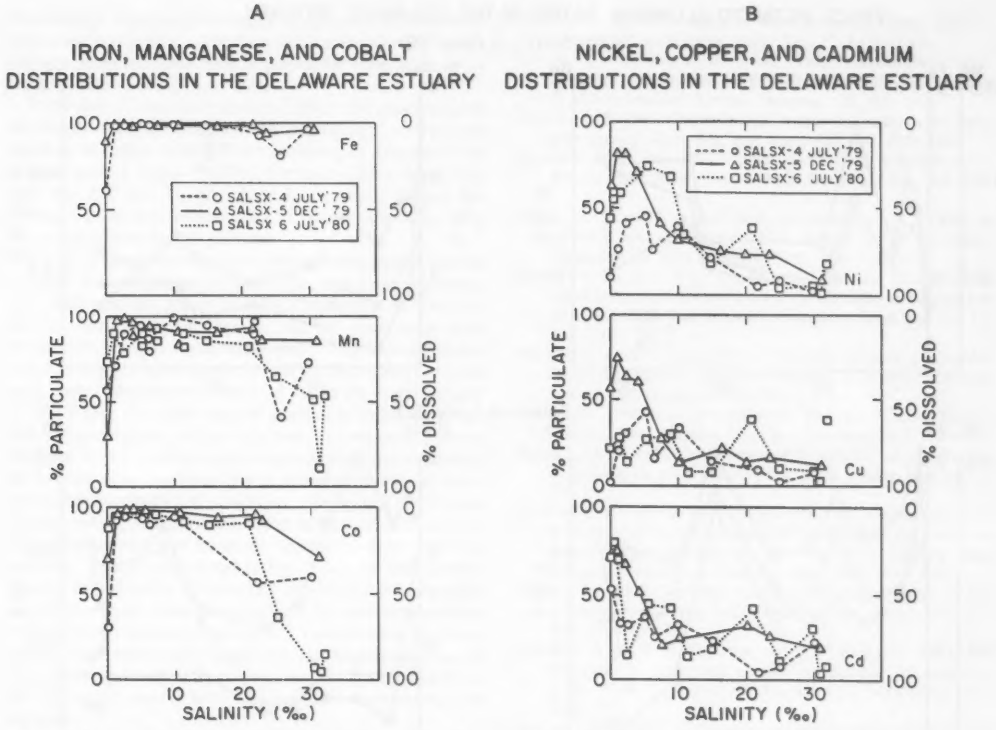

FIG. 4. Dissolved-particulate metal fractionation in Delaware Estuary surface waters.

The river, upper turbidity maximum, and lower bay formed a continuum, even though the lower bay contained relatively large suspended particles. The lower turbidity maximum, however, formed a distinct zone on the graph, consistent with the larger particle sizes found in the seston there. Values of the beam attenuation coefficient, α, exhibited similar behavior at all wavelengths, though in the low salinity reach of the estuary, pronounced absorption occurred in the yellow region.

The phenomenon of the turbidity maximum has been attributed by some workers (e.g. Krone 1972) to flocculation. Others (e.g. Nelson 1960) have suggested deflocculation as the principal cause. In estuaries with strong tidal currents, sediment resuspension by bottom scour has been advanced as a mechanism for turbidity maximum formation (Postma 1967; Schubel 1972). Nichols (1974) suggested an estuarine circulation mechanism involving near-bottom convergence where downstream river flow and upstream estuarine flow meet (the null region) and where upward vertical mixing slightly exceeds sediment settling rate. Officer and Nichols (1980) have proposed that gravitational circulation effects and tidal resuspension are both important phenomena, and that either or both may be necessary for the formation of the turbidity maximum. We cannot now determine the mechanisms responsible for the turbidity maxima in Delaware Bay, though we suspect that some combination of gravitational circulation and tidal resuspension may be responsible.

A general view of the seston showed a marked increase in the salinity range from 1 to 10‰, as compared to the freshwater end and the remainder of the estuary. The ratio of particulate carbon to seston, expressed as a percentage, exhibited a minimum in the same 1−10‰ salinity range (Fig. 2A). These minimal values were as low as 1−2% carbon, while the lower estuary usually had values in the 5−10% carbon range. The double turbidity maxima can be seen here as double percent carbon minima.

In Sharp et al. (1982), the phosphate buffer effect described by Morris et al. (1981) was identified as a nonconservative estuarine phosphate source. That is, in the mid-estuary, there is an exchange from particulate to dissolved phosphorus. Figure 2B is a composite plot of dissolved nitrate/phosphate ratios against salinity, using averaged values from 13 cruises. This demonstrates a deficiency in dissolved inorganic phosphorus in the mid-estuary. If this interpretation is correct, one might expect that suspended matter was enriched with phosphorus. By comparing particulate carbon/phosphorus ratios, relative particulate phosphorus enrichment can be seen in Fig. 2C, which gives average particulate C/P ratios for 10

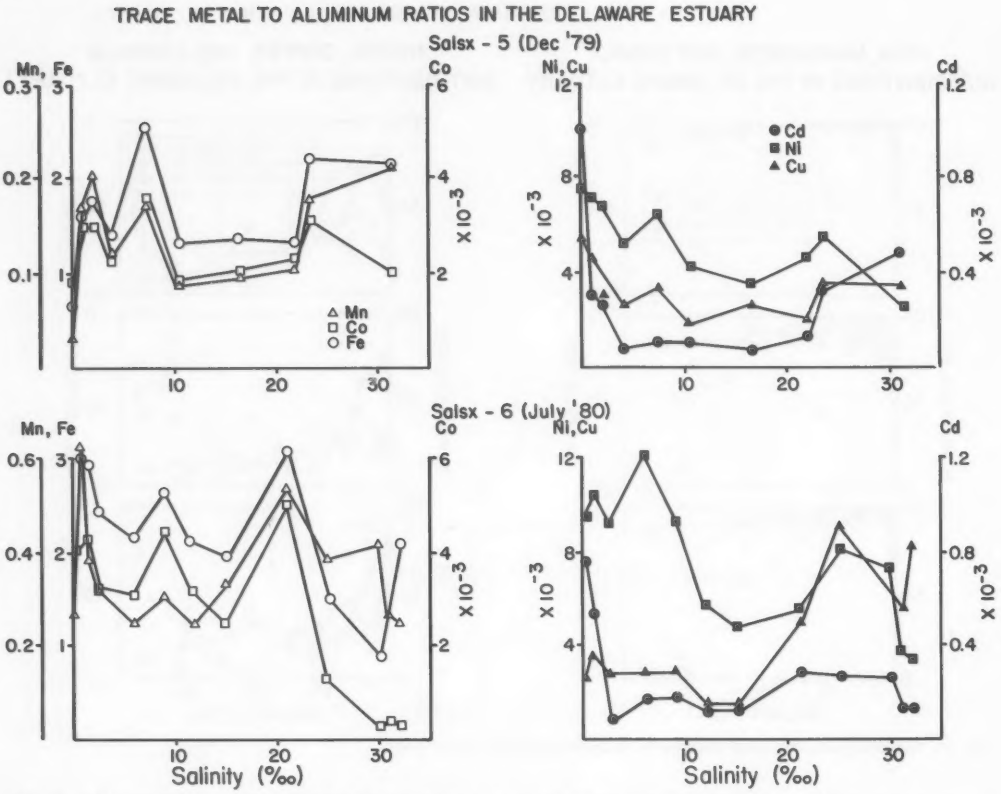

FIG. 5. Metal–aluminum ratios for Delaware Estuary surface seston plotted as a function of salinity.

cruises. One might expect a ratio of 106/1 if the particulates were similar to plankton (Redfield et al. 1963). Values near this ratio occurred only in the lower estuary, while considerably lower values (P-enrichment) were found in the upper estuary. Individual cruise data gave considerable scatter in the ratio but there is strong evidence of P-enrichment. No distinct deviation appeared in the regions of the turbidity maxima.

In contrast to C/P ratios, C/N ratios showed values close to the expected Redfield ratio throughout the estuary (Fig. 2C). Seasonal averages for the entire estuary for C/N and C/P were made by combining cruises Salsx 4 and 6 as summer; Salsx 3 and 5 and Salt 2 and 3 as winter; and Salt 1, 4, 5, and 6 as transitional (between summer and winter). Salt 7 was not included in the calculations because of evidence of relatively high detritus giving very high C/N and C/P ratios in the upper estuary. The averages are shown in Table 2. The trend in C/N is indicative of particulate matter that is richer in nitrogen in the summer than in the winter. The reverse trend is seen for the C/P ratio, which showed less P-enrichment in the summer, but this is not surprising since the average C/P was considerably lower than the Redfield ratio.

Figure 3 shows two characteristic patterns for phytoplankton production; on cruise Salt 5, low upriver production was typical of winter while cruise Salt 6 exhibited higher production at the freshwater end during late springtime. The production maximum occurred downstream from the turbidity maxima during all seasons. Light limitation of phytoplankton production was suggested by production patterns, which were correlated with light attenuation, by low production/chlorophyll ratios in the turbidity maxima (chlorophyll levels during non-bloom conditions did not rise proportionally with observed production), by the presence of major nutrients in high concentration in the turbidity maxima, and by a significant rise in chlorophyll levels for incubated samples.

As the Delaware River enters the upper reaches of the estuary, trace metals showed general removal to the particulate phase, which apparently represents physical/geochemical behavior ascribed to the processes of colloidal destabilization, flocculation, and/or precipitation. Figure 4 shows this redistribution as a decrease of percent dissolved accompanied by an increase percent particulate with increasing salinity. The metals Fe, Mn, Co demonstrated this most dramatically as a sharp increase from 50 to 90% in the particulate fraction, by

5‰ salinity. However, the metals Cd, Cu, and Ni showed an increasing dominance by the dissolved burden with increasing salinity, from less than 50% in particulate form in the river water to more than 75% by 30‰.

Particulate Al was quite uniform (300 ± 100 μmol/g) over the entire estuary in both the winter and summer, with a slight decrease at higher salinities due, perhaps, to dilution of the detrital load by organic matter. Particulate trace metal (Fe, Mn, Co, Cd, Cu, Ni) to Al ratios showed a general enrichment relative to average crustal (shale) abundance over the entire estuary for all seasons.

Figure 5 illustrates the trace metals undergoing a distinct increase in their ratio to Al at 0−2‰, and a sharp increase (especially for the group Fe, Mn, Co) at 8‰ as well, reflecting particulate enrichment. All the particulate trace metals then showed a gradual decrease relative to aluminum which reached a minimum at 10−20‰. The return to higher trace metal enrichment relative to Al in the lower estuary (>20‰) (Fig. 5) might suggest association with the particulate organic material originating from the estuarine primary biomass, which reached maximum proportions in this reach of the estuary (Fig. 3). From Fig. 4 it might be argued that a decreasing percentage of particulate trace metals simply represents particle settling in the lower estuary. If this were so, one might suppose that the metal−aluminum ratios would be constant. The data presented in Fig. 5 suggest that there is specific enrichment of trace metals on particulates because the metal−aluminum ratios increased and the increase coincided with maximum primary productivity. Two potential processes which could supply trace metals for such regeneration might be estuarine sediment diagenesis in general, or specifically for the Delaware, export from the extensive surrounding salt marshes.

Acknowledgments

This research was partially supported by the Office of Sea Grant (NA80AA-D-00106) of the U.S. National Oceanic and Atmospheric Administration and by a grant from the Delaware River and Bay Authority.

BIGGS, R. B. 1978. Coastal bays. *In* R. A. Davis [ed.] Coastal sedimentary environments. Springer-Verlag, New York, NY.

BOPP, F., III, AND R. B. BIGGS. 1981. Metals in estuarine sediments: factor analysis and its environmental significance. Science 214: 441−443.

BOULEGUE, J., C. LORD, AND T. CHURCH. 1981. Sulfur speciation and associated trace metals (Fe, Cu) in the pore waters of Great Marsh, Delaware. Geochim. Cosmochim. Acta.

CULBERSON, C. H., J. H. SHARP, T. M. CHURCH, AND B. W. LEE. 1982. Data from the Sals X cruises. May 1978−July 1980. Univ. Delaware Oceanogr. Data Rep. 2: 53 p.

DITORO, D. M. 1978. Optics of turbid estuarine waters: approximations and applications. Water Res. 12: 1059−1068.

EPPLEY, R. W., AND J. H. SHARP. 1975. Photosynthetic measurements in the central North Pacific: The dark loss of carbon in 24-h incubations. Limnol. Oceanogr. 20: 981−987.

JORDAN, R. R. 1969. Suspended and bottom sediments in the Delaware estuary. Geol. Soc. Am. Spec. Pap. 121: 357−369.

KETCHUM, B. H. 1952. The distribution of salinity in the estuary of the Delaware River. Woods Hole Oceanogr. Inst. 52−103: 1−52.

KRONE, R. B. 1972. A field study of flocculation as a factor in estuarial shoaling processes. U.S. Army Corps of Engineers, Committee on Tidal Hydraulic. Tech. Bull. 19: 125 p.

MORRIS, A. W., A. J. BALE, AND R. J. M. HOWLAND. 1981. Nutrient distributions in an estuary: evidence of chemical precipitation of dissolved silicate and phosphate. Estuarine Coastal Mar. Sci. 12: 205−216.

NEILHEISEL, J. 1973. Source of detrital heavy minerals in estuaries. Ph.D. dissertation, School of Geophysical Sciences, Georgia Inst. of Technology, Atlanta, GA. 112 p.

NELSON, B. 1960. Clay mineral of the bottom sediments, Rappahannock River, Virginia. Clays and Clay Minerals 7: 135−147.

NICHOLS, M. M. 1974. Development of the turbidity maximum in the Rappahannock estuary. Mem. Inst. Geol. Bassan Aquitaine 7: 19−25.

OFFICER, C. B., AND M. M. NICHOLS. 1980. Box model application to a study of suspended sediment distributions and fluxes in partially mixed estuaries, p. 329−340. *In* V. Kennedy [ed.] Estuarine perspectives. Academic Press, New York, NY.

POSTMA, H. 1967. Sediment transport and sedimentation in the estuarine environment. *In* G. Lauff [ed.] Am. Assoc. Adv. Sci. Pub. 83: 158−179.

REDFIELD, A. C., B. H. KETCHUM, AND F. A. RICHARDS. 1963. The influence of organisms on the composition of seawater, p. 26−77. *In* M. N. Hill [ed.] The sea, V. 2. Interscience, New York, NY.

SCHUBEL, J. R. 1972. Distribution and transportation of suspended sediment in upper Chesapeake Bay. *In* B. W. Nelson [ed.] Environmental framework of coastal plain estuaries. Geol. Soc. Am. Mem. 133: 91−117.

SHARP, J. H., AND C. H. CULBERSON. 1982. The physical definition of salinity: A chemical evaluation. Limnol. Oceanogr. 27: 385−387.

SHARP, J. H., C. H. CULBERSON, AND T. M. CHURCH. 1982. The chemistry of the Delaware Estuary. General considerations. Limnol. Oceanogr. 27: 1015−1028.

U.S. ARMY CORPS OF ENGINEERS. 1968. Long Range Disposal Study, Sub-study No. 2. Nature and Source of Shoal. U.S. Army Corps of Engineers, Philadelphia District, Philadelphia, PA. 118 p. + Appendix.

U.S. GEOLOGICAL SURVEY. 1975. Surface Water Quality of the United States: Water Supply Paper 1271.

WEIL, C. B. 1977. Sediments, structural framework and evolution of Delaware Bay, a transgressive estuarine delta. University of Delaware Sea Grant Publication DEL-SG-4-77, Newark, DE. 199 p.

Les flux de sels nutritifs dans l'estuaire de la Seine (France); rôle et importance du bouchon vaseux au cours du mélange estuarien[1]

JEAN-FRANÇOIS GUILLAUD

Centre Océanologique de Bretagne — C.N.E.X.O.[2], B.P. 337, 29273 — Brest Cédex — France

GUILLAUD, J.-F. 1983. Les flux de sels nutritifs dans l'estuaire de la Seine (France); rôle et importance du bouchon vaseux au cours du mélange estuarien. Can. J. Fish. Aquat. Sci. 40(Suppl. 1): 180 – 187.

Les apports fluviaux en sels nutritifs dissous dans l'estuaire de la Seine ont été étudiés au cours de la période 1976 à 1979; ils sont directement proportionnels au débit de la Seine, à l'exception des apports plus constants en phosphates. Les apports annuels moyens sous forme minérale dissoute sont de l'ordre de 37 600 t/année pour la silice, 10 300 t/année pour le phosphore et 66 000 t/année pour l'azote. Des échantillons de sels nutritifs ont aussi été recueillis le long de l'estuaire durant les mois de mars 1978, mars et septembre 1979; les résultats montrent que, dans l'estuaire, les sels nutritifs se diluent généralement de façon conservative; les seules exceptions notables à ce schéma concernent : une addition limitée de silicates au niveau du fond en période de crue, et une production d'ammoniaque et de nitrites en période estivale. Les résultats montrent aussi que le phosphore particulaire et l'azote organique particulaire sont stockés dans le bouchon vaseux, mais que ce phénomène n'affecte qu'une faible part des apports fluviaux de sels nutritifs. Il apparaît, enfin, que les fortes turbidités et le temps de renouvellement assez court des eaux sont deux facteurs qui limitent la production primaire phytoplanctonique et, donc, la consommation des sels nutritifs dans l'estuaire.

Mots clés : sels nutritifs, estuaire de la Seine, apports, dilution, bouchon vaseux

GUILLAUD, J.-F. 1983. Les flux de sels nutritifs dans l'estuaire de la Seine (France); rôle et importance du bouchon vaseux au cours du mélange estuarien. Can. J. Fish. Aquat. Sci. 40(Suppl. 1): 180 – 187.

Dissolved nutrient loadings from the Seine River as it enters the Seine Estuary were examined for the period 1976 – 79; these are directly related to river flow, except for more constant phosphate loading. Mean annual inputs of dissolved inorganic nutrients attain 37 600 t/yr for silica, 10 300 t/yr for phosphorus and 66 000 t/yr for nitrogen. Nutrients samples were also collected along the estuary during March 1978 and March and September 1979; results show that in the estuary the dissolved nutrients are generally mixed in a conservative way; a few exceptions can be noticed — addition of silicate to the bottom water during high river flow periods and production of ammonia and nitrites during the summer months. Results also indicate that particulate phosphorus and particulate organic nitrogen can be trapped within the area of the turbidity maximum but this process affects only a small fraction of the total inputs of nutrients from the river. Finally it is suggested that high turbidity levels and rapid flushing time are two significant factors limiting the primary production and the removal of dissolved nutrients within the estuary.

L'ESTUAIRE de la Seine, situé dans la partie Nord Ouest des côtes françaises, est le point d'arrivée en mer des eaux d'un bassin versant de 78 650 km^2. Sur ce bassin se trouvent 30% de la population française (dont l'agglomération parisienne) et 40% de l'activité économique nationale.

La Seine, à son arrivée dans l'estuaire, a un débit moyen de 400 m^3/s et peut atteindre 2000 m^3/s en crue (décembre à mars) et 100 m^3/s en étiage (juillet à octobre); par ailleurs, l'estuaire est soumis à la marée semi-diurne, dont l'amplitude est de 7,5 m dans l'embouchure en vive eau. L'onde de marée qui se déforme en pénétrant dans l'estuaire parvient jusqu'au barrage de Poses, alors que le front de salinité (0,5 ‰) ne remonte en étiage que jusqu'aux environs de Courval (Fig. 1).

Dans l'estuaire, les sédiments en suspension forment un

[1]Cet article fait partie des comptes rendus du Colloque sur la dynamique des environnements côtiers troubles tenu à l'Institut océanographique de Bedford, à Dartmouth (Nouvelle-Écosse), Canada, du 29 septembre au 1er octobre 1981.

[2]Centre National pour l'Exploitation des Océans.

Printed in Canada (J6684)
Imprimé au Canada (J6684)

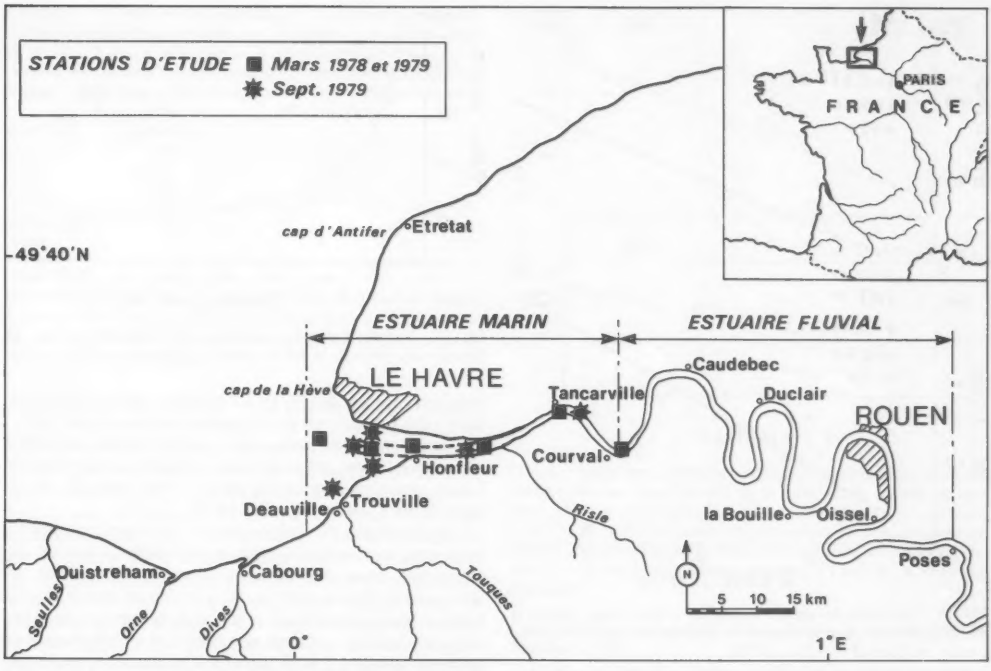

FIG. 1. L'estuaire de la Seine. Position des stations d'échantillonnage.

bouchon vaseux très turbide, où les concentrations en matières en suspension varient de 0,05 à plus de 1 g/L. L'existence de ce bouchon vaseux apparaît essentiellement liée aux remises en suspension des sédiments par les courants de marée. Le cycle vive eau – morte eau joue de ce fait un rôle prépondérant sur la dynamique sédimentaire de cet estuaire à fort marnage. La masse de matières en suspension varie aussi au cours de la marée; elle est importante au moment des vitesses maximales de courants, et plus faible au cours des étales qui permettent une décantation rapide, notamment à pleine mer (Avoine et al. 1981). La masse maximale du bouchon vaseux, évaluée par Avoine (1981) à 200 000 t, est atteinte lors des marées de vive eau d'étiage, au cours desquelles les vitesses de courant sont élevées (2,5 m/s).

Les variations saisonnières du débit fluvial entraînent un déplacement de la zone turbide; en période d'étiage, le bouchon vaseux est maintenu dans l'estuaire par l'asymétrie de l'onde de marée, et il occupe une zone comprise entre Courval et Honfleur; dans ce secteur, les salinités moyennent passent de 0,5 ‰ à l'amont à 25 ‰ à l'aval. Par contre, en période de crue, sous l'effet des forts débits, le bouchon vaseux migre vers l'aval, et une partie des matières en suspension est évacuée plus au large; il occupe alors une zone dont la limite amont est située entre Tancarville et Honfleur, et dont la limite aval se trouve dans l'embouchure, au large du Havre; dans ce secteur, les salinités moyennes passent de 5 ‰ à l'amont à 30 ‰ à l'aval.

La présente étude des sels nutritifs dans l'estuaire de la Seine fait partie d'un ensemble d'études océanographiques pluridisciplinaires entreprises de 1977 à 1980 dans le cadre du «Schéma d'Aptitude et d'Utilisation de la Mer» (S.A.U.M.) de l'estuaire de la Seine.

La réalisation de ce schéma a été coordonnée par la Mission d'Aménagement de la Basse-Normandie, et la Mission d'Etudes de la Basse-Seine, avec l'assistance scientifique du département Environnement Littoral et Gestion du Milieu Marin du Centre National pour l'Exploitation des Océans (C.N.E.X.O.).

Les objectifs de cette étude sont de déterminer, en fonction des conditions hydrologiques, les variations des apports fluviaux en sels nutritifs dans l'estuaire de la Seine, et de préciser le rôle éventuel des fortes teneurs en matières en suspension sur les concentrations et la dilution de ces mêmes sels dans l'estuaire.

Ce travail vise aussi à compléter, d'une part les premières estimations d'apports fluviaux en sels nutritifs faites par Lassus et al. (1980) à partir des données du Service de la Navigation de la Seine (4e section — Cellule Antipollution) et, d'autre part, les études faites plus en aval, dans l'embouchure et la baie de Seine (C.O.B. 1979).

Matériel et méthodes

Les mesures hydrologiques réalisées dans l'estuaire de la

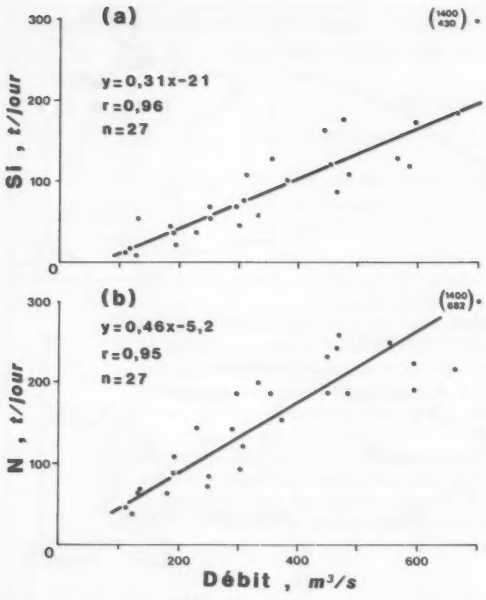

FIG. 2. Variations des apports journaliers en (a) silicates dissous et en (b) azote total minéral dissous, en fonction du débit de la Seine (station de Courval — 1976 à 1979).

Seine et utilisées dans cette étude, proviennent de deux types de campagnes :

1) les campagnes du Port Autonome de Rouen (Service de la Navigation de la Seine — 4e section — Cellule Antipollution), qui effectue tous les deux mois, depuis 1964, un prélèvement à mi-profondeur, au cours de la basse mer, en 23 stations réparties entre Honfleur et Poses; seules les mesures réalisées depuis 1975 ont été utilisées pour étudier les apports en sels nutritifs par la Seine.
2) les campagnes organisées dans le cadre du S.A.U.M., en 1978 et 1979, qui comprenaient des stations de mesures à point fixe durant un cycle de marée, réparties dans l'estuaire en aval de Courval. L'étude de la dilution des sels nutritifs dans l'estuaire est fondée sur les résultats des mesures effectuées en vive eau et en morte eau, à poste fixe en six stations (Fig. 1), en période de crue (mars 1978 et 1979) en période d'étiage (septembre 1979). Les prélèvements étaient faits à chaque point fixe toutes les deux heures en surface et au fond, durant un cycle de marée (12h15'), à l'aide d'une bouteille Niskin de 5 L.

Les échantillons de sels nutritifs ont été conservés au froid (4°C) et dans l'obscurité à bord des bateaux, puis congelés à leur arrivée au laboratoire; les analyses ont été faites dans les 48 h après les prélèvements. Les concentrations en matières en suspension ont été déterminées par filtration sur disque en fibre de verre et par pesée (AFNOR, norme T90-105, 1972). Les concentrations en sels nutritifs dissous ($Si(OH)_4$, NO_2, NO_3, PO_4^{3-}) ont été mesurées suivant les méthodes de

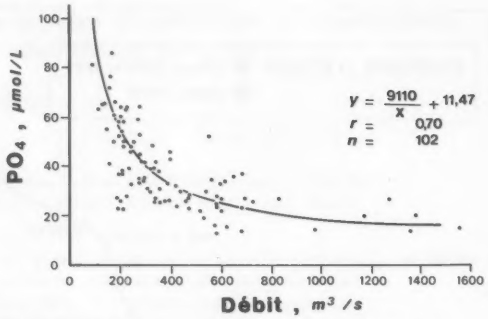

FIG. 3. Variations des concentrations en phosphates dissous, en fonction des débits de la Seine (station aval-Rouen — 1975 à 1978).

Strickland et Parsons (1972), à l'exception de l'ammoniaque (NH_4^+) qui fut analysée par la méthode de Koroleff (1969).

L'azote organique particulaire a été déterminé par différence entre l'azote organique total (échantillon non filtré) et l'azote organique dissous (échantillon filtré), mesurés par la méthode de Kjeldahl (Koroleff 1976).

Les phosphates particulaires ont été déterminés par différence entre les phosphates totaux et les phosphates dissous; les phosphates totaux ont été analysés suivant la méthode de Strickland et Parsons (1972), mais en faisant agir le réactif habituel (molybdate d'ammonium, acide sulfurique, acide ascorbique, émetite) sur l'eau non filtrée, et en effectuant ensuite une filtration à 0,45 µm afin d'effectuer la mesure de densité optique sans être gêné par la turbidité; le blanc de turbidité a été fait sur l'eau de l'échantillon filtrée sans réactif. Cette méthode permet de déterminer, d'après Koroleff (1976) et Strickland et Parsons (1972), les phosphates particulaires inorganiques contenus dans les matières en suspension et qui sont libérés par la solution acide de molybdate; les phosphates particulaires ainsi dosés ne sont pas tous librement échangeables avec la fraction dissoute, car ils comprennent aussi des phosphates de calcium, tels que l'apatite. Néanmoins, cette mesure garde tout son intérêt pour l'évaluation ultérieure des apports et du stock de phosphates particulaires inorganiques dans l'estuaire, étant donnés les rejets importants effectués en Basse-Seine par les industries de fabrication d'engrais phosphatés (minerai de fluorapatite).

Résultats

Les Apports en Sels Nutritifs

Les apports fluviaux en sels nutritifs dissous dans l'estuaire de la Seine ont été calculés en multipliant les débits de la Seine par les concentrations observées tous les deux mois à l'amont de l'estuaire et, donc, en amont de l'intrusion saline (station de Courval).

Les apports en silicates — L'étude de la variation des apports en silicates dissous en fonction des conditions hydrologiques montre que ces apports sont directement propor-

TABLEAU 1. Evolution des concentrations moyennes et des pourcentages moyens d'ammoniaque dans les apports d'azote total minéral dissous, à Poses, et évolution des concentrations moyennes en oxygène dissous dans l'estuaire de la Seine (entre Rouen et Honfleur).

Année	NH_4 µmol/L	NH_4/Ntotal %	O_2 mg/L
1976	230	55	2,6
1977	126	38	3,5
1978	101	28	3,8
1979	92	22	4,4
1980	72	19	5,2

tionnels au débit (Fig. 2a); ils varient de 10 t/jour en étiage, à plus de 400 t/jour de silicium, en crue; pour un débit moyen annuel de 400 m^3/s, les apports annuels en silicium sont de l'ordre de 37 600 t/année.

Les apports en phosphates — La relation qui lie les apports en phosphates dissous au débit de la Seine est beaucoup moins nette que pour les silicates; ces apports tendent cependant à croître légèrement avec le débit de la Seine; pour un débit moyen annuel de 400 m^3/s, les apports annuels de phosphore dissous sont de l'ordre de 10 300 t/année. Cette faible augmentation des apports en fonction du débit fluvial vient du fait que les concentrations en phosphates tendent à diminuer lorsque le débit augmente; ceci est confirmé par les nombreuses mesures de concentrations en phosphates réalisées tous les 15 jours en aval de Rouen, et dont la décroissance en fonction du débit traduit le fait que la part des rejets constants, industriels ou urbains, est prépondérante dans les apports en phosphates par la Seine (Fig. 3).

Les apports en azote — Les apports en azote total minéral dissous ($N \cdot NO_3 + N \cdot NO_2 + N \cdot NH_4$) croissent, comme dans le cas des silicates, de façon linéaire avec le débit (Fig. 2b) et peuvent dépasser 500 t/jour en période de forte crue. Pour un débit moyen annuel de 400 m^3/s, les apports annuels d'azote total minéral dissous sont de l'ordre de 66 000 t/année. L'ammoniaque et les nitrates constituent l'essentiel de ces apports azotés et l'étude de la variation temporelle de la proportion d'ammoniaque dans ces apports montre que le pourcentage d'azote ammoniacal à Courval, par rapport à l'azote total minéral dissous, est plus faible en périodes estivales (0 à 16 %) qu'en périodes hivernales (32 à 65 %) car les processus d'oxydation en nitrates se trouvent accélérés au cours de l'été par les températures plus élevées. Par ailleurs, il existe une décroissance pluriannuelle des concentrations annuelles moyennes en ammoniaque et des pourcentages annuels moyens d'azote ammoniacal dans les apports d'azote total minéral dissous, mesurés à Poses durant la période 1976 à 1980 (Tableau 1). Cette décroissance s'accompagne d'une augmentation des concentrations moyennes annuelles en oxygène dissous mesurées dans l'estuaire (entre les stations de Honfleur et Rouen) par le Port Autonome de Rouen; l'ammoniaque est, en effet, lors de son oxydation en nitrates, une source importante de déficit en oxygène; les causes de cette évolution sont sans doute à rechercher dans un meilleur fonctionnement des stations d'épuration du Bassin Parisien; les mêmes phénomènes ont été constatés lors de l'amélioration de la qualité des eaux dans la Tamise (Dart et Sheldon 1980).

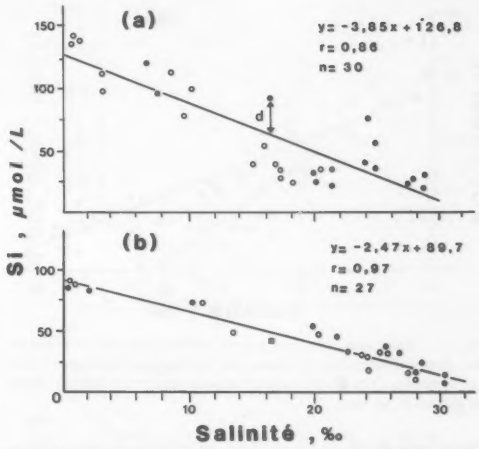

FIG. 4. Variations, en fonction de la salinité, des concentrations en silicates dissous dans l'estuaire de la Seine en (a) période de crue (mars 1979) et en (b) période d'étiage (septembre 1979). Les symboles ○, ● et *d* représentent respectivement les concentrations en surface, les concentrations au fond, et l'écart entre les concentrations observées et les concentrations calculées à l'aide de la droite de régression.

Enfin, les mesures des concentrations en azote organique, réalisées depuis 1978 dans les eaux de la Seine, ont aussi permis de calculer les apports en azote organique total (dissous, plus particulaire) à Courval. Ces apports croissent avec le débit et sont de l'ordre de 13 500 t/an pour un débit moyen annuel de 400 m^3/s; le pourcentage d'azote organique particulaire par rapport à l'azote organique total est en moyenne de 73 %.

LA DILUTION DES SELS NUTRITIFS DANS L'ESTUAIRE

Les eaux fluviales qui arrivent dans l'estuaire de la Seine vont être confrontées à deux phénomènes qui sont le mélange avec les eaux marines plus pauvres en sels nutritifs, et le passage dans un milieu beaucoup plus chargé en matières en suspension. Nous examinerons pour chaque type de sels nutritifs (silice, phosphore et azote) le rôle des fortes concentrations en matières en suspension sur les teneurs en sels nutritifs au cours de la dilution des eaux douces dans les eaux marines.

Le cas des silicates — L'examen des concentrations en silicates dans l'estuaire de la Seine montre que, tant en période d'étiage qu'en période de crue, les silicates ont, au cours de la dilution des eaux douces dans les eaux marines, un comportement apparemment conservatif; il est, en effet, impossible de distinguer nettement une production ou une consommation de silicates dans la zone estuarienne, qui se traduirait par des écarts notables par rapport à la droite de dilution (Fig. 4). Néanmoins, si l'on prend en compte les

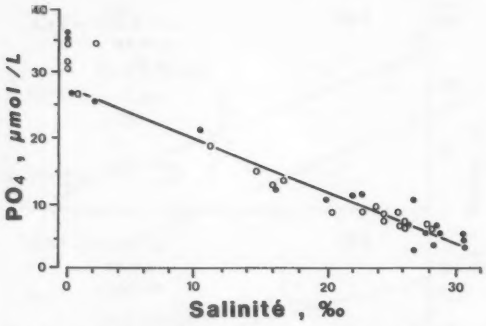

FIG. 5. Variations, en fonction de la salinité, des concentrations en phosphates dissous dans l'estuaire de la Seine, en septembre 1979. Les symboles ○ et ● représentent respectivement les concentrations en surface et au fond.

concentrations observées au fond, en période de crues (mars 1978 et 1979) et que l'on calcule l'écart d entre ces concentrations et les valeurs théoriques déduites, à salinité égale, de la droite de régression, il apparaît que cet écart d (µmol/L) est positivement corrélé avec le logarithme naturel de la teneur en matières en suspension des échantillons (M.E.S.; mg/L); l'équation de la régression est la suivante (avec $r = 0{,}82$ et $P < 0{,}01$) :

$$d = 8{,}40 \ln \text{MES} - 26{,}85$$

Il semble donc exister, en période de crue, une source limitée de silicates qui influence plus spécifiquement les eaux de fond et qui pourrait être liée à la remise en suspension des sédiments superficiels au sein du bouchon vaseux. Cette observation est à rapprocher de celle que Van Bennekom et al. (1974) ont faite en mer de Wadden; ces auteurs constatent, en effet, qu'il existe, du fait des processus de reminéralisation, une source de silicates au niveau des sédiments superficiels par échange turbulent entre les eaux interstitielles et les eaux de fond lorsque ces sédiments sont remobilisés.

Le cas des phosphates — L'étude des concentrations en phosphates dissous dans l'eau révèle un comportement essentiellement conservatif de ce sel nutritif dans l'estuaire au cours du mélange des eaux douces et des eaux marines (Fig. 5). Seule peut être observée au niveau des très faibles salinités, une chute rapide des concentrations en phosphates dissous; il est peu probable que cette décroissance résulte d'une consommation par les organismes phytoplanctoniques car les autres sels nutritifs ne montrent pas du tout la même évolution; il pourrait s'agir, par contre, d'une adsorption rapide du phosphore lorsque les eaux fluviales rentrent en contact avec les matières en suspension du bouchon vaseux dans la zone des faibles salinités; Edzwald et al. (1976) ont expérimentalement mis en évidence de tels phénomènes d'adsorption sur les minéraux argileux et ont montré que ce processus pouvait être rapide. Les mesures de phosphates particulaires, réalisées au cours des campagnes de septembre 1979, montrent qu'il existe une corrélation hautement significative entre les concentrations en matières en suspension et les teneurs en

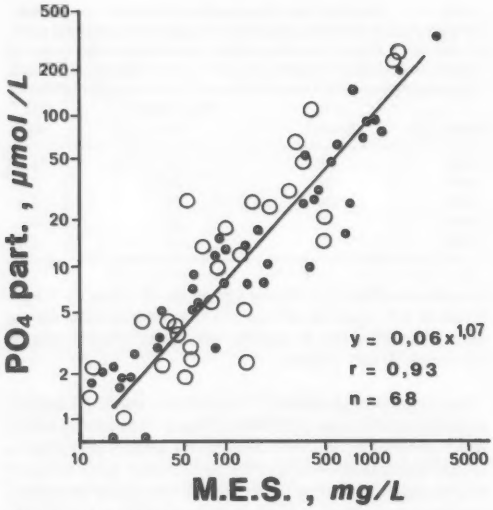

FIG. 6. Variations des concentrations en phosphates particulaires, en fonction des concentrations en matières en suspension (M.E.S.) dans l'estuaire de la Seine en septembre 1979. Les symboles ○ et ● représentent respectivement les mesures en morte eau et en vive eau.

phosphates particulaires dans l'estuaire (Fig. 6). Cette relation est très voisine de celles mises en évidence par De Jonge et Postma (1979) en mer de Wadden. De plus, l'étude de la variation des teneurs en phosphore particulaire inorganique des matières en suspension en fonction de la salinité, montre qu'il existe une légère décroissance de ces teneurs lorsque la salinité augmente; cette relation est décrite par l'équation de régression suivante (avec $r = 0{,}69$ et $P < 0{,}01$) :

$$\text{P.P.} = 4\,182\ S^{-0{,}24}$$

où P.P. est la teneur en phosphore particulaire inorganique des matières en suspension (exprimée en p.p.m.), et S la salinité (exprimée en ‰). Cette relation peut traduire le fait qu'il y a, au sein de l'estuaire, mélange entre des particules fluviatiles chargées en phosphates et des particules estuariennes ou marines plus pauvres. Cette relation montre aussi que les éventuels phénomènes d'adsorption évoqués précédemment, et qui auraient lieu dans la zone des faibles salinités, ne sont pas suffisamment importants vis-à-vis de la masse du bouchon vaseux pour faire croître significativement les concentrations en phosphates des matières en suspension estuariennes. Ces observations sont à rapprocher de celles que Boust (1981) fait en ce qui concerne les métaux dans l'estuaire de la Seine; cet auteur met en évidence une décroissance rapide des concentrations en métaux dissous dans l'eau, limitée à la zone des faibles salinités, et une diminution d'amont en aval de la charge en métaux des matières en suspension; il attribue ce dernier phénomène à des mécanismes de désorption et de mélanges entre particules marines et fluviatiles.

Il existe donc, au sein de l'estuaire, un stock de phosphore particulaire qui peut être évalué à partir de la charge moyenne

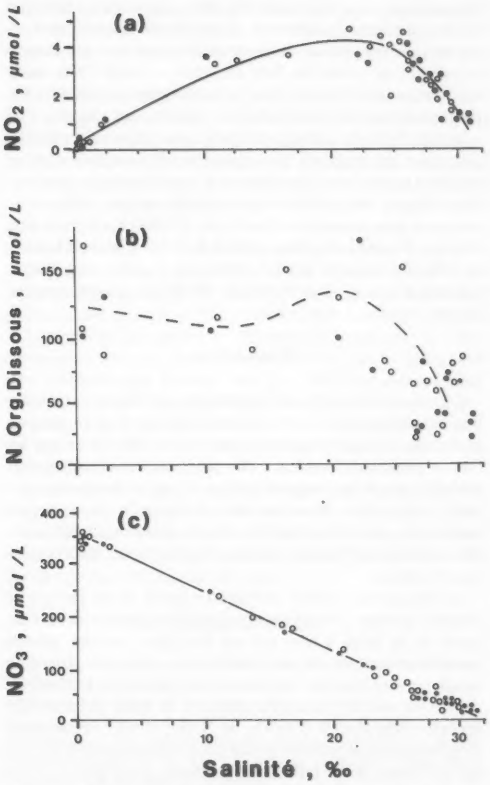

FIG. 7. Variations, en fonction de la salinité, des concentrations en (a) nitrites, en (b) azote organique dissous et en (c) nitrates dans l'estuaire de la Seine, en septembre 1979. Symboles identiques à la Fig. 5.

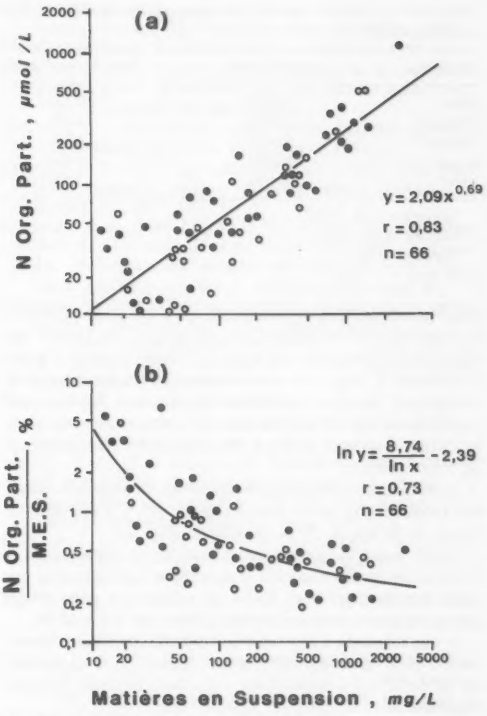

FIG. 8. Variations, en fonction des concentrations en matières en suspension (M.E.S.), (a) des teneurs en azote organique particulaire dans l'eau et (b) du pourcentage d'azote organique particulaire dans les matières en suspension, dans l'estuaire de la Seine, en septembre 1979. Symboles identiques à la Fig. 6.

en phosphore des matières en suspension (3 540 ppm) et de la masse du bouchon vaseux qui est au maximum de 200 000 t en vive eau d'étiage; ce stock de phosphore particulaire est donc égal au maximum à 700 t, ce qui représente de l'ordre de 7 % des apports annuels en phosphore sous forme dissoute. La comparaison avec les apports annuels de phosphore particulaire est plus difficile, car l'on ne dispose pas de mesure régulière en Seine du phosphore particulaire; néanmoins, la mesure de la charge en phosphore des matières en suspension, en septembre 1979, au niveau de l'eau douce (6 000 ppm) et la connaissance des apports annuels moyens de matières en suspension par la Seine, estimés à 530 000 t par Avoine et al. (1981), permettent d'évaluer le flux moyen annuel de phosphore particulaire à 3 180 t. Le phosphore particulaire stocké dans le bouchon vaseux représente donc de l'ordre de 22 % des apports fluviaux sous forme particulaire.

Malgré la présence de ce stock de phosphore particulaire dans l'estuaire, les concentrations en phosphates dissous ne présentent pas d'excès par rapport aux droites de dilution théorique; il n'y a donc pas, dans l'estuaire, de phénomène important de production de phosphore à partir des matières en suspension, ou de l'eau interstitielle des sédiments; ceci rejoint les observations faites par Taft et Taylor (1976) dans la zone turbide de la baie de Chesapeake; de plus, les nombreux travaux entrepris sur le relargage du phosphore par les sédiments montrent que ce phénomène prend place en milieu estuarien lorsque les concentrations en phosphates dissous sont inférieures à un seuil qui est compris, suivant les auteurs, entre 0,67 et 1,19 µmol/L (Pomeroy et al. 1965; Stefansson et Richards 1963; Butler et Tibbitts 1972); ces valeurs sont bien inférieures aux concentrations en phosphates dissous mesurées dans l'estuaire de la Seine et expliqueraient l'absence de phénomène de désorption dans l'estuaire. Ces désorptions, à partir des matières en suspension, devraient se produire beaucoup plus au large lorsque les eaux fluviales auront été suffisamment diluées par l'eau de mer pour que les concentrations en phosphates dissous tombent à un niveau égal ou inférieur aux seuils précédemment cités.

Le cas de l'azote — Les différents sels minéraux azotés (NH_4, NO_2, NO_3) présentent, durant la période hivernale de

TABLEAU 2. Apports moyens en azote et en phosphore dans quelques grands estuaires.

Estuaires	Azote, t/année	Phosphore, t/année
Seine	66 000	10 300
Potomac[a]	16 500	4 850
Hudson[b]	58 400	4 740
Escaut[c]	18 500	1 400
Rhin[d]	263 000	13 500

[a]Jaworsky et al. (1972).
[b]Malone et al. (1980).
[c]Wollast (1976).
[d]R.N.O. (1978).

crue, un comportement conservatif vis-à-vis de la salinité et ce sont donc essentiellement des mécanismes de dilution qui régissent les concentrations de ces sels dans l'estuaire. Durant les périodes d'étiage, les concentrations en ammoniaque et en nitrites sont souvent très faibles dans les eaux fluviales, car ces éléments ont été oxydés dans la rivière; par contre, dans l'estuaire, il apparaît au cours du mélange des eaux douces et des eaux marines:

1) une augmentation des concentrations en nitrites et, donc, une production de ce sel dans l'estuaire suivie d'une dilution rapide au-dessus de 20 ‰ de salinité (Fig. 7a),

2) une augmentation des concentrations en ammoniaque et du pourcentage d'ammoniaque par rapport à l'azote total minéral dissous entre 0 et 30 ‰ de salinité; ce pourcentage passe, entre ces deux valeurs de salinité, de 0,5 à 12 %,

3) une tendance à la production d'azote organique dissous entre 0 et 20 ‰ de salinité mise en évidence par la stagnation, ou même la légère augmentation des concentrations en azote organique dissous entre ces salinités (Fig. 7b),

4) un comportement conservatif des nitrates vis-à-vis de la salinité (Fig. 7c).

Il existe donc, en période estivale, une production d'azote organique dissous et d'azote minéral sous forme réduite (ammoniaque et nitrite) au sein de l'estuaire ou dans sa partie aval; cette production a très probablement pour origine l'hydrolyse des matières organiques particulaires suivie de leur minéralisation en ammoniaque et en nitrites. Par contre, la production de nitrates ne peut être mise en évidence car les concentrations dans l'estuaire sont essentiellement régies par le phénomène de dilution dans les eaux marines des très fortes teneurs en nitrates présentes dans les eaux fluviales. Cette minéralisation de la matière organique dans l'estuaire peut être due à une accélération estivale de l'activité bactérienne, du fait des températures plus élevées, et à une augmentation du temps de séjour des eaux dans l'estuaire, due aux plus faibles débits.

Par ailleurs, les mesures d'azote organique particulaire montrent qu'il existe, dans l'estuaire, un stock de matières organiques particulaires dont l'importance est liée à la masse du bouchon vaseux; en effet, les concentrations en azote organique particulaire dans l'eau augmentent avec les concentrations en matières en suspension (Fig. 8a). Le calcul des pourcentages d'azote organique particulaire dans les matières en suspension et le report de ces pourcentages en fonction des concentrations en matières en suspension montrent que la charge en azote organique des particules décroît rapidement lorsque la turbidité augmente (Fig. 8b); ceci est lié au fait que, lors des remises en suspension au sein du bouchon vaseux, il y a une augmentation de la granulométrie des particules, notamment au niveau du fond (Dupont et David 1980, données non publiées) et que ces particules plus grossières sont très probablement moins riches en matières organiques.

Le calcul du pourcentage moyen d'azote organique particulaire dans les matières en suspension du bouchon vaseux (0,53 %) permet d'estimer le stock d'azote organique particulaire contenu dans l'estuaire en considérant que le bouchon vaseux a une masse maximale de 200 000 t en vive eau d'étiage. Ce stock maximum serait de 1 070 t, soit de l'ordre de 2 % des apports annuels fluviaux d'azote sous forme minérale dissoute, et de l'ordre de 11 % des apports annuels d'azote organique particulaire.

Discussion

L'étude des variations des apports en sels nutritifs, en fonction des débits de la Seine, a montré que les flux de silicates et d'azote croissent régulièrement avec le débit, alors que les flux de phosphates tendent à être plus stables; il est donc fort probable que le lessivage du bassin versant et des terres agricoles joue un rôle important dans l'apport de ces deux premiers sels, alors que, dans le cas des phosphates, les rejets plus constants, d'origines urbaine et industrielle, sont la principale source.

Le calcul des apports moyens en azote et en phosphore minéral dissous permet de comparer les apports dans l'estuaire de la Seine à ceux qui ont lieu dans quelques grands estuaires européens ou nord-américains, et qui possèdent un bassin versant fortement industrialisé et urbanisé (Tableau 2).

Seul, parmi les estuaires recensés, le Rhin présente des apports supérieurs à ceux de la Seine; il faut, cependant, rappeler que la population vivant sur le bassin versant du Rhin est de l'ordre de 55 millions d'habitants, alors que celle occupant le bassin de la Seine est de 15 millions d'habitants.

L'étude des concentrations en sels nutritifs, lors du mélange estuarien des eaux douces et des eaux marines, montre qu'il existe, dans la plupart des cas, des phénomènes de dilution de type conservatif; seules peuvent être mises en évidence une production limitée de silicates (en période de crue, au niveau du fond), et une production d'azote ammoniacal et nitreux (en période estivale) due au processus de minéralisation de l'azote organique; les matières en suspension doivent constituer, ici, un excellent support pour les bactéries capables de dégrader la matière organique. Par contre, la minéralisation éventuelle du phosphore organique particulaire (non mesurée dans cette étude) n'apparaît pas, au vu des diagrammes de dilution des phosphates, comme une source significative de phosphates dissous dans l'estuaire, car les concentrations de ce dernier sel sont dominées par le simple phénomène de dilution dans l'eau de mer des très fortes concentrations rencontrées dans l'eau fluviale; de plus, il faut remarquer que les teneurs en matières organiques du bouchon vaseux dans l'estuaire de la Seine sont relativement faibles puisque Boust (1981) a déterminé que les concentrations moyennes en carbone organique particulaire des matières en suspension varient de 3 à 5,7 %. Les quantités d'éléments nutritifs stockés sous forme particulaire dans le

bouchon vaseux apparaissent comme faibles, non seulement vis-à-vis des apports fluviaux sous forme particulaire mais, surtout, en comparaison des apports de la Seine sous forme dissoute.

Enfin, le comportement essentiellement conservatif des sels nutritifs dans l'estuaire de la Seine, même en période estivale, laisse supposer que les processus de consommation de ces sels par le phytoplancton sont limités; cette hypothèse se trouve confirmée par les mesures de production primaire qui ont été réalisées dans l'estuaire de la Seine par Romaña (1981), et qui ont montré l'existence d'une production minimale au niveau du bouchon vaseux; ce même auteur a aussi mis en évidence le fait que, lorsque la charge en matières en suspension croît dans l'estuaire, le pourcentage de chlorophylle active décroît.

La production primaire phytoplanctonique et la consommation des sels nutritifs dans l'estuaire de la Seine sont très probablement limitées par les turbidités élevées, qui gênent la pénétration de la lumière, et par le temps de renouvellement assez court des eaux douces dans l'estuaire : Avoine (1981) évalue ce temps à 2 ou 3 jours en crue, et de 10 à 20 jours en étiage.

L'estuaire de la Seine est donc caractérisé par des apports importants en sels nutritifs, mais la consommation de ces sels est faible dans l'estuaire; elle se fait pour la plus grande part à l'extérieur de l'estuaire, et plus particulièrement dans la partie orientale de la baie de Seine.

Remerciements

Je désire remercier M. Yves Monbet pour son aide dans la réalisation de ce travail, ainsi que les laboratoires d'analyses municipaux de Rouen, du Havre et de Caen, qui ont effectué les nombreuses analyses dans le cadre de S.A.U.M. Par ailleurs, ce travail a été rendu possible grâce à la participation de l'Agence Financière de Bassin Seine-Normandie et de M. Lesouef en particulier (Convention CNEXO/COB/AFBSN n° 97 9046).

AFNOR. 1972. Détermination des matières en suspension. Norme T 90-105. *In* Dir. de la Prév. des Poll. et des Nuis. [ed.] Analyse de l'eau. Méthodes et instructions. Environnement, Paris.

AVOINE, J. 1981. L'estuaire de la Seine. Sédiments et dynamique sédimentaire. Thèse, Université de Caen, France. 236 p.

AVOINE, J., G. P. ALLEN, M. NICHOLS, J. C. SALOMON ET C. LARSONNEUR. 1981. Suspended sediment transport in the Seine Estuary, France: effects of man-made modifications on estuary-shelf sedimentology. Mar. Geol. 40: 119 – 137.

BOUST, D. 1981. Les métaux-traces dans l'estuaire de la Seine et ses abords. Thèse, Université de Caen, France. 237 p.

BUTLER, E. I. ET S. TIBBITTS. 1972. Chemical survey of the Tamar Estuary. I. Properties of the waters. J. Mar. Biol. Assoc. U.K. 52: 681 – 699.

C.O.B. 1979. Les éléments nutritifs en baie de Seine, p. 187 – 193. *In* Rapport Scientifique. Centre National pour l'Exploitation des Océans. Paris.

DART, M. C. ET D. SHELDON. 1980. Management of the Thames Estuary. Report for NATO/CCMS. 62 p. Thames Water. Directorate of Scientific Services. London.

DE JONGE, V. N. ET H. POSTMA. 1974. Phosphorus compounds in the Dutch Wadden Sea. Neth. J. Sea Res. 8: 139 – 153.

EDZWALD, J. K., D. C. TOENSING ET M. C. Y. LEUNG. 1976. Phosphate adsorption reactions with clay mineral. Environ. Sci. Technol. 10: 485 – 490.

JAWORSKY, N. A., D. W. LEAR ET O. VILLA. 1972. Nutrient management in the Potomac Estuary, p. 246 – 273. *In* G. E. Likens [ed.] Nutrient and Eutrophication: the Limiting Nutrient Controversy. Special symp., Vol. 1. Allen Press. Lawrence, KS.

KOROLEFF, F. 1969. Direct determination of ammonia in natural waters as indophenol blue. ICES Interlab. Report 3: 19 – 22.

1976. Determination of nutrients, p. 118 – 181. *In* K. Grasshof [ed.] Methods of seawater analysis. Verlag Chemie, New York, NY.

LASSUS, P., P. MAGGI ET C. BESSINETON. 1980. Les phénomènes d'eaux colorées de la baie de Seine en 1978. Science et Pêche, Bull. Inst. Pêches marit. 298: 1 – 28.

MALONE, T. C., P. J. NEALE ET D. BOARDMAN. 1980. Influences of estuarine circulation on the distribution and biomass of phytoplankton size fraction, p. 249 – 262. *In* V. Kennedy [ed.] Estuarine Perspectives. Academic Press, New York, NY.

POMEROY, L. R., E. E. SMITH ET C. M. GRANT. 1965. The exchange of phosphate between estuarine water and sediments. Limnol. Oceanogr. 10: 167 – 172.

R.N.O. 1978. Synthèse des observations 1975, 1976 et 1977. Bull. trimestriel n° 9. CNEXO/COB, Ministère de l'Environnement et du Cadre de Vie, Paris. 195 p.

ROMAÑA, L. A. 1981. Rôle du bouchon vaseux dans un écosystème estuarien, p. 121 – 138. *In* E.D.F. [ed.] 2e Journée de la Thermoécologie. Influence des rejets thermiques sur le milieu vivant en mer et en estuaire. I.S.T.P.M. Nantes. 1979.

SERVICE DE LA NAVIGATION DE LA SEINE. 4e Section. 1964 à 1980. Reconnaissances hydrologiques. Port Autonome de Rouen. France.

STEFANSSON, H. ET F. A. RICHARDS. 1963. Processes contributing to the nutrient distributions of the Columbia River and Strait of Juan de Fuca. Limnol. Oceanogr. 8: 394 – 410.

STRICKLAND, J. D. H. ET T. R. PARSONS. 1972. A practical handbook of sea water analysis. Fish. Res. Board Can. Bulletin 167: 310 p.

TAFT, J. L. ET W. R. TAYLOR. 1976. Phosphorus distribution in the Chesapeake Bay. Chesapeake Sci. 17: 67 – 73.

VAN BENNEKOM, A. J., E. KRIJGSMAN-VAN HARTINGSVELD, G. C. M. VAN DER VEER ET H. F. J. VAN VOORST. 1974. The seasonal cycles of reactive silicate and suspended diatoms in the Dutch Wadden Sea. Neth. J. Sea Res. 8: 174 – 207.

WOLLAST, R. 1976. Transport et accumulation de polluants dans l'estuaire de l'Escaut. 191 – 218. *In* C. J. Nihoul et R. Wollast [ed.] L'estuaire de l'Escaut. Vol. 10. Projet Mer. Rapport Final. Bruxelles.

Behavior of Nitrogen Nutrients and Dissolved Silica in the Ems–Dollard Estuary[1]

W. HELDER, R. T. P. DE VRIES, AND M. M. RUTGERS VAN DER LOEFF

Netherlands Institute for Sea Research, P.O. Box 59, Texel, The Netherlands

HELDER, W., R. T. P. DE VRIES, AND M. M. RUTGERS VAN DER LOEFF. 1983. Behavior of nitrogen nutrients and silica in the Ems–Dollard Estuary. Can. J. Fish. Aquat. Sci. 40(Suppl. 1): 188–200.

Using natural fluorescence and salinity as tracers to distinguish between two freshwater inputs (River Ems, 125 $m^3 \cdot s^{-1}$; and River WWA, 12.5 $m^3 \cdot s^{-1}$) in the Ems–Dollard Estuary, deviations from conservative behavior for nutrients (ammonia, nitrite, nitrate, and silicate) were calculated. With the aid of time scales, derived from a one-dimensional mixing and flushing model, rates of net nitrification (2.5 $mmol \cdot m^{-2} \cdot d^{-1}$), net denitrification (2.0 $mmol \cdot m^{-2} \cdot d^{-1}$), and silica dissolution (2.3 $mmol \cdot m^{-2} \cdot d^{-1}$) were estimated. The observed production of dissolved silica during estuarine mixing has not been reported in most studies on other estuaries.

Key words: estuaries, denitrification, nitrification, silica-dissolution, mixing and flushing model, natural fluorescence, Wadden Sea, Ems–Dollard Estuary

HELDER, W., R. T. P. DE VRIES, AND M. M. RUTGERS VAN DER LOEFF. 1983. Behavior of nitrogen nutrients and silica in the Ems–Dollard Estuary. Can. J. Fish. Aquat. Sci. 40(Suppl. 1): 188–200.

À l'aide de la fluorescence naturelle et de la salinité comme marqueurs, il a été possible de séparer deux arrivées d'eau douce (rivière Ems, 125 $m^3 \cdot s^{-1}$; rivière WWA, 12,5 $m^3 \cdot s^{-1}$) dans l'estuaire Ems–Dollard et de calculer les déviations par rapport à un comportement conservateur des nutriments (ammoniac, nitrites, nitrates et silicates). Grâce à des échelles chronologiques dérivées d'un modèle unidimensionnel de mélange et de vidange, on a pu estimer les taux de nitrification nette (2,5 $mmol \cdot m^{-2} \cdot jour^{-1}$), de dénitrification nette (2,0 $mmol \cdot m^{-2} \cdot jour^{-1}$) et de dissolution de la silice (2,3 $mmol \cdot m^{-2} \cdot jour^{-1}$). La plupart des études d'autres estuaires ne mentionnent pas la production de silice dissoute lors du mélange estuarien.

Received October 14, 1981
Accepted August 17, 1982

Reçu le 14 october 1981
Accepté le 17 août 1982

THE exchange of dissolved constituents between sediments and overlying water has been the subject of much research and many reviews (e.g. Lerman 1978). To estimate nutrient release rates from the sediment, bell-jars are widely used (Pamatmat 1968; Rowe et al. 1975; Propp et al. 1980) and have been used in the Ems–Dollard Estuary (Rutgers van der Loeff et al. 1981).

The aim of this study is to compare the results from the earlier bell-jar experiments with estimates of these fluxes from a hydrographical approach in which parts of the Ems–Dollard Estuary are considered as "open bell-jars." In this approach, deviations from conservative mixing behavior of the nutrients in the overlying water are estimated, and by combination with residence time scales derived from a one-dimensional mixing and flushing model of the estuarine water, it becomes possible to calculate nutrient production or consumption rates.

The deviation of conservative behavior of a dissolved constituent is usually estimated by comparing its behavior with a conservative indicator of mixing between seawater and freshwater (e.g. Burton and Liss 1976). To be useful as such an indicator or tracer, any dissolved constituent has to obey three basic rules. Firstly, the difference in tracer concentrations between the sources must be large enough to allow an accurate determination of the relative contributions. Secondly, the tracer must behave conservatively, i.e. breakdown or formation of the tracer must be slow with respect to the residence time of freshwater parcels in the study area. Thirdly, the time-dependent variation of the source concentrations of the tracer must be slow compared to the residence time of freshwater.

Salinity is the most commonly used tracer. By plotting the dissolved constituent of interest against the salinity, deviations from conservative behavior can be detected. In the mixing plots, the source concentrations of the constituents

[1]This paper forms part of the Proceedings of the Dynamics of Turbid Coastal Environments Symposium convened at the Bedford Institute of Oceanography, Dartmouth, N.S., Canada, September 29–October 1, 1981.

Printed in Canada (J6675)
Imprimé au Canada (J6675)

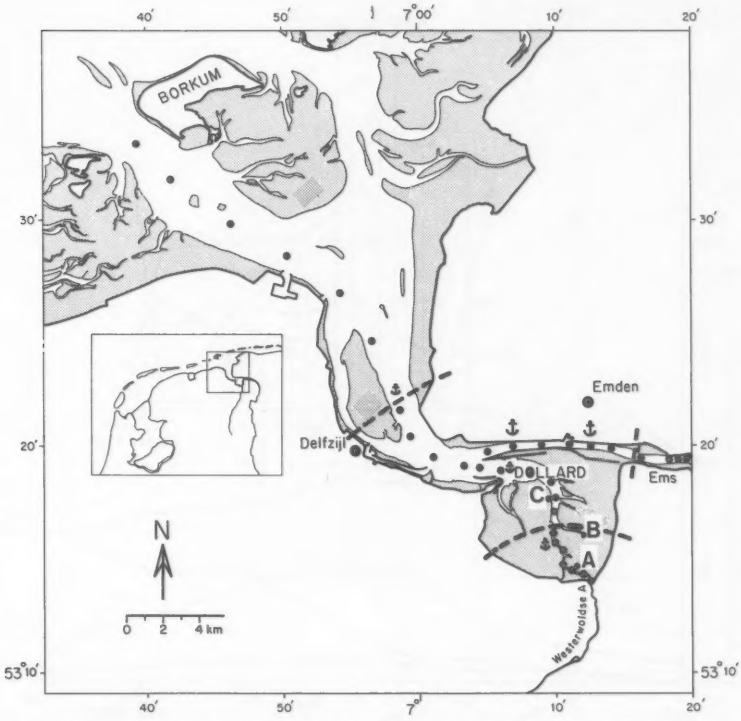

FIG. 1. Ems–Dollard Estuary with locations of stations and of cores A, B, and C. --- Partition between "Southern part Dollard" (0–15‰), "Northern part Dollard and adjacent Ems-Estuary" (15–25‰) and outer estuary. ● Sample station; A, B, C core locations; ⚓ Anchor station.

play an important role. Temporal changes of the source concentrations, relevant with respect to the residence time of the water parcels in the study area, may easily result in misinterpretation of the mixing plots (Boyle et al. 1974; Loder and Reichard 1981). When there is more than one source of freshwater, a second tracer is needed to discriminate between them.

Natural fluorescence (caused by polyphenolic compounds) has been used successfully to discriminate between different river inputs in coastal waters (Otto 1967; Zimmerman and Rommets 1974; Laane 1981; Willey and Atkinson 1982). To study the behavior of inorganic nitrogen nutrients and dissolved silica in the Ems–Dollard Estuary, we used salinity and natural fluorescence as conservative tracers. With the aid of these tracers we are able to calculate relative contributions of water from the sea, the River Ems, and the River WWA at our sampling stations and, together with their source concentrations, calculate the deviations from conservative behavior for these nutrients.

Apart from calculation of residence times, the mixing and flushing model is used to make independent calculations of the water composition in terms of volume percentages of sea-, Ems-, and WWA-water in the estuary. In doing so, it is possible to compare the water composition as calculated from the mixing plots, based on the use of fluorescence and salinity as tracers, with the calculation of the same water composition using the mixing and flushing model, based only on longitudinal salinity distribution and freshwater discharges.

A review of one-dimensional mixing and flushing models is given by Officer (1976), while definitions of residence time and other time-scales are given by Bolin and Rohde (1973) and discussed by Zimmerman (1976).

In an estuary like the Ems–Dollard that is dominated by tidal flats, the behavior of dissolved constituents in the water column cannot be understood without considering interactions with the underlying sediments. For this reason, concentrations of nitrogen compounds and dissolved silica were also measured in the porewaters of the sediments. Nitrifying bacteria were enumerated both in the water and in the sediment.

Hydrography

The Ems–Dollard Estuary is situated between the Dutch and German parts of the Wadden Sea (Fig. 1) and, like the

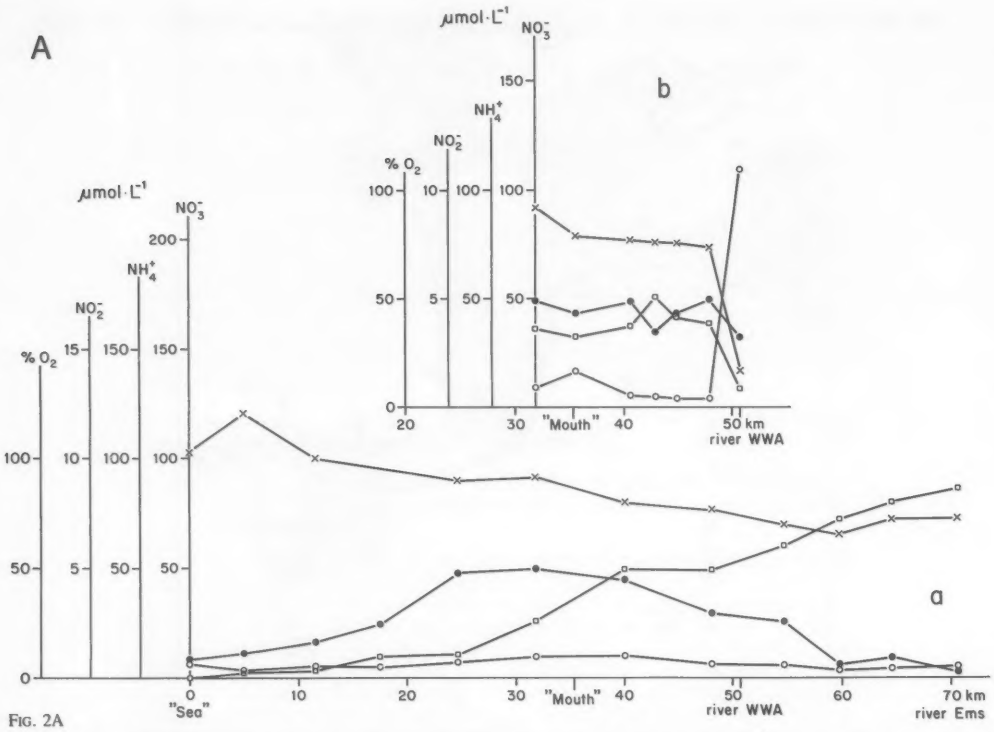

FIG. 2A

Wadden Sea as a whole, is characterized by having extensive tidal flats. The flats comprise 40–50% of the area of the total estuary and 80% in the case of the Dollard. The tidal volume of the whole estuary is about 1100×10^6 m^3 of which 100×10^6 m^3 is contained in the Dollard. Mean tidal amplitude is about 2.5–3 m and the tide is semidiurnal. The hydrographical characteristics have been described by Dorrestein (1960) and Dorrestein and Otto (1970). From these studies it can be concluded that the estuary has no permanent stratification and can be considered as well-mixed. Main freshwater inputs are the River Ems that discharges about 4×10^9 m$^3 \cdot$a^{-1} (125 m$^3 \cdot$s^{-1}) and the Westerwoldse A (WWA), a canalized river in the southeast corner of the Dollard, which has a discharge rate of 0.4×10^9 m$^3 \cdot$a^{-1} (12.5 m$^3 \cdot$s^{-1}). Exchange between water at the mouth of the Ems and in the Dollard is restricted by an artificial dam (Fig. 1).

The first attempt to determine the mixing and flushing of water types present in the estuary was made by Dorrestein and Otto (1960), who developed a one-dimensional mixing and flushing model. However, they omitted any freshwater inflow from the WWA into the Dollard and consequently their model cannot be used to predict transport processes in this region. Moreover, their model was based on only four surveys and they did not collect data in the Dollard. Using the same assumptions and computations, we have developed a more accurate and sophisticated model using salinity data collected on 12 surveys in 1970–72.

Chemical Composition of Freshwater

The chemical composition of Ems water is significantly different from that of the WWA. In the River Ems, oxygen saturation shows an annual variation of 60–100%. Dissolved inorganic nitrogen is mainly present as nitrate and shows an annual variation in concentration from 320 µmol$\cdot$L^{-1} in early spring to 70 µmol$\cdot$L^{-1} in summer. In contrast, the WWA is a heavily polluted river that brings 33×10^6 kg$\cdot$a^{-1} of organic carbon into the Dollard (van Es 1977; de Wolf 1978). Consequently, nitrate and oxygen are absent throughout the year. Approximately 75% of the nitrogen in the WWA is composed of ammonia and the remaining 25% is in dissolved and particulate organic forms. The concentration of ammonia in the WWA is 60–150 µmol$\cdot$L^{-1} in summer but increases to over 5500 µmol$\cdot$L^{-1} from October to December when the river is loaded with potato mill wastewater (Fig. 2). The distribution of suspended matter in the Ems–Dollard Estuary is dominated by a strongly developed turbidity maximum (Fig. 3). The suspended matter is mainly of marine origin (van Straaten 1960) and both inorganic and organic matter appear to originate from the North Sea (Postma 1961, 1967).

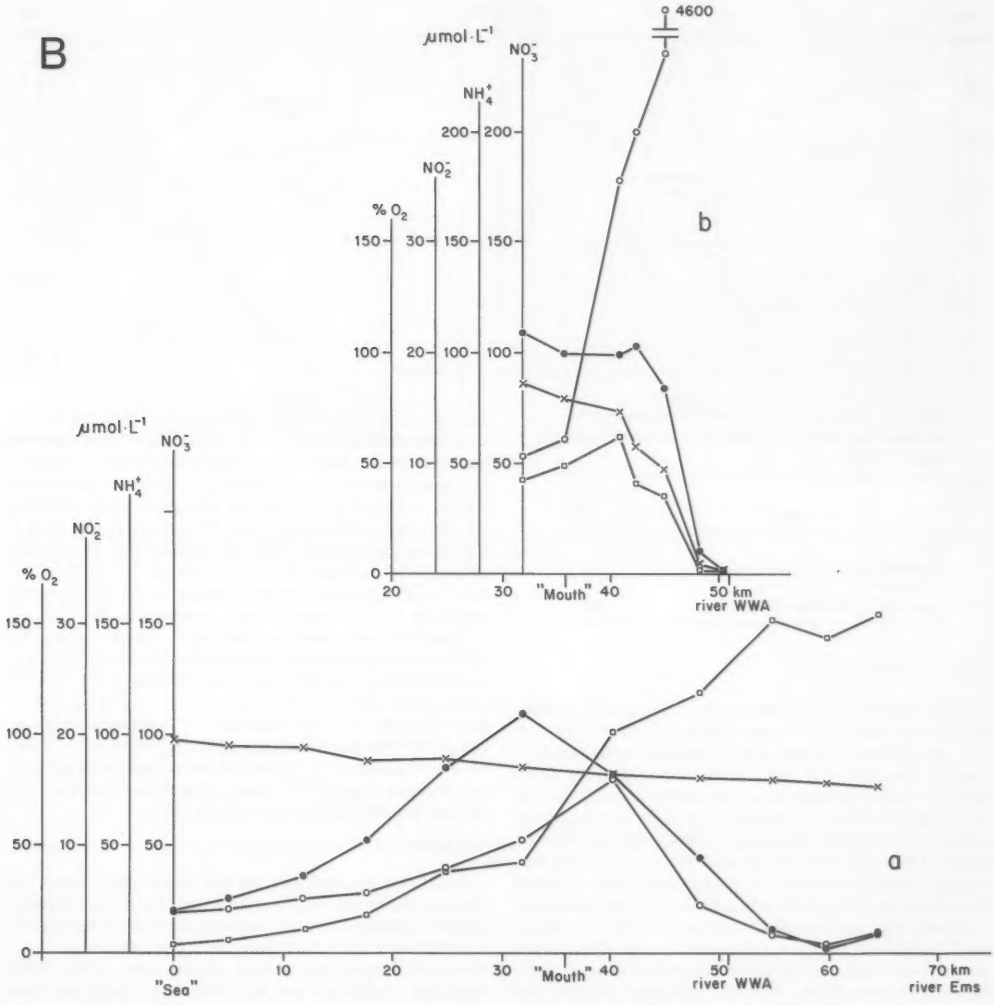

FIG. 2. Distribution of NH_4^+ (○), NO_2^- (●), NO_3^- (□), O_2 (×) in (A) November and (B) July. (a) Ems Estuary; (b) Dollard.

Methods

SURVEYS

In the period 1970–72, monthly surveys were conducted covering the estuary from the island of Borkum to Leer on the River Ems and including the main Dollard channel from its mouth to the freshwater input (Fig. 1). Subsurface water samples (1–2 m depth) were taken at about 30 stations (Fig. 1) for the analyses of salinity, oxygen, fluorescence, nitrate, nitrite, ammonia, and silicate.

From 1973 to 1978, field work was carried out over periods of 14 d in summer and winter. During these periods, observations were made at anchor stations (Fig. 1). Sediments were collected and chemical analyses of the porewater were conducted. Most probable number counts (MPN) of nitrifying bacteria were also made. These field excursions always started and finished with an overall survey in the area to permit detection of any changes in source concentrations which might have occurred during the working period.

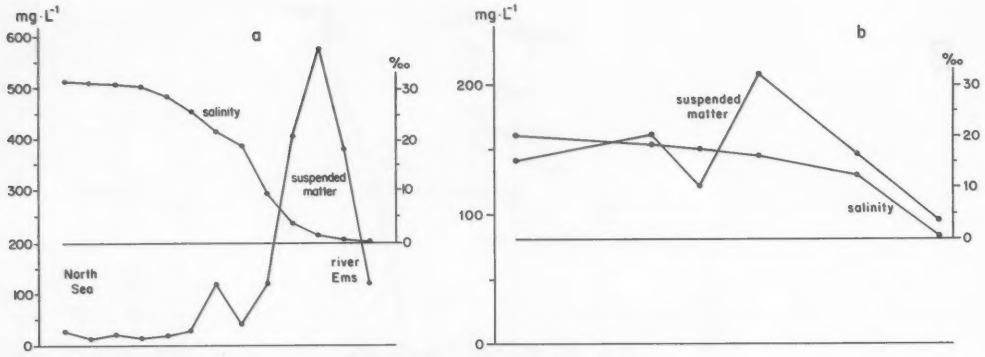

FIG. 3. Distribution of suspended matter and salinity. (a) Ems Estuary; (b) Dollard.

TABLE 1. Residence time of water in different parts of the Ems–Dollard Estuary (calculated from mixing and flushing model).

Part of estuary	Residence time (days)
Entire	38
Ems and lower half of Dollard (15–25‰)	14.2
Upper half of Dollard (0–15‰)	4.8

CHEMICAL AND PHYSICAL

Water samples for the determination of nutrient concentrations were taken with Nansen bottles and filtered through 0.45 μm cellulose–acetate filters. Samples were stored in carefully cleaned (acid and distilled water washed) polyethylene flasks, stored frozen, and usually analyzed within 2 wk after collection. Originally, nutrient analyses were carried out manually according to Strickland and Parsons (1968). From 1973 onwards an auto-analyzer was used employing standard methods. A phenol-hypochlorite method (Helder and de Vries 1979) was used to determine ammonia.

Salinity was measured either with an "Autolab" or "Guildline" inductively coupled salinometer using Copenhagen standard seawater for calibration. Dissolved oxygen determination followed the Winkler technique (Carrit and Carpenter 1966). Fuorescence was measured at room temperature on a Turner-III fluorometer equipped with a primary filter 7-60 (maximum transmission 358 nm) and a secondary filter combination of a Wratten 48 and a 2A filter (maximum transmission 457 nm) (Duursma and Rommets 1961).

Sediment cores (5 cm diameter) were collected by hand on the tidal flats just before emersion. Squeezing of cores was done immediately afterwards at approximately in situ temperature in a Reeburgh type squeezer, under N_2 pressure (Reeburgh 1967). Samples were stored frozen until analyses in the laboratory about 1 wk later. Position of the core stations is indicated in Fig. 1. Core A was taken in the immediate neighbourhood of the WWA input into the Dollard, an environment that is devoid of dissolved oxygen throughout the year. Organic carbon in the sediment is > 40 mg·g^{-1} (dry sediment) (Schröder and van Es 1980). Core B was taken in a tributary of the main Dollard tidal channel (Fig. 1). Organic carbon content was about 20 mg·g^{-1}. The overlying water had an averaged yearly oxygen saturation value of about 20–40% and a salinity of about 15‰. Core C was from a location in the northern part of the Dollard (Fig. 1). Organic carbon in this sediment was about 5–10 mg·g^{-1}. In the overlying water dissolved oxygen reaches values of 40–80% saturation and the averaged yearly salinity was 20–25‰.

Counts of viable nitrifying bacteria (ammonia- as well as nitrite-oxidizing bacteria) in water and sediment samples were made according to an MPN procedure (Rodina 1972). Salinity of the media used was 20‰ and dilutions of 1 to 10^{-5} were used. The tubes were incubated at 20°C and tested for nitrite and nitrate with paper indicator strips (Merckoquant). About 60 d were necessary to permit definite separation of positive and negative tubes. MPN counts of nitrifying bacteria were derived from the tabulation of Brock (1974).

MODELING AND CALCULATIONS

A detailed description of our one-dimensional mixing and flushing model will be given elsewhere (Helder and Ruardij, unpublished data). Briefly, exchange coefficients between 17 compartments, each 5 km long, were calculated from quasi-stationary longitudinal salinity distributions. Using these exchange coefficients and the freshwater discharges from both rivers, it was possible to calculate the average volumes of sea-, Ems-, and WWA-water in the estuary. Residence time in a compartment is defined as the time a parcel of water or dissolved constituent needs to pass through that compartment. Calculation for the different parts of the estuary followed the procedure of Zimmerman (1976).

The calculation of volume percentages of sea-, Ems-, and WWA-water at field stations during particular surveys, using salinity and fluorescence as tracers, was carried out according to Zimmerman and Rommets (1974). With these volumes and source concentrations of the nutrients in sea-, Ems-, and WWA-water, the conservative mixing concentrations at sample stations were calculated. By comparing with the measured field concentrations, deviations from conservative behaviour

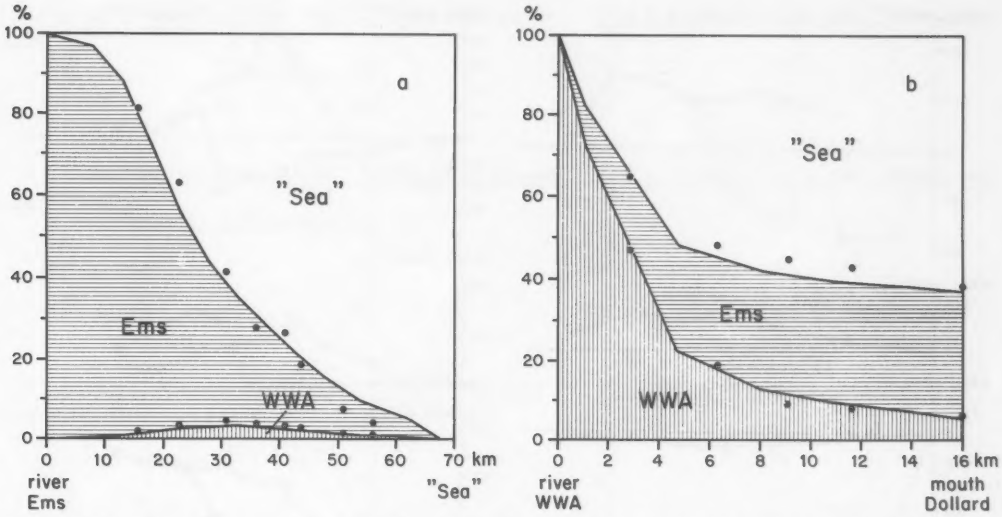

FIG. 4. Quasi-stationary water composition as calculated from one-dimensional mixing- and flushing model, and salinity–fluorescence diagrams. (a) Ems Estuary; (b) Dollard. Lines: model results, ●: results from S–mFl graphs.

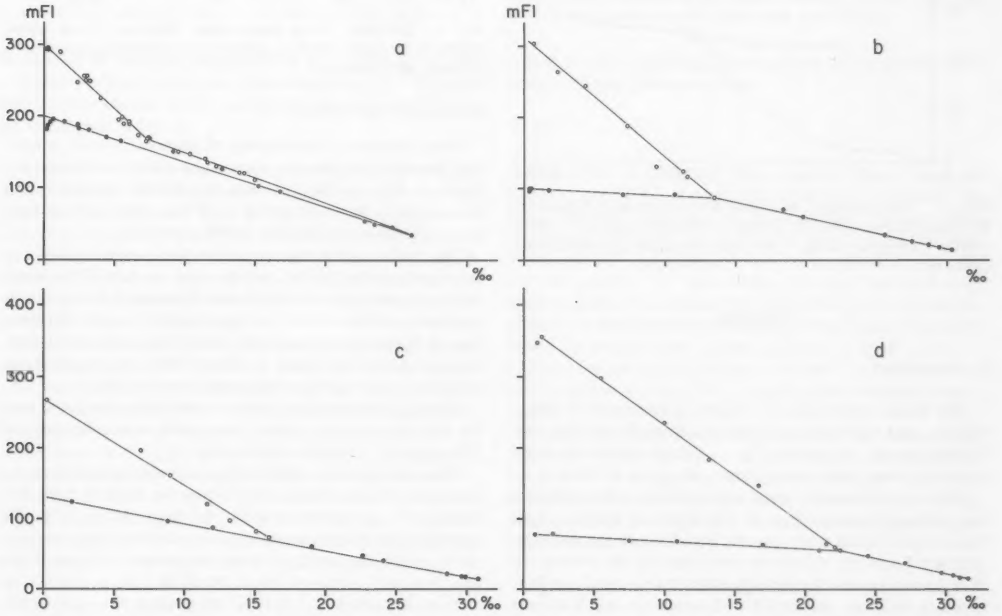

FIG. 5. Distribution of fluorescence (mFl) as a function of salinity (‰). (● Ems Estuary, ○ Dollard; (a) January, (b) April, (c) August, (d) October.)

were calculated (Δ values). Combination of these Δ values with the residence time of water in a particular area of the estuary makes it then possible to calculate nutrient production or consumption rates.

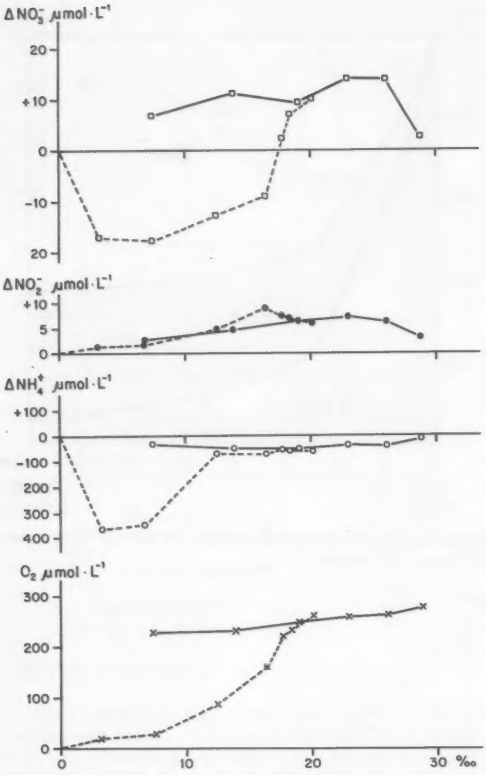

FIG. 6. Yearly averaged deviations from conservative behavior in the Ems Estuary (—) and the Dollard (---) for nitrate (ΔNO_3^-), nitrite (ΔNO_2^-), ammonia (ΔNH_4^+) and yearly averaged O_2 concentrations ($\mu mol \cdot L^{-1}$).

Results

HYDROGRAPHY

The water composition in volume percentages of Ems-, WWA-, and seawater as calculated from the mixing and flushing model, is given in Fig. 4. The most relevant timescales for some parts of the estuary are given in Table 1.

Plots of fluorescence versus salinity show a linear relationship during all seasons (Fig. 5). The inflow of relatively high fluorescent Dollard water into the Ems Estuary can easily be detected. From Fig. 4 it can be concluded that the volumes of WWA water outside the Dollard are relatively small and their accuracy becomes questionable. Zimmerman and Rommets (1974) estimated the accuracy of the method in their study of Dutch coastal water to be 1% volume fraction. For this reason, the calculations were only applied to that part of the Dollard and the adjacent Ems Estuary where the volume of WWA water is > 2%.

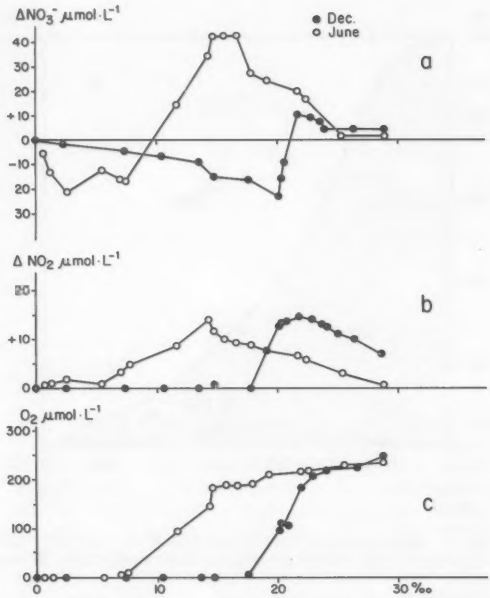

FIG. 7. Deviations from conservative behavior of (a) nitrate (ΔNO_3^-), (b) nitrite (ΔNO_2^-), and (c) O_2-concentrations ($\mu mol \cdot L^{-1}$) (○ June, ● December.)

NITROGEN COMPONENTS

Water column — Distributions of ammonia, nitrite, nitrate, and dissolved oxygen in summer and winter conditions are given in Fig. 2. The ammonia distribution in winter was dominated by the small inflow of WWA-water with its very high ammonia concentration (4600 $\mu mol \cdot L^{-1}$).

The nitrite distribution showed highest concentrations in the mouth of the Dollard and the adjacent part of the Ems. Obviously nitrite concentration was determined also by in situ processes and not only by mixing of source waters. The maxima of nitrite in summer and winter were associated with oxygen saturation values of about 90% and therefore an oxidative origin of the nitrite maximum was likely.

Nitrate distributions in summer and winter are dominated by the River Ems, where maximum concentrations of 320 $\mu mol \cdot L^{-1}$ occur in winter (Fig. 2).

There are only few nutrient data available from the past to compare with our observations. From the work of Kühl and Mann (1954) it can be concluded that from 1954 to 1970–72 ammonia concentrations in the estuary did not change significantly, while the maximum nitrate concentrations in the River Ems in winter increased almost threefold. (113 $\mu mol \cdot L^{-1}$ in 1953 to 320 $\mu mol \cdot L^{-1}$ in 1972). In general, the same trends are visible for Rivers Rhine and IJssel (Helder 1974; van Bennekom et al. 1975).

Averaged over the year (surveys regularly distributed over the seasons), ammonia, nitrite, and nitrate did not behave conservatively in the estuary (Fig. 6). Because formation and

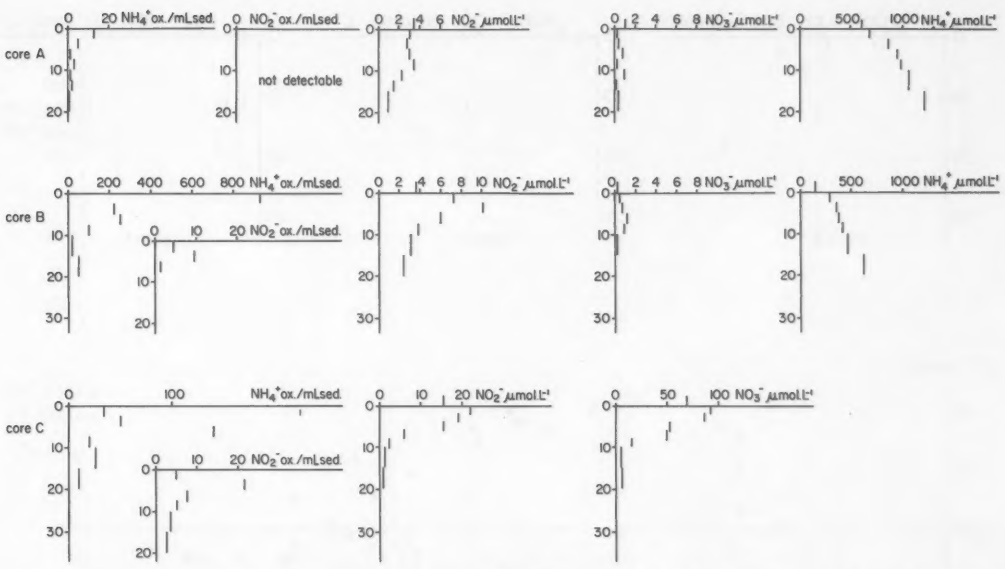

FIG. 8. Porewater concentrations of NO_2^-, NO_3^-, NH_4^+ (µmol·L^{-1}) and ammonia oxidizing and nitrite oxidizing bacteria (MPN/ml sediment) as a function of depth in the sediment (cm) for core A, B, and C. Vertical bars represent depth interval of sample.

breakdown of nitrogen compounds is dependent on oxygen availability, dissolved oxygen concentrations are also given in Fig. 6. Summer and winter conditions for nitrite and nitrate are contrasted in Fig. 7.

Sediments — Porewater concentrations of ammonia, nitrite, nitrate, and abundance of nitrifying bacteria are plotted against sediment depth in Fig. 8. Core A is from an area (Fig. 1) that is devoid of dissolved oxygen throughout the year. Ammonia concentrations increased with depth and were high, even compared to the concentration in the overlying water. Nitrate and nitrite concentrations in the porewater of core A were low.

Core B is from an area (Fig. 1) where the average yearly oxygen saturation was 20–40%. As in core A, ammonia concentration increased with depth, but the concentrations were low compared to core A. The porewater concentrations of nitrate were low as well. The nitrite concentration showed a maximum at 2–4 cm depth. The numbers of especially ammonia, and nitrite oxidizing bacteria were considerable.

Core C is from an area (Fig. 1) with an average yearly oxygen saturation value of 40–80%. Porewater concentrations of nitrite as well as nitrate reached their highest values at 0–2 cm sediment depth and were also high compared to the overlying water.

When comparing the results of core A, core B, and core C, it is obvious that, together with increasing oxygen availability from the overlying water, the number of ammonia oxidizing bacteria was increasing. At higher oxygen concentrations, the number of nitrite oxidizing bacteria was also increasing. In the water column, the number of ammonia-oxidizing bacteria was ≤ 5 cm^{-3}; nitrite-oxidizers were not detected in the overlying water by MPN-procedure.

SILICA

The inputs of dissolved silica into the estuary from the Ems and the WWA showed considerable variation over the year. Maxima were reached in December–January when the concentration in the Ems and WWA were 210 and 315 µmol·L^{-1}, respectively; minima occurred in June (30 and 80 µmol·L^{-1}). In addition to input by freshwater sources, there was a marked in situ production of silica in the estuary as demonstrated by higher concentration than predicted by conservative mixing behavior (Fig. 9). Concentrations in porewater at Stations A, B, and C were greater than in overlying water (Fig. 9), indicating that sediments were a source.

For the data of the northern part of the Dollard and adjacent Ems (15–25‰), the averaged Δ Si values are given as a function of the season (Fig. 10). All available data were used to construct Fig. 10, which essentially gives the same results as in an earlier published version based on less data (Rutgers van der Loeff et al. 1981).

Discussion

HYDROGRAPHY

The linear relationships between fluorescence and salinity that exist throughout the year in the Ems–Dollard Estuary (Fig. 5) suggest that fluorescence is behaving conservatively.

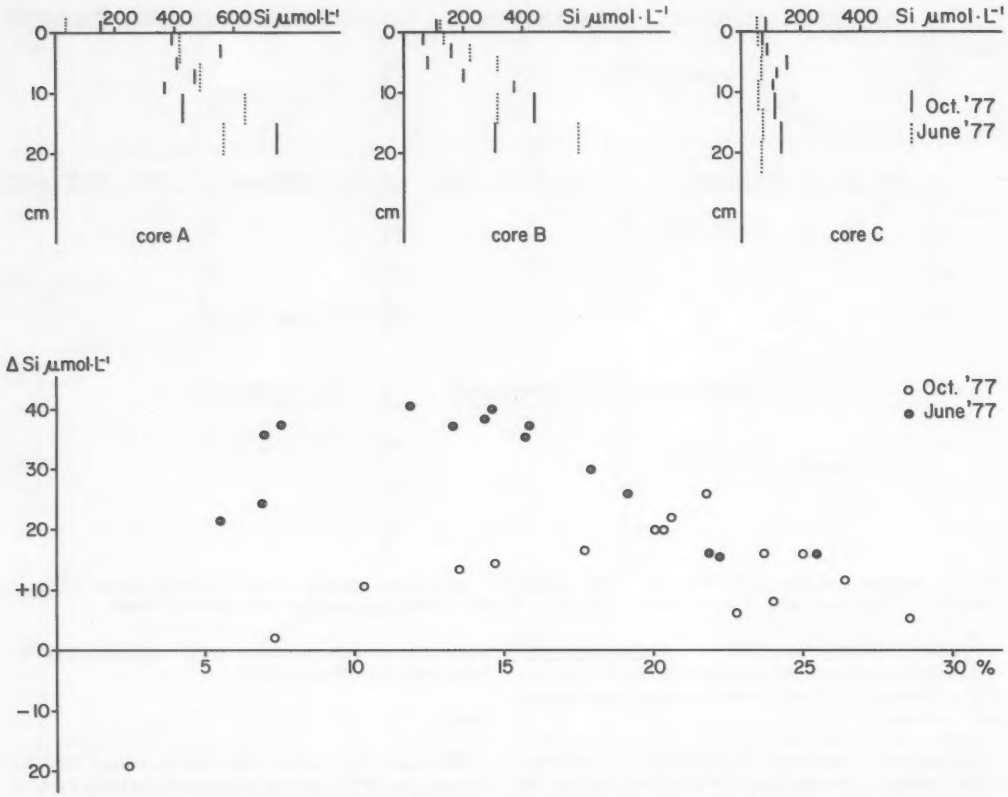

FIG. 9. Vertical distribution of Si ($\mu mol \cdot L^{-1}$) in sediment porewater and deviations from conservative behavior (ΔSi) for water column concentrations in the Dollard and adjacent Ems Estuary.

Laane (1981) has also observed conservative behavior of fluorescence in the Ems–Dollard Estuary plus the western Wadden Sea. In decomposition experiments, van Es and Laane (1982) could not detect changes in fluorescence of Ems–Dollard water over a 30-d incubation period at room temperature. Willey and Atkinson (1982) also reported conservative behavior of fluorescence in waters off the coasts of Georgia and North Carolina.

The average distributions of three water types present in the area, as calculated by using salinity and fluorescence as conservative mixing indicators, correspond well with the distribution as calculated from a one-dimensional mixing and flushing model based on quasi-stationary salinity distributions in the same period (1970–72) (Fig. 4). This correspondance also indicates that fluorescence is a suitable tracer.

NITRATE

Deviation from conservative behavior of nitrate concentration is the net result of nitrification, nitrate reduction, and assimilation by primary producers. The last process probably plays a minor role in the estuary because of the general preference of algae for ammonia (Eppley et al. 1969, 1970; McCarthy et al. 1975) and its abundance (Fig. 2) throughout the year. Nitrification and nitrate reduction are important processes in the estuary (Fig. 6, 7). In the southern part of the Dollard, where low oxygen saturation values occur, nitrate is probably used as electron acceptor in the absence of oxygen. Nitrate is nearly absent from the porewater in this area (Fig. 8).

In marine and estuarine ecosystems an important part of nitrogen recycling occurs in the benthic phase rather than in the water column (Billen 1978; Fenchel and Blackburn 1979) and therefore production and consumption rates of nutrients are often, as in bell-jar experiments, associated with the underlying sediment surface. Aided by residence time calculations from the mixing and flushing model, the rate of the nitrate reduction process was estimated at 2.0 mmol $N \cdot m^{-2} d^{-1}$ in the oxygen-poor part of the estuary (ranging from 1.0–6.1 mmol $N \cdot m^{-2} \cdot d^{-1}$). From the bell-jar

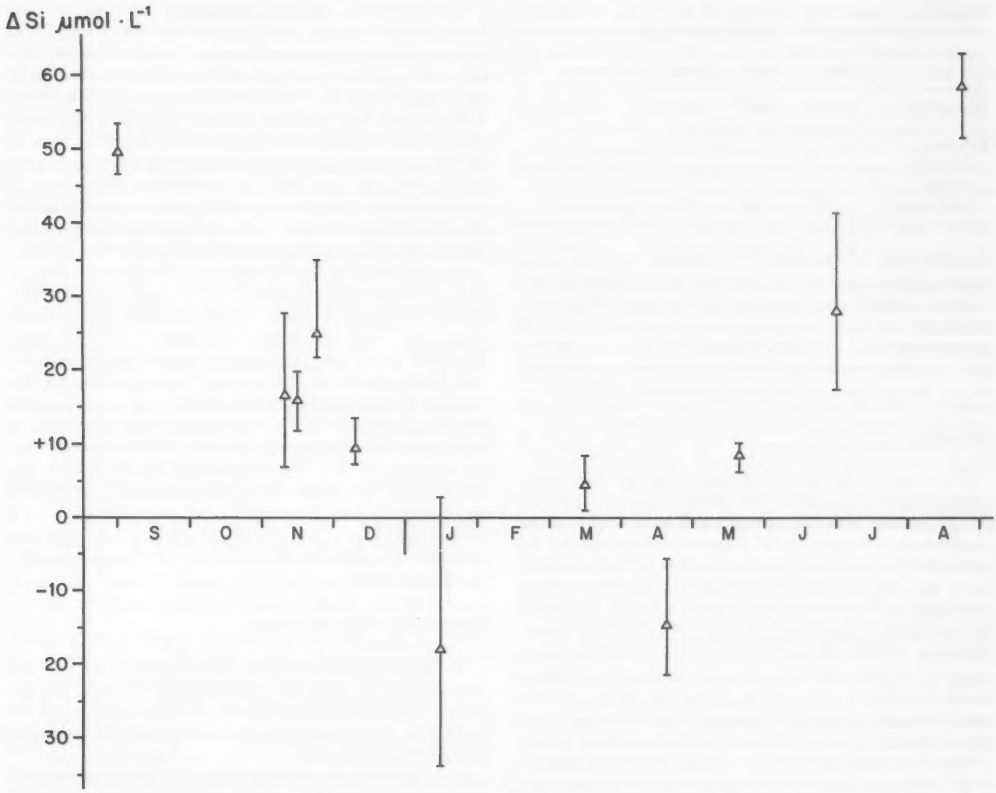

FIG. 10. Deviations from conservative behavior of Si (ΔSi) in Dollard and adjacent Ems Estuary (15–25‰ S versus time). Δ average of all data. Vertical bars represent range of data.

experiments (Rutgers van der Loeff et al. 1981), a maximum rate of 5 mmol·m^{-2}·d^{-1} was calculated. Values of 0.26–5.19 mmol N·m^{-2}·d^{-1} were calculated by Fenchel and Blackburn (1979) from the data of Vanderborght and Billen (1975) in the Sluice Dock of Ostend.

In the northern part of the Dollard and adjacent part of the Ems Estuary, nitrate concentrations were in excess of predictions based on conservative mixing behavior. The onset of net nitrification ($+\Delta NO_3^-$ values) along the axis of the estuary lies at dissolved oxygen concentrations of about 100 µmol $O_2 \cdot L^{-1}$ (Fig. 7). Using the residence time of water in the area and surplus nitrate values, net nitrification was estimated at 2.5 mmol N·m^{-2}·d^{-1} (ranging from 0.5–6.0 mmol N·m^{-2}·d^{-1}). Our rates are very similar to those given by Billen (1975 and 1978) who, by indirect nitrification activity measurements, found a rate of 1.6 mmol N·m^{-2}·d^{-1} in the seaward end of the Scheldt estuary, and to those of Tijssen et al. (1974) who, with budget calculations, found net nitrification rates of 1.4–2.1 mmol N·m^{-2}·d^{-1} in September and October in the Southern Bight of the North Sea. Henriksen et al. (1981) found rates of 0.3–1.4 mmol N·m^{-2}·d^{-1} in Danish coastal waters.

NITRITE

The in situ production of nitrite ($+\Delta NO_2^-$ values) occurred at those stations where dissolved oxygen was present in the overlying water (Fig. 6 and 7). Maximum surplus nitrite values were found at about 175 µmol $O_2 \cdot L^{-1}$. Probably the difference in oxygen sensitivity of the two nitrification steps was responsible for the high concentrations of nitrite in the porewater at stations B and C. Knowles et al. (1965) concluded that 62.5 µmol $O_2 \cdot L^{-1}$ is necessary for maximum rate of the oxidation of ammonia to nitrite, while 125 µmol·L^{-1} is needed for maximum oxidation of nitrite to nitrate. Van Bennekom et al. (1978) found that in the deep waters of the Zaire Canyon nitrite accumulated at oxygen concentrations of 35–70 µmol $O_2 \cdot L^{-1}$. The greater abundance of ammonia oxidizers compared to nitrite oxidizers, as found in Core B (Fig. 8), may have also contributed to the high nitrite

TABLE 2.

	NH_4^+	NO_2^-	NO_3^-	Dissolved Si ($mmol \cdot m^{-2} \cdot d^{-1}$)
This study	−5.0	+0.5	+1.2	+2.3
Bell-jars (Rutgers van der Loeff et al.)	−3.0	−0.3	−3.7	−2.2

concentrations in porewater. For oxidation of ammonia to nitrate, without accumulation of nitrite, this ratio of ammonia to nitrite oxidizers should be about 5 (Alexander 1965). Similar results of nitrite accumulation and anomalous ratio of ammonia oxidizers to nitrite oxidizers have been recorded by Landner and Larsson (1973) in the Swedish Bay of Köping which, like the Dollard, is nitrogen-enriched.

AMMONIA

There was a large loss of ammonia from the water, especially in the southern part of the Dollard (Fig. 6). With bell-jar experiments, Rutgers van der Loeff et al. (1981) found simultaneous consumption of ammonia and nitrate by the sediments in the Dollard. An explanation for the ammonia losses that may be valid for the observations in the bell-jar experiments as well as for those from this study, consists of the following elements (Rutgers van der Loeff et al. 1981). Nitrifying and denitrifying bacteria reach their highest abundance in the upper few centimetres of the sediment (Rutgers van der Loeff et al. 1981 in Fig. 5) and the activity of both kinds of bacteria might be separated in time as a response to diurnal (Revsbeck et al. 1980) or seasonal (Jørgensen 1977a) changes in the penetration depth of oxygen into the sediment. Nitrification and denitrification can also occur simultaneously (Wilson 1978). When ammonia is oxidized to nitrate or nitrite first and, after diffusion to a denitrifying micro-environment (Jørgensen 1977b) is reduced to gaseous N_2 or N_2O, ammonia is lost from the sediments and overlying waters without an apparent change in nitrite or nitrate concentration. This kind of mechanism has been described earlier for deepsea sediments by Barnes et al. (1975).

Postma (1966) and Helder (1974) have studied the behavior of nitrogen nutrients in the Dutch Wadden Sea, where small net increases of ammonia and nitrite were detected in water passing through. Losses of ammonia and/or nitrate, in contrast to the observations in the Dollard, did not occur in the Wadden Sea; obviously as a consequence of lower input of organic matter and higher oxygen concentrations.

DISSOLVED SILICA

In most estuaries, dissolved silica is reported to behave conservatively during the mixing of freshwater and seawater, but removal of dissolved silica from estuarine water has been also observed (Liss 1976). Our data show considerable reactivity with both removal and addition at different periods of the year (Fig. 10).

The observed seasonal periodicity of ΔSi in the Ems−Dollard Estuary, with maximum in situ production in August−September and small removal (−ΔSi values) in January and April, is in good agreement with the observations of van Bennekom et al. (1974) in the western part of the Dutch Wadden Sea. The observed seasonal periodicity with high surplus silica values in summer and low or negative values in winter and spring suggests that a temperature dependent process is going on. It is likely that temperature dependence of the equilibrium concentration as well as the dissolution rate of dissolved silicate in contact with clay minerals is responsible for the observed seasonal pattern (Fanning and Pilson 1971).

From the data of Fig. 10, and with the residence time of 14.2 d for the northern part of Dollard and adjacent Ems Estuary, a yearly averaged production rate of 2.3 mmol $Si \cdot m^{-2} \cdot d^{-1}$ was calculated. Maximum rates of about 9.2 mmol $Si \cdot m^{-2} \cdot d^{-1}$ occurred in August and September. Van Bennekom et al. (1974) found average values for the Western Wadden Sea of 1.7 mmol $Si \cdot m^{-2} \cdot d^{-1}$ with maxima of 3.3 mmol $Si \cdot m^{-2} \cdot d^{-1}$ in September. The smaller rates in the Western Wadden Sea compared to the Ems−Dollard may be attributed to the lower suspended matter load in the Wadden Sea. The results in the northern part of the Dollard are in contrast with the results of bell-jar experiments on a Dollard tidal flat, where a net consumption of Si by the sediments was observed throughout the year (Rutgers van der Loeff et al. 1981).

COMPARISON WITH BELL-JARS

In Table 2, yearly averaged results of production (+) and consumption (−) rates are compared for this study and the bell-jar experiments on a Dollard tidal flat (Rutgers van der Loeff et al. 1981). Only data originating from the same area in the Dollard are used.

Both methods give similar results for ammonia, but contrasting results for nitrite and nitrate. In the hydrographical approach applied in this study, both nitrite and nitrate were estimated to have been produced. Production of both nutrients coincided with relatively high oxygen concentration in the overlying water (Fig. 6, 7). In the bell-jars, nitrate and nitrite were consumed by reduction (Rutgers van der Loeff et al. 1981). Apparently production of nitrite and nitrate occurs in the turbid water column. Bell-jars have the disadvantage of isolating the enclosed sediment from tidal currents and wave action (e.g. the turbulence is inhibited compared to natural circumstances). Consequently under bell-jar conditions the supply of oxygen to the sediment is also restricted.

The results of the calculations for dissolved Si are also contrasting. It must be concluded that dissolution of clay minerals and/or diatom skeletons in the turbid water column and at the bottom of the tidal channels more than balances the silica consumption by diatoms on the tidal flats.

The conclusion from our comparison is that bell-jar experiments have limited value. Firstly, sediment−water exchange rates are underestimated and secondly, the processes in the water column are evidently ignored. For estimation of overall nutrient production or consumption rates, results from other methods (e.g. a hydrographical approach) must be considered more reliable.

Acknowledgments

Of the many colleagues and students that participated in some part of the fieldwork we want to thank especially skipper J. Oversluizen of R.V. *Eider*. For discussions and critical reading of the manuscript, we are indebted to H. Postma, S. B. Tijssen, P. Ruardy, and to D. C. Gordon Jr. who also improved the English text substantially.

ALEXANDER, M. 1965. Nitrification, p. 307–343. *In* W. V. Bartholomew and F. E. Clark, [ed.] Soil nitrogen. American Society of Agronomy, Madison, WI.

BARNES, R. O., K. K. BERTINE, AND E. D. GOLDBERG. 1975. N_2: Ar, nitrification and denitrification in southern California borderland basin sediments. Limnol. Oceanogr. 20: 962–970.

BENNEKOM VAN, A. J., G. W. BERGER, W. HELDER, AND R. T. P. DE VRIES. 1978. Nutrient distribution in the Zaire estuary and riverplume. Neth. J. Sea Res. 12: 296–323.

BENNEKOM VAN, A. J., W. W. C. GIESKES, AND S. B. TIJSSEN, 1975. Eutrophication of Dutch coastal waters. Proc. R. Soc. Lond. B. 189, 359–374.

BENNEKOM VAN, A. J., E. KRIJGSMAN-VAN HARTINGSVELD, G. C. M. VAN DER VEER, AND H. F. J. VAN VOORST. 1974. The seasonal cycles of reactive silicate and suspended diatoms in the Dutch Wadden Sea. Neth. J. Sea Res. 8: 174–207.

BILLEN, G. 1975. Nitrification in the Scheldt estuary. Estuarine Coastal Mar. Sci. 3: 79–89.

1978. A budget of nitrogen recycling in North Sea sediments off the Belgian coast. Estuarine Coastal Mar. Sci. 7: 127–146.

BOLIN, B., AND H. ROHDE. 1973. A note on the concepts of age distribution and transit time in natural reservoirs. Tellus 25: 58–62.

BOYLE, E., R. COLLIER, A. T. DENGLER, J. M. EDMOND, A. C. NG, AND R. F. STALLARD. 1974. On the chemical mass balance in estuaries. Geochim. cosmochim. Acta 38: 1719–1728.

BROCK, T. D. 1974. Biology of microorganisms. Prentice Hall, New York, NY.

BURTON, J. D. AND P. S. LISS. 1976. Estuarine chemistry. Academic Press, New York, NY.

CARRITT, D. E., AND J. H. CARPENTER. 1966. Comparison and evaluation of currently employed modifications of the Winkler method for determining dissolved oxygen in seawater; a NASCO report. J. Mar. Res. 24: 286–318.

DORRESTEIN, R. 1960. On the distribution of salinity and of some other properties of the water in the Ems-estuary. Verh. K. Ned. geol. Mijnb. Genoot. 19: 43–74.

DORRESTEIN, R., AND L. OTTO. 1960. On the mixing and flushing of the water in the Ems-estuary. Verh. K. Ned. Geol. Mijnb. Genoot. 19: 83–102.

DUURSMA, E. K., AND J. W. ROMMETS. 1961. Interprétation mathématique de la fluorescence des eaux douces, saumâtres et marines. Neth. J. Sea Res. 1: 391–405.

EPPLEY, R. W., J. L. COATSWORTH, AND L. SOLORZANO. 1969. Studies of nitrate reductase in marine phytoplankton. Limnol. Oceanogr. 14: 194–210.

EPPLEY, R. W., T. T. PACKARD, AND J. J. MC ISAAC. 1970. Nitrate reductase in Peru Current phytoplankton. Mar. Biol. 6: 195–199.

VAN ES, F. B. 1977. A preliminary carbon budget for a part of the Ems-estuary: the Dollard. Helgolander Wiss. Meeresunters. 30: 283–294.

VAN ES, F. B., AND R. W. P. M. LAANE. 1982. Utility of organic matter in the Ems–Dollard estuary. Neth. J. Sea Res. (in press).

FANNING, K. A. AND M. E. Q. PILSON. 1971. Interstitial silica and pH in marine sediments: Some effects of sampling procedure. Science N.Y. 173: 1228–1231.

FENCHEL, T., AND T. H. BLACKBURN. 1979. Bacteria and mineral cycling. Academic Press: 225 p.

HELDER, W. 1974. The cycle of dissolved inorganic nitrogen compounds in the Dutch Wadden Sea. Neth. J. Sea Res. 8: 154–173.

HELDER, W., AND R. T. P. DE VRIES. 1979. An automatic phenol-hypochlorite method for the determination of ammonia in sea- and brackish waters. Neth. J. Sea Res. 13: 154–160.

HENRIKSEN, K., J. I. HANSEN, AND T. H. BLACKBURN. 1981. Distribution of nitrifying bacteria and nitrate fluxes in different types of sediment from Danish waters. Mar. Biol. 61: 299–304.

JØRGENSEN, B. B. 1977a. The sulfur cycle of a coastal marine sediment. (Limfjorden, Denmark). Limnol. Oceanogr. 22: 814–832.

1977b. Bacterial sulfate reduction within reduced microniches of oxidized marine sediments. Mar. Biol. 41: 7–17.

KNOWLES, G., A. L. DOWNING, AND M. J. BARRETT. 1965. Determination of kinetic constants for nitrifying bacteria in mixed culture, with the aid of an electronic computer. J. Gen. Microbiol. 38: 263–278.

KÜHL, H., AND H. MANN. 1954. Über die Hydrochemie der unteren Ems. Veroff. Inst. Meeresforsch. Bremerhaven III: 126–146.

LAANE, R. W. P. M. 1981. Composition and distribution of dissolved fluorescent substances in the Ems–Dollard estuary. Neth. J. Sea Res. 15: 88–99.

LANDNER, L. AND T. LARSSON. 1973. Indications of disturbances in the nitrification process in a heavily nitrogen polluted water body. Ambio 11: 154–157.

LERMAN, A. 1978. Chemical exchange across sediment water interface. Ann. Rev. Earth Planet. Sci. 6: 281–303.

LISS, O. S. 1976. Conservative and non-conservative behaviour of dissolved constituents during estuarine mixing, p. 93–130. *In* B. Liss [ed.] Estuarine chemistry. Academic Press, New York, NY.

LODER, T. C., AND R. P. REICHARD. 1981. The dynamics of conservative mixing in estuaries. Estuaries 4: 64–69.

MCCARTHY, J. J., W. R. TAYLOR, AND J. L. TAFT. 1975. The dynamics of nitrogen and phosphorus cycling in the open waters of the Chesapeake Bay, p. 664–881. *In* T. M. Church [ed.] Marine chemistry in the coastal environment. ACS Symposium Series No. 28.

OFFICER, C. B. 1976. Physical oceanography of estuaries (and associated coastal waters). John Wiley and Sons, New York, NY. 465 p.

OTTO, L. 1967. Investigations on optical properties and watermasses of the southern North Sea. Neth. J. Sea Res. 3: 532–552.

PAMATMAT, M. N. 1968. Ecology and metabolism of a benthic community on an intertidal sandflat. Int. Rev. Gesamten Hydrobiol. 53: 211–298.

POSTMA, H. 1961. Transport and accumulation of suspended matter in the Dutch Wadden Sea. Neth. J. Sea. Res. 1: 148–190.

1966. The cycle of nitrogen in the Wadden Sea and adjacent areas. Neth. J. Sea Res. 3: 186–221.

1967. Sediment transport and sedimentation in the estuarine environment, p. 158–159. *In* G. H. Lauff [ed.] Estuaries. AAAS publ. 83.

PROPP, M. V., V. G. TARASOFF, I. I. CHERBADGI, AND N. V. LOOTZIK. 1980. Benthic–pelagic oxygen and nutrient exchange in a coastal region off the Sea of Japan, p. 265–284. *In* K. R. Tenore and B. C. Coull. [ed.] Marine benthic dynamics. Belle W. Baruch Library in Marine Science 11.

REEBURGH, W. S. 1967. An improved interstitial water sampler. Limnol. Oceanogr. 12: 163–165.

REVSBECK, N. P., J. SØRENSEN, T. H. BLACKBURN, AND J. P. LOMBOLT. 1980. Distribution of oxygen in marine sediments measured with microelectrodes. Limnol. Oceanogr. 25:

403–411.

RODINA, A. G. 1972. Methods in aquatic microbiology. Butterworths. London.

ROWE, G. T., C. H. CLIFFORD, K. L. SMITH, AND P. L. HAMILTON. 1975. Benthic nutrient regeneration and its coupling to primary productivity in coastal waters. Nature (Lond.) 255: 215–217.

RUTGERS VAN DER LOEFF, M. M., F. B. VAN ES, W. HELDER, AND R. T. P. DE VRIES. 1981. Sediment water exchanges of nutrients and oxygen on tidal flats in the Ems–Dollard estuary. Neth. J. Sea Res. 15: 113–129.

SCHRÖDER, H. G. J., AND F. B. VAN ES. 1980. Distribution of bacteria in intertidal sediments of the Ems–Dollard estuary. Neth. J. Sea Res. 14: 268–287.

STRAATEN, L. M. J. U. VAN. 1960. Transport and composition of sediments. Verh. K. Ned. Geol. Mijnb. Genoot. 19: 279–292.

STRICKLAND, J. D. H., AND T. R. PARSONS. 1968. A practical handbook of seawater analysis. Bull. Fish. Res. Board Can. 167.

TUSSEN, S. B., A. J. VAN BENNEKOM, AND W. HELDER. 1974. Contribution of in situ production to the budget of dissolved inorganic nutrients (P, N, and Si) in the eastern part of the Southern Bight of the North Sea. ICES C. M. C26: 1–5.

VANDERBORGHT, J. P., AND G. BILLEN. 1975. Vertical distribution of nitrate in interstitial water of marine sediments with nitrification and denitrification. Limnol. Oceanogr. 20: 953–961.

WILLEY, J. C., AND L. P. ATKINSON. 1982. Natural fluorescence as a tracer for distinguishing between Piedmont and coastal plain riverwater in the nearshore waters off Georgia and North Carolina. Estuarine Coastal Shelf Sci. 14: 49–59.

WILSON, T. R. S. 1978. Evidence for denitrification in aerobic pelagic sediments. Nature (Lond.) 274: 354.

WOLF, P. DE. 1978. "Biologisch Onderzoek Veenkoloniaal Afvalwater": An introduction and a review of a waste-water research project. Hydrobiol. Bull. 11: 7–11.

ZIMMERMAN, J. T. F. 1976. Mixing and flushing of tidal embayments in the western Dutch Wadden Sea. Part I: Distribution of salinity and calculation of mixing time scales. Neth. J. Sea Res. 10: 149–191.

ZIMMERMAN, J. T. F., AND J. W. ROMMETS. 1974. Natural fluorescence as a tracer in the Dutch Wadden Sea and the adjacent North Sea. Neth. J. Sea Res. 8: 117–125.

Chemical Composition of Suspended Particles in an Estuarine Turbidity Maximum Zone[1]

D. H. LORING AND R. T. T. RANTALA

Department of Fisheries and Oceans, Atlantic Oceanographic Laboratory, Bedford Institute of Oceanography, Dartmouth, N.S. B2Y 4A2

AND A. W. MORRIS, A. J. BALE, AND R. J. M. HOWLAND

Natural Environment Research Council, Institute for Marine Environmental Research, Prospect Place, The Hoe, Plymouth, U.K. PL1 3DH

LORING, D. H., R. T. T. RANTALA, A. W. MORRIS, A. J. BALE, AND R. J. M. HOWLAND. 1983. Chemical composition of suspended particles in an estuarine turbidity maximum zone. Can. J. Fish. Aquat. Sci. 40(Suppl. 1): 201 – 206.

The detrital and nondetrital elemental compositions of suspended particles in the Tamar Estuary, U.K., have been examined when the estuarine turbidity maximum was well developed and also when high river flow restricted the development of a turbidity maximum. Correlation matrices and '*r*'-mode factor analyses were used to identify significant relationships within and between the variances in the fractionated particulate compositions and in the ambient physico-chemical conditions. Marked temporal and spatial differences in the elemental composition of suspended particles were found. At high river flow, suspended particulate compositions throughout the estuary were dominated by dilution and dispersion of an overwhelming flux of riverborne material. Under normal conditions of low riverine particle flux, internal cycling of particles, especially within the turbidity maximum region, controlled the spatial distributions of suspended particle compositions and subsidiary inputs were of greater significance.

Key words: estuaries, suspended sediment, particle transport, trace elements

LORING, D. H., R. T. T. RANTALA, A. W. MORRIS, A. J. BALE, AND R. J. M. HOWLAND. 1983. Chemical composition of suspended particles in an estuarine turbidity maximum zone. Can. J. Fish. Aquat. Sci. 40(Suppl. 1): 201 – 206.

La composition élémentaire détritique et non détritique de particules en suspension dans l'estuaire de la Tamar (R.-U.) a été examinée au moment où le maximum de turbidité estuarien était bien établi et aussi quand le fort débit de la rivière limitait l'établissement d'un maximum de turbidité. Les matrices de corrélation et des analyses factorielles sur matrice *r* ont servi à identifier les relations intra et intervariances des compositions particulaires fractionnées et des conditions physico-chimiques ambiantes. On a trouvé des différences temporelles et spatiales marquées de composition élémentaire des particules en suspension. À un fort débit de la rivière, ces particules dans tout l'estuaire sont dominées par la dilution et la dispersion d'un matériel considérable transporté par la rivière. Dans des conditions normales de faible débit de particules fluviales, le recyclage interne des particules, surtout dans la région de turbidité maximale, règle leur distribution spatiale, et les entrées auxiliaires ont une plus grande importance.

Received October 26, 1981
Accepted June 15, 1982

Reçu le 26 octobre 1981
Accepté le 15 juin 1982

THE combination of hydrodynamic and hydraulic processes that leads to the development and maintenance of a high turbidity zone in the low salinity region of partially mixed estuaries is particle selective (Postma 1967; Schubel 1969). Particles within a restricted range of settling velocities, as determined by their size, shape, and density, are preferentially retained within the zone of high turbidity (Festa and Hansen 1978; Officer 1980). Also, both the abundance of selected particles in suspension and the preferred range of their settling velocities vary considerably in response to changes in hydrodynamic conditions: principally, river flow and tidal state. These factors also control the contribution to

[1]This paper forms part of the Proceedings of the Dynamics of Turbid Coastal Environments Symposium convened at the Bedford Institute of Oceanography, Dartmouth, N.S., Canada, September 29–October 1, 1981.

Printed in Canada (J6703)
Imprimé au Canada (J6703)

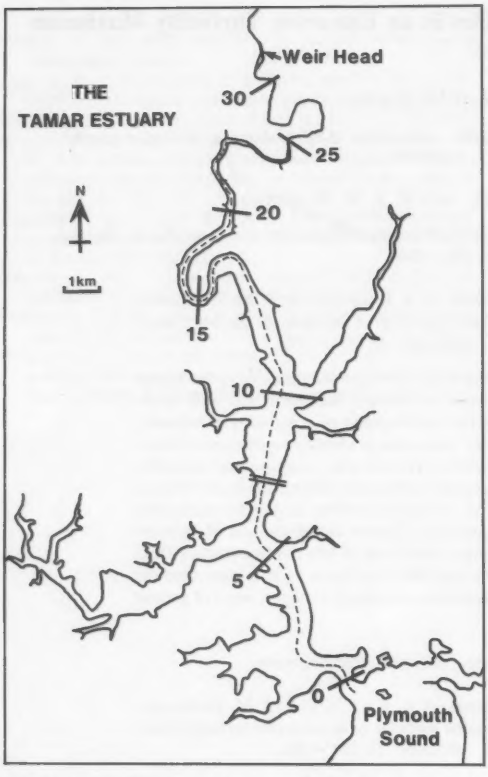

FIG. 1. Tamar Estuary — Bars down at 5-km intervals from the estuary mouth define the distance scale used in Fig. 2 and 3.

the turbidity maximum made by the instantaneous balance of continuous local resuspension and deposition of sediment (Schubel 1969). Corresponding variability in the chemical composition and hence the reactivity of estuarine suspended particulate material (SPM), which is implicit in these observations, has not been investigated systematically. Substantial temporal and spatial variability in the chemical composition of estuarine SPM is, however, generally evident (d'Anglejan and Smith 1973; Sholkovitz 1979; Sholkovitz and Price 1980; Gobeil et al. 1981). An understanding of this variability and its causes is fundamental to estuarine geochemical studies because the majority of chemical transformations in estuaries is mediated at the surface of particles.

Here, data on the fractionated composition of SPM obtained when a well-defined turbidity maximum was present in the low salinity region of the Tamar Estuary, southwest England, are compared with data obtained when the development of a turbidity maximum was restricted by high river flow. Ambient aquatic physico-chemical characteristics were recorded simultaneously. Correlation matrices and '*r*'-mode factor analyses (Cameron 1968, 1969) have been used to identify significant interrelationships indicative of processes controlling the composition and characteristics of the SPM.

The Tamar Estuary Environment

The Tamar Estuary (Fig. 1) is 31.7 km long from its seaward boundary with Plymouth Sound to the weir at Weir Head which physically restrains further landward intrusion of saline water. Saline water reaches the weir only when there is extremely low river flow. Normally, the limit of salt intrusion is located 5–15 km seaward of the weir. Monthly averaged river flow ranges from 38 $m^3 \cdot s^{-1}$ in January to 5 $m^3 \cdot s^{-1}$ in June, with an annual mean of 18 $m^3 \cdot s^{-1}$, but instantaneous flows often exceed 100 $m^3 \cdot s^{-1}$ during periods of heavy rainfall. The annual mean flow gives rise to an estuarine freshwater replacement time of about 1 wk.

Tides in the estuary are predominantly semidiurnal with mean neap and spring ranges of 2.2 and 4.7 m, respectively. The middle estuary is generally partially mixed, with a vertical salinity range typically of 1–2 ‰, although vertically mixed conditions are produced when low river flows coincide with a spring tide.

A pronounced turbidity maximum prevails in the low salinity (<1 to 5 ‰) region of the estuary, irrespective of the geographical siting of the saline intrusion. This maximum comprises a background population of hydrodynamically trapped particles persisting in suspension which is augmented cyclically by resuspension of local sediments around times of maximum flood and ebb tidal currents, with net deposition at other times. The tidally averaged suspended load correlates positively with tidal amplitude. Suspended loads within the turbidity maximum range from around 50 $mg \cdot L^{-1}$ to more than 1000 $mg \cdot L^{-1}$. These levels contrast markedly with the generally low loads (<5 $mg \cdot L^{-1}$) prevalent in the marine and freshwater inputs to the estuary. However, under river spate conditions, the freshwater loading is considerably enhanced, often reaching 50 $mg \cdot L^{-1}$ or more. Coincidentally, high river flows can restrict the development of a pronounced turbidity maximum.

The information given above has been abstracted from George (1975), Morris et al. (1982a, b), and Uncles et al. (1982). Additional information on the chemistry and physics of the estuary is available in Butler and Tibbits (1972), Morris (1978), Morris et al. (1978), Knox et al. (1981), Morris et al. (1981), Morris et al. (1982c), and Readman et al. (1982).

Materials and Methods

FIELD SAMPLING

The sampling and analytical methods used for characterization of the basic physico-chemical properties (salinity, temperature, pH, turbidity, and dissolved oxygen) by continuous recording have been described elsewhere (Morris 1978; Morris et al. 1978; Morris et al. 1982b).

Surface SPM samples were collected with a polyethylene bucket during an axial traverse along the estuarine channel at intervals selected such that about 20 samples covered the full range of salinity and turbidity conditions encountered in the estuary. Triplicate SPM samples were isolated, immediately

TABLE 1. A comparison of the overall mean concentrations (w/w), ranges, and standard deviations for selected components of the suspended particulate material in the Tamar Estuary on two separate occasions. On December 20, 1979, river flow was abnormally high and the freshwater particulate contribution dominated the system. The data for April 11, 1980, was recorded under normal flow conditions, with internal cycling of estuarine particles ascendant.

	December 10, 1979			April 11, 1980		
	Mean	Range	± SD	Mean	Range	± SD
Total dry weight, $mg \cdot L^{-1}$	63.0	10.0 −268	60.8	26.8	3 − 75	28.2
Si, total, %	24.4	21.7 − 26.7	1.47	18.5	13.7 − 24.1	2.93
Al, total, %	10.7	8.7 − 12.0	0.82	8.86	6.2 − 10.8	1.06
Na, total, %	0.44	0.3 − 0.6	0.06	0.44	0.3 − 0.7	0.1
Ca, nondetrital, %	1.04	0.34− 3.36	0.84	1.03	0.43− 3.63	0.85
Ca, detrital, %	0.18	0.1 − 0.3	0.06	0.16	0.1 − 0.3	0.09
Mg, nondetrital, %	0.27	0.12− 0.47	0.09	0.29	0.14− 0.43	0.09
Mg, detrital, %	0.72	0.62− 0.86	0.06	0.65	0.44− 0.90	0.11
Fe, nondetrital, %	1.08	0.94− 1.20	0.07	1.61	0.9 − 3.7	0.69
Fe, detrital, %	4.79	4.32− 5.23	0.21	4.24	3.67− 4.72	0.27
Mn, nondetrital, $\mu g \cdot g^{-1}$	475	362 −633	71	762	388 −1000	236
Mn, detrital, $\mu g \cdot g^{-1}$	335	293 −367	23	299	220 − 342	30
Mn, total, $\mu g \cdot g^{-1}$	810	713 −967	68	1060	622 −1300	249
Zn, nondetrital, $\mu g \cdot g^{-1}$	334	271 −388	32	781	400 −1610	387
Zn, detrital, $\mu g \cdot g^{-1}$	162	106 −202	26	132	90 − 183	24
Zn, total, $\mu g \cdot g^{-1}$	496	432 −578	37	913	530 −1763	389
Cu, nondetrital, $\mu g \cdot g^{-1}$	235	183 −316	44	653	405 −1854	347
Cu, detrital, $\mu g \cdot g^{-1}$	114	95 −147	16	110	86 − 145	15
Cu, total, $\mu g \cdot g^{-1}$	349	279 −458	53	763	518 −1945	343
Cd, total, $\mu g \cdot g^{-1}$	3.3	1.5 − 8.2	2.0	8.5	1.1 − 27	6.9

following collection, by filtration onto preweighed 47 mm Nuclepore® 0.40 μm pore-sized membranes and washed with deionized water to remove occluded dissolved sea salt. Samples were stored dry in plastic envelopes during transport.

Samplings were carried out on December 20, 1979 (river flow, 42.3 $m^3 \cdot s^{-1}$) and on April 4, 1980 (river flow, 12.8 $m^3 \cdot s^{-1}$).

CHEMICAL ANALYSIS

Weights of sediment collected on the filters, per unit volume of water, were measured gravimetrically. The SPM samples were then analyzed for total Si, Al, Fe, Mn, Ca, Mg, Na, Cd, Zn, and Cu. An acetic acid leach, which selectively solubilizes carbonates and amorphous oxides of Fe and Mn as well as mobilizing weakly adsorbed and ion-exchangeable material (Hirst 1962), was used to determine the Fe, Mn, Ca, Mg, Zn, and Cu content of the nondetrital fraction. The acetic acid insoluble material is defined as the detrital fraction. All analyses were carried out using validated atomic absorption spectrophotometric techniques (Rantala and Loring 1977, 1978, 1980).

DATA ANALYSIS

Correlation matrices and '*r*'-mode factor analyses were used to identify significant relationships ($P < 0.01$ and $P < 0.02$) within and between the variances in the fractionated particulate compositions and in the corresponding ambient physico-chemical conditions.

The statistical relationships were interpreted in the same way as reported by Loring (1978, 1979) in which variables are grouped on the basis of their degree of correlation into factors that are associations of highly correlated variables. For this study, the principal factor (correlation) matrices were rotated to produce normal and logarithmic varimax orthogonal solutions. The varimax matrix of six factors of the winter (December) data set ($n = 20$) accounted for 84.4% of the total problem variance and six factors accounted for 91.1% of the total problem variance of the spring (April) data set ($n = 19$). The statistical loadings of the variables on each factor is considered to represent the roles played by the various components in controlling the abundance and distribution of the elements in each data set. The similarities and differences of these factors are discussed in the following section.

Results and Discussion

A summary of the analytical data from each of the two surveys is provided in Table 1 as overall means, ranges and standard deviations. Data on the composition of suspended particles is reported throughout this paper as weight of element per unit weight of suspended solids. The estuarine axial distributions of a selected range of components are illustrated in Fig. 2 and 3; these are scaled identically to facilitate comparison.

The total particle mass within the estuarine mixing region during the winter spate (December 20, 1979) was almost twice that found in the late spring (April 4, 1980) when the river discharge was normal and the turbidity maximum was well developed. SPM composition throughout the estuary in winter was quite uniform, as shown by the limited concentration ranges and low standard deviations about the average values (Table 1). This contrasted sharply with the high internal variation in particle composition in spring. The winter correlation matrices principally demonstrated significant

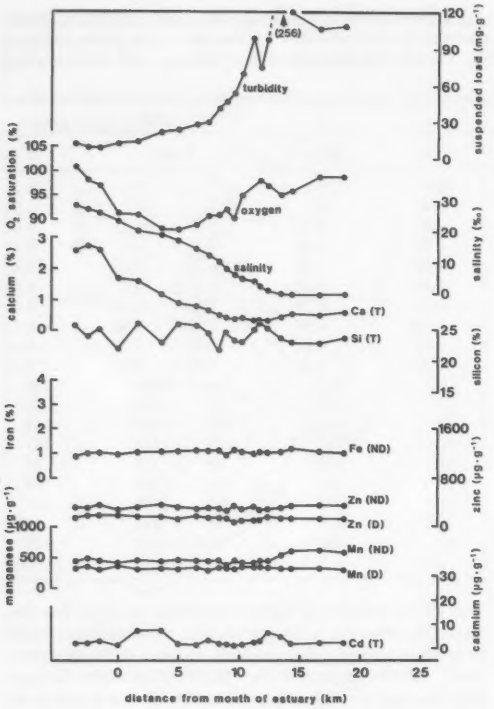

FIG. 2. Variations in turbidity, dissolved oxygen saturation, salinity, and the composition of suspended particles (w/w) along the axis of the Tamar Estuary during high river flow (December 20, 1979). (T), (ND), and (D) refer to the total, nondetrital, and detrital fractions, respectively. At this time, internal recycling of particles was minimal and the abundance and composition of particles throughout the estuary was dominated by the immediate riverine supply. Hence, apart from Ca (see text), the composition of the suspended particulate material was relatively constant.

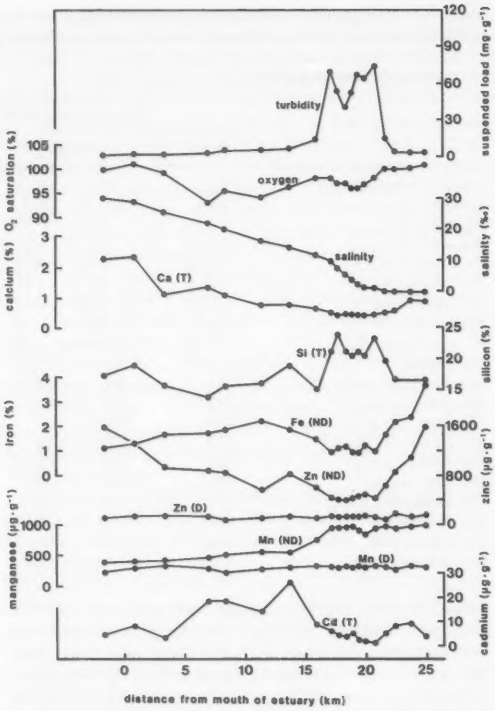

FIG. 3. Variations in turbidity, dissolved oxygen saturation, salinity, and the composition of suspended particles (w/w) along the axis of the Tamar Estuary during normal flow conditions (April 11, 1980). (T), (ND), and (D) refer to total, nondetrital, and detrital fractions, respectively. At this time, a pronounced turbidity maximum was present in the low salinity region of the estuary. Increasing Si (T) and decreasing Fe (ND) and Zn (ND) were strongly correlated with increasing suspended particle mass; Zn (D) and Mn (D) were relatively invariant. Increases in Cd (T) in the lower estuary correlated with a decrease in O_2 saturation. Ca (T) variations relative to salinity were remarkably similar to those found under high flow conditions (cf. Fig. 1).

($P < 0.01$) inverse particle mass–salinity and Ca–Mg–salinity relationships which reflected dilution within the estuary of the relatively high freshwater particulate loading (ca. 100 mg·L^{-1}) although deposition of the riverine flux was also evident. Apart from Ca and Mg, there was little evidence for spatial variability in SPM composition. Thus, the distribution and composition of the SPM during the spate was dominated by dilution and dispersion of an overwhelming flux of river transported material.

In spring, riverine SPM concentrations were low (<5 mg·L^{-1}) although particulate concentrations within the turbidity maximum reached 75 mg·L^{-1}. However, because it resided in the low salinity region, this marked feature did not entirely mask an overall inverse correlation ($r = -0.50$, $P < 0.02$) of particle mass with salinity. Hence, some significant inverse component–salinity relationships attributable to mixing within the estuary were present. On average, total Si and Al were appreciably lower in concentration and relatively more variable than in the winter set (Table 1). Total Cd, Mn, Zn, and Cu concentrations also displayed considerably increased mean concentrations and expanded ranges of occurrence. These compositional differences resulted predominantly from an increase in the nondetrital component. The mean nondetrital concentration of Mn was almost doubled, and that of Zn and Cu more than doubled, compared with their winter levels (Table 1). The detrital contributions of Mn, Zn, and Cu, however, were mainly consistent with the winter data in both concentrations and variability. This demonstrated a seasonal constancy in the composition of the detrital inputs to the estuary.

Total Na and detrital and nondetrital particulate Ca and Mg showed closely comparable means and ranges of occurrence for the two samplings. Total Ca, which was predominantly located in the nondetrital fraction, and total Mg correlated

positively ($P < 0.01$) with salinity on both occasions. It follows that the fractional contributions made by these components to the total particulate load were substantially indifferent to changes in particle transport mechanisms and associated chemical processes within the estuary. Their distributions are compatible with the dilution of marine particles of relatively high carbonate content by riverine particles of relatively low carbonate content, although they also accord with salinity controlled ion-exchanged accumulations of Ca and Mg by freshly discharged riverine particles, as proposed by Russell (1970). However, the results of Sayles and Mangelsdorf (1979) suggest that, for Ca, the second mechanism may not always operate.

The correlation matrices for the spring data showed that significant ($P < 0.01$) increases in the proportion of total Si and of total and nondetrital Mn accompanied an increase in particle mass. Particle mass, however, correlated inversely with total Zn ($P < 0.01$) and Cd ($P < 0.02$), and with nondetrital Fe ($P < 0.01$), Zn ($P < 0.01$), and Cu ($P < 0.02$). Since Si reached maximum levels within the turbidity maximum and its dominant host was undoubtedly quartz, it appears that the depressed concentrations of nondetrital Fe, Zn, Cu, and of total Cd in this zone (Fig. 2) resulted from the dilutant effect of fine sand grains. Present data, however, do not allow us to differentiate selective retention in suspension from immediate local resuspension of sand grains as the basic cause. The recorded increase in the proportion of inorganic material accords with previous observations, on a number of other occasions, that both the ignition loss and the fractional contribution made by organic carbon to the total suspended particulate carbon are depressed within the turbidity maximum zone (Morris et al. 1982c).

Significant ($P < 0.01$) relationships also occurred between nondetrital Fe and nondetrital Zn and Cu in the spring data set. These correlations, together with high loadings of these elements on the same factor of the varimax matrix, suggest that iron oxide particles and/or grain coatings were the main hosts for particulate nondetrital Zn and Cu in the high turbidity zone. These particles were apparently supplied from adjacent mineralized areas and may also have been selectively removed from solution within the high turbidity zone by salinity induced aggregation of riverine Fe-containing microcolloids to particle sizes retained by a 0.4 μm pore size filter. This process is a common and well documented feature of the low salinity region of estuaries (Boyle et al. 1977; Sholkovitz et al. 1978; Moore et al. 1979; Bale and Morris 1981).

Although not varying extensively within either data set, the percentage O_2 saturation was the dominant covariant physicochemical factor associated with the variances in nondetrital Fe and Mn. This may reflect the sensitivity of Fe and Mn speciation to changes in ambient redox conditions. In both data sets, O_2 concentrations in the marine and freshwater mixing components were essentially in equilibrium with the atmosphere. Furthermore, both data sets (Fig. 2 and 3) showed two estuarine minima in O_2 saturation. One has been attributed to hydrodynamic localization of river transported O_2 demand in the very low salinity region, the other to domestic and industrial waste disposal into the lower estuary (Morris et al. 1978). The reduced oxygen concentrations in the lower estuary were associated with an increased fractional contribution of organic carbon to the total particulate carbon and with high (19–26 $\mu g \cdot g^{-1}$) particulate Cd. Sewage discharges to the lower estuary have been reported previously (Eagle et al. 1979) to contain high concentrations of particulate Cd. The correlation of high particulate Cd concentrations with low O_2 saturation in the lower estuary during spring is therefore attributable to their common source.

In the winter data, a decrease in O_2 saturation was one of the principal varimax factors associated with a decrease in nondetrital and total Mn and an increase in nondetrital Fe. In the spring, a decrease in O_2 saturation appeared to be the principal factor associated with a decrease in nondetrital Fe. $Mn-O_2$ saturation relationships at this time were masked by a dominant inverse total Mn–salinity (mixing controlled) relationship. The apparently contradictory results for nondetrital Fe can be explained by a geographical localization of SPM sources coupled with temporal changes in their relative effectiveness. Both data sets exhibited an increase in nondetrital Fe associated with a decrease in O_2 saturation within the lower estuary. This relationship dominated the overall statistics for the winter data, when effects associated with the turbidity maximum were minimized. In the spring data set, however, the decrease in nondetrital Fe within the zone of maximum turbidity, which coincided with reduced O_2 saturation, dominated the overall statistics.

These results confirm the general conclusion from a number of estuarine studies that physical transport processes acting on marine and riverine sources exert a major influence on the spatial variability in the composition of SPM. Evidence for significant control of particle composition through aquatic heterogeneous chemical reactivity is generally lacking, restricted, or equivocal. The distributions and chemical compositions of SPM in the Tay (Sholkovitz 1979), the Amazon (Sholkovitz and Price 1980), the Rhine (Duinker and Nolting 1978), the St. Lawrence (Gobeil et al. 1981), and the Varde A (Duinker et al. 1980) are all basically consistent with mixing of particles derived from the river and from the outer estuary, modified to a greater or lesser extent by localized sediment deposition and/or resuspension.

Conclusions

Fractionation of the particulate composition allows deductions to be made as to the site of the elements and their source, and the chemical response of the particles to their physico-chemical environment. It is evident that both the quantity and composition of SPM undergo considerable temporal and spatial variations in the Tamar Estuary. With abnormally high river flow, freshwater particulate inputs predominate and control the distribution, abundance, and composition of the estuarine particulate matter. As a result, spatial variations in estuarine particulate composition are mainly limited to seaward increases in Ca and Mg concentrations as riverine particulates mix increasingly with marine particles of high carbonate content carried by the intruding saline flow. Under normal flow conditions, however, riverine particulate inputs are reduced and the turbidity maximum becomes well defined. At this time, internal particle cycling and resuspension of sediments override the riverine effects, and control as well as modify the particulate composition. Within the high

turbidity zone, enhancement of particulate Si and the depression of particulate nondetrital Fe, Zn, and Cu carried into the zone from adjacent mineralized areas is evident. Despite these seasonal changes, there is an underlying consistency in the detrital element composition of particles irrespective of changes in particle transport mechanisms and associated chemical processes within the estuary. Superimposed on these natural variations in composition is the additional input of anthropogenic Cd-rich organic wastes to the lower estuary that modifies the natural chemical conditions and processes of the lower estuary.

Acknowledgments

The I.M.E.R. contribution to this collaborative study with M.E.L. forms part of the Estuarine Ecology Program of the Natural Environment Research Council. The work was partly supported by the Department of the Environment (U.K.).

BALE, A. J., AND A. W. MORRIS. 1981. Laboratory simulation of chemical processes induced by estuarine mixing: the behaviour of iron and phosphate in estuaries. Estuarine Coastal Shelf Sci. 13: 1–10.

BOYLE, E. A., J. M. EDMOND, AND E. R. SHOLKOVITZ. 1977. The mechanism of iron removal in estuaries. Geochim. Cosmochim. Acta 41: 1311–1324.

BUTLER, E. I., AND S. TIBBITS. 1972. Chemical survey of the Tamar Estuary. I. Properties of the waters. J. Mar. Biol. Assoc. U.K. 52: 681–699.

CAMERON, E. M. 1968. A geochemical profile of Swan Hills reef. Can. J. Earth Sci. 5: 287–309.

1969. Regional geochemical study of the Slave Point carbonates, western Canada. Can. J. Earth Sci. 7: 1346–1349.

D'ANGLEJAN, B. F., AND E. C. SMITH. 1973. Distribution, transport and composition of suspended matter in the St. Lawrence estuary. Can. J. Earth Sci. 10: 1380–1396.

DUINKER, J. C., M. T. J. HILLEBRAND, R. F. NOLTING, S. WELLERHAUS, AND N. KINGO JACOBSEN. 1980. The river Varde A: processes affecting the behaviour of metals and organochlorines during estuarine mixing. Neth. J. Sea. Res. 14: 237–267.

DUINKER, J. C., AND R. F. NOLTING. 1978. Mixing, removal and mobilization of trace metals in the Rhine estuary. Neth. J. Sea Res. 12: 205–223.

EAGLE, R. A., P. A. HARDIMAN, M. G. NORTON, AND R. S. NUNNY. 1979. The field assessment of effects of dumping wastes at sea. 4. A survey of the sewage sludge disposal off Plymouth. Fish. Res. Tech. Rep. 50, MAFF Lowestoft, 24 p.

FESTA, J. F., AND D. V. HANSEN. 1978. Turbidity maxima in partially mixed estuaries: a two-dimensional numerical model. Estuarine Coastal Mar. Sci. 7: 347–359.

HIRST, D. M. 1962. The geochemistry of modern sediments from the Gulf of Paria. Geochim. Cosmochim. Acta 26: 1147–1187.

GEORGE, K. J. 1975. The tides and tidal streams of the Tamar Estuary. Ph.D. Thesis, University of London, U.K. 555 p.

GOBEIL, C., B. SUNDBY, AND N. SILVERBERG. 1981. Factors influencing particulate matter geochemistry in the St. Lawrence Estuary turbidity maximum. Mar. Chem. 10: 123–140.

KNOX, S., D. R. TURNER, A. G. DICKSON, M. I. LIDDICOAT, M. WHITFIELD, AND E. I. BUTLER. 1981. Statistical analysis of estuarine profiles: application to manganese and ammonium in the Tamar Estuary. Estuarine Coastal Shelf Sci. 13: 357–371.

LORING, D. H. 1978. Geochemistry of zinc, copper and lead in the sediments of the estuary and Gulf of St. Lawrence. Can. J. Earth Sci. 15: 757–772.

1979. Geochemistry of cobalt, nickel, chromium and vanadium in the sediments of the estuary and open gulf of St. Lawrence. Can. J. Earth Sci. 16: 1196–1209.

MOORE, R. M., J. D. BURTON, P. J. LEB. WILLIAMS, AND M. L. YOUNG. 1979. The behaviour of dissolved organic material, iron and manganese in estuarine mixing. Geochim. Cosmochim. Acta 43: 919–926.

MORRIS, A. W. 1978. Chemical processes in estuaries: the importance of pH and its variability, p. 179–187. *In* W. E. Krumbein [ed.] Environmental biogeochemistry and geomicrobiology. Vol. 1, The aquatic environment. Ann Arbor Science, Ann Arbor, MI.

MORRIS, A. W., A. J. BALE, AND R. J. M. HOWLAND. 1981. Nutrient distributions in an estuary: evidence of chemical precipitation of silicate and phosphate. Estuarine Coastal Shelf Sci. 12: 205–217.

1982a. The dynamics of estuarine manganese cycling. Estuarine Coastal Shelf Sci. 14: 175–192.

1982b. Chemical variability in the Tamar Estuary, southwest England. Estuarine Coastal Shelf Sci.

MORRIS, A. W., D. H. LORING, A. J. BALE, R. J. M. HOWLAND, R. F. C. MANTOURA, AND E. M. S. WOODWARD. 1982c. Particle dynamics, particulate carbon and the oxygen minimum in an estuary. Oceanolog. Acta.

MORRIS, A. W., R. F. C. MANTOURA, A. J. BALE, AND R. J. M. HOWLAND. 1978. Very low salinity regions of estuaries: important sites for chemical and biological reactions. Nature (London) 274: 678–680.

OFFICER, C. B. 1980. Discussion of the turbidity maximum in partially mixed estuaries. Estuarine Coastal Mar. Sci. 10: 239–246.

POSTMA, H. 1967. Sediment transport and sedimentation in the estuarine environment, p. 159–179. *In* G. H. Lauff [ed.] Estuaries. Am. Assoc. Adv. Sci., Washington.

RANTALA, R. T. T., AND D. H. LORING. 1977. A rapid determination of 10 elements in marine suspended particulate matter by atomic absorption spectrophotometry. At. Absorp. Newsl. 16: 51–52.

1978. Atomic absorption analysis of USGS reference sample marine mud MAG-1 for selected trace elements. Geostandards Newsl. 2: 125–127.

1980. Direct determination of cadmium in silicates from a fluoboric-boric acid matrix by graphite furnace atomic absorption spectrometry. Atomic Spectrosc. 1: 163–165.

READMAN, J. W., R. F. C. MANTOURA, M. M. RHEAD, AND L. BROWN. 1982. Aquatic distribution and heterotrophic degradation of polycyclic aromatic hydrocarbons (PAH) in the Tamar Estuary. Estuarine Coastal Mar. Sci. 14: 369–389.

RUSSELL, K. L. 1970. Geochemistry and halmyrolysis of clay minerals, Rio Ameca, Mexico. Geochim. Cosmochim. Acta 34: 893–907.

SAYLES, F. L., AND P. C. MANGELSDORF. 1979. Cation-exchange characteristics of Amazon River suspended sediment and its reaction with seawater. Geochim. Cosmochim. Acta 43: 767–780.

SHOLKOVITZ, E. R. 1979. Chemical and physical processes controlling the chemical composition of suspended material in the River Tay Estuary. Estuarine Coastal Mar. Sci. 8: 523–545.

SHOLKOVITZ, E. R., AND N. B. PRICE. 1980. The major-elemental chemistry of suspended matter in the Amazon Estuary. Geochim. Cosmochim. Acta 44: 163–171.

SHOLKOVITZ, E. R., E. A. BOYLE, AND N. B. PRICE. 1978. The removal of dissolved humic acids and iron during estuarine mixing. Earth Planet. Sci. Lett. 40: 130–136.

SCHUBEL, J. R. 1969. Size distributions of the suspended particles of the Chesapeake Bay turbidity maximum. Neth. J. Sea Res. 4: 283–309.

UNCLES, R. J., A. J. BALE, R. J. M. HOWLAND, AND A. W. MORRIS. 1982. Variations in the salinity of surface water in the Tamar Estuary. Oceanolog. Acta (unpublished).

Sediments and Metal Pollutants in a Turbid Tidal Estuary[1]

M. F. C. THORN AND T. N. BURT

Hydraulics Research Station, Wallingford, Oxfordshire 0X10 8BA, England

THORN, M. F. C., AND T. N. BURT. 1983. Sediments and metal pollutants in a turbid tidal estuary. Can. J. Fish. Aquat. Sci. 40(Suppl. 1): 207–215.

An engineering study has been carried out in the tidal River Parrett, U.K., to investigate to what extent metals are trapped and stored within the estuary in its sediments. The River Parrett is a muddy estuary for which the sedimentary regime has been thoroughly studied and is quite well understood. Recently deposited bank sediments and sediments in suspension were sampled in a regular seasonal program, and their metal concentrations analyzed. In general, the relative magnitudes of metal concentrations correlated with the known annual inputs and the spatial distributions of all the metals within the estuary system were similar. The metal pollutants were found to have an affinity for the finer, cohesive sediment particles, and all comparisons of results are therefore based on concentrations on the same particle size fraction of the samples. The longitudinal distribution of metal pollutants in the tidal River Parrett was found to show a systematic seasonal variation. This variation is also mirrored in the layered depth variation of metal concentrations in accumulated sediment in a disused riverside berth. The results are consistent with the hypothesis that metal adsorption is enhanced by increased water salinity. There is no detectable long-term increase in metal concentrations in the sediments of the tidal River Parrett: the metal input is being adsorbed by the much larger sediment resources of the Severn Estuary without any noticeable effect on concentration levels.

Key words: estuary, metals, mud, pollution, sediment

THORN, M. F. C., AND T. N. BURT. 1983. Sediments and metal pollutants in a turbid tidal estuary. Can. J. Fish. Aquat. Sci. 40(Suppl. 1): 207–215.

Une étude de génie a été menée dans la rivière à marée Parrett (R.-U.) afin de déterminer le degré auquel les métaux sont emprisonnés et emmagasinés dans les sédiments de l'estuaire. La rivière Parrett est un estuaire vaseux dont le régime sédimentaire a été étudié à fond et est assez bien connu. Les sédiments récemment déposés ainsi que ceux en suspension ont été échantillonnés lors d'un programme saisonnier régulier, on a déterminé leurs teneurs en métaux. En général, il y a corrélation entre la teneur relative en métaux et les apports annuels, et la distribution spatiale de tous les métaux dans le système estuarien est identique. On a constaté que les contaminants métalliques ont une affinité pour les particules plus fines et cohésives du sédiment. La comparaison des résultats est donc toujours fondée sur les concentrations de particules de même taille dans les échantillons. On a observé, dans cet estuaire, une variation saisonnière systématique de la distribution longitudinale des contaminants métalliques. Cette variation se reflète également dans les différences bathymétriques par couches des concentrations de métaux dans le sédiment accumulé à un poste de mouillage abandonné du bord de la rivière. Ces résultats confirment l'hypothèse que l'absorption des métaux est plus prononcée quand augmente la salinité de l'eau. Il n'y a pas d'augmentation à long terme détectable des concentrations de métaux dans les sédiments de la rivière Parrett : les apports sont absorbés par les sédiments beaucoup plus importants de l'estuaire de la Severn, sans qu'il y ait d'effet notable sur les niveaux de concentration.

Received October 14, 1981
Accepted July 12, 1982

Reçu le 14 octobre 1981
Accepté le 12 juillet 1982

[1]This paper forms part of the Proceedings of the Dynamics of Turbid Coastal Environments Symposium convened at the Bedford Institute of Oceanography, Dartmouth, N.S., Canada, September 29–October 1, 1981.

Printed in Canada (J6686)
Imprimé au Canada (J6686)

THE United Kingdom has obligations under international conventions and the directives of the European Economic Community to control the pollution of the aquatic environment resulting from the discharge of dangerous substances. Legislative control of marine pollution from freshwater sources demands a more thorough understanding of the transmission of pollutants through a tidal estuary, from the point where

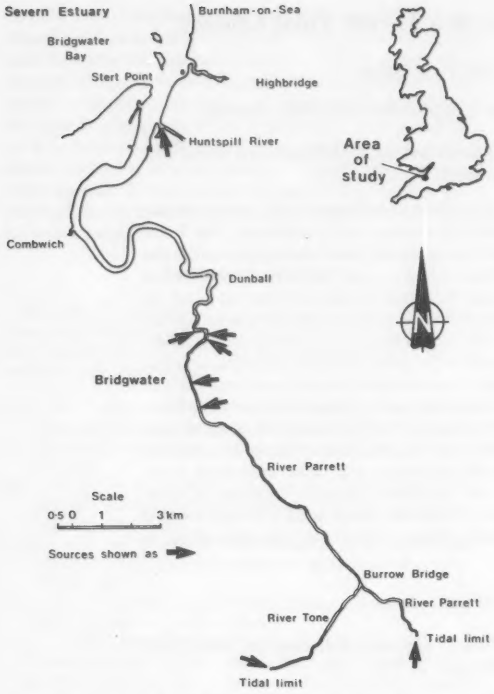

FIG. 1. Location of River Parrett and metal pollutant sources.

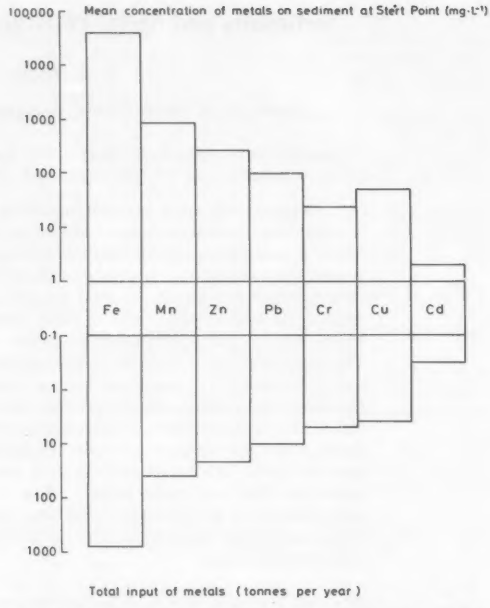

FIG. 2. Comparison of metal inputs and concentrations on sediments.

they may be monitored in an outfall or a freshwater river to the point where they are absorbed by marine sediments or organisms.

Metals in both dissolved and particulate form enter an estuary by way of the river input at the tidal limit and domestic and industrial outfalls discharging from the banks. It is generally thought that many metals have an affinity for fine sediment particles, which may act as a trap removing them from solution and suspension. Hence, based on its expertise and experience in the study of sedimentary processes in estuaries, the Hydraulics Research Station (HRS) has been engaged on a 2-yr pilot field study of the estuarine transmission of heavy metal pollutants. This has been an engineering study using standard methods of measurement and analysis to determine, as far as is practicable, to what extent metals are trapped and stored within the estuary in the sediments, and how much passes out to sea. It has not been concerned with the intrinsic chemistry of metal pollutants but with the apparent determinate interaction of metal pollutants and cohesive sediments in a dynamic sedimentary regime.

The estuary chosen for the pilot study was the tidal River Parrett, which is a tributary of the Severn Estuary in Southwest England (Fig. 1). The reasons for the choice were:

a) There is a sufficient input of heavy metals to produce measurable concentrations in the rivers and outfalls entering the estuary.
b) Most of the effluent discharges are concentrated in a fairly short stretch of the tidal river near Bridgwater (see Fig. 1) so that upriver and downriver distribution is not unduly complicated by intervening sources of pollutants.
c) There is a large amount of fine sediment in the estuary with the potential to scavenge the metals.
d) A large bank of field data was previously obtained by HRS from the River Parrett for a study of a proposed barrier scheme, so there was already a basic understanding of the hydraulic and sedimentary regimes of the estuary (Thorn and Maskell 1980).

The tidal rivers Parrett and Tone meet at Burrow Bridge (Fig. 1) and the combined river flows through Bridgwater to Stert Point, where it enters the Severn Estuary through Bridgwater Bay. Over its entire length from Stert Point to the tidal limits it is characterised by steep-sided muddy banks and a relatively flat bottom; the channel width is about 250 m at Combwich reducing to about 50 m at Bridgwater. Bridgwater Bay is an area of extensive mudflats. The mean Spring and Neap tidal ranges at Stert Point are 11.1 and 6.0 m, respectively, and large quantities of mud are transported up and down the estuary by the tides. Suspended solids concentrations observed during Spring tides are very high, often reaching 100000 $mg \cdot L^{-1}$. The River Parrett may thus be categorised as a well-mixed, turbid estuary with an abundant supply of cohesive sediments.

The field program was based on sampling and analysis of sediments, both deposited and in suspension, in the estuary system. Concentrations of Fe, Mn, Zn, Pb, Cr, Cu, and Cd

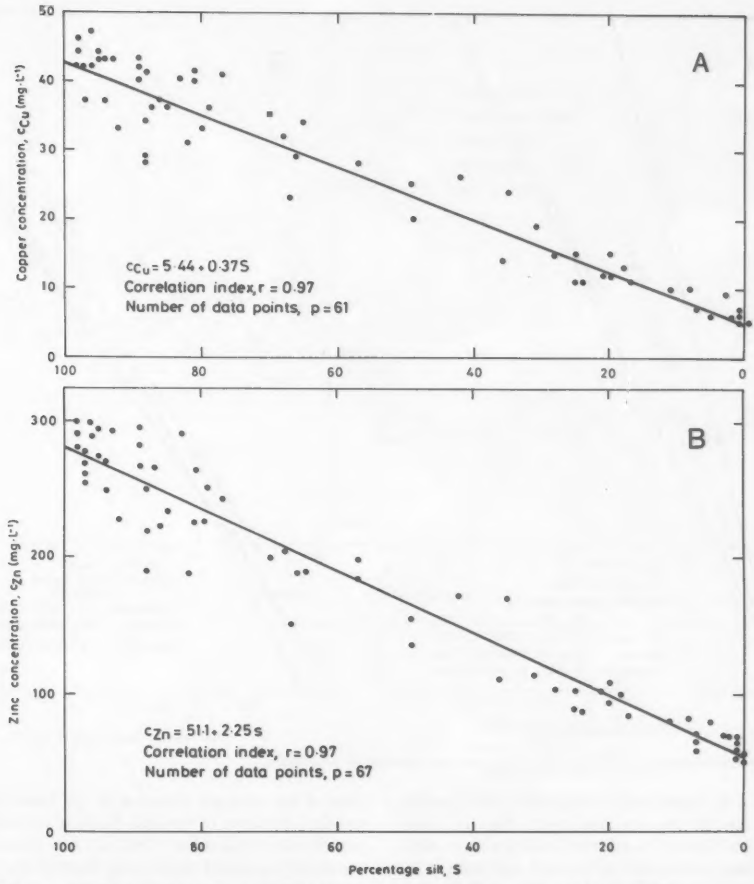
A
Copper concentration, c_{Cu} (mg·l⁻¹)
c_{Cu} = 5·44 + 0·37S
Correlation index, r = 0·97
Number of data points, p = 61
B
Zinc concentration, c_{Zn} (mg·l⁻¹)
c_{Zn} = 51·1 + 2·25s
Correlation index, r = 0·97
Number of data points, p = 67
Percentage silt, S

FIG. 3. Correlation of (A) Cu concentration and (B) Zn concentration and sediment particle size.

were determined for each sample using the method of acid digestion and atomic absorption. Sediment samples were dried and sieved before a mixture of nitric and perchloric acids were added. Digestion was started at a low temperature to destroy organics present, followed by a strong heat to evaporate all the perchloric acid. The resulting mixture was leached with 50% hydrochloric acid and diluted with metal-free water. The required metals were determined on the settled solution by atomic absorption using a two point (plus blank) linear calibration. The concentrations are quoted as milligrams per litre in the dried sample.

In addition, all the sediment samples were analyzed for particle size distribution by the methods described by Kiff (1973). Samples were first separated by wet-sieving to 0.075 mm. The particle size distribution of the coarser fraction was then determined by drying at 120−130°C and dry-sieving to 0.060 mm. The size distribution of the fraction passing the wet sieve at 0.075 mm or the dry sieve at 0.060 mm was determined by the bottom withdrawal tube method (Kiff 1973). The smallest size of determination by this method was 0.002 mm.

Occurrence of Metal Pollutants

The sources of input of metals into the estuary are shown in Fig. 1, and the estimated total annual input of each of the seven metals studied is given in Fig. 2. The inputs are calculated from monitored values of metal concentration and water discharge obtained by the Wessex Water Authority as part of Phases I and II of the Severn Estuary Inputs program (Severn Estuary Survey and Systems Panel 1977). The percentages of the total estimated input that enter in the combined river flows at the tidal limits are as follows:

Metal	Fe	Mn	Zn	Pb	Cr	Cu	Cd
River input as % of total input	75	75	50	37	75	84	89

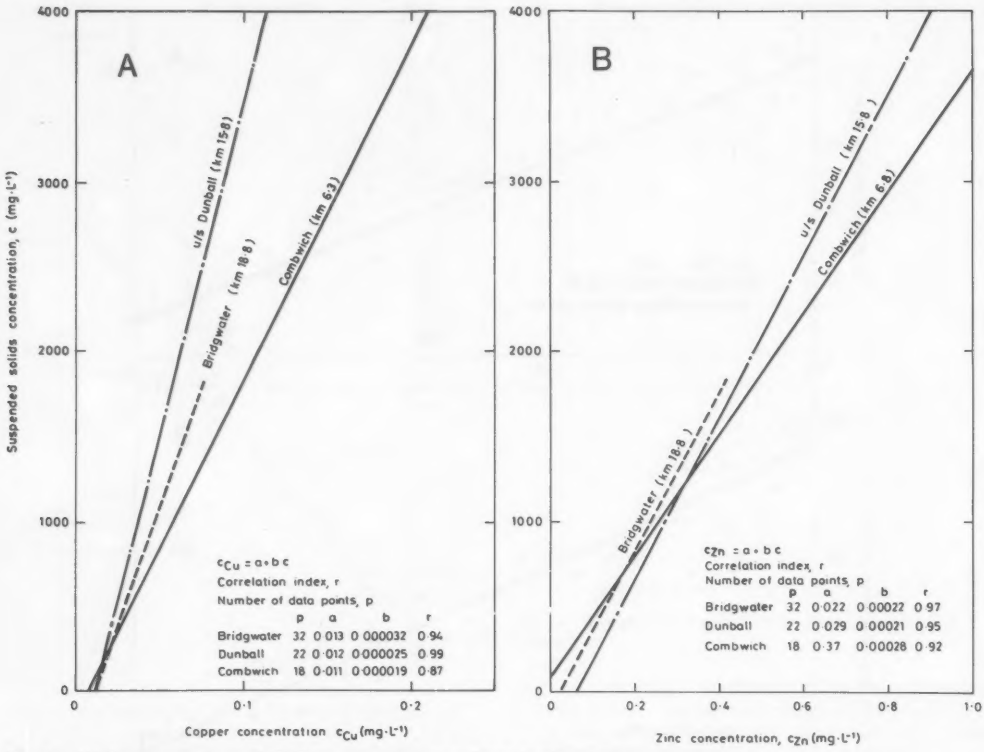
A
B
u/s Dunball (km 15·8)
Bridgwater (km 18·8)
Combwich (km 6·3)
Suspended solids concentration, c (mg·L⁻¹)
Copper concentration c_{Cu} (mg·L⁻¹)
Zinc concentration, c_{Zn} (mg·L⁻¹)
$c_{Cu} = a + b\,c$
Correlation index, r
Number of data points, p
p a b r
Bridgwater 32 0·013 0·000032 0·94
Dunball 22 0·012 0·000025 0·99
Combwich 18 0·011 0·000019 0·87
$c_{Zn} = a + b\,c$
Correlation index, r
Number of data points, p
p a b r
Bridgwater 32 0·022 0·00022 0·97
Dunball 22 0·029 0·00021 0·95
Combwich 18 0·37 0·00028 0·92

FIG. 4. (A) Cu concentrations and (B) Zn concentrations on sediment in suspension.

The remainder of the inputs enter through the several outfalls that discharge directly into the tidal river (Fig. 1). Comparison in Fig. 2 of the total metal inputs with the mean metal concentrations measured on the surface bed sediments at the mouth of the estuary at Stert Point shows that, with the marginal exception of Cr, the concentrations correspond to the inputs. Thus the sediment appears to be absorbing all the different available metals to the same degree. Indeed, the distributions and proportions of all the sediment-attached metal pollutants have been found to be similar throughout the study, and will be represented in this paper by the data for Cu and Zn.

The published results of De Groot et al. (1976) show that the metal pollutants have a particular affinity for the finer, cohesive sediment particles. In the course of this study, 86 samples of the bed surface material were taken from 40 ha of mudflats in Bridgwater Bay. The samples consisted of a wide variety of sediment size distributions, encompassing clay, silt, and fine/medium sand. Metal concentrations were plotted as a function of percentage (by weight) of fine "silt" particles smaller than 0.060 mm, and correlations were obtained as shown in Fig. 3. The least-squares regression coefficients, the correlation index (r), and the sample size (p) are given in each case. The correlation index is defined as the ratio of the standard deviation of the fitted function to the standard deviation of the data (Beckett and Hurt 1967). The particle size threshold of 0.060 mm was chosen because it is a generally accepted engineering basis of discrimination between granular and cohesive sediments, amenable to standard size analysis techniques. De Groot et al. (1976) chose a lower threshold of 0.016 mm, but did not obtain a significantly better correlation. Both sets of results demonstrate the importance, when making comparisons of metal concentrations in estuary sediments, of comparing the concentrations associated with a similar size fraction. Any variations in particle size distribution are otherwise likely to produce spurious apparent variations in metal attachment. In this study all comparisons of results are based on the metal concentrations found on the sample size fraction smaller than 0.060 mm.

The availability of metal pollutants in the tidal waters of the estuary was investigated by taking water samples throughout a complete tidal cycle at Bridgwater, Dunball, and Combwich. Each sample was divided, and the suspended solids concentration of one half was determined by laboratory photoabsorptiometer. The total metal concentrations in the water and solids of the other half was determined by the method of acid digestion and atomic absorption previously described, the results being expressed as weight of metal per unit sample

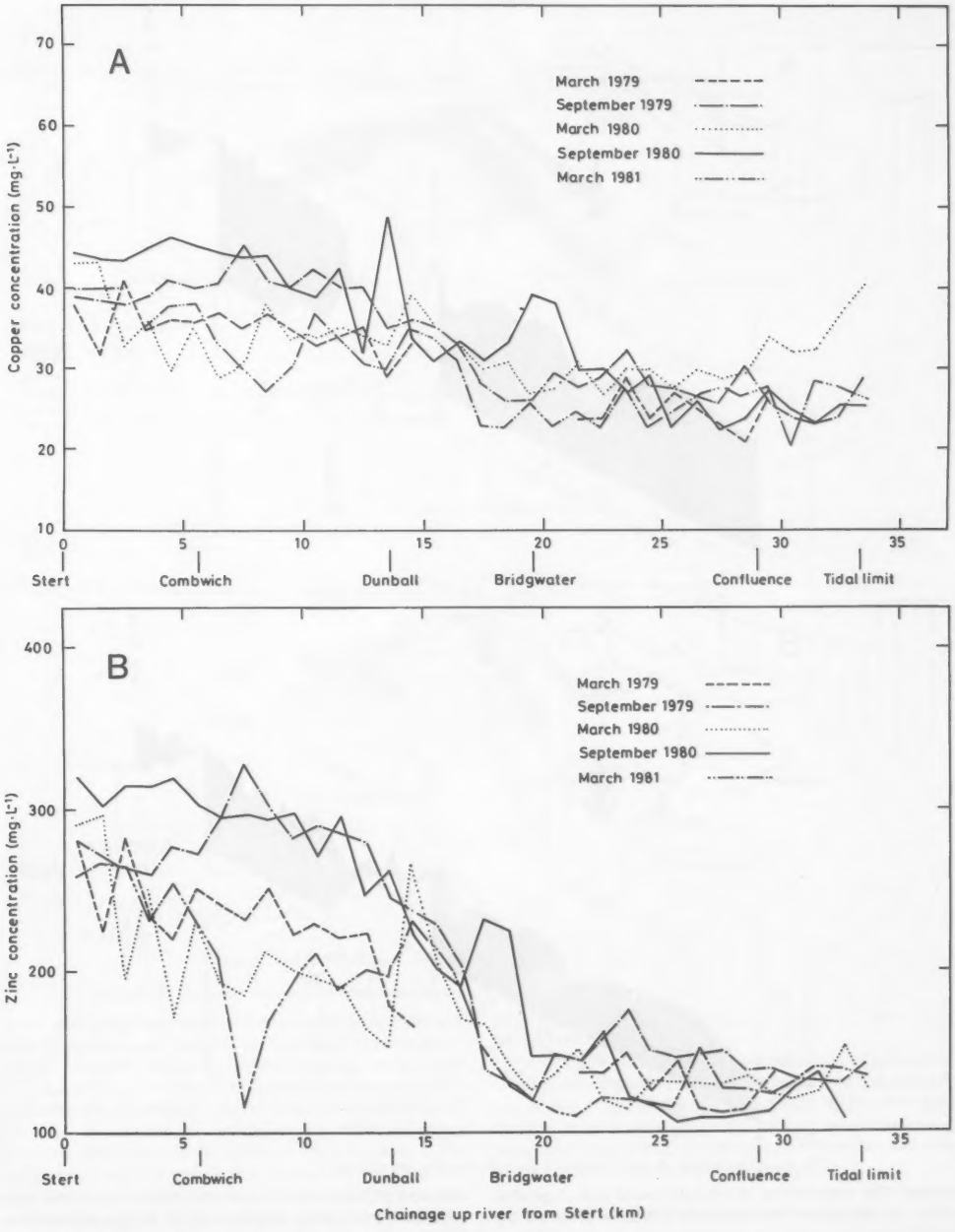

FIG. 5. Longitudinal distributions of (A) Cu and (B) Zn in the tidal River Parrett.

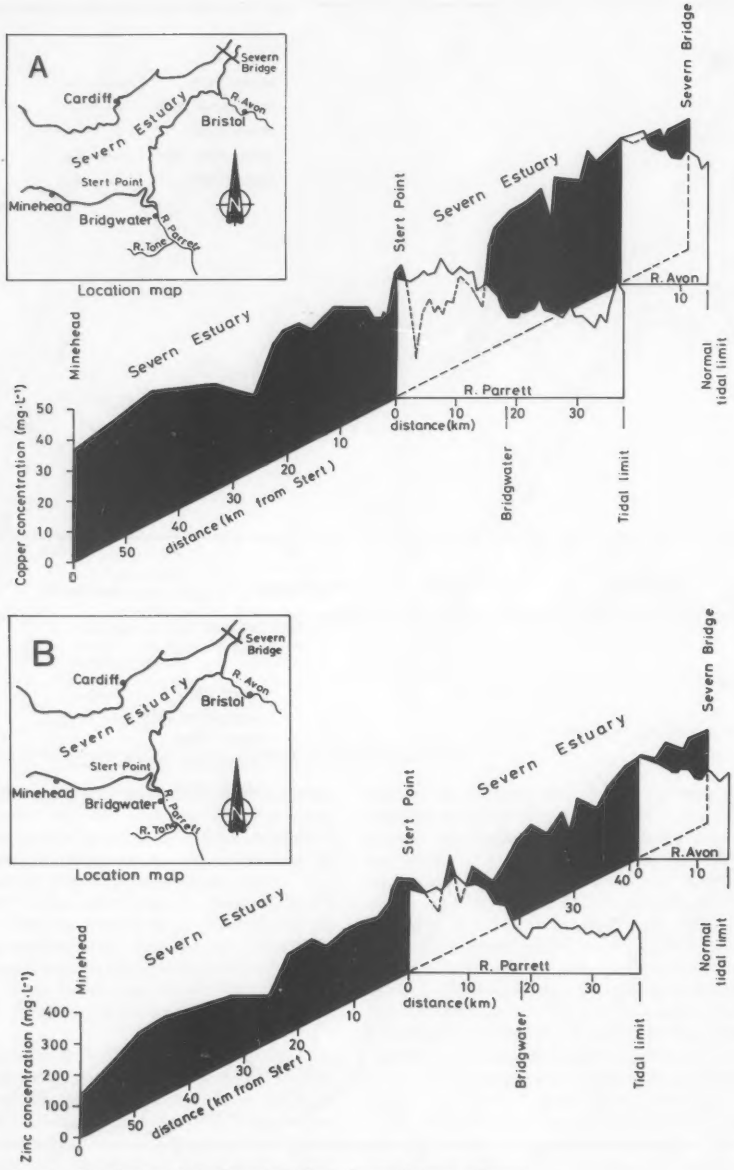

FIG. 6. Distribution of (A) Cu and (B) Zn in Severn Estuary sediments.

volume. The correlations of the total metal and suspended solids concentrations are illustrated in Fig. 4 in which the best-fit lines of correlation are reproduced and the statistical parameters defined above are tabulated. It is clear that the metal pollutants are principally attached to the suspended sediment particles (all of which are smaller than 0.060 mm).

In the upper reaches of the estuary at Bridgwater and Dunball there is a consistent residual concentration at zero suspended solids, which is taken to indicate metals in solution. Note that in the case of Cu, which predominantly enters the

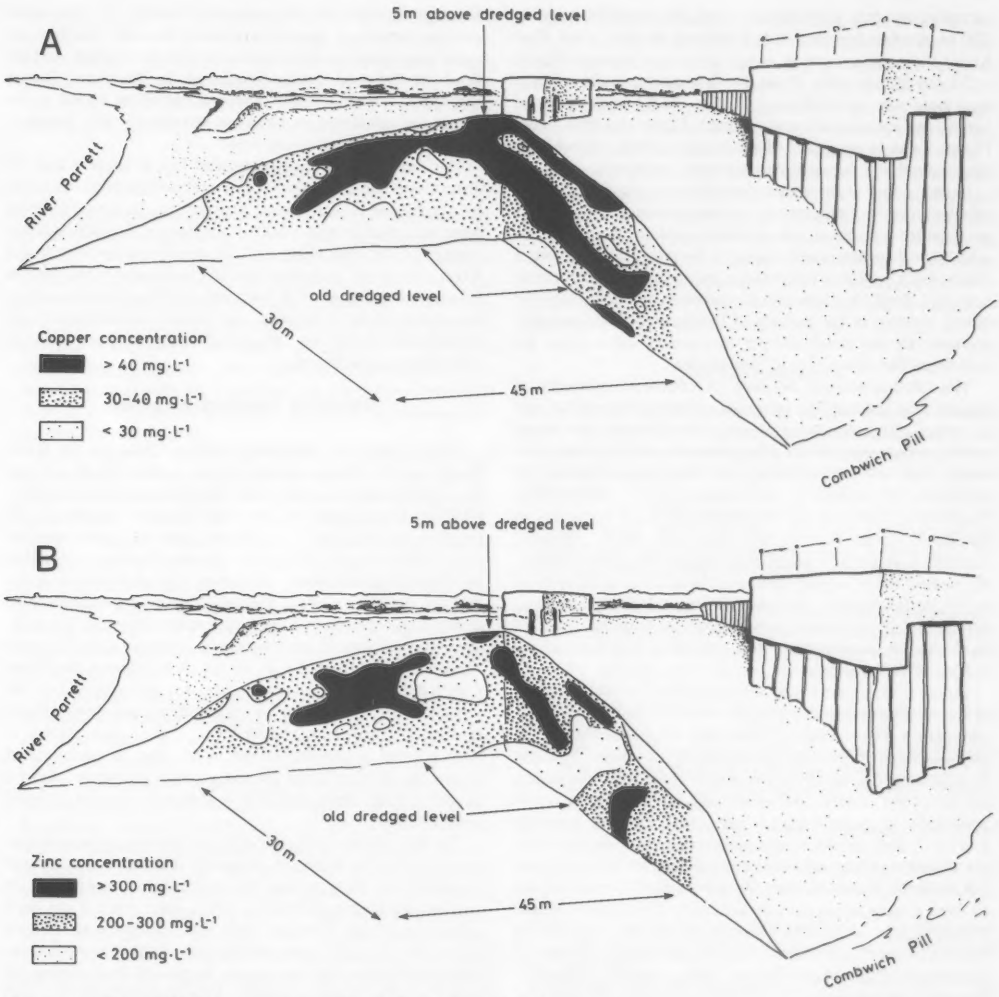

FIG. 7. (A) Cu and (B) Zn concentration profiles of Combwich mud bank.

estuary at the tidal limit, the zero intercepts at Bridgwater and Dunball are the same, and that at Combwich is not significantly different. In the case of Zn which has significant inputs lower down the estuary the zero intercepts are different. The higher intercept at Dunball is almost certainly caused by metal in solution in the effluent outfalls upriver which discharge during the ebbing tide. In the lower estuary at Combwich, the correlation line passes inside the origin, indicating that the metal has become totally adsorbed by the sediments. This was subsequently confirmed by a further tidal water sampling exercise at Stert Point. The weight of Zn in the water samples was 0.33×10^{-3} times the weight of suspended solids with very little variation through the tide, during which time the suspended solids concentration varied in the range $300-77\,000$ mg·L^{-1}.

These results indicate that metal pollutants in solution become adsorbed by the estuarine sediments within the estuary, and do not escape in solution through the mouth. Any transmission of pollutants out of the estuary must therefore be associated with the transportation of fine-grain bed sediments in the context of the sedimentary regime.

Distribution of Metal Pollutants

The longitudinal and seasonal distribution of metal pollutants in the tidal River Parrett has been determined by

sampling recently deposited silt from the intertidal banks at 250 m intervals between Stert Point and the tidal limit. Five March/September surveys were carried out between March 1979 and March 1981. From the first survey it was evident that there was no difference in the results from opposite banks, and subsequent surveys sampled from one bank only. Figure 5 shows examples of the results, which exhibit both longitudinal and seasonal characteristic variations.

Looking first at the longitudinal distribution of sediment-attached metals, a progressive increase in concentration from the tidal limit to the mouth at Stert is evident. Note that Cu, which has its predominant source at the tidal limits exhibits a much more uniform progressive increase in concentration than Zn, of which a substantial proportion enters through the outfall sources in the vicinity of Bridgwater. This probably accounts for the much sharper increase in sedimentary Zn concentrations downriver of Bridgwater.

The electrochemical bonding of cohesive sediments is known to be enhanced by increased salinity (Owen 1970), and a similar effect has been observed by Bewers and Yeats (1978) with respect to the adsorption of metals by bed sediments. The influence of salinity on adsorption of metals by sediments is disputed in the literature (e.g. Eaton 1979; Sholkovitz 1980), but the distribution of metal pollutants in the River Parrett supports the view that salinity enhances adsorption. In the well-mixed tidal waters of the River Parrett, the overall mean salinity decreases from 26‰ at Stert Point to 5‰ at Bridgwater. The general seaward increase in concentrations of sediment-attached metals on both the intertidal banks and in suspension is thus consistent with the salinity regime of the estuary.

Figure 5 shows a marked and repetitive seasonal variation in the metal concentrations in the estuary. At the end of the summer the concentrations in the lower reaches of the estuary are consistently higher than at the end of the winter. This can be explained in terms of the known hydraulic and sedimentary regime of the estuary. During the summer months the freshwater input at the tidal limit is very small, typically less than 3 $m^3 \cdot s^{-1}$. The salinity of the estuary increases and there is a net accretion of bed sediments brought into the estuary by the tide from the Severn Estuary. Hence surface sediment deposits from a more saline environment with consequently higher concentrations of adsorbed metals are found in the lower reaches of the River Parrett. During the winter months the occurrence of freshwater floods, with an annual frequency magnitude of approximately 125 $m^3 \cdot s^{-1}$, causes the accumulated bed sediments to be flushed out of the estuary, and the estuary salinity to be reduced. Hence the sediments carrying higher metal concentrations are no longer found on the intertidal banks at the end of the winter and the salinity regime is less favourable towards metal adsorption.

In view of the apparent interchange of metal-bearing sediments between the lower reaches of the River Parrett and the Severn Estuary, more extensive sampling and analysis of cohesive sediments on the southern and western shores of the Severn Estuary was carried out. In addition a sampling survey of the next upstream tidal tributary of the Severn, the River Avon, was carried out in the same way as for the River Parrett to see whether similar metal distributions were reproduced in another similar situation. Isometric diagrams of the results for the autumn condition are reproduced in Fig. 6. The most striking features of these diagrams are the way in which the metal concentrations in all three estuaries fit together, and the similarity between similar lengths of the Avon and Parrett tributaries. The reaches of low concentrations found in the Parrett are not found in the Avon because its tidal length is interrupted by a controlling weir.

The concentration distributions of Fig. 6 suggest that the distribution and transmission of metal pollutants in the River Parrett cannot be considered in isolation. In both examples there are concentration peaks in the Severn Estuary distributions at points coinciding with the mouths of the Parrett and Avon tributaries. It appears that the sediments of the Severn Estuary are acting as a sink for heavy metal pollutants entering the system in the tributaries, and metal concentrations near the tributary mouths are influenced by the tidal and seasonal interchange of sediments.

Historical Sediment Deposits

The exchange of suspended sediment between the River Parrett and the Severn Estuary during a mean Spring tide has been estimated from continuous tidal survey measurements as 60 000 t. For comparison, the mean input of sediment in the rivers at the tidal limits is estimated from long-term monitor data as about 5 t per tidal cycle, and may thus be neglected in the tidal sediment balance. Assuming from available evidence that the top 0.3 m of the Parrett sediment deposits are also dynamically involved in the sedimentary regime of the estuary, the total weight of sediment in dynamic equilibrium is approximately 200 000 t. If all the zinc entering the River Parrett through the known sources was accumulated in the estuary, the concentration on active surface sediments should increase by approximately 80 $mg \cdot L^{-1}$ each year. Hence if even a small proportion of the metal input is accumulated within the River Parrett by the estuary sediments, over a period of years there should be a detectable change in metal concentrations.

The opportunity to sample historic deposits is presented at a small riverside berth at Combwich. The berth was created artificially by dredging and was in regular use until 1972. It was last dredged in September 1972, since when it has been allowed to silt up. Detailed study and calculation of siltation rates in the estuary (Thorn and Maskell 1980) estimate that the Combwich berth silted up to near its present level during the first 2 yr after dredging ceased. At its highest point the mud bank is now 5 m above the original dredged level. The mud deposits within the bank thus provide a snap-shot of mud as it was at the time of deposition, between 10 and 8 yr ago.

A special tool was designed to extract small, undisturbed, and uncontaminated samples at precise depths up to 5 m. It was used to probe the mud bank along two section lines 45 and 30 m long, over the whole range of depths. From the results, it is possible to construct contoured profiles of the distributions of metal pollutants within the mud bank (Fig. 7). The profiles show fairly broad bands of high and low concentrations, with a low concentration band at the bottom. They are consistent with an accumulation of sediment over a period of $1\frac{1}{2}$–2 yr, beginning in the winter of 1972/73 when metal concentrations would be at a seasonal minimum. There is,

however, no evidence of generally lower concentrations of metals than those measured on present-day sediments. This means that the adsorption of the metals is by a much greater quantity of sediment than is estimated to be active during the tidal cycle within the tidal River Parrett itself: it seems likely that the whole of the Severn sedimentary system is involved.

Discussion

This study has provided a more coherent and complete view of the interaction of sediments and metal pollutants in a muddy estuary. It raises questions about the chemistry of sediment adsorption of metals that are not satisfactorily answered in the current literature and which are outside the scope of this study to explore. The results lead us to formulate a rational model for the transmission of metal pollutants in the River Parrett/Severn Estuary system that is consistent with our observations, and with the hypothesis (as yet unresolved in the chemistry literature) that metal adsorption is enhanced by increased water salinity.

Metals enter the tidal River Parrett in the freshwater rivers and the domestic and industrial outfalls. As they enter the progressively more saline environment of the estuary they become attached to the fine, cohesive sediment particles. This appears to happen within the River Parrett itself, but the tidal exchange of fine sediments between the River Parrett and the Severn Estuary is such that adsorbed metal concentrations are not rising within the tidal River Parrett. Metals entering through the tributaries such as the Parrett and the Avon are dispersed into the incomparably larger sediment deposits of the Severn Estuary system as a whole.

The Severn Estuary sediments thus provide a second source of metal pollutants entering the tidal River Parrett by tidal exchange. Since the whole of the tidal reaches of the River Parrett are involved in the sedimentary regime, this should lead to uniformity of sediment metal concentrations throughout the estuary. In fact, sedimentary metal concentrations are found to be lower in the less saline upper reaches. It appears that the freshwater environment loosens the bonding between metals and sediment, so that metals are desorbed and sedimentary metal concentrations are reduced. As the desorbed metals travel in solution down the estuary they return to a more saline environment where they reattach themselves to the silt. It follows from this that any fluctuations in saline penetration of the Parrett should be reflected in the distribution of metal concentrations. This is observed to be so, for at the end of the summer when river flows are low and saline penetration is greater, the metal concentrations in the lower reaches are high and equal to those nearby in the Severn Estuary. During the winter, river flows are high and saline penetration is reduced, which gives rise to lower metal concentrations on the sediment in the lower reaches.

Investigation of historical sediment deposits shows no detectable change in adsorbed metal concentrations over a period of 9 yr. It is concluded that there is no significant accumulation of sediment-attached metal pollutants within the tidal River Parrett, and that the total quantity of fine sediment in the Severn Estuary system is large enough to receive the existing inputs without noticeable effect on concentration levels.

This pilot engineering study of the transmission of metal pollutants through a turbid tidal estuary has given an insight into the overall framework of the process, but does not pretend to be an exhaustive investigation of the mechanisms involved. In particular, a clearer understanding of the chemistry of adsorption and desorption of pollutants by cohesive sediments is needed before metal pollution can be fully integrated into models of the estuary regime.

Acknowledgments

The authors have been grateful for the advice and assistance of Mr P. R. Kiff of the HRS Sedimentation Laboratory who carried out all particle size and suspended solids determinations and prepared all the sediment samples for analysis. Chemical analysis was by Charter Consolidated Services Ltd., Ashford, Kent. This study was carried out as part of the research program of the Hydraulics Research Station, Wallingford with the support of the Water Data Unit, Reading and the Department of the Environment, London. It is published with the permission of the Director of Hydraulics Research.

BECKETT, R., AND J. HURT. 1967. Numerical calculations and algorithms, Ch. 8, McGraw-Hill Book Company, New York, NY.

BEWERS, J. M., AND P. A. YEATS. 1978. Trace metals in the waters of a partially mixed estuary. Estuarine Coastal Mar. Sci. 7: 147–162.

EATON, A. 1979. Removal of 'soluble' iron in the Potomac River Estuary. Estuarine Coastal Mar. Sci. 9: 41–49.

DE GROOT, A. J., W. SALOMONS, AND E. ALLERSMA. 1976. Processes affecting heavy metals in estuarine sediments, Ch. 5. *In* J. D. Burton and P. S. Liss [ed.] Estuarine chemistry. Academic Press, New York, NY.

KIFF, P. R. 1973. Particle size analysis of sediments. Laboratory Practice (April 1973): 259–266.

OWEN, M. W. 1970. A detailed study of the settling velocities of an estuary mud. Hydraulics Research Station, Wallingford, Rep. No. INT 78.

SEVERN ESTUARY SURVEY AND SYSTEMS PANEL. 1977. First report to the technical working party of the Severn Estuary Joint Committee.

SHOLKOVITZ, E. R. 1980. Removal of 'soluble' iron in the Potomac River Estuary: Comments. Estuarine Coastal Mar. Sci. 11: 585–587.

THORN, M. F. C., AND J. M. MASKELL. 1980. River Parrett tidal barrier: hydraulic investigations. Public Health Eng. 8(1): 11–19.

Heterotrophic Bacterial Biomasses, Activities, and Productivities Within The Fraser River Plume[1]

L. J. ALBRIGHT

Department of Biological Sciences, Simon Fraser University, Burnaby, B.C. V5A 1S6

ALBRIGHT, L. J. 1983. Heterotrophic bacterial biomasses, activities, and productivities within the Fraser River plume. Can. J. Fish. Aquat. Sci. 40(Suppl. 1): 216–220.

Most of the microorganisms within the silt-laden Fraser River water are bacteria, the majority of which are attached to detritus and suspended silt. However, within surface water of the Strait of Georgia bacteria constitute only about 4% of the microbial biomass; most are free-living. Within the plume, which results when the freshwater of the Fraser River mixes with the seawater of the Strait of Georgia (salinity of about 27‰ and containing mainly phytoplankton) stimulations of bacterial glucose heterotrophic activity and productivity occur throughout the year. Bacterial production is a relatively greater proportion of the total microbial, i.e. both algal and bacterial production, in the winter than in the spring or fall. Preliminary evidence indicates that the stimulation of bacterial activity and productivity may be, at least partially, due to entrainment of nitrate and phosphate-rich deep water of the Strait of Georgia into the Fraser plume.

Key words: Fraser plume, bacteria, production, heterotrophic activity, Strait of Georgia

ALBRIGHT, L. J. 1983. Heterotrophic bacterial biomasses, activities, and productivities within the Fraser River plume. Can. J. Fish. Aquat. Sci. 40(Suppl. 1): 216–220.

La plupart des micro-organismes dans le fleuve Fraser, chargé de limon, sont des bactéries, en grande partie fixées sur les détritus et le limon en suspension. Cependant, dans l'eau de surface du détroit de Géorgie, les bactéries ne représentent que 4 % de la biomasse microbienne, la plupart étant libres. Dans le panache formé quand l'eau douce du fleuve Fraser se mélange à l'eau salée du détroit de Géorgie (salinité d'environ 27 ‰ et contenant surtout du phytoplancton), l'activité hétérotrophe et la productivité de glucose des bactéries sont stimulées à l'année longue. La production bactérienne représente une proportion relativement plus forte du total, c.-à-d. à la fois des algues et des bactéries, en hiver qu'au printemps ou à l'automne. Des données préliminaires indiquent que la stimulation de l'activité et de la productivité des bactéries seraient dues, au moins en partie, à l'entraînement des eaux profondes, riches en phosphates et en nitrates, du détroit de Géorgie dans le panache du fleuve Fraser.

Received October 14, 1981
Accepted July 15, 1982

Reçu le 14 octobre 1981
Accepté le 15 juillet 1982

VALDES and Albright (1981) and Bell and Albright (1981) found that a stimulation of the heterotrophic activity of the bacterioplankton occurs where the freshwater of the Fraser River mixes with seawater of the Strait of Georgia in the Fraser plume. These authors reasoned that the stimulation in activity may be caused by an enhancement of the nutritive quality of the plume water, compared to either of the parent waters. It was speculated that the enriching nutrients may be mineralized components, e.g. NO_3 and PO_3, entrained into the plume from deep Strait of Georgia water. Because increased bacterial activities are often associated with increases in rates of cell division and growth, the observed stimulation of bacterial heterotrophic activity in these plume waters may be indicative of a stimulation of bacterial productivity, which possibly contributes significantly to total plume microbial production.

Since the above studies indicate that the bacterioplankton in the Fraser plume is a significant portion of the total microbial (including phytoplankton) biomass, this study was initiated to determine: (1) factors which cause stimulation of heterotrophic bacterial activity; and (2) the relative contribution of bacteria and phytoplankton to microbial production.

Materials and Methods

SAMPLING TECHNIQUES

Water samples (one per station) were collected from depths of 1–3 m using a 6-L Van Dorn sampler within the lower

[1]This paper forms part of the Proceedings of the Dynamics of Turbid Coastal Environments Symposium convened at the Bedford Institute of Oceanography, Dartmouth, N.S., Canada, September 29–October 1, 1981.

Printed in Canada (J6672)
Imprimé au Canada (J6672)

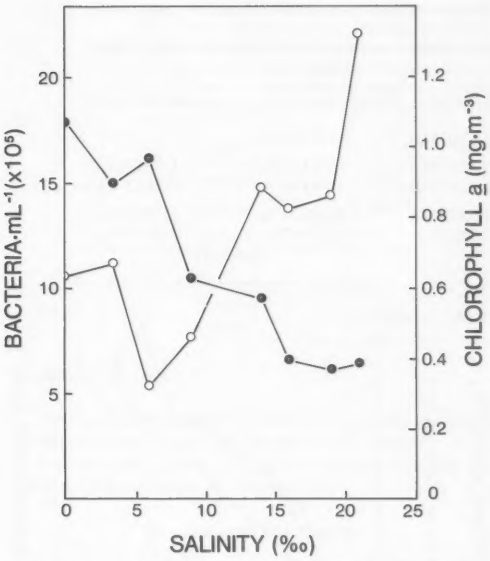

FIG. 1. Bacterial (●) and chlorophyll *a* (○) content of Fraser plume water as assayed on February 2, 1981.

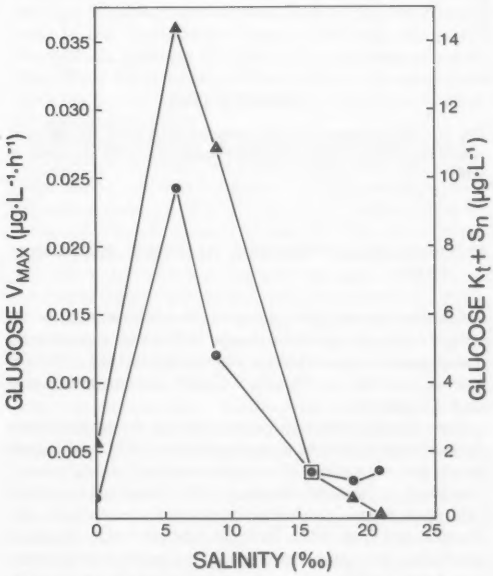

FIG. 2. Bacterial glucose heterotrophic activities (V_{max}, ●) and $K_t + S_n$ values (▲) of Fraser plume water as determined on February 2, 1981.

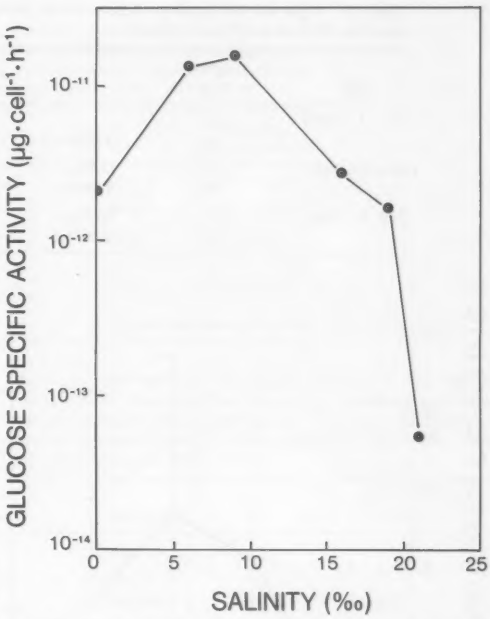

FIG. 3. Glucose specific activities of bacteria contained within the Fraser plume water (a replot of the data of Fig. 2 and 3).

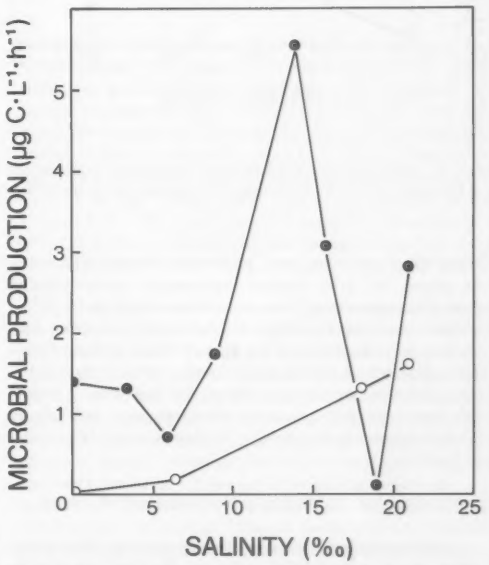

FIG. 4. Bacterial (●) and phytoplankton (○) production within the Fraser plume as determined February 25, 1981.

TABLE 1. Light and dark productivities within the Fraser Plume as determined at various times of the year. Corresponding salinities are given in parentheses.

Date	Light (L) or Dark (D)	Production ($\mu g\ C \cdot L^{-1} \cdot h^{-1}$)			
Nov. 11, 1979	L				
	D	1.03(0‰)	2.15(6.0‰)	4.67(14.5‰)	
Feb. 25, 1981	L	0(0‰)	0.18(6.4‰)	1.32(18.2‰)	1.62(21.1‰)
	D	1.36(0‰)	0.72(6.0‰)	5.54(14.0‰)	2.81(21.2‰)
June 27, 1981	L	0(0‰)	0.6(6.2‰)	30.6(12.6‰)	25.8(17.6‰)
	D	0.8(0‰)	1.5(6.2‰)	6.2(14.5‰)	5.6(17.6‰)

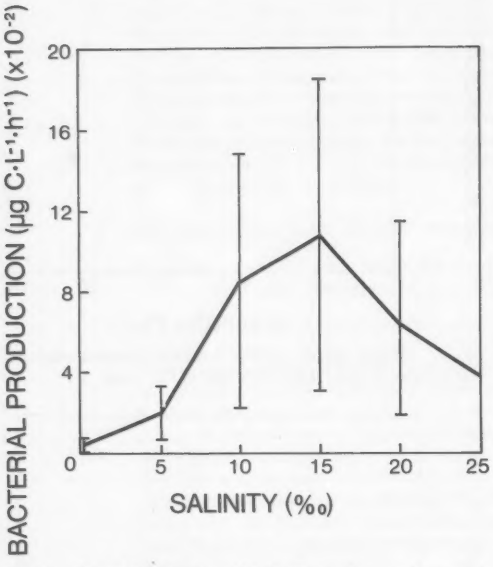

FIG. 5. Bacterial production within the Fraser plume as determined on February 25, 1981 by the technique of Fuhrman and Azam (1980).

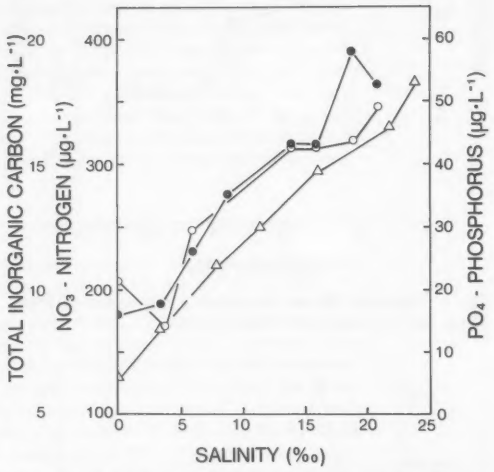

FIG. 6. NO_3-nitrogen (○), PO_4-phosphorus (▲), and TIC (●) content of Fraser plume water sampled February 25, 1981 at a depth of 1 m.

Fraser River, its plume, and the Strait of Georgia adjacent to the plume. All 0 ‰ salinity water samples were collected about 5 km upstream of Steveston whereas the high (> 21‰) salinity waters were collected, at variable distances (depending upon the extent of the plume) WNW of Sand Heads light. Samples of intermediate salinities were collected between the Strait of Georgia stations and Steveston. All samples were immediately assayed for temperature and salinity (Yellow Springs Instrument Co., Yellow Springs, OH, model 33 S-C-T).

DETERMINATION OF MICROBIAL NUMBERS AND BIOMASSES

Total bacterial numbers were determined using the acridine orange direct count (AODC) technique as described by Hobbie et al. (1977) and Daley and Hobbie (1975) and chlorophyll *a* concentrations by Strickland and Parsons (1972).

DETERMINATION OF MICROBIAL ACTIVITIES AND PRODUCTIVITIES

Glucose heterotrophic activities were determined as described by Azam and Holm-Hansen (1973) with experimental manipulations as per Valdes and Albright (1981). D-6-^{3}H glucose, specific activity 22.5 $Ci \cdot mM^{-1}$ (Amersham) was used as substrate.

Dark (mainly bacterial) production was determined using the method described by Romanenko et al. (1972) and sodium bicarbonate substrate (^{14}C - specific activity 8.4 $mCi \cdot mM^{-1}$, New England Nuclear). The factor, 16.6, was used to convert ^{14}C uptake rate to bacterial biomass production rate (Romanenko et al. 1972; Bell and Albright 1981). Bacterial production was also determined by the method of Fuhrman and Azam (1980) using a thymidine substrate (methyl-^{3}H-thymidine, specific activity 74.1 $Ci \cdot mM^{-1}$, New England nuclear).

Primary production was measured by the ^{14}C technique using the sodium bicarbonate substrate described above.

TABLE 2. The influence of glucose (2.5×10^{-8} M), $NaNO_3$ (100 μg $N \cdot L^{-1}$) and $NaHPO_4$ (50 μg $P \cdot L^{-1}$) additions to 500 mL Fraser River freshwater (salinity 0‰) upon bacterial glucose heterotrophic activity and production. Heterotrophic activities and productivities were assayed on February 18 and 20, 1981, respectively. Bacterial productivities were determined by the technique of Fuhrman and Azam (1980).

Water	$K_t + S_n$ ($\mu g \cdot L^{-1}$)	V_{max} ($\mu g \cdot L^{-1} \cdot h^{-1}$)	T_t (h)	Production ($\mu g\ C \cdot L^{-1} \cdot d^{-1}$)
Untreated	0.128	0.21×10^{-2}	59.4	1.82–11.81
Glucose	0.277	0.28×10^{-2}	98.4	1.28–8.34
Nitrogen + Phosphorus	0.582	0.31×10^{-2}	186.0	1.24–8.03
Nitrogen + Phosphorus + Glucose	0.235	0.24×10^{-2}	97.2	1.19–6.63

NUTRIENT ANALYSES

The levels of NO_3 and PO_4 were measured using methods described by Strickland and Parsons (1972).

Total inorganic carbon (TIC) levels were determined by the gas-stripping technique of Stainton (1973).

Results and Discussion

When the heterotrophic bacteria dominated Fraser River water enters the saline water of the Strait of Georgia, which is phytoplankton dominated, significant changes in bacterial and algal biomasses and activities occur in the zone of mixed water of the Fraser plume. Figure 1 illustrates the pattern observed on February 2, 1981. The bacterial dominated Fraser River water became altered to a microalgae-dominated saline water of the Strait of Georgia, with plume waters showing intermediate values.

Significant increases in glucose heterotrophic activity (V_{max}) occurred within the plume waters over the salinity range of 0–15‰. In this instance, maximal potential activity occurred at about 6‰ (Fig. 2). The $K_t + S_n$ values (which are a sum of the cell uptake constant (K_t) plus the substrate concentration (S_n)) closely followed the changes in V_{max} values. When activities per cell were calculated (Fig. 3), an increase in specific activity was noted for bacteria in water of salinities of about 5–10‰. Although the precise reason(s) for this increase in bacterial activity and specific activity is not known it may be indicative of enriched nutrient conditions in intermediate salinity plume waters.

In many microcosms, a direct causal relationship has been noted between bacterial activity and cell production. Therefore, assays of bacterial production were also done to determine if they correlated with the observed increases in heterotrophic activities. In this instance (February 25, 1981), a stimulation in dark (mainly bacterial) production occurred over the plume salinity range of about 10–15‰ (Fig. 4). Since primary production was also determined at the same time, a relatively direct comparison of the bacterial (dark) and microalgae (light) productivities could be made (Fig. 4). Dark production exceeded that of the phytoplankton within river and plume waters over the salinity range of 0 to 17‰.

When both light and dark productivities within the Fraser plume were determined at various times of the year, the phytoplankton were clearly more productive in late spring (Table 1). In winter, production by bacterioplankton appeared to exceed that of the microalgae. Moreover, dark production was not so clearly seasonally dependent and tended to remain within the range of 1–6 μg $C \cdot L^{-1} \cdot h^{-1}$ in the plume waters. Maximum dark productivities occurred at salinities of 5–15‰ in the Fraser plume, being maximum at about 5–6 μg $C \cdot L^{-1} \cdot h^{-1}$ throughout the year. This observed temporal "stability" in dark production throughout the year may be a reflection of only minor temporal changes in nutrient concentrations within plume water.

TABLE 3. The influence of glucose (2.5×10^{-8} M), $NaNO_3$ (100 μg $N \cdot L^{-1}$) and $NaHPO_4$ (50 μg $P \cdot L^{-1}$) additions to 500 mL surface Strait of Georgia water (salinity 26‰) upon bacterial production. Productivities were assayed on March 4, 1981 by the technique of Fuhrman and Azam (1980).

Water	Production ($\mu g\ C \cdot L^{-1} \cdot d^{-1}$)
Untreated	13.17–20.27
Nitrogen + Phosphorus	15.75–24.23
Nitrogen + Phosphorus + Glucose	17.06–26.25

The dark production data were treated with caution since several investigators have found that this assay has relatively large experimental errors (e.g. Overbeck and Daley 1973). Therefore, the ^{3}H-thymidine uptake assay of Fuhrman and Azam (1980) was employed as another assay of bacterial production, since the growth of only those microorganisms which can utilize exogenous thymidine is determined, i.e. the growth of bacteria. However, only a portion of the active and growing bacteria in a natural population can utilize this exogenous substrate. Hence the assay tends to underestimate total bacterial production. Although bacterial production was lower (Fig. 5) the productivity curve was similar to that previously noted (the Romanenko technique) with a peak at about 15‰ salinity. Thus, the actual bacterial production of these waters is between values obtained following each technique.

It may be significant that bacterial production per unit volume of water was relatively constant at a given plume salinity, when assayed at various times of the year, whereas primary production was not (Takahashi et al. 1973), implying that bacterial production may be supplying a greater proportion of the microbial biomass to the food web in the plume during the winter when primary production is low.

What causes stimulation of glucose heterotrophic activity and production in plume water? The most likely explanation is that plume water is more nutrient rich than either parent water, with regard to organic and inorganic nutrients, although Valdes and Albright (1981) and Bell and Albright (1981) found that concentrations of organic matter (both dissolved and particulate) were greater in the surface water of the Strait of Georgia than in the Fraser River or plume. However, the Fraser plume water contains increased levels of the mineralized compounds of NO_3, PO_4, and TIC (total inorganic carbon) as the river is diluted with Strait of Georgia water (Fig. 6). Water sampled at 100 m below the plume on February 25, 1981 contained 430 $\mu g \cdot L^{-1}$ NO_3 - nitrogen, 62 $\mu g \cdot L^{-1}$ PO_4 - phosphorus and 27 $mg \cdot L^{-1}$ TIC. Hence, it is likely that deep (i.e. depths greater than about 100 m) Strait of Georgia water is entrained into the Fraser plume enriching this water with its mineralized components.

To test this hypothesis, 500 mL portions of Fraser River water were treated with 1.25×10^{-8} moles of glucose, 50 μg of NO_3 - nitrogen, or 25 μg of PO_4 - phosphorus and combinations thereof. The untreated control and treated waters were allowed to stand for 4 h at in situ temperatures and then assayed for glucose heterotrophic activities and bacterial productivities (Table 2). There were no apparent increases in either of these bacterial processes following these nutrient treatments.

When Strait of Georgia surface water was treated with these nutrients at similar combinations and concentrations, there was a stimulation in bacterial production (Table 3). Valdes and Albright (1981) have previously found that most of the indigenous freshwater bacteria of the lower Fraser River are activity-inhibited upon exposure to the saline water of the Strait of Georgia whereas the bacteria of surface Strait of Georgia water remain viable and active as they are mixed into Fraser River freshwater. Therefore, one possible explanation of the increased bacterial productivities in the Fraser plume may be that this water is more nutritive with regard to essential metabolities such as NO_3 and PO_4.

Acknowledgments

I acknowledge the financial support of the Natural Sciences and Engineering Research Council of Canada for this research and I thank Dr C. R. Bell and Mr D. Stroh for technical assistance. I am grateful to Dr T. R. Parsons for chlorophyll *a*, primary production, NO_3 and PO_4 analyses and the officers and crews of M/V *Pandora II*, CSS *Vector*, and MSSV *John Strickland* for aid in sampling.

AZAM, F., AND O. HOLM-HANSEN. 1973. Use of tritiated substrates in the study of heterotrophy in seawater. Mar. Biol. 23: 191–196.

BELL, C. R., AND L. J. ALBRIGHT. 1981. Attached and free-floating bacteria in the Fraser River estuary, British Columbia, Canada. Mar. Ecol. Prog. Ser. 6: 317–327.

DALEY, R. J., AND J. E. HOBBIE. 1975. Direct counts of aquatic bacteria by a modified epi-fluorescent technique. Limnol. Oceanogr. 20: 875–881.

FUHRMAN, J. A., AND F. AZAM. 1980. Bacterioplankton secondary production estimates for coastal waters of British Columbia, Antarctica and California. Appl. Environ. Microbiol. 39: 1085–1095.

HOBBIE, J. E., R. J. DALEY, AND S. JASPER. 1977. Use of Nuclepore filters for counting bacteria by fluorescent microscopy. Appl. Environ. Microbiol. 33: 1225–1228.

OVERBECK, J., AND R. J. DALEY. 1973. Some precautionary comments on the Romanenko technique for estimating heterotrophic bacterial production. Bull. Ecol. Res. Comm. 17: 342–344.

ROMANENKO, V. I., J. OVERBECK, AND Y. I. SOROKIN. 1972. Estimation of production of heterotrophic bacteria using ^{14}C, p. 82–85. *In* Y. I. Sorokin and H. Kadota [ed.] Microbial production and decomposition in fresh waters. Blackwell Scientific, Oxford.

STAINTON, M. P. 1973. A syringe gas stripping procedure for gas chromatographic determination of dissolved inorganic and organic carbon in freshwater and carbonates in sediment. J. Fish. Res. Board Can. 30: 1441–1445.

STRICKLAND, J. D. H., AND T. R. PARSONS. 1972. A practical handbook of seawater analyses. 2nd ed. Bull. Fish. Res. Board Can. 167: 310 p.

TAKAHASHI, A., K. FUJII, AND T. R. PARSONS. 1973. Simulation study of phytoplankton photosynthesis and growth in the Fraser River estuary. Mar. Biol. 19: 102–116.

VALDES, M., AND L. J. ALBRIGHT. 1981. Survival and heterotrophic activities of Fraser River and Strait of Georgia bacterioplankton within the Fraser River plume. Mar. Biol. 64: 231–241.

Vertical Mixing and its Effects on Phytoplankton Growth in a Turbid Estuary[1]

R. J. UNCLES AND I. R. JOINT

Natural Environment Research Council, Institute for Marine Environmental Research, Prospect Place, The Hoe, Plymouth PL1 3DH, England

UNCLES, R. J., AND I. R. JOINT. 1983. Vertical mixing and its effects on phytoplankton growth in a turbid estuary. Can. J. Fish. Aquat. Sci. 40(Suppl. 1): 221–228.

Using a hydrodynamical model, in conjunction with current meter observations, vertical eddy diffusivities, and associated vertical mixing time-scales are estimated for the Bristol Channel, U.K. In this shallow region, the mixing time-scale appears to be more useful than the commonly employed stratification parameter in assessing the potential for thermal stratification of the water column.

Chlorophyll *a* concentrations in the Bristol Channel are observed to be vertically well-mixed throughout the year. This is shown to be a consequence of the short vertical mixing time-scales in comparison with phytoplankton generation times. These time-scales are of particular importance to phytoplankton in the region because the mixed depth is much greater than the depth of the euphotic zone. Photoinhibition is unlikely to occur in the rapidly mixing water column because phytoplankton cells experience high light conditions for only very short periods. In addition, the rapid mixing does not appear to allow time for photosynthetic adaptation of the phytoplankton population of the Bristol Channel.

Key words: Bristol channel, phytoplankton growth, vertical mixing, vertical eddy viscosity

UNCLES, R. J., AND I. R. JOINT. 1983. Vertical mixing and its effects on phytoplankton growth in a turbid estuary. Can. J. Fish. Aquat. Sci. 40(Suppl. 1): 221–228.

À l'aide d'un modèle hydrodynamique, concurremment avec des observations au courantomètre, nous estimons les propriétés diffusibles des tourbillons verticaux et les périodes de mélange verticaux qui lui sont associées dans le chenal de Bristol (R.-U.). Dans cette région peu profonde, l'échelle temporelle de mélange semble plus utile que le paramètre de stratification communément utilisé pour évaluer le potentiel de stratification thermale de la colonne d'eau.

On constate que les concentrations de chlorophylle *a* dans le chenal de Bristol sont verticalement bien mélangées tout au long de l'année. Nous démontrons que ceci est la conséquence de courtes périodes de mélange vertical, comparativement aux temps de génération du phytoplancton. Ces périodes de mélange sont particulièrement importantes pour le phytoplancton de la région, car la zone mélangée se trouve à une profondeur beaucoup plus grande que la zone euphotique. Il est peu probable qu'il y ait photoinhibition dans la colonne d'eau se mélangeant rapidement, car les cellules phytoplanctoniques rencontrent des conditions de forte intensité lumineuse pendant de courtes périodes seulement. En outre, le mélange rapide ne semble pas donner à la population phytoplanctonique du chenal de Bristol suffisamment de temps pour une adaptation photosynthétique.

Received June 22, 1982
Accepted August 17, 1982

Reçu le 22 juin 1982
Accepté le 17 août 1982

PHYTOPLANKTON respond to variations in light intensity on two different time-scales. A variation in light intensity produces rapid change in the rate of photosynthesis (i.e., a photochemical time-scale); longer term changes in light intensity may induce a physiological response in the algal cell as it accommodates to the new light conditions (a biochemical and physiological time-scale). There have been many studies of the physiological changes induced by varying solar illumination, but it is only recently that the effect of vertical movement within the water column has been investigated (Marra 1978, 1980a). Vertical movement may result in changes in light available to a phytoplankton cell as great as, or greater than, those caused by variation in cloud cover or seasonal and daily irradiance curves. It is particularly important to discount whether the time-scale of vertical mixing is sufficiently long for phytoplankton cells to become biochemically and physiologically adapted to this varying light regime.

[1]This paper forms part of the Proceedings of the Dynamics of Turbid Coastal Environments Symposium convened at the Bedford Institute of Oceanography, Dartmouth, N.S., Canada, September 29–October 1, 1981.

Printed in Canada (J6972)
Imprimé au Canada (J6972)

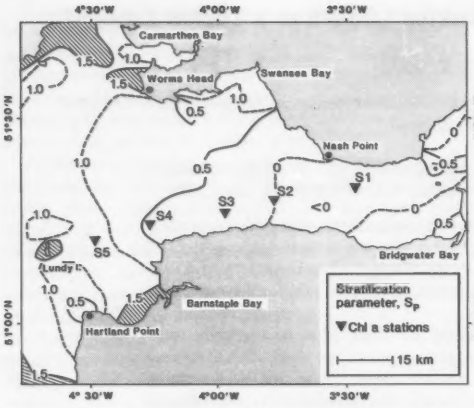

FIG. 1. Stratification parameter, S_p. Areas with $S_p > 1.5$ are hatched. Vertical profiles of chlorophyll *a* were observed at stations S1 to S5 during April 1976.

Recent work suggests that physiological changes which allow cells to adapt to new light regimes may occur over relatively short periods. Marra (1980b), working with a diatom in continuous culture, found a physiological adaptation to reduced irradiance within 10 h. Prezelin and Matlick (1980) found full photosynthetic adaptation within 12 h of a shift from high to low light and a very rapid change, within 3 h, of a chlorophyll *a*–pigment complex. Physiological changes occurring within such short time-scales would be very important processes for inclusion in models of primary production, and at least as important as the effect of diel variations in irradiance. However, there have been few studies of the importance of vertical mixing to phytoplankton, because of the absence of physical models which can be used to set time-scales to the mixing process.

The purpose of this paper is to determine vertical eddy diffusivities and associated time-scales of vertical mixing for the Bristol Channel, which is a large, turbid estuary in the southwest of the U.K. Vertical mixing in this estuary is very relevant to the phytoplankton because the substantial turbidity of the water results in a euphotic zone which is often much shallower than the mixed layer; in the turbid regions of the estuary, phytoplankton are severely light-limited and vertical mixing results in transport from surface light into darkness. Water samples taken from the turbid regions of the Bristol Channel show significant photosynthesis when incubated under simulated in situ conditions, that is under conditions equivalent to a static depth within the water column (Joint and Pomroy 1981). However, as discussed by Joint and Pomroy (1981), the significance of such static light regime incubations is dependent on the time-scale of vertical mixing.

Vertical mixing and stabilization of water on the continental shelf determine the availability of light and nutrients required for phytoplankton growth. A convenient measure of the relative degree of vertical mixing where tidally induced turbulence dominates is given by the Simpson–Hunter stratification parameter, S_p (Simpson and Hunter 1974):

$$S_p = \log_{10}[\rho h/\epsilon], \qquad \text{(c.g.s. units)}$$

where ϵ is the tidally averaged rate at which energy is dissipated by seabed friction, ρ is the density of seawater, and h is the depth of water. S_p has been derived for the case of M_2 tidal flows in the Bristol Channel using a hydrodynamical model (Uncles 1981), and is contoured in Fig. 1. During summer months, the boundary between vertically well-mixed and thermally stratified shelf water is given by $S_p = 1.5$. Regions having $S_p > 1.5$, and which should, therefore, be subject to seasonal stratification, are hatched in Fig. 1. The stratified region in the southwest corner of Fig. 1 extends across the Celtic Sea, and has also been identified in previous theoretical and experimental studies (Fearnhead 1975; Simpson 1976; Pingree 1978). Other regions where $S_p > 1.5$, in Fig. 1, lie in bays and off Lundy Island; however, these areas do not exhibit stratification. This is possibly because of horizontal tidal advection effects, or wind–wave mixing. An alternative explanation is that, despite large values of S_p, the vertical mixing time-scales in these regions are too short to allow stratification to occur. This possibility is examined later. Elsewhere in the Bristol Channel the stratification parameter shows that the water column does not stratify due to summer heating, and that vertical mixing becomes intense as S_p decreases rapidly progressing into the Severn Estuary.

Methods

Vertical mixing depends on the vertical eddy diffusivity, K_z. In the well-mixed water of the Bristol Channel, K_z can be estimated from the vertical eddy viscosity, N_z. Values of N_z are deduced from current meter data obtained at the stations shown in Fig. 2, and are parameterized in terms of local water depth and depth-averaged currents. A numerical model of the depth-averaged M_2 (principal lunar semidiurnal) tide is then used to draw contours of the depth-averaged and tidal cycle-averaged vertical eddy viscosity and vertical mixing time-scale in the Bristol Channel and Severn Estuary (west and east of Nash Point, respectively, in Fig. 2). The numerical model has been verified for the M_2 tide by comparing computed and observed water elevations and currents (Uncles 1981). Data for the elevations were taken from tide-gauge stations shown in Fig. 2.

Vertical Chlorophyll *a* Distributions

Chlorophyll *a* was routinely measured on 64 cruises, covering the Bristol Channel and western Severn Estuary, at all seasons between 1972 and 1980, and was always homogeneously distributed with depth. Vertical profiles of chlorophyll *a* sampled during April 1976 at stations S1 to S5 (see Fig. 1) are shown in Fig. 3A; overall, there were no systematic variations with depth, and the distributions may be considered essentially vertically homogeneous. Simulated in situ, depth-integrated primary production varied from 0.20 mg C fixed$\cdot m^{-2}\cdot h^{-1}$ at S1, to 15 mg C$\cdot m^{-2}\cdot h^{-1}$ at S5. Secchi disc depths, D, for these profiles are also shown in Fig. 3A; D decreased from 6 m at station S5 in the western Bristol Channel (see Fig. 1) to less than 1 m at station S1 in the Severn Estuary, in response to the much higher turbidity of

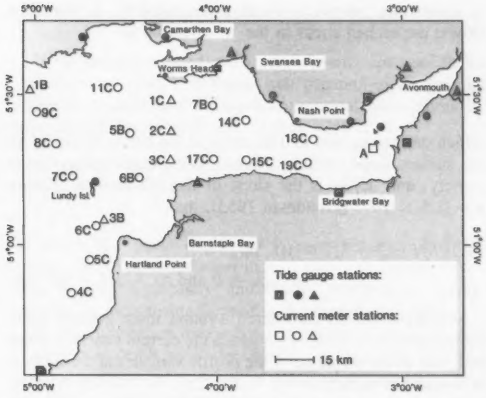

FIG. 2. Locations of tide-gauge stations (■, ●, ▲), and current meter stations (□, ○, △). (■, ●, ▲) denote observations over 15 d, 1 mo, and 1 yr, respectively. (○, △) denote stations at which two or three recording current meters were deployed on a mooring for a few tidal cycles and 1 mo, respectively. A direct reading current meter was used for current profiling over three tidal cycles at station A (□).

the Severn. D is generally a very small fraction of the depth, h. We define a scale depth:

$$h_D = h/D,$$

and a scaled "critical depth":

$$h_{CD} = h_C/D,$$

where h_C is the maximum value of h for which the depth-averaged light intensity is sufficiently high to initiate rapid growth for a homogeneous distribution of phytoplankton. Both h_D and h_{CD} are easily related to the incident light intensity, I_O, and the depth-averaged intensity over the water column, $\bar{I}$. The light intensity at any depth is:

$$I = I_O \exp - (1 - \eta)\kappa h,$$

where η is non-dimensional depth, with $\eta = 0$ at the bed and $\eta = 1$ at the surface, and κ is extinction coefficient, which is related to Secchi disc depth by (Sinclair et al. 1981):

$$\kappa = 1.44/D.$$

The depth-averaged light intensity is:

$$\bar{I} = I_O[1 - \exp(-\kappa h)]/\kappa h \simeq I_O/\kappa h,$$

using $\kappa h = 1.44h/D \gg 1$.

It follows that:

$$h_D = h/D = 0.69I_O/\bar{I}.$$

In a well-mixed water column, rapid production occurs when

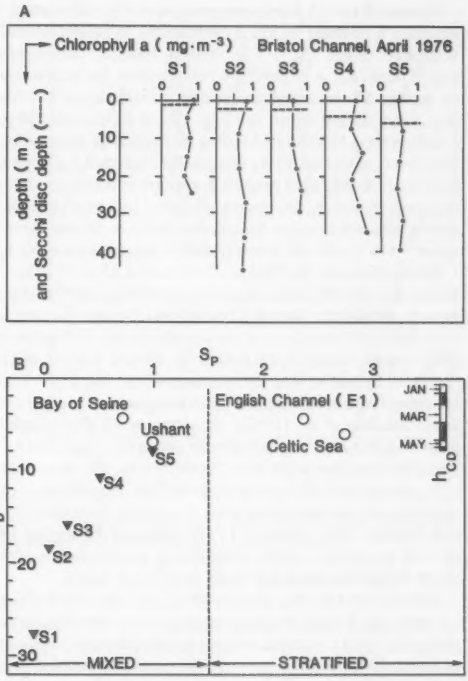

FIG. 3. Vertical profiles of chlorophyll a and the physical conditions governing phytoplankton growth: A, Profiles at stations S1 to S5; B, Stratification parameter, S_p, against scaled depth, h_D, for S1 to S5 and other coastal and shelf stations. Also shown is the scaled critical depth, h_{CD}.

a critical, depth-averaged light intensity is exceeded, $\bar{I}_C$ (Sinclair et al. 1981):

$$\bar{I} > \bar{I}_C \simeq 19\ W\ m^{-2}$$

so that:

$$h_{CD} = h_C/D = 0.69I_O/\bar{I}_C \simeq 3.6 \times 10^{-2}I_O,$$

where I_O has units $W\ m^{-2}$. For a stratified water column, the depth, h, must be taken as the thickness of the surface mixed layer.

Pingree (1978) has shown that the scaled depth and the stratification parameter provide a useful physical framework for a study of processes governing phytoplankton growth. Accordingly, h_D and S_p were plotted in Fig. 3B for stations S1 to S5 and for four stations in the English Channel and Celtic Sea (taken from Pingree 1978, and also applicable to M_2 tides). The diagram divides into either a mixed or seasonally stratified regime according to whether S_p is less than or greater than 1.5. Scaled critical depths (h_{CD}), typical for the area, are shown as approximate values for the months January to mid-June in Fig. 3B.

Stations S1 to S5 form a progression in Fig. 3B: station S5 occupies a position which is comparable to other thermally, vertically mixed ($S_p < 1.5$) coastal stations, although its scaled depth h_D, is slightly greater. Because the scaled depth of station S5 exceeded the scaled critical depth for April ($h_D > h_{CD}$ during April, see Fig. 3B), it follows that phytoplankton were light limited during this period of observations. Moreover, at station S5 h_D marginally exceeded h_{CD} even for mid-June, so that light limitation appears to occur throughout the year; however, the degree of light limitation is reduced during summer because Secchi disc depth at S5 increases to about 10 m (Joint and Pomroy 1981), hence decreasing h_D.

Progressing into the channel from station S5 to S1, Fig. 3B shows that the physical conditions governing phytoplankton growth within the Bristol Channel and Severn Estuary are very different from those generally applicable to coastal and shelf waters, being characterized by intense vertical mixing ($S_p \ll 1.5$) and severe light-limitation ($h_D \gg h_{CD}$). These conditions also seem atypical when compared with other estuaries: Sinclair et al. (1981), in a review of phytoplankton growth cycles in a large number of estuaries, show that h_D is typically less than about five. Nevertheless, the large values of h_D do not preclude primary production. Significant standing stocks of phytoplankton exist throughout the region (Joint and Pomroy 1981; Radford 1981), although the annual production decreases rapidly progressing up-channel — from about 150 to less than 5 g $C \cdot m^{-2} \cdot yr^{-1}$.

Despite the fact that photosynthesis in the eastern Bristol Channel and Severn Estuary can occur only in a thin surface layer ($h_D \gg 1$), vertical mixing is, nevertheless, sufficient to maintain vertical homogeneity of the phytoplankton population (see Fig. 3A). To understand why this is the case, it is necessary to estimate time-scales for vertical mixing (rather than merely compute the thermal stratification parameter) and compare these with cell division times. The following sections are concerned with the derivation of vertical eddy diffusivities arising from tidal currents, and with the estimation of associated mixing time-scales.

Eddy Viscosity

A brief review of available formulations for the vertical eddy viscosity, N_z, is given in Bowden and Hamilton (1975). For vertically mixed conditions the eddy diffusivity, K_z, applicable to tidal flows, can be equated to N_z.

For steady, homogeneous, unidirectional flow in a wide channel of depth h, Rossby and Montgomery (1935) proposed an eddy viscosity of the form:

$$(1) \quad N_z = k_O h u_* \eta(1 - \eta),$$

where k_O is Von Karman's constant (0.41), u_* is friction velocity, h is depth, and η is again the nondimensional depth ($\eta = 0$ at the bed and $\eta = 1$ at the surface); in the absence of surface stress this leads to a logarithmic velocity profile throughout the column. N_z is a quadratic function of depth, with a maximum value, $(N_z)_{max} = k_o u_* h/4$, at mid-depth ($\eta = \frac{1}{2}$), and minimum values, $(N_z)_{min} = 0$, at surface and bed; the depth-mean value is $\bar{N}_z = k_O u_* h/6$. Friction velocity is commonly related to depth-mean velocity, $\bar{u}$, for such flows; the seabed stress in the 'x' direction is:

$$(2) \quad \tau = \rho u_*^2 = \rho k \bar{u}^2 = -\rho h g \frac{\partial \zeta}{\partial x},$$

which defines u_* and k. The stress at the bed is balanced by the surface slope forcing, where g is the acceleration due to gravity, and $\partial\zeta/\partial x$ is the slope of the sea surface. Taking $k = 2.5 \times 10^{-3}$ (Proudman 1953), then:

$$(3) \quad (N_z)_{max} = 5.1 \times 10^{-3} h\bar{u},$$
$$(N_z)_{min} = 0 \text{ and } \bar{N}_z = 3.4 \times 10^{-3} h\bar{u}.$$

McGregor (1972) considered a rather more general logarithmic profile of velocity, in which the current vanishes at the bed, and where the slope of the profile vanishes at the surface in absence of surface stress. In this case the maximum value of N_z again occurs at mid-depth, and the small (but nonzero) minimum values occur at surface and bed.

For tidal flows the definition of N_z is uncertain because of the importance of accelerations in the momentum balance. However, near times of maximum flood or ebb streams in homogeneous water there are indications that a logarithmic, or similar power-law profile is applicable. From a considerable number of observations of tidal streams near their maximum flood and ebb, Van Veen (1938) concluded that:

$$(4) \quad u = \beta \eta^{\delta}$$

where δ varies somewhat according to location, but typically has the value $\delta = 1/5.2$. The eddy viscosity is:

$$(5) \quad N_z = \{\eta^{1-\delta}(1 - \eta)/\delta(1 + \delta)\} \cdot kh\bar{u},$$

which reaches a maximum near mid-depth (at $\eta = 0.45$ for $\delta = 1/5.2$) and a minimum at surface and bed:

$$(6) \quad (N_z)_{max} = 3.1 \times 10^{-3} h\bar{u},$$
$$(N_z)_{min} = 0 \text{ and } \bar{N}_z = 2.1 \times 10^{-3} h\bar{u},$$

using $k = 2.5 \times 10^{-3}$ and $\delta = 1/5.2$.

Dyer (1970), observing current profiles near a dune field, found that up-stream of the dunes the profiles were logarithmic throughout the column, whereas some distance from the field the profiles followed a power law, with $\delta \simeq 1/5$ at high flow rates. Bowden (1967) used observations of tidal currents in homogeneous water to show that the maximum value of N_z occurred near mid-depth during peak streams, and had the value:

$$(7) \quad (N_z)_{max} = 2.5 \times 10^{-3} h\bar{u}.$$

From equations (3), (6), (7), and other investigations, the agreement between coefficients of $(N_z)_{max}/h\bar{u}$ is within a factor of two. Current meter data from the vertically homogeneous Bristol Channel are subsequently used to improve knowledge of this coefficient for the region.

N_z from Bristol Channel Data

If the depth-averaged momentum balance for semidiurnal tides is considered, with the 'x' axis pointing in the direction of the maximum depth-averaged semidiurnal tidal current, $\bar{u}_m$, then at maximum flood (see equation (2)):

$$g\frac{\partial\zeta}{\partial x} = -\frac{k\bar{u}_m{}^2}{h}$$

in which the mean depth, h, is used because maximum streams occur near midwater in an estuary, and where advection, horizontal viscosity, and density gradients are ignored because of their insignificance to the semidiurnal tide.

If the momentum balance is considered now at any nondimensional depth, η, in the column, and if a new 'x' axis is defined to be in the direction of the local maximum current, u_m, then at maximum streaming:

$$g\frac{\partial\zeta}{\partial x} = \frac{1}{h^2}\frac{\partial}{\partial\eta}\left(N_z\frac{\partial u_m}{\partial\eta}\right).$$

Therefore, the equations reduce to those for steady, unidirectional flow provided the orientations of the semidiurnal tidal currents and their phases do not vary appreciably down the column. For most stations in Fig. 2 the differences in current orientation and phase through the column are less than 4°; at the western, seaward end of the Bristol Channel, however (stations 6C, 7C, 8C, and 9C), the differences can be in the range 10°−20°. Nevertheless, there is reasonable indication from those stations where three or more observations were made (see Fig. 4), that a logarithmic profile is applicable near times of maximum streaming, although such data can be made to fit a power law of Van Veen form, equation (4), equally well. For the remaining stations in Fig. 2 only two observations were made down the column, so that these fit exactly any two-parameter representation of the profile.

If the data are fitted to equation (4), with an eddy viscosity of the form of equation (5), then the results are (using 95% confidence intervals):

$$\delta = 1/(5.2 \pm 0.3)$$

in agreement with Van Veen's (1938) data. The maximum value of N_z occurs at $\eta = 0.45 \pm 0.03$, which with $k = 2.5 \times 10^{-3}$ gives:

$$(8)\quad (N_z)_{\max} = (3.3 \pm 0.5) \times 10^{-3}h\bar{u}_m,\ (N_z)_{\min} = 0,$$

and $$\bar{N}_z = (2.3 \pm 0.3) \times 10^{-3}h\bar{u}_m.$$

This result is not significantly different from either equation (6), or from results obtained by fitting a logarithmic profile of McGregor's (1972) form to the data. Therefore, at maximum tidal streams, the vertical mixing deduced from data fitted to logarithmic or power law profiles in the Bristol Channel is essentially the same as that predicted from data presented by Van Veen (1938) for the Straits of Dover, and for areas in the neighborhood of the Dutch coast.

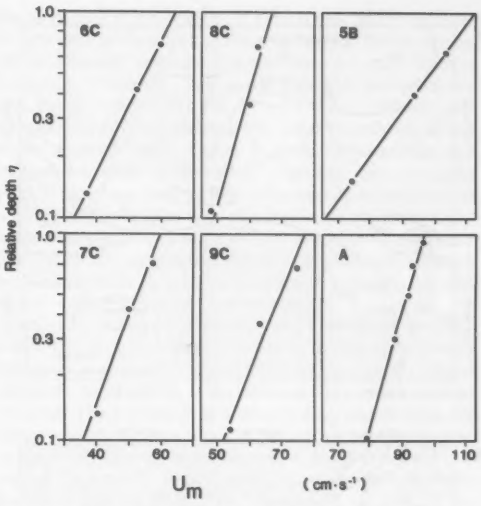

FIG. 4. Maximum semidiurnal tidal currents, u_m, against nondimensional depth. See Fig. 2 for station positions.

Tidal Averages and Vertical Mixing

Equation (8) for N_z applies during maximum streams, and is based on the assumption that a power law profile is applicable throughout the column. During other times in the tidal cycle, N_z may have a very different profile shape from that predicted by equation (5), and will also probably have smaller values at lower current speeds. Therefore, in estimating an effective N_z over a tidal cycle with the limited data available, it seems reasonable to ignore vertical variations in N_z and consider an instantaneous depth mean value of the form (see equation (8)):

$$\bar{N}_z = 2.3 \times 10^{-3}h|\bar{u}| = 2.3 \times 10^{-3}h\bar{u}_m|\sin\omega t|,$$

where ω is the semidiurnal tidal angular frequency, and where tidal currents are taken to be rectilinear for this region (Uncles 1981). The average value over a tidal cycle is:

$$(9)\quad \langle\bar{N}_z\rangle = 1.5 \times 10^{-3}h\bar{u}_m,$$

which is contoured in Fig. 5A for the case of M_2 tidal streams. Values range from 100 $cm^2 \cdot s^{-1}$ in the shallow bays where currents are low, to 700 $cm^2 \cdot s^{-1}$ in the region of intense tidal streaming and moderately deep water near Nash Point.

A time-scale for vertical mixing can now be derived from equation (9) by assuming that "Reynolds analogy" holds in the vertically homogeneous water of the Bristol Channel, so that the vertical eddy diffusivity, K_z, equals N_z. Ignoring vertical variations in K_z, then a typical time-scale for complete mixing of a passive tracer released from mid-depth is (Fischer et al. 1979):

$$T = 0.1h^2/\langle\bar{K}_z\rangle.$$

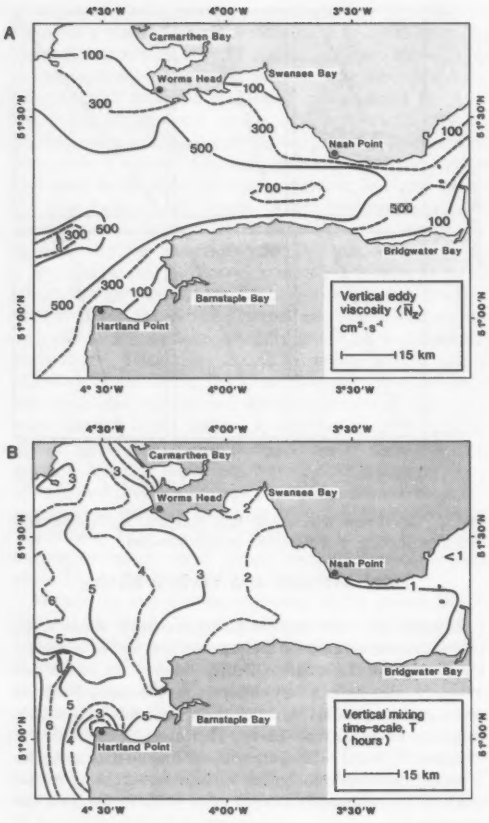

FIG. 5. Vertical eddy viscosity and vertical mixing times: A, $\bar{N}_z$ ($cm^2 \cdot s^{-1}$); B, Time-scale, T(hours).

However, because phytoplankton photosynthesis occurs in a thin layer near the surface (see Fig. 3A), it is more appropriate to investigate the time-scale for complete mixing of a passive tracer released at the surface, which is:

$$(10) \quad T = 0.4h^2/\langle \bar{K}_z \rangle = 2.7 \times 10^2 h/\bar{u}_m,$$

using equation (9). This time-scale is contoured in Fig. 5B. In the Severn Estuary the mixing time is between 1 and 2 h. Progressing down-channel, T increases, exceeding 7 h in the southwest of the region where seasonal stratification can occur. This time-scale is an effective value over a tidal cycle; naturally, at peak currents the mixing will be faster than depicted in Fig. 5B, and near slack water it will be slower (see later).

Discussion

During maximum tidal streams, the vertical eddy viscosity deduced from current meter data in the Bristol Channel and Severn Estuary has a similar form, and magnitude, to that observed for other shallow, well-mixed coastal regions. The associated time-scales for vertical mixing in the Channel, T (equation (10) and Fig. 5B), can be compared with the stratification parameter, S_p, in Fig. 1. The Celtic Sea front, a segment of which is shown in the southwest corner of Fig. 1, occurs at $T \sim 8$ h. Plotting T for the whole of the northwest European shelf (using modeled currents and depth data supplied by R. D. Pingree, personal communication) shows that the observed seasonal frontal regions on the shelf occur for mixing time-scales between 8 to 12 h. No attempt has been made to define a "critical" T at which fronts develop. On this basis, one would expect the short mixing time-scales in Carmarthen Bay and Barnstaple Bay (less than about 5 h, see Fig. 5B) to result in vertically homogeneous conditions, as was observed. S_p (Fig. 1) indicates that stratification can occur in these bays, which suggests that, in shallow water at least, the mixing time-scale may be a more useful indicator of stratification than S_p.

This paper has shown the physical reason for the observed homogeneous distribution of phytoplankton within the water column of the Bristol Channel. Even at the seaward end of the Channel, where the euphotic zone may be 15 m deep or more, tidally induced mixing has a time-scale of the order of 5 h; this is significantly less than the generation time of phytoplankton. We have no measurements of carbon:chlorophyll a ratios for Bristol Channel phytoplankton that would allow us to calculate precise cell division times. Nevertheless, a reasonable value to assume for the carbon:chlorophyll a ratio is 25. Dividing the depth-integrated chlorophyll a concentrations at stations S1 and S5 by the respective rates of primary production, gives doubling times of the order of 70 d at the turbid station, S1, and one day at S5. A cell division time of 1 d is comparable with that found from a number of other investigations, and is supported by work with cultures of phytoplankton (Brand and Guillard 1981). Therefore, even at station S5, generation times are much longer than the vertical mixing time-scales in the Bristol Channel, and there is no possibility of a chlorophyll maximum developing at any depth in the water column.

Consideration should also be given to whether sinking of phytoplankton cells can affect the vertical distribution in this estuary. Bienfang (1981) observed sinking rates for natural populations of temperate phytoplankton in a CEPEX bag; these were in the range 0.32–1.69 $m \cdot d^{-1}$, and the mean sinking rate, w, was 0.64 $m \cdot d^{-1}$ (7×10^{-4} $cm \cdot s^{-1}$). Walsby and Reynolds (1980) have briefly reviewed a number of models which take into account the effects of sinking in the presence of vertical mixing. If growth and decay are ignored, and if the phytoplankton concentration, P, is in a steady-state, then a balance exists between sinking and mixing in the form (Walsby and Reynolds 1980, p. 400):

$$\langle \bar{K}_z \rangle \frac{\partial^2 P}{\partial \eta^2} + hw \frac{\partial P}{\partial \eta} = 0,$$

which has the solution:

$$P = P_O \exp(-hw\eta/\langle \bar{K}_z \rangle),$$

where P_O is the concentration at the bed ($\eta = 0$). The relative surface ($\eta = 1$) to bed difference in concentration is thus:

$$\delta P/P_O = -1 + \exp(-hw/\langle\bar{K}_z\rangle) \simeq -0.4\%$$

using $w = 7 \times 10^{-4}$ cm·s^{-1}, $h \simeq 30m$, and $\langle\bar{K}_z\rangle \simeq 500$ cm^2·s^{-1} as typical values for the region (see Fig. 5A). The effects of sinking are thus negligible in the presence of this intense vertical mixing.

It is of interest to enquire how phytoplankton achieve net production in the severely light-limited conditions that exist in the turbid region of the Bristol Channel. Joint and Pomroy (1981) estimated the yearly averaged primary production in this region to be only 6.8 g C·m^{-2}·yr^{-1}. The observed low production at station S1, coupled with the estimated doubling time of about 70 d, implies that only marginally more energy is assimilated by the phytoplankton than is needed to meet the maintenance energy requirement. Moreover, this long doubling time means that advection and dispersion by currents effectively determines phytoplankton concentrations in this region. In deriving estimates of primary production, Joint and Pomroy (1981) assumed that the depth-integrated production for a well-mixed water column was equivalent to the integration of a number of static-depth incubations. Support for this assumption comes from Platt and Gallegos (1980) and Gallegos and Platt (1982), who attempted to simulate the effect of vertical motion on photosynthesis using a conceptual model and an analogue incubation technique. They concluded that vertical mixing has very little quantitative effect on primary production in the column. However, they were considering the Canadian Arctic, where the surface mixed layer is shallower than the euphotic zone. The opposite situation applies in the Bristol Channel, and further work is required to study the effect of vertical mixing (with time-scales determined in this paper) on estimates of depth-averaged primary production in a turbid water column.

Such rapid mixing times have obvious implications for phytoplankton physiology. With time-scales of 5 h or less, physiological changes of the type described by Marra (1980b), and Prezelin and Matlick (1980), are unlikely to occur in the Bristol Channel. Photoinhibition is also unlikely to occur in a well-mixed water column, because of the short time that phytoplankton cells are in high light levels. Marra (1978) found an enhancement of integral photosynthesis in incubations when bottles were moved vertically when compared with bottles incubated at fixed depths; part, but not all, of this enhancement was assumed to be due to the absence of photoinhibition in the vertically cycled bottles. Generally, Joint and Pomroy (1981) could not detect photoinhibition in surface incubations of less than 2 h, although photoinhibition sometimes occurred within this time-scale on summer days with very high irradiance. Therefore, for a well-mixed water column, simple models of primary production may be appropriate; models of the type recently derived to describe both the linear and the photoinhibited part of the photosynthesis irradiance curve (Platt et al. 1980) may be unnecessarily complex.

In the Bristol Channel, vertical mixing brings phytoplankton cells from darkness into high irradiance in a random way, and processes other than photosynthesis may be important for the survival of phytoplankton. If a cell is only briefly exposed to light once an hour, as may occur in the most turbid regions of the Channel, respiratory losses from the cells become important. Intuitively, one would expect a phytoplankton cell that is exposed to light for only a few minutes each hour to have difficulty in surviving, yet the population seems viable — water samples taken from the turbid estuary and incubated at constant light show substantial rates of carbon fixation (Joint and Pomroy 1981). We have no information on whether phytoplankton from this region are physiologically adapted to long periods in the dark by alteration of respiration rate, but clearly maintenance requirements of the cells are met by brief exposure to light; the population remains viable and able to exploit longer exposure to light.

Individual cells may experience longer periods of illumination if they are in the euphotic zone at slack tide, when vertical mixing is negligible; however, they will be quickly mixed within the water column as the tide turns and currents increase in speed. The population as a whole cannot benefit from the longer periods of illumination at the surface because the rest of the population will spend longer in darkness at times of low mixing. In general, vertical mixing is more rapid than that shown in Fig. 5B (time-scale less than T) for 60% of the time. Mixing time-scales are less than $2T$ for 80% of the time, and less than $3T$ for 90% of the time. On hot, windless days at slack water, it is possible that stabilizing temperature gradients might form just beneath the surface, but these would escape detection on the scale of our observations. In any event, such gradients would have a small effect on the water column as a whole; and would rapidly decrease with increasing current speed.

Finally, there appears to be no photosynthetic adaptation of the phytoplankton population of the Bristol Channel. Demers and Legendre (1982) suggest that increased vertical mixing in an estuarine water column results in a lower assimilation number (P'_{max}). Nevertheless, P'_{max} values determined in the turbid region of the Bristol Channel, with mixing times of 1 h or less, are not significantly different from those in regions with euphotic depths in excess of 10 m, and with mixing times longer than 5 h (I. R. Joint unpublished data). However, the degree of vertical mixing occurring in the Bristol Channel is greater than that studied by Demers and Legendre (1982), and differences in physiological adaptation may only be obvious in regions with a wider range of vertical mixing than is found in the Bristol Channel. Such regions would include partially mixed estuaries in which vertical stratification (and thus the stability of the water column) depends strongly on freshwater inputs, as well as tidal currents (Bowden 1967).

Acknowledgments

This work, which forms part of the estuarine ecology programme of the Institute for Marine Environmental Research, a component of the Natural Environment Research Council (NERC), was partly supported by the Department of the Environment on Contract No DGR 480/48.

BIENFANG, P. K. 1981. Sinking rates of heterogeneous temperate phytoplankton populations. J. Plankton Res. 3: 235–253.

BOWDEN, K. F. 1967. Stability effects on turbulent mixing in tidal

currents. Phys. Fluids Suppl., p. 278–280.

BOWDEN, K. F., AND P. HAMILTON. 1975. Some experiments with a numerical model of circulation and mixing in a tidal estuary. Estuarine Coastal Mar. Sci. 3: 281–301.

BRAND, L. E., AND R. R. L. GUILLARD. 1981. The effects of continuous light and light intensity on the reproduction rates of twenty-two species of marine phytoplankton. J. Exp. Mar. Biol. Ecol. 50: 119–132.

DEMERS, S., AND L. LEGENDRE. 1982. Water column stability and photosynthetic capacity of estuarine phytoplankton: Long-term relationships. Mar. Ecol. Prog. Ser. 7: 337–340.

DYER, K. R. 1970. Current velocity profiles in a tidal channel. Geophys. J. R. Astr. Soc. 22: 153–161.

FEARNHEAD, P. G. 1975. On the formation of fronts by tidal mixing around the British Isles. Deep Sea Res. 22: 311–321.

FISCHER, H. B., E. J. LIST, R. C. Y. KOH, J. IMBERGER, AND N. H. BROOKS. 1979. Mixing in inland and coastal waters. Academic Press, New York, NY. 484 p.

GALLEGOS, C. L., AND T. PLATT. 1982. Phytoplankton production and water motion in surface mixed layer. Deep Sea Res. 29: 65–76.

JOINT, I. R., AND A. J. POMROY. 1981. Primary production in a turbid estuary. Estuarine Coastal Shelf Sci. 13: 303–316.

MARRA, J. 1978. Phytoplankton photosynthetic response to vertical movement in a mixed layer. Mar. Biol. 46: 203–208.

1980a. Vertical mixing and primary production, p. 121–137. *In* P. G. Falkowski [ed.] Primary productivity in the sea. Plenum Press, New York, NY.

1980b. Time course of light intensity adaptation in a marine diatom. Mar. Biol. Lettr. 1: 175–183.

MCGREGOR, R. C. 1972. The influence of eddy viscosity on the vertical distribution of velocity in the tidal estuary. Geophys. J. R. Astr. Soc. 29: 103–108.

PINGREE, R. D. 1978. Mixing and stabilization of phytoplankton distributions on the northwest European continental shelf, p. 181–220. *In* J. H. Steele [ed.] Spatial pattern in plankton communities. Plenum Press, New York, NY.

PLATT, T., AND C. L. GALLEGOS. 1980. Modelling primary production, p. 339–362. *In* P. G. Falkowski [ed.] Primary productivity in the sea. Plenum Press, New York, NY.

PLATT, T., C. L. GALLEGOS, AND W. G. HARRISON. 1980. Photoinhibition of photosynthesis in natural assemblages of marine phytoplankton. J. Mar. Res. 38: 687–701.

PREZELIN, B. B., AND H. A. MATLICK. 1980. Time course of photoadaptation in the photosynthesis–irradiance relationship of a dinoflagellate exhibiting photosynthetic periodicity. Mar. Biol. 58: 85–96.

PROUDMAN, J. 1953. Dynamical oceanography. Methuen. 409 p.

RADFORD, P. J. 1981. Modelling the impact of a tidal power scheme on the Severn Estuary ecosystem, p. 235–247. *In* W. J. Mitsch, R. W. Bosserman, and J. M. Klopatek [ed.] Energy and ecological modelling. Elsevier Scientific Pub. Co., Amsterdam.

ROSSBY, C. G., AND R. B. MONTGOMERY. 1935. The layer of frictional influence in wind and ocean currents. Pap. Phys. Oceanogr. Meteorol. 3(3): 1–101.

SIMPSON, J. H. 1976. A boundary front in the summer regime of the Celtic Sea. Estuarine Coastal Mar. Sci. 4: 71–81.

SIMPSON, J. H., AND J. R. HUNTER. 1974. Fronts in the Irish Sea. Nature 250: 404–406.

SINCLAIR, M., D. V. SUBBA RAO, AND R. COUTURE. 1981. Phytoplankton temporal distributions in estuaries. Oceanol. Acta 4: 239–246.

UNCLES, R. J. 1981. A numerical simulation of the vertical and horizontal M_2 tide in the Bristol Channel and comparisons with observed data: Limnol. Oceanogr. 26: 571–577.

VAN VEEN, J. 1938. Water movements in the Straits of Dover. J. Cons. Int. Explor. Mer 13: 7–36.

WALSBY, A. E., AND C. S. REYNOLDS. 1980. Sinking and floating. *In* I. Morris [ed.] The physiological ecology of phytoplankton. Studies in ecology, Vol. 7. Blackwell. 625 p.

Primary Production and Respiration in Pelagic and Benthic Communities at Two Intertidal Sites in the Upper Bay of Fundy[1,2]

B. T. HARGRAVE, N. J. PROUSE, G. A. PHILLIPS, AND P. A. NEAME

Department of Fisheries and Oceans, Marine Ecology Laboratory, Ocean Sciences and Surveys, Bedford Institute of Oceanography, P.O. Box 1006, Dartmouth, N.S. B2Y 4A2

HARGRAVE, B. T., N. J. PROUSE, G. A. PHILLIPS, AND P. A. NEAME. 1983. Primary production and respiration in pelagic and benthic communities at two intertidal sites in the upper Bay of Fundy. Can. J. Fish. Aquat. Sci. 40(Suppl. 1): 229–243.

Primary production by microalgae on intertidal sediments during ebb tide at two sites in Cumberland and Minas Basin, Bay of Fundy, amounted to 47–83 g $C \cdot m^{-2} \cdot yr^{-1}$. Phytoplankton production measured during flood tide over intertidal sediments in Cumberland Basin varied from 4–10 g $C \cdot m^{-2} \cdot yr^{-1}$ with respiration in the water column between 6 and 12 g $C \cdot m^{-2} \cdot yr^{-1}$ depending on concentrations of suspended matter. Respiration by undisturbed sediments (47–62 g $C \cdot m^{-2} \cdot yr^{-1}$) was measured at both locations to estimate aerobic metabolic consumption of organic matter.

Maximum rates of benthic primary production occurred during early and late summer at both locations but values at the Cumberland Basin sites were two to three times greater than those observed in Minas Basin. Chlorophyll *a* in surface sediments was also lower at the stations in Minas Basin where coarser grained deposits reflect extensive sediment transport. Annual benthic respiration at the two stations in Cumberland Basin, however, was only slightly greater than that at four stations in Minas Basin. *Spartina* marshes, phytoplankton, and benthic microalgae may provide supplies of organic matter for aerobic consumption in these intertidal sediments which are more similar than are measures of benthic primary production.

Key words: benthic microalgae, primary production, intertidal community metabolism, Bay of Fundy

HARGRAVE, B. T., N. J. PROUSE, G. A. PHILLIPS, AND P. A. NEAME. 1983. Primary production and respiration in pelagic and benthic communities at two intertidal sites in the upper Bay of Fundy. Can. J. Fish. Aquat. Sci. 40(Suppl. 1): 229–243.

La production primaire par les micro-algues sur les sédiments intertidaux au moment du jusant à deux sites des bassins de Cumberland et des Mines, dans la baie de Fundy, est de 47–83 g $C \cdot m^{-2} \cdot an^{-1}$. La production phytoplanctonique mesurée pendant le flot sur les sédiments intertidaux du bassin de Cumberland varie de 4–10 g $C \cdot m^{-2} \cdot an^{-1}$, la respiration dans la colonne d'eau variant entre 6 et 12 g $C \cdot m^{-2} \cdot an^{-1}$ selon les concentrations de matière en suspension. Nous avons mesuré la respiration de sédiments non dérangés (47–62 g $C \cdot m^{-2} \cdot an^{-1}$) aux deux endroits afin d'estimer la consommation métabolique aérobie de matière organique.

Les taux de production primaire benthique les plus élevés se rencontrent au début et à la fin de l'été aux deux endroits, mais les valeurs du bassin de Cumberland sont de deux à trois fois plus élevées dans celles du bassin des Mines. La chlorophylle *a* dans les sédiments superficiels est également inférieure aux stations du bassin des Mines, où des dépôts de particules plus grosses reflètent un transport intensif de sédiments. La respiration benthique annuelle aux deux stations du bassin de Cumberland n'est toutefois que légèrement supérieure à celle des quatre stations du bassin des Mines. Les marais de *Spartina*, le phytoplancton et les micro-algues benthiques peuvent être une source de matière organique pour consommation aérobie dans ces sédiments intertidaux, plus semblables que ne le sont les mesures de production primaire benthique.

Received October 14, 1981
Accepted June 18, 1982

Reçu le 14 octobre 1981
Accepté le 18 juin 1982

[1]This paper forms part of the Proceedings of the Dynamics of Turbid Coastal Environments Symposium convened at the Bedford Institute of Oceanography, Dartmouth, N.S., Canada, September 29–October 1, 1981.
[2]BIO Contribution.

Printed in Canada (J6670)
Imprimé au Canada (J6670)

ALTHOUGH there have been several estimates of benthic primary production in various marine intertidal locations (Pomeroy 1959; Pamatmat 1968; Steele and Baird 1968; Leach 1970; Cadée and Hegeman 1974a, 1977; Van Raalte et al. 1976; and Van Es 1977), only one study (Joint 1978) has simultaneously measured annual primary production in the water column and on exposed intertidal sediments. Also, Pomeroy (1959), Pamatmat (1968), and Hartwig (1978) measured changes in dissolved oxygen in light and dark chambers placed over the sediment to simultaneously estimate gross production by benthic microalgae and benthic respiration. Other studies, which have utilized ^{14}C uptake as a measure of primary production, have not quantified both gross production and community respiration. Understanding of the dynamics of organic matter production and utilization requires that these measurements be made simultaneously.

This paper describes in situ measurements of primary production and respiration in the water column and on intertidal sediments in Cumberland and Minas Basin in the Bay of Fundy. Both of these sites are within regions of the Bay of Fundy identified as having potential for tidal power development (Gordon and Longhurst 1979). No information concerning rates of primary production by either phytoplankton or benthic microalgae existed for these areas. Measurements of ^{14}C uptake were used to quantify rates of phytoplankton production at the Cumberland Basin site where high turbidity severely limits light penetration. In situ oxygen production and uptake in undisturbed light and dark cores of sediment and incubation of surface sediment resuspended in oxygenated water provided estimates of gross and net primary production by microalgae in the sediment, benthic respiration, and potential respiration in the water column.

Materials and Methods

STUDY SITES

The upper reaches of the Bay of Fundy extend inland as two large embayments — Chignecto Bay to the north, Minas Basin to the south. Two intertidal locations [Anthony Park on the south side of Cobequid Bay — an eastern extension of Minas Basin, described in Hargrave (1978) and Pecks Cove on the northwest side of Cumberland Basin — a northeastern extension of Chignecto Bay, described in Gordon et al. (1980)] were visited at irregular frequencies (from weekly during the summer to once every 4–8 wk during winter) between May 1977 and October 1980. Ice prevented sampling in January and February each year. A transect of four stations at 50-m intervals from mean high water (15 m above chart datum) was established at Anthony Park as described in Hargrave (1978). Two stations, one near the upper intertidal zone approximately 50 m beyond the lower edge of a *Spartina alterniflora* marsh (Station A) and a second 100 m further down the intertidal zone (Station C), were used to conduct experiments at Pecks Cove. Both of these stations were approximately 10 m above chart datum.

Sediments at both locations consisted of well-sorted coarse to medium silt (mean grain size of 10–30 μm) within and below a fringing *Spartina* marsh. A wharf at Anthony Park has apparently created an area where sediment deposition is enhanced since the distribution of silt and *Spartina* is restricted to the eastern side of the wharf. Three of the intertidal sites at Anthony Park were located adjacent to the wharf (13 m above chart datum) with the fourth station in coarser sand 50 m further along the transect (12 m above chart datum).

Both locations experience large tides (11–14 m) with a mean tidal range near Anthony Park of 11.7 m. Water covered the intertidal stations at Anthony Park for 2–5 h (Station 1 and 4) at each high tide while Station A at Pecks Cove was flooded for 4 h during each tide (average of spring and neap cycles). Highest current velocities occur over the outer portions of both intertidal flats where silt deposits grade to fine-sand sediments. Sand ripples and waves are present in the lower intertidal zone of both sites. Those at Anthony Park are more extensive indicative of the high velocity of tidal currents present in this region of Minas Basin (Dalrymple et al. 1975). In the upper intertidal zone, however, a soft sediment layer from 5 to 10 cm thick with a high water content (40–50%) (E. MacDormand, unpublished data) overlies a compact subsurface layer with lower water content (≈30%) (Andrews 1980). Physical characteristics of the intertidal areas have been described in greater detail in Hargrave (1978) and Gordon et al. (1980).

PLANKTONIC AND BENTHIC MICROALGAL PRIMARY PRODUCTION

Phytoplankton production was measured at Pecks Cove using the conventional ^{14}C method described in Strickland and Parsons (1972). Water was collected from the well-mixed water column during a rising tide with sampling days chosen so that high tide occurred near noon. Water was used to fill 125 mL bottles, without filtering and 5 μCi of $H^{14}CO^{-3}$ was added to each bottle. Three light and one dark bottle were suspended in situ during the period of flood tide (2–4 h) at 0, 0.5, and 1 m depth. Turbidity usually limited light penetration at 1 m to a few percent of surface flux. A relationship between suspended particulate matter concentration and light penetration was derived to permit conversion of measurements of production carried out only at the surface at Pecks Cove during 1979 to an integral value over 1 m depth calculated from measurements made at three depths over 1 m during 1980. No measurements of phytoplankton production were carried out at Anthony Park.

Contents of all bottles were filtered immediately after the end of the exposure period onto Millipore 0.45 μm pore diameter filters, rinsed with 5 mL filtered seawater and placed directly into glass scintillation vials containing 10 mL of Aquasol-2 (New England Nuclear). Fuming filters over HCL in a dessicator did not alter counts on filters and so rinsing was assumed to have removed unfixed ^{14}C. Counts from a Beckman liquid scintillation counter were corrected for quenching with the channels ratio method (counting efficiency 75–90%) and net carbon fixation (mg $C \cdot m^{-2} \cdot h^{-1}$) calculated as the difference between light and dark bottles (Strickland and Parsons 1972).

Preliminary measurements of oxygen production and uptake in gas trapped within capped light and dark cores, by taking time series samples with gas-tight syringes for injection

into a Fisher–Hamilton gas partitioner, showed that rates of oxygen production and consumption were similar ($P > 0.05$) to those determined by simultaneous in situ incubation of water-filled cores. Except for several experiments at Pecks Cove in 1979 initiated just before the intertidal area was flooded for 4 h, experiments were usually begun shortly after exposure when a film of water was still present at the sediment surface. Fine sand at station 4 at Anthony Park drained rapidly and water was never present before cores were inserted. All measurements described here were made with water covering the sediment surface and effects of drying on prolonged exposure to air were not considered.

Measurements of changes in dissolved oxygen in water contained in plexiglass cores (5.5 cm diameter) pressed into intertidal sediments, described by Neame in Hargrave (1978), were used to calculate gross epibenthic primary production. In each experiment, at least three clear and three dark (tape and foil wrapped) cores were pushed 10 cm into the sediment to leave a 1–4 cm head space. Filtered seawater which had been cooled to below ambient temperature was gently bubbled with nitrogen to lower dissolved oxygen concentrations to 70–80% of saturation before siphoning onto sediment contained in cores. This treatment reduced the problem of supersaturation and bubble formation which may arise when oxygen is produced by photosynthesis in light-exposed cores (Hunding and Hargrave 1973). Cores were capped with tight-fitting clear plexiglass lids and sealed with Vaseline to avoid air bubbles after making initial measurements of dissolved oxygen (sensitivity 0.1 mg $O_2 \cdot L^{-1}$) and temperature (sensitivity 0.2°C) using a portable oxygen meter (54A Yellow Spring Instruments). Exposure periods varied (between 30 min during mid-summer to 2 h during late fall and winter months) after which lids were removed from cores and a final measurement of dissolved oxygen and temperature made.

Experiments at Pecks Cove during 1980 were used to quantify relationships between incident light and primary production by benthic microalgae. Four or five groups of five cores each were incubated simultaneously with tinted plexiglass shade covers used to vary the amount of incident radiation reaching the sediment (70, 20, 14, and 1%). Three separate dark cores were also incubated to measure total oxygen uptake. The quantum sensor, described below, was placed within clear plexiglass cores in several experiments with different intensities and angles of incident radiation. Cores with lids transmitted an average of 86% of incident light. Estimates of photosynthetically available light in all cores were corrected for this decrease.

Water in cores was not stirred during experiments. Experiments to quantify effects of water circulation within cores, described below, showed that oxygen production in light exposed cores was unaltered by stirring. Water volume (usually 20–40 mL) was estimated in each core by multiplying the depth of water measured to the nearest millimetre with a plastic ruler by 25.5 (the cross-sectional core area in cm^2). Values were within 8% of those determined by actual volume measurement. Changes in oxygen produced or consumed were calculated on an hourly and m^{-2} basis. Gross oxygen production was calculated as the average value of oxygen produced in cores exposed to light plus the mean of total oxygen consumed in dark cores calculated as mg $O_2 \cdot m^{-2} \cdot h^{-1}$. Oxygen production was converted to carbon assimilation by assuming P.Q. = 1.0 and multiplying by 0.375 (Strickland and Parsons 1972). Although photosynthetic quotients are variable, the presence of inorganic nitrogen as ammonia in interstitial pore water (discussed below) implies that nitrate would not be preferentially utilized. A P.Q. value of 1.0 is reasonable if nitrate is not reduced during photosynthesis (Ryther 1956).

Oxygen Uptake in the Water Column and by Sediment

Plexiglass cylinders (internal diam 3.1 cm, height 31 cm) fixed 1 m above the sediment over one flood-ebb tidal cycle (4 h) were used to collect settled particles from the water column. Aliquots of this material were added to glass stoppered flasks (30 mL) filled with filtered seawater and used for measurements of oxygen uptake in the laboratory as described in Hargrave (1978). Control flasks (without sediment) and replicate flasks with sediment filled with a 1% buffered formalin solution (equilibrated for 24 h) were used to meaure chemical oxygen demand. Flasks were rotated at 30 rpm in the dark at 3–5°C during the winter and 18–20°C during summer months for at least 24 h. Changes in dissolved oxygen, calculated as the difference between initial and final measurement using a Radiometer Blood Gas Analyzer (sensitivity 0.1 mg $\cdot L^{-1}$), were expressed g^{-1} dry weight of sediment.

Concentrations of particulate matter in suspension during the flood–ebb tidal cycle were measured by filtering water samples, collected by a pump at Pecks Cove with an intake fixed 10 cm above the sediment or by water bottles, through preweighed filters. Oxygen uptake in the water column at Pecks Cove (Station A) was calculated over 4 h for comparison with phytoplankton production by multiplying the sediment weight-specific consumption by the total concentration (per m^2) of particulate matter suspended through the water column (approximately 2–4 m during neap and spring tides, respectively). No vertical concentration gradients in the well-mixed column were ever observed. Particulate matter filtered from water samples was used for chlorophyll *a* and organic carbon analysis as described below.

Oxygen uptake of undisturbed sediments as mg $O_2 \cdot m^{-2} \cdot h^{-1}$ was separated into biological respiration and chemical oxidation. Six darkened cores, three with filtered water and three with filtered seawater containing 1% buffered formalin, were incubated during periods of exposure of the sandflats simultaneously with transparent cores used to measure oxygen production. Aluminum foil, used to cover cores after caps were put in place, prevented temperature increase caused by solar heating. Incubation times were identical to or shorter than those for cores exposed to the light. Prolonged incubations of more than a few hours during summer caused oxygen depletion (>30%) and resulted in reduced rates of uptake. Incubation times were adjusted throughout the year so that oxygen depletion in dark cores did not exceed this value. Incubation of cores over short (1–2 h) periods throughout the day with all cores filled with filtered seawater did not show any periodicity in uptake rates nor were these significantly different before and after flood tide. Thus, hourly rates were multiplied by 24 to calculate daily totals. A respiratory quotient to 1.0 was assumed to convert measures of oxygen

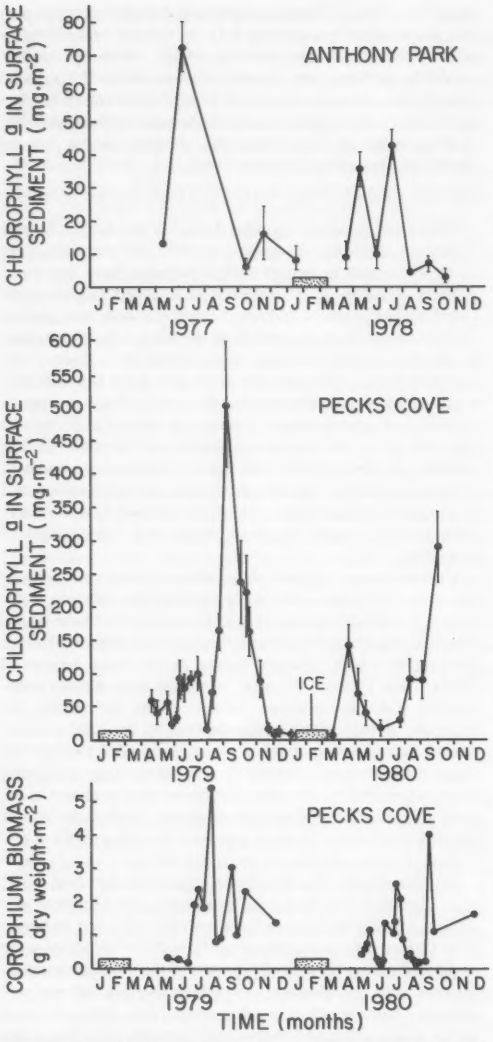
ANTHONY PARK
CHLOROPHYLL a IN SURFACE SEDIMENT (mg·m⁻²)
J F M A M J J A S O N D J F M A M J J A S O N D
1977
1978
PECKS COVE
ICE
1979
1980
COROPHIUM BIOMASS (g dry weight·m⁻²)
TIME (months)

FIG. 1. Seasonal changes in chlorophyll *a* in surface (upper 2 mm) sediment at Anthony Park (station 3) and Pecks Cove (station A) during consecutive years. *Corophium volutator* biomass (to 5 cm depth) measured only at Pecks Cove. Vertical lines represent + 1 SD of average chlorophyll *a* measurements determined from five replicate samples. Values for *Corophium* biomass (provided by C. Hawkins and D. Peer) are derived from two to five measurements.

uptake (corrected for chemical demand) to carbon respired (mg O_2 consumed $h^{-1} \times 0.375$ = mg C respired h^{-1}).

TEMPERATURE AND SOLAR RADIATION

Air, surface sediment, and flood tide water temperature were recorded with a glass hand-held thermometer (sensitivity 0.1°C) at various times during each sampling day. The temperature probe on the portable oxygen meter (accuracy 0.2°C) was used to record water temperature in each core before and after incubation. Incident solar radiation was recorded continuously during in situ production experiments. A Li-Cor underwater quantum sensor (Li-192S) measuring photosynthetically available radiation (450–700 nm, accuracy of 0.05% maximum surface radiation) was connected to a Li-Cor printing integrator (Li-550) during phytoplankton production experiments. Integrals (10 min) from the sensor exposed in air were summed for the duration of each incubation. A measure of light penetration into the water at flood tide was taken by lowering a spherical quantum sensor (Li-193S) connected to a Li-Cor quantum photometer (Li-185A). A Belfort recording pyrheliograph (sensitivity 0.1 g-cal·cm^{-2}·min^{-1}) was also used to continuously measure total incident radiation. Photosynthetically available energy was assumed to be 50% of the total. Integral values were derived by planimeter for total daily radiation during the period of tidal exposure and for periods of incubation during each day.

Total daily radiation was not recorded continuously at either Anthony Park or Pecks Cove during the 4 years of investigation, yet this data was needed to extrapolate estimates of primary production between days of measurement. Solar radiation data collected by pyranometer (KIPP-CM6) at Kentville, Nova Scotia by the Canadian Department of Agriculture is compiled and published as total hourly radiation for each day by the Atmospheric Environment Service. Data for the years 1977–80 were used to derive values for comparison with actual measurements on particular days during experiments. A linear correlation of daily total values at Kentville with those at Anthony Park and Pecks Cove (n=29) produced a slope value of 0.86 and an r^2 coefficient of 0.82. Thus, for the purposes of calculation, it has been assumed that radiation received at Kentville is equivalent to that received throughout the region generally. Light quanta reaching the sediment surface during exposure each day was estimated from daily records of hourly radiation at Kentville and times of high tide (Canadian Hydrographic Service Tide and Current Tables).

TABLE 1. Above-ground biomass (g dry weight m^{-2}) of *Spartina alterniflora* in upper intertidal areas at Anthony Park (Station 1) and Pecks Cove. Numbers in parenthesis are ±1 SD of adjacent mean values derived by removing all blades from three randomly chosen areas (225 cm^2). Samples taken at Pecks Cove are single determinations (data provided by P. Cranford).

Date	Anthony Park ($g \cdot m^{-2}$)	Date	Pecks Cove ($g \cdot m^{-2}$)
1977		1981 Apr. 27	2.3
		May 29	11.5
June 23	111.1 (16.2)	June 26	80.5
July 25	326.7 (54.8)	July 24	235.0
Aug. 24	368.4 (136.9)	Aug. 15	152.3[a]
Sept. 22	388.6 (18.2)	Sept. 23	115.7
Oct. 21	235.8 (23.5)	Nov. 20	52.5
Nov. 21	325.1 (80.1)		

[a]Mean of three samples.

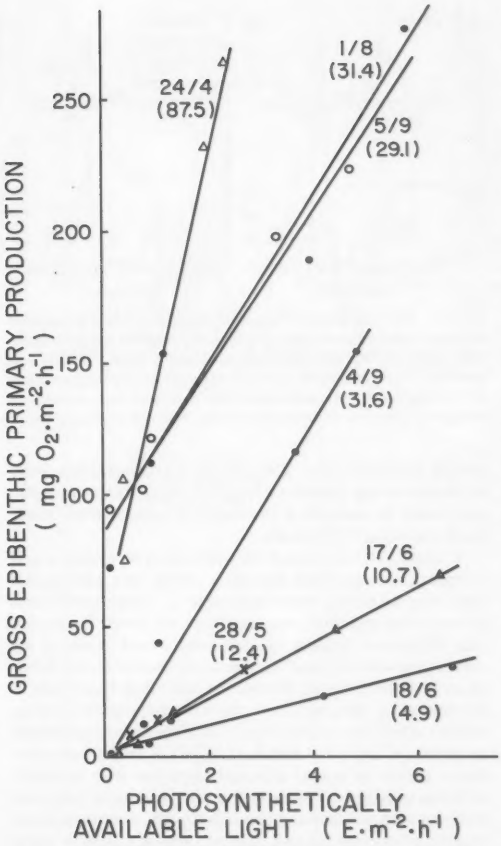

FIG. 2. Relationship between photosynthetically available radiation (400–700 nm) and in situ gross production by benthic microalgae measured a two stations on several different days during 1980 at Pecks Cove. Numbers in parentheses indicate the slope of the linear regression lines. Points are each means of five cores exposed to various light levels during simultaneous incubation.

These were combined to calculate total radiation received at experimental sites and to estimate the fraction of the total received by the exposed sediment. Daily averages on a weekly basis were then calculated.

SEDIMENTARY PLANT PIGMENTS

Surface sediment (0–2 mm) for chlorophyll *a* was collected with a metal spatula adjacent to cores used for measurements of oxygen production and consumption immediately after experiments were completed. On several occasions a 1 cm^2 corer was used to take 1–2 cm plugs of sediment which were either extracted in total or used to examine fine-scale vertical distrubutions of pigments (as described in Hargrave 1978). Samples of sediment and suspended matter on Millipore HA filters for chlorophyll *a* analysis were placed immediately into 10 mL of 85% acetone (15% distilled water) containing two drops of saturated $MgCO_3$ solution. Extracts were stored (24 h in the dark) at 5°C, centrifuged (5 min) and chlorophyll *a* determined by fluorometric methods described in Brown et al. (1981). Estimated concentrations of chlorophyll *a* are uncorrected for phaeopigments and other compounds which fluoresce at wavelengths used in the analyses.

MACROFAUNA AND *SPARTINA* BIOMASS

Cores incubated for measurements of oxygen production and consumption were stoppered at the termination of experiments, removed from the sediment and placed in plastic bags. Each core was sieved through a 420 μm mesh and all macrofauna were preserved for identification, counting, and dry weight determination. The mollusc *Macoma balthica* and the amphipod *Corophium volutator* were the predominant benthic macrofauna at Anthony Park and Pecks Cove, respectively. Other animals (*Nereis virens*, *Hydrobia* spp., *Heteromastus filiformis*, *Nassarius obsoletus*) also occur at the study sites but these species were either not present throughout the year or the size of core (25.5 cm^2) and mesh used for sampling was inadequate to quantify their biomass. *Spartina* was harvested throughout the growing season in the upper intertidal zone at both locations by quantitavely clipping above-ground shoots from a measured area (225–400 cm^2). Material was dried at 60°C for several days before dry weight determinations.

Results

SEASONAL CHANGES IN SEDIMENTARY CHLOROPHYLL *a* MACROFAUNA AND *SPARTINA* BIOMASS

Large seasonal changes in chlorophyll *a* with maximum concentrations during September and October were observed in surface sediments at Pecks Cove (Fig. 1). Although measurements were made in different years, concentrations were generally much lower at corresponding times of the year at Anthony Park and there was no increase during the fall comparable to that at Pecks Cove. Measurements of sedimentary chlorophyll *a* before and after periods of flood tide on several occasions showed no short-term changes in concentrations. Samples collected by vertical sectioning of cores at mm intervals from the surface to 2 cm showed that chlorophyll *a* concentrations decreased with depth, yet no clear pattern of changes in depth profiles during the day were obtained.

The mollusc *Macoma* was the dominant macrobenthic species at Anthony Park stations 1, 2, and 3. One to four animals of 1–2 cm length were present in each 25.5 cm^2 core. The amphipod *Corophium* was not abundant at Anthony Park but this was the dominant macrobenthic species at Pecks Cove with 20–40 animals per core at peak abundance, equivalent to 3 to 5 g dry weight m^{-2} (Fig. 1). Overwintering adults produced a new generation during spring with a subsequent cohort which reached maximum biomass during late July. This coincided with the arrival of large numbers of migrating semipalmated sandpipers (*Ereunetes pusillus*). Predation by these birds on amphipods >4 mm in length reduced biomass

TABLE 2. Quantum yield values for measures of oxygen production by benthic microalgae at two stations at Pecks Cove during 1980. Numbers derived from individual experiments or from multiple experiments (n = 3) during the day expressed as a mean and one standard deviation.

Date	mg $O_2 \cdot E^{-1}$	
	Station A	Station C
May 27	21.3	—
May 28	9.6 (3.5)	—
May 29	13.8	11.9
July 31	15.5 (2.1)	60.7
Aug. 1	19.0	47.8 (1.0)
Aug. 14	74.1	116.8
Aug. 15	61.7	113.6
Sept. 4	49.3 (4.1)	30.0 (9.3)
Sept. 5	52.3 (8.1)	—

greatly during August after which the birds departed. Small amphipods remaining increased in length (and weight) but no further generations were produced and no further biomass increases occurred during fall months.

Spartina was restricted to the upper part of the intertidal zone above the LHW mark at both locations. Ice scour removed the bulk of above-ground biomass during the winter with growth resuming slowly after April. Harvested weights throughout the summer and fall showed that growth occurred early in the growing season with total biomass (living and dead) increasing up to September (Table 1). Organic carbon in fragments of *Spartina* debris sieved from surface sediments in the upper intertidal zone at a site near Anthony Park varied between 30.1 and 39.1% of dry weight. If annual maximum above-ground biomass of *Spartina*, with an average of 35% dry weight as organic carbon, decomposed at the site of production, 82 and 136 g $C \cdot m^{-2} \cdot yr^{-1}$ would be added to sediments within the marsh zones at Pecks Cove and Anthony Park, respectively.

Calculation of Annual Rates of Gross Epibenthic and Planktonic Primary Production

Linear regression analyses were used to compare mean hourly rates of gross production by benthic microalgae and net carbon fixation by phytoplankton with chlorophyll *a* concentrations in surface (0−2 mm) sediment and suspended in the water column and with hourly incident radiation at the sediment surface and penetrating to 0.5 m depth. Positive correlations (r=0.20 − 0.48, n=48−78) existed between measures of benthic microalgal primary production and chlorophyll *a* in sediments. Phytoplankton production was unrelated (P >0.05 for a slope significantly different from zero, n=27) to suspended chlorophyll *a* concentration. Incident radiation; on the other hand, was positively correlated (r=0.35 − 0.59, n=58−95) with both benthic and planktonic primary production.

The importance of incident light received during in situ experiments was evident when measurements were made throughout the day. Oxygen production changed markedly over short-term incubations (1 h) early in the day as incident light rapidly increased. Also, no significant oxygen production occurred when light and dark-exposed cores were incubated during periods of high tide (4 h). No measurable light could be detected at the sediment surface when water depth exceeded 1.5 m depth.

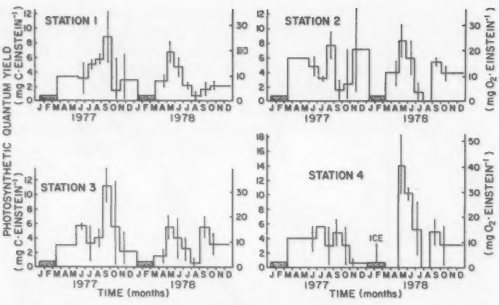

FIG. 3. The ratio of gross oxygen production or carbon assimilation by benthic microalgae to photosynthetically available radiation (quantum yield) at four intertidal sites at Anthony Park. Vertical bars indicate ± 1 SD of a mean value calculated from in situ experiments of three light and three dark cores. The horizontal lines forming the histogram extend to the midpoint of time between each experiment.

A linear relation existed between incident radiation and oxygen production when plexiglass covers were used to alter light received during experiments (Fig. 2). Slope coefficients derived from regression analyses were not tested for significant differences because the few points used to derive the curves preclude statistical interpretation. However, the differences in slopes indicate that factors other than light (such as chlorophyll *a* concentrations, species composition, grazing effects) affect microalgal production. Experiments performed at stations C (4/9/80) and A (5/9/80) at Pecks Cove produced curves of almost identical slope but with markedly different intercepts. Chlorophyll *a* concentrations were also different at these stations when experiments were performed. Highest production per unit light occurred at station A where chlorophyll *a* concentrations of 89 $mg \cdot m^{-2}$ were less than the 264 $mg \cdot m^{-2}$ measured at station C. The higher quantum yield at station A reflects increased oxygen uptake which occurred in dark cores incubated at that site. Rates of total oxygen consumption in this experiment were more variable at station A (37−77 mg $O_2 \cdot m^{-2} \cdot h^{-1}$) and higher than those observed at station C (29−31 mg $O_2 \cdot m^{-2} \cdot h^{-1}$). Estimates of gross oxygen production are thus increased due to higher values of oxygen consumption. In addition to these differences, extrapolation of regression lines to the y axis in three of the seven experiments results in positive intercept values. Either oxygen continued to be released despite reduced light or a marked nonlinear relation between photosynthesis and light existed at low light levels. Temperature did not change differentially in cores under various plexiglass shades and thus changes in dissolved oxygen concentration were not the result of solubility changes due to temperature increase.

Within and between day variation in quantum yield of benthic microalgal production was assessed at Pecks Cove during 1980 by conducting sequential experiments throughout the day on consecutive days (Table 2). The average coeffi-

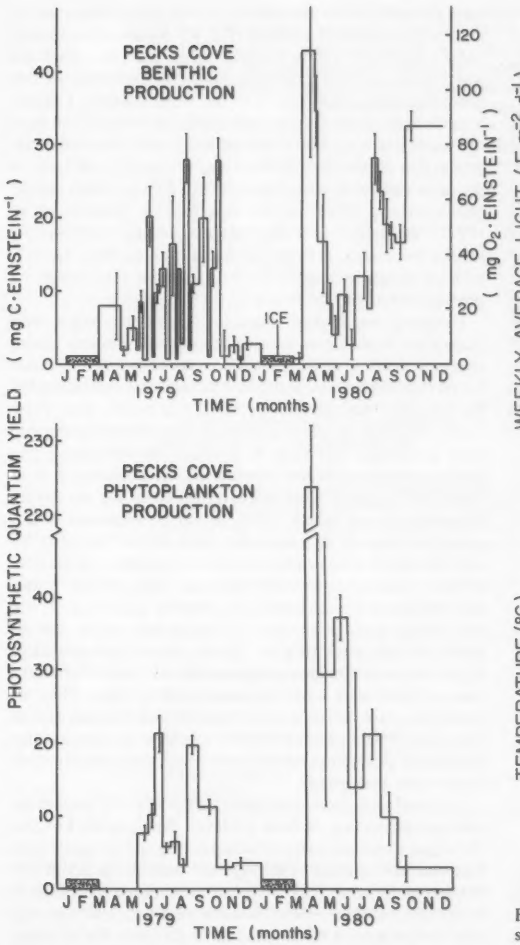
PECKS COVE
BENTHIC
PRODUCTION
ICE
(mg C·EINSTEIN⁻¹)
(mg O₂·EINSTEIN⁻¹)
J F M A M J J A S O N D J F M A M J J A S O N D
1979
1980
TIME (months)
PECKS COVE
PHYTOPLANKTON
PRODUCTION
PHOTOSYNTHETIC QUANTUM YIELD
J F M A M J J A S O N D J F M A M J J A S O N D
1979
1980
TIME (months)

FIG. 4. Photosynthetic quantum yield of benthic and planktonic primary production at Pecks Cove. Vertical bars and horizontal lines as described in Fig. 3.

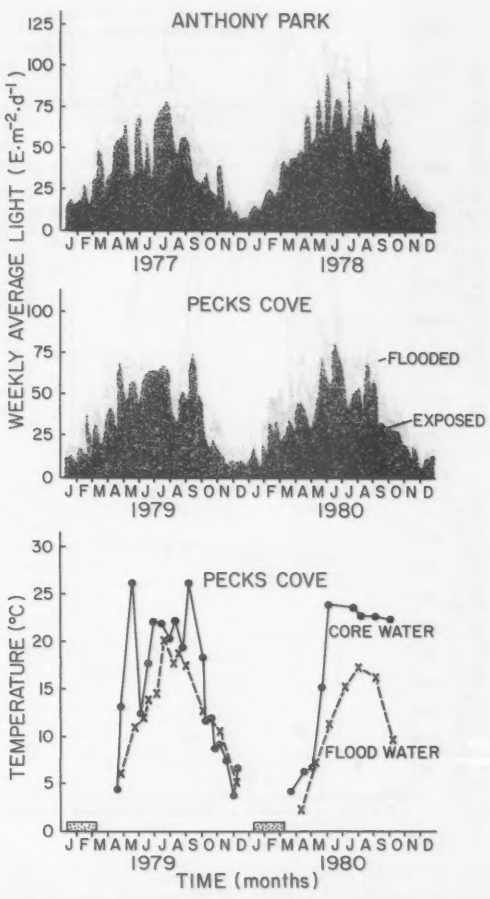
ANTHONY PARK
WEEKLY AVERAGE LIGHT (E·m⁻²·d⁻¹)
J F M A M J J A S O N D J F M A M J J A S O N D
1977
1978
PECKS COVE
FLOODED
EXPOSED
J F M A M J J A S O N D J F M A M J J A S O N D
1979
1980
PECKS COVE
CORE WATER
FLOOD WATER
TEMPERATURE (°C)
J F M A M J J A S O N D J F M A M J J A S O N D
1979
1980
TIME (months)

FIG. 5. Daily total incident radiation as weekly average photosynthetically available light, taken from Atmospheric Environment Service measurements at Kentville, N.S. Hourly records were corrected for daily variation in tidal periodicity at intertidal sites at Anthony Park (station 3 upper panel) and Pecks Cove (middle panel) to calculate light received during periods of exposure (dark stippled area). Temperature of water in cores and in flood-tide water at Pecks Cove was measured at the termination of in situ experiments.

cient of variation ($\sigma/\bar{x}$) for four sets of experiments at station A, where three or four experiments were carried out during one day, was 0.18 (0.08–0.36). There was no statistically significant trend to the data relative to time of day or duration of exposure before experiments were initiated. This within day variation gives a maximum error of up to 36% for estimates of quantum yield derived from a single experiment on one day. Values derived from experiments on consecutive days usually differed by less than this maximum within day variation (Table 2).

Phytoplankton production was measured at three depths (with a reduction in light dependent on suspended particulate matter concentrations) at Pecks Cove in six experiments during 1980. Photosynthetically available radiation decreased by an average of 96% between the surface and 1 m while phytoplankton production decreased by an average of 59%. A nonlinear (asymptotic) relation between light and carbon fixation was observed in only one experiment. In all other cases, photosynthesis decreased linearly with decreasing light over depth.

These observations showed that hourly rates of benthic oxygen production and ^{14}C uptake by phytoplankton could be combined with measures of radiation received during incubation (as $E \cdot m^{-2} \cdot h^{-1}$) to compare the photosynthetic

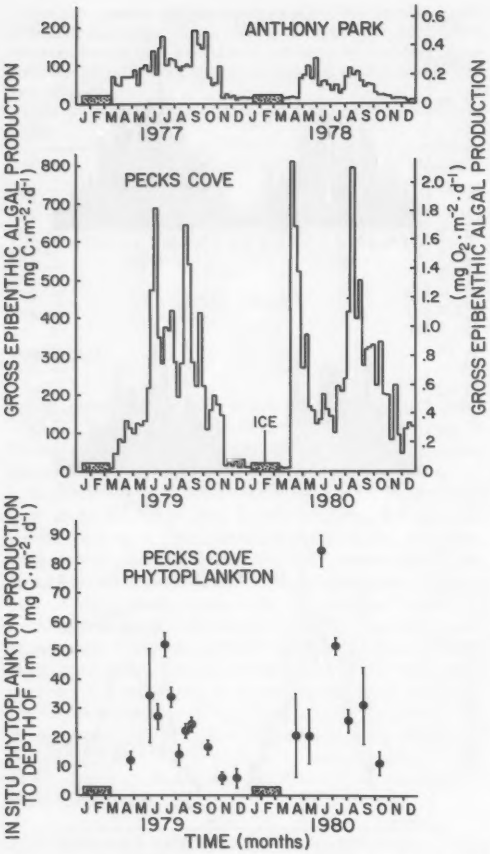
ANTHONY PARK
PECKS COVE
ICE
PECKS COVE
PHYTOPLANKTON
GROSS EPIBENTHIC ALGAL PRODUCTION (mg C·m⁻²·d⁻¹)
GROSS EPIBENTHIC ALGAL PRODUCTION (mg O₂·m⁻²·d⁻¹)
IN SITU PHYTOPLANKTON PRODUCTION TO DEPTH OF 1m (mg C·m⁻²·d⁻¹)
J F M A M J J A S O N D J F M A M J J A S O N D
1977
1978
1979
1980
TIME (months)

FIG. 6. Weekly averages of daily gross production by benthic microalgae calculated from measures of photosynthetic quantum yield and incident radiation on exposed intertidal sediment at Anthony Park (station 3) and Pecks Cove. Daily phytoplankton production is that which occurred in the water column over four hours of flood tide during the day. Vertical lines represent ± 1 SD. Points cannot be joined because of lack of information on in situ light levels in the water column on intervening days between experiments.

quantum yield throughout the year and between areas (Fig. 3 and 4). Maximum values occurred during spring and summer at all sites, with minimum values during fall and winter. Values from experiments at Pecks Cove were similar to those observed during 1978 at an adjacent site (Gordon et al. 1980) and these were generally higher than those determined at Anthony Park. This is consistent with the lower concentrations of chlorophyll *a* in surface sediments at Anthony Park stations. Maximum values (115 ± 40 mg $O_2 \cdot E^{-1}$) during April and minimum values (7 ± 4 mg $O_2 \cdot E^{-1}$) during June in 1980 were similar for both station A and C at Pecks Cove.

Quantum yield values for phytoplankton at Pecks Cove were generally lower than those calculated for benthic microalgae except in one experiment (Fig. 4). An anomalously high value (April 15, 1980) occurred when vigorous wind and wave action created extremely high concentrations of suspended material ($1.6\ g \cdot L^{-1}$) in the water column. Concentrations in the water column at floodtide were usually an order of magnitude less. Maximum quantum yield for epibenthic production observed at Pecks Cove occurred 1 wk later. If quantum yield values are converted to a dimensionless ratio of photosynthetic efficiency as described in Parsons et al. (1977), the highest efficiency (as a percentage) observed for benthic microalgae at Pecks Cove and Anthony Park was 0.77 with an annual average value 0.31. Similar calculations for phytoplankton yielded values of 0.09 and 0.04.

Hourly quantum yield values for benthic microalgae were multiplied by radiation received throughout the day during exposure to calculate daily rates of oxygen production. Values for phytoplankton was multiplied by radiation received while the sediment was covered by flood tide water. This yields values for daily production only on days when experiments were performed and there is no basis for calculating production on days between experiments. If, however, it is assumed that quantum yield values measured on any one day are representative of values which would be measured over a period of time of at least a few days before and after the measurements, then production can be calculated on the basis of daily variation in incident radiation. Daily average values for radiation were calculated on a weekly basis (Fig. 5) and the average daily production of benthic microalgae was derived for each week (Fig. 6). In the case of phytoplankton, however, no continuous measurements of suspended matter concentration were made between sampling dates. Thus, although incident radiation could be calculated for each day, no measures of light penetration were available to calculate phytoplankton production for days other than those when experiments were performed.

Seasonal changes in calculated values of daily benthic microalgal production at both Anthony Park and Pecks Cove show that maximum rates occurred during spring–early summer and late summer–fall (Fig. 6). Seasonal peaks in production at Anthony Park were less pronounced than those at Pecks Cove and there were between year differences at each site. Differences in April–May at Pecks Cove, for example, arose from marked changes in quantum yield values during the corresponding period (Fig. 4 and Fig.6). Different annual patterns in incident radiation between years (Fig. 5) also occurred but no clear correlation existed between periods of enhanced radiation and increased weekly average values of benthic primary production. Maximum values of solar radiation occurred between June and July but reduced quantum yield values resulted in lower values of production.

Stepwise multiple linear regression analyses were used to compare calculated daily rates of gross benthic microalgal production (mg $O_2 \cdot m^{-2} \cdot d^{-1}$) for various stations at Anthony Park and Station A at Pecks Cove with temperature and chlorophyll *a* in surface sediment. Temperature and chlorophyll *a* accounted for 36.6 and 17.9%, respectively, of the total variance ($MR^2 = 0.54$, $n = 28$) in the regression when all data from Pecks Cove were combined. No significant correlation ($P > 0.05$) between these variables existed for data from

TABLE 3. Comparison of measures of phytoplankton production and chlorophyll *a* biomass in surface water samples exposed to natural light[a] in situ at the surface (Pecks Cove) or in a deck incubator (in Minas Basin during *Dawson* cruise 79-023) during July and August 1979 at two locations in the upper reaches of the Bay of Fundy.

Location and date	Phytoplankton production mg $C \cdot m^{-3} \cdot h^{-1}$	Chlorophyll *a* concentration mg $\cdot m^{-3}$	Specific production mg $C \cdot (mg\ chlorophyll\ a)^{-1} \cdot h^{-1}$
Pecks Cove (in situ)			
July 9	19.6	5.3	3.7
July 24	12.4	1.7	7.3
Aug. 8	5.0	2.0	2.5
Aug. 21	8.5	2.0	4.3
Minas Basin (deck incubation)			
Aug. 13	6.2	1.1	5.6
Aug. 14	9.8	1.5	6.5
Aug. 15	5.2	0.8	6.5

[a]Incident radiation varied between 400 and 500 $\mu E \cdot m^{-2} \cdot s^{-1}$ in Minas Basin and between 400 and 1800 $\mu E \cdot m^{-2} \cdot s^{-1}$ in Cumberland Basin.

TABLE 4. Annual benthic microalgal primary production and respiration of undisturbed sediments at Anthony Park and Pecks Cove. Phytoplankton production and respiration in the water column were not measured throughout the year at Anthony Park.

		Anthony Park					
		1	2	3	4		
		(g $C \cdot m^{-2} \cdot yr^{-1}$)				Pecks Cove	
Gross benthic	(1977)	32.0	30.0	23.2	20.2	(1979)	62.5
Microalgal production	(1978)	25.9	29.2	24.7	27.4	(1980)	83.5
Phytoplankton						(1979)	4.2
Production						(1980)	9.8
Benthic respiration	(1977)	9.6	34.4	47.4	—	(1979)	49.3
	(1978)	11.5	40.9	49.4	33.0	(1980)	62.5
Water column						(1979)	11.6
Respiration						(1980)	12.8

Anthony Park (treated as single stations or by combining all observations). Comparison of benthic primary production and chlorophyll *a* using Pecks Cove data yielded a significant regression ($r^2 = 0.76$) with a higher coefficient ($r^2 = 0.88$) after logarithmic transformation of both variables. Significant regressions ($P > 0.10$) could not be derived from similar observations at Anthony Park.

Phytoplankton production for days between those on which experiments were performed was not estimated and thus detailed seasonal changes are not observable. However, maximum values of carbon assimilation occurred at Pecks Cove during June and July, the period of maximum incident radiation in both years of study (Fig. 5 and 6). This was not reflected in enhanced values of photosynthetic quantum yield which were reduced during these periods (Fig. 4). No measurements of phytoplankton production were made on a regular basis at Anthony Park, but water samples collected offshore in Minas Basin (N. Prouse, unpublished data from *Dawson* cruise 79-023) provided an estimate of in situ phytoplankton production at the surface (Table 3). Although these production experiments were conducted in deck incubators, estimates or total and specific production are similar to in situ measures at Pecks Cove at the same time of year.

Annual values for benthic microalgal primary production at Anthony Park and Pecks Cove (Table 4) were calculated by integrating areas under histograms (Fig. 6) on a monthly basis. Between 65 and 85% of the annual total production occurred between May and September at both sites, although rates were always higher at Pecks Cove. There was not a large difference in gross annual microalgal production between stations at Anthony Park, despite small differences in elevation and duration of tidal cover. Average annual production of benthic microalgal at Pecks Cove (73.4 g $C \cdot m^{-2} \cdot yr^{-1}$) was 2.7 times higher than the mean value for four stations at Anthony Park. Average annual phytoplankton production during periods of flooding at Pecks Cove, calculated by integrating the area under a curve formed by joining the points in Fig. 6, amounted to 7 g $C \cdot m^{-2} \cdot yr^{-1}$.

ANNUAL RATES OF BENTHIC RESPIRATION

Total oxygen uptake was greatest at station 1 at Anthony

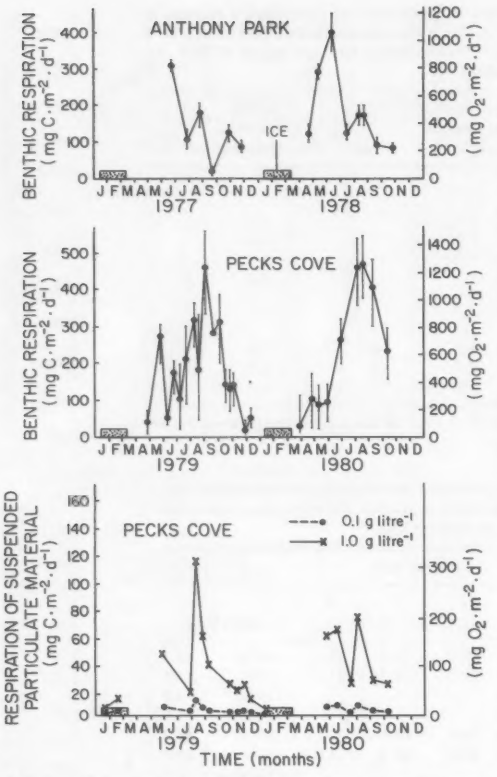

FIG. 7. Oxygen uptake (corrected for chemical oxygen consumption) of undisturbed cores of sediment incubated in situ at Anthony Park (station 3) and Pecks Cove between 1977 and 1980. Sedimented particulate matter, collected in settling tubes during one period of flood tide, was used in laboratory experiments to measure oxygen uptake by known weights of resuspended particles. Benthic respiration was assumed to be zero during periods of ice cover for purposes of calculating annual integrals.

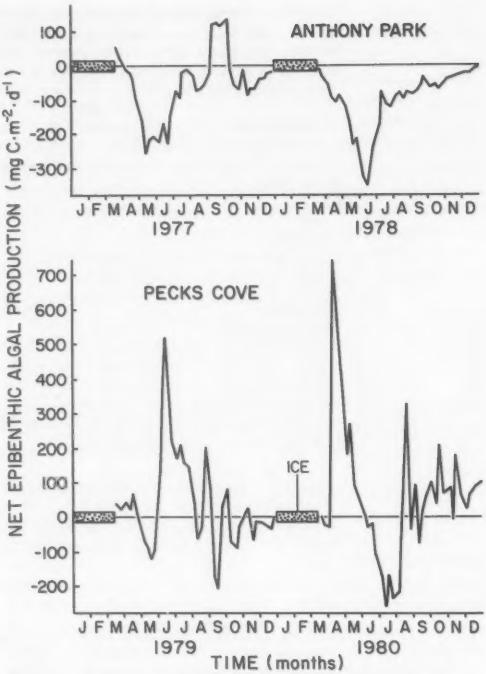
ANTHONY PARK
NET EPIBENTHIC ALGAL PRODUCTION (mg C·m⁻²·d⁻¹)
J F M A M J J A S O N D J F M A M J J A S O N D
1977
1978
PECKS COVE
ICE
1979
1980
TIME (months)

FIG. 8. Calculated values of "net" benthic microalgal production (the difference between gross microalgal production and benthic community respiration both expressed as daily carbon flux) for intertidal sediments at Anthony Park (station 3) and Pecks Cove during consecutive years. Calculations based on weekly average daily rates derived from data presented in Fig. 6 and 7.

Park where formalin addition reduced consumption by an average of 18%. Respiration amounted to 50% of total uptake at all other stations at Anthony Park with values between 70 and 85% at Pecks Cove. There were insufficient measurements at Anthomy Park to observe seasonality in relative rates of biological and chemical oxidation, but no significant correlations ($P > 0.10$) existed between this ratio and temperature or chlorophyll *a* in surface sediment at Pecks Cove.

Annual estimates of biological respiration by sediments and particulate matter suspended in the water column (Table 4) were calculated by integration of daily rates plotted over time (Fig. 7). Since observations did not cover a full year at either location, curves were extrapolated to zero at the beginning and end of each year. Respiration rates observed at stations A and C at Pecks Cove differed by less than 15% in five of nine experiments performed simultaneously. Large differences between stations, with rates up to 60% higher at station C, occurred in late June and July, coincident with similar differences in quantum yield of benthic microalgae. This increase, combined with that which might have occurred had cores been stirred during incubation (discussed above) shows that we have underestimated benthic respiration during the months of rapid increase in rates. Correction of measures of oxygen uptake for this underestimate would increase annual values by 15%.

Annual benthic respiration at Pecks Cove (integrals of curves in Fig. 7) exceeded estimates for all Anthony Park stations except station 3 where equivalent values were observed (Table 4). Calculations of monthly integrals showed that from 70 to 80% of total annual respiration occurred between May and September when maximum production by benthic microalgal and highest seasonal temperatures also occurred. Stepwise multiple regression with and without logarithmic transformation of variables was performed using individual daily measurements of monthly totals of benthic respiration with corresponding values for water temperature, chlorophyll *a* in surface sediments and estimates of gross primary produciton by microalgae. Temperature was the sin-

gle most important variable in all cases, but this accounted for less than 50% of the variance (r^2 values varied from 0.14 at Anthony Park to 0.50 at Pecks Cove). Although additional variables (chlorophyll *a*, gross microalgal production) were added to regressions in a stepwise manner, this only raised the r^2 coefficients slightly (less than 0.15). Different slope coefficients were calculated for different variables in each regression.

Rates of formalin sensitive oxygen uptake (respiration) varied from 0.002 to 0.02 mg $O_2 \cdot g^{-1} \cdot h^{-1}$ with minimum and maximum values in winter and midsummer, respectively. Estimates of annual oxygen uptake in the water column depend on the concentration of suspended particulate matter used in the calculation. Measurements during periods of flood-tide varied from 0.05 to 2.0 $g \cdot L^{-1}$ (E. MacDormand, unpublished data). Highest concentrations occurred at the flood tide wave front, but these levels were only sustained for a short time (30 min) after which resuspended sediment settled. Cylinders used to collect deposited material would intercept these particles as well as those settled during the rest of the period of tidal cover. Average values for suspended matter concentration during this time varied from 200 to 500 $mg \cdot L^{-1}$. Annual oxygen uptake for a maximum concentration of 1.0 $g \cdot L^{-1}$ in a 2.5 m water column over a 4 h (a daily time period comparable to that for phytoplankton production) would be equivalent to a respiration rate of 12 g $C \cdot m^{-2} \cdot yr^{-1}$ (Table 4). A lower concentration of 500 $mg \cdot L^{-1}$ would result in a correspondingly reduced rate (6 g $C \cdot m^{-2} \cdot yr^{-1}$). Since two periods of high tide occur every 24 h, actual daily rates would be double this estimate derived for high tide periods during the day.

"Net" Production by Benthic Microalgae

Estimates of benthic respiration as daily average rates (mg $C \cdot m^{-2} \cdot d^{-1}$) over weekly intervals throughout the year were calculated from Fig. 7. These values, which are assumed to represent a measure of metabolic carbon release by the entire community of aerobically respiring organisms present in the sediment, were subtracted from corresponding daily average values of gross benthic microalgal production . The resultant ("net") rates provide a measure of the balance between benthic autotrophic production and respiration.

Negative values of net production by benthic microalgal (daily benthic respiration > benthic algal production) occurred in all months except September 1977 at Anthony Park (Fig. 8). Oscillating periods of surplus and deficits in gross production over consumption occurred at Pecks Cove. Greatest deviations from a balance occurred in late spring and early summer at both locations, with a dampened oscillation or gradual approach to a balance throughout the fall and winter. The timing and duration of intervals of enhanced production or respiration varied between years (as was observed for measures of gross microalgal algae production) but the general seasonal pattern was similar over 2 yr at each site. The curves illustrate an annual deficiency of organic carbon supply from production by benthic microalgae for benthic respiration at Anthony Park and an excess of production over consumption at Pecks Cove. This is also shown by annual rates summarized in Table 4.

Discussion

Previous estimates of annual rates of benthic microalgae production on various intertidal sandflats and shallow subtidal sediments, tabulated in Parsons et al. (1977) show that values vary between 0 and 300 g $C \cdot m^{-2} \cdot yr^{-1}$. Recent studies in the Dutch Wadden Sea (Cadée and Hegeman 1977; Cadée 1980) and in the Lyhner estuary (Joint 1978) provide estimates between 30 and 188 g $C \cdot m^{-2} \cdot yr^{-1}$. Annual values at Anthony Park (20–30 g $C \cdot m^{-2} \cdot yr^{-1}$) and Pecks Cove (60–80 g $C \cdot m^{-2} \cdot yr^{-1}$) are within this range. Estimates of phytoplankton production at Pecks Cove (7 g $C \cdot m^{-2} \cdot yr^{-1}$), where high concentrations of suspended matter severely limited light penetration, are lower than rates observed in other turbid nearshore waters. For example, Cadée and Hegeman (1974b) cite values of 13 g $C \cdot m^{-2} \cdot yr^{-1}$ for the Dollard Estuary, and higher estimates (100–120 g $C \cdot m^{-2} \cdot yr^{-1}$) in adjacent waters of the Wadden Sea. Production of above-ground biomass by *Spartina* at our study sites (82–136 g $C \cdot m^{-2} \cdot yr^{-1}$) is less than that of Great Sippewissett marsh (423 g $\cdot m^{-2} \cdot yr^{-1}$) (Valiela et al. 1976). This is equivalent to a production of 148 g $C \cdot m^{-2} \cdot yr^{-1}$ if organic carbon content is 35% of dry biomass. These figures do not consider root and rhizome production which Valiela et al. (1976) observed to be from 2.5 to 7.7 times that of annual above-ground growth.

Differences in annual estimates of primary production by benthic microalgae, phytoplankton, and emergent plants in various locations reflect seasonal differences in absolute rates and variation in shapes of annual production curves. Maximum rates of gross production by benthic microalgae in our study (200 and 800 mg $C \cdot m^{-2} \cdot d^{-1}$ at Anthony Park and Pecks Cove, Fig. 6) are similar to rates observed in previous studies (Van Raalte et al. 1976, Cadée and Hegeman 1977; Cadée 1980) but less than the highest rates reported for a Georgia salt marsh by Pomeroy (1959). However, the seasonal duration of periods of high production is restricted in the upper reaches of the Bay of Fundy.

Light availability is a critical factor for the determination of the shape of the annual primary production cycle. The assumed linear relation between primary production and light in our calculations of daily and annual rates also determined the absolute magnitude of production. Pamatmat (1968), Van Raalte et al. (1976), and Hartwig (1978) also reported a linear correlation between in situ production by benthic microalgae and light. McIntire and Wulff (1969) and Wulff and McIntire (1972), using laboratory experiments with estuarine diatom assemblages attached to artificial substrates not exposed to dessication, also concluded that gross oxygen production could be described as a linear function of light. Curvilinear relations do appear in their data as well as that presented by Pamatmat (1968). Light saturation of photosynthesis can occur (Taylor 1964; Gargas 1971; Colijn and Buurt 1975) and nonlinear photosynthesis–light curves have been observed for gross oxygen production by benthic microalgae (Hunding 1973; Gallagher and Daiber 1973). It is possible that photosynthesis–light curves change in shape under conditions of varying light (Gallegos et al. 1980) and that with limited data nonlinearity is not apparent.

The relation between light and gross production by benthic microalgae at Pecks Cove was not constant throughout the

year. The variation in photosynthetic quantum yield (Table 2, Fig. 3 and 4) and the relatively low values of photosynthetic efficiency show that factors other than only light are involved in determining rates of primary production. Thus, although similar seasonal patterns are attributable to similar amounts of radiation received during the year at both sites, higher annual production estimates at Pecks Cove reflect higher values of photosynthetic quantum yield measured at this site. This is consistent with the higher concentration of chlorophyll *a* usually present in surface sediments at Pecks Cove (Fig. 1).

Cadée and Hegeman (1977) observed a linear correlation (r=0.8) between annual production of benthic microflora on tidal flats in the Wadden Sea and annual average concentrations of chlorophyll *a* in surface sediment despite an earlier observation of a weak correlation between daily production and chlorophyll content. Hartwig (1978) also did not observe a significant ($P > 0.05$) linear correlation between gross microalgal production and chlorophyll content in subtidal sediments. Our data show that fluctuations in quantum yield and daily production at Pecks Cove were not closely correlated with major peaks in chlorophyll *a* throughout the year (Fig. 1 and 4). Higher values of quantum yield were not simply related to increased chlorophyll concentrations. No single regression common to both Anthony Park and Pecks Cove between daily production by benthic microalgal and chlorophyll *a* concentration could be derived, although the multiple regression to compare production with temperature and chlorophyll showed significant ($P > 0.05$) seasonal effects of both of these variables.

Some form of a positive relationship would be expected between rates of primary production and chlorophyll *a* biomass once corrections are made for varying light intensity. In effect, this is achieved when annual total production rates are compared with average pigment concentrations in different areas within a region which receives similar amounts of radiation annually. Thus, the higher average chlorophyll *a* content in sediments at Pecks Cove over that present at Anthony Park (Fig. 1) is consistent with the observation that average annual production by benthic microalgal is approximately three times greater at Pecks Cove (Table 4). Exposure to longshore currents and ice scour at Anthony Park, and the coarse grain sand sediments which tidal scour produces at this site, could account for reduced concentrations of chlorophyll *a* in these sediments in comparison to those at Pecks Cove.

Specific production rates (mg C·(mg chlorophyll *a*)$^{-1}$·h^{-1}) (assimilation numbers) may be used to compare carbon assimilation by algae at saturating light levels. Steele and Baird (1968) and Admiraal and Peletier (1980) reported values of 0.1−1.4 for benthic microalgae growing at a sediment surface with higher numbers (3.4−13) for cells in suspension. In situ experiments on cloudless days during summer (photosynthetically available radiation of 6 E·m^{-2}·h^{-1}) at Pecks Cove and Anthony Park yield values between 0.1 and 7. Assimilation numbers for phytoplankton when water samples were incubated at the surface (2.5−7.3) (Table 3) are similar to those reported for phytoplankton grown in culture without nutrient limitation (Parsons et al. 1977).

Nutrient concentrations in the water and in pore water extracted from sediments by centrifugation at these intertidal locations will be described elsewhere, but dissolved silicate, nitrate and ammonia were present at concentrations >1 μm even during periods of maximum primary production (P. Keizer, unpublished data). Light rather than nutrient supply appears to be critical for production of these benthic and planktonic algal populations. Values for photosynthetic efficiency (<0.1% for phytoplankton and 0.3−0.8% for benthic microalgal) indicate that algal cells in suspension utilize light less efficiently during photosynthesis than do cells on the sediment surface. Pomeroy (1959) and Pamatmat (1968) also observed relatively high values (0.1−3.0%) for photosynthetic efficiency of algae on intertidal sediments. Presumably the presence of solid surfaces which allows movement to optimal light conditions and a nonlimiting nutrient supply contribute to increased photosynthetic efficiency.

Measurements of oxygen uptake by undisturbed sediments do not provide estimates of total benthic metabolism (Pamatmat 1977). Oxygen uptake will underestimate total metabolic activity by the fraction of respiration which does not use oxygen as a terminal electron acceptor when anaerobic metabolism occurs. Aerobic respiration can be measured as oxygen uptake but only if a correction is made for chemical oxygen uptake by reduced materials accumulated in sediment. Dale (1979) criticized the use of formalin poisoning to separate biological and chemical oxygen uptake in sediments. Simultaneous observations of oxygen and carbon dioxide flux across undisturbed sediments, however, have shown that a conservative estimate of aerobic respiration may be made using this approach, even if total metabolism is not measured (Hargrave and Phillips 1981).

Diel and tidal rhythms observed in benthic respiration in some intertidal or shallow water sediments (Pamatmat 1968; Hunding 1973; Gallagher and Daiber 1973) were not apparent in our study. Rates of oxygen uptake over 24 h at Pecks Cove using benthic chambers which maintained water over the sediment (Hargrave and Connolly 1978) showed no tidal or diel periodicity. No experiments were performed where desiccation due to exposure to air occurred during the measurements. However, incubations of cores before, after and during periods of high tide did not demonstrate any pattern of differences in rates of oxygen uptake.

Maximum rates of benthic respiration at both of our study sites are low relative to rates often observed in intertidal deposits (Hargrave 1969). The occurrence of highest seasonal rates during summer months (Fig. 7) accounts for positive correlations with temperature observed in the present and many previous studies (Pamatmat 1977). However, a single regression equation to describe seasonal changes in respiration as a function of temperature at both Pecks Cove and Anthony Park could not be derived. Fluctuations (usually increases over ambient or initial values) in temperature in water over cores during short-term experiments might have contributed to this lack of a consistent relationship.

Factors correlated with temperature, such as the seasonal supply of organic matter which provides substrates for metabolism, could also control benthic respiration rates. There were significant ($P > 0.05$) linear correlations (r^2 = 0.28−0.64) between daily rates of gross production by benthic microalgae and benthic respiration at Pecks Cove and Anthony Park. Chlorophyll *a* concentrations in surface sediments were partially correlated with benthic respiration at Pecks Cove, but

the relationship was only significant ($P > 0.05$) after variation due to temperature and microalgal production was removed. Average annual rates of respiration at Pecks Cove were not appreciably higher than rates at stations 2 and 3 at Anthony Park, despite increased rates of production by benthic microalgae observed at these stations (Table 4). If respiration reflects the supply of oxidizable material which is decomposed aerobically, this rate is more similar at our study sites than are measures of primary production by microalgae.

The inadequacy of oxygen uptake as a measure of total metabolism in sediments was apparent in observations at station 1 at Anthony Park. Above-ground biomass production by *Spartina* could contribute up to 136 g $C \cdot m^{-2} \cdot yr^{-1}$ at this station. Some fraction of this biomass is exported, however, since the presence of *Spartina* debris at stations further down the intertidal zone indicates that organic fragments are widely distributed. Also, observations of stable carbon isotopes at Pecks Cove (Schwinghammer et al. 1983) show that organic carbon in surface sediments is probably derived in part from *Spartina* detritus. Biomass remaining is enhanced by annual root and rhizome production which may exceed above-ground growth by several times (Valiela et al. 1976). High rates of chemical oxidation (an average of 82% of total oxygen uptake) in these sulfide-rich sediments attests to the importance of anaerobic metabolism. Although compounds of below-ground growth may also be transported laterally as solubilized material, most of this is probably degraded in situ (Howarth and Teal 1980).

Despite the incomplete measure of organic carbon oxidation in sediments provided by estimates of oxygen uptake, relative rates of gross production by benthic microalgae and benthic community respiration can be compared to consider if primary production at the sediment surface can at least supply organic carbon decomposed aerobically in the underlying sediments. Calculations of the "net" value as the difference between primary production and respiration for stations 2, 3, and 4 at Anthony Park illustrated that annual production was insufficient to meet demands of aerobic respiration (Table 4). Exceptions to this imbalance occurred only at station 3 (Fig. 8) and 4 during the fall of 1977.

Organic carbon production of benthic microalgae at station 1 at Anthony Park and at Pecks Cove, on the other hand, exceeded benthic aerobic respiration as Pomeroy (1959) and Pamatmat (1968) also observed in their studies. However, the ratio of benthic autotrophic production to aerobic heterotrophic consumption was not constant through the year at either Anthony Park or Pecks Cove (Fig. 8). The deficit in production over respiration at station 3 at Anthony Park, for example, gradually increased during spring and early summer. This was a period of enhanced production over respiration at Pecks Cove when chlorophyll *a* in surface sediments increased (Fig. 1).

Evidence for the utilization of products of benthic microalgal production by the amphipod *Corophium* existed at Pecks Cove during the early summer. Amphipod biomass increased during July (Fig. 1) which coincided with a sharp reduction in rates of production by benthic microalgae (Fig. 6) while net production decreased to near zero or became negative (Fig. 8). Chlorophyll *a* content of the sediment also decreased during this period in 1979 and throughout the entire spring and early summer of 1980 implying that cropping by amphipods exceeded rates of benthic microalgal production. The low biomass of *Corophium* during August, caused by bird predation, released this cropping pressure and the standing crop of chlorophyll *a* in the sediment increased rapidly. Daily consumption of microalgae after this period of intense predation (late August) was apparently less than daily rates of production since peaks in chlorophyll *a*, gross and "net" production occurred during this time (Fig. 6 and 8). By mid-September, however, cropping rates must have equalled or exceeded daily production and both benthic microalgal standing crop and production decreased rapidly.

Absolute rates of oxygen uptake by particulate matter settled into cylinders at Pecks Cove (0.002–0.02 mg $O_2 \cdot g^{-1} \cdot h^{-1}$) are within the lower range of values observed for small (10–30 μm) particles of sand with relatively low amounts (<1%) of organic matter (Hargrave 1972). Highest rates of oxidation during midsummer corresponded to the period of most intense benthic and pelagic primary production as would be expected if the supply of oxidizable substrates was linked to short-term rates of primary production. Since only settled particles were incubated in our experiments, no measure of respiration of planktonic organisms which remain in suspension was provided. However, estimates of annual carbon fixation by phytoplankton at Pecks Cove were approximately half of calculated rates of annual carbon respiration (Table 4). Organic matter respired in the water column must be derived from sources in addition to phytoplankton production.

Resuspended benthic microalgae and *Spartina* debris could contribute material to the water column for oxidation. At Pecks Cove, for example, average annual production by benthic microalgae exceeded aerobic benthic respiration by 17.5 g $C \cdot m^{-2}$. Although total benthic metabolism was underestimated because anaerobic respiration was not measured, the magnitude of this difference shows that some of the estimated carbon demand in the water column could be provided by products of primary production by benthic microalgae. Detritus produced by *Spartina* is distributed over an unknown area, but particulate matter from this source could also contribute material respired in the water column. Pelagic and benthic respiration in these turbid water environments would then reflect the combined input of organic material from different sources. Cadée (1978, 1980) and Wolff (1977) also concluded that organic matter supply to intertidal sediments in the western Wadden Sea and Grevelingen Estuary arose from various sources.

Lack of knowledge of rates of import and export of particulate matter through tidal flushing precludes calculations of a complete organic carbon budget at Anthony Park and Pecks Cove. Horizontal movement of material equals or exceeds in situ planktonic and benthic primary production in some estuaries and subtidal sediments (Wolff 1977; Hartwig 1978). Further, we have not quantified all sources of input and loss of dissolved organic carbon. Van Es (1977) attributed a discrepancy between measured input and output of organic carbon in the Dollard Estuary to loss (export or microbial utilization) of organic matter in this form. Teal and Valiela (1978) also emphasized the importance of tidal water export of dissolved organic and inorganic nitrogen from a salt marsh,

although not all estuaries show a net annual loss (Heinle and Flemer 1976; Woodwell et al. 1979). The magnitude of flux of both particulate and dissolved organic carbon through tidal action must be determined before a complete carbon budget of any intertidal ecosystem can be constructed.

Acknowledgments

We are grateful to J. Walker, E. MacDormand, D. Peer, P. Cranford, J. Dale, D. Gordon, and P. Keizer who helped with various aspects of the field program and provided analytical assistance. D. Peer, C. Hawkins, P. Keizer, P. Cranford, and E. MacDormand kindly shared unpublished data. D. Gordon, C. Hawkins, and V. de Jonge read the manuscript and offered useful comments.

ADMIRAAL, W., AND H. PELETIER. 1980. Influence of seasonal variations of temperature and light on the growth rate of cultures and natural populations of intertidal diatoms. Mar. Ecol. Prog. Ser. 2: 35–43.

ANDREWS, D. 1980. The prediction and measurement of dissolved silicate flux across marine sediments. Ph.D. thesis, Dalhousie Univ. Halifax, N.S. 195p.

BROWN, L. M., B. T. HARGRAVE, AND M. D. MACKINNON. 1981. Analysis of chlorophyll *a* in sediments by high-pressure liquid chromatography. Can. J. Fish. Aquat. Sci. 38: 205–214.

CADÉE, G. C. 1978. On the origin of organic matter accumulating on tidal flats of Balgzand, Dutch Wadden Sea. Hydrobiol. Bull. 12: 145–150.

1980. Reappraisal of the production and import of organic carbon in the western Wadden Sea. Neth. J. Sea Res. 14: 305–322.

CADÉE, G. C., AND J. HEGEMAN. 1974a. Primary production of the benthic microflora living on tidal flats in the Dutch Wadden Sea. Neth. J. Sea Res. 8: 260–291.

1974b. Primary production of phytoplankton in the Dutch Wadden Sea. Neth. J. Sea Res. 8: 240–259.

1977. Distribution of primary production of the benthic microflora and accumulation of organic matter on a tidal flat area, Balgzand, Dutch Wadden Sea. Neth. J. Sea Res. 11: 24–41.

COLIJN, F., AND G. VAN BUURT. 1975. Influence of light and temperature on the photosynthetic rate of marine benthic diatoms. Mar. Biol. 32: 209–214.

DALE, T. 1979. Total, chemical and biological oxygen consumption of the sediments in Lindåspollene, Western Norway. Mar. Biol. 49: 333–341.

DALRYMPLE, R. W., R. J. KNIGHT, AND G. V. MIDDLETON. 1975. Intertidal sand bars in Cobequid Bay (Bay of Fundy), p. 293–307. *In* L. E. Cronin [ed.]. Estuarine research, International Estuarine Research Conference. Vol. 2. Academic Press, New York, N.Y.

GALLAGHER, J. L., AND F. C. DAIBER. 1973. Diel rhythms in edaphic community metabolism in a Delaware salt marsh. Ecology 54: 1160–1163.

GALLEGOS, C. L., A. M. HORNBERGER, AND M. A. KELLY. 1980. Photosynthesis–light relationships of a mixed culture of phytoplankton in fluctuating light. Limnol. Oceangr. 25: 1082–1092.

GARGAS, E. 1971. "Sun-shade" adaptation in microbenthic algae from the Øresund. Ophelia 9: 107–112.

GORDON, D. C. JR., AND A. R. LONGHURST. 1979. The environmental aspects of a tidal power project in the upper reaches of the Bay of Fundy. Mar. Pollut. Bull. 10: 38–45.

GORDON, D. C. JR., P. D. KEIZER., J. DALE, AND P. J. CRANFORD. 1980. Pecks Cove mudflat ecosystem study: observations in 1978. Can. Tech. Rep. Fish. Aquat. Sci. 928: 17 p.

HARGRAVE, B. T. 1969. Similarity of oxygen uptake by benthic communities. Limnol. Oceanogr. 14: 801–805.

1972. Aerobic decomposition of sediment and detritus as a function of particle surface area and organic content. Limnol. Oceanogr. 17: 583–596.

[ed.] 1978. Geochemical and biological observations in intertidal sediments from Cobequid Bay, Bay of Fundy, Nova Scotia. Fish. Mar. Ser. Tech. Rep. 782: 43 p.

HARGRAVE, B. T., AND G. F. CONNOLLY. 1978. A device to collect supernatant water for measurements of the flux of dissolved compounds across sediment surfaces. Limnol. Oceanogr. 23: 1005–1010.

HARGRAVE, B. T., AND G. A. PHILLIPS. 1981. Annual *in situ* carbon dioxide and oxygen flux across a subtidal marine sediment. Estuarine Coastal Shelf. Sci. 12: 725–737.

HARTWIG, E. O. 1978. Factors affecting respiration and photosynthesis by the benthic community of a subtidal siliceous sediment. Mar. Biol. 46: 283–293.

HEINLE, D. R., AND D. A. FLEMER. 1976. Flows of materials between poorly flooded tidal marshes and an estuary. Mar. Biol. 35: 359–373.

HOWARTH, R. W., AND J. M. TEAL. 1980. Energy flow in a salt marsh ecosystem: the role of reduced inorganic sulfur compounds. Am. Nat. 116: 862–872.

HUNDING, C. 1973. Diel variation in oxygen production and uptake in a microbenthic littoral community of a nutrient-poor lake. Oikos 24: 352–360.

HUNDING, C., AND B. T. HARGRAVE. 1973. A comparison of benthic microalgal production measured by C^{14} and oxygen methods. J. Fish. Res. Board Can. 30: 309–312.

JOINT, I. R. 1978. Microbial production of an estuarine mudflat. Estuarine Coastal Mar. Sci. 7: 185–195.

LEACH, J. H. 1970. Epibenthic algal production in an intertidal mudflat. Limnol. Oceanogr. 15: 514–521.

MCINTIRE, C. D., AND B. L. WULFF. 1969. A laboratory method for the study of marine benthic diatoms. Limnol. Oceanogr. 14: 667–678.

PAMATMAT, M. M. 1968. Ecology and metabolism of a benthic community on an intertidal sand flat. Rev. Ges. Hydrobiol. 53: 211–298.

1977. Benthic community metabolism: a review and assessment of present status and outlook., p. 89–111. *In* B. C. Coull [ed.] Ecology of marine benthos. Univ. J. Carolina Press, CA.

PARSONS, T. R., M. TAKAHASHI, AND B. T. HARGRAVE. 1977. Biological oceanographic processes. Pergamon Press, Toronto, Ont.

POMEROY, L. R. 1959. Algal productivity in salt marshes of Georgia. Limnol. Oceanogr. 4: 386–397.

RYTHER, J. H. 1956. The measurement of primary production. Limnol. Oceanogr. 1: 72–84.

SCHWINGHAMER, P., F. TAN, AND D. C. GORDON JR. 1983. Stable carbon isotope studies on the Pecks Cove mudflat ecosystem in the Cumberland Basin, Bay of Fundy. Can. J. Fish. Aquat. Sci. Suppl. 40. (This issue)

STEELE, J. H., AND I. E. BAIRD. 1968. Production ecology of a sandy beach. Limnol. Oceanogr. 13: 14–25.

STRICKLAND, J. D. H., AND T. R. PARSONS. 1972. A practical handbook of seawater analysis. Bull. Fish. Res. Board Can. 167: 311 p.

TAYLOR, W. R. 1964. Light and photosynthesis in intertidal benthic diatoms. Helgol. Wiss. Meeresunters. 10: 29–37.

TEAL, J. M., AND I. VALIELA. 1978. Nitrogen budget of a coastal marine ecosystem. Rapp. P.-V. Réun. Cons. Int. Explor. Mer 173: 101–105.

VALIELA, I., J. M. TEAL, AND N.Y. PERSSON. 1976. Production and

dynamics of experimentally enriched salt marsh vegetation: below ground biomass. Limnol. Oceanogr. 21: 245–252.

VAN ES, F. B. 1977. A preliminary carbon budget for a part of the Ems estuary: The Dollard. Helgol. Wiss. Meeresunters. 30: 283–291.

VAN RAALTE, C. D., I. VALIELA, AND J. M. TEAL. 1976. Production of epibenthic salt marsh algae: light and nutrient limitation. Limnol. Oceanogr. 21: 862–872.

WOLFF, W. J. 1977. A benthic food budget for the Grevelingen estuary. The Netherlands, and a consideration of the mechanisms causing high benthic secondary production in estuaries, p. 267–280. *In* B. C. Coull [ed.] Ecology of marine benthos. Univ. S. Carolina Press, SC.

WOODWELL, G. M., C. A. S. HALL, D. E. WHITNEY, AND R. A. HOUGHTON. 1979. The Flax Pond ecosystem study: exchanges of inorganic nitrogen between an estuarine marsh and Long Island Sound. Ecology 60: 695–702.

WULFF, B. L., AND C. D. MCINTIRE. 1972. Laboratory studies of assemblages of attached estuarine diatoms. Limnol. Oceanogr. 17: 200–214.

Spatial and Temporal Variability of Dinoflagellate Cyst Abundance in a Tidal Estuary[1,2]

WILLIAM M. BALCH

Institute of Marine Resources, A-018, Scripps Institution of Oceanography, La Jolla, CA 92093, USA

PHILIP C. REID AND SONIA C. SURREY-GENT

Institute for Marine Environmental Research, Prospect Place, The Hoe, Plymouth, Devon PL1 3DH, England

BALCH, W. M., P. C. REID, AND S. C. SURREY-GENT. 1983. Spatial and temporal variability of dinoflagellate cyst abundance in a tidal estuary. Can. J. Fish. Aquat. Sci. 40(Suppl. 1): 244–261.

A study of dinoflagellate cysts was made in an estuary near Plymouth, England for 1 yr. The data show that the cysts were most concentrated in sediments near the entrance of the estuary (3000 cysts (mL·flocculant^{-1})) and less concentrated upstream (<500 cysts (mL·flocculant^{-1})). Dinoflagellate cysts were observed in 99% of the plankton samples with an average concentration of 9.2 cysts·L^{-1}. Thirty percent of the variance in planktonic cyst concentration was associated with tidal range, wind stress, and river flow. The potential for inoculation of nearshore dinoflagellate populations by estuarine populations is discussed.

Key words: benthic resting cyst, dinoflagellate, estuary, frontal convergence, sediment trap, spring tides, turbulence

BALCH, W. M., P. C. REID, AND S. C. SURREY-GENT. 1983. Spatial and temporal variability of dinoflagellate cyst abundance in a tidal estuary. Can. J. Fish. Aquat. Sci. 40(Suppl. 1): 244–261.

Une étude des kystes de dinoflagellés, d'une durée d'un an, a été menée dans un estuaire du voisinage de Plymouth, en Angleterre. Les données recueillies indiquent que les kystes sont les plus concentrés dans le sédiment situé près de l'entrée de l'estuaire (3 000 kystes (mL de floculat^{-1})) et les moins concentrés en amont (<500 kystes (mL de floculat^{-1})). Des kystes de dinoflagellés ont été observés dans 99 % des échantillons de plancton, la concentration moyenne étant de 9,2 kystes·L^{-1}. La variance de la concentration est associée, dans une proportion de 30 %, à l'amplitude de la marée, à la force du vent et au débit de la rivière. Nous examinons le potentiel d'inoculation des populations de dinoflagellés du voisinage de la côte par les populations estuariennes.

Received October 14, 1981
Accepted August 31, 1982

Reçu le 14 octobre 1981
Accepté le 31 août 1982

THE distribution of dinoflagellate resting cysts has been the topic of considerable research since extant cysts were first associated with thecate dinoflagellates (Evitt and Davidson 1964; Wall 1965). A summary of work on cyst distribution in relation to environment and climate was given in Reid and Harland (1977) and Wall et al. (1977). The formation of these cysts and their subsequent distribution in bottom sediments could be tightly coupled with the dispersion of motile dinoflagellates in nature. To examine this possibility, a comprehensive sampling of the seafloor for cysts was necessary for comparison with the distribution of motile dinoflagellates. A survey made by Lewis et al. (1979) in the Gulf of Maine for cysts of the toxic dinoflagellate *Gonyaulax excavata*, a survey by Anderson and Morel (1979) of *G. tamarensis*, and earlier studies by Reid (1972, 1974) of cysts in intertidal sediments around the British Isles all showed some correlation between the distributions of cyst and thecate forms.

Dinoflagellate cysts have been observed to accumulate in the sediments of fjords, estuaries, and shallow embayments (Anderson and Morel 1978; Anderson et al. 1982; Dale 1976; Steidinger 1975; Tyler et al. 1981). It is a point of contention whether or not these dormant dinoflagellates serve as an inoculum for nearshore red tides because so little is known about the coastal hydrographic processes that affect a cyst's location in space and time. There would have to be either sufficient turbulence to resuspend cysts and carry them out of the estuary or advective processes capable of carrying thecate cells from the estuary into neritic waters for inoculation of the neritic waters to occur. The most likely place to observe the

[1]This paper forms part of the Proceedings of the Dynamics of Turbid Coastal Environments Symposium convened at the Bedford Institute of Oceanography, Dartmouth, N.S., Canada, September 29–October 1, 1981.

[2]Bigelow Laboratory Contribution No. 81001.

Printed in Canada (J6682)
Imprimé au Canada (J6682)

occurrence of such an inoculation phenomenon would probably be in a tidal estuary rather than in a fjord since turbulence would vary with water depth and would be more intense in an estuary. Obviously, working in such a complex environment as an estuary limits the conclusions one can draw and necessitates asking very basic questions.

Much of the previous sampling of benthic resting cysts has been qualitative in nature. Wall et al. (1977) and Dale (1976) used a semiquantitative method of counting the cysts in a given dry weight of sediment. Problems arose, however, when sampling with grabs and gravity corers since these can severely disrupt the flocculant layer at the sediment–water interface. This is the most interesting layer in terms of resuspension, since cysts in the flocculant layer are the first to be mixed into the upper water column. A description of cyst distribution (e.g. in terms of hydrography) has been somewhat difficult with old techniques. Thus, one objective of the first part of this study was to develop a semiquantitative method for measuring the number of cysts per unit volume of surface sediment. It involved the use of a nondisturbing corer. Our major questions were: (1) Are there cysts in the sediments of the Tamar Estuary? (2) Is it possible to map the cyst distribution in the sediments of the estuary?

Also fundamental to dinoflagellate ecology is the passive cycling of dinoflagellate cysts between marine sediments and the plankton. Cysts are ubiquitous in marine sediment (Wall et al. 1977) and may also be common in surface plankton (Dale 1976; Reid 1977), though little data exist on the actual numbers or the temporal variation in the concentration of cysts in the water column. Encystment of thecate dinoflagellates in the water column is one obvious explanation for the cysts one observes in the plankton; resuspension of cysts from the sediment is another, yet undocumented, mechanism. The timing and location of either a resuspension or an encystment event has never been examined. Therefore, the second part of this study addresses two basic questions: (1) Are cysts present in the water column of neritic and estuarine areas close to Plymouth, England? (2) If so, does the concentration of these waterborne cysts vary over time? The second question is asked in an attempt to define what events caused the cysts to be present in the water column (i.e. by resuspension or by recent encystment of waterborne thecate dinoflagellates). Knowledge of the timing of cyst appearance might help identify causal event(s).

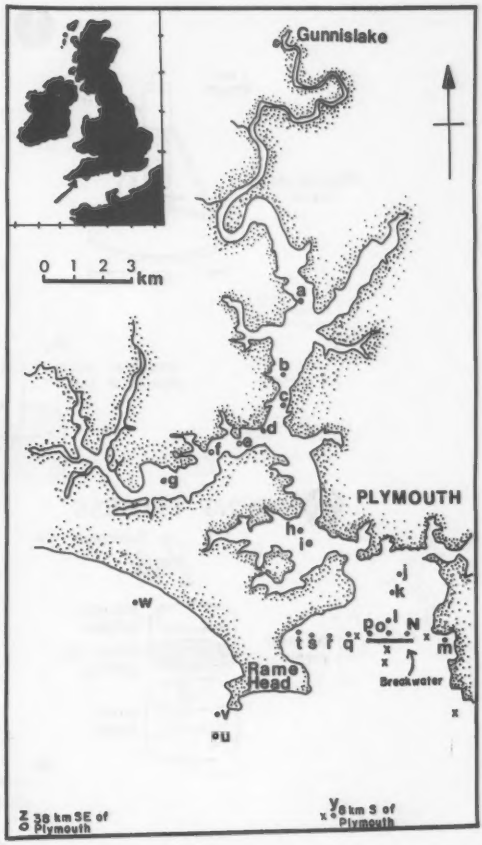

FIG. 1. Tamar Estuary and adjacent English Channel showing locations of stations A to Z. Inset shows the location of the sample area in the British Isles. Solid dots represent successful coring attempts. ×'s mark where the sediment was too hard for the corer to penetrate (rock or hard sand). Circles represent supporting data from previous cores.

Methods

Spatial Distribution of Dinoflagellate Cysts

Samples were taken between February 14 and June 30, 1980 in the Tamar River Estuary (50°20.5′N; 4°9.0′W), Plymouth Sound (confluent with the Tamar River), and the western approaches to the English Channel (Fig. 1). Bottom sediment was sampled with a Craib corer (Craib 1965), a coring device designed to take short cores in mud or sand while retaining the surface flocculant layer and overlying water. Upon gently lowering the corer onto the bottom, a plexiglass core tube (20 cm long and 5 cm diameter) was pushed into the sediment at a velocity of 0.3 $m \cdot min^{-1}$. The plexiglass coring tube remained open at both ends as it slowly penetrated the sediment. After 1 min, tension was applied to the winch cable, a watertight cover sealed the top of the coring tube and the corer was carefully lifted off the bottom. As soon as the bottom of the coring tube was clear of the sediment, a rubber ball sealed the aperture so that the contents were not lost during ascent. After recovery, the core tube was carefully resealed with rubber stoppers and withdrawn from the device. Clear plexiglass coring tubes allowed visual inspection of the contents to assure that the flocculant layer was undisturbed.

Each core was subsampled with an Eppendorf micropipette with the clear plastic tip marked off in 0.05 mL graduations (the opening of the tip was 2 mm in diameter). Initially, 0.25 mL of mud or 0.50 mL of sand was gently drawn into the pipette as it was pushed into the core. Visual inspection of the clear pipette showed that this subsampling technique

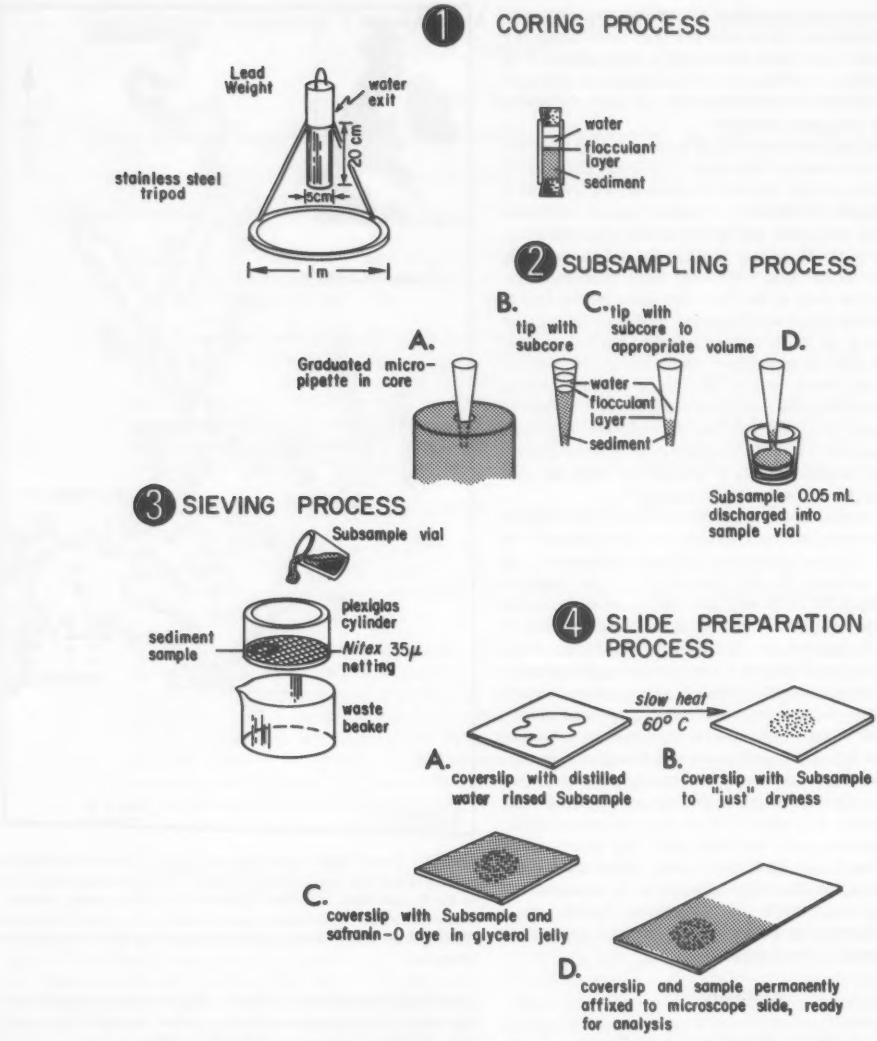

FIG. 2. Summary of the semiquantitative method for sampling cysts and the preparation of microscope slides.

retained the same vertical structure of the sediments as in the original core sample. After taking the initial subsample, all but 0.05 mL of sediment was squeezed out of the pipette tip and discarded; the remaining 0.05 mL of sediment was the sample which would be examined. Such a sample represented a slightly tapered cylinder of 3.5 mm mean diameter and 5 mm depth. Several replicate subsamples could be taken from one core to test for precision. All samples were preserved in 3-mL serum vials with a solution of approximately 90% filtered seawater and 10% buffered formalin.

Preparations for microscopic examination were made with each 0.05 mL sample. First, the samples were sonicated in the serum vial with a Branson sonifier for 5 s at the lowest intensity and amplitude settings. After sonication, the samples were rinsed onto a 35-μm sieve with distilled water, and then were carefully washed back into the original serum vial with distilled water. Filtrate from the sieving process was washed through 20 μm mesh and saved in a serum vial for microscopic examination. This was to ensure that no cysts were lost during the 35 μm screening. Microscope prepara-

tions were made according to Reid (1974). The technique is summarized in Fig. 2.

Cysts were examined and counted on one-third of the prepared slide using 100× magnification. Species identification was made with higher magnifications. Some caution should be used in interpreting the counts since they were scaled up 62.5× to calculate the number of cysts per millilitre of flocculant material. "Living" cysts (containing protoplasm) could be differentiated more easily from empty cysts by background staining with Saffranin-O dye. Thirty-two cores were examined from the Tamar River and Plymouth Sound areas and five cores were examined from the western approaches to the English Channel. Temporary cysts were not enumerated in the counts because they are easily induced to form by harsh sampling conditions. Thus, their numbers on the microscope slide would probably not represent their true concentration in nature (Dale 1979).

Temporal Variation of Dinoflagellate Cysts in the Plankton

Temporal variability in abundance of planktonic cysts was monitored at station N in Plymouth Sound (50°20.5'N; 4°9.0'W) (Fig. 1). Daily or twice-a-week samples were taken at the eastern end of the Plymouth Sound breakwater (station "N") from March to June and August to December of 1980. Depth at this station over one tidal cycle varied from 9 to 14 m during spring tides and 10–12 m during neap tides.

Three types of quantitative measurements were made for waterborne cysts: discrete water samples, integrated water samples, and sediment trap samples. In all of the procedures, care was taken to avoid outside contamination since the actual number of cysts in a water sample was frequently very low.

Daily or bi-daily surface samples were taken as close to high tide as possible during daylight hours. A 5-L bucket sample was poured through a 20-μm Nitex(r) sieve. Contents on the sieve were carefully rinsed with filtered seawater into a 50-mL snapcap jar which contained 2 mL of formalin. Sonication, re-sieving on 35 μm mesh, microscope slide preparation, and cyst counts were done as previously described.

Three vertical profiles of cysts were made at station N using 5-L Niskin bottles set at discrete depths. The profiles were taken on March 27, April 10, and April 18 at station N. A fourth vertical profile was taken at station Y (Fig. 1) on April 18. Water samples were sieved, sonicated, preserved, and prepared for the microscopic examination as described above. Temperature and salinity profiles were taken concurrently with the cyst profiles using an MC-5 thermosalinograph.

A series of water samples, integrated with depth, was taken hourly through one half of a semidiurnal tidal cycle (high to low tide). A hand operated pump with a 15 m long intake hose was used for this. The intake hose was lowered to 1 m off the bottom and water was pumped until the intake hose was filled with only bottom water (30 strokes). At this time, the pump outflow was directed into a 50-L tub and the hose was raised 2 m. Every subsequent 30 strokes of the pump, the hose was slowly raised 2 m while still directing all outflow into the tub. This was repeated until the hose intake was raised from the surface of the water and all water pumped out of it. The tub

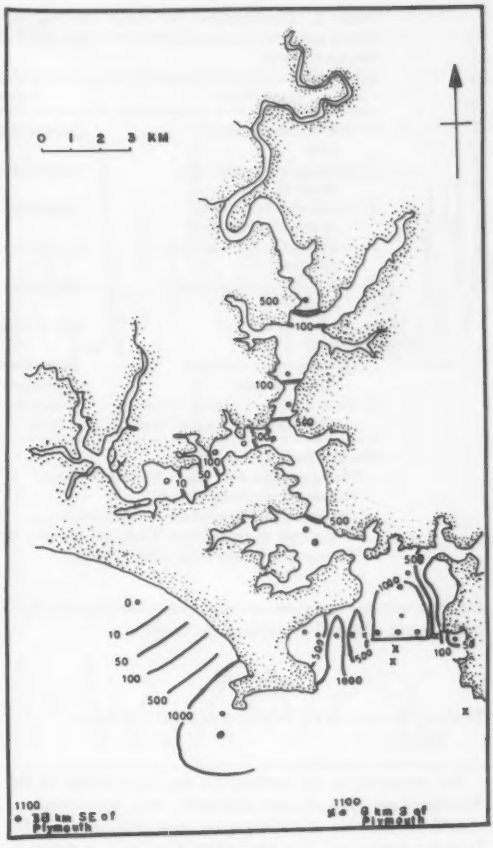

FIG. 3. Sampling area showing log contours of cyst concentration in the flocculant layer (values are in numbers per mL flocculant).

now contained a 25-L "integrated" water sample. A 5-L subsample was taken from the tub, sieved with 20-μm mesh, rinsed, sonicated, resieved with 35-μm mesh and prepared for microscope examination as outlined previously.

A sediment trap was deployed 4 m above the bottom at station N (average water depth = 11 m) for 2–4-d intervals between April 23, 1980 and March 3, 1981 to check for the settling rates of dinoflagellate cysts. Zooplankton feces, tintinnid cysts, benthic diatoms, and copepod eggs were also counted and organic and inorganic sediment was measured using the methods of Holme and McIntyre (1971). The cylindrical sediment trap had a diameter of 11.4 cm and length of 57.0 cm which gave it an 85% collection efficiency (Hargrave and Burns 1979; Gardner 1980). A messenger-operated closing device was triggered before recovery of the trap. After retrieving the trap, the contents were rinsed into a bucket and diluted to 2 L. Vigorous stirring suspended all of the particulate debris. This suspension was subsampled volumetrically

TABLE 1. Dinoflagellate cyst species observed in the sediments (listed in order of decreasing dominance). Station data have been grouped into the three major areas sampled, the Tamar River, Plymouth Sound, and the English Channel.

Tamar River	Plymouth Sound	English Channel
1) *Dubridinium cavatum*[a] Reid	*Quinquecuspis concretum*	*Quinquecuspis concretum*
2) *Quinquecuspis concretum* (Reid) Harland	*Dubridinium cavatum*[a]	*Dubridinium cavatum*[a]
3) *Spiniferites bulloideus*[b] Deflandre & Cookson	*Spiniferites bulloideus*[b]	cyst of *Polykrikos schwartzii* Butschli
4) *Brigantedinium cariacoense*[c] (Wall) Reid	*Spiniferites septentrionalis*	*Operculodinium centrocarpum*[d]
5) *Spiniferites septentrionalis* Harland	*Spiniferites belerius*[b]	*Spiniferites bulloideus*[b]
6) *Spiniferites belerius*[b] Reid	*Operdulodinium centrocarpum*[d]	*Spiniferites septentrionalis*
7) *Quinquecuspis sabrinum* (Reid) Harland	*Multispinulosa quanta*[c] Bradford ex Harland & Reid	*Multispinulosa quanta*[c]
8) *Operculodinium centrocarpum*[d] (Deflandre & Cookson) Wall	*Spiniferites elongatus*[b] Reid	*Brigantedinium caricoense*[c]

Thecal affinities when known:
[a]*Diplopsalopsis orbicularis* (Paulsen) Lebour.
[b]*Gonyaulax scrippsae* Kofoid.
[c]*Protoperidinium punctulatum* (Paulsen) Balech.
[d]*Protoceratium reticulatum* (Clap. and Lachm.) Balech.
[e]*Protoperidinium conicum* (Gran) Balech.

for cyst counts, sediment analysis, etc. Samples for cyst counts were prepared as outlined previously.

Results

SPATIAL VARIATION OF DINOFLAGELLATE CYSTS IN SEDIMENTS

The precision of the method for the examination of the dinoflagellate cysts in the sediments, was approximately ±23% (coefficient of variation for nine replicate samples from the same core). The coefficient of variation at station N over 6 mo was 36.2% ($\bar{x}$ = 2349 cysts·mL^{-1} sediment, n = 6, s = ±851 cysts·mL^{-1} of sediment).

The raw data from the cores, consisting of cyst species, actual numbers of cysts counted and calculated cyst concentrations, is shown in Appendix 1. A description of the sediment type at each station is given as well.

Figure 3 shows the sampling area with logarithmic contours of cyst concentrations. Data spanning 6 months were pooled to construct this figure. Repeated counts of cores from station N over 6 mo had a coefficient of variation of 36.2%, 13.2% greater than the precision of the measuring technique (see Appendix 1). Therefore, contours were plotted logarithmically to emphasize only major changes in concentration. Highest abundances of cysts were observed near Rame Head (see Fig. 3) and inshore of the Plymouth Sound Breakwater. Dinoflagellate resting cysts occurred in 33 of the 35 cores examined (Fig. 3, Appendix 1). Values of 49−3000 cysts (mL·sediment)$^{-1}$ were observed, representing a variation spanning almost two orders of magnitude. Samples which contained the highest cyst concentrations were usually fine-grained mud. However, it was not always true that fine-grained sediments had high cyst concentrations. Most of the fine-grained muds upstream of station I had lower concentrations of cysts than those at the mouth of the estuary. Qualitative estimates of the cyst species composition did not vary substantially between the Tamar River, Plymouth Sound, and the English Channel except for a greater relative abundance of *Operculodinium centrocarpum* (= *Protoceratium reticulatum*) and the cyst of *Polykrikos schwartzii* in the English Channel and a greater abundance of *Dubridinium cavatum* (= *Diplopsalopsis orbicularis*) and *Brigantedinium cariacoense* (= *Protoperidinium punctulatum*) in the estuary. Although *Gonyaulax tamarensis* was first described in the Tamar Estuary (Lebour 1925), few of its cysts were found in this study. The species composition observed in this study agrees quite well with the species composition given by Reid (1974, 1977) for the same region. A list of the species found, ranked from highest to lowest abundance, is shown in Table 1.

TEMPORAL VARIATION OF DINOFLAGELLATE CYSTS IN THE PLANKTON

The precision for the examination of the temporal variability in planktonic cyst concentrations was calculated to be ±28% (coefficient of variation for 10 different 5-L subsamples from the same sample). There were planktonic dinoflagellate cysts in 113 out of 114 water samples taken near Plymouth, England, but there was considerable variability in the data ($\bar{x}$ = 9.2 cysts·L^{-1}, coefficient of variation = 0.86). This variability is greater than the precision of the sampling technique. The cyst species counts are presented in Appendix 2 along with the total concentrations of planktonic cysts. Figure 4 shows a chronological plot of the Plymouth

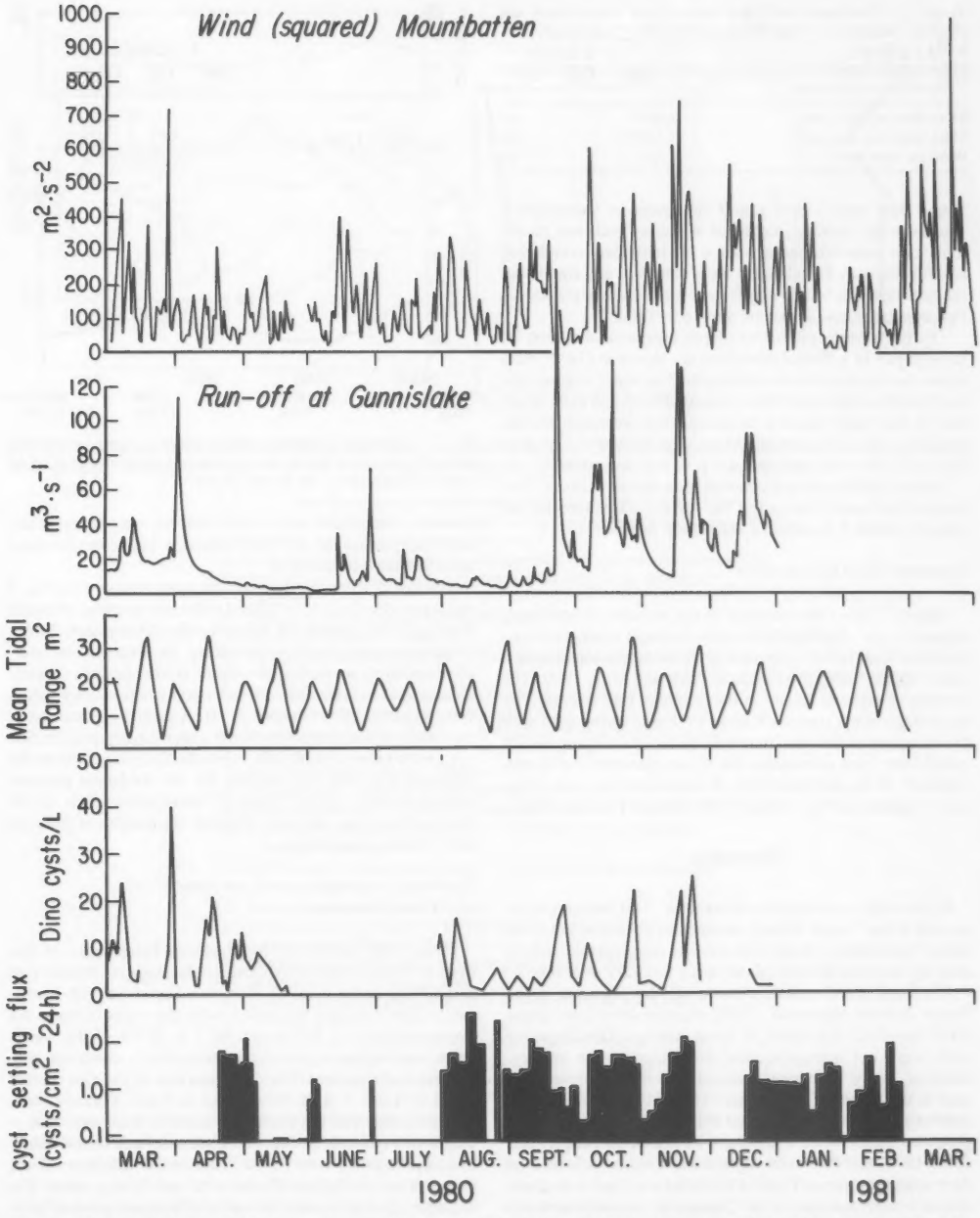

FIG. 4. Chronological plots of tidal range, river runoff, squared wind velocity, planktonic cyst concentration, and cyst settling flux at the mouth of the Tamar Estuary.

TABLE 2. Correlation coefficient between cyst concentration and physical parameters. (*significant, $P < 0.05$; **significant, $P < 0.001$.)

	r	n
River flow vs. cyst conc.	0.281*	60
Tidal range vs. cyst conc.	0.424**	60
Wind vs. cyst conc.	0.221	60

Sound tidal range, river runoff (measured at Gunnislake), squared wind velocity (measured at Rame Head) and planktonic cyst concentration at station N. Individual correlation coefficients were calculated to see if there was any significant relation between wind, runoff, and tides versus planktonic cyst concentration. These are shown in Table 2.

The planktonic cyst counts (depth integrated at station N) through part of a diurnal tidal cycle are shown in Fig. 5. Also shown are sigma-*t* values with depth. The water column was least stratified one hour before maximum ebb and most stratified at low water when a freshwater lens intruded into the sampling area. Cyst concentrations were highest 1−2 h after high and low water and lowest 1 h before low water.

Vertical profiles of cyst concentration appear in Fig. 6. The species that were observed in the surface water samples are listed in Table 3 in order of decreasing dominance.

SEDIMENT TRAP COLLECTIONS

Figure 7 shows the variation in the amounts of sediment, copepod eggs, dinoflagellate cysts, tintinnid cysts, and zooplankton fecal pellets recovered in the sediment trap during a neap−spring−neap tidal cycle in April and May, 1980. The amount of material caught in the sediment trap increased by an average of 8× (range 3× to 11×) during spring tides with the exception of the data from the first day of sampling (which could have been extraneous due to inexperience with a new method). A chronological plot of downward cyst flux at station N appears in Fig. 4 (April 1980 through February 1981).

Discussion

In this study, we wanted to determine: (1) if there are cysts present in the Tamar Estuary sediments, (2) where are cysts most concentrated, (3) are there cysts in the plankton, and (4) does the concentration of planktonic cysts vary over time?

We found dinoflagellate cysts to be very abundant in the Tamar Estuary sediments. Their concentration approached 3000 cysts/mL flocculant at some stations. Dinoflagellate cysts were not homogeneously distributed in the estuary, however. They were most concentrated in the fine-grained mud at the mouth of the estuary. The fact that high concentrations of cysts were associated with fine-grained muds suggests that the cysts were settling with fine sediment particles (Dale 1976) and that water motion was a major influence on their spatial position. Tyler et al. (1981) suggest that *Gyrodinium uncatenum* cysts in the Chesapeake Bay sediments are deposited at frontal convergences. This same mechanism might be occurring in the Tamar Estuary. The hydrographic profile in Fig. 5 shows the presence of a frontal convergence at station N during low tide. In contrast to Tyler et al. (1981),

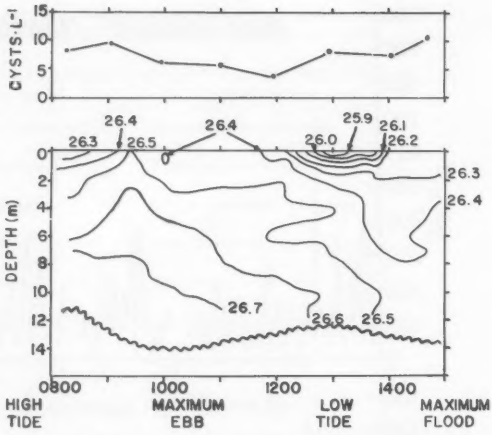

FIG. 5. High tide to low tide vertical profile of sigma-*t* isopleths at station N. Integrated planktonic cyst concentration through this tidal series is shown above the density profile.

however, integrated cyst counts did not vary dramatically with the passage of the front although cyst concentrations were greater seaward of it.

The low cyst concentrations in the upper estuary (see Fig. 3 and Appendix 1) could be related to the low numbers of motile dinoflagellates reported in the same area (Mommaerts 1969). Compared to the mouth of the estuary, he observed low overall abundances as well as two-thirds fewer species of motile dinoflagellates in the Tamar River water where salinity values were less than 25‰ (stations A−I). A further explanation of the low cyst concentrations in the upper estuary may be that cysts were more concentrated below the flocculant layer of the sediment and were not sampled (D. M. Anderson personal communication). Heavy input of terrigenous debris in the upper estuary may also have "diluted" the number of cysts per unit volume of sediment.

TEMPORAL VARIATION OF PLANKTONIC CYST CONCENTRATIONS

Cysts were present in the plankton. Percentages of live cysts as well as species composition data suggest that the cyst assemblage in the muds of Plymouth Sound was not significantly different from that observed in the water column. An average of 45.5 ± 20.3% and 48.7 ± 20.7% of the waterborne and sediment assemblages respectively contained protoplasm and appeared "live." Comparison of the cyst species listed in Table 1 with those listed in Table 3 shows some similarity between the planktonic and sediment cyst assemblages in Plymouth Sound. Moreover, several of the planktonic cyst species were found in either the sediments of the Tamar River or English Channel, but not in both areas. For example, *Dubridinium cavatum* (= *Diplopsalopsus orbicularis*) was a dominant species found in the Plymouth Sound plankton and in the Tamar River sediments. The cyst of *Polykrikos schwartzii* was a dominant species in the Plymouth Sound plankton and the English Channel sediments.

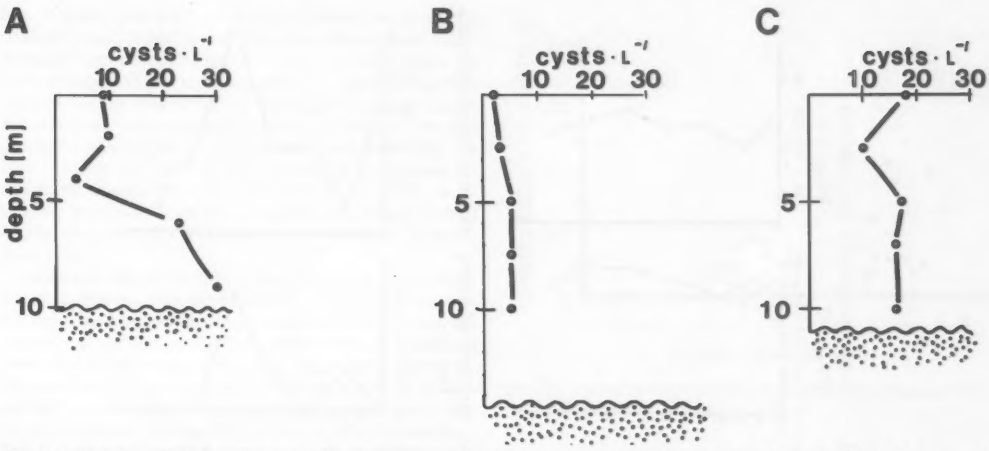

FIG. 6. Vertical profiles of planktonic dinoflagellate cysts at station N at the mouth of the Tamar Estuary (sediment at this station averaged 2000 cysts/mL flocculant). Profiles A, B, and C were made on March 27, April 10, and April 18, 1981, respectively.

TABLE 3. Dinoflagellate cyst species observed in the plankton at the Plymouth Sound breakwater (listed in order of decreasing dominance). When known, the corresponding motile thecate species are given.

1)	*Dubridinium cavatum* Reid = *Diplopsalopsis orbicularis* (Paulsen) Lebour
2)	*Quinquecuspis concretum* (Reid) Harland
3)	*Polykrikos schwartzii* Butschli
4)	*Multispinula quanta* Bradford = *Protoperidinium conicum* (Gran) Balech
5)	*Operculodinium centrocarpum* (Deflandre & Cookson) Wall = *Protoceratium reticulatum* (Clap. and Lachm.)
6)	*Spiniferites bulloideus* Deflandre & Cookson = *Gonyaulax scrippsae* Kofoid
7)	*Bitectatodinium tepikiense* Wilson
8)	*Quinquecuspis sabrinum* (Reid) Harland
9)	*Brigantedinium* sp. = *Protoperidinium* sp.?
10)	*Brigantedinium auranteum* sp. nov. = *Protoperidinium avellana* (Meunier) Balech
11)	*Stelladinium stellatum* comb. nov. = *Protoperidinium compressum* (Abé) Balech
12)	*Spiniferites septentrionalis* Harland
13)	*Brigantedinium cariacoense* (Wall) Reid = *Protoperidinium punctulatum* (Paulsen) Balech
14)	*Spiniferites elongatus* Reid = *Gonyaulax scrippsae* Kofoid?
15)	*Spiniferites* sp. = *Gonyaulax* sp.
16)	*Trinovantedinium capitatum* Reid = *Protoperidinium pentagonum* (Gran) Balech
17)	*Spiniferites belerius* Reid = *Gonyaulax scrippsae* Kofoid
18)	*Lejeunia paratenella* Benedek
19)	*Spiniferites membranaceus* (Rossignol) Sarjeant

If we assume that the cyst assemblages in the plankton and in the sediment are the same (since it cannot be demonstrated that they are significantly different) then we can postulate that a dynamic equilibrium may exist between the sediments and the plankton, where frequent exchange of cysts between the two environments takes place. Other observations also suggested such an exchange of cysts between the sediments and the plankton. For example, vertical profiles of cysts showed (albeit with low precision) that cysts were found at all depths sampled. Two of the profiles (Fig. 6B and 6C) showed that cyst numbers throughout the water column did not change markedly. Higher concentrations of waterborne cysts were found near the bottom in one profile (Fig. 6A), suggestive of cyst resuspension.

Assuming such a dynamic equilibrium does take place, it is difficult to determine with certainty what specific physical processes were responsible for cyst resuspension. Three somewhat different sources of turbulence may have been

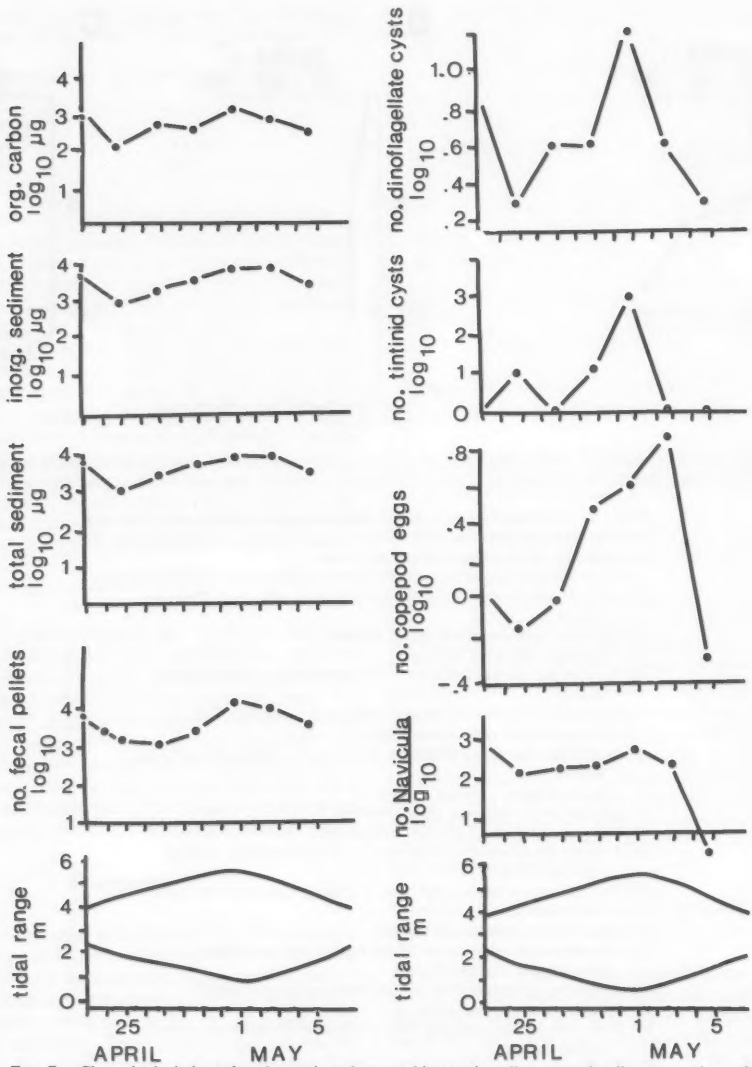

FIG. 7. Chronological plots of total organic carbon, total inorganic sediment, total sediment, numbers of fecal pellets, numbers of dinoflagellate cysts, numbers of tintinnid cysts, numbers of copepod eggs, and numbers of *Navicula* sp. (benthic diatom) caught in the sediment trap. Values represent numbers caught per cm^2 − 24 h or in the case of sediment, 1/40 total µg caught per 24 h.

involved in cyst resuspension: wind, river and tidal mixing. It is not necessary to consider diurnal tidal mixing because the daily planktonic cyst samples were taken at high tide. An initial attempt has been made to determine what physical parameters are important for cyst resuspension by calculating correlation coefficients between the measured physical parameters and cyst concentration. Multiple correlation coefficients cannot be calculated due to significant intercorrelation between the independent variables (e.g. wind velocity and river flow).

Thirty-one percent of the variance in cyst concentration can be accounted for by changes in the wind velocity squared, river runoff and tidal range (this is the sum of the r^2 values in Table 2). Tidal range appeared to be the most important of these parameters for resuspending cysts ($r = 0.42$, $P < 0.001$). Although this correlation is highly significant,

Fig. 8 shows that there is merely a greater range of cyst concentrations during spring tides than during neap tides. Sediment trap collection rates of cysts increased almost an order of magnitude during spring tides. Perhaps dinoflagellate cysts as well as tintinnid cysts, fecal pellets, copepod eggs, and sediment were resuspended into the water column and deposited in the sediment trap as a function of tidal range (see Fig. 7). Only one third of the variance in planktonic cyst concentration remained accounted for by the physical parameters we measured. Therefore, we cannot make any definitive conclusion as to what regulates the concentration of planktonic cysts.

Anderson and Wall (1978) suggested that many dinoflagellate blooms may be initiated by the displacement of motile estuarine populations into nearshore areas by tidal advection and surface runoff. Our observations are consistent with this idea and suggest that in the region near Plymouth, resuspension of overwintering cysts may occur in shallow coastal and estuarine waters, probably where mixing processes are intense. Subsequent inoculation of nearshore dinoflagellate populations from these estuarine cyst beds might reasonably follow.

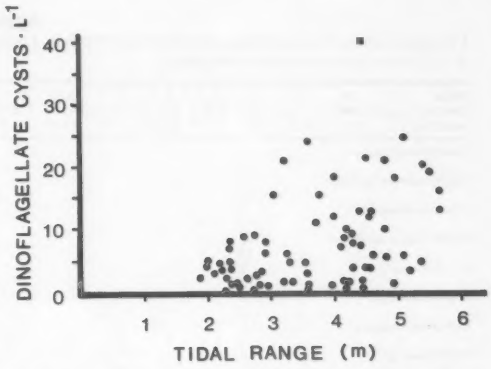

FIG. 8. Plot of the concentration of planktonic dinoflagellate cysts against tidal range ($r = 0.424$, $n = 59$, $P < 0.001$).

Acknowledgments

Many thanks go to Captain Frank Hutchings and his crew of the R/V *Sepia* for their bi-daily sampling, A. W. G. John and A. J. Pomroy for help with sampling and analysis, and the support staff of the Plymouth Marine Biological Association and Institute for Marine Environmental Research for help with cruise preparation. R. W. Eppley, S. Horrigan, G. Jackson, D. Redalje, and D. M. Anderson kindly reviewed the manuscript. The comments of two referees were greatly appreciated. J. Rollins and J. Carleton-Walker drafted the figures. Doris Osborn, Mary Anne Ogle, and Janice Stearns typed the final manuscript. We are especially grateful to C. M. Yentsch and P. M. Holligan for initiating this study, and supplying much effort and many ideas. Finally, we would like to thank the Director of the Plymouth Marine Biological Association who provided laboratory space to us during our sampling. This work was supported by Food and Drug Administration Contract No. 233-77-2314; 6S-005-86307; and NIEH R01-ES 01329 State of Maine, and the Institute of Marine Environmental Research and Marine Biological Association.

ANDERSON, D. M., D. M. KUHS, J. A. ORPHANAS, AND A. R. CEURVELS. 1982. Distribution of the toxic dinoflagellate *Gonyaulax tamerensis* in the southern New England region. Estuarine Coastal Shelf Sci. 14: 447–458.

ANDERSON, D. M., AND F. M. MOREL. 1979. Toxic dinoflagellate blooms in the Cape Cod region of Massachusetts, p. 145–150. *In* D. L. Taylor and H. H. Seliger [ed.] Toxic dinoflagellate blooms. Elsevier-North Holland, Inc., New York, NY.

ANDERSON, D. M., AND D. WALL. 1978. Potential importance of benthic cysts of *Gonyaulax tamerensis* in initiating toxic dinoflagellate blooms. J. Phycol. 14: 224–234.

CRAIB, J. J. 1965. A sampler for taking short undisturbed marine cores. J. Cons. Perm. Int. Explor. Mar. 30: 34–39.

DALE, B. 1976. Cyst formation, sedimentation and preservation: factors affecting dinoflagellate assemblages in recent sediments from Trondheimsfjord, Norway. Rev. Paleobot. Palynol. 22: 39–60.

1979. Collection, preparation and identification of dinoflagellate resting cysts, p. 443–452. *In* D. L. Taylor and H. H. Seliger [ed.] Toxic dinoflagellate blooms. Elsevier-North Holland, Inc., New York, NY.

EVITT, W. R., AND S. E. DAVIDSON. 1964. Dinoflagellate studies. I. Dinoflagellate cysts and thecae. Stanford Univ. Publ. 6 ed. Geol. Sci. 10: 1–12.

GARDNER, W. 1980. Field assessment of sediment traps. J. Mar. Res. 38: 41–52.

HARGRAVE, B. T., AND N. M. BURNS. 1979. Assessment of sediment trap efficiency. Limnol. Oceanogr. 24: 1124–1136.

HOLME, N. A., AND A. D. MCINTYRE. 1971. Methods for the study of marine benthos. IBP Handbook No. 16.

LEBOUR, M. V. 1925. The dinoflagellates of northern seas. J. Mar. Biol. Assoc. U.K., Plymouth. 250 p.

LEWIS, C. M., C. M. YENTSCH, AND B. DALE. 1979. Distribution of *Gonyaulax excavata* resting cysts in the sediments of the Gulf of Maine, p. 235–238. *In* D. L. Taylor and H. H. Seliger [ed.] Toxic dinoflagellate blooms. Elsevier-North Holland, Inc., New York, NY.

MOMMAERTS, J. P. 1969. On the distribution of major nutrients and phytoplankton in the Tamar Estuary. J. Mar. Biol. Assoc. U.K. 49: 749–765.

REID, P. C. 1972. Dinoflagellate cyst distribution around the British Isles. J. Mar. Biol. Assoc. U.K. 52: 939–944.

1974. Gonyaulacacean dinoflagellate cysts from the British Isles. Nova Hedwigia 25: 579–637.

1977. Peridineacean and Glenodiniacean dinoflagellate cysts from the British Isles. Nova Hedwigia 24: 429–463.

REID, P. C., AND R. HARLAND. 1977. Studies of quaternary dinoflagellate cysts from the North Atlantic, p. 147–169. *In* W. C. Elsik [ed.] Zenozoic palynology, v. 1. Am. Assoc. Stratigraphic Palynologists, Contr. Ser. 4A.

STEIDINGER, K. A. 1975. Basic factors influencing red tides, p. 153–162. *In* D. L. Taylor and H. H. Seliger [ed.] Toxic dinoflagellate blooms. Elsevier-North Holland, Inc., New York, NY.

TYLER, M. A., D. W. COATS, AND D. M. ANDERSON. 1981. Encystment in a dynamic environment: deposition of dinoflagellate cysts by a frontal convergence. Mar. Ecol. Prog. Ser. 7: 163–178.

WALL, D. A. 1965. Modern hystrichospheres and dinoflagellate cysts from the Woods Hole region. Grana Palynologica 6: 297–314.

WALL, D., B. DALE, G. P. LOHMANN, AND W. K. SMITH. 1977. The environmental and climatic distribution of dinoflagellate cysts in modern marine sediments from regions in the north and south Atlantic Oceans and adjacent seas. Mar. Micropaleont. 2: 121–200.

Appendix 1

Cyst species counts from sediment cores taken near Plymouth, England. L or X after species name means "live" or "excysted," respectively. A "/" means data unavailable or not taken.

Station		A	B	C	D	E	F	G	H	I	J	K	L	M	N	N
Date (day–mo) All 1980		8–5	8–5	8–5	18–4	6–2	6–2	6–2	6–2	18–4	6–3	6–3	6–3	6–3	6–3	14–2
Depth (m)		7.3	18.3	/	3.7	2.4	3.0	6.1	4.3	2.5	11.9	12.8	14.6	11.9	13.7	11.3
Ataxiodinium choanum	L															
	X															
Bitechtatodinium tepikiense	L															
	X															
Bitechtatodinium sp.	L										2				1	1
	X									2						
Brigantedinium auranteum	L															
	X															3
B. cariacoense	L															
	X											1			1	
Brigantedinium sp.	L													1		
	X												1			5
Dubridinium cavatum	L	1		1						1						
	X	6	1	2	1							1				2
Dubridinium sp.	L												1			
	X						2				1		3		1	2
Gonyaulax tamarensis	L								1							1
	X															
Multispinula quanta	L															
	X				1											
Operculodinium centrocarpum	L			1							2		2		3	1
	X															1
Operculodinium sp.	L	1														
	X															
Polykrikos schwartzii	L															1
	X				1											
Quinquecuspis concretum	L															
	X															
Q. sabrinum	L															
	X															
Scrippsiella faroense	L												4		4	3
	X												3			7
Spiniferites belerius	L			1							1	1			1	
	X												1			
Spiniferites bentori	L										1					
	X															
S. bulloideus	L	1								1			2		1	4
	X				1											1
S. elongatum	L														1	
	X												1			
S. membranaceus	L						1									
	X															
S. mirabilus	L															
	X															
S. ramuliferus	L											1			2	
	X										1				1	
Spiniferites sp.	L	3			2		1				2	1	2		1	
	X									1		1				
Stelladinium stellatum	L															
	X															
Trinovantedinium capitum	L					1				1						2
	X														1	
T. concretum	L												1			1
	X	2							3	3		3	7		2	12
T. olivum	L											1				
	X															
T. sabrinum	L									1						2
	X			1	1											
Trinovantedinium sp.	L															1
	X			1								1				
Unidentified cysts	L															
	X															
Xandarodinium xanthum	L															
	X				1											
		Muddy sand/mussel banks	Muddy sand	Muddy/sand w/rock	Muddy sand	Muddy sand	Fine grain mud	Fine grain mud	Fine grain mud	Fine grain mud	Coarse shell gravel	Coarse shell gravel	Fine grain mud	Compact sand	Fine grain mud	Fine grain mud
% slide counted		32.7	32.7	32.7	34.9	8.0	80.0	16.0	16.0	34.9	31.7	34.9	34.9	40.8	34.9	34.9
Total number cysts counted		14	1	6	9	1	4	0	4	10	10	15	28	1	20	51
% live cysts		35.7	0	33.0	33.3	/	/	/	/	40.0	63.6	40.0	42.9	100	70	31.4
Total conc. cysts (mL·Flocculent)$^{-1}$		856	61	367	516	250	100	0	500	573	630	859	1605	49	1146	2923

N	N	N	N	N	N	N	O	O	O	P	Q	R	S	T	U	V	W	Y	Z
27–3	27–3	10–4	18–4	8–5	2–7	2–7	6–3	14–2	27–3	6–3	6–3	14–2	14–2	6–3	14–2	14–2	2–6	18–4	1–5
10.0	10.0	/	13.0	11.0	11.5	11.5	16.5	14.6	/	18.3	20.1	8.5	7.6	9.1	41.5	38.4	11.5	59.0	72.0
								1											
1																			
			1																
2	2	1	1	3	1		1	1	1			1		1					
								2											
1														1	1				
						1						1						1	
						2			1										
			1				2				1			1		1			
	2	2	1	1	1		2	2				2				1			
1			5	5		1										1			
1	1		10	7	9	8				1						4		5	1
1		1			1					1					1			1	
							1		2						2			1	2
																1			
		1	1	6		2										1		2	
	2	2	6	3	1	1						1			1	1			
2	1	2	8	4	1		3		2						1			3	1
1		2	1	3			2		2										
						1													
1	1				1			2							1				2
2	1		3		1	1		1							1			1	6
	5		1	1				4	2	1	1	1			1				
8	3	3					6	11	2	3		4	1		7	8			
1	1	1	1					2		1		1				2		1	1
	1				1							1							
1	1	5	9	4	4		3	5	4	2		1			2	2		1	1
1	2	1	2	6	1	2		3	1	1						3		1	2
	1	1				2		1	1	1					1	1			
2	2				1					1									
					1														
										1									1
1							3	3	4	1					1	3			
3		2	2			1	3		1			1							
	1	3	2	5		1		2	4	2		1		1					
		1	2	2	1	1	1		1			1							1
1								2											
1				1															
1		1																	
1								4				1			2				
10	5	2	4	5	4	4	5	9	7	5		2		2	6	2		1	
	1		1	1						1									1
		4	1															1	1
					1														
		1			1													1	
1																			
1																			
		1																	

Fine grain mud	Fine grain mud	Fine grain mud	Fine grain mud	Fine grain mud	Fine grain mud	Fine grain mud	Fine grain mud	Fine grain mud	Fine grain mud	Muddy sand	Compact sand	Silty sand	Silty sand	Silty sand	Muddy sand	Muddy sand	Compact sand	Soft sand	Course shell gravel
34.9	34.9	34.9	34.9	32.7	32.7	32.7	34.9	34.9	34.9	34.9	34.9	34.9	34.9	34.9	34.9	34.9	34.9	34.9	34.9
46	33	39	63	60	31	29	33	56	35	22	2	20	3	7	28	31	0	20	20
36.9	36.4	33.3	47.6	50.0	29.0	31.0	36.4	50.0	48.6	50	100	35.0	66.6	28.6	35.7	61	/	45.0	30.0
2636	1891	2234	3610	3670	1896	1774	1891	3209	2006	1261	115	1146	172	401	1604	1776	0	1146	1146

Appendix 2

Cyst species counts from plankton samples taken near Plymouth, England. L or X after species name means "live" or "excysted," respectively. been listed as "live" but they are actually totals of live and excysted counts. A "/" means data unavailable or not taken. An "I0–12" in the row

Station N	Date (d–mo)	29–2	3–3	5–3	6–3	7–3	10–3	11–3	12–3	13–3	14–3	26–3	27–3	27–3	27–3	27–3	27–3
	Time		1315				1210	1110	1225	1510	1235	1215	1130	1130	1130	1130	1130
	Depth of sample	0	0	0	0	0	0	0	0	0	0	0	0	2	4	6	8
	Station	N	N	N	N	N	N	N	N	N	N	N	N	N	N	N	N
Ataxiodinium choanum	L																1
	X																
Biitechtatodinium tepikiense	L																
	X																
Biitechtatodinium sp.	L																
	X				3	1	1						1	1		6	1
Brigantedinium auranteum	L		2														
	X							3			1						
B. cariacoense	L																
	X						1										
Brigantedinium sp.	L						3										
	X			1	1									2		2	1
Dubridinium caperatum	L																
	X																
Dubridinium cavatum	L				1	2	2	1		2							
	X				4		1	1		1	1						
Dubridinium sp.	L				1								1				1
	X				3	3							1	1			2
Gonyaulax tamerensis	L			1	1												
	X																
Hystrichosphaeridium choanophorum	L			1													
	X																
Multispinula quanta	L	1				1											
	X																
Operculodinium centrocarpum	L												2		1		2
	X																
Operculodinium sp.	L		1											1			
	X											1					
Polykrikos schwartzii	L		1		1	2	1										
	X																
Quinquecuspis concretum	L																
	X																
Q. sabrinum	L																
	X																
Scrippsiella faroense	L			1	7	4		1	1	1	2	1	4	1		2	
	X				8		2	1	2		1	2	1	4	4	7	10
Spiniferites belerius	L				1	1											2
	X																
S. bentori	L			1													
	X																
S. bulloideus	L					1							2	1		2	2
	X													1			3
S. delicatus	L																
	X																
S. elongatum	L															3	2
	X												1			2	1
S. membranaceus	L													1			
	X																
S. mirabilus	L				1												
	X																
S. ramuliferus	L					1					1						
	X												1			2	1
Spiniferites sp.	L	3		2	3	1			1					1			2
	X	2			2												1
Stelladinium stellatum	L															1	
	X																
Trinovantedinium capitum	L																
	X	1		1													
T. concretum	L	1	1		4	3									1	2	4
	X	1		2	4	14	2		2	1	2	2	1	1	2	10	14
T. olivum	L					1											
	X																
T. sabrinum	L		1											2			
	X													1			
Trinovantedinium sp.	L																
	X																
Unidentified cysts	L			2						1	1	1	1	1			
	X		1		1												
Votadinium calvum	L																
	X																
Xandarodinium xanthum	L																
	X																
Litres filtered		5	5	5	5	5	5	5	5	5	5	5	5	5	5	5	5
% of microscope slide counted			25	25	25	28	34.9	34.9	34.9	34.9	34.9	34.9	34.9	34.9	34.9	34.9	34.9
Total cysts counted		9	7	11	46	35	13	7	6	6	9	7	16	19	8	39	50
% live		55.0	14.0	58.3	35.7	51.4	46.1	28.6	33.3	66.6	44.0	28.5	62.5	36.8	75.0	25.6	30.0
Total cysts·L^{-1}		7.2	12	9.0	18.4	24	7.4	4.0	3.4	3.4	5.2	4.0	9.2	10.9	4.58	22.4	28.7

Note that after June 30, 1981, counts did not include the L or X determination. For convenience, all the species counts after June 30 have labeled "Depth of sample" means "Integrated water sample from 0 to 12 metres."

31–3	1–4	2–4	9–4	10–4	10–4	10–4	10–4	10–4	10–4	11–4	15–4	15–4	16–4	16–4	17–4	17–4	18–4	18–4	18–4	18–4
	0755	0805	1250	1300	1230	1230	1230	1230	1230	0950	0750	0750	0750	0750	0750	0750	1030	1030	1000	1000
0	0	0	0	0	2.5	5.0	7.5	10	0	0	0	0	0	0	0	0	0	0	2.5	5.0
N	N	N	N	N	N	N	N	N	N	N	N	N	N	N	N	N	N	N	N	N
																		1		1
1	2									1	3	1		2	2	3		1	2	
	4										2									
												1								
3	1					1										2				
4			1		1										1		3	1		
7						2		1					1					1		1
1																				
9											5	4	1	1	3	3	5	4	2	1
20						1		1			9	7	3	10	5	10	7	13	2	6
	1				1							1			1				1	
	1							1						1			1	1		
				1							2	1	1	2		3		1	2	
	1										1			3	2					
1	1	1									1	1		1	2	1				
											1									
2	2	1												2	2		1	1	2	3
2	2			1								1				1		1	1	
	6		1		1	1	3	1		1	1			2	2					
			1			3	3			1	1				1					
1													1			1	1			
	1										1	1	3	4	1	2				
		1	1											1		1				
			1													1				
	1			1				1							1	1				
					1										1					
1																				
2																				
1															2	1				
			1																1	
1																		1		
1																		1		
	1																	1		
			1																	
1	1				1	2		1			1	4		3	1		1			4
5	1			1	2		3	3			5	1		1	5	6	3	2	1	3
			1										1							
3	2														1		1	3	1	
8	3						1								1	1	1	4	2	
								1						1						
							1	1									1	1		
										1			1							
5	5	5	5	5	5	5	5	5		5	5	5	5	5	5	5	5	5	5	5
34.9	34.9	34.9	34.9	34.9	40.7	34.9	34.9	34.9		34.9	34.9	34.9	34.9	34.9	34.9	34.9	34.9	34.9	34.9	23.3
74	37	3	8	4	6	10	11	11		3	31	25	12	34	34	37	25	38	19	19
31.1	43.2	66.6	50.0	50.0	50	40	27.2	27.3		0	32.2	52.0	58.3	50.0	50.0	29.7	52.0	36.8	36.8	52.6
42.4	21.2	1.7	4.58	2.29	2.95	5.7	6.3	6.3		1.72	17.8	14.3	6.9	19.5	19.5	21.2	14.3	21.8	10.9	16.3

APPENDIX 2. (*Continued.*)

Station N	Date (d–mo)		18–4	18–4	18–4	18–4	18–4	18–4	18–4	18–4	22–4	23–4	24–4	25–4	28–4	29–4	30–4	1–5
	Time		1000	1000	1115	1115	1115	1130	1130	1130	1140	1345	1045	/	0850		0750	0755
	Depth of sample		7.5	10	0	10	15	30	45	55	0	0	0	0	0	0	0	0
	Station		N	N	Y	Y	Y	Y	Y	Y	N	N	N	N	N	N	N	N
Ataxiodinium choanum		L																
		X																
Bitechtaxodinium tepikiense		L																
		X																
Bitechtatodinium sp.		L									1					1		
		X	3	2	2	2	1	2		2								
Brigantedinium auranteum		L							1									
		X																
B. cariacoense		L		1		1												
		X			1													1
Brigantedinium sp.		L		1		1												
		X	1	2		2	1		2									
Dubridinium caperatum .		L																
		X																
Dubridinium cavatum		L	6	2	4	2	2	7	3	5	1		2		4	4	4	
		X	8	10	8	10	1	3	9	6	4	3			8	7	7	3
Dubridinium sp.		L																8
		X						4										
Gonyaulax tamerensis		L											1					
		X																
Hystrichosphaeridium choanophorum		L																
		X																
Multispinula quanta		L	1							1				1	1			
		X	1								1							
Operculodinium centrocarpum		L		1		1					1		1		1			
		X																
Operculodinium sp.		L																
		X																
Polykrikos schwartzii		L	1							1			1				1	
		X		1		1			2	1	1							1
Quinquecuspis concretum		L																1
		X																
Q. sabrinum		L																
		X																
Scrippsiella faroense		L																
		X																1
Spiniferites belerius		L																
		X																
S. bentori		L																
		X																
S. bulloideus		L							1	1								
		X		1		1												1
S. delicatus		L																
		X																
S. elongatum		L							1									
		X																
S. membranaceus		L																
		X																
S. mirabilus		L																
		X																
S. ramuliferus		L																
		X																
Spiniferites sp.		L						1	3		1		1		3			
		X							1									
Stelladinium stellatum		L									1	1						
		X																
Trinovantedinium capitum		L												1				
		X																1
T. concretum		L		2		2	2		1						1			
		X	1	5		5	1	3	4	3					2	2	1	2
T. olivum		L									1							2
		X																
T. sabrinum		L	1				1	3	2	1						1		
		X	4	1	1	1			2									1
Trinovantedinium sp.		L			1													1
		X	1	1		1				2								
Unidentified cysts		L								1								
		X																
Votadinium calvum		L																
		X																
Xandarodinium xanthum		L																
		X																
Litres filtered			5	5	5	5	5	5	5	5	5	5	5	5	5	5	5	5
% of microscope slide counted			34.9	23.3	34.9	23.3	23.3	34.9	23.3	34.9	34.9	34.9	34.9	34.9	34.9	34.9	34.9	34.9
Total cysts counted			28	30	17	30	9	23	32	23	12	4	6	2	21	15	13	23
% live			32.1	23.3	29.4	24.1	55.5	47.8	37.5	43.5	50	25.0	100	100	52.4	40.0	38.5	47.8
Total cysts·L^{-1}			16.0	25.8	9.7	25.8	7.7	13.2	27.5	13.2	6.9	2.3	3.4	1.15	12.0	8.6	7.4	13.2

2–5 0755 0 N	6–5 1045 0 N	7–5 0755 0 N	7–5 0755 0 N	9–5 1330 0 N	15–5 1105 0 N	19–5 1110 0 N	21–5 1115 0 N	30–5 0815 10–10 N	30–5 0815 10–10 N	30–5 0905 10–13 N	30–5 0955 10–13 N	30–5 1058 10–12 N	30–5 1155 10–12 N	30–5 1255 10–11 N	30–5 1405 10–12 N	30–5 1440 10–12 N	30–6 / 0 N	4–8 / 0 N	7–8 / 0 N	11–8 / 0 N
					1											1			1	2?
				1																
														1						
1									1		1						11		4	2
1	1	1			1				1						1					
														9	3	7				
	1	4	5	4	2		2	2	4	8	4	4	3		3	3				
6	3	4	4	4	3		1	3	3	7	1	2	1				12	1	2	1
1																				
1																	1			
											1								1	
	1		1								1			1	1	1	1		2	
1																	2		5	
																			1	
															1		1?		2	4
						1						1					2			1
															1					
				1							1									
	1											1					1	1	6	
										1							1		1	
1		4		2	1			1			1	1	2	1	2	5				
1					2									1						
	2			1				1												
	2			1		1	1	1											2	1
*	5	5	5	5	5	5	5	5	5	5	5	5	5	5	5	5	4	4	5	5
32.9	32.9	32.9	32.9	32.9	32.9	32.9	32.9	32.7	16.3	32.7	32.7	32.7	32.7	32.7	32.7	32.7	33.3	33.3	33.3	33.3
13	10	13	10	15	10	2	4	8	9	16	10	9	6	13	12	17	14	3	26	11
15.4	70.0	69.2	60.0	53.3	50.0	0	75.0	50	55.5	56.2	80.0	66.6	83.3	92.0	58.3	82.0	/	/	/	/
8.0	6.1	8.0	6.1	9.2	6.1	1.22	2.4	4.9	11	9.8	6.1	5.5	3.7	8.0	7.34	10.4	10	2	16	7

APPENDIX 2. (*Concluded.*)

Station N	Date (d–mo) / Time / Depth of sample / Station	14–8 / 0 N	18–8 / 0 N	27–8 / 0 N	1–9 / 0 N	4–9 / 0 N	9–9 / 0 N	11–9 / 0 N	15–9 / 0 N	18–9 / 0 N	22–9 / 0 N	25–9 / 0 N	29–9 / 0 N	2–10 / 0 N	6–10 / 0 N	9–10 / 0 N
Ataxiodinium choanum	L															
	X															
Bitechtatodinium tepikiense	L									1	12	1			2	
	X															
Bitechtatodinium sp.	L															
	X															
Brigantedinium auranteum	L															
	X															
B. cariacoense	L															
	X															
Brigantedinium sp.	L			1							3				1	
	X															
Dubridinium caperatum	L															
	X															
Dubridinium cavatum	L															
	X															
Dubridinium sp.	L				1			2	1	3	4		4		1	3
	X															
Gonyaulax tamerensis	L															
	X															
Hystrichosphaeridium choanophorum	L															
	X															
Multispinula quanta	L					1										
	X															
Operculodinium centrocarpum	L															
	X							2	1	1	1		4		1	
Operculodinium sp.	L															
	X					1						2			2	
Polykrikos schwartzii	L															
	X					2	2	1			4	3	1	2	4	
Quinquecuspis concretum	L			2												
	X					1										
Q. sabrinum	L															
	X					1						3				2
Scrippsiella faroense	L	1	2	2?	1											
	X															
Spiniferites belerius	L	2														
	X															
S. bentori	L															
	X															
S. bulloideus	L															
	X															
S. delicatus	L															
	X															
S. elongatum	L															
	X															
S. membranaceus	L															
	X															
S. mirabilus	L															
	X															
S. ramuliferus	L															
	X							1	2	2	2	2			2	1
Spiniferites sp.	L															
	X										1					
Stelladinium stellatum	L															
	X															
Trinovantedinium capitum	L	+		1												
	X															
T. concretum	L															
	X															
T. olivum	L															
	X															
T. sabrinum	L															
	X															
Trinovantedinium sp.	L															
	X															
Unidentified cysts	L									1	3			2	6	
	X															
Votadinium calvum	L															
	X															
Xandarodinium xanthum	L															
	X															
Litres filtered		5	5	5	5	5	5	5	5	5	5	5	5	5	5	5
% of microscope slide counted		33.3	33.3	33.3	33.3	33.3	33.3	33.3	33.3	33.3	33.3	33.3	33.3	33.3	33.3	33.3
Total cysts counted		3	2	6	2	6	2	6	4	8	31	6	13	4	19	6
% live		/	/	/	/	/	/	/	/	/	/	/	/	/	/	/
Total cysts·L^{-1}		2	1	4	1	4	1	4	2	5	19	4	16	2	11	4

13–10 / 0 N	16–10 / 0 N	23–10 / 0 N	27–10 / 0 N	30–10 / 0 N	3–11 / 0 N	6–11 / 0 N	10–11 / 0 N	13–11 / 0 N	18–11 / 0 N	20–11 / 0 N	24–11 / 0 N	27–11 / 0 N	18–12 / 0 N	22–12 / 0 N	29–12 / 0 N
			+?		1	1					2			1	
			8	2				3	7		5	1			
											2				
1		5	12					2	8	4	12	1	1		
			1												
								1?	2?		2				
					1				3						
2		1	4		1			1	2		2		1		1
			2					1		1	8	1	5	1	1
			2	1?	2	1	1?		4?						
			1							1					1
1		2	2						2		5				
			1						2		2				
		1		1		2	1	1	6	4		2	1	2	1
											1				
5 33.3 4 / 2	5 33.3 0 / 0	5 33.3 9 / 5	5 33.3 35 / 22	5 33.3 4 / 2	5 33.3 5 / 3	5 33.3 4 / 2	5 33.3 2 / 1	5 33.3 9 / 5	5 33.3 36 / 22	5 33.3 10 / 6	5 33.3 41 / 25	5 33.3 5 / 3	5 33.3 8 / 8	5 33.3 4 / 2	5 33.3 5 / 3

Stable Carbon Isotope Studies on the Pecks Cove Mudflat Ecosystem in the Cumberland Basin, Bay of Fundy[1]

PETER SCHWINGHAMER[2]

Department of Biology, Dalhousie University, Halifax, N.S. B3H 4J1

FRANCIS C. TAN

Department of Fisheries and Oceans, Atlantic Oceanographic Laboratory, Bedford Institute of Oceanography, P.O. Box 1006, Dartmouth, N.S. B2Y 4A2

AND DONALD C. GORDON JR.

Department of Fisheries and Oceans, Marine Ecology Laboratory, Bedford Institute of Oceanography, P.O. Box 1006, Dartmouth, N.S. B2Y 4A2

SCHWINGHAMER, P., F. C. TAN, AND D. C. GORDON JR. 1983. Stable carbon isotope studies on the Pecks Cove mudflat ecosystem in the Cumberland Basin, Bay of Fundy. Can. J. Fish. Aquat. Sci. 40(Suppl. 1): 262–272.

Ratios of stable carbon isotopes ($\delta\ ^{13}C$) have been measured in components of an intertidal mudflat ecosystem located near the head of the Bay of Fundy. Special attention was given to the isolation and analysis of carbon source materials including phytoplankton, benthic algae, marsh grass (*Spartina alterniflora*), size-fractionated detritus, and "mineral" sediment. Bulk sediment and suspended matter were also analyzed. For most of the year the two major primary producers, *Spartina* and benthic diatoms (dominated by *Gyrosigma* spp.), had similar $\delta\ ^{13}C$ values (−13 to −14‰). Some *Spartina* detritus, presumably "fresh" material, also had similar $\delta\ ^{13}C$ values. It was therefore imposible to estimate the relative importance of carbon from these sources to the nutrition of consumer organisms. Zooplankton, benthic-feeding fish, and benthic fauna had $\delta\ ^{13}C$ values mostly in the range of −12 to −15‰, suggesting that live *Spartina*, "fresh" detritus, and benthic diatoms could be major carbon sources. Phytoplankton and other isotopically light carbon sources including "aged" detritus, bulk and "mineral" sediment, do not appear to be major carbon sources for mudflat organisms. We found *Spartina* detritus to be abundant both in sediments and suspended matter outside the salt marshes, but the $\delta\ ^{13}C$ values of most of the detritus were much lighter (−17 to −20‰) than those of live *Spartina*. The mechanism of this isotopic alteration is not known and we were not able to demonstrate it clearly in laboratory experiments. Although the $\delta\ ^{13}C$ method has helped to assess the relative importance of some isotopically distinct carbon sources, we were unable to detect any ^{13}C enrichment in various trophic levels of mudflat organisms and benthic-feeding fish.

Key words: stable carbon isotope ratio, detritus, decomposition, mudflat ecosystem, Pecks Cove, Bay of Fundy

SCHWINGHAMER, P., F. C. TAN, AND D. C. GORDON JR. 1983. Stable carbon isotope studies on the Pecks Cove mudflat ecosystem in the Cumberland Basin, Bay of Fundy. Can. J. Fish. Aquat. Sci. 40(Suppl. 1): 262–272.

Les rapports d'isotopes de carbone stables ($\delta\ ^{13}C$) ont été mesurés sur des composantes d'un écosystème de vasière intertidale située près de la tête de la baie de Fundy. On s'est attaché surtout à isoler et analyser les sources de carbone, y compris phytoplancton, algues benthiques, herbe salée (*Spartina alterniflora*), détritus fractionnés d'après la grosseur et sédiment «minéral». On a également analysé le sédiment en vrac et la matière en suspension. Pendant la plus grande partie de l'année, les deux principaux producteurs primaires, *Spartina*

[1]This paper forms part of the Proceedings of the Dynamics of Turbid Coastal Environments Symposium convened at the Bedford Institute of Oceanography, Dartmouth, N.S., Canada, September 29–October 1, 1981.

[2]Present address: Department of Fisheries and Oceans, Marine Ecology Laboratory, Bedford Institute of Oceanography, P.O. Box 1006, Dartmouth, N.S. B2Y 4A2.

Printed in Canada (J6724)
Imprimé au Canada (J6724)

et diatomées benthiques (dominées par *Gyrosigma* spp.) ont des valeurs de $\delta\ ^{13}C$ identiques (−13 à −14‰). Certains détritus de *Spartina*, probablement du matériel «frais», ont aussi des valeurs identiques de $\delta\ ^{13}C$. Il a donc été impossible d'estimer l'importance du carbone provenant de ces sources dans l'alimentations des organismes consommateurs. Les valeurs de $\delta\ ^{13}C$ du zooplancton, des poissons se nourrissant au fond, et enfin de la faune benthique sont comprises surtout dans la fourchette de −12 à −15‰, ce qui donne à penser que *Spartina* vivante, les détritus «frais» et les diatomées benthiques pourraient être des sources de carbone majeures. Par contre, le phytoplancton et les autres sources de carbone isotopiquement léger, y compris les détritus «âgés», les sédiments en vrac et «minéraux» ne semblent pas être d'importantes sources de carbone pour les organismes des vasières. On a constaté que les détritus de *Spartina* étaient abondants à la fois dans les sédiments et dans la matière en suspension en dehors des marais salés, mais que, pour la plupart des détritus, les valeurs de $\delta\ ^{13}C$ sont beaucoup moindres (−17 à −20‰) que celles observées dans *Spartina* vivante. On ignore le mécanisme de cette altération isotopique et on n'a pu le démontrer clairement dans des expériences de laboratoire. Bien que la méthode de $\delta\ ^{13}C$ nous ait aidés à évaluer l'importance relative de sources de carbone isotopiquement distinctes, nous n'avons pu détecter d'enrichissement de ^{13}C dans divers niveaux trophiques des organismes des vasières et des poissons ne nourrissant de benthos.

Received November 10, 1981
Accepted June 19, 1982

Reçu le 10 novembre 1981
Accepté le 19 juin 1982

In 1978, the Marine Ecology Laboratory initiated a comprehensive study of a mudflat ecosystem located at Pecks Cove, N.B., in the Cumberland Basin, at the head of the Bay of Fundy. The purpose of the study is twofold: to elucidate the structure and dynamics of the unperturbed mudflat ecosystem, and to use the ecological information obtained to help predict likely environmental impacts of tidal power projects being considered in the upper Bay of Fundy (Bay of Fundy Tidal Power Review Board 1977).

In a turbid coastal ecosystem such as the Cumberland Basin, planktonic primary production is severely limited by the shallow euphotic zone (Hargrave et al. 1983). There is, however, a considerable amount of particulate organic carbon in the form of waterborne detritus which is potentially available to heterotrophic organisms in both the water column and the mudflat. The importance of *Spartina alterniflora*, which grows in extensive marshes around the head of Cumberland Basin, as a source of detrital carbon has not been well investigated, but may be significant (Morantz 1976). Additionally, production by epibenthic diatoms on intertidal mudflats (Hargrave et al. 1983) may contribute substantial amounts of carbon to consumers in the Cumberland Basin.

We undertook a study that included careful isolation and isotopic analysis of various carbon source-materials from bulk sediment and suspended material in an attempt to assess the relative contributions of *Spartina*, benthic diatoms, and detritus to the nutrition of organisms in the Pecks Cove mudflat. Through laboratory experiments, in which we monitored the ratio of stable carbon isotopes ($\delta\ ^{13}C$) of *Spartina* as it decomposed, we hoped to determine whether or not the ratio is conservative over a period longer than that covered by Haines' (1977) experiment.

The method of stable carbon isotope ratios has been used in numerous recent studies to define carbon sources and, implicitly or explicitly, food chains in coastal ecosystems (Haines 1976, 1977; DeNiro and Epstein 1978; Thayer et al. 1978; Fry and Parker 1979; Haines and Montague 1979; McConnaughy and McRoy 1979a, b; Kneib et al. 1980; and Hackney and Haines 1980). Based on comparison of $\delta\ ^{13}C$ of consumer organisms with that of carbon sources available to them, the conclusions of these studies are critically dependent upon a number of inadequately verified assumptions. Benthic algae have been assumed to be isotopically distinct from *Spartina* and its detritus, based on only three analyses of material containing benthic algae (Haines 1976). Fractionation of carbon isotopes in metabolism of consumers has been assumed important in some studies (McConnaughy and McRoy 1979a), not in others. Plant detritus has been assumed to maintain the $\delta\ ^{13}C$ of the living organism (Haines 1977). Single or few carbon sources have been assumed in many ecosystems, based on inadequate isolation of the various possible source materials.

Our purpose in the present study has been to reduce the number of untested assumptions by careful isolation and measurement of as many components of the Pecks Cove ecosystem as we could handle, especially the phytal and detrital source materials. If the various carbon sources are isotopically distinct, and if metabolic fractionation of ^{12}C and ^{13}C is insignificant in consumers, then the relative importance of the various carbon sources to the benthic community at Pecks Cove could be assessed. We have included the results of approximately 200 isotopic analyses of sediment, suspended material, and isolated plant, animal, and detrital material collected in the field over a 3-yr period or resulting from laboratory experiments. Our interpretation includes an evaluation of the usefulness of the $\delta\ ^{13}C$ method as applied to food web studies.

Site Description

The Pecks Cove mudflat is located near the head of the Bay of Fundy just inside Cumberland Basin (Fig. 1). The tides are semidiurnal and the average range is 11 m (14 m for large spring tides). At low tide, the mudflat is approximately 1 km wide and 4 km long. Pecks Cove is just one of many large intertidal mudflats in Cumberland Basin (Fig. 1) which together comprise 40% of the total area below the highest tides.

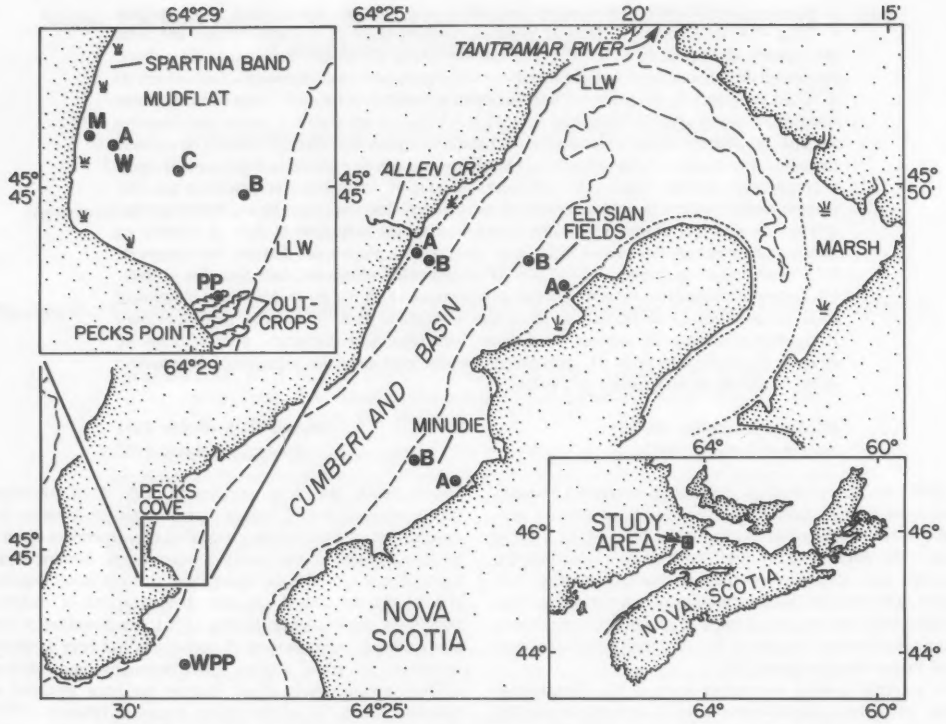

FIG. 1. Location of sampling sites in Cumberland Basin. Inset shows location of sampling sites at Pecks Cove. Station M is in a band of *Spartina alterniflora* just below mean high water. Stations A and B are upper and lower intertidal sites, respectively, on all mudflats studied. Station W and WPP are the locations of collection of suspended material.

The mudflat is composed of fine sediment, mostly silt and clay. A soft surface layer, about 5–10 cm deep and having a water content of 40–50% by weight, is underlain by a denser, more compact sediment layer of similar grain size. Sediment organic carbon concentrations vary seasonally between about 0.3 and 1% by weight (Gordon et al. 1980). Landward, the mudflat terminates at a beach composed primarily of sand and gravel. A narrow band of *Spartina alterniflora*, up to 100 m wide, grows along the upper edge of the mudflat. More extensive saltmarshes (17.3 km^2) are found further up the Cumberland Basin (Fig. 1). Annual primary production by *S. alterniflora* in the Cumberland Basin is estimated to be 2.1×10^6 kg $C \cdot yr^{-1}$ (D. C. Gordon Jr. and P. J. Cranford, unpublished data). Rock ledges are restricted to near the headlands between mudflats and support the growth of macrophytic algae, primarily *Fucus*.

The water flooding the mudflat twice daily is very turbid and suspended sediment concentrations generally range from 0.1 to 1 g/L. Light penetration is severely restricted such that the euphotic zone is limited to approximately 1 m or less. Accordingly, phytoplankton primary production in Cumberland Basin is only estimated at 5.0×10^5 kg $C \cdot yr^{-1}$ (D. C. Gordon Jr. and P. J. Cranford, unpublished data).

On each tide, a thin film of surface sediment is suspended and subsequently deposited. Heavy storms can result in extensive sediment shifting, especially noticeable at Station B, and there is an apparent relationship between storms and carbon influx into the sediment (Schwinghamer 1981b). The flow of river water into the Basin is negligible compared to the rate of tidal flushing and carbon from terrestrial sources carried via river flow into the Basin is also probably of minor importance to the system (D. C. Gordon Jr. unpublished data).

Biomass estimates of benthic organisms at Pecks Cove Station A are given by Schwinghamer (1981b). Bacteria biomass ranged between 3.3 and 6.3 g $C \cdot m^{-2}$, contributing an average of approximately 1.3% to the total organic carbon in the sediment. Only during blooms of benthic diatoms did the biomass of any other group exceed that of bacteria. The biomass of benthic algae was more variable than that of bacteria, ranging from less than 0.2 g $C \cdot m^{-2}$ in February and March 1980 to a peak of 12.6 g $C \cdot m^{-2}$ in September 1979. Even at peak biomass, however, algae only accounted for 2.8% of the total organic carbon in the sediment. Primary production by benthic microalgae on Cumberland Basin mudflats is about 1.5×10^6 kg $C \cdot yr^{-1}$ (D. C. Gordon and P. J. Cranford unpublished data). Macrophytic algae were only incidental on

occasional ice-rafted rocks or wooden stakes and probably contribute little organic carbon to the system. Meiofauna and macrofauna had lower biomasses than bacteria or benthic algae. Meiofaunal carbon ranged from 0.09 to 2.45 g $C \cdot m^{-2}$ while that of macrofauna ranged from near 0 during the winter to 3.0 g $C \cdot m^{-2}$ in June 1979.

A tellinid bivalve, *Macoma balthica*, a tubicolous amphipod, *Corophium volutator*, and a capitellid polychaete, *Heteromastus filiformis* are the dominant macrofaunal species on the mudflat (Hicklin et al. 1980). *M. balthica* is restricted to the area near the *Spartina* band for most of the year. The mud snail, *Hydrobia minuta*, is common at Stations M, A, and C but the periwinkle, *Littorina* sp., is restricted to the *Spartina* band. *Ilyanassa obsoleta*, a dogwhelk, occurs in small numbers at Stations A and B.

The meiofauna is dominated by Nematoda, with Harpacticoida, Foraminifera, and Oligochaeta contributing relatively small proportions of the total biomass (Schwinghamer 1981b). Testate Foraminifera were common at Station B, but an allogromiid, *Rhynocogromia* sp., which lacked a mineral test, was the dominant foraminiferan at the other Pecks Cove stations.

No good estimates of biomass of benthic feeding fish are available for Pecks Cove, but Schwinghamer (1981b) has shown that predation upon the macrofauna by smooth flounder (*Liopsetta putnami*) and tomcod (*Microgadus tomcod*) may affect macrofaunal abundance, especially that of *Macoma balthica*. Predation by benthic feeding shorebirds has been shown to reduce the biomass of *Corophium volutator* in the Minas Basin (Boates and Smith 1979), and Schwinghamer (1981b) also showed that the presence of these shorebirds has a negative effect upon total macrofaunal biomass at Pecks Cove.

Most benthic production at Pecks Cove occurs during the ice-free season, usually from early April to mid-December. Ice of various forms is present on the mudflat during the winter and causes considerable erosion (Gordon and Desplanque 1981). Mortality of meiofauna and macrofauna may also be related to ice scouring of the sediment surface.

Though planktonic primary production is limited, zooplankton are abundant in the Cumberland Basin. Several species of mysids (*Neomysis americana*, *Mysis* spp.) dominate the zooplankton (M.Dadswell personal communication). The sand shrimp *Crangon septemspinosa*, Calanoid copepods, and suspended benthic organisms such as harpacticoid copepods, nematodes, isopods, and *Corophium* also occurred in plankton samples.

Methods

Sample Collection and Treatment

Most of the samples analyzed in this study were collected at Stations A, B, C, and M when the mudflat was exposed (Fig. 1). Station A is located in the upper intertidal zone just seaward of the *Spartina* band and is flooded about 4 h per tide. Station B is located in the lower intertidal zone about 100 m landward of the mean low tide mark and is exposed about 4 h per tide. Station C is intermediate. Station M is located within the fringing *Spartina* band. Samples of suspended particulate material (SPM) were collected from CSS *Dawson* near the mouth of Cumberland Basin in February 1980. Zooplankton and suspended detritus were collected with plankton nets from a fishing boat at the same location in July and August 1981. A set of core samples of surface sediment collected at other mudflats by helicopter in September 1980 was also analyzed. In all, the samples were collected over a 3-yr period with the majority in May and September 1980. Sediment and SPM samples were collected at Pecks Cove all seasons of the year.

Live and dead leaves, shoots, roots, and rhizomes of *Spartina alterniflora* were collected from Station M. Epiphytes and other adherent materials were removed from the *Spartina* by rinsing and wiping. The cleaned material was rinsed with organic-free, distilled water (Super Q), dried at 60°C and stored at −20°C in rinsed, glass scintillation vials with foil-lined caps. This final rinsing, drying, and storage procedure was the same for all samples collected from the field.

Larger macrofaunal organisms were picked from the mud, rinsed with filtered (0.2 μm) seawater from Pecks Cove, and placed in mason jars containing filtered Pecks Cove seawater. Smaller macrofauna were sieved onto a 420 μm mesh screen, hand sorted, and placed in mason jars. All species were kept separately in several changes of water for 24−36 h to allow them to void their gut contents. Only active, intact animals were retained for analysis. Body tissues of molluscs were removed from the shells prior to analysis.

Meiofauna were separated from the sediment by first sieving onto a 63 μm mesh screen. Harpacticoids, Foraminifera (*Rhyncogromia* sp.), and, where abundances of individual taxa were low, mixed meiofauna were separated from detritus and benthic algae by density-gradient centrifugation in a silica sol−sorbitol mixture as described by Schwinghamer (1981a). The small amount of contaminating material was removed by hand.

Nematodes and oligochaetes were collected by placing 64 μm sieved material in funnels lined with 56 μm mesh nylon screen and covering with filtered, Pecks Cove seawater. Clear vinyl tubing attached to the funnel outlet was clamped shut. The worms crawled through the mesh and settled in the tubing above the clamp. They were drawn off periodically over the following 24 h, and separated into size fractions by sieving (505, 253, 130, and 64 μm meshes). All meiofauna were held in filtered Pecks Cove seawater for 24 h prior to final rinsing and drying.

Benthic diatoms were collected by a multi-step concentration and separation procedure. Diatoms were concentrated at the sediment surface by shading areas of the surface using inverted plastic pans or plywood boxes placed soon after the areas were exposed at receding tide. The surface few millimeters of sediment was then scraped with a garden trowel into plastic buckets just before inundation by incoming tide. In the lab, the sediment was spread in shallow enamel pans and placed under fluorescent lights for at least 12 h. The surface layer of sediment was then removed and sieved onto 20 μm mesh nylon screen. Material retained on the sieve was placed in 250 mL centrifuge tubes, and approximately 100 mL of filtered Ludox silica−sol was added. Organic-free, distilled water (Super Q) was poured onto the surface of the silica sol to prevent it from crystallizing, and to set up a density gradient where the water and silica sol mixed. The tubes were centrifuged at 1500−2000 rpm for 30 min. Diatoms collected

TABLE 1. Mean $\delta\ ^{13}C$ values and individual measurements of material collected from Pecks Cove and in other areas of the Cumberland Basin, Fig. 1. M, A, C, and B are the Pecks Cove marsh and mudflat stations. W indicates material collected by pump from the overflooding water at Pecks Cove; WPP, suspended material collected in the Basin off Pecks Point; ACA and ACB, Allan Creek upper and lower intertidal; MA and MB, Minudie upper and lower intertidal; EFA and EFB, Elysian Fields upper and lower intertidal; and PP, the rocky intertidal at Pecks Point.

Material	Location	$\delta\ ^{13}C$ Determinations	Mean $\delta\ ^{13}C$
Ulva sp.	A	−4.9	−4.9
Enteromorpha sp.	M	−9.6	−9.6
Ilyanassa obsoleta	A	−8.9, −10.0, −11.1	−10.7
	B	−12.7	
Hydrobia minuta	M	−13.1	−11.1
	A	−11.3, −11.6	
	C	−9.6, −10.1	
Aglaophamus circinata plus other small Polychaeta	C	−12.1	−12.5
	B	−12.9	
Littorina sp.	M	−12.1, −12.4, −13.4	−12.6
Oligochaeta	A	−13.1	−12.8
	C	−12.4	
Nereis diversicolor	A	−11.8, −13.9	−12.9
Microgadus tomcod	W	−12.8, −12.9	−12.9
Liopsetta putnami	W	−12.6, −13.3	−12.9
Eteone trilineata	A	−12.1	−13.0
	B	−13.8	
Macoma balthica	M	−12.7, −13.0, −13.5	−13.1
	A	−13.0, −13.1, −13.6	
	C	−12.8, −12.9	
	B	−13.3	
Nematoda, 125−500 μm	A	−12.8, −13.4	−13.1
	C	−13.2	
Spartina alterniflora, alive	M	−12.9, −13.2, −13.1	−13.1
Spartina alterniflora, dead	M	−12.6, −12.9, −13.3, −14.0	−13.2
Crangon septemspinosa	WPP	−12.1, −13.3, −13.6, −14.1	−13.3
Spionids plus other small Polychaeta	A	−12.9, −13.8	−13.4
Cerebratulus sp.	A	−13.6	−13.5
	B	−13.3	
Nematoda, > 500 μm	A	−13.3, −13.4	−13.6
	C	−14.1	
Gyrosigma sp., other	A	−14.2, −13.3, −13.2, −13.3, −14.1	−13.6
Nematoda, all sizes	C	−12.3	−13.9
	B	−13.8, −15.5	
Mixed meiofauna, mostly Nematoda	M	−13.1, −14.3	−14.1
	A	−14.8	
Harpacticoida	A	−13.9, −15.0	−14.1
	C	−14.3	
	B	−13.7, −13.8, −13.8	
Nematoda, < 125 μm	A	−13.4, −13.9, −14.1, −15.2	−14.2
Mysidacea, with shell	WPP	−13.6, −13.7, −15.6	−14.3
Rhyncogromia sp.	A	−14.6	−14.6
Corophium volutator	M	−13.1	−14.6
	A	−14.1, −14.7, −14.8	
	C	−15.6, −15.7	
	B	−13.7, −14.0, −15.4	

TABLE 1. (*Concluded*).

Material	Location	$\delta^{13}C$ Determinations	Mean $\delta^{13}C$
Gammarus sp.	M	−14.8	−14.8
Menidia menidia	A	−14.8, −15.0	−14.9
Heteromastus filiformis	A	−15.0, −15.5	−15.1
	C	−13.2, −14.4	
	B	−16.1, −16.6	
Mysidacea, without shell	WPP	−15.3, −17.8	−16.6
Spartina detritus, > 500 μm, in sediment	M	−15.1	−17.4
	A	−13.6, −17.0, −19.4	
	C	−19.8	
	B	−18.1, −18.6	
Fucus vesiculosus	M	−13.4, −15.1, −16.2, −18.2, −21.9	−17.6
	PP	−20.7	
Suspended *Spartina* detritus	W	−18.0	−17.7
	WPP	−16.1, −17.1, −17.3, −17.3, −18.1, −19.8	
Gyrosigma sp., May 1981	A	−17.6, −18.5	−18.1
Spartina sediment detritus, < 125 μm, in sediment	A	−18.1, −18.2, −18.5, −18.6, −20.2	−18.8
	C	−18.9	
Spartina detritus, 125−500 μm in sediment	A	−17.2, −18.5, −17.7, −21.1	−18.9
	C	−19.6	
	B	−18.0, −20.1	
Phytoplankton	W	−18.7, −19.6	−19.2
Copepoda	W	−17.1, −21.5	−19.3
Bulk sediment, surface	M	−19.7	−20.0
	A	−17.9, −18.3, −19.1, −19.2, −19.2, −19.3, −20.0, −20.0, −20.3, −20.7, −20.8, −20.8, −20.9, −20.9, −21.2	
	B	−20.3, −20.4	
	ACA	−19.7	
	ACB	−20.6	
	MA	−19.9	
	MB	−20.7	
	EFA	−20.2	
	EFB	−20.5	
Bryozoa	B	−20.1	−20.1
Bulk sediment, deep	M (5 cm)	−18.5	−20.3
	A (5 cm)	−20.7	
	A (10 cm)	−20.9	
	A (15 cm)	−21.0	
Bulk SPM	W	−20.6, −21.9, −22.2, −22.8	−21.1
	WPP	−19.6, −20.0, −20.4	
Mineral SPM	W	−21.2, −21.4	−21.3
Mineral sediment	M	−21.3	−21.8
	A	−21.4, −23.1	
	C	−22.4	
	B	−20.9, −21.8	
Alosa sapidissima	W	−28.2	−28.2

near the base of the density gradient in a clearly defined dark green band. They were siphoned off using a suction apparatus as described by Schwinghamer (1981a) and rinsed to remove the silica sol. To obtain a "pure" diatom sample, the material was placed in a glass Petri dish and Super Q water added. Surface tension caused the diatoms to float on the surface film while detritus and meiofauna remained at the bottom. A Pasteur pipette was used to remove the diatoms to pre-ignited silver or glass-fibre filters.

Detritus, with algae and fauna removed, was rinsed with Super Q water and separated into size fraction by sieving. It was visually inspected to ensure that no organisms remained,

TABLE 2. Results of *Spartina* decomposition experiments. All samples were run in triplicate.

Experiment	Sample	Live		Dead	
		Mean $\delta^{13}C$	SD	Mean $\delta^{13}C$	SD
Initial	Freshly collected	−13.3	0.7	−12.4	0.3
Leaching	In Super Q water	−12.0	0.3	—	—
	In filtered seawater	−11.8	0.1	—	—
Aerobic in seawater	Initial	−13.0	1.4	−13.5	0.6
	1 w	−13.4	0.5	−13.1	0.1
	1 mo	−12.1	0.5	−13.3	1.0
	2 mo	−12.5	0.8	−11.1	1.3
	3 mo	−13.7	0.3	−13.7	2.1
Anaerobic in sediment	Initial	−16.8	0.7	−16.2	0.9
	1 w	−17.8	0.1	−16.9	0.5
	1 mo	−16.2	1.7	−16.8	1.0
	2 mo	−17.8	1.0	−17.8	0.1
	3 mo	−17.4	0.9	−18.4	0.2

and to ascertain the nature of its origin. In all cases it consisted mostly of fragments of vascular plant material often identifiable as grass blades,stems, and rhizomes. The only abundant source of such material around the Cumberland Basin is *Spartina alterniflora* in the lower salt marshes (D. C. Gordon and P. J. Cranford, unpublished data).

"Mineral sediment", (mineral grains free of detritus, benthic algae, and meiofauna) was obtained from the material remaining at the bottom of the centrifuge tubes after separating the organic material. This was dispersed and rinsed well with Super Q water, then decanted several times to remove any remaining detritus. The material that remained was mostly fine sand with attached micro-organisms and sorbed or otherwise adherent organic matter.

Suspended material was collected from approximately 10^3 L of seawater, which was pumped ashore from 1 m above the sediment surface at Station A using a centrifugal pump. The pump discharge was directed onto a 20 μm mesh nylon screen to concentrate suspended material. Most zooplankton was removed immediately after collecting by sieving the bulk material through a 256 μm mesh screen. Smaller zooplankton was hand picked from the detritus and phytoplankton. The latter two components in the May 1980 sample were isolated by density gradient centrifugation as described above. Large detritus was separated from phytoplankton in the September 1980 sample by sieving onto a 130 μm mesh screen. The smaller size fraction contained both phytoplankton and detritus but there was insufficient material to allow further separation. Zooplankton and detritus collected in plankton net tows during 1981 were hand-picked and sorted from the bulk sample.

Suspended "mineral" sediment was collected by directing approximately 20 L of pump effluent through a 256 μm screen to plastic buckets. The suspended material was allowed to settle and the supernatant poured off. "Mineral" sediment was then concentrated as described above.

SPARTINA DECOMPOSITION EXPERIMENTS

We attempted to assess, in vitro, the magnitude of any shift of $\delta^{13}C$ values associated with leaching or anaerobic decomposition of *Spartina* detritus. All materials (live and dead *Spartina alterniflora*, seawater, and subsurface sediment) were collected on May 29, 1981 in Cumberland Basin. Initially, *Spartina* was washed to remove sediment and then cut into fine pieces with scissors. Subsamples of both live and dead grass were taken for initial analysis.

The first experiment examined rapid leaching. Two grams of live *Spartina* were placed in 200 mL of Super Q water and filtered Bedford Basin seawater, both in triplicate. The flasks were plugged, shaken and autoclaved daily. At the end of 1 wk, the contents were filtered and analyzed.

The second experiment examined aerobic decomposition in seawater. After mashing *Spartina* in a blender with filtered seawater, 2 g of the mash was added to 200 mL of *unfiltered* Cumberland Basin seawater, 15 replicates for both live and dead grass. Containers were kept in the dark at room temperature (≈21 C) and purged frequently with oxygen. Three replicates, both live and dead, were sampled at the following intervals: initial; 1 wk; and 1, 2, and 3 mo.

The final experiment focused on anaerobic decomposition in sediment. Sixty grams of *Spartina* mash was added to 0.5 L of subsurface (>3 cm depth) Pecks Cove sediment, with enough filtered seawater to make a slurry, and mixed well. About 15 mL of the *Spartina* sediment mixture were placed in a glass vial, 15 replicates for both live and dead grass. Before sealing, vials were purged with nitrogen to remove oxygen. Vials were kept undisturbed in the dark at room temperature and were sampled at the same intervals as the aerobic experiment.

ANALYTICAL PROCEDURES

The procedures for isotopic analysis of organic carbon were described by Tan and Strain (1979a,b). Briefly, the samples were acidified with 10% HCl for a minimum of 5 h at 50°C in a precombusted (500°C for 1 h) porcelain combustion boat to remove carbonates. Conversion of organic carbon to CO_2 was accomplished in a combustion line similar to that used by Craig (1953). The CO_2 was purified in a separate vacuum line containing Cu and MnO_2 at 470°C for the removal of nitrogen and sulfur oxides (Sackett and Thompson 1963). The yield of

CO_2 was measured on a calibrated mercury manometer. The $^{13}C/^{12}C$ ratios were determined with a Nuclide 6–60 RMS mass spectrometer equipped with a triple collector and a small sample inlet system. The raw data are corrected for instrument effects and mass spectral cross terms and reported in the standard $\delta\ ^{13}C$ notation relative to the Pee Dee Belemnite (PDB) standard. The overall analytical precision for sedimentary organic carbon is ±0.2‰ (1 SD).

Results

The results of all $\delta\ ^{13}C$ determinations made in this study are tabulated in Tables 1 and 2. Mean $\delta\ ^{13}C$ values, ±2 standard deviations, of carbon sources and consumer organisms in Pecks Cove and the Cumberland Basin are plotted in Fig. 2.

Carbon Sources

1) *Spartina* — Living and dead *Spartina* had similar $\delta\ ^{13}C$ values, ranging from −12.6‰ (dead leaves, December 1979) to −14.0‰ (dead leaves, February 1980), and averaging −13.2‰. Roots and rhizomes were isotopically similar to the above-ground parts. The values are similar to those of *Spartina* in the southeastern United States (Haines 1976; Hackney and Haines 1980).

2) *Benthic diatoms* — Most of the benthic diatom samples, which were collected during June–September 1981 and September 1980, were isotopically indistinguishable from living *Spartina*, their $\delta\ ^{13}C$ values being mostly in the range of −13.2 to −14.2‰. Two samples taken in May 1981 from Station A were much lighter than the others, having values of −17.6 and −18.5‰. The same genus of pennate diatom (*Gyrosigma* sp.) was dominant in all samples and no contamination of the May samples was suspected. It is not known whether two isotopically distinct forms of *Gyrosigma* were sampled or whether a wide range of carbon isotope ratios was exhibited by one species. Figure 2 illustrates the results as two distinct forms with means of −13.6 and −18.1‰. Analysis of triplicate samples of diatoms collected on August 15, 1981 indicates the standard error of replicate samples to be ± 0.5‰.

3) *Phytoplankton* — Two samples of phytoplankton had $\delta\ ^{13}C$ values of −18.7‰ (May 1980) and −19.6‰ (September 1980). The September sample contained detritus (roughly 25% of the particles in the sample), but considering the similarity of the two values the effect of contamination probably is not serious.

4) *Macrophytic algae* — The green algae *Ulva* and *Enteromorpha* had $\delta\ ^{13}C$ values of −4.9 and −9.6‰, respectively, and were isotopically the heaviest carbon sources on the mudflat. The brown algae, *Fucus* was isotopically lighter, and extremely variable, ranging from −13.4 to −21.9‰ with a mean of −17.6‰.

5) *Detritus* — With the exception of one sample from Station A, *Spartina* detritus was isotopically much lighter than the living plant. The heaviest detrital samples were coarse material (>500 μm) from Station A (−13.6‰) and Station M (−15.1‰). All other values for sediment detritus were in the range of −17.0 to −20.2‰. *Spartina* detritus

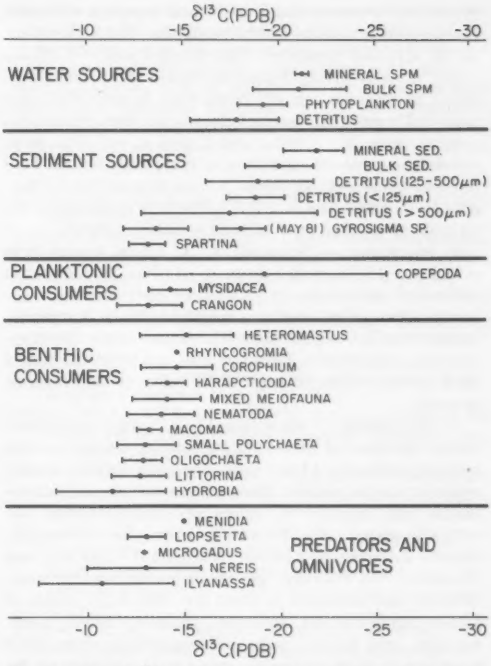

FIG. 2. Mean $\delta\ ^{13}C$ (± 2 SD) of components in the Pecks Cove mudflat ecosystem. All field data are tabulated in Table 1.

suspended in the water column was isotopically similar to sediment detritus, ranging from −16.1 to −19.8‰.

6) *Bulk sediment and suspended organic matter* — The $\delta\ ^{13}C$ values of organic carbon in bulk sediments from four mudflats in the Cumberland Basin were all in the range of −17.9 to −21.2‰. Values of subsurface sediments, including an anaerobic sample from Station M, were indistinguishable from surface sediments. The mean value of surface and subsurface bulk sediments was −20.1‰, slightly but significantly ($P < 0.02$) heavier than that of bulk suspended organic matter, −21.1‰. There is a consistent trend of lighter values in the lower intertidal sediments than in the sediments of corresponding upper intertidal sites, possibly reflecting a lesser input of heavy carbon from fresh *Spartina* and benthic diatoms at the lower intertidal sites. Bulk sediment values tended to be slightly heavier during the summer when benthic diatoms were most abundant.

7) *"Mineral" sediment and suspended matter* — The $\delta\ ^{13}C$ of this fraction is assumed to represent the isotope ratio of attached micro-organisms plus sorbed or otherwise adherent organic material on the surfaces of sediment grains. Suspended and in situ "mineral" sediments were isotopically similar. The mean ratio of all samples was −21.7‰, making this the lightest carbon source material that we observed.

Consumers

1) *Zooplankton* — Zooplankton collected by pump at

Pecks Cove consisted mostly of calanoid copepods with some resuspended nematodes and harpacticoids. The $\delta^{13}C$ values of the May and September 1980 samples were −17.0 and −21.5‰, respectively. Planktonic mysids and *Crangon* collected by plankton nets off Pecks Point in July 1981 were isotopically much heavier. Including exoskeleton, mysids had a mean value of −13.6‰, and *Crangon*, −13.3‰. With exoskeleton removed, mysids were isotopically lighter. Four replicate samples of individual *Crangon* indicate that the standard error of replicates is ± 0.8‰ similar in magnitude to the estimate of standard error of benthic diatom samples.

2) *Meiofauna* — Nematode $\delta^{13}C$ values ranged from −12.3 to −15.5‰ with a mean of −13.7‰. No significant differences attributable to location or body size were observed, although the smallest worms tended to be isotopically lighter than the largest ones. The mean values for harpacticoids, oligochaetes, *Rhyncogromia*, and mixed meiofauna were all well within the range of the values of the nematode samples.

3) *Macrofauna* — Macrofaunal $\delta^{13}C$ values varied more widely than those of meiofaunal but centered around a similar midrange of about −13 to −15‰. The dominant macrofaunal organisms on the mudflat, *Macoma*, *Corophium*, and *Heteromastus* had mean $\delta^{13}C$ values of −13.1, −14.6, and −15.1‰, respectively. The heavier mean values of the gastropods *Littorina* (−12.6‰), *Hydrobia* (−11.1‰), and *Ilyanassa* (−10.7‰) may indicate carbonate contamination, although care was taken to avoid this. The $\delta^{13}C$ values of known carnivores and omnivores, including *Nereis*, *Cerebratulus*, and *Eteone*, were indistinguishable from other macrofauna. *Ilyanassa* was the only known carnivore on the mudflat whose isotopic composition was noticeably heavier than that of the nonpredatory benthic fauna.

4) *Benthic feeding fish* — The smooth flounder, *Liopsetta putnami*, tomcod, *Microgadus tomcod*, and silversides, *Menidia menidia* were the three most common benthic feeding fish on the Pecks Cove mudflat. Flounder and tomcod had very similar $\delta^{13}C$ values, −12.9‰ for both species. Silversides were lighter, having an average ratio of −14.9‰. A juvenile American shad, *Alosa sapidissima*, had the lightest $\delta^{13}C$ of any component of the Pecks Cove ecosystem, −28.2‰, indicative of a freshwater (terrestrial) carbon source (Tan and Strain 1979a).

Spartina Decomposition Experiments

Results in Table 2 illustrate that in vitro leaching and microbial decomposition of *Spartina* did not result in an observable negative shift in the $\delta^{13}C$ value of the detrital carbon. Values for the anaerobic samples were all lighter than the initial *Spartina* owing to the presence of organic carbon in the sediment used in the experiment. The question of whether the presence of light, *Spartina*-derived detritus in the field results from processes in the sediment (anaerobic) or in the water column (aerobic) remains unanswered, though there is some evidence in the dead anaerobic samples of decreasing $\delta^{13}C$ values. Longer incubation times and, perhaps, more loading of the sediment with *Spartina* carbon may be required to demonstrate adequately any negative shift in the isotope ratio.

Discussion

To our knowledge, this is the first study in which both sediment and suspended matter were fractionated into relatively "pure" carbon source materials for the determination of $\delta^{13}C$. Contrary to results of previous studies, our observations indicate the presence of several carbon sources that are potentially available to consumers but not all of which are isotopically distinct.

Haines (1976) found that *Spartina* and benthic diatoms had significantly different $\delta^{13}C$ values. Other authors subsequently have assumed that the benthic diatom values given in Haines (1976) are typical. Our results clearly show that such an assumption cannot be made. Even though one genus of pennate diatom, *Gyrosigma*, dominated all of the samples, two distinct mean values were obtained. The May 1980 mean value is close to the range (−18 to −16‰) given by Haines (1976) but other values, taken over most of the productive season, are indistinguishable from those of fresh *Spartina*. This is unfortunate because, owing to the stresses of high turbidity and sediment instability placed upon phytoplankton and seaweeds, *Spartina* and intertidal benthic diatoms account for most of the primary production at Pecks Cove (Hargrave et al. 1983). Thus the relative importance of two major carbon sources in the Pecks Cove ecosystem cannot be assessed by the $\delta^{13}C$ method.

Detritus is the most abundant form of particulate organic matter in the sediments of Pecks Cove (Schwinghamer 1981b) and primarily originates from *Spartina*. In further contrast to results of previous studies (Haines 1977, 1979), we find that most *Spartina* detritus, both suspended and in the sediments, is isotopically lighter than live *Spartina*. The caution expressed by Cousins (1980), that detritus not be considered a single resource, is well advised. The state of decomposition of detritus varies, and may be reflected in the wide range of $\delta^{13}C$ values exhibited. There appears to be some tendency for finer detrital fractions, which are probably highly decomposed, to be more negative than the larger detrital fragments of *Spartina*. It is probably useful to differentiate "fresh" detritus, with $\delta^{13}C$ values similar to those of live *Spartina* and benthic diatoms, from "aged" detritus, with $\delta^{13}C$ values in the range of −17 to −20‰.

Haines (1977, 1979) has used $\delta^{13}C$ values to support the contention that *Spartina* contributes little detrital carbon to estuarine and coastal food chains. Peterson et al. (1980) argued that although the evidence of $\delta^{13}C$ studies implies little direct contribution of *Spartina* carbon to coastal ecosystems outside salt marshes, *Spartina* detritus can supply energy in the form of reduced sulfur compounds to coastal ecosystems via anaerobic bacterial metabolism. We have found that *Spartina* detritus is physically transported to sediments and suspended material outside the salt marshes, but because of the multiplicity of carbon sources available to consumers, we cannot assess the importance of detritus in the planktonic or benthic food web. Most consumer organisms had $\delta^{13}C$ values similar to those of live *Spartina*, fresh detritus and benthic diatoms. If detrital carbon is a nutritional source in the mudflat ecosystem, it must be mostly as "fresh" rather than "aged" material.

It is clear from our data that there are no nonselective deposit feeders at Pecks Cove. The mean $\delta\ ^{13}C$ values of all benthic organisms were, in all cases, at least 5‰ heavier than the mean bulk sediment value. Further, there is little indication of assimilation of any of the isotopically light carbon sources including "aged" detritus, phytoplankton, and "mineral" particulate matter. Even within the zooplankton, only the small copepods were light enough to assume that these sources are important. Mysids and *Crangon* apparently derived most of their nutrition from isotopically heavier material such as "fresh" detritus or benthic diatoms.

It must be noted that the value for mysids value shown in Fig. 2 represents whole animals. Body tissue without the chitinous exoskeleton was considerably lighter, with a value of −16.5‰. It is not known whether the chitinous material is isotopically heavy or whether carbonates, not removable by acidification, are incorporated into the chitinous exoskeleton as in larger decapods. Whether or not to include the exoskeleton in the determination of mysid $\delta\ ^{13}C$ values depends upon the resolution of this question.

There remains the question of the origin of the light carbon which dominates both the SPM and the sediment. This carbon is isotopically similar to that found in sediments of the open Gulf of St. Lawrence (Tan and Strain 1979b) and in suspended organic matter on the Continental Shelf of eastern North America (Haines 1977; F. C. Tan, unpublished data). One can only conclude that we have not identified an abundant, isotopically light fraction of organic carbon in our analysis, probably in the form of dissolved or colloidal organic material that is readily sorbed onto silt−clay or detrital surfaces, or used by surface bacteria. Such would serve as an ad hoc explanation of the failure of our decomposition experiments, and those of Haines (1977), to demonstrate the negative shift of $\delta\ ^{13}C$ values of *Spartina* detritus that occurs in situ. At present too little is known of the relevant parameters to design an experimental microcosm from which multiple, unknown interactions could be excluded and in which all relevant variables could be included and measured.

We have seen little evidence of ^{13}C enrichment along food chains as described by DeNiro and Epstein (1978) and McConnaughy and McRoy (1979a,b). It is unlikely that such an effect would be discernable in a system like Pecks Cove where numerous, isotopically variable carbon sources are available and food chains are blurred by opportunistic feeding habits of consumers. In these respects, Pecks Cove is probably similar to most coastal ecosystems. Thus it is clear that food web studies using $\delta\ ^{13}C$ as a tracer must be interpreted with caution.

We can conclude by noting that, even in the biologically "simple" benthic community of Pecks Cove, a bewildering complexity of processes precludes the possibility of simple analysis of carbon transfer by the use of a single tracer. However, relatively simple $\delta\ ^{13}C$ techniques can, used properly and carefully, provide useful insight into some aspects of system behavior.

Acknowledgments

We wish to thank P. Cranford, N. Prouse, W. Ross, and the Helicopter Division of the Canadian Coast Guard for their assistance in collecting some of the samples. I. Salinas provided flounder and tomcod for analysis. P. Cranford and W. Ross also assisted in preparing samples for isotopic analysis and conducting the decomposition experiment. We especially thank J. Abriel and C. Cunningham for conducting the $\delta\ ^{13}C$ analyses. This project has benefitted from fruitful discussions with many people, most importantly P. Keizer. B. Hargrave, C. Hawkins, P. Strain, and J. M. Bewers kindly reviewed the manuscript.

BAY OF FUNDY TIDAL REVIEW BOARD. 1977. Reassessment of Fundy Tidal Power. Ottawa, Ont. 57 p.

BOATES, J. S., AND P. C. SMITH. 1979. Length−weight relationships, energy content and the effects of predation on *Corophium volutator* (Pallas) (Crustacea: Amphipoda). Proc. N.S. Inst. Sci. 29: 489−499.

COUSINS, S. H. 1980. A trophic continuum derived from plant structure, animal size, and a detritus cascade. J. Theor. Biol. 82: 607−618.

CRAIG, H. 1953. The geochemistry of the stable carbon isotopes. Geochim. Cosmochim. Acta. 3: 53−92.

DENIRO, M. J., AND S. EPSTEIN. 1978. Influence of diet on the distribution of carbon isotopes in animals. Geochim. Cosmochim. Acta 42: 495−506.

FRY, B., AND P. L. PARKER. 1979. Animal diet in Texas seagrass meadows: $\delta\ ^{13}C$ evidence for the importance of benthic plants. Estuarine Coastal Mar. Sci. 8: 499−510.

GORDON, D. C. JR., AND C. DESPLANQUE. 1981. Ice dynamics in the Chignecto Bay region of the Bay of Fundy. *In* Workshop on ice action on shores. National Research Council. Associate Committee for Research on Shoreline Erosion and Sedimentation, p. 35−52.

GORDON, D. C. JR., P. D. KEIZER, J. DALE, AND P. CRANFORD. 1980. Pecks Cove mudflat ecosystem study: observations in 1978. Can. Tech. Rep. Fish. Aquat. Sci. 928: 17 p.

HACKNEY, C. T., AND E. B. HAINES. 1980. Stable carbon isotope composition of fauna and organic matter collected in a Mississippi estuary. Estuarine Coastal Mar. Sci. 10: 703−708.

HAINES, E. B. 1976. Stable carbon isotope ratios in the biota, soils, and tidal water of a Georgia saltmarsh. Estuarine Coastal Mar. Sci. 4: 609−616.

1977. The origins of detritus in Georgia salt marsh estuaries. Oikos 29: 254−260.

1979. Interactions between Georgia salt marshes and coastal waters: a changing paradigm, p. 35−46. *In* R. I. Livingston [ed.] Ecological processes in coastal and marine systems, Plenum, New York, NY.

HAINES, E. B., AND C. L. MONTAGUE. 1979. Food sources of estuarine invertebrates analyzed using C^{13}/C^{12} ratios. Ecology 60: 48−56.

HARGRAVE, B. T., N. J. PROUSE, G. PHILLIPS, AND P. NEAME. 1983. Primary production and respiration in pelagic and benthic communities at two intertidal sites in the upper Bay of Fundy. Can. J. Fish. Aquat. Sci. Suppl. 40. (This issue)

HICKLIN, P. W., L. E. LINKLETTER, AND D. L. PEER. 1980. Distribution and abundance of *Corophium volutator* (Pallas), *Macoma balthica* (L.) and *Heteromastus filiformis* (Clarapede) in the intertidal zone of Cumberland Basin and Shepody Bay, Bay of Fundy. Can. Tech. Rep. Fish. Aquat. Sci. 965: 56 p.

KNEIB, R. T., A. E. STIVEN, AND E. B. HAINES. 1980. Stable carbon isotope ratios in *Fundulus heteroclitus* (L.) muscle tissue and gut contents from a North Carolina Spartina marsh. J. Exp. Mar. Biol. Ecol. 46: 89−98.

MCCONNAUGHEY, T., AND C. P. MCROY. 1979a. Food web structure and the fractionation of carbon isotopes in the Bering Sea. Mar. Biol. 53: 257−262.

1979b. ^{13}C label identifies eelgrass (Zostera marina) carbon in an Alaskan estuarine food web. Mar. Biol. 53: 263–269.

MORANTZ, D. L. 1976. Productivity and export from a march with a 15 m tidal range, and the effect of impoundment of selected areas. M.Sc. thesis, Dalhousie Univ., Halifax, N.S. 77 p.

PETERSON, J. B., R. W. HAWORTH, F. LIPSCHULTZ, AND D. ASHENDORF. 1980. Salt marsh detritus: an alternative interpretation of stable carbon isotope ratios and the fate of *Spartina alterniflora*. Oikos 34: 173–177.

SACKETT, W. M., AND R. R. THOMPSON. 1963. Isotopic organic carbon composition of recent continental derived clastic sediments of east Gulf of Mexico. Bull. Am. Assoc. Pet. Geol. 47: 525.

SCHWINGHAMER, P. 1981a. Extraction of living meiofauna from marine sediments by centrifugation in a silica sol-sorbitol mixture. Can. J. Fish. Aquat. Sci. 38: 476–478.

1981b. Size distributions of benthic organisms in the Bay of Fundy, Canada. Ph.D. thesis, Dalhousie Univ., Halifax, N.S. 122 p.

TAN, F. C., AND P. M. STRAIN. 1979a. Carbon isotope ratios of particulate organic matter in the Gulf of St. Lawrence. J. Fish. Res. Board Can. 36: 678–682.

1979b. Organic carbon isotope ratios in recent sediments in the St. Lawrence estuary and the Gulf of St. Lawrence. Estuarine Coastal Mar. Sci. 8: 213–225.

THAYER, G. W., P. L. PARKER, M. W. LACROIX, AND B. FRY. 1978. The stable carbon isotope ratio of some components of an eelgrass, *Zostera marina*, bed. Oecologia 35: 1–12.

Suspended Particulate Loading on the Macrobenthos in a Highly Turbid Fjord: Knight Inlet, British Columbia[1]

GEORGE E. FARROW

Department of Geology, University of Glasgow, Glasgow G12 8QQ, U.K.

JAMES P. M. SYVITSKI

Geological Survey of Canada, Bedford Institute of Oceanography, Dartmouth, N.S. B2Y 4A2

AND V. TUNNICLIFFE

Department of Fisheries and Oceans, Ocean Ecology Laboratory, Institute of Ocean Science, Patricia Bay, Sidney, B.C. V8L 4B2

FARROW, G. E., J. P. M. SYVITSKI, AND V. TUNNICLIFFE. 1983. Suspended particulate loading on the macrobenthos in a highly turbid fjord: Knight Inlet, British Columbia. Can. J. Fish. Aquat. Sci. 40(Suppl. 1): 273–288.

Knight Inlet is a deep, low-energy but well-oxygenated fjord. The effects of turbidity are principally those of seasonally very high vertical flux from the sediment-laden surface layer. Submersible observations of the benthos are related to suspended load and sedimentation rate data. The bayhead delta slope receives a continual rain of glacial silt (30 cm/yr) and has summer sedimentation rates of 4 $kg \cdot m^{-2} \cdot d^{-1}$.

The epifauna of the steep fjord walls shows a marked down-inlet increase in abundance, and the number of species increases from 9 to 45. Brachiopods (*Laqueus californianus*), solitary corals (*Caryophyllia/Cyathoceros*), and encrusting sponges are remarkably tolerant of high turbidity. The high sedimentation rates affect the epifauna in three ways: (1) subjection to the ubiquitous "gentle rain" of flocs and agglomerates; (2) more locally, microturbidity flows set off by biological resuspension of unstable slope sediment; and (3) major slides of rock and/or sediment. Submarine soil-creep limits the slope infauna, by burrows requiring repeated reexcavation.

Down-inlet decrease in sedimentation rate is accompanied by a change in feeding type. In the upper inlet, suspension feeders taking particles <8 μm (e.g. sabellids, brachiopods) probably utilize bacteria associated with the high vertical flux of SPM. In the middle inlet, selective suspension feeders (e.g. crinoids, gorgonians) sort the SPM for larger particles. In the lower inlet, filter feeders (e.g. barnacles, glass sponges) increase, especially where currents are stronger. The soft-bottom detritus feeders also show a change: from epibenthic forms (e.g. pandalid shrimp, spider crabs) in the upper inlet, through burrowing shrimp in the middle inlet, to ophiuroids in the lower inlet. These changes are correlated with the greater amounts of organic carbon preserved in bottom sediments as they are less diluted by glacially derived inorganic material.

The modern-day "turbid association" of brachiopods, solitary corals, and sponges recalls typical outer shelf-basinal shale facies of the Palaeozoic. Turbid, low-energy environments were thus colonized early but faunas have since become less diverse.

Key words: fjord, benthos, sedimentation, submersible

FARROW, G. E., J. P. M. SYVITSKI, AND V. TUNNICLIFFE. 1983. Suspended particulate loading on the macrobenthos in a highly turbid fjord: Knight Inlet, British Columbia. Can. J. Fish. Aquat. Sci. 40(Suppl. 1): 273–288.

L'inlet Knight est un fjord profond, à faible énergie mais bien oxygéné. La turbidité se fait surtout sentir au moment du flux vertical saisonnièrement très élevé en provenance de la couche superficielle chargée de matière en suspension. La submersion du benthos est liée à la charge en suspension et au taux de sédimentation. La pente du delta de la tête de la baie

[1]This paper forms part of the Proceedings of the Dynamics of Turbid Coastal Environments Symposium convened at the Bedford Institute of Oceanography, Dartmouth, N.S., Canada, September 29–October 1, 1981.

Printed in Canada (J6706)
Imprimé au Canada (J6706)

reçoit un apport continu de vase glaciaire (30 cm/an) et la sédimentation en été se fait au taux de 4 $kg \cdot m^{-2} \cdot d^{-1}$.

L'épifaune des parois escarpées du fjord devient sensiblement plus abondante vers l'aval, et le nombre d'espèces passe de 9 à 45. Les brachiopodes (*Laqueus californianus*), les coraux solitaires (*Caryophyllia/Cyathoceros*) et les éponges incrustantes ont une remarquable tolérance à une forte turbidité. Les taux de sédimentation élevés influent sur l'épifaune de trois manières: (1) exposition à une "petite pluie" omniprésente de flocs et d'agglomérats; (2) plus localement, flux de microturbidité déclenchés par la resuspension biologique du sédiment de pentes instables; et (3) glissements majeurs de roches et (ou) de sédiments. La reptation des sols sous-marins limite l'endofaune des pentes, les tunnels devant être continuellement réparés.

La diminution du taux de sédimentation vers l'aval est accompagnée d'un changement de type d'alimentation. Dans la partie supérieure du fjord, les organismes se nourrissant de particules en suspension de moins de 8 μm (p. ex., sabellidés, brachiopodes) utilisent probablement des bactéries associées au flux vertical de matière particulaire en suspension. Dans la portion moyenne, les organismes se nourrissant sélectivement de particules en suspension (p. ex., crinoïdes, gorgones) trient le matériel et choisissent les plus grosses particules. Dans le bas du fjord, les filtreurs (p. ex., bernaches, éponges siliceuses) augmentent, surtout là où les courants sont plus forts. Les animaux se nourrissant de détritus de fonds mous varient également: depuis des formes épibenthiques (p. ex., crevettes pandalides, crabes-araignées) dans la partie supérieure du fjord jusqu'aux ophiurides dans la partie inférieure, en passant par les crevettes fouisseuses dans le secteur moyen. Ces variations sont reliées aux plus grandes quantités de carbone organique conservé dans les sédiments benthiques, moins dilués par du matériel organique d'origine glaciaire.

L'« association turbide » des temps modernes de brachiopodes, coraux solitaires et éponges rappelle les facies typiques du plateau extérieur-schistes argileux du bassin de la période paléozoïque. Les milieux turbides, à faible énergie, ont donc été colonisé tôt, mais leurs faunes ont depuis perdu de leur diversité.

Received October 30, 1981
Accepted August 16, 1982

Reçu le 30 octobre 1981
Accepté le 16 août 1982

DROWNED-river estuaries and glacier-fed fjords are both highly turbid environments but they differ in other parameters, particularly flux (Table 1). In drowned-river estuaries, tidal currents regularly resuspend the bottom sediments: suspended particulate matter (SPM) is very high yet the rate of accumulation of sediment is relatively low. In fjords, tidal flux, except over the sills, is minimal: levels of SPM are considerably less, yet rates of sedimentation can markedly exceed those in estuaries.

In this paper, therefore, we are dealing with a system dominated by the *vertical* flux of a turbid suspension, sharply seasonal, whereas the papers dealing with estuaries sensu stricto are concerned with a system driven by *horizontal* flux, with year-round turbidity.

The oceanographic characteristics of British Columbian fjords have been summarized by Pickard (1961) and Pickard and Stanton (1980). Data for Alaskan fjords may be found in Kinney et al. (1970) and Hoskin et al. (1976), the latter paper relating sediment flux to benthic biomass.

Knight Inlet is the northernmost of a group of fjords on

TABLE 1. Comparison of environmental parameters between drowned-river estuaries and glacier-fed fjords.

Parameter	Drowned-river estuaries	Glacier-fed fjords
Physiography	Alluvial plain (soft-sediments — low slopes)	Mountainous (rocky — high slopes)
World location	All latitudes	High latitude only
Depth of water	Shallow	Deep
Wave activity	Low	Low — moderate
Tidal flux	High	Low
Tidal resuspension	High	None
Salinity	Widely fluctuating (short term)	Stable
Stratification	Generally well-mixed	Highly stratified
Oxygenation	Moderate — low	Moderate — low
Total suspended particulate matter ($mg \cdot L^{-1}$)	1000–2000 (typical)[a] 50000 (maximum)[b]	1350 (Cook Inlet: maximum)[c] 285 (Bute Inlet: maximum)[d]
Turbidity maxima	Year-round	June–September
Sedimentation rates ($mm \cdot yr^{-1}$)	1–2[e]	11–14[f]

[a]Moore (1977); [b]Kirby and Parker (1977); [c]Kinney et al. (1970); [d]Pickard and Giovando (1960); [e]Rusnak (1967); [f]this paper.

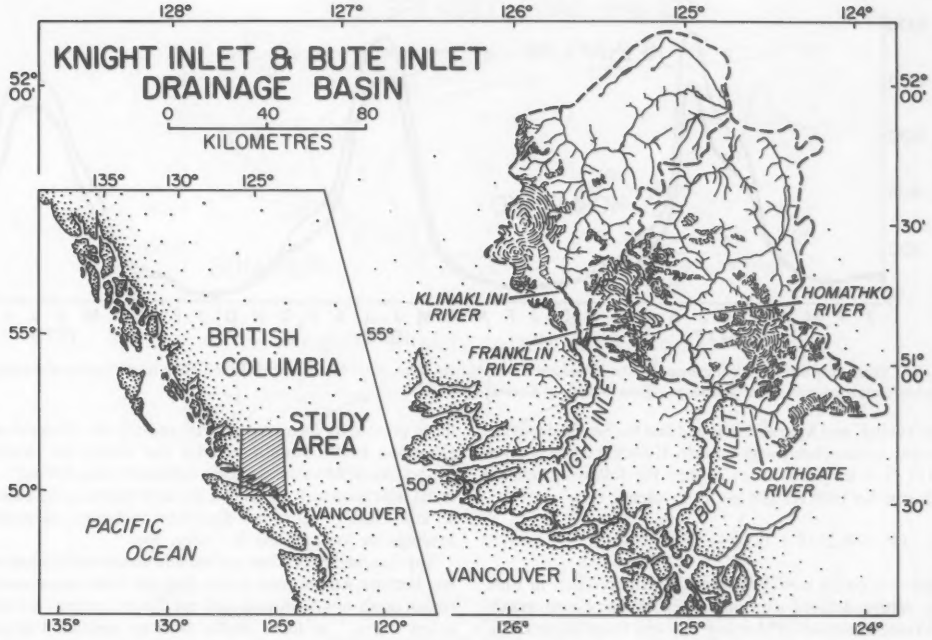

FIG. 1. Location of the study area and major drainage basins of Knight and Bute inlets, British Columbia, Canada.

mainland British Columbia whose drainage basins include ice fields (Fig. 1). Discharge (Fig. 2) and resultant turbidity reach a maximum in Knight and Bute inlets. Sill depths vary, Knight Inlet being shallower (70 m) than Bute Inlet (240 m) for instance, but both are well oxygenated compared with Saanich Inlet in Vancouver Island, where a shallow sill and low discharge lead to anoxic bottom waters (Herlinveaux 1962).

Knight Inlet provides an ideal, unpolluted site for studying the effects of high seasonal turbidity on the distribution of macrobenthos. Our results were obtained principally from submersible observations in comparatively deep water (to 530 m). They thus provide an extension of the type of SCUBA study carried out by Evans et al. (1980) in a Norwegian fjord. Faunal distribution is related to an empirically derived gradient in suspended load and to the flux and preservation of organic carbon.

Suspended Load Model

Knight Inlet is typical of a British Columbian fjord having pronounced seasonal variation in runoff with high summer discharge (Pickard 1961). Two rivers at the inlet head, the Klinaklini and Franklin, provide 95% of the freshwater input (85 and 10%, respectively). The average annual freshwater discharge of the Klinaklini River ranges from 230 to 440 $m^3 \cdot s^{-1}$ with summer maxima of 680 to 1100 $m^3 \cdot s^{-1}$, respectively, and winter lows of $\simeq 50$ $m^3 \cdot s^{-1}$ (W.S.C. 1979). The freshwater source is from melting winter snow, which peaks in June, and from glacial meltwater, which peaks in August. Variations in these two sources provide modal departures from an otherwise Gaussian distribution of discharge (Fig. 2). The Klinaklini River drains some of Canada's largest west coast ice-fields, in its 6462 km^2 drainage basin.

Suspended load data for Knight Inlet consist mostly of Secchi disk readings and submersible observations. However, it is possible to generate data for Knight Inlet by using a deterministic/empirical loading model developed for Bute Inlet (Syvitski 1983). The main similarities between the inlets upon which the model relies are: (1) Bute Inlet drains adjacent icefields (Fig. 1). (2) Bute Inlet also has two rivers at its head, the Homathko and Southgate, that supply 94% of its freshwater input (75 and 19%, respectively). (3) The discharge from the Homathko plus Southgate Rivers is 100 ± 2% of the discharge from the Klinaklini plus Franklin Rivers of Knight Inlet. (4) The major river of Knight Inlet, the Klinaklini, is highly correlated in terms of monthly discharge ($r = 0.996$, $P < 0.001$, $n = 36$ mo) with the major river from Bute Inlet, the Homathko. (5) In both inlets, the major source of sediment is fluvially derived glacial flour. (6) In both cases the sediment plume moves quickly down the inlet as a well defined surface-layer, slowly mixing with the underlying marine water.

The loading model is based on the premise that surface-layer salinity can be used to indicate the freshwater sediment

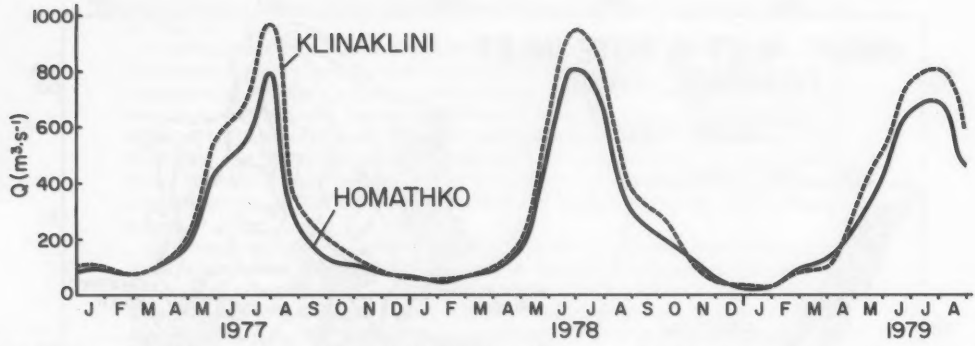

FIG. 2. Three-year discharge comparison of the Klinaklini River, Knight Inlet, with the Homathko River, Bute Inlet. Sediment discharge is highly correlated with water discharge (Water Survey of Canada 1979).

load (Syvitski and Murray 1981) and that the Secchi depth can therefore be correlated with salinity. If Secchi depth is given as $1/\tau$ (τ = turbidity) in m^{-1}, then the following relation holds true for both Knight and Bute inlets:

$$(1) \quad 1/\tau = 0.23 \cdot S + 0.34$$

with $r = 0.94$ for $n = 49$ where S is salinity (‰). In Bute Inlet, where detailed data on suspended particulate matter (SPM) are available, SPM in $mg \cdot L^{-1}$ was found to vary with salinity (‰) as

$$(2) \quad \log(\text{SPM}) = -0.9 \cdot \log(S) + 1.36$$

with $r = 0.99$ for $n = 40$. Combining equations (1) and (2) we have

$$(3a) \quad 1/\tau = 7.12 \cdot \text{SPM}^{-1.1} + 0.34$$

or

$$(3b) \quad \text{SPM} = [0.14 \cdot (1/\tau) - 0.05]^{-0.9}$$

for $0.3 < 1/\tau \leq 6.0$. This relationship compares favorably with those previously published (Postma 1961; Manheim et al. 1972). Finally, the surface-layer suspended load can be predicted to depth based on the dilution model of Syvitski and Murray (1981) and their general relationship relating SPM values below the halocline, SPM($\bar{x}bh$), to SPM values above the halocline, SPM($\bar{x}ah$), of

$$(4) \quad \text{SPM}(\bar{x}bh) = 0.12 \cdot \text{SPM}(\bar{x}ah) + 0.7$$

Equation (4) is based on data from another nearby glacial-fed inlet, Howe Sound, B.C., of similar freshwater input to Knight and Bute inlets.

The above equations describe the SPM pattern in a fjord as a perforated-conveyor-belt of sediment in the surface layer causing a continual rain of sediment to the bottom depending on the concentration in the surface layer (Fig. 3). The model expresses suspended load patterns and values similar to those previously measured in west coast fjords (Pickard and Giovando 1960). Results indicate that during the summer freshet, the SPM values decrease from more than 200 $mg \cdot L^{-1}$ at the inlet head to 1 $mg \cdot L^{-1}$ at the inlet mouth, a distance of 83 km. During the winter discharge minimum, suspended loadings are low, 1.5 $mg \cdot L^{-1}$ (Fig. 3b).

This loading model does not include resuspension phenomena because Knight Inlet is too deep for wave resuspension (mean depth of 420 m) and tidal oscillatory currents are only a few $cm \cdot s^{-1}$ at these depths with no residual transport (Pickard and Rodgers 1959). Sediment gravity flows which may occur on a yearly basis would be short-lived events although bottom turbidity would be greatly increased.

Sedimentation Models

Two sedimentation models are developed here, and their results compared. The first was derived from sediment trap data or Pb^{210} data from Bute Inlet (Syvitski 1983), Howe Sound (Syvitski and Murray 1981), Blue Fjord (Hoskin et al. 1978), and Saguenay Fjord (Smith and Walton 1980); all are similar sediment-laden fjords. The model consists of a two-stage exponential decay of sedimentation rates with distance from the source, the inlet head, such that:

$$(5a) \quad \log(\text{ST}) = m \cdot x + \log b, \text{ for } \text{ST} > 10^{-2} \cdot b$$

$$(5b) \quad \log(\text{ST}) = \frac{m}{10} \cdot x + \log c \text{ for } \text{ST} \leq 10^{-2} \cdot b$$

where ST is the sedimentation rate at a given distance, x, from the source; m is the empirical decay slope; b is the sedimentation rate near the source (delta station); and $c = 10^{-2} \cdot b$. Considering that the water and sediment discharge signature and quantities are identical between Knight and Bute inlets, values of b for Knight will be assumed equal to Bute Inlet. The value for m is set at -0.1, the same as calculated for the other sediment-laden fjords. Figure 3a shows the summer sedimentation rates calculated using $b = 3700$. The values range from 3700 down to 6 $g \cdot m^{-2} \cdot d^{-1}$ (at the inlet mouth). In winter (Fig. 3b), the sedimentation rates decrease dras-

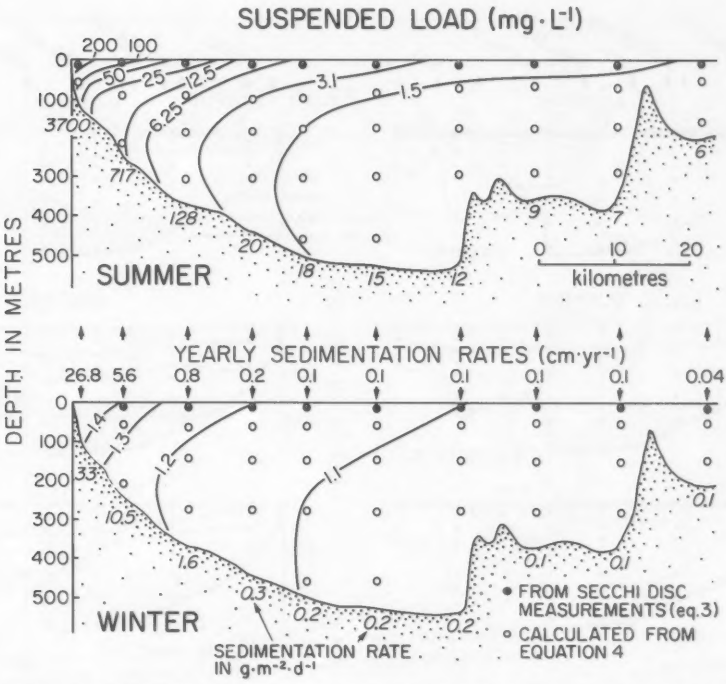

FIG. 3. Predicted turbidity and sedimentation rates for Knight Inlet, showing seasonal variation, from equations in text.

tically to range from 33 to 0.1 $g \cdot m^{-2} \cdot d^{-1}$. The yearly rates are calculated in terms of $cm \cdot yr^{-1}$ (assuming a bulk density of 1.75 $g \cdot cm^{-3}$), and are based on $b = 26.8\ cm \cdot yr^{-1}$ (summation of monthly values from trap data at the delta station). The values decrease down inlet from 26.8 to 0.04 $cm \cdot yr^{-1}$.

A second sedimentation model based on discharge was used to check the exponential decay model. This model relates the water discharge Q, $m^3 \cdot s^{-1}$, to sediment discharge Q_s, $kg \cdot s^{-1}$, based on the following empirical formula from Howe Sound data:

$$(6) \quad Q_s = 0.34 \cdot Q^{1.05}$$

Using the average discharge (over 25 yr) of the Klinaklini River of 330 $m^3 \cdot s^{-1}$, Q_s is then 150 $kg \cdot s^{-1}$. In 1 yr the total sediment discharge is $4.73 \times 10^9\ kg \cdot yr^{-1}$. Next we assume that the inlet is a closed sedimentation system with no sediment escaping, (a good assumption based on Fig. 3a). Using the bulk density of 1750 $kg \cdot m^{-3}$, then the average accumulation rate over the fjord bottom is 1.1 $cm \cdot yr^{-1}$. When equation (5) is integrated over the fjord bottom and over a 1-yr period, then the first method predicts an average accumulation rate of 1.4 $cm \cdot yr^{-1}$. Both methods are in agreement, and considering that the discharge model is based on a 25-yr average, the two methods are in very good agreement.

Near the delta and river source, the SPM is mostly sand and silt grains with attached clay particles, and clay clasts possibly derived from river mudballs. In the main fjord body, the SPM settles in the form of mineral-bearing fecal pellets from pelagic zooplankton, large grain and colloidal floccules, and inorganic–biogenic agglomerates. The description of these SPM types is given in detail elsewhere (Zabawa 1978; Syvitski and Murray 1981). In addition, streamers or stringers of bacterially bound sediment appear to be nearly ubiquitous and abundant in the water below 100 m. The streamers vary in size up to 30 cm in length and contain agglomerate globules attached to their surface. They are common in west coast turbid environments where small-scale turbulence is negligible, but their role in the vertical flux of sediment has yet to be determined.

Physical Oceanography

Figure 4 shows 1975 temperature, salinity, and dissolved oxygen values for winter and summer. The stenotopic bottom conditions contrast sharply with the classically eurytopic estuarine situation. Bottom temperatures vary annually by less than 1°C and salinity by less than 0.2‰. Dissolved oxygen shows more variation in annual bottom conditions (4.9 $mL \cdot L^{-1}$ in summer, 3.3 $mL \cdot L^{-1}$ in winter). Deepwater exchanges over the Knight sill increase the dissolved oxygen

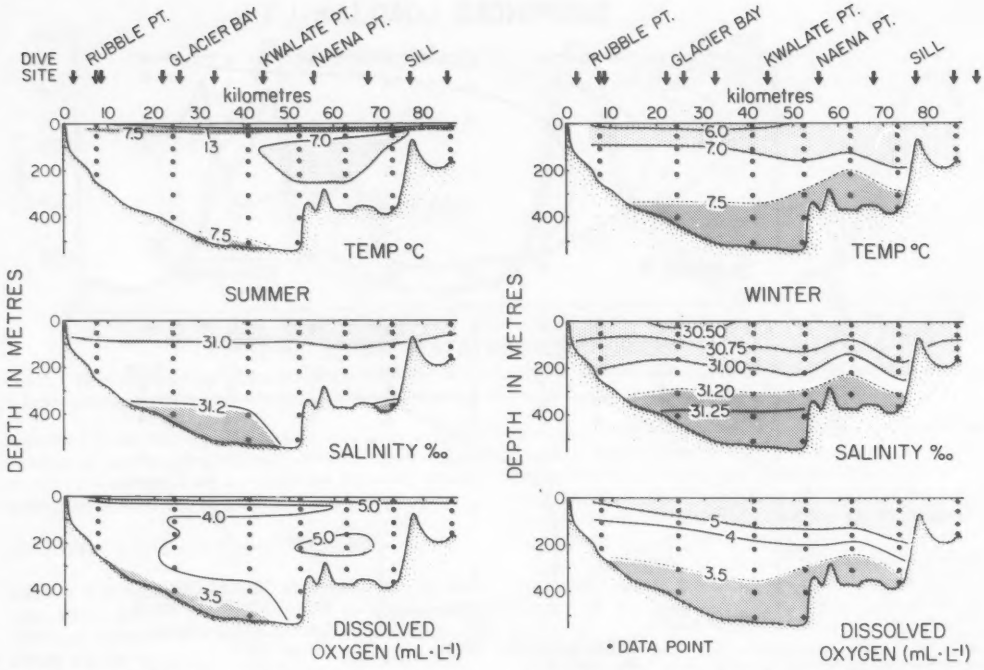

FIG. 4. Synoptic physical oceanography of Knight Inlet showing seasonal variations of temperature, salinity, and dissolved oxygen. Data from 1975 cruise reports of the Institute of Oceanography, University of British Columbia.

content (to 6.85 $mL \cdot L^{-1}$ in July 1956) and decrease the bottom temperature (6.2°C in July 1956).

Current measurements in the fjord proper are to be found in Pickard and Rodgers (1959). At station 5 (Fig. 5) the maximum near-bottom currents recorded at spring tides were 15 $cm \cdot s^{-1}$, (Pickard and Rodgers 1959, p. 656). No current of greater speed was experienced during *Pisces* operations in 1980/81, except on the sill and near the bayhead delta. A significant residual up-inlet flow occurs at 300 m (Pickard and Rodgers 1959, p. 662).

It is clear then that the dominant variables in these glacier-fed fjords are turbidity and suspended sediment loading. In contrast, in estuaries, it is difficult to perceive these effects through a background of widely fluctuating temperature, salinity, and tidal current activity.

Materials and Methods

Marine operations consisted of the CNAV *St. Anthony* towing the barge *Pender* which housed the submersible *Pisces IV*. During descents in *Pisces*, at about 0.3 $m \cdot s^{-1}$, recorded observations of macroplankton and nekton were made, together with descriptions of SPM. Plankton down to the size of large copepods could be distinguished. Bottom transects were run at submersible speeds of 0.2–0.3 $m \cdot s^{-1}$, with many stops for site investigation. On the cliff face, a 30 by 30 cm scale was extended to the rock face. Photographs were taken every 10–20 m with an internal camera and external stobe. Photographs were analyzed for faunal identification, diversity, abundance, and dispersion.

Benthos gravity cores and Shipek grab samples were collected from the *St. Anthony*. Cores were subjected to X-radiography. Grabs were size analyzed by Coulter Counter® and organic carbon was determined by a LECO® carbon analyzer. Figure 5 shows the sample density and submersible tracks.

Soft Substrate Fauna and Bioturbation

X-radiographs were taken of sediment cores from along the axis of the fjord (Fig. 5): their structures are shown on Fig. 6. Away from the delta small burrows predominated. The surrounding mud sometimes took on a "clotted" appearance that probably represented compaction caused by the burrowing. Close to the delta, parallel- or cross-lamination produced by regular sand intercalations predominated: little burrowing was observed. Occasional convoluted intervals probably indicate downslope movement.

These observations show that as the bayhead delta is approached, the rate of sedimentation increases to the point where sediment is accumulating more rapidly than it can be completely reworked by organisms. This sharp difference in

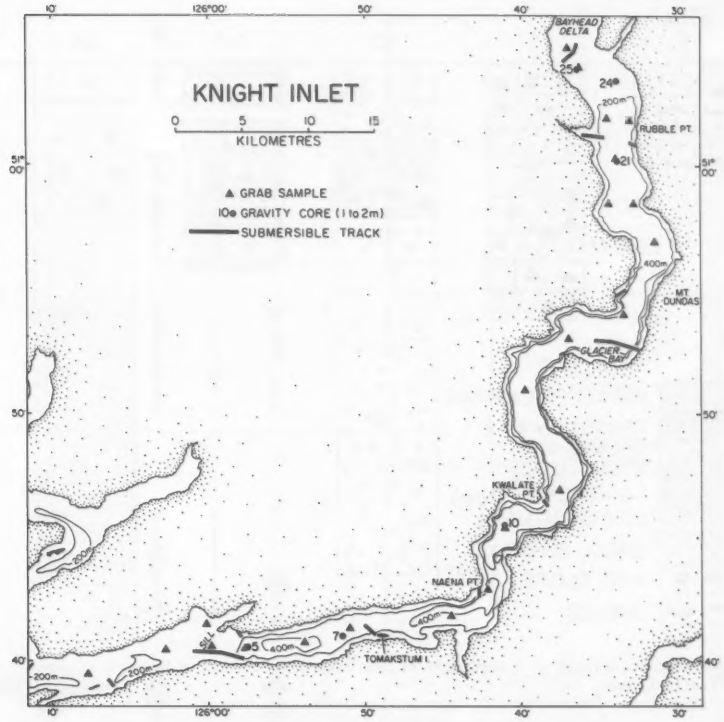

FIG. 5. Station locations and *Pisces IV* submersible tracks.

the nature of the preserved record between the delta slope and the level bottom was not mirrored by the submersible observations: the soft substrate fauna was not notably reduced on the delta slope compared with the level bottom. In fact certain organisms like the sea pen *Ptilosarcus gurneyi* were only to be found on the delta slope, despite the loading of suspended matter (>100 $mg \cdot L^{-1}$ in summer), showing that some other factor such as an increase in current speed may be more significant. The restriction of preserved lamination to the delta-slope cores, where annual sedimentation rates are greater than 5.6 $cm \cdot yr^{-1}$, supports Moore and Scruton's (1957) curve derived from the Mississippi which gives an upper limit of about 20 $cm \cdot yr^{-1}$ before bioturbation ceases and infauna is limited.

Clearly defined burrows seen on the X-rays were made by polychaetes. Grab samples from the axial floor were frequently devoid of fauna, except immediately inside the sill, where the scaphopod *Dentalium* and the sipunculid *Golfingia vulgaris* were collected. The presence of an irregular echinoid (*Brisaster townsendi*) from station 22 and brittle stars near Rubble Point affirmed the long-term stability of favorable oxygenation (Pearson 1980) indicated by the oceanographic data.

In the upper inlet (Fig. 7) surface traces, that would destroy lamination yet leave no clearly defined structure, were formed by several demersal fish: gadoids probably pollack (*Theragra chalcogramma*); flounder, longnose skate, and salmon (*Oncorhynchus* sp.). Red shrimp (either *Pandalus borealis* or *Pandalopsis dispar*) were ubiquitous, imparting a micro-pockmarked appearance to the seabed. Their density increased from around 1 to 2/m^2 on the deep level bottom to 4/m^2 in the vicinity of woody debris. On certain areas of the bottom, logs, branches, and even whole trees resembled a submerged forest, but with everything prone. Also of wide distribution were grazing trails of errant gastropods (buccinids or neptuneids?), spidercrab traces (*Hyas* sp.), and fecal coils and pellets.

Deeper bioturbation was effected principally by the burrowing eelpout (*Lycodes diapterus*) and by burrowing shrimp (?*Axiopsis spinulcauda*) responsible for burrow pits and mud volcanoes. Burrows appeared to have multiple openings about 6 cm in diameter.

In the middle inlet, the sediment surface consisted of fecal pellets and planktonic debris: bioturbation was lower. Epibenthic shrimp were fewer but infaunal shrimp increased. The tubes of a sedentary polychaete appeared with the occasional anemone and holothurian.

In the lower inlet, where localized bottom currents were

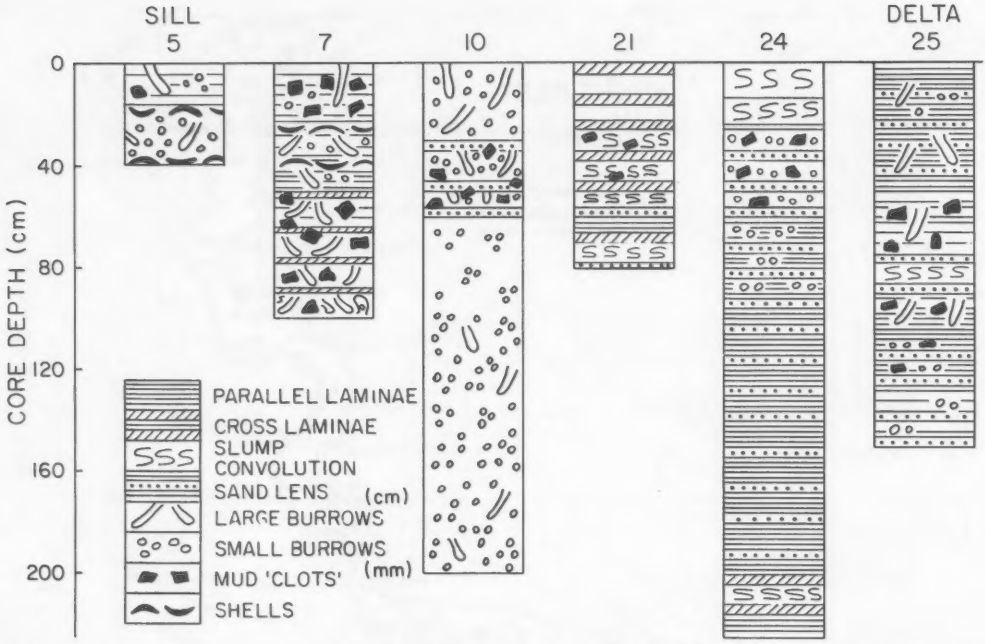

FIG. 6. Sedimentary structures revealed by X-radiographs of cores taken along the axis of Knight Inlet, Stations shown on Fig. 5. Generalized over 25 cm increments.

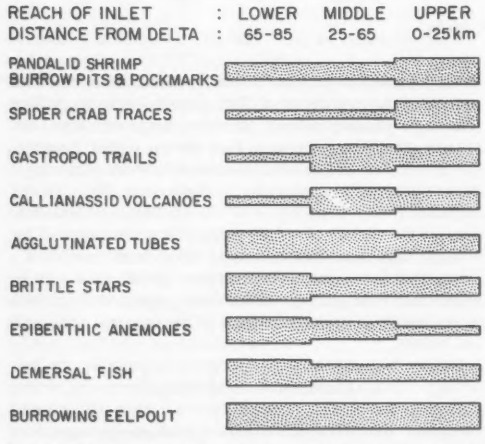

FIG. 7. Trace makers and bioturbators on the level bottom; Knight Inlet: based on *Pisces* observations and grab samples. Width of bar corresponds to rare, frequent and abundant occurrences.

high enough to resuspend the bottom mud, shell debris was exposed and infauna absent. However, epibenthic shrimp and shrimp burrows were present in areas of deposition, but in reduced numbers. Worm tubes became more abundant and an ophiuroid (*Ophiura leptoctenia*) appeared, particularly near the sill.

Outside the sill, a marked drop in numbers of shrimp, burrows, and worm tubes was found; ophiuroids dominated the benthic fauna (Fig. 7), with echinoderms such as the asteroid *Ceramaster patagonicus* and the urchin *Strongylocentrotus pallidus*.

In addition to infaunal changes along the axis of the inlet, a broad vertical zonation was also evident. Throughout the inlet, sabellids appeared between 70 and 200 m. Shrimp species changed from *Pandalopsis dispar* and *Pandalus borealis* below 200 m to *Pandalus platyceros* above 200 m. In the lower inlet, ophiuroids and agglutinated worm tubes were rarely seen on the fjord slopes, though *Munida quadrispina* and *Pachycerianthus* sp. appeared above 150 m.

The fauna bears a striking resemblance, perhaps predictably, to that described from Prince William Sound in Alaska by Feder and Paul (1977). There the shortfin eelpout *Lycodes brevipes* is abundant with *Pandalus borealis* at 60–70 m depth, and analysis of stomach contents has shown that pollack feed widely on the shrimp, from 36 to 235 m (Feder and Paul 1977, p. 17).

Epilithic Benthos

The hard substratum fauna of Knight Inlet showed marked

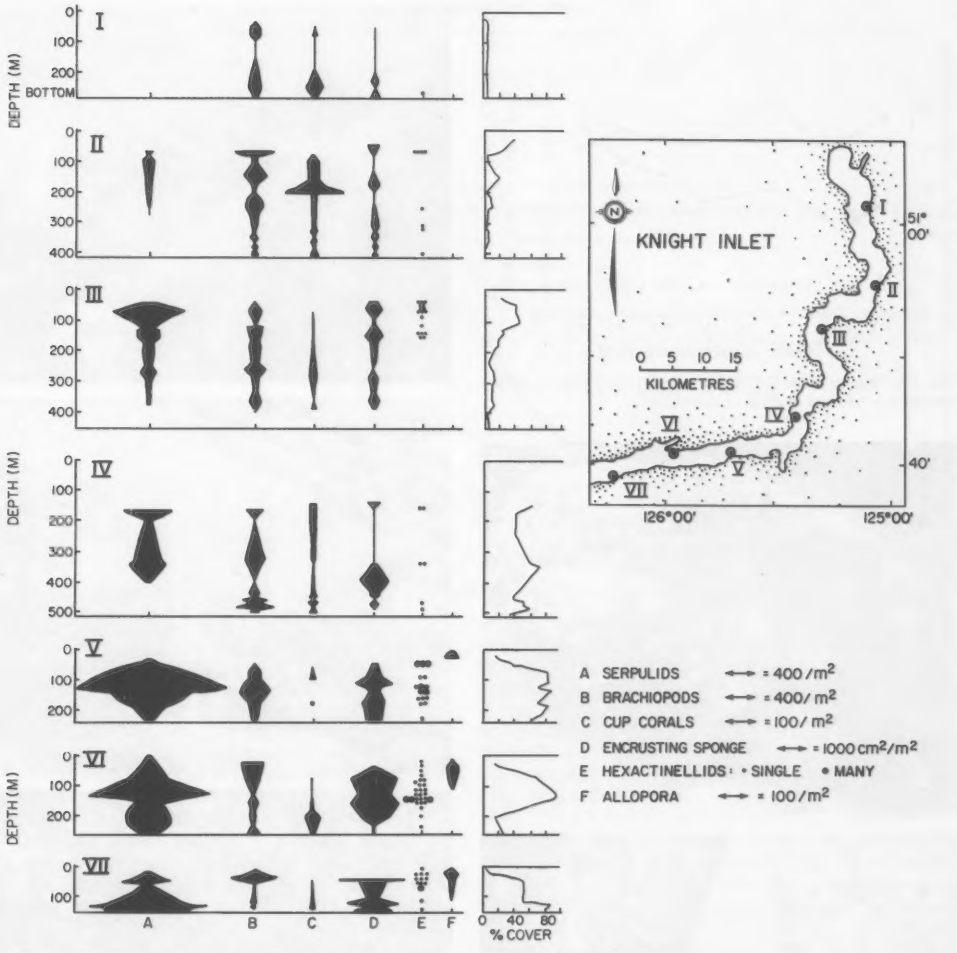

FIG. 8. Distributions of selected epilithic benthos seen along *Pisces* transects in Knight Inlet.

variations in composition, abundance, and diversity along the transects. The dominant constituents are two species of encrusting sponge, an articulate brachiopod, three species of serpulid polychaete, and a solitary scleractinian coral: these animals were found on most transects.

Figure 8 shows the distribution of six animals chosen for their varying responses to sediment loading. The epilithic community was dominated by serpulids, which reached maximum numbers of 2200/m^2 at transect V. Their populations increased in size down-inlet but they were absent from the uppermost dive site. Numbers may have been overestimated as the tubes of dead individuals remain in situ.

Brachiopods were next in abundance. The dominant species was *Laqueus californianus*, but a few *Terebratulina unguicola* were also present. They were ubiquitous with little variation in numbers except for shallow sites near the fjord mouth, where a maximum of 610/m^2 was recorded.

Small cup corals (*Caryophyllia alaskensis* and/or *Cyathoceros quaylei*) were particularly evident on the mud-draped slopes of the upper inlet. Highest numbers (100/m^2) occurred at 200 m on transect II, with a steady decline toward the inlet mouth.

The encrusting sponges consisted almost entirely of two species: *Lophoplakortis* sp. nov. and an unidentified species. Individuals covered areas up to 500 cm^2 but most were less than 10 cm^2. Both species were found at the first transect and then showed an increase in both size and numerical abundance down-inlet.

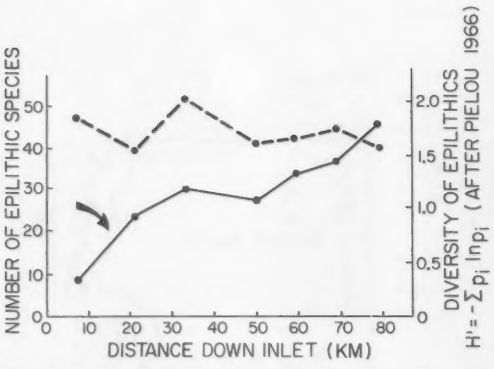

FIG. 9. Number (solid line) and diversity (dashed line) of epilithic species as a function of distance down-inlet.

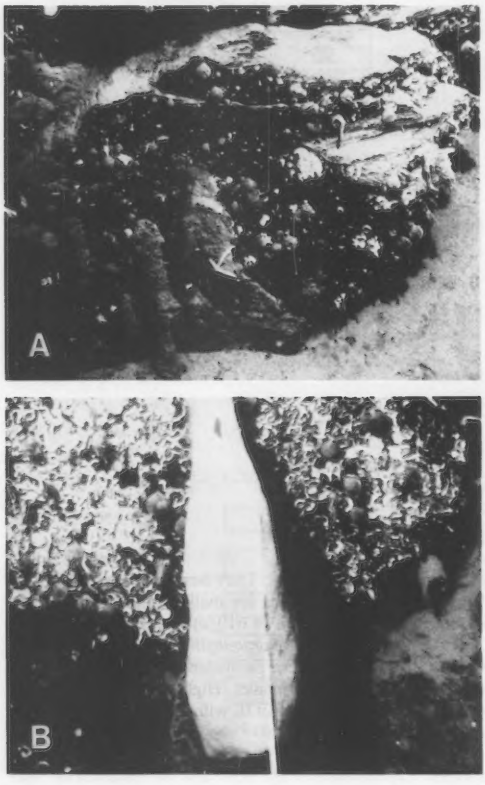

FIG. 10. The effect of current winnowing: (A) 69 m, transect II off Mt. Dundas, showing sediment-laden sponges; (B) 75 m, transect III off Tsukola Pt., showing clean sponge and denser epilithic fauna.

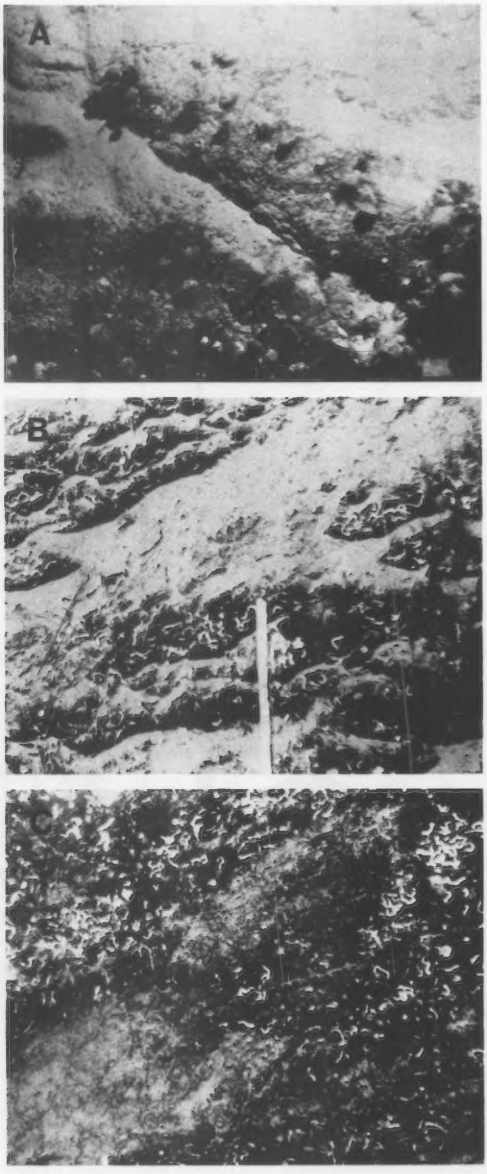

FIG. 11. Decrease in sediment drape down-inlet: (A) 250 m depth, transect I, off Rubble Pt., corals and brachiopods; (B) 107 m depth, transect III, serpulids under ledges; (C) 330 m depth, transect IV off Naena Pt., increase in serpulid cover with little sediment drape.

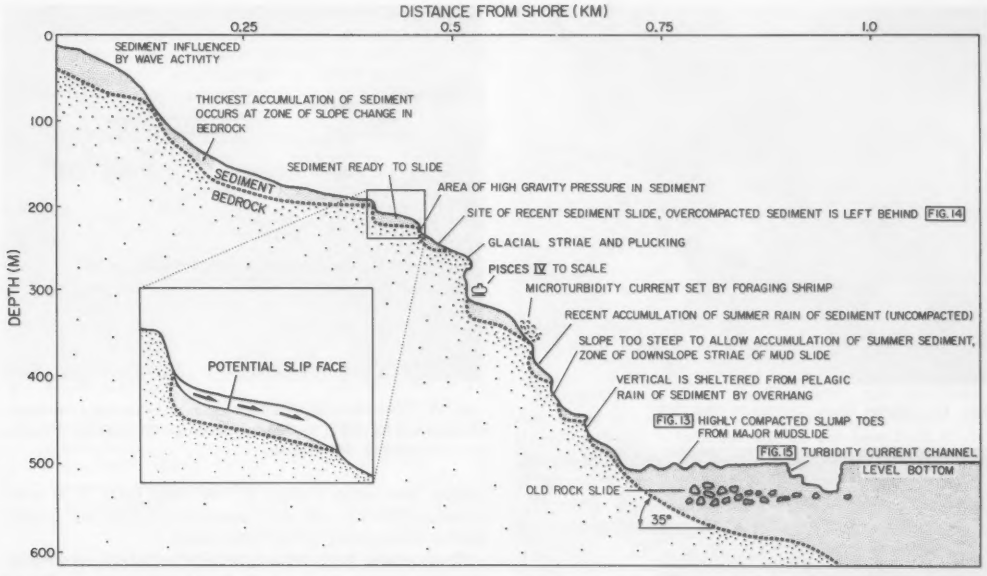
DISTANCE FROM SHORE (KM)
0.25
0.5
0.75
1.0
DEPTH (M)
0
100
200
300
400
500
600
SEDIMENT INFLUENCED BY WAVE ACTIVITY
THICKEST ACCUMULATION OF SEDIMENT OCCURS AT ZONE OF SLOPE CHANGE IN BEDROCK
SEDIMENT
BEDROCK
SEDIMENT READY TO SLIDE
AREA OF HIGH GRAVITY PRESSURE IN SEDIMENT
SITE OF RECENT SEDIMENT SLIDE, OVERCOMPACTED SEDIMENT IS LEFT BEHIND FIG. 14
GLACIAL STRIAE AND PLUCKING
PISCES IV TO SCALE
MICROTURBIDITY CURRENT SET BY FORAGING SHRIMP
RECENT ACCUMULATION OF SUMMER RAIN OF SEDIMENT (UNCOMPACTED)
SLOPE TOO STEEP TO ALLOW ACCUMULATION OF SUMMER SEDIMENT, ZONE OF DOWNSLOPE STRIAE OF MUD SLIDE
POTENTIAL SLIP FACE
VERTICAL IS SHELTERED FROM PELAGIC RAIN OF SEDIMENT BY OVERHANG
FIG. 13 HIGHLY COMPACTED SLUMP TOES FROM MAJOR MUDSLIDE
FIG. 15 TURBIDITY CURRENT CHANNEL
LEVEL BOTTOM
OLD ROCK SLIDE
35°

FIG. 12. Fjord slope environment showing sedimentary processes and position of following photographs. Glacier Bay, Knight Inlet.

The siliceous hexactinellid sponges, normally rare in coastal waters, are common in British Columbian fjords. These sponges, *Aphrocallistes vastus*, *Rhabdocalyptus dawsoni*, *Acanthascus platei*, and *Staurocalyptus dowlingi*, may extend more than a metre from the cliff. The few sponges that were seen on the upper two transects were very small and sediment laden (*A. vastus* and *R. dawsoni*). Again, their abundance and size increased down the inlet to reach a maximum at 130 m at transect VI just inside the sill.

Allopora verrilli, a stylasterine coral found in shallow water, was not found on the upper four transects but appeared on the final three in increasing numbers.

There were numerous other organisms on the cliffs. Most appear to be sediment intolerant and increased in abundance down the inlet. Figure 9 indicates the increase in number of species encountered. Despite large variations in cliff size, the curve does not show species per area effects. The diversity curve hardly varies at all because as the total number of animals increases down the inlet, so do the chances of encountering new species. Tubes of what appeared to be a chaetopterid worm were common in the upper inlet, most abundant at transect IV (max. 1000/m^2) and absent from the lower inlet; similarly, a benthic hydromedusa was also common here. A few encrusting sponge species were found near the head of the inlet, but molluscs, echinoderms, hydroids and anemones were not widely represented until beyond transect III.

Other animals that appeared only in the middle and lower portion of the inlet included a comatulid crinoid (*Florometra serratissima*), two species of gorgonian coral (*Paragorgia arborea* and *Primnoa willeyi*), several species of ascideans, and some large bryozoans. Despite the increase in species, the community remained dominated by either serpulids or encrusting sponges.

Apart from the distributional gradients seen along the inlet, the epifauna showed distinctive variations with respect to depth. Most animals were more abundant in shallow water, although the cup coral was commonest near the bottom. Dramatic increases in numbers of serpulids and hexactinellid sponges were found at particular depths on transects III, V, VI, and VII (Fig. 8); wherever currents strong enough to resuspend sediment were experienced (Fig. 10). A distinct shallow water association formed in the lower inlet in water less than 50 m; here in the photic zone, coralline algae dominated, with a subordinate fauna of bryozoans, echinoderms, *Allopora*, and encrusting sponges. In the very shallow water about 10 m, barnacles and mussels were common, but there was a marked paucity of macrophytic algae, probably because of seasonal low salinities.

Sediment drapes on rock surfaces appeared to deter settlement of nearly all the sessile benthos; they were living almost exclusively on surfaces greater than 90° in slope (Fig. 11). The most sediment-tolerant animal was the cup coral which at transect II ventured onto upward-facing slopes. Encrusting sponges and serpulids remained in cracks and overhangs while brachiopods and chaetopterid worms were somewhat less restricted (Fig. 11A). Organisms that grew into the "third dimension" such as gorgonians and glass sponges were particularly susceptible to fouling (Fig. 10A). The coralline algae appeared tolerant of transitory deposition, and it would be of interest to establish whether they could survive the 3-mo freshet buried with silt.

FIG. 13. Recent slump covered by mud clasts.

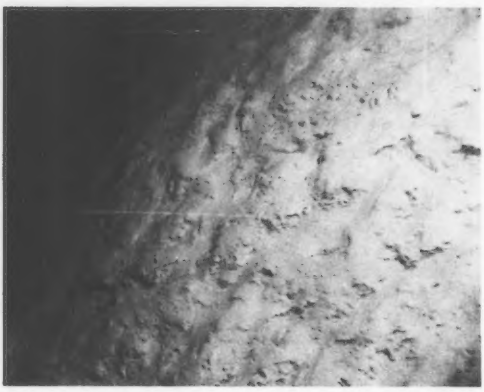

FIG. 14. Overcompacted slip plane with "fluted" microrelief showing no faunal activity.

Figure 8 indicates the extent to which the epibenthos occupies the substratum; these estimates include only the "usable" rock, i.e. >90° slope. Cover is generally less than 20% below 100 m on the three transects nearest the delta; a marked increase occurs in the lower reaches of the inlet where competition for space may become intense. Serpulids grow out from the wall with overgrowth common; many organisms such as corals are excluded entirely. Again, the areas of highest cover are those of current winnowing.

Because of the absence of many sessile forms that are common in other inlets (e.g. larger ascideans in Saanich Inlet; Tunnicliffe 1981) the serpulids and sponges in Knight Inlet can flourish. Predators like rockfish, crustaceans and starfish are also scarce, and they too may modify patterns of space competition.

Processes Affecting Slope Fauna

Knight Inlet has 20% of its submerged area as side-wall

FIG. 15. Two-metre high cutbank generated by turbidity current(s). Channel was located at the 500-m level on the fjord bottom. Note the turbidite bedding. Mt. Dundas.

slopes. Wall slopes average 35° and range from 15° to near-vertical cliffs (Fig. 12), with outcrops of granite and granite gneiss, sedimentary and volcanic rocks.

Rock walls have been glacially modified, producing polished surfaces (some with striae) and areas of plucked bedrock. The latter afford organisms steep to vertical slopes occasionally capped by overhangs which shelter the benthos from the continual pelagic rain of sediment and from downslope movement (Fig. 11A).

In contrast, the polished rock walls have a wide range of slope values and the benthos is subjected to the normal rain of pelagic detritus as well as the downslope movement of sediment. Benthic colonization becomes possible on the slopes when reduced friction limits accumulation. Rock outcrops that have a roughened surface (i.e. numerous striae or a dense benthic community) will increase the likelihood of sediment accumulation. The thickness of this accumulation will then depend on physical and biological factors.

Biological activity is a major factor controlling the geotechnical properties of slope sediments (Richardson and Young 1980). Bioturbation and in situ pelletization normally decrease the shear strength by respectively increasing the water content and decreasing the soil cohesion, except where mucoid adhesion is involved (Nowell et al. 1981). Epibenthic shrimp, up to $6/m^2$, were the major bioturbators on Knight Inlet slopes. They were also the largest cause of sediment resuspension. Their crawling and jumping on the steep slopes commonly generated microturbidity flows that have been observed to move downslope many tens of metres. Flows were generally tens to hundreds of centimetres wide and deep, and must increase local turbidity by an order of magnitude. Other sediment resuspenders that produce similar flows were spider crabs and burrowing fish.

Slope sediment has a short residence time. Where rock slopes were steep (>40°) and local currents strong enough to dislodge grains, sediment was seen sliding down the slope in a traction carpet. Elsewhere, mass movement processes were very important. We have witnessed possibly the first

TABLE 2. Trends of abundance of the animals of Knight Inlet proceeding down the fjord. D = detritovore; NS = nonselective suspension feeder; SS = selective suspension feeder; F = filter feeder; C = carnivore. (Categories from Jørgensen 1966 and Moore 1977.)

A. Decrease and or constant	C. Increase
spider crabs (D)	serpulids (NS)
mud snails (D)	ophiuroids (D)
shrimp (D)	tube worms (D or NS)
copepods (D & D)	soft corals (SS)
ctenophores (NS)	stylasterine coral (SS)
hydromedusae (NS)	hydroids (SS)
sabellids (SS)	most molluscs (F)
brachiopods (SS)	glass sponges (F)
cup corals (SS)	most demosponges (F)
brain sponges (F)	ascideans (F)
	barnacles (F)
B. Middle maximum	amphipods (F)
	arrow worms (C)
burrowing shrimp (SS/D)	asteroids (C)
crinoids (SS)	fish (C)
siphonophores (SS)	
Paragorgia (Gorgonacea) (SS)	
?chaetopterids (F)	

direct evidence of submarine soil creep, a process largely underestimated (Sherif et al.1980). *Axiopsis* burrow openings, normally 10 cm in diameter, were extended 60 cm downslope. These burrowing crustaceans must continually reexcavate the surface sediment as it creeps over the deeper, more stable sediments that house their permanent tunnel system.

Other more dramatic types of mass movement of slope sediment occurred in the high sedimentation areas near the major bayhead delta and on the smaller fanglomerate deltas prograding from side-entry creeks. Evidence of mass movement could be observed along the entire fjord, as was predicted by Flaate and Janbu (1975). Movement may be triggered internally, when the mass of accumulating sediment can no longer be supported, or externally by earthquakes and/or rock slides. The Pacific coastline is perennially subject to low intensity quakes, occasionally reaching 6 or more on the Richter scale. Landslides are frequent, with many fresh slide-scars on the fjord mountains. Large talus blocks from the mountain slopes above were scattered along the side-wall slopes. Compressional slump toes ($\lambda \geq 60$ m, $h \leq 15$ m) were commonly observed. On the slopes angular blocks of compacted mud up to 1 m across or larger (Fig. 13), were common, with tensional joints in the upper slopes. The fault-slip plane occurred either along the bedrock wall or through the sediment (as witnessed by exposed overcompacted sediment surfaces). Such surfaces were very rough, microrelief of 10 cm, with high angle gouge marks — as if the slumped surface sediment was ripped away (Fig. 14).

Submarine soil-creep and slope failure appears to be a major factor in limiting infaunal development on the side-walls of the fjord. The perennially unstable surfaces support only a sparse infauna. Animal burrows may be limited by compaction of the sediment or by the recent nature of the slumping.

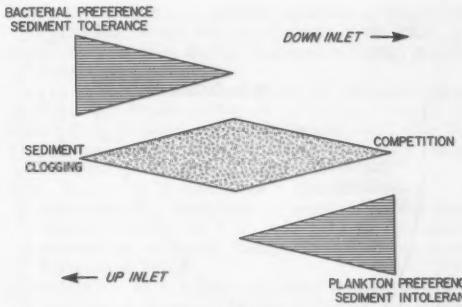

FIG. 16. Animal distribution in Knight Inlet based on feeding types in response to sedimentation rate and turbidity.

Sediment gravity flows (fluidized flows, turbidity flows) may occur in conjunction with slumping (Middleton and Hampton 1976). A turbidite channel was seen from *Pisces* near the base of slope (Fig. 15). Other channels with widths of 30–50 m and depths of 10 m are revealed by detailed bathymetry. Such channels could be fed by slumping from the bayhead delta or localized wall-slope failure.

Multiple Limiting Factors

The Knight Inlet sessile epilithic fauna and much of its infauna appear to follow one of three distribution patterns (Table 2; Fig. 16). These patterns are most readily explained in terms of variation in feeding categories, with many suspension feeders capturing certain particle sizes more effectively than others (Jørgensen 1975; Rubenstein and Koehl 1977). In general, the common animals up-inlet are either nonselective suspension feeders, or those selecting the finest detritus (e.g. sabellids, 3–8 μm, Fauchald and Jumars 1979, p. 244) or bottom detritus feeders; in mid-inlet selective suspension feeders taking larger particles (e.g. crinoids) while filter feeders (e.g. molluscs, barnacles) predominate near the mouth of the inlet.

It is likely that the turbid waters at the fjord-head support large populations of microfauna and bacteria on the suspended sediment (Syvitski and Lewis 1980; Syvitski and Murray 1981); fluorescing inorganic particles indicate the presence of organic activity. The vertical flux of organic matter is highest near the fjord-head, although the percent organic matter incorporated in the sediment is the lowest due to the inorganic dilution factor (Fig. 17). The nonselective suspension feeder is able to take advantage of this nutrient source as all captured particles are passed through for digestion. Organisms selecting the smaller particle sizes are also at an advantage because the SPM is finer here than farther down inlet. The "impingement" method of feeding ensures that the particle catching filaments do not become clogged; Steele-Petrovic (1975) describes the advantages of this design for brachiopods — animals that are particularly common at the head of Knight Inlet. The scarcity of infauna in these sediments reflects the low levels of incorporated total organic matter. In the middle inlet, zooplankton productivity is higher and

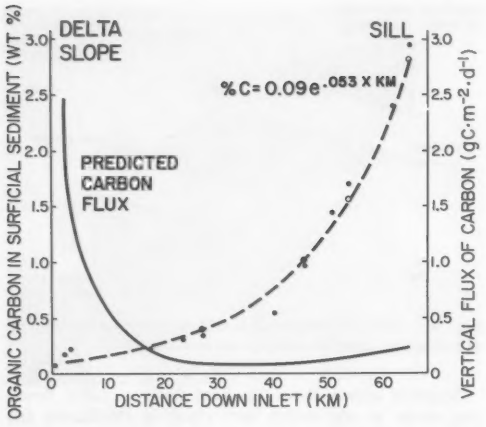

FIG. 17. Amount of organic carbon incorporated into bottom sediment, with predicted vertical flux of organic carbon, as a function of distance down-inlet.

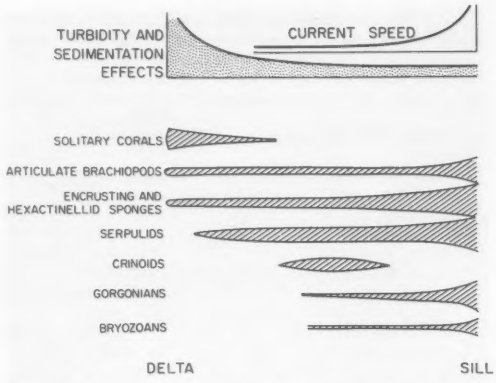

FIG. 18. Approximate distribution of epilithic benthos in Knight Inlet, in relation to sediment loading and current speed.

numerous selective suspension feeders could take advantage of this.

The filter feeders that appear at the mouth of the inlet may be precluded from the upper reaches by the high sediment load. Numerous studies on sponges (Gerrodette and Fleschig 1979), ascideans (Bakus 1968), and bivalves (Loosanoff 1962; Jørgensen 1966) indicate the lowered tolerance of such filter feeders for highly turbid environments. Estuarine bivalves such as *Mytilus* and *Modiolus*, however, flourish in areas of high turbidity, indicating that their rarity in Knight Inlet may be due more to lack of adequate current movement than to high SPM. *Mytilus*, for instance, produces the maximum number of fecal pellets when filtering water with a Secchi disc reading of 0.05 m (Dodgson 1928) and is only absent from such extremely turbid areas as Minas Basin (Moore 1977, p. 301). *Modiolus*, too, is present in the Severn Estuary wherever the current is suitable except in "fluid mud" regions where quite exceptional suspended loads (10^4 mg·L^{-1}) exist (Warwick and Uncles 1980). Sedimentation effects rather than turbidity per se must therefore be a major limiting factor, particularly in larval settlement, as is indicated by Lang et al. (1975), Konnecker (1973) and by Evans et al.'s (1980) evidence from overhangs in Balsfjord, Norway.

The overwhelming effects of sediment blanketing in prohibiting settling on almost all upward-facing rock surfaces can be seen through Knight Inlet, even beyond the sill (Fig. 11) and it is tempting to relate faunal distributions (Fig. 18) primarily to the conspicuous gradient in suspended sediment (Fig. 3). It must also be borne in mind, however, that not only do the effects of sedimentation and turbidity increase as one progresses up-inlet, but so does the distance that the larvae of nonindigenous stock must travel increase. The viability of larvae probably contributes greatly to the maintenance of the observed community structure. The larvae of many epilithic invertebrates avoid silted surfaces (Withers and Thorpe 1977) and others may die after metamorphosis (Davis and Hidu 1969). The seasonal heavy sedimentation in Knight Inlet coincides with the period of reproduction of the majority of these temperate invertebrates. As a result, surfaces less than 90° in slope tend to remain unpopulated. Thus the majority of nonindigenous larvae will have either settled out on a cleaner surface closer to the sill or will have been consumed while in the plankton, so that only small numbers eventually reach the head of the inlet, encountering largely inhospitable silt-smothered surfaces except beneath overhangs — but at least they seem to encounter few predators.

From the visible evidence it is clear that the larvae of solitary corals and brachiopods must be able to withstand the most turbid environments far better than the bivalves, for instance, that are conspicuous by their absence from B.C. fjords today, as they were from Palaeozoic outer shelf-basinal facies where solitary corals and brachiopods were dominant.

Conclusions

Turbidity and sedimentation rate decrease along the length of Knight Inlet according to the perforated conveyor belt model; from an initial rate of 30 cm/yr at the delta, which corresponds to a freshet loading of 4 kg·m^{-2}·d^{-1}. There is also a down-inlet gradient of faunal change, more conspicuous in the rock epifauna than in the sediment infauna. Selective settling is observed throughout the fjord, only solitary scleractinian corals, and to a lesser extent articulate brachiopods and sponges, being able to adapt to sediment laden slopes. Most epifauna seek the shelter afforded by overhangs, with serpulids the dominant group. The epilithic benthos may be ranked in the following order of their decreasing tolerance to the combined effects of high turbidity and sedimentation: (1) solitary corals; (2) articulate brachiopods; (3) ?chaetopterid worms; (4) encrusting sponges; (5) serpulid worms; (6) hexactinellid sponges; (7) ascideans and stylasterine corals. Figure 16 shows three patterns of faunal distribution that can be discerned. Nonselective or fine-selecting suspension feeders are common in the upper inlet where they proba-

bly feed on bacteria associated with the high vertical flux of SPM. Coarser-selecting suspension feeders, less sediment-tolerant, are found in mid-inlet feeding on zooplankton and larger SPM. Filter feeders are confined to the lower inlet where organic matter represents a higher proportion of the SPM and where currents are stronger.

Submersible observations have revealed that the slope fauna is subject to a wide range of localized turbidity maxima or catastrophes that operate with increasing scale and decreasing frequency as follows: (*i*) microturbidity currents, set off by foraging pandalid shrimp; (*ii*) submarine soil-creep, causing burrowing shrimp continually to reexcavate burrow entrances; (*iii*) turbidity currents, at the base of slope, possibly emanating from mudslides or from the main delta slope; (*iv*) mudslides, that periodically sweep across both rock and mud bottoms (see Prior et al. 1981); and (*v*) rock falls that originate from above sea level.

There are thus a great many secondary effects that result from the two primary factors of high vertical sediment flux and low current energy that typify the fjord environment and separate it so distinctively from other turbid coastal regions.

Acknowledgments

This research was funded by the Natural Science and Engineering Research Council of Canada and the Geological Survey of Canada through Dr J. P. M. Syvitski, and the Department of Fisheries and Oceans, Canada through Dr V. Tunnicliffe. Dr G. E. Farrow was supported by a grant from the Royal Society of London. Mr G. Hodge and K. Asprey are thanked for the collection and X-radiography of cores, respectively. We would like to thank the *Pisces* pilots whose combined expertise allowed us to perform some of the most intricate submersible manoeuvres to date.

BAKUS, G. J. 1968. Sedimentation and benthic invertebrates of Fanning Island, Central Pacific. Mar. Geol. 6: 45–51.

DAVIS, H. C., AND H. HIDU. 1969. Effects of turbidity producing substances in sea water on eggs and larvae of three genera of bivalve mollusks: *Crassostrea virginea, Ostrea edulis* and *Mercenaria merceharia*. Veliger 11: 316–323.

DODGSON, R. W. 1928. Report on mussel purification. Fish. Invest. Lond. Ser. II, 10: 498 p.

EVANS, R. A., B. GULLIKSEN, AND O. K. SANDRES. 1980. The effect of sedimentation on rocky bottom organisms in Balsfjord Northern Norway, p. 603–607. *In* H. J. Freeland, D. M. Farmer, and C. D. Levings [ed.] Fjord oceanography. Plenum Press, New York, NY.

FAUCHALD, K., AND P. A. JUMARS. 1979. The diet of worms: a study of polychaete feeding guilds. Oceanogr. Mar. Bio. Ann. Rev. 17: 193–284.

FEDER, H. M., AND A. J. PAUL. 1977. Biological cruises of the R/V *Acona* in Prince William Sound, Alaska (1970–73). Inst. Mar. Sci. Univ. Alaska, Rep. 77–4: 76 p.

FLAATE, K., AND N. JANBU. 1975. Soil exploration in a 500 m deep fjord, Western Norway. Mar. Geotech. 1: 117–139.

GERRODETTE, T., AND A. O. FLESCHIG. 1979. Sediment-induced reduction in the pumping rate of the tropical sponge *Verongia lacunosa*. Mar. Biol. 55: 103–110.

HERLINVEAUX, R. H. 1962. Oceanography of Saanich Inlet in Vancouver Island, British Columbia. J. Fish. Res. Board Can. 19: 1–37.

HOSKIN, C. M., D. C. BURREL, AND G. R. FREITAG. 1978. Suspended sediment dynamics in Blue Fjord, Western Prince William Sound, Alaska. Estuarine Coastal Mar. Sci. 7: 1–16. 1976. Suspended sediment dynamics in Queen Inlet, Glacier Bay, Alaska. Mar. Sci. Commun. 2: 95–108.

JØRGENSEN, C. B. 1966. Biology of suspension feeding. Pergamon Press, Oxford. 357 p. 1975. Comparative physiology of suspension feeding. Annu. Rev. Physiol. 37: 57–79.

KINNEY, P. J., J. GROVES, AND D. K. BUTTON. 1970. Cook Inlet environmental data. R/V *Acoria* cruise 065 — May 21–28, 1968. Inst. Mar. Sci. Univ. Alaska R-70-2: 120 p.

KIRBY, R., AND W. P. PARKER. 1977. Sediment dynamics in the Severn estuary: a background for studies of the effects of a barrage, p. 41–52. *In* T. L. Shaw [ed.] An environmental appraisal of the Severn Barrage. Dep. Civil Engineering, University of Bristol.

KONNECKER, G. 1973. Littoral and benthic investigations on the west coast of Ireland — I (Section A: Faunistic and ecological studies). The sponge fauna of Kilkievan Bay and adjacent areas. Proc. R. Ir. Acad. B73: 451–472.

LANG, J. C., W. D. HARTMAN, AND L. S. LAND. 1975. Sclerosponges — primary framework constructors on Jamaican deep fore-reef. J. Mar. Res. 33: 223–231.

LOOSANOFF, V. L. 1962. Effects of turbidity on some larval and adult bivalves. Proc. Gulf Carib. Fish. Inst. 14: 80–95.

MANHEIM, F. T., J. C. HATHAWAY, AND E. UCHUPI. 1972. Suspended matter in surface waters of the Northern Gulf of Mexico. Geol. Oceanogr. 17: 17–27.

MIDDLETON, G. V., AND M. A. HAMPTON. 1976. Subaqueous sediment transport and deposition by sediment gravity flows, p. 197–218. *In* D. J. Stanley and D. J. P. Swift [ed.] Marine sediment transport and environmental management. Wiley-Intersci. Publ., New York, NY.

MOORE, P. G. 1977. Inorganic particulate suspensions in the sea and their effect on marine animals. Oceanogr. Mar. Biol. Ann. Rev. 15: 225–363.

MOORE, P. G., AND P. C. SCRUTON. 1957. Minor internal structures of some recent unconsolidated sediments. Am. Assoc. Petrol. Geol. Bull. 41: 2723–2751.

NOWELL, A. R. M., P. A. JUMARS, AND J. E. EKMAN. 1981. Effects of biological activity on the entrainment of marine sediments. Mar. Geol. 42: 133–153.

PEARSON, T. H. 1980. The macrobenthos of fjords, p. 569–609. *In* H. J. Freeland, D. M. Farmer, and C. D. Levings [ed.] Fjord oceanography. Plenum Press, New York, NY.

PICKARD, G. L. 1961. Oceanographic features of inlets in the British Columbia mainland coast. J. Fish. Res. Board Can. 18: 907–999.

PICKARD, G. L., AND L. F. GIOVANDO. 1960. Some observations of turbidity in British Columbia inlets. Limnol. Oceanogr. 5: 162–170.

PICKARD, G. L., AND K. RODGERS. 1959. Current measurements in Knight Inlet, British Columbia. J. Fish. Res. Board Can. 16: 635–678.

PICKARD, G. L., AND B. R. STANTON. 1980. Pacific fjords — a review of their water characteristics, p. 1–51. *In* H. J. Freeland, D. M. Farmer, and C. D. Levings [ed.] Fjord oceanography. Plenum Press, New York, NY.

PIELOU, E. C. 1966. Measurement of diversity in different biological collections. J. Theor. Biol. 13: 131–144.

POSTMA, H. 1961. Suspended matter and secchi disc visibility in coastal waters. Neth. J. Sea Res. 1: 359–390.

PRIOR, D. B., W. J. WISEMAN JR., AND W. R. BRYANT. 1981. Submarine chutes on the slopes of fjord deltas. Nature 290: 326–328.

RICHARDSON, M. D., AND D. K. YOUNG. 1980. Geo-acoustic models and bioturbation. Mar. Geol. 38: 205–218.

RUBENSTEIN, D. I., AND M. A. R. KOEHL. 1977. The mechanisms

of filter feeding: some theoretical considerations. Am. Nat. III: 981–996.

RUSNAK, G. A. 1967. Rates of sediment accumulate in modern estuaries. *In* G. H. Lauff [ed.] Estuaries. Am. Assoc. Adv. Sci. 83: 180–190.

SHERIF, M. A., I. ISHIBASHI, AND D. HEYER. 1980. Undrained creep characteristics of deep-ocean sediments. Mar. Geotechnol. 4: 107–124.

SMITH, J. N., AND A. WALTON. 1980. Sediment accumulation rates and geochronologies measured in the Saguenay Fjord using the Pb-210 dating method. Geochim. Cosmochim. Acta 44: 225–240.

STEELE-PETROVIC, H. M. 1975. An explanation for the tolerance of brachiopods and relative intolerance of filter-feeding bivalves for soft muddy bottoms. J. Paleontol. 49: 552–556.

SYVITSKI, J. P. M. 1983. Sedimentology of suspended particulate matter in a turbid west coast fjord; Bute Inlet, B.C. Environmental Marine Geology, AGC, Dartmouth, N.S.

SYVITSKI, J. P. M., AND A. G. LEWIS. 1980. Sediment ingestion by *Tigriopus californicus* and other zooplankton: Mineral transformations and other sedimentological considerations. J. Sediment. Petrol. 50: 869–880.

SYVITSKI, J. P. M., AND J. W. MURRAY. 1981. Particle interaction in fjord suspended sediment. Mar. Geol. 39: 215–242.

TUNNICLIFFE, V. 1981. Epilithic community of a deep oxygen-deficient basin. Nature 294: 354–356.

WARWICK, R. M., AND R. J. UNCLES. 1980. Distribution of benthic macrofauna associations in the Bristol Channel in relation to tidal stress. Mar. Ecol. Prog. Ser. 3: 97–103.

Water Survey of Canada. 1979. Historical streamflow summary, British Columbia. Environment Canada, Ottawa, Ont. 861 p.

WITHERS, R. G., AND C. H. THORP. 1977. Studies on shallow sublittoral epibenthos of Langstone Harbour, Hampshire, using settlement panels, p. 595–604. *In* Biology of benthic organisms. B. F. Keegan and P. O. Ceidigh [ed.] Pergamon, Oxford.

ZABAWA, C. F. 1978. Microstructure of agglomerated suspended sediments in northern Chesapeake Bay Estuary. Science 202: 49–51.

Relations Between Annual Dredging Activities, Suspended Matter Concentrations, and the Development of the Tidal Regime in the Ems Estuary[1]

V. N. DE JONGE[2,3]

Biological Research Ems–Dollard Estuary, Netherlands Institute for Sea Research, Texel, The Netherlands

JONGE, V. N. DE 1983. Relations between annual dredging activities, suspended matter concentrations, and the development of the tidal regime in the Ems Estuary. Can. J. Fish. Aquat. Sci. 40(Suppl. 1): 289–300.

This paper challenges Kühl and Mann's suggestion (1973) that an increase in organic matter in the Ems Estuary between 1950 and 1970 caused a five- to tenfold increase in the turbidity in that period. Their hypothesis is refuted because: (a) during that period the discharge of organic matter via both the River Ems and the River Westerwoldsche A did not change significantly; (b) the increase in particulate organic carbon in the western Dutch Wadden Sea and possibly also in the Ems Estuary resulting from eutrophication of the North Sea by the River Rhine during 1950–70 is unlikely to have been more than twofold; and (c) Secchi-disc data do not support the five- to tenfold increase in turbidity. It is suggested that dredging is probably responsible for the increase in turbidity because the volume of material dredged annually increased fourfold between 1950 and 1970. The mean annual concentration of suspended matter increased by a factor ranging from 1.3 to 2.1 between 1954 and the period 1970 to 1979. The fluctuations in concentrations of suspended matter showed a statistically significant correlation with the distance dredged annually and not with the volume dredged annually. This indicated that the relation depended more on how "extensive" rather than on how "intensive" the dredging was. The fluctuations in concentrations of suspended matter are caused by the intensified erosion and sedimentation cycle that is initiated after the local natural equilibrium between channel morphology and current pattern is disturbed. This explanation is supported by the morphological changes that occurred in part of the study area between 1975 and 1979. Further support for this hypothesis was found in the changes of the tidal regime in the estuary. It is postulated that the complete cessation of dredging would probably be accompanied by the concentrations of suspended solids falling from the 1979 levels to values nearer those obtained in 1954. The biological implications of the processes described are discussed.

Key words: dredging, suspended matter, tidal regime, Ems Estuary, turbidity

JONGE, V. N. DE 1983. Relations between annual dredging activities, suspended matter concentrations, and the development of the tidal regime in the Ems Estuary. Can. J. Fish. Aquat. Sci. 40(Suppl. 1): 289–300.

Dans l'article qui suit, l'auteur met en doute la suggestion de Kühl et Mann (1973) qu'une augmentation de matière organique dans l'estuaire de l'Ems entre 1950 et 1970 a été responsable d'une augmentation, pendant cette période, de cinq à dix fois de la turbidité. On réfute leur hypothèse pour les raisons suivantes : (a) pendant cette période, le déversement de matière organique, à la fois de la rivière Ems et de la rivière Westerwoldsche A, n'a pas varié notablement; (b) l'augmentation de carbone organique particulaire dans le secteur hollandais occidental de la mer Wadden et peut-être aussi dans l'estuaire de l'Ems à la suite d'une eutrophisation de la mer du Nord par le Rhin entre 1950 et 1970 n'a probablement pas plus que doublé; (c) les mesures au disque de Secchi n'indiquent pas d'augmentation de turbidité de cinq à dix fois. Étant donné que le volume de matériel dragué annuellement a quadruplé entre 1950 et 1970, l'auteur suggère que ce draguage est responsable de l'augmentation de turbidité. On a constaté que la concentration annuelle moyenne de matière en suspension a augmenté d'un facteur allant de 1,3 à 2,1 entre 1954 et la période de 1970 à 1979. Les

[1]This paper forms part of the Proceedings of the Dynamics of Turbid Coastal Environments Symposium convened at the Bedford Institute of Oceanography, Dartmouth, N.S., Canada, September 29–October 1, 1981.

[2]Author's address: Biological Centre, Kerklaan 30, 9751 NN Haren, The Netherlands.

[3]Publication No. 53 of Biological Research Ems–Dollard Estuary.

Printed in Canada (J6729)
Imprimé au Canada (J6729)

fluctuations de concentration de matière en suspension sont en corrélation statistiquement significative avec la distance mais non le volume draguée annuellement. Ceci indique que la relation dépend davantage de l'étendue que de l'intensité du dragage. Nous démontrons que les fluctuations de concentration de matière en suspension sont causées par une érosion plus intense et un cycle de sédimentation déclenchés par la perturbation de l'équilibre naturel local entre la morphologie du chenal et les courants. Les changements morphologiques qui se sont produits dans une partie de la région étudiée entre 1975 et 1979 sont en accord avec cette explication. Il en est de même des modifications du régime des marées de l'estuaire. Nous croyons qu'un arrêt complet du dragage serait accompagné d'un abaissement des concentrations de solides en suspension des niveaux de 1979 à ceux de 1954. Nous analysons les implications biologiques des processus en cause.

Received November 13, 1981
Accepted August 13, 1982

Reçu le 13 novembre 1981
Accepté le 13 août 1982

THE Wadden Sea in northwestern Europe is a shallow coastal sea separated from the North Sea by barrier islands. It is approximately 600 km long and extends from north Denmark to the northwestern part of the Netherlands. A number of rivers enter the North Sea via the Wadden Sea, one of them being the River Ems (Fig. 1) whose estuary forms the border between the Federal Republic of Germany and the Netherlands.

The estuary is approximately 100 km long and its area is approximately 600×10^6 m^2 (including the outer delta). The tide is semidiurnal with a diurnal inequality and the tidal prism in the inlet near Borkum is approximately 1250×10^6 m^3 over the flood or ebb, respectively. At the cross section near Knock (Fig. 1) the tidal prism is reduced to approximately 280×10^6 m^3. The mean tidal amplitude near Borkum is 2.25 m and near Knock it is 2.87 m.

In the estuary the gradient of suspended matter, and consequently of turbidity, rises steeply upstream of Knock (Fig. 2). This gradient primarily results from an accumulation mechanism caused by the tide-generated estuarine circulation (Postma and Kalle 1955). Secondly, it is due to an accumulation mechanism described by Postma (1954, 1961) and van Straaten and Kuenen (1957). The result of the estuarine circulation is a turbid region (Fig. 1; between Emden and Leer) with extremely high but greatly fluctuating concentrations of suspended matter. This turbidity results from tidal influences (Postma and Kalle 1955) and varying river discharges in that part of the river where brackish and river water meet (Postma 1981). The accumulation mechanism also builds up a gradient in suspended matter between the deeper tidal inlet and the shallower water on the high tidal flats (Fig. 1). In this estuary, this gradient is well developed between the tidal inlet and the Dollard area (Fig. 1). It partly interferes with the gradient formed by the estuarine circulation. In the Dollard area the concentrations of suspended matter near the water surface reach high values ranging from 50 to 200 mg·L^{-1}. Strong tidal and seasonal fluctuations also occur here.

In 1973 Kühl and Mann reported a five- to tenfold increase in the turbidity of the Ems Estuary between approximately 1950 and 1970, which they attributed to an increase in organic matter. They used a photometer to assess turbidity, i.e. they measured the combined values of the amounts of dissolved compounds and of inorganic and organic suspended materials. Consequently, changes in any of these components or combinations of components could be responsible for the observed increase in turbidity. In this paper some processes that could have had particular influence on changing the concentrations of organic and/or inorganic suspended matter in the area will be briefly discussed.

Extensive morphological changes can lead to a change in the salinity gradient and consequently to a change in the gradient of fine suspended matter (Postma 1967). Bathymetric charts show that this did not occur between 1950 and 1970.

Increased eutrophication of natural fresh waters such as the River Ems could also have led to an increase in the particulate organic carbon entering the estuary. However, the particulate organic carbon entering the Ems Estuary seems to be barely

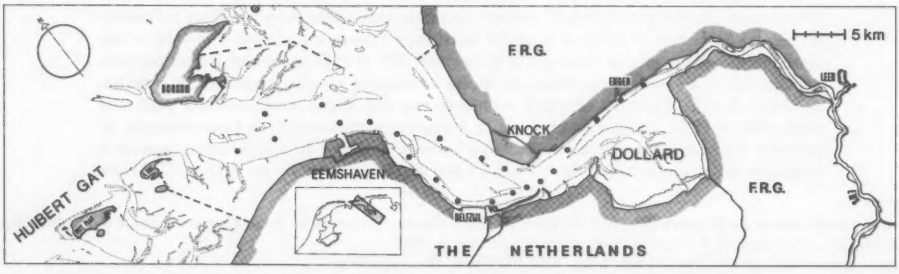

FIG. 1. Ems Estuary showing sampling stations and the divides (---) between the estuary and other tidal basins of the Wadden Sea formed by high tidal flats.

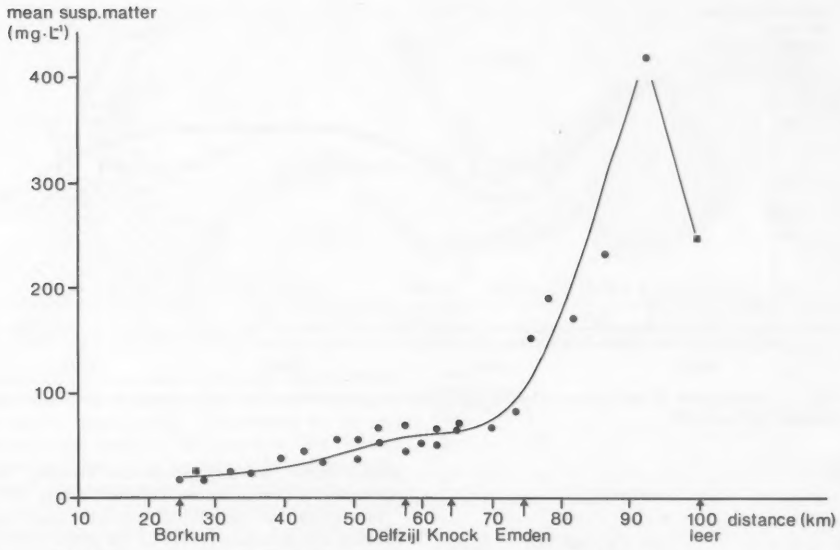

FIG. 2. Surface values of mean suspended matter for the Ems Estuary between the barrier islands and the River Ems, excluding the Dollard.

degradable. This was concluded from experiments done by van Es and Laane (1982) who demonstrated that the degradation of particulate organic matter in a water mass close to the River Ems was lower than in the other parts of the estuary. It is known (de Smet 1960) that the River Ems flows through soils containing peat. Thus, the results of van Es and Laane (1982) support a hypothesis that the particulate organic matter entering the estuary from the River Ems is mainly non-degradable erosion material and that the eutrophication of the River Ems has not led to a strong increase in the degradable particulate organic carbon. We can assume that the amount of the erosion material entering the Ems annually did not change between 1950 and 1970 because the Ems is a rain-fed river and the land use of the river-basin did not change during that period.

An increase in eutrophication of the North Sea, and consequently an increase in the content of suspended organic carbon in the estuary, is possible. Although the organic matter content was not determined in the early 1950s, this parameter can be roughly estimated, enabling the recent situation in the Ems Estuary to be compared with the recent and former situations in the western Dutch Wadden Sea. Data from the surface water collected by Manuels and Postma (1974) in 1970 and 1971 showed that the mean annual content of particulate organic carbon in the part of the estuary lying roughly between Borkum and the mouth of the River Ems (Fig. 1) was 2.2 $mg \cdot L^{-1}$. This was in the same order of magnitude as the mean value they calculated for the western Dutch Wadden Sea (1.5 $mg \cdot L^{-1}$ particulate organic carbon). The difference in mean carbon content between the Ems Estuary and the Wadden Sea may have been caused by the input of the barely degradable organic matter from the River Ems and the large discharge of organic matter in the southeastern part of the Dollard. The discharge in the Dollard is mainly from the potato–flour industry, and, to a lesser extent, strawboard factories as well as domestic sewage (de Wolf 1978). On the basis of the phosphor cycle in the eastern Dutch Wadden Sea, de Jonge and Postma (1974) calculated that between 1950 and 1970 the particulate organic carbon could have doubled. They attributed this development to an increasing eutrophication of the North Sea, mainly by the River Rhine, resulting in an increase in the transport of organic carbon from the North Sea into the Wadden Sea. The eutrophication of the North Sea may also have influenced the transport of particulate organic carbon to the Ems Estuary during the same period. Consequently, it is feasible to attribute a doubling of the mean particulate organic carbon to an increased input of carbon into the Ems Estuary. This increase, however, does not even roughly correspond with the increase in turbidity reported by Kühl and Mann (1973).

Published (Anon. 1965) and unpublished data of the RIZA showed that the large annual waste water discharge of organic matter in the southeastern part of the Dollard did not change greatly between 1960 and the period 1970–79. Although no values are available for 1950, it is assumed here that the waste discharges also remained fairly constant between 1950 and 1960.

Figure 3 shows the changes in total annual dredging activities, including sand extraction, carried out by The Netherlands and Germany in the Ems Estuary. It can be seen that the total volume of removed and/or replaced sediment increased between 1950 and 1970 from approximately 2.3 to 9.2×10^6 m^3 per year. This is an approximately fourfold increase and therefore seems to be a likely explanation for the

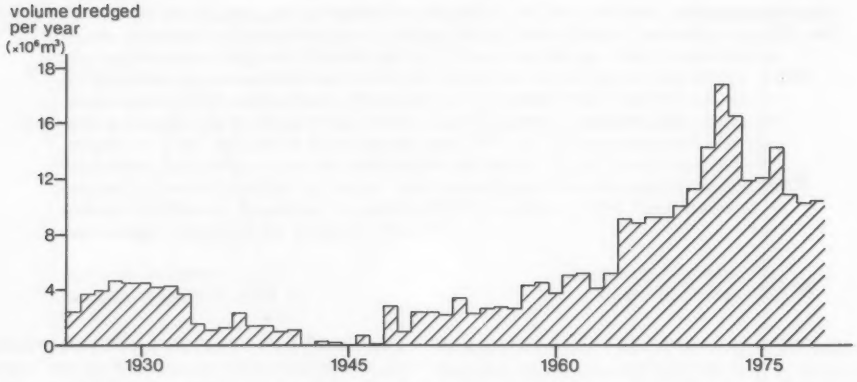

FIG. 3. Development of the combined German and Dutch dredging activities and sand extraction in the Ems Estuary between 1925 and 1979.

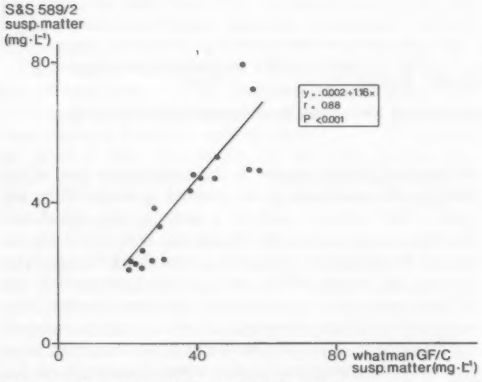

FIG. 4. Comparison of the suspended matter content determined using S&S 589/2 filters and Whatman GF/C glass fibre filters.

five- to tenfold increase in turbidity observed by Kühl and Mann (1973).

The possibilities outlined above indicate that the turbidity changes observed by Kühl and Mann (1973) cannot merely be attributed to an increase in organic matter alone but might also have arisen from an increase in total suspended material resulting from dredging. The increase in turbidity reported by Kühl and Mann was, however, not supported by the increase in suspended matter calculated from data published by Manuels and Rommets (1972) and unpublished Secchi-disc data from NIOZ (Netherlands Institute for Sea Research). This inspired a new, detailed study on changes in turbidity and concentrations of total suspended matter in relation to dredging activities, the results of which are reported in this paper.

Materials and Methods

COLLECTION OF DATA

The primary data used were the concentrations of suspended matter, turbidity (Secchi-disc visibility values) and chlorophyll *a* concentrations, collected during 1975–79.

In addition, concentrations of suspended matter reported by Manuels and Rommets (1972) for the period 1970–72 were used. Chlorophyll *a* concentrations for 1972 were obtained from Cadée (NIOZ) who discussed standing stock and primary production of the estuary of the River Ems in Cadée and Hegeman (1974). Unpublished Secchi-disc observations for the period 1970–72 were obtained from the NIOZ data file. Data on concentrations of suspended matter and chlorophyll *a* concentrations for 1954 were obtained from Postma (1960), and data on Secchi-disc visibilities for 1954 and 1956 were obtained from Dorrestein (1960).

Samples were usually taken in duplicate at 1 m below the water surface irrespective of the tidal phase or bimonthly cycle. This was done because it was impossible to sample the whole estuary between Leer and Borkum (Fig. 1) at the same tidal phase. No data from surveys carried out during high wind were used for this study. Some high values (outliers) for suspended matter resulting from resuspension of sand from the bottom of the channels were omitted.

The authorities in The Netherlands (Rijkswaterstaat, Delfzijl) and the Federal Republic of Germany (Wasser und Schiffahrtsamt, Emden) provided mean annual tidal amplitudes for the period 1960–80. The Rijkswaterstaat supplied bathymetric data for the outer part of the estuary of the River Ems and data on changes in time lag between high water and slack high water. Data on dredging activities and sand extraction were obtained from the Rijkswaterstaat and the Wasser und Schiffahrtsamt. Over the years the technique of dredging has changed. Before 1960 all dredging was done by a bucket dredge. In 1965 suction dredging was introduced and since 1973 has been the only method used. However, it is assumed that the different dredging techniques had similar effects on suspended matter or turbidity. Bucket dredging accounted for 21.8, 7.5, and 4.0% of the total dredging activity in 1970, 1971, and 1972. After 1972 bucket dredging was unimportant.

Float observations were carried out to determine the dis-

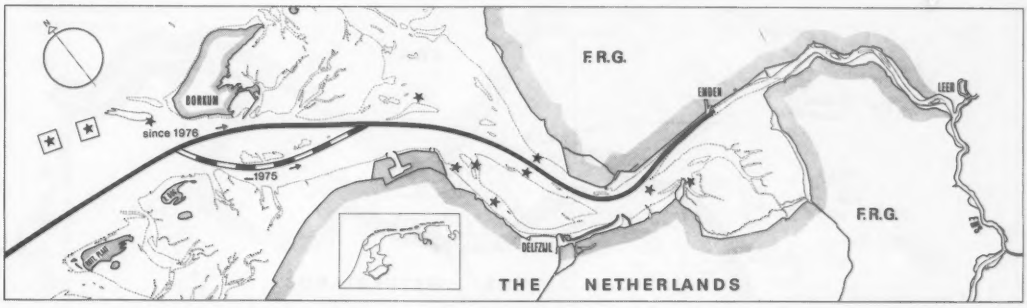

FIG. 5. The navigation route dredged until 1975 and from 1976 to the present. Locations of spoil (mainly sand) dumps are asterisked.

tance travelled by the water mass in the main channel system in the outer part of the estuary.

For the present investigation, data available for the area from Borkum to the mouth of the River Ems (Fig. 1) were used to investigate changes in the mean values of suspended matter, Secchi-disc observations and concentrations of chlorophyll *a*. The choice of this area was primarily based on the geographical distribution of available data. Furthermore, the values for suspended matter in the Dollard and in the Ems are very high and variable because of the influence of the accumulation mechanisms described in the introduction. Moreover, these areas lay outside the region that had been dredged.

ANALYTICAL PROCEDURES

Concentrations of suspended matter were determined gravimetrically using Whatman GF/C glass fibre filters. In 1954, suspended matter was determined using S&S 589/2 paper filters (Postma 1960). Therefore, a comparison between these filters was made for the suspended matter retained. Figure 4 shows that only a slight difference exists between both series of observations. The results show that the S&S 589/2 filters used in 1954 gave, on average, a 13% higher dry weight than the Whatman GF/C filters that were used subsequently. This relatively slight difference was not taken into account in the calculations, because the annual mean for 1954 given in Table 1 was an estimate obtained by calculations using a linear regression equation. Secchi-disc visibilities were obtained using a 30 cm diameter white disc. Chlorophyll *a* content was determined according to the method described in Lorenzen (1967). The volumes dredged were calculated to be the net volume of wet sediment transported by the ships. Dredged distances were expressed per annum and calculated to be the total length of the main channel where any operation (dredging or sand extraction) was carried out, irrespective of the depth to which or the breadth over which sediment was removed. The fine-grained sediment obtained from the area between Knock and Emden (Fig. 1) was usually brought on land while most of the coarse-grained sediment was either deposited at one of the localities indicated in Fig. 5 by a square containing an asterisk, or, if it was derived from sand mining, was also brought on land. Only small amounts of dredged material were dumped at the localities indicated by

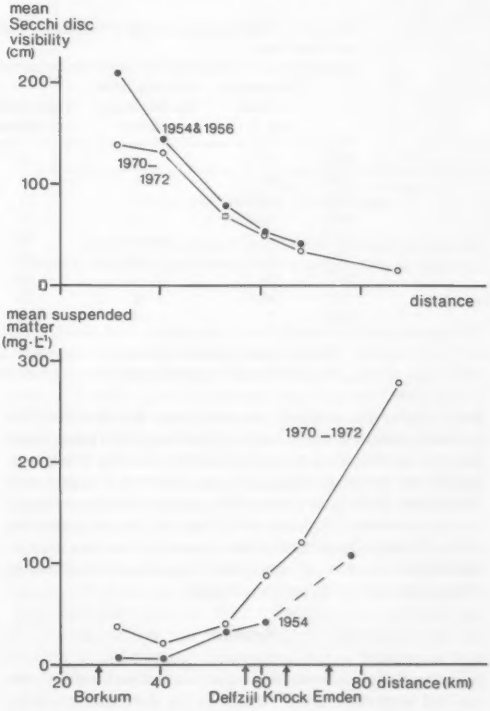

FIG. 6. Comparison between 1954 and 1970–72 for the mean concentrations of suspended matter and between 1954 and 1956 and 1970–72 for the mean Secchi-disc visibilities.

asterisks on Fig. 5. Usually, the dredging along the navigation route (Fig. 5) was done round the clock. The sand mining involved different numbers of ships at different localities. The mean annual content of suspended matter in the study area was calculated by averaging the annual station means. For sampling surveys that had been carried out over less than four quarters per year, the annual area mean was estimated using

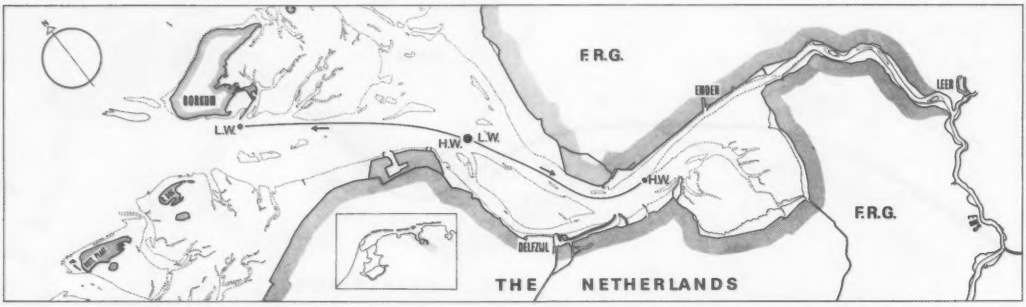

FIG. 7. Results of float observations for two half tidal cycles starting at the same station. Observations were undertaken in the main channel. The length of the float was at least two thirds of the channel depth.

TABLE 1. Mean annual content of suspended matter in the Ems Estuary between the barrier islands and the River Ems.

	Suspended matter ($mg \cdot L^{-1}$)	Data available for following quarters	Total number of stations	Total no. of observations	Correlation coefficient (r)	Significance level (P) using correlation test[b]
1954	45.8[a]	3	9	16	0.69	0.06
1970	61.3[a]	3, 4	9	29	0.92	0.02
1971	60.4	1–4	11	104		
1972	90.4[a]	1–3	11	51	0.83	0.01
1975	58.2	1–4	21	178		
1976	57.6	1–4	19	140		
1977	68.3[a]	3, 4	15	57	0.92	0.02
1978	96.6	1–4	10	50		
1979	76.5	1–4	13	90		

[a]Mean annual content estimated by regression analysis.
[b]Correlation test was only applied to the data from which some annual means were estimated.

linear regression analysis. A correlation test was used to ascertain statistical significance. A test based on a linear combination of Wilcoxon test statistics (van Elteren 1960) was applied to compare changes in the suspended matter and Secchi-disc visibilities for the third quarter of the year, based on the combined 1954 and 1956 data and on the combined 1970–72 data. Spearman's rank correlation test was used to investigate whether a statistically significant relationship existed between different parameters.

Results

Figure 6 shows a comparison for Secchi-disc visibility values and suspended matter values for the third quarter of the years 1954 and 1956 and of the period 1970–72. The suspended matter values calculated for 1954 were significantly lower than those in 1970–72 ($P = 0.0011$; the test based on a combination of Wilcoxon test statistics). The mean value for the whole area under consideration increased from 24.0 to 44.9 $mg \cdot L^{-1}$. The Secchi-disc values for the third quarter of the years 1954 and 1956 were significantly higher than those for the period 1970–72 ($P = 0.042$; same test). However, the difference for the Secchi-disc values was less significant than for suspended matter, because of a smaller decrease in mean value (from 101 to 83 cm). Note that for both parameters, the values in the outer region deteriorated relatively sharply (Fig. 6).

Results of float experiments undertaken in the outer region of the estuary are presented in Fig. 7. If dredging at a certain site increases the concentrations of suspended matter, then this effect should be spread out by tidal water movements over a long distance in the main channel. Such an effect should, of course, only be seen from the fine material and/or suspended material of low density that will remain in suspension for relatively long periods. The float observations indicated that the maximum distance over which effects should be measurable was approximately 35 km within one full tidal cycle, i.e. approximately 75% of the area under consideration.

Table 1 gives the results of the mean values for suspended matter per annum. The asterisked annual values were estimated using regression analysis between annual mean values and means calculated for single quarters or combinations of quarters.

Figure 8 gives the relation between volume dredged per year including sand extraction and the mean suspended matter values for the area under consideration. It can be concluded that the mean content of suspended matter increased after 1954 and fluctuated clearly from year to year. These fluctuations were not similar to the fluctuations in dredging operations. The same picture was obtained if spoil (mainly sand)

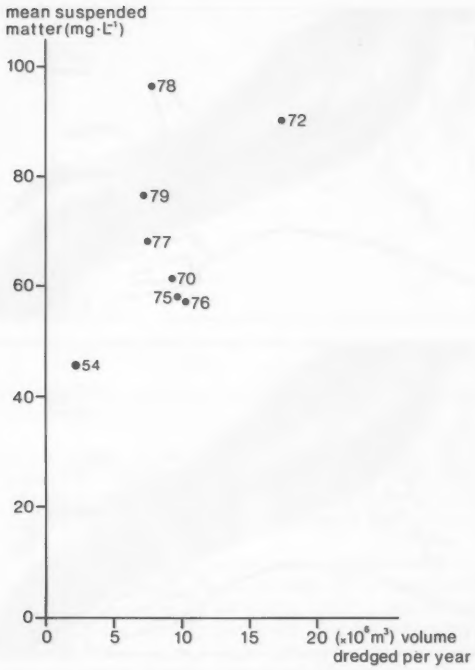

FIG. 8. Relation between volume dredged per year (including sand extraction) and mean annual concentrations of suspended matter.

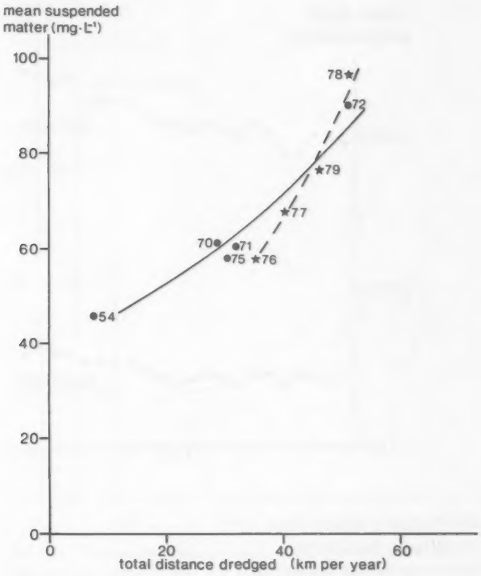

FIG. 9. Relation between total length of bars removed and channels widened or deepened and mean annual concentrations of suspended matter.

partly dumped into the estuary was also taken into account. The Spearman rank correlation test carried out on the values given in Fig. 8 showed that the rank correlation coefficient between volume dredged and mean suspended matter concentrations was low ($r = 0.08$) and statistically not significant ($P > 0.10$).

Figure 9 gives the relation between the total distance dredged and the mean values for suspended matter. The total distance dredged represents approximately the total length of bars removed and widened or deepened channels. Here, a consistent picture emerges. Depending on a dredging distance that increased from 8 km in 1954 to approximately 53 in 1972 and 1978, suspended matter increased from approximately 45 to 95 mg·L^{-1}. However, after 1975 the values seem to show a somewhat different relationship than those for the period 1954–75. A Spearman's rank correlation test using all the annual values resulted in a high ($r = 0.83$) rank correlation coefficient between distance dredged and mean suspended matter concentrations, which was statistically significant ($P = 0.01$).

To ascertain why the relationship between distance and suspended matter provided a better correlation than the relationship between volume dredged and suspended matter, changes in tidal characteristics were examined near Borkum, Knock, and Emden (Fig. 1) for the period 1960–80. It was found (Fig. 10) that the time lag between high water and high slack water near Knock decreased from 25.5 min to approximately 14 min during this period. Further, it was found that the mean tidal amplitude at Borkum increased between 1960 and 1972 while a greater increase was observed for the period 1972–80. The difference between the mean tidal amplitude at Emden and Borkum also increased. The decrease in time lag between 1960 and 1980 indicates that the bottom friction within the estuary decreased progressively during that period. This is confirmed by the increases in mean tidal amplitudes near Borkum and Emden. The increase at Emden as compared with the almost unchanged mean tidal amplitude at Borkum between 1960 and 1972 indicates that the bottom friction between Borkum and Emden had decreased. The increase in mean tidal amplitude after 1972 for both stations indicates that the bottom friction near the tidal inlet (outer delta) also decreased. It can therefore be assumed that an increase in tidal amplitude resulted in increased current velocities and changed current pattern.

Bathymetric changes for part of the estuary between 1970 and 1979 are illustrated in Fig. 11. Here the estuary remained relatively stable until 1975. In 1976 some bars in the upper channel were removed by dredging. This subsequently resulted in the channel migrating over a much broader area than the 200-m wide navigation route which was dredged. The area deeper than 12.5 m below mean sea level was greatly enlarged.

The changes in phytoplankton standing stock expressed as chlorophyll *a* concentrations over the study period are given in Fig. 12. For 1954 data were only available for the third

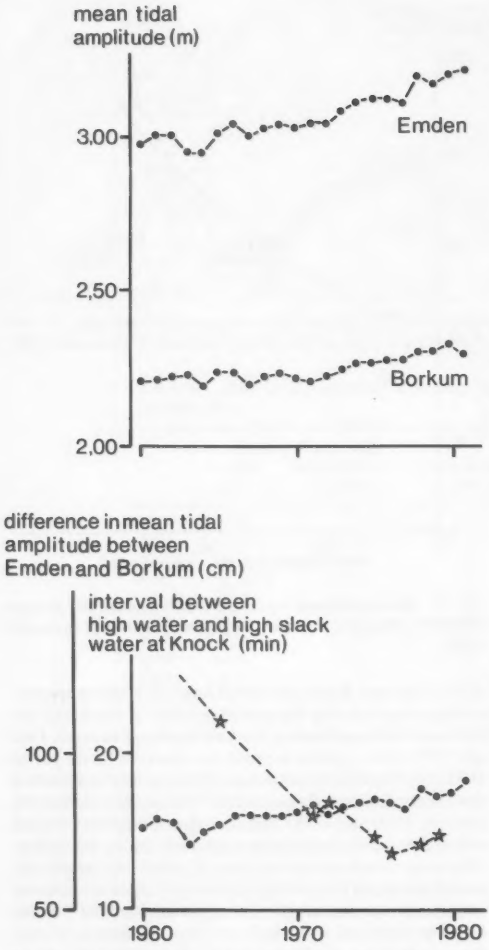

FIG. 10. Changes in time lag between high water and high slack water (asterisk), mean annual tidal amplitudes and difference between mean annual tidal amplitudes for stations Emden and Borkum for the time period 1960–80.

FIG. 11. Morphological development between 1970 and 1979 of the channels in part of the estuary near Eemshaven (see also Fig. 1). Five depth zones below mean sea level are shown. The arrowed open circles indicate the location of bars.

quarter. Therefore, phytoplankton standing stock is represented per year for only the third quarter. The chlorophyll *a* values declined between 1954 and 1972. Furthermore, there seems to be a continuing decline in chlorophyll *a* for the period 1972 to 1979. However, no clear relationship could be found between suspended matter and chlorophyll *a*.

Discussion

TURBIDITY

The reasons for challenging Kühl and Mann's (1973) assertion that the five- to tenfold increase in turbidity in the estuary of the River Ems between 1950 and 1970 was due to an increase in organic matter and for proposing that dredging was more likely to have been responsible for these changes were stated in the introduction. They were that: (a) the increase in transport of particulate organic carbon from the North Sea to the estuary of the River Ems during the period would be unlikely to have been more than twofold, (b) the discharge of

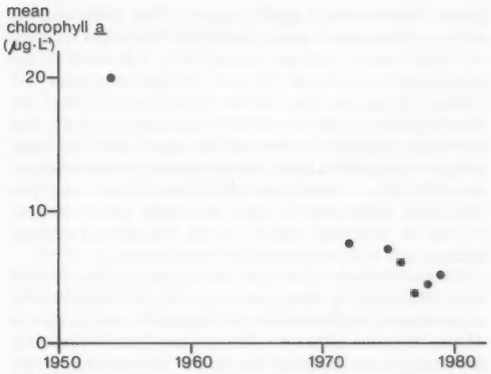

FIG. 12. Mean concentrations of chlorophyll *a* in the study area in the third quarter of certain years.

organic matter via both the River Ems and the River Westerwoldsche A did not change significantly, (c) Secchi-disc data did not support the five- to tenfold increase in turbidity, and (d) the annual volume of material dredged increased fourfold between 1950 and 1970.

The statistical analyses of levels of suspended matter and degree of turbidity (Secchi-disc visibility values) between the years 1954 and 1956 and the period 1970–72 showed that both parameters differed significantly over the time periods reviewed. However, the mean increase in the suspended matter in certain stretches of the estuary (Fig. 6) ranged from 120 to 590% and the decrease in Secchi-disc values ranged from 8.3 to 31.5%. The increase in turbidity reported by Kühl and Mann (1973) for approximately the same period was not of the same magnitude. To ascertain that this discrepancy was not caused by differences in the method of calculation, I used the original data collected by Kühl and Mann (1954, 1972) in 1951–53 and 1968–70 to recalculate the turbidity in the part of the Ems Estuary I studied using the procedure described in Materials and Methods. I found a fivefold increase in turbidity for the period 1950–70. Although Kühl and Mann's reported increase in turbidity seems reasonable, it is not in accordance with the 20% decrease of the light penetration I calculated using the Secchi-disc data (Fig. 6). These differences cannot satisfactorily be explained: although the methods used were different, it is unlikely that this led to the observed discrepancy. The most probable reason could be the limited number of surveys carried out by Kühl and Mann (1973), mainly in one season.

The five- to tenfold increase in turbidity found by Kühl and Mann (1973) also disagrees with the increase in suspended matter (1.3–2.1 times higher) found in the present study. Because the dry weight content of the suspended material can be determined more accurately than the Secchi-disc values, only the former will be considered in discussing the mechanism thought to be responsible for increases in suspended matter (turbidity).

In the introduction it was suggested that the changes in dredging activities, including sand extraction, could be responsible for the observed temporal changes in the suspended

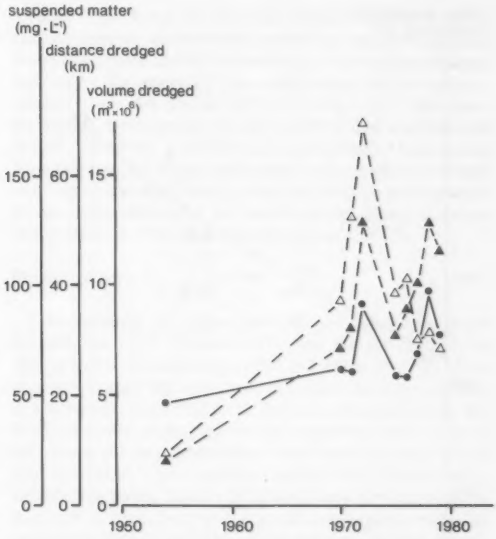

FIG. 13. Mean annual concentrations of suspended matter (●), annual distance dredged (▲), and annual volume dredged (△), plotted as a time series.

matter content. However, Postma (1981) showed that a good inverse correlation was present between the mean monthly river discharges of the Ems and the maximum values of concentrations of suspended matter in the turbid zone. This suggested that, for the present, a relationship between river discharge and concentrations of suspended matter in the more seaward part of the estuary should not be overruled. Although not reported here, statistical analysis of the available data sets for the period 1954–79 showed no significant relationship between both parameters and consequently did not show that river discharges also influenced concentrations of suspended matter in the more seaward parts of the estuary.

DREDGING

Much effort was spent to obtain a detailed picture of the possible relation between changes in concentrations of suspended matter and dredging activity. The estuary was divided into seven sections and possible relations between mean annual suspended matter, volumes dredged, spoil disposed, and distance dredged were investigated. This was done per section and per combination of sections. Not all these attempts shed new light on the relation between dredging and suspended material.

Windom (1976) reviewed the effects of dredging on turbidity and concluded that they have temporal and spatial restrictions. The total annual dredging activity in the estuary of the River Ems, about 17.6×10^6 m^3, is high compared with, for example, the total activity in the USA (approximately 300×10^6 m^3 per annum; Windom 1976), particularly considering that the part of the Ems that is dredged is only 0.2% of the total length of waterways maintained by dredging in the

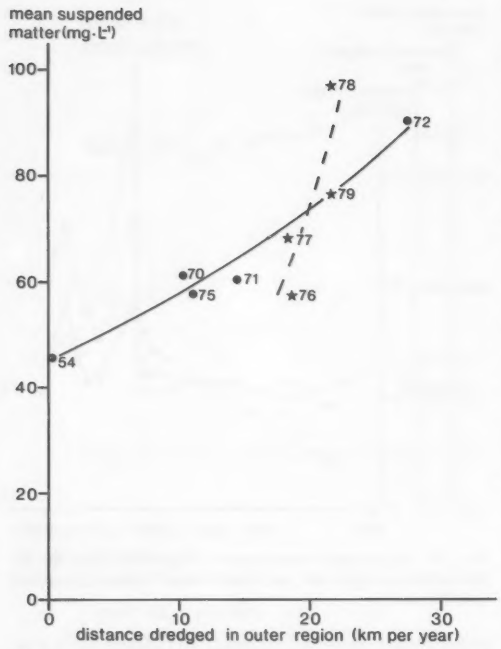

FIG. 14. Relation between length of bars removed and channels widened or deepened seaward from Eemshaven and the mean annual concentrations of suspended matter for the whole study area.

USA (approximately 35 000 km). Although the dredging expressed in m^3 in the estuary of the River Ems is relatively intensive, its effects can be restricted, as discussed by Windom (1976).

The float observations described earlier indicated that an increase in suspended material resulting from dredging operations should be measurable over a long distance. Baretta et al. (1980) showed that an increase in suspended matter content resulting from spoil dumping was only measurable over a distance of a few kilometres. But if dredging is carried out at one site for a longer time period, which is usually the case, then a cumulative increase in suspended matter concentrations cannot be dismissed. Various processes could have influenced the suspended matter content: the possible positive contribution of dredging on concentrations of suspended matter; the long distance travelled by the water mass; the unknown magnitude of the interaction between the increase in suspended matter brought about by dredging and the decrease caused by the suspended matter accumulation mechanisms described; and the continuous dredging operations varying in intensity from place to place. In view of this, and the limited number of observations available, a less detailed comparison of the available data was undertaken. The most realistic approach seemed to be to compare data obtained over longer time periods and over relatively long distances, to ascertain the relation between changes in the concentrations of suspended matter and dredging activity. The mean concentrations of suspended matter, total annual distances dredged, and total annual volumes dredged were calculated as described in Materials and Methods. A Spearman rank correlation test on the data for annual suspended matter and dredging (Figs. 8 and 9) confirmed my supposition: the rank correlation coefficient between the mean annual concentrations of suspended matter and the annual volumes dredged was low and statistically not significant, whereas the rank correlation coefficient between the mean annual concentrations of suspended matter and the total annual distance dredged was high and statistically significant.

To interpret these results, the values given in Figs. 8 and 9 were replotted as a time series (Fig. 13). It is clear that the mean annual concentrations of suspended matter for the 45 km long channel between Borkum and Emden were more dependent on the length of the channel dredged than on the volume of material removed, i.e. on how "extensive" rather than on how "intensive" the dredging was. For the time period 1970–75 both dredging parameters (volume and distance) clearly varied concomitantly, while after 1975 only suspended matter varied concomitantly with distance dredged. The transition between both time periods coincided with the dredging of another channel near the tidal inlet in 1976 as before (Fig. 5). This suggested that dredging activity influenced concentrations of suspended matter mainly indirectly by disturbing the equilibrium between morphology and current pattern when sediment is removed, and that the longer the distance over which sediment was removed the greater this disturbance. This explanation also satisfies the contention (Windom 1976; Baretta et al. 1980) that the direct effects of spoil dumping on suspended matter are usually restricted. The relation between suspended matter and distance dredged seems to be different for the time period 1970–75 as compared with the subsequent period (Fig. 9). It seems that after 1975, the estuary was more sensitive to dredging operations than before that year. This observed difference in trend is not unexpected, because different estuarine channels were modified over both periods. The relation between distance dredged and suspended matter became more evident when only the mean annual suspended matter content was plotted against the distance of channel improvements in the outer estuary (seaward of Eemshaven, Fig. 1) (Fig. 14). This suggests that channel modifications near the tidal inlet of the estuary were especially important in determining the levels of suspended matter over the whole estuary.

The hypothesis that dredging activity influences the estuarine sediment cycle by disturbing the existing equilibrium between morphology and current pattern and that operations near the tidal inlet have a particularly strong influence on the whole suspended matter gradient between Borkum and Emden, can be supported by the changes observed in certain tidal characteristics (Fig. 10). The progressive change in tidal propagation (i.e. diminishing of the bottom friction within the system) that accompanied dredging in the 1960s–76 is demonstrated by the decrease in the time lag between high water and slack high water. It is interesting that this change in time lag is related to the increase in the channel length that was dredged. Between 1960 and 1968 the area between Eemshaven and the island of Borkum (Fig. 1) was modified,

and after 1968 the Huibertgat channel between the island of Borkum and the North Sea was also included in the area modified to meet changing navigational requirements. In 1976, another estuarine channel was dredged, possibly resulting in minimal bottom friction and consequently a minimal time lag (Fig. 10), maybe because no natural bars were present in either the southern or northern estuarine channels in the outer part of the estuary (Fig. 11, 1976). The slightly increased time lag after 1976 could have resulted from a readjustment of the morphology of the channel bed in the southern channel.

The progressive change in tidal propagation is also apparent from the development of the mean tidal amplitudes between 1960 and 1980 near Borkum and Emden (Fig. 10). The tidal amplitudes near Borkum remained virtually constant between 1960 and 1972. After that year, a clear increase was observed. The development of the tidal amplitudes near Emden was different from that of Borkum: between 1960 and 1972 a slight increase in the mean tidal amplitude was calculated, probably mainly the result of the extension of dredging activities between Eemshaven and Borkum. After 1972 the tidal amplitudes near Emden increased further, but more in accordance with the changes in the tidal amplitudes near Borkum. This was probably mainly the result of the further improvements made to the Huibertgat navigation route seaward from Borkum. Because the tidal amplitudes near Emden are a complex function of those near Borkum, the increase near Emden was more pronounced than that near Borkum. The differences in tidal propagation and tidal amplitude must also have resulted in changes in the complex current patterns (Zimmerman 1976) within the estuarine channels. Thus, after the channels were deepened, there was a decrease in the bottom friction and an increase in the tidal propagation, a shortening of the time lag between high water and slack high water, an increase in tidal range and, consequently, increased current velocities with new local current patterns. This means that the bed is continuously adjusting to the new regime. For this to happen erosion must occur elsewhere and an increase in fine suspended sediment would be expected as a result of sorting (because coarse-grained material will mainly settle in the channels whereas fine sediment remains in suspension for a longer time). This supposition is confirmed by the morphological development of the area near Eemshaven between 1975 and 1979. The morphology of the area between Borkum and Eemshaven remained relatively stationary between 1965 and 1975 (Fig. 11; 1975). After 1976, when a new channel was adapted to navigation requirements, the initial channel improvements (Fig. 11; 1976 arrows) within the navigation route led to much greater changes in the total channel morphology (note the changes in the −12.5 m isobath). This strongly suggests the interference of local changes in channel morphology and changes in current patterns, leading to an intensified cycle of erosion and sedimentation followed by a further widening of the main channels (Fig. 11; 1979) until a new bed equilibrium has been reached. A complicating factor is that after 1976 (Fig. 10; 1979 arrow), the bed levels in the southern formerly dredged channel readjusted. This could also have had a positive influence on the concentrations of suspended matter (see high 1978 values in Figs. 9 and 14). However, the reasonable correspondence between distance dredged (Figs. 9 and 14) and mean suspended matter suggests that the increase in suspended matter was mainly caused by the improvements carried out annually in the northern channel and not by the relatively slow readjustment of the southern channel over the period 1975−79 (Fig. 11). The morphological development clearly confirms that readjustment occurs. Therefore, it would not be unreasonable to postulate from this that, all things being equal, the complete cessation of dredging and sand-mining would probably be accompanied by the concentrations of suspended matter falling to values nearer those in 1954 than those measured in 1979.

Productivity

Unfortunately, no values for primary production were available for 1954. However, it is clear that the decrease in chlorophyll *a* values between 1954 and 1972−79 (Fig. 12) is of approximately the same order of magnitude as the increase in suspended matter (Table 1). Because chlorophyll *a* is the most important photo pigment this must also have led to a decrease in primary production. This means less food for the total ecosystem. This conclusion seems to be of importance, because van Es and Laane (1982) have shown by experiments that only a small part of the particulate organic matter is degradable within 1 mo. This clearly indicates that the organic matter from the North Sea is of relatively low nutritional quality. However, it is not certain that the chlorophyll *a* decrease was entirely caused by the increase in mean concentrations of suspended matter and that turbidity increased as a result: this can be demonstrated by the fact that the chlorophyll *a* values did not vary inversely with dredging activities or concentrations of suspended matter. Furthermore, it is well known that the chlorophyll *a* concentrations are not only solely determined by the light regime but reflect a number of factors (de Jonge 1980).

The increase in suspended matter and decrease in algal standing stock has consequences for the fauna. From transplantation experiments, Vrins (1978) concluded that in the Ems Estuary the bivalve *Cerastoderma edule* grows poorly compared with specimens taken to the western Dutch Wadden Sea. She attributed this to the lower organic carbon content of the suspended matter in the Ems Estuary as compared with the reference station in the western Wadden Sea. However, her determinations of the particulate organic carbon content in the Ems Estuary and in the western Dutch Wadden Sea were based on relatively few observations. In the introduction, it was indicated that during 1970−71 the content of particulate organic carbon in the Ems Estuary was somewhat higher than that in the Wadden Sea area, partly because of the peaty soils through which the Ems flows. As a result, the organic matter in the Ems Estuary mineralizes very slowly. It is not unlikely that bivalves are unable to use the remains of phanerogams because even freshly prepared detritus derived from *Spartina foliosa* and *Salicornia viriginica* appear to have low food value for *Mytilus edulis* (Williams 1981). Thus, it seems that the unselective suspension feeders must invest so much energy in filtering large quantities of suspended matter that they cannot grow very well in the more inner parts of the estuary. Today these populations must filter approximately four times as much suspended matter as in 1954 to obtain the same

amount of usable organic carbon, e.g. in the form of phytoplankton and phytobenthos (compare Table 1 and Fig. 12).

Chervin et al. (1981) maintained that copepod production was directly dependent on the assimilation of phytoplankton, even though nonphytoplankton organic matter accounted for most organic carbon assimilated on average. It was stated earlier that the particulate organic matter is barely degradable and consequently is nutritionally inferior to phytoplankton organic carbon. Thus, a higher content of suspended matter and lower phytoplankton standing stock could also have negatively influenced the development of zooplankton populations in the Ems Estuary.

Acknowledgments

I am indebted to the Rijkswaterstaat, Meet en Adviesdienst, Delfzijl, The Netherlands and to the Wasser und Schiffahrtsamt, Emden, Federal Republic of Germany, to Dr G. C. Cadée, Dr R. Dorrestein, and Dr H. Postma for providing data. I am indebted to M. Rademaker and W. H. Uitman-Knol for taking samples and doing analyses. I would like to thank Ph. van Elteren and J. Mulder for statistical advice, and G. Kamstra and E. Leeuwinga for preparing the figures. I am very much obliged to Mr H. Boorsma (Rijkswaterstaat, MAD, Delfzijl) who extracted some important data for me from the available Rijkswaterstaat data file and to Mr D. van Parreeren for discussions on changes in the tidal regime published in this paper. Further, I would like to thank Mr L. A. Bouwman, Dr M. P. Kendrick, Dr H. Postma, and Dr P. de Wolf for their valuable comments on the manuscript.

ANON. 1965. Het estuarium als ontvangend water van grote hoeveelheden afvalstoffen — Afvoer van het veenkoloniale afvalwater naar de Eems. RIZA, Mededelingen no. 2, 144 p, Staatsdrukkerij, 's Gravenhage.

BARETTA, J. W., J. G. BARETTA-BEKKER, V. N. DE JONGE, L. A. VILLERIUS, AND P. DE WOLF. 1980. Slib specielozingen in het Eems estuarium nabij Delfzijl, zoals gemeten volgens verschillende meetmethoden. BOEDE publikaties en verslagen no. 4 — 1980.

CADÉE, G. C., AND J. HEGEMAN. 1974. Primary production of phytoplankton in the Dutch Wadden Sea. Neth. J. Sea Res. 8: 240–259.

CHERVIN, M. B., T. C. MALONE, AND P. J. NEALE. 1981. Interactions between suspended organic matter and copepod grazing in the plume of the Hudson River. Estuarine Coastal Mar. Sci. 13: 169–183.

DORRESTEIN, R. 1960. On the distribution of salinity and of some other properties of the water in the Ems-estuary. *In* J. H. van Voorthuysen. Das Ems-Estuarium. Verh. Kon. Ned. Geol. Mijnb.k. Gen. 19: 103–110.

ELTEREN, P. VAN. 1960. On the combination of independent two sample test of Wilcoxon. Bull. Inst. Int. Stat. 37: 1–13.

ES, F. B. VAN, AND R. W. P. M. LAANE. 1982. The utility of organic matter in the Ems–Dollard estuary. Neth. J. Sea Res. 16: 300–314.

JONGE, V. N. DE. 1980. Fluctuations in the organic carbon to chlorophyll-*a* ratios for estuarine benthic diatom populations. Mar. Ecol. Prog. Ser. 2: 345–353.

JONGE, V. N. DE, AND H. POSTMA. 1974. Phosphorus compounds in the Dutch Wadden Sea. Neth. J. Sea Res. 8: 139–153.

KÜHL, H., AND H. MANN. 1954. Protokolle zur Hydrochemie der unteren Ems auf Grund der Untersuchungsfahrten 1951–1953. Veröffentlichungen des Instituts für Küsten- und Binnenfischerei nr. 8/1954, Bundesforschungsanstalt für Fischerei, Hamburg, 32 p.

1972. Protokolle zur Hydrochemie des Ems auf Grund von drei Untersuchungsfahrten 1968–1970. Veröffentlichungen des Instituts für Küsten- und Binnenfischerei nr. 52/1972, Bundesforschungsanstalt für Fischerei, Hamburg, 14 p.

1973. Untersuchungen zur Hydrobiologie der unteren Ems. Arch. Fischereiwiss. 23: 243–268.

LORENZEN, C. J. 1967. Determination of chlorophyll and pheopigments: spectro-photometric equations. Limnol. Oceanogr. 12: 343–346.

MANUELS, M. W., AND H. POSTMA. 1974. Measurements of ATP and organic carbon in suspended matter of the Dutch Wadden Sea. Neth. J. Sea Res. 8: 292–311.

MANUELS, M. W., AND J. W. ROMMETS. 1972. Metingen van zoutgehalte, temperatuur en zwevend materiaal in de Waddenzee, april 1970 — oktober 1972. NIOZ, publikaties en verslagen 1973–6.

POSTMA, H. 1954. Hydrography of the Dutch Wadden Sea. Arch. néerl. Zool. 10: 405–511.

1960. Einige Bemerkungen über den Sinkstofftransport im Ems–Dollard Gebiet. *In* J. H. van Voorthuysen: Das Ems-Estuarium. Verh. Kon. Ned. Geol. Mijnb.k. Gen. 19: 103–110.

1961. Transport and accumulation of suspended matter in the Dutch Wadden Sea. Neth. J. Sea Res. 1: 148–190.

1967. Sediment transport and sedimentation in the estuarine environment, p. 158–179. *In* G. H. Lauff [ed.] Estuaries. Am. Ass. Adv. Sci. Washington. 757 p.

1981. Exchange of materials between the North Sea and the Wadden Sea. Mar. Geol., 40: 199–215.

POSTMA, H., AND K. KALLE. 1955. Die Entstehung von Trübungszonen im Unterlauf der Flüsse, speziell im Hinblick auf die Verhältnisse in der Unterelbe. Deutschen Hydrogr. Z. 8: 137–144.

SMET, L. A. H. DE. 1960. Die holozäne Entwicklung des niederländischen Randgebietes des Dollarts und der Ems. *In* J. H. van Voorthuysen: Das Ems-Estuarium. Verh. Kon. Ned. Geol. Mijnb.k. Gen. 19: 15–23.

STRAATEN, L. M. J. U. VAN, AND PH. H. KEUNEN. 1957. Accumulation of fine grained sediments in the Dutch Wadden Sea. Geologie-Mijnb. 19: 329–354.

VRINS, A. 1978. De groei en populatiedichtheid van kokkels op enkele plaatsen in de Eems-Dollard. BOEDE publikaties en verslagen no. 6-1978, 69 p.

WILLIAMS, P. 1981. Detritus utilisation by *Mytilus edulis*. Estuarine Coastal Shelf Sci. 12: 739–746.

WINDOM, H. L. 1976. Environmental aspects of dredging in the coastal zone. Crit. Rev. Environ. Cont. 91–109.

WOLF, P. DE. 1978. Effects of organic waste on primary and secondary production in the Ems–Dollard estuary. Hydrobiol. Bull. 12: 260–272.

ZIMMERMAN, J. T. F. 1976. Mixing and flushing of tidal embayments in the western Dutch Wadden Sea, part II: analysis of mixing processes. Neth. J. Sea Res. 10: 397–439.

Particle Resuspension in the Benthic Boundary Layer Induced by Flow around Polychaete Tubes[1]

DREW A. CAREY[2]

Gatty Marine Laboratory and Department of Geology, University of St. Andrews, Scotland

CAREY, D. A. 1983. Particle resuspension in the benthic boundary layer induced by flow around polychaete tubes. Can. J. Fish. Aquat. Sci. 40(Suppl. 1): 301–308.

The effect of the projecting tubes of *Lanice conchilega* (Terebellidae) on particle flux in the benthic boundary layer was studied in laboratory flume experiments. Intact tubes, worms, and flume sediment were collected from an ebb channel of the Tay Estuary. Experiments were performed with dye and high contrast, near-neutral density particles to determine flow patterns and net particle movement in individual tube wakes. Projecting tubes produced characteristic vortex patterns which may increase resuspension of sediment particles. These vortex patterns were not strongly dependent on obstacle shape or flow regime and resulted in pronounced upward motion of fluid from the bed. Particle velocities within the wake were lower than ambient free stream velocity. Results of flume observations reported are consistent with detailed visualization studies of small-scale disturbances within a laminar boundary layer.

Key words: resuspension, boundary layer, benthos, tubes, polychaete, *Lanice conchilega*, flow visualization

CAREY, D. A. 1983. Particle resuspension in the benthic boundary layer induced by flow around polychaete tubes. Can. J. Fish. Aquat. Sci. 40(Suppl. 1): 301–308.

Des expériences avec flumes en laboratoire ont servi à déterminer l'effet des tubes en saillie de *Lanice conchilega* (Terebellidae) sur le flux des particules dans la couche limite benthique. Des tubes intacts, des vers et des sédiments de flume ont été recueillis dans un chenal de jusant de l'estuaire de la Tay. Les expériences ont été menées à l'aide de colorants de particules de densité presque neutre et à fort contraste pour déterminer les caractéristiques des flux et le mouvement net des particules dans le sillage de tubes individuels. Les tubes en saillie produisent des tourbillons caractéristiques susceptibles d'augmenter la resuspension des particules du sédiment. La configuration de ces tourbillons dépend étroitement de la forme des obstacles et du débit, et cause un mouvement prononcé du fluide, du lit vers le haut. La vitesse des particules dans le sillage est inférieure à celle du cours d'eau ambiant. Les résultats des essais avec flumes présentés dans cet article s'accordent avec les observations de perturbations à petite échelle dans une couche limite laminaire.

Received October 26, 1981
Accepted August 16, 1982

Reçu le 26 octobre 1981
Accepté le 16 août 1982

MANY marine organisms build cylindrical tubes that project vertically from the surface of mobile substrata but which remain within the benthic boundary layer (e.g. amphipods: Mills 1967; polychaetes: Fauchald and Jumars 1979). In benthic environments subjected to predictable fluid motion, the interaction of the fluid, tubes, and substratum is a complex process that until recently has received little attention. The flow disturbance associated with projections in boundary layer flow is likely to have important effects on sediment movement in a variety of dynamic benthic environments.

The objective of the study was to describe the influence of the tubes of the polychaete *Lanice conchilega* on the paths of suspended particles. The purpose of this description was to provide a background for elucidating the effects of tubes on near-bottom sediment transport and the feeding behavior of tube-building animals in unidirectional flow. The experiments were designed to measure trajectories of suspended particles and to test the multiple hypotheses that the presence of the tube with and without the fringe can cause:

1) increased numbers of particles with a trajectory towards the bed;
2) no significant change in particle trajectories;
3) increased numbers of particles with a trajectory away from the bed.

This paper reports the results of laboratory experiments on

[1]This paper forms part of the Proceedings of the Dynamics of Turbid Coastal Environments Symposium convened at the Bedford Institute of Oceanography, Dartmouth, N.S., Canada, September 29–October 1, 1981.

[2]Present address: Earth and Environmental Sciences, Wesleyan University, Middletown, CT 06457, USA.

Printed in Canada (J6702)
Imprimé au Canada (J6702)

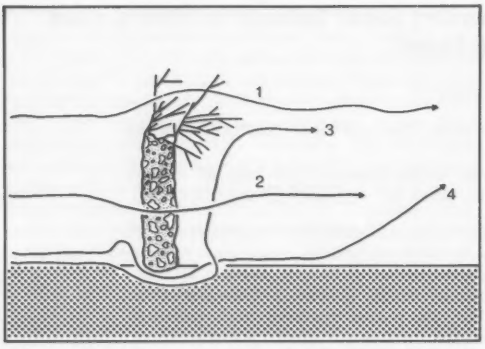

FIG. 1. Flow disturbance by a tube of *Lanice conchilega* in turbulent channel flow. The tube end is extended into two semicircular plates arranged normal to the dominant flow direction. The plates are adorned with a branched fringe which provides support for highly extensile, mucus-coated tentacles. *Lanice* captures food particles resuspended by flow disturbance. Arrows represent generalized flow patterns observed in flume experiments. Numbers refer to description in text. Tube is 0.5 cm wide.

boundary layer flow disturbance by *Lanice* tubes projecting from the natural sediment substratum (fine-medium sand, mean diameter 2.36 phi 195 μm). A recirculating flume was used to produce repeatable flow conditions roughly similar to those observed in the collection area (turbulent flow with a dominant flow direction). A new substance to seed flow for visualization (denatured egg albumen) is described and was used to mimic particulate organic matter for measurement of particle velocities and trajectories.

The tube of *Lanice conchilega* is constructed through mucoidal binding of shell fragments and mineral grains (Ziegelmeier 1952, 1969). Below the sediment there is no selection of material, and the burrow is lined with layers of muco-polysaccharides which bind the sediments of the burrow wall (Bielakoff et al. 1975). Above the sediment surface, the tube is built of selected grains and fragments of shell carefully attached with muco-polysaccharides (Wunderlich 1970). Generally, *Lanice* selects large grains and shell fragments to construct the projecting tube, and small grains and narrow fragments to build prolonged filaments that comprise a fan-shaped "fringe." The precise nature of the tube top varies according to the material available, but the general form studied here consisted of two semicircular plates extending above the circular opening of the tube (4−5 mm outside diameter). The plates and the cylindrical tube ended in irregular branching filaments (1−5 times as long as the diameter of the tube, Fig. 1). The diameter of the filaments was dependent on the particle size available, but when a wide range of sizes was present, the worm selected particles 0.5−1.0 mm in the narrowest dimension and attached them lengthwise to build the fringe elements.

Materials and Methods

FIELD AND EXPERIMENTAL CONDITIONS

Worms and tubes were collected at low spring tides from sand flats bordering a tidal channel at Tentsmuir Beach, N.E. Fife, Scotland. This channel receives moderately turbid water from the Tay Estuary on ebb tides and from St. Andrews Bay on flood tides (Ferentinos and McManus 1983). St. Andrews Bay has a gently sloping bottom topography and is subject to considerable wave action and resuspension. The channel itself is protected from most wave activity by an intertidal sand deposit, the Abertay Sands.

Adult *Lanice* with well-developed tube tops were collected with rectangular can-cores (20 × 20 cm, 30 cm long) and the contents of the cores (tubes, worms, and sediment) were immediately placed in sediment boxes. These boxes (fiberglass boxes 20 × 20 × 30 cm with a 2 cm lip to accommodate brass bolts and a sealing ring) were maintained in a continuous seawater system at 12°C until needed. They were then mounted with the sediment surface level with the flume bed and the tubes projecting into the test section of the flume.

Some boxes were placed in the flume after removing all the tube tops. *Lanice* will rebuild the tube top if provided with sediment and exposed to a gentle current (6−10 $cm \cdot s^{-1}$: Ziegelmeier 1969). Observations of particle behavior were conducted with natural tube tops and with reconstructed tube tops before the fringes were constructed. This procedure allowed evaluation of the hydrodynamic effects of the fringe and tube separately.

FLUME

A free standing water channel, constructed of reinforced fiberglass with a return circuit of PVC pipe, was used in all experiments (Fig. 2). This recirculating flume was filled with 100 L of fresh seawater obtained from the surface of settling tanks. The test section had a working cross section of 250 cm^2 (10 cm deep, 25 cm wide) and the length to width ratio of the channel was 4:1 (settling length and test section). The flow was produced by a DC shunt wound motor (Parvalux 1/4 h.p.) and variable speed gearbox turning a perspex propellor mounted on a brass shaft. The speed of flow was controlled with a thyristor DC controller (Parvalux) and measured by timing suspended particles near the bed. One hundred PVC pipes (2 cm diameter × 10 cm long) served as a collimator, and a 50 W aquarium heater and thermostat maintained the seawater at 12°C. The walls of the test section were composed of a plate glass view port and a black plastic background, both flush with the walls of the flume. The floor of the flume was spread with a 5 mm layer of sediment collected from Tentsmuir Beach (mean diameter 2.40 phi 190 μm) to provide a roughness equivalent to the floor of the tidal channel where it was smooth (e.g. devoid of any other tubes or bedforms).

In a recirculating flume with a rough floor, where any free stream turbulence generated is recirculated, it is very likely that the flow is turbulent throughout the length of the flume. For a turbulent boundary layer and mean cross sectional flow velocity (U) of at least 10 $cm \cdot s^{-1}$ (conditions of experiments reported here) the minimum boundary layer thickness (δ) would be 3.8 cm ($\delta = 0.38l\left(\frac{\nu}{Ul}\right)^{1/5}$ Schlichting 1960, where l is the length downstream from the formation point of the boundary layer and ν is the kinematic viscosity of seawater)

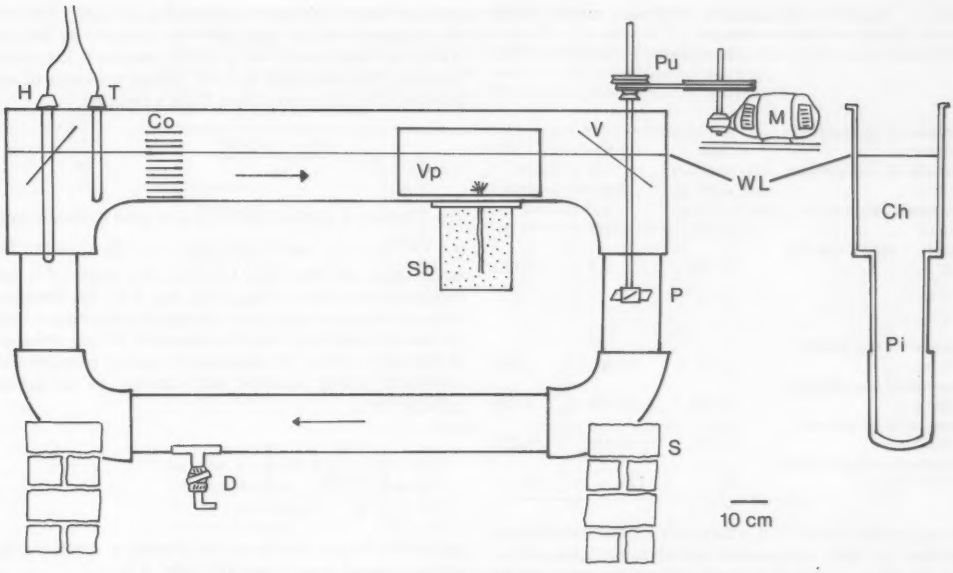

FIG. 2. Free standing saltwater flume constructed from fiberglass reinforced with polyester resin used to produce repeatable flow conditions. The flume is an open channel design with a closed return circuit of standard PVC drain pipe. A DC motor was used to turn a plastic propellor mounted on a brass shaft via a belt and pulley system. The flow direction is indicated by arrows. The flume was supported on brick plinths and held against a wall with angle brackets. (Legend: WL — water level, H — heater, T — thermostat, Co — collimator, Vp — viewport, Sb — sediment box, V — vane, Pu — pulley, M — motor, P — propellor, S — support, D — drain. Cross-section: Ch — channel, Pi — pipe.)

and the Reynolds number $\left(\mathrm{Re} = \frac{U\delta}{\nu}\right)$ would be at least 3800. In this calculation of minimal thickness, the boundary layer is assumed to begin forming at the upstream limit of the flume channel (see Fig. 2). These flow conditions were selected to approximate mean time-averaged flow over the sand-flat collection area. Bed shear stress in the flume was sufficient to transport natural organic particulates in bedload but not to entrain the fine sand of the bed. Observations of the sand flat at low tides and by diving supported this assumption. The sand flat was subject to sand transport in the small ripple regime during spring tide cycles (maximum mean velocities), while large suspended organic particles were seen at neap tides (minimum mean velocities).

FLOW VISUALIZATION

Milk was used as a non-toxic dye to observe flow conditions and patterns of flow disturbance (Crisp and Southward 1956). Milk was carefully injected into the upstream flow with a pipette (1 mm tip diameter). The pipette was held in an electrode manipulator and racked up and down to inject milk at different depths. Observations with the dye confirmed the presence of turbulent channel flow and a thin (< 5 mm) sublayer close to the bed with the flow conditions detailed above. The sublayer, although not strictly laminar due to disturbance by the small-scale roughness (sand-size) of the bed, exhibited slower flow velocities and the milk was maintained in a distinct layer until it encountered larger roughness elements. In practice, the flume produced turbulent flow throughout the depth of the channel apart from thin layers at the free surface (contaminated with dust particles), rough floor, and smooth walls.

The qualities necessary to mimic organic particulates and fine sediment for visualization purposes were met with suspensions of denatured egg albumen (high contrast, net density in seawater low relative to natural particles : $\rho_{egg} - \rho_{seawater} = 0.010\ g \cdot cm^{-3}$, discrete form, non-diffusing, insoluble, inexpensive). Particles of denatured egg albumen were prepared by rinsing 60 g of hard-boiled egg white in distilled water and pressing it twice through a plastic mesh sieve (two sizes used: 0.5 and 1.0 mm). The particles were rinsed three times with distilled water on plastic mesh one phi grade smaller (0.25 or 0.5 mm) and then once through plastic mesh one phi grade larger (1.0 or 2.0 mm) onto the finer mesh to remove irregularly sized particles. The residue was then rinsed thoroughly with filtered seawater and washed through a clean sieve of the original mesh size with 1.5 L of filtered seawater into suspension in a beaker. This procedure resulted in subspherical particles with grain sizes of 0.5−1.0 and 0.25−0.5 mm.

The most useful particles for visualization of fluid movement are large (particles > 0.25 mm are easy to photograph) and neutrally buoyant. To successfully mimic the movement

TABLE 1. Diameters with equivalent (A) terminal settling velocity and (B) Shields threshold criterion.

A.

Diameter of egg particles (mm)	0.25	0.50	1.00
Diameter of oma particles (mm)	0.15	0.31	0.61
Diameter of qtz particles (mm)	0.046	0.092	0.183
Shields threshold criterion θ_r	0.150	0.068	0.052

B.

Diameter of egg particles (mm)	0.25	0.50	1.00
Diameter of oma particles (mm)	0.135	0.320	0.750
Diameter of qtz particles (mm)	0.020	0.039	0.070
Theoretical settling velocity (10^{-3} cm·s^{-1})	32	128	325

of small natural particles, it is necessary for the visualization particles to have comparable hydrodynamic characteristics; thus they must have a density somewhat greater than seawater. To determine the appropriate size and density, a theoretical approach was used as a precursor to extensive empirical measurement.

Two hydrodynamic characteristics widely used in studies of sediment transport dynamics (terminal settling velocity and Shields threshold criterion) were calculated for spheres of egg albumen density immersed in seawater (Table 1A and B, respectively). The derivation of these characteristics was based on denatured albumen density of 1035 kg·m^{-3} (ρ_{egg}) and seawater density of 1025 kg·m^{-3} (ρ_w). The Shields threshold criterion (θ_r) was obtained from Yalin curve (Miller et al. 1977, fig. 4) knowing $\left[\frac{(\rho_{egg} - \rho_w)gd^3}{\rho_w \nu^2}\right]^{1/2} = \sqrt{\Xi}$ (Yalin parameter).

$$\theta_r = \frac{\tau_{o\,crit}}{(\rho_s - \rho_w)gd}$$

where ρ_s = density of particles
ρ_w = density of fluid
g = grav. constant
d = equivalent sphere diameters
ν = dynamic viscosity
$\tau_{o\,crit}$ = critical threshold stress

Knowing the value of the Yalin parameter, diameters of particles with higher densities were obtained by solving for d

$$\left[\frac{\Xi(\rho_w \nu^2)}{g(\rho_s - \rho_w)}\right]^{1/3} = d \qquad \begin{aligned} \rho_{oma} &= 1068 \text{ kg·m}^{-3} \\ \rho_{qtz} &= 2650 \text{ kg·m}^{-3} \end{aligned}$$

In this way the egg particles could be compared with large organic-mineral aggregates (oma) and quartz (qtz). The density of organic-mineral aggregates was estimated by McCave (1975); the value used is that given for particles 0.181 mm in diameter. The theoretical terminal settling velocities of egg particles were determined from Yalin's equation

$$\omega = 0.056 \frac{(\rho_{egg} - \rho_\omega)gd^2}{\nu\rho_\omega}$$

This equation is valid for particles with grain Reynolds number $\left(\frac{\omega D}{V}\right) < \approx 1$ and Yalin parameter $(\Xi) < \approx 18$. For larger grains (in this case 1.00 mm) the value of ω was obtained from a curve (Yalin 1972, fig. 3.2). The diameters of organic-mineral aggregates with equivalent settling velocities were interpolated from the estimated settling velocities of McCave (1975). The diameters of quartz particles with equivalent settling velocities were obtained by solving the equation for d

$$d = \left[\frac{\left(\frac{\omega}{0.056}\right)\nu\rho_\omega}{(\rho_s - \rho_\omega)g}\right]^{1/2}$$

and for the largest particle size by plotting ω versus d using values obtained from Yalin (1972, fig. 3.2).

The procedure for calculating theoretical settling velocity and Shields threshold criterion for novel conditions is described in detail in Miller and Komar (1977).

The particles produced by the method described above were not spheres but angular, subspherical shapes. This should reduce the accuracy of the predicted values; Baba and Komar (1981) reported that while grain roundness had no significant effect on settling velocities, nonspherical particles had a settling velocity lower than that of spheres. This listing of hydrodynamic characteristics (Table 1) is not intended as an accurate measure but rather as a preliminary guide to the mesh sizes of egg particles useful for mimicking natural particles.

PARTICLE PATHS

Photographs of egg particle paths were analysed for movement towards or away from the bed. Path angles were determined by measuring 5–10 tangents along the length of the path, taking the mean tangential angle as the instantaneous path angle. Observations of particle movement during experiments usually allowed definition of direction; any paths with indeterminate direction were not measured. Particles were not observed to descend vertically to the bed as any particles that struck the bed had a greater component of streamwise movement than vertical movement. Some particles leaving the bed near the tube were observed to have vertical path angles (little or no streamwise movement). This allowed discrimination of path direction near the bed in most cases. Flow within the wake was subject to upstream movement and shedding of complex vortices and was consequently more difficult to analyze. Measurements were made of long pathlines on long exposure photographs ($\frac{1}{2}$ s) and only relate to pathlines near the bed. An upstream vector parallel to the bed was taken as

TABLE 2. Increase in resuspension of egg particles within wake envelope of *Lanice conchilega* tubes. Total of results from six photographs ($\frac{1}{2}$ s) taken at 30-s intervals in recirculating flume with a mean channel flow velocity of 10 cm·s^{-1}. Wake envelope is directly downstream of tube, height = tube, width = twice tube diameter and downstream length = five tube diameters. Count with no tubes present made on equivalent areas (tube diameter 0.5 cm).

Experimental conditions	Egg particle grain size μm	Particle pathlines with net movement towards bed	Particle pathlines with net movement away from bed
1 tube, no fringe	250−500	8	17
1 tube, no fringe	250−500	5	10
1 tube, no fringe	500−1000	11	17
1 tube, fringe	250−500	10	21
1 tube, fringe	500−1000	9	17
2 tubes, fringes	250−500	7	10
2 tubes, fringes	250−500	6	11
2 tubes, fringes	500−1000	12	17
2 tubes, fringes	500−1000	10	17
	(Total)	(78)	(137)
No tubes present	250−500	13	12
No tubes present	250−500	17	15
No tubes present	500−1000	8	9
No tubes present	500−1000	10	6
	(Total)	(48)	(42)

0°, downstream 180°, vertical away from the bed 90° and vertical towards the bed 270°. Net movement towards the bed was defined as pathlines in contact with the bed with mean tangential angles of 180°−270° and net movement away from the bed as pathlines in contact with the bed with mean tangential angles of 90°−180°.

Results

Flow past tubes produced a characteristic pattern of disturbance (Fig. 1) at all velocities observed (1−25 cm·s^{-1}).

1) Fluid near the top of the tube was accelerated over the tube and encountered some disturbance near the top of the wake.

2) Fluid that encountered the tube between the base and the top was accelerated around the tube and only rarely entrained in the wake.

3) Some of the fluid near the bed was accelerated around the base of the tube and entrained in an area of slow moving fluid in the lee of the tube (the wake). The entrained fluid rose in an erratic spiral to the top of the tube and was accelerated downstream by the disturbed flow near the top of the wake, or captured in eddies behind the tube which were periodically shed downstream.

4) Part of the fluid near the bed not entrained near the tube was entrained in the downstream portion of the wake, rose from the bed at a relatively shallow angle and was rapidly transported downstream. Particles and dyed fluid observed in the wake were found to result from entrainment of particles of the upstream bedload and fluid from the upstream near-bed sublayer. This may indicate "resuspension" of saltating or rolling grains and slow-moving fluid, rather than "capture" of higher velocity suspended particles of fluid.

Observed patterns of flow disturbance in the tube wake increased movement of egg particles away from the bed (Table 2). Data were pooled for each set in Table 2, because no significant departure from homogeneity was found within the tube-present data ($\chi^2 = 1.1302$ with 8 df, $P > 0.995$; expected values from marginal totals), or within the tubes-not-present data ($\chi^2 = 0.2659$, with 3 df, $P > 0.95$). Each set was tested against the null hypothesis of equal frequencies of movement away from and movement towards the bed. The results from experiments with tubes present showed a highly significant departure from the expected frequencies ($\chi^2 = 15.842$, with 1 df, $P < 0.001$); the departure was an increase over the expected frequency for movement away from the bed.

Results from experiments with tubes not present showed a significant departure from the expected frequencies ($\chi^2 = 4.850$ with 1 df, $P < 0.05$); in this case, however, the departure was an increase over the expected frequency for movement toward the bed.

Mean time-averaged particle velocities were determined by measuring relative lengths of pathlines to eliminate inconsistencies of experimental conditions. Pathline lengths were related to mean length of undisturbed pathlines calculated from 10 to 15 paths above the tubes for each photograph. Thus, particle velocities were expressed as percentages of an approximation of mean channel flow velocities. Velocities of particles within the wake were about 30% of the velocities of particles in undisturbed flow (Fig. 3). This lower velocity was not significantly different between the wake of a single tube with no fringe and the wakes of two tubes with fringes ($P = 0.1660$, $n = 30$, $m = 46$, Wilcoxon rank sum text).

Pathlines of particles within the wake were observed to fall into two classes (Fig. 4 and Table 3). Particles moving away

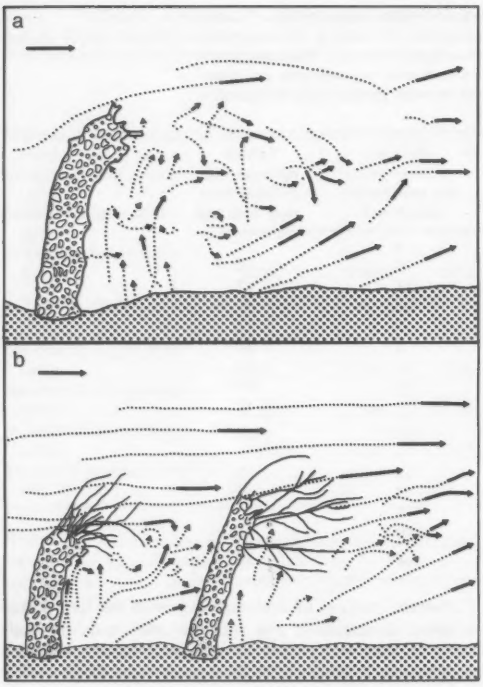

FIG. 3. Velocities of egg particles resuspended in the wake envelopes of *Lanice conchilega* tubes, measured from pathlines on flume photographs. Vector length represents length of pathlines relative to mean length of undisturbed pathlines calculated for each photograph. Lengths of pathlines are equivalent to time averaged velocities of particles. Reference vector (100% of channel flow velocity) in upper left. Dot lines are observed pathlines. Channel flow velocity 10–11 cm·s^{-1} in all photographs. (a) Adult tube, built in tank, fringe not present. Summary of eight photographs ($\frac{1}{4}$ to $\frac{1}{2}$ s exposure). Mean percentage of channel flow velocity of particles within wake envelope is 35.08 ± 6.27 (at 95% confidence level, n = 46). (b) Adult tubes, natural spacing, orientation and fringes. Summary of six photographs ($\frac{1}{4}$ to $\frac{1}{2}$ s). Mean percentage of channel flow velocity of particles within wake envelopes is 31.47 ± 7.64 (95% CL, n = 30). Tubes are 0.5 cm wide.

from the bed within four tube diameters had low velocities and steep trajectory angles. Particles moving away from the bed between 4 and 10 tube diameters had higher velocities and shallow trajectory angles.

The observed trajectory angles for pathlines within four downstream tube diameters were significantly steeper than those further downstream ($P << 0.0003$, n = 32, m = 38, Wilcoxon rank sum test). Pathlines with the steepest trajectories (maximum 90°) appeared to be concentrated within two downstream diameters (Fig. 3), but a value for the distribution was not measured.

At moderate flow velocities ($\bar{u}$ = 2–15 cm·s^{-1}), worms were observed extending their tentacles into the wake, using the branched fringe as a support, and capturing resuspended

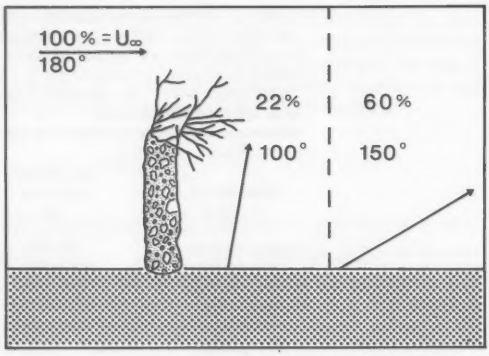

FIG. 4. Mean angles and relative velocities of pathlines downstream of tube of *Lanice conchilega*. Summary of results from 26 photographs (angles) and using velocities from Fig. 3. Length of arrows is not significant. Downstream is defined as 180°, and undisturbed channel flow as U (100%).

egg particles and natural organic particulates. Worms in tubes without fringes were also observed extending tentacles into the current but achieved less spread of the tentacles both vertically and horizontally and appeared to be less successful in particle capture.

Discussion

The characteristic flow disturbance patterns observed for tubes of *Lanice conchilega* in turbulent channel flow do not appear to be very sensitive to ambient flow velocities or fine details of tube geometry. Similar patterns have been observed for isolated projections in laminar boundary layer flow (Gregory and Walker 1951; Mochizuki 1961; Tani et al. 1962), and these patterns were not strongly dependent on flow regime, flow speed, or obstacle shape (Sedney 1973).

Flow perturbations induced by flow past a three-dimensional obstacle have been described by reference to vorticity. Lighthill (1963), Richardson (1968), and Tritton (1977) have provided useful summaries of the meaning and value of arguments utilizing vorticity. Vortex filaments are tubular regions of rotating fluid and are used mathematically and graphically to define and illustrate patterns of flow.

The particle trajectories observed within the wake of the individual tubes of *Lanice* can be related to descriptions of vortex systems summarized by Morkovin (1972) and Sedney (1973). These systems represent an idealized flow pattern past a three-dimensional object in a laminar boundary layer (Fig. 5) and are based on empirical evidence. In this model, the near wake (region close behind the obstacle) is fed by the near bed upstream flow and emptied by the spiral vortex system. This means that momentum is transported towards the bed by the horseshoe vortex (3 in Fig. 5) and away from the bed by the spiral filaments (2 in Fig. 5). Thus, particles carried in near bed flow or scoured from the bed by the horseshoe vortex can be resuspended by the spiral vortex system and carried downstream by the trailing filaments (1 in Fig. 5).

TABLE 3. Mean velocities of egg particle pathlines relative to undisturbed channel flow velocities and mean trajectory angles of pathlines relative to downstream flow direction. Velocities were obtained from pathlines and vectors in Fig. 3 and are expressed as a percentage of channel flow velocity (100%). Trajectory angles were obtained from 26 photographs and are expressed in degrees where 180° is downstream and 0° is upstream. The results were grouped in two classes related to distance downstream of a tube.

	Point of departure from the bed (in tube diameters downstream)	
	< 4	> 4, < 10
Velocity	22.6±2.6% n=53	$60.5 \overset{\times}{\div} 1.2\%$[a] n=11
Trajectory	100.3±5.6% n=38	149.7 ± 4.1% n=32

[a]Confidence limits from log transformation.

Although these detailed patterns of flow disturbance are described from laminar boundary layers, Morkovin (1972) stated that "Scattered evidence suggests that similar rising and sharp rearward bending of a mean flow-through takes place when the obstacle is immersed in a turbulent boundary layer." Apparently, enhanced local scour and resuspension of bedload are likely consequences of isolated small disturbances on erodable beds in the benthic boundary layer (see also Allen 1965).

Lanice conchilega is known to capture and ingest suspended particles, but the nature and source of the particles and the mechanism of capture has not been adequately described (Ziegelmeier 1969; Buhr 1976; Buhr and Winter 1977). Buhr (1979) has suggested that the reduction in near-bottom current velocity produced by arrays of tubes will result in increased sedimentation. The effect of individual tubes of *Lanice conchilega* on flow clearly produces an area of reduced flow velocity (20% of the free stream velocity in the near wake, Fig. 4) but equally clearly does not result in direct sedimentation of suspended particulates (Table 2 and Fig. 3). The flow disturbance created by the tubes could enhance particle capture efficiency through reduced flow speed and chaotic motion alone (Rubenstein and Koehl 1976; Meyer 1973). Perhaps more importantly, the flux of particulates from the sediment surface into the tube wake and the specific geometry of the flow patterns might enable the worms to place their tentacles in a position of maximum capture efficiency.

When the tentacles are extended along the top of the wake parallel to the ambient flow (Ziegelmeier 1969), they should experience minimum drag. The movement of the resuspended particles with the lowest velocity, although chaotic, is generally up the lee of the tube perpendicular to ambient flow and then sharply rearward upon reaching the top of the wake (Fig. 1 and 3). These circumstances would produce maximum particle capture efficiency (Rubenstein and Koehl 1976) and have been observed to occur with natural organic particulates and egg particles in the flume.

The spatial limits of the wake envelope, and concomitantly the flow effects described above, are not known in detail. It would appear, however, that four tube diameters downstream

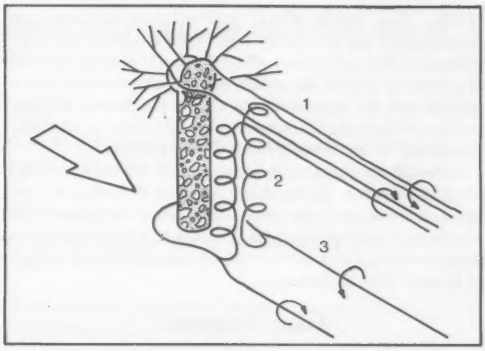

FIG. 5. Diagrammatic representation of flow disturbance by a tube of *Lanice conchilega*. Lines represent vortex filaments and arrows indicate sense of rotation, broad arrow represents dominant flow direction (derived from Gregory and Walker 1951; Thwaites 1960; Mochizuki 1961; Tani et al. 1962). (1) Trailing vortex filaments, (2) Spiral vortex filaments, (3) Horseshoe vortex filaments.

represents a rough limit to the distribution of the spiral filaments which may result in strong resuspension of bedload and entrainment directly behind the tube. The spiral filaments and trailing filaments may, however, be shed periodically; the effect of the vortices travelling slowly downstream within the wake can be seen in Fig. 3a in the lower middle of the diagram.

These speculations on spatial limits ignore any harmonic effects between tube wakes which can have a profound influence on the flow disturbance (Zdravkovich 1977), particularly when vortex shedding occurs (Tritton 1977). Arrays of tubes (or roughness elements) may produce effects which at present are unpredictable, but they are likely to increase bed movement up to a critical density (one-twelfth of the plan area of the bottom occupied by tubes or elements) and decrease bed movement above that density (Nowell and Church 1979). Eckman et al. (1981) provided a plot of this critical density expressed as a relationship between tube size and density. Reported maximum densities and estimated tube diameters for *Lanice* tubes (20 000 m^{-2} × 2 mm, 10 000 m^{-2} × 4 mm, Buhr and Winter 1977; 4 000 m^{-2} × 5 mm, personal observation 1978) fall on or slightly above this critical level. Experiments reported by Eckman et al. (1981) failed to produce bed stabilization widely assumed to result from dense arrays of tubes. Rhoads et al. (1978), however, reported observations that supported the suggestion that arrays of tubes may have a stabilizing effect on fine sediments by increasing the thickness of the viscous sublayer.

It is important to emphasize that roughness elements that produce flow disturbances have two primary effects on boundary layer flow: they create localized areas of increased and decreased flow velocity with a net loss of flow energy through friction, and they produce flow perturbations (shed vortices, trailing filaments, turbulent wakes) that extend downstream. It seems logical that arrays of roughness elements should also produce a net loss of flow energy and result in net sedimentation as predicted by Buhr (1979) and Warner

(1979). This "baffle effect" sedimentation has not been demonstrated and the poorly understood effects of flow disturbance within arrays may affect the result. It is not possible at present to predict the effects of tube arrays on net resuspension and net deposition, but clearly the density and dispersion of individual roughness elements must be carefully considered in any investigations of this problem.

Although the conclusions are at present limited to isolated projections within the boundary layer on noncohesive substrata, it seems clear that small-scale flow of disturbance can resuspend organic particulates. There is no direct evidence in these results that indicates increased sedimentation as a result of isolated flow disturbance.

Acknowledgments

This work was supported by grants from Conoco Ltd. and The University of St. Andrews. Dr J. A. Charlton assisted with the design and R. Jack assisted in installation of the flume. C. Hannan reviewed an earlier version of this manuscript. I would like to especially thank Dr A. R. MacGregor and Professors E. K. Walton and M. S. Laverack for providing support and facilities and Drs A. D. D. Craik, A. Okubo, and H. Bokuniewicz for helpful discussions. I would also like to thank two anonymous reviewers for helpful criticism and advice.

ALLEN, J. R. L. 1965. Scour marks in snow. J. Sediment. Petrol. 35: 331–338.

BABA, J., AND P. D. KOMAR. 1981. Settling velocities of irregular grains at low Reynolds numbers. J. Sediment. Petrol. 51: 121–128.

BIELAKOFF, J., D. DAMAS, AND J. VOVELLE. 1975. Histologie et histochimie des formations glandulaires impliquées dans l'élaboration du tube chez *Lanice conchilega* (Annélide Polychète). Arch. Zool. Exp. Gen. 116: 499–520.

BUHR, K.-J. 1976. Suspension-feeding and assimilation efficiency in *Lanice conchilega* (Polychaeta). Mar. Biol. 38: 373–383.

1979. Eine massensiedlung von *Lanice conchilega* (Polychaeta Terebellidae) in Weder-Aestuar. Veroeff. Inst. Meeresforsch. Bremerhaven 17: 101–149.

BUHR, K.-J., AND J. E. WINTER. 1977. Distribution and maintenance of a *Lanice conchilega* association in the Weser Estuary (FRG), with special reference to the suspension-feeding behaviour of *Lanice conchilega*, p. 101–113. *In* B. F. Keegan, P. O. O'Ceidigh, and P. J. S. Boaden [ed.] Biology of benthic organisms: Proc. 11th European Symp. on Marine Biology, Galway, Oct. 1976. Pergamon Press. 633 p.

CRISP, D. J., AND A. J. SOUTHWARD. 1956. Demonstration of small-scale water currents by means of milk. Nature 178: 1076.

ECKMAN, J. E., A. R. M. NOWELL, AND P. A. JUMARS. 1981. Sediment destabilization by animal tubes. J. Mar. Res. 39: 361–374.

FAUCHALD, K., AND P. A. JUMARS. 1979. The diet of worms: a study of polychaete feeding guilds. Oceanogr. Mar. Biol. Ann. Rev. 17: 193–284.

FERENTINOS, G., AND J. MCMANUS. 1983. Nearshore processes and shoreline development in St. Andrews Bay, Scotland, U.K. Sedimentology. (In press)

GREGORY, N., AND W. S. WALKER. 1951. The effect on transition of isolated surface excrescences in the boundary layer. Rep. Memo. Aero. Res. Coun., Lond. 2779. 10 p.

MCCAVE, I. N. 1975. Vertical flux of particles in the ocean. Deep-Sea Res. 22: 491–502.

MEYER, D. L. 1973. Feeding behaviour and ecology of shallow-water unstalked crinoids (Echinodermata) in the Caribbean Sea. Mar. Biol. 22: 105–129.

MILLER, M. C., AND P. D. KOMAR. 1977. The development of sediment threshold curves for unusual environments (Mars) and for inadequately studied materials (foram sands). Sedimentology 24: 709–721.

MILLER, M. C., I. N. MCCAVE, AND P. D. KOMAR. 1977. Threshold of sediment motion under unidirectional currents. Sedimentology 24: 507–527.

MILLS, E. L. 1967. The biology of an ampeliscid amphipod crustacean sibling species pair. J. Fish. Res. Board Can. 24: 305–355.

MOCHIZUKI, M. 1961. Smoke observation on boundary layer transition caused by a spherical roughness element. J. Phys. Soc. Japan 16: 995–1008.

MORKOVIN, M. V. 1972. An approach to flow engineering via functional flow modules. Beitr. Stromungsmechanik, insbesondere zur Grenzschichttheorie Teil 2, Deutsche Luft-und Raumfahrt Forschungsbericht. 72-27: 270–301.

NOWELL, A. R. M., AND M. CHURCH. 1979. Turbulent flow in a depth-limited boundary layer. J. Geophys. Res. 84: 4816–4824.

RHOADS, D. C., J. Y. YINGST, AND W. J. ULLMAN. 1978. Sea floor stability in central Long Island Sound: Part I. Temporal changes in erodibility of fine-grained sediments, p. 221–224. *In* M. Wiley [ed.] Estuarine interactions. Academic Press, NY. 603 p.

RICHARDSON, P. D. 1968. The generation of scour marks near obstacles. J. Sediment. Petrol. 38: 965–970.

RUBENSTEIN, D. I., AND M. A. R. KOEHL. 1976. The mechanisms of filter-feeding: some theoretical considerations. Am. Natur. 111: 981–994.

SCHLICHTING, H. 1960. Boundary layer theory. McGraw-Hill, NY. 647 p.

SEDNEY, R. 1973. A survey of the effects of small protuberances on boundary-layer flows. A.I.A.A. Journal 11: 782–792.

TANI, I., H. KOMODA, Y. KOMATSU, AND M. IUCHI. 1962. Boundary-layer transition by isolated roughness. Aero. Res. Inst., Univ. of Tokyo, Rep. 375: 129–142.

THWAITES, B. [ed.] 1960. Incompressible aerodynamics. Clarendon Press, Oxford. 636 p.

TRITTON, D. J. 1977. Physical fluid dynamics. Van Nostrand Reinhold, NY. 362 p.

WARNER, G. F. 1979. Aggregation in echinoderms, p. 375–396. *In* G. Larwood and B. R. Rosen [ed.] Systematics Association Special Volume No. 11, Biology and systematics of colonial organisms. Academic Press, London and NY.

WUNDERLICH, F. 1970. Korngrössenverschiebung durch *Lanice conchilega* (Pallas). Senckenbergiana Marit. 2: 119–125.

YALIN, M. S. 1972. Mechanics of sediment transport. 1st ed. Pergamon Press, Oxford. 290 p.

ZDRAVKOVICH, M. M. 1977. Review of flow interference between two circular cylinders in various arrangements. J. Fluids Eng., Trans. A.S.M.E. 99: 618–633.

ZIEGELMEIER, E. 1952. Beobachtungen uber den Rohrenbau von *Lanice conchilega* (Pallas) un experiment und am natürlichen standort. Helgol. Wiss. Meeresunters. 4: 107–129.

1969. Neue untersuchen uber die Wohnrohren-Bau-wiese von *Lanice conchilega* (Polychaeta, Sedentaria). Helgol. Wiss. Meeresunters. 19: 216–229.

Tidal Current Speed and Production of Benthic Macrofauna in the Lower Bay of Fundy[1]

D. J. WILDISH

Department of Fisheries and Oceans, Fisheries and Environmental Sciences, Biological Station, St. Andrews, N.B. E0G 2X0

AND D. PEER

Department of Fisheries and Oceans, Marine Ecology Laboratory, Bedford Institute of Oceanography, Dartmouth, N.S. B2Y 4A2

WILDISH, D. J., AND D. PEER. 1983. Tidal current speed and production of benthic macrofauna in the lower Bay of Fundy. Can. J. Fish. Aquat. Sci. 40(Suppl. 1): 309–321.

The benthic production of the lower Bay of Fundy, which has an area of 8620 km^2, was estimated to be 166.7 × 10^4 t wet biomass in summer 1978, equivalent to an average benthic production of 193 g·m^{-2}·yr^{-1}. Over 88% of the production was by suspension feeders of which the horse mussel, *Modiolus modiolus* (Linnaeus, 1758), was by far the largest contributor.

The geographic distribution of production of the major, soft-sediment, epi- and infaunal trophic groups in the lower Bay of Fundy was in general agreement with the hypothesis that tidal currents are a major determinant of benthic distribution and production in the lower Bay. Tidal currents control sediment dynamics, as well as settlement, growth, and feeding of benthic animals.

Key words: benthos, benthic production, trophic groups, lower Bay of Fundy

WILDISH, D. J., AND D. PEER. 1983. Tidal current speed and production of benthic macrofauna in the lower Bay of Fundy. Can. J. Fish. Aquat. Sci. 40(Suppl. 1): 309–321.

La production benthique de la portion inférieure de la baie de Fundy, d'une superficie de 8 620 km^2, a été estimée à 166,7 × 10^4 t de biomasse humide pendant l'été 1978, ce qui équivaut à une production benthique moyenne de 93 g·m^{-2}·an^{-1}. Plus de 88 % de la production provenait d'espèces se nourrissant d'organismes en suspension, la moule géante, *Modiolus modiolus* (Linnaeus, 1758), étant de beaucoup le plus important contributeur.

La répartition géographique de la production des principaux groupes trophiques épi et infauniques du sédiment mou de la portion inférieure de la baie de Fundy s'accorde en général avec l'hypothèse que, dans ce secteur, les courants de marée sont un important facteur déterminant la distribution et la production benthique. Les courants de marée règlent la dynamique des sédiments de même que la déposition, la croissance et l'alimentation des animaux benthiques.

Received November 10, 1981
Accepted August 6, 1982

Reçu le 10 novembre 1981
Accepté le 6 août 1982

TWO major, interlocking, production pathways occur in the Bay of Fundy. One involves pelagic and benthic *primary production* — the latter inclusive of attached algae and benthic diatoms. Necessary requirements are radiation energy, dissolved nutrients released by decomposer microorganisms, and a photosynthetic capability. The other involves *secondary production* inclusive of pelagic, e.g. zooplankters, and benthic components, both requiring transported detritus consisting of organic matter from primary producers and decomposer microorganisms.

This paper presents the first description of geographic distribution of sublittoral benthic epi- and infauna of the lower part of the Bay of Fundy, with an estimate of secondary benthic production for this area based on wet biomass and annual turnover ratios. The patterns of distribution and production by the major trophic groups are related to tidal current speed and sediment erodibility throughout the Bay.

Materials and Methods

The grab used was designed by Hunter and Simpson

[1]This paper forms part of the Proceedings of the Dynamics of Turbid Coastal Environments Symposium convened at the Bedford Institute of Oceanography, Dartmouth, N.S., Canada, September 29–October 1, 1981.

Printed in Canada (J6723)
Imprimé au Canada (J6723)

(1976). It had a sampling surface area of 0.1 m^2 and typically sampled to a depth of 16 cm; quantitative samples contained 10–16 L of sediment. Two replicate grabs were taken at each location and from one a surface subsample was removed for plant pigment and particle size analysis. Replicates were combined for sieving through 0.8-mm mesh and macrobenthos was preserved in a 10% formalin solution in seawater. In the laboratory, organisms were handpicked from the sediment, tentatively identified, counted, and weighed to the nearest milligram. The taxonomic identity of each species was checked by the Identification Centre, St. Andrews. The resulting station × species × number^{-1} × biomass^{-1} matrix (Peer et al. 1980) was used to produce density (number·m^{-2}) and biomass (wet weight g·m^{-2}) by multiplying the number or biomass per sampling area, 0.2 m^2, by 5. Wet biomass values are for formalin-preserved weights inclusive of shells in the case of molluscs. These values would be variably related to fresh weights (see Mills et al. 1982) making a correction problematical and, in fact, this error has not been accounted for throughout this work.

Secondary production per square metre was calculated by multiplying the biomass value of each species by the estimated P:B values and summing for all species at the station. P:B ratios were taken directly from literature sources or estimated according to the curve derived by Robertson (1979). The curve depends on the inverse logarithmic relationship between life span (x) and P:B(y) of the form $\log_{10} Y = 0.66 - 0.726 \log_{10} X$. Thus, known or estimated life spans used in this study are given in Table 1. Species were also categorized by trophic type as follows: S — suspension feeding, D — deposit feeding, A — algal scraper, C — carnivore, and O — omnivorous scavenger, based on literature sources (Fauchald and Jumars 1979; Bousfield 1973; Biernbaum 1979; Wildish 1983) or as inferred from mouthpart morphology and gut content analysis.

The position of each of the 98 benthic sampling stations occupied in the lower Fay of Fundy is shown in Fig. 1. The limits of the lower Bay used throughout this work are lines joining Martin Head–Cape Chignecto–Morden at the landward limit and Beaver Harbour–Grand Manan–northern tip of Long Island at the seaward limit (Fig. 1). The area within these limits was estimated by counting dots on an Areagraph Chart. Isolines joining areas of equal productivity or percentage of deposit feeders were contoured by hand and the area within each isoline determined as above. The average production of each station occurring within the isoline was then multiplied by the area to give the annual production for each production unit.

The stations were sampled during May 1978 from the research vessel, *J. L. Hart*, and were chosen to correspond with the grid system used in the Greenberg (1979) model of tidal energy behavior. Data from the model were obtained in the form of graphs of current speed (x) against percentage of time a particular speed was exceeded (y), inclusive of both M_2 and solar semidiurnal tidal components for 1978. Calculations were made to estimate the average shear stress, τ_o, (Warwick and Uncles 1980) and turbulent supply of seston, N_A, (Wildish and Kristmanson 1979) as follows:

$$\tau_o = 1/2\ \gamma p V_{max}^2, \text{ units dynes cm}^2$$

where $\gamma = 3 \times 10^{-3}$ is a dimensionless coefficient dependent on bottom roughness, here treated as a constant,

$p = 1.03$ g·cm^{-3} is the density of seawater, also a constant,

V_{max} = maximum current velocity in cm·s^{-1}, a variable for each station,

and

$$N_A = \gamma V(C - C^*) \text{ in units of } \mu g \text{ ATP}\cdot m^{-2}\cdot s^{-1},$$

where V is the mean tidal velocity in $m^{-1}\cdot s^{-1}$ integrated throughout the water column, taken from Greenberg (1979),

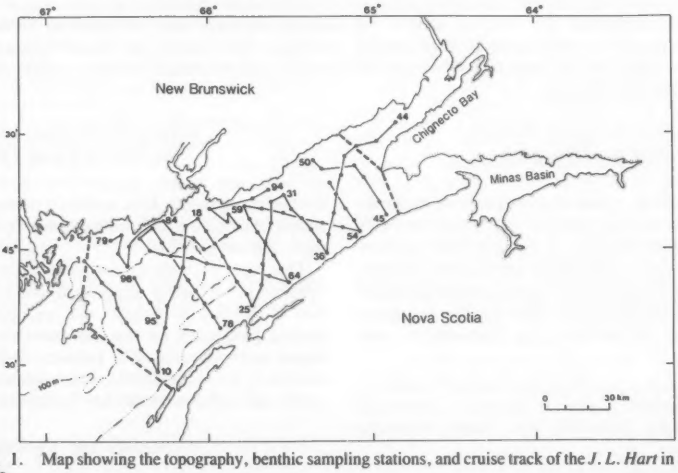

FIG. 1. Map showing the topography, benthic sampling stations, and cruise track of the *J. L. Hart* in May 1978.

TABLE 1. Taxonomic list, trophic type, estimated life span, and wet biomass production ($g \cdot m^{-2} \cdot yr^{-1}$) in the Bay of Fundy

Taxa	Trophic type	Life span, yr^{-1}	Production	
			Mean	Max.
Porifera				
Isodictya deichmannae (deLaubenfels, 1949)	S	100.0	54.70	107.90
Cnidaria, Anthozoa				
Edwardsia elegans Verrill, 1869	S	4.5	1.26	1.28
Cerianthus borealis Verrill, 1873	S	20.0	12.07	22.88
Stomphia coccinea (Müller, 1776)	S	5.0	5.36	34.16
Cnidaria sp.	S	4.0	1.05	1.82
Rhynchocoela				
Lineus sp.	D	3.0	1.07	3.82
Cerebratulus sp.	D	3.0	1.08	3.01
Tetrastemma vittatum Verrill, 1874	D	2.0	0.85	1.17
Brachiopoda				
Terebratulina septentrionalis (Couthony, 1839)	S	7.0	42.25	180.08
Mollusca, Aplacophora				
Chaetoderma sp.	C	1.5	0.42	0.85
Mollusca, Polyplacophora				
Hanleya mendicaria (Mighels and Adams, 1842)	A	2.5	1.24	2.06
Ischnochiton albus (Linnaeus, 1767)	A	3.0	2.49	4.29
Mollusca, Gastropoda				
Puncturella noachina (Linnaeus, 1771)	A	2.5	1.94	4.37
Torellia vestita Jeffreys, 1867	A	4.0	2.70	4.76
Crucibilum striatum Say, 1824	A	6.0	3.39	5.27
Natica clausa Broderip and Sowerby, 1829	C	8.0	2.68	6.29
Mollusca, Scaphopoda				
Dentalium entale Henderson, 1920	D	3.0	5.30	26.58
Mollusca, Bivalvia				
Nucula proxima Say, 1822	D	2.5	1.30	2.02
N. tenuisulcata (Couthony, 1838)	D	3.5	1.07	2.07
Yoldia myalis (Couthony, 1838)	D	4.0	5.80	15.74
Bathyarca pectunculoides (Scacchi, 1833)	S	2.5	3.35	6.53
Placopecten magellanicus (Gmelen, 1791)	S	20.0	202.88	326.53
Chlamys islandica (Müller, 1776)	S	20.0	164.48	326.53
Musculus niger (Gray, 1824)	S	4.0	1.47	1.86
Crenella glandula (Totten, 1834)	S	4.0	2.55	8.43
Modiolus modiolus (Linnaeus, 1758)	S	20.0	485.33	1769.23
Anomia squamula Linnaeus, 1758	S	2.0	0.79	3.42
Astarte undata (Gould, 1841)	S	5.0	30.38	68.22
A. subaequilatera Sowerby, 1854	S	5.0	48.62	87.24
Cyclocardia borealis (Conrad, 1831)	S	5.0	19.36	109.93
Hiatella arctica (Linnaeus, 1767)	S	5.0	2.84	6.41
Thyasira flexuosa (Montagu, 1803)	S	2.5	1.27	1.62
Cerastoderma pinnulatum (Conrad, 1831)	S	7.0	4.89	17.80
Annelida, Polychaeta				
Phyllodoce maculata (Linnaeus, 1767)	D	3.0	0.28	1.57
P. mucosa Oersted, 1843	D	3.0	0.68	1.96
Aphrodita hastata Moore, 1905	O	6.0	9.11	27.59
Laetmonice filicornis Kinberg, 1855	D	1.0	5.90	19.19
Antinoella sarsi (Malmgren, 1865)	C	1.0	1.58	7.61
Lepidonotus squamatus (Linnaeus, 1758)	C	2.0	2.99	6.66
Harmothoe imbricata (Linnaeus, 1767)	C	2.0	0.21	0.22
H. extenuata (Grube, 1840)	C	3.0	1.59	3.14
Sthenelais limicola (Ehlers, 1864)	C	3.0	0.13	0.23
Glycera capitata Oersted, 1843	D	7.0	0.69	4.17
Goniada maculata Oersted, 1843	D/C	2.5	0.64	7.59
G. norvegica Oersted, 1845	C	3.0	2.40	8.74
Ophioglycera gigantea Verrill, 1885	D/C	3.0	1.57	2.27
Nephtys bucera Ehlers, 1868	C	2.0	0.51	1.10
N. incisa Malmgren, 1865	D/C	3.0	2.66	49.41
N. ciliata (O. F. Müller, 1789)	C	3.0	1.98	7.23
N. caeca (Fabricius, 1780)	C	3.0	3.69	10.97

TABLE 1. (*Continued*).

Taxa	Trophic type	Life span, yr^{-1}	Production	
			Mean	Max.
N. picta Ehlers, 1868	C	3.0	0.74	0.78
Aglaophamus circinata (Verrill, 1874)	C	2.0	1.23	4.86
Notomastus latericeus Sars, 1850	D	3.0	0.68	2.45
Heteromastus filiformis (Claparède, 1864)	D	3.0	0.60	1.82
Mediomastus ambiseta (Hartman, 1944)	D	2.0	2.88	9.94
Scalibregma inflatum Rathke, 1843	D	2.0	0.55	2.30
Polyphysia crassa (Oersted, 1843)	D	3.0	10.24	30.21
Nicomache lubricalis (Fabricius, 1780)	D	1.0	0.35	0.73
Rhodine loveni Malmgren, 1865	D	2.0	1.15	5.22
Euclymene zonalis (Verrill, 1874)	D	2.0	0.67	3.59
Maldane sarsi Malmgren, 1865	D	2.0	0.19	0.44
Ophelia limacina Rathke, 1843	D	2.0	0.52	1.05
Travisia carnea Verrill, 1873	D	3.0	1.09	2.11
Ophelina acuminata Oersted, 1843	D	1.5	0.37	1.48
Sternaspis scutata (Renier, 1817)	D	3.0	7.24	21.61
Spio filicornis (O. F. Müller, 1776)	D/C	1.0	0.46	0.84
Laonice cirrata Sars, 1851	D	2.0	0.84	2.57
Scolelepis squamatus (Mueller, 1806)	D	1.0	0.41	0.80
Spiophanes bombyx (Claparède, 1870)	D	2.0	1.41	7.40
Aricidea suecica Eliason, 1920	D	2.0	0.39	1.52
Sabellaria vulgaris Verrill, 1873	D	2.0	2.16	10.08
Eunice pennata (O. F. Müller, 1776)	C	2.0	5.61	22.97
E. norvegica (Linnaeus, 1767)	C	2.0	14.61	20.07
Lumbrineris fragilis (O. F. Müller, 1776)	C	3.0	1.55	6.83
L. impatiens (Claparède, 1868)	A	1.0	0.20	0.45
Ninoe nigripes Verrill, 1873	D	2.0	2.78	14.95
Drilonereis magna Webster and Benedict, 1887	C	2.0	0.98	3.05
Scoloplos armiger (O. F. Müller, 1776)	D	2.0	0.72	3.02
S. acutus (Verrill, 1873)	D	1.0	0.10	0.22
Chaetozone setosa Malmgren, 1867	D	1.0	0.11	0.11
Tharyx acutus Webster and Benedict, 1887	D	3.0	0.34	2.67
Owenia fusiformis Delle Chiaje, 1841	S/D	1.0	0.74	3.40
Ampharete arctica Malmgren, 1866	D	2.0	0.90	2.65
Melinna cristata (Sars, 1851)	D	2.0	1.31	11.05
Anabothrus gracilis (Malmgren, 1866)	D	2.0	0.57	4.07
Amphitrite figulus (Dalyell, 1853)	D	3.5	1.56	2.63
Trichobranchus glacialis Malmgren, 1866	D	2.0	0.75	2.11
Terebellides stroemi Sars, 1835	D	1.0	1.04	3.45
Pista maculata (Dalyell, 1853)	D	3.0	0.20	0.38
Streblosoma spiralis (Verrill, 1874)	D	3.0	1.73	3.08
Pherusa plumosa (Müller, 1776)	D	5.0	2.36	3.41
Brada granosa Stimpson, 1854	D	1.0	2.07	5.59
B. inhabilis (Rathke, 1843)	D	7.0	2.71	3.06
B. villosa (Rathke, 1843)	D	3.0	1.02	2.52
Chone infundibuliformis Kroyer, 1856	S	1.0	0.58	0.89
Sabella crassicornis Sars, 1851	S	4.0	2.33	5.65
Potamilla neglecta (Sars, 1851)	S	1.0	1.84	5.89
Syllis cornuta Rathke, 1843	C	1.0	0.28	0.75
Nereis pelagica Linnaeus, 1758	C	4.0	3.36	11.04
N. zonata Malmgren, 1867	C	2.0	0.51	1.24
N. grayi Pettibone, 1956	C	2.0	0.75	3.66
Sipunculida				
Phascolion strombi (Montagu, 1804)	D	2.0	0.63	1.54
Arthropoda, Crustacea				
Balanus balanus (Linnaeus, 1758)	S	5.0	9.61	21.05
B. crenatus Bruguiere, 1789	S	5.0	77.02	410.76
Eudorella truncatula (Bate, 1856)	D	1.0	0.07	0.20
Calathura branchiata (Stimpson, 1853)	D	1.0	0.75	2.03
Cirolana polita (Stimpson, 1853)	D	2.0	0.83	1.24
Janira alta (Stimpson, 1853)	D	1.0	0.25	0.41
Byblis gaimardi Kroyer, 1846	S/D	1.0	0.16	0.34

TABLE 1. (*Concluded*).

Taxa	Trophic type	Life span, yr^{-1}	Production Mean	Production Max.
Haploops setosa Boeck, 1871	S	2.0	1.70	7.95
H. fundyensis Wildish and Dickinson, 1982	S	2.0	0.40	1.61
Corophium bonelli (Milne-Edwards, 1830)	S/D	1.0	0.30	0.48
Erichthonius rubicornis (Stimpson, 1853)	S	1.0	0.29	0.91
E. difformis Milne-Edwards, 1830	S	1.0	0.18	0.27
Unciola irrorata Say, 1818	D	1.0	0.52	1.78
U. leucopis (Kroyer, 1845)	D	2.0	0.30	0.73
Casco bigelowi (Blake, 1929)	D	2.0	0.47	1.17
Monoculodes nitida Smith, 1873	D	1.0	0.16	0.18
Maera danae Stimpson, 1853	D	2.0	0.34	0.77
M. loveni (Bruzelius, 1859)	D	2.0	1.99	3.92
Argissa hamatipes (Norman, 1869)	D	1.0	0.83	1.64
Ischyrocerus anguipes Kroyer, 1838	S	1.0	0.16	0.41
Anonyx sarsi Steele and Brunel, 1968	D/C/O	2.0	0.13	0.41
Psammonyx nobilis (Stimpson, 1853)	D	2.0	0.56	1.07
Gammaropsis melanops G. O. Sars, 1882	D	1.0	0.17	0.45
Podoceropsis nitida (Stimpson, 1853)	D	1.0	0.34	0.84
Protomedia fasciata Kroyer, 1842	D	1.0	0.34	1.09
Leptocheirus pinguis (Stimpson, 1853)	S	2.0	1.35	7.95
Phoxocephalus holbolli (Kroyer, 1842)	D	1.0	0.27	0.91
Harpinia propingua G. O. Sars, 1895	D	2.0	0.10	0.38
H. truncata G. O. Sars, 1890	D	2.0	0.06	0.12
Pleusymtes glaber (Boeck, 1861)	D/A	1.0	0.10	0.16
Dyopedos porrectus Bate, 1857	S	1.0	0.33	0.82
D. monacantha (Metzger, 1875)	S	1.0	0.29	0.91
Aeginina longicornis (Kroyer, 1842–3)	D	2.0	0.62	1.79
Pandalus montagui Leach, 1813	O	5.0	1.75	3.09
Eualus pusiolus (Kroyer, 1841)	O	5.0	0.56	2.38
Axius serratus Stimpson, 1852	O	5.0	0.19	0.24
Pagurus acadianus Benedict, 1901	O	10.0	15.13	29.56
P. pubescens Kroyer, 1838	O	10.0	1.67	5.63
Echinodermata, Holothuroidea				
Psolus fabricii Duben and Moren, 1844	D	3.0	2.74	6.26
Molpadia oolitica (Pourtales, 1857)	D	25.0	107.58	213.61
Echinodermata, Echinoidea				
Strongylocentrotus droebachiensis	A	10.0	7.60	15.11
Echinarachnius parma (Lamarck, 1816)	D	18.0	11.49	53.33
Briaster fragilis (Duben and Moren, 1844)	D	20.0	26.63	74.62
Echinodermata, Stelleroidea				
Asterias sp.	C	10.0	12.03	23.70
Ophiura robusta (Ayres, 1851)	C	3.0	2.86	6.42
O. sarsi Lutken, 1858	C	5.0	7.19	61.93
Ophiacantha bidentata (Retzius, 1805)	S	3.0	2.59	7.96
Ophiopholis aculeata (Linnaeus, 1767)	S	5.0	4.36	15.48
Amphipholis squamata (Delle Chiaje, 1828)	S	5.0	1.88	2.67

C is the ATP-seston concentration 1 m above the sediment–water interface, in $\mu g \cdot m^{-3}$, estimated from the summer temperature of bottom water at each station (unpublished) and the water temperature–ATP–seston relationship for Bay of Fundy estuaries given in Wildish and Kristmanson (1979),

C^* is the concentration of ATP-seston 1 cm above the sediment–water interface, in $\mu g \cdot m^{-3}$.

The assumption was made in all calculations of N_A that $C^* = 0.5C$, although C^* is unlikely to be a constant. To our knowledge, no measurements of C^* have yet been made although, if the food limitation hypothesis for suspension feeders of Wildish and Kristmanson (1979) is correct, this is a plausible value.

Sediment grain size and sorting characteristics were determined as described in Akagi and Wildish (1975) on a few of the samples (Peer et al. 1980) and sediment chlorophyll *a* determined following 90% acetone-extraction and measurement by fluorescence according to the method of Holm-Hansen et al. (1965).

Results

Benthic Species Distribution and Productivity

Density and wet formalin weights per square metre of the

TABLE 2. List of species used in the production estimates with numbers of stations occupied by species and wet biomass production for each taxon.

Taxa	No. of species	Stations occupied	Production, $g \cdot m^{-1} \cdot yr^{-1}$ Total	Production, $g \cdot m^{-1} \cdot yr^{-1}$ Mean
Porifera	1	3	164	54.7
Cnidaria	4	14	78	5.6
Rhynchocoela	3	23	25	1.1
Brachiopida	1	19	802	42.2
Mollusca, Aplacophora	1	10	4	0.4
Polyplacophora	2	9	17	1.9
Gastropoda	4	15	39	2.6
Scaphopoda	1	44	233	5.3
Bivalvia	16	137	17 180	125.4
Annelida, Polychaeta	69	620	1 116	1.8
Sipunculida	1	16	10	0.6
Arthropoda, Crustacea	38	243	802	3.3
Echinodermata, Holothuroidea	2	5	223	44.6
Echinoidea	3	10	153	15.3
Stelleroidea	6	58	307	5.3

TABLE 3. The top ten species for three trophic groups in the lower Bay of Fundy, arranged in decreasing order of total wet biomass production (P, $g \cdot m^{-2} \cdot yr^{-1}$) at the total number of stations (n) occupied by that species.

Active suspension feeders	n	P	Passive suspension feeders	n	P	Deposit feeders	n	P
Modiolus modiolus	30	14560	*Balanus crenatus*	8	616	*Dentalium entale*	44	233
Terebratulina septentrionalis	19	803	*Placopecten magellanicus*	3	609	*Sternaspis scutata*	22	159
Astarte subaequilatera	14	681	*Chlamys islandica*	2	329	*Nephthys incisa*	38	101
Astarte undata	18	547	*Isodictya diechmannae*	3	164	*Briaster fragilis*	3	80
Clyclocardia borealis	15	290	*Ophiopholis aculeata*	12	52	*Polyphysia crassa*	6	61
Cerastoderma pinnulatum	9	44	*Potamilla neglecta*	27	50	*Yoldia myalis*	10	58
Leptocheirus pinguis	21	28	*Stomphia coccinea*	7	37	*Echinarachnius parma*	5	57
Crenella glandula	6	15	*Cerianthus borealis*	3	36	*Melinna cristata*	37	48
Hiatella arctica	3	9	*Balanus balanus*	3	29	*Laetmonice filicornis*	7	41
Anomia squamula	7	6	*Ophiocantha bidentata*	9	23	*Ninoe nigripes*	10	28

245 taxa identified in this study are reported in Peer et al. (1980). From this list, 152 species were selected for production estimation based on whether they occurred at two or more stations (Table 1). Taxa occurring at only one of the 98 stations sampled were considered to be rare and presumed to make a small contribution to overall benthic production, and therefore excluded from further analysis.

The trophic type classification used inTable 1 is recognized to be tentative and probably more species are facultative than is indicated (see Mills 1967; Buhr and Winter 1977; Taghon et al. 1980). The largest group were deposit feeders (68 species), followed by suspension feeders (38 species), carnivores (29 species), and with algal scrapers (8 species) and omnivorous scavengers (7 species) being relatively poorly represented. The estimates summarized in Table 2 indicate that the number of polychaetes was greatest. Polychaetes, which are mostly deposit feeders, had the widest distribution in the Bay, with 620 individual records from 69 species (total possible is 69×98 stations $= 6762$). The next most widely distributed group was Crustacea, followed by bivalve molluscs. In considering contributions to production however, bivalve molluscs, which are mostly suspension feeders, were by far the greatest, followed by polychaetes, Crustacea, and the single species of brachiopod present.

The top 10 individual species' contribution to productivity of both active and passive suspension feeders and deposit feeders is shown in Table 3. This table includes most of the species with significantly large contributions to production, although the list of significant producers is longer than shown for deposit feeders. In addition, a few species with quite large contributions to production, such as the echinoderm *Ophiura sarsi* ($P = 180$, $n = 25$) and polychaetes *Eunice pennata* ($P = 90$, $n = 16$), *Lumbrineris fragilis* ($P = 49$, $n = 32$), *Eunice norvegica* ($P = 44$, $n = 3$), *Nephtys ciliata* ($P = 40$, $n = 20$), were omitted from Table 3 because they are classified trophically as carnivores. Quite possibly this classification is in error and these species are deposit feeders or at least facultative carnivores/deposit feeders. A few others with a relatively small contribution to production are ecologically "key" species. An example is *Haploops fundiensis* whose 1- to 2-cm tubes protrude from the sediment–water interface in great quantities and which must influence other benthos by their presence.

GEOGRAPHIC DISTRIBUTION OF THE TROPHIC GROUPS

The distribution of the two major trophic types, suspension feeders (S) and deposit feeders (D), was calculated as follows:

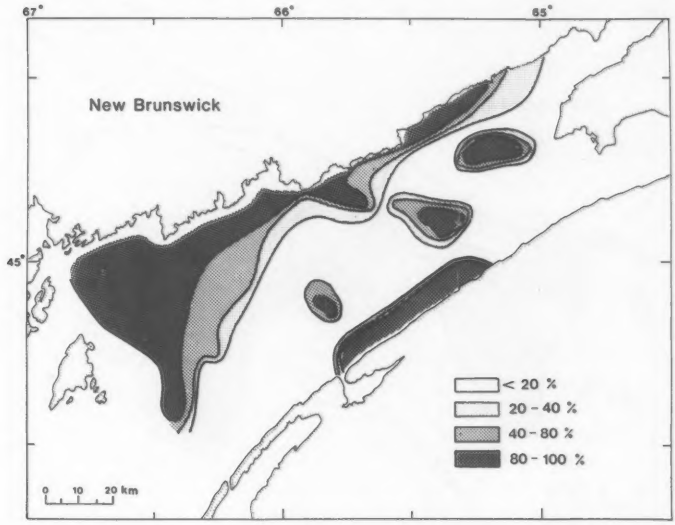

FIG. 2. Trophic ratio (*TR*) values for numbers of species present in the lower Bay of Fundy. $TR = D/D + S \times 100$ where D is the number of species of deposit feeders and S is the number of suspension feeders.

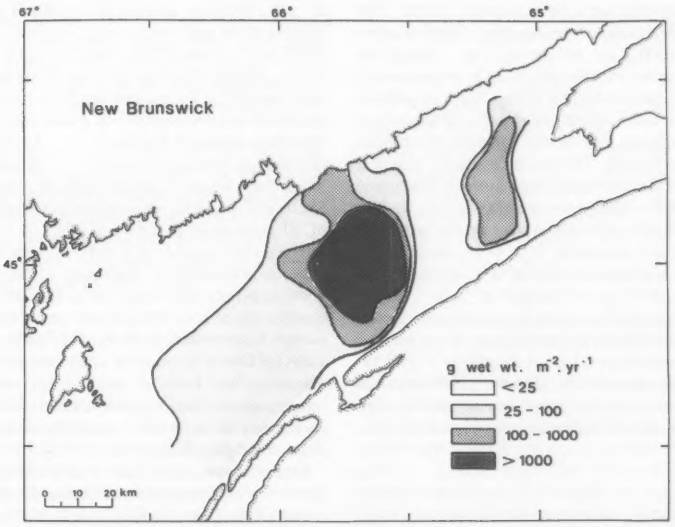

FIG. 3. Production by macrobenthic suspension feeders in the lower Bay of Fundy.

$$TR = \frac{D}{D + S} \times 100,$$

where *TR* is the trophic ratio and the units used are numbers of species in each trophic group. The results of plotting *TR* values (Fig. 2) show that high proportions of deposit feeders occurred in the southwestern mouth of the bay and in a narrow coastal strip extending along much of the New Brunswick shore. By contrast, a nearshore strip high in deposit feeders was absent on the Nova Scotia coast except downstream, according to the residual circulation pattern described by Godin (1968), from Digby Gut. There were also three isolated

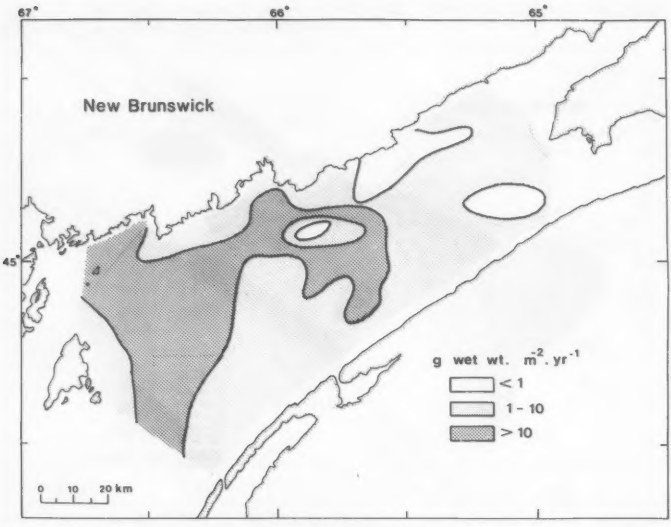

FIG. 4. Production by macrobenthic deposit feeders in the lower Bay of Fundy.

patches in the center of the bay where a high proportion of deposit feeders occurred.

Highest production rates were by suspension feeders concentrated in two central areas of the bay (Fig. 3). Production values in excess of 1000 g wet weight $\cdot m^{-2} \cdot yr^{-1}$, largely by the horse mussel, *Modiolus modiolus*, occur in an area northeast of a line joining Saint John and Digby. Stretching down the center of the bay to the southeast mouth was an area of lesser production, mainly due to the infaunal brachiopod *Terebratulina septentrionalis*. The second epicenter was near the limit of the lower Bay of Fundy, with average production values in the range 100−1000 g wet weight $\cdot m^{-2} \cdot yr^{-1}$. Production by deposit feeders throughout the bay was generally in the range 1−10 g wet weight $\cdot m^{-2} \cdot yr^{-1}$. However, in the southwestern mouth and center of the bay (Fig. 4) production reached an average of 32 g wet weight $\cdot m^{-2} \cdot yr^{-1}$. In the center of the bay, high deposit feeding production overlapped the area of high suspension-feeder production. There are also three areas of low production (<1 g wet weight $\cdot m^{-2} \cdot yr^{-1}$) as shown in Fig. 4. Because of the sizeable contribution of carnivores to production and the possibility of error in their trophic classification, we also included a plot of their distribution (Fig. 5).

DISTRIBUTION OF BENTHIC SPECIES IN RELATION TO SEDIMENTS

Following the last ice age, the whole of the Bay of Fundy floor was covered with glacial till laid down as a submarine deposit beneath the ice at depths greater than 37 m (Fader et al. 1977). Early postglacial tidal ranges were small, of the order of 2 m, because Georges and Browns Banks were then emergent, thus protecting the Bay from Atlantic tidal and wave dynamics. During this period and until 8000 yr BP, tidal current speeds were low and fine deposits were deposited on the till. Following submergence of the Banks, increased tidal amplification and hence tidal currents commenced about 6000 yr BP (Grant 1970). This resulted in a shift in sedimentation patterns. The main features of this are areas of erosion, most marked in the case of the Sambro sand litho-facies and an area of net deposition — LaHave clay (Fader et al. 1977). The chart produced by Fader et al. (1977) shows the modern distribution of these two surficial sediment units plus Scotian Shelf drift, which is geologically the older deposit. Scotian Shelf drift is glacial till consisting of poorly sorted sediments of all sizes from boulders to clays in various proportions. LaHave clay consists of a silty clay derived from reworked material originating in other parts of the Bay and from estuaries, generally overlying glacial till and which may be gas-charged due to accumulation and partial breakdown of organic matter. Sambro sand in the Bay of Fundy is contemporaneous with LaHave clay, and is characterized by extensive tidal reworking and fields of sand waves, small ripple-like features, isolated megaripples, and is still undergoing modification. This sediment is generally devoid of silt- and clay-sized sediments (Fader et al. 1977).

One obvious concordance with surficial sediment distribution is the high proportion of deposit feeders in the southwest mouth of the Bay (see Fig. 2) in the LaHave clay. The distribution of chlorophyll *a* in sediments (Fig. 6) was also highest here where most benthic species are deposit feeders. However, the three isolated patches of deposit feeders which were found in the center of the Bay (Fig. 2) do not correlate with sediment distribution patterns.

An examination of the production-dominant benthic species occurring in the bay for occurrence on particular surficial sediment types (Table 4) produced interesting results. Eight

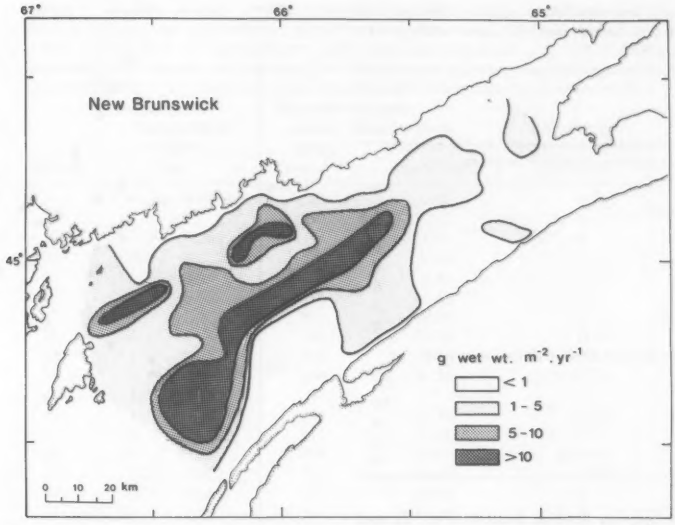

FIG. 5. Production by macrobenthic carnivores in the lower Bay of Fundy.

species present at four or more stations were absent from LaHave clay and, with the single exception of the deposit feeder *Echinarachnius parma*, all were suspension feeders. Of five species absent from Sambro sand, three were deposit feeders and the two *Haploops* spp. are possibly facultative for suspension/deposit feeding. By contrast, no dominant species present at four or more stations was absent from Scotian Shelf drift.

The dominant suspension feeder of Scotian Shelf drift was the brachiopod *Terebratulina septentrionalis*. Of 13 stations at which this species was present, nine were on Scotian Shelf drift, three on Sambro sand, and one on LaHave clay, although the latter four stations were all near Scotian Shelf drift. By contrast, horse mussel maximum production occurred both on Scotian Shelf drift and Sambro sand.

Distribution of Benthic Species in Relation to Tidal Currents

Maximum tidal current velocities in the bay were, in general, inversely related to depth (Fig. 7). Thus, at the shallower locations landward in the bay, current speeds were fastest and sediment reworking on Sambro sand most marked. Intermediate current velocities were found centrally in the bay on Scotian Shelf drift and the slowest currents over LaHave clay. For the latter sediment the relationship between V_{max} and depth is poorest.

The correlation between N_A (x) and suspension-feeder benthic production (y) at each station for which the benthic data are quantitative is a semilogarithmic linear one. The fitted line for this relationship is:

$$\text{Log}_{10} y = 0.121 + 0.134x$$

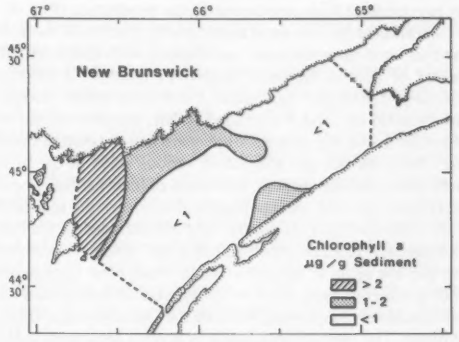

FIG. 6. Distribution of sediment chlorophyll *a* in units of µg/g sediment dry weight in the lower Bay of Fundy.

where: $n = 40$, $r = 0.82$, and there is significant correlation at $P > 99\%$.

If the data are partitioned by surficial sediment type, a similar significant regression is given for each, with the exception of LaHave clay. This relationship supports the food limitation hypothesis for suspension feeders of Wildish and Kristmanson (1979).

Nineteen of the 59 quantitative stations did not follow the fitted line. These stations have reduced (8 stations) or absent (11 stations) suspension-feeding macrofauna (Table 5). Two of the stations, 7 and 10, occur on LaHave clay where there was no correlation between N_A and suspension-feeder production. Included in Table 5 is the available information relating to an assessment of the erodibility of the sediment at each of these stations, viz. particle size and shear stress.

TABLE 4. Faithfulness of dominant benthic species to three surficial sediment types: LaHave clay, Scotian Shelf drift, and Sambro sand as defined by Fader et al. (1977)

Species	No. of stations occupied
Sambro sand–Scotian Shelf drift locations only	
Modiolus modiolus	19
Cerastoderma pinnulatum	12
Ophiopholis squamata	10
Balanus crenatus	8
Yoldia myalis	8
Crenella glandula	6
Anomia aculeata	5
Echinarachnius parma	4
LaHave clay–Scotian Shelf drift locations only	
Sternaspis scutata	20
Haploops fundiensis	16
Laetmonice filicornis	6
Haploops setosa	6
Polyphysia crassa	5

The three patches high in deposit feeders (Fig. 2) had relatively low biomasses and production values for both deposit and suspension feeders and were sandwiched between the two areas of high suspension-feeder production (Fig. 4). We interpreted the two most northeasterly patches of these as impoverished macroinfaunal associations with characteristic species of deposit feeders: *Spiophanes bombyx*, *Scoloplos armiger*, *Scolelepis squamatus*, *Echinarachnius parma*, *Cerebratulus* sp., and *Psammonyx nobilis* that live below, or otherwise avoid, the strong sediment erosion-deposition cycle here. Such species are adapted in various ways to the high shear stress and the unstable sediments of their habitat. Shear stress values and the median particle diameter of the sediment of the four stations (33, 40, 51, and 56) included in the two northeasterly patches confirmed that an unstable sediment was present in these locations which could limit suspension feeding macroinfauna. With the observational data to hand we were unable to unequivocally decide the causal physical factor involved. The most seaward patch of deposit feeders included only two stations (22 and 23) and its faunal composition of five to nine deposit-feeding species indicated a normal deposit feeding association, although lacking in suspension feeders.

Discussion

The field assessment of benthic macrofauna production, particularly in sublittoral waters, has been recognized to be difficult to accomplish satisfactorily, partly because there is no way to check the accuracy of the measure and partly because of likely systematic sampling errors and inadequacies in available field methods for assessment of secondary production.

Systematic sampling errors include: insufficient sampling depth or surface area with which to quantitatively estimate some species with the grab used (see Wildish 1983). This might result in either inaccurate biomass estimations or total absence of some dominant species. In a continuation of our work in the upper bay we have used a heavier 0.5 m^2 grab to help check this potential source of error at some stations. Another possibility is that some areas may have been recently cropped by groundfish and, consequently, yield low biomass value, resulting in a low production estimate.

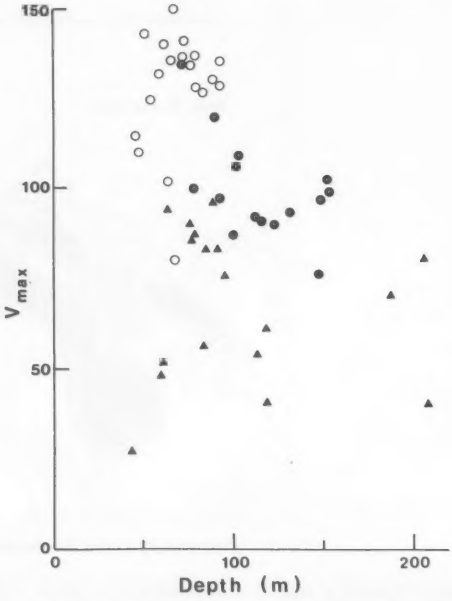

FIG. 7. Relationship of maximum tidal velocities (V_{max} in $cm \cdot s^{-1}$) to sampling depth in the lower Bay of Fundy. Open circles, Sambro sand; closed circles, Scotian Sheld drift; and triangles, LaHave clay quantitative sampling locations.

Detailed assessment of macrofauna production is not possible when geographic areas are involved. This is because of the time required to temporally analyze growth, recruitment, and mortality of even a few dominant species (Warwick 1980). Several authors (Zaika 1973; Parsons et al. 1977; Robertson 1979) have demonstrated a relationship between annual P:B and life span, and between P:B and body mass (Banse and Mosher 1980), which may be used in estimating geographical population production from knowledge of average and individual adult biomass and life span. The approach followed here of estimating production from biomass and life-span estimates for individual species (Table 1) is recognized to be a first, crude attempt which will require modification in the future. A critique of this approach was given by Warwick (1980).

Total production by macrobenthos in the lower bay, exclusive of Annapolis Basin and St. Mary's Bay, (Table 6) was 166.7×10^4 t from a total area of 8620 km^2, of which 580 km^2 is a 2-km wide coastal strip. Three trophic groups were included in this estimate (Table 6) plus the coastal strip which was not sampled during our study. The coastal strip consists of a mixed trophic group whose production was based on biomass values from a range of New Brunswick estuaries

TABLE 5. Stations lacking, or with reduced, suspension-feeding macrofaunal production. Only stations quantitatively sampled, that is classified as 1 or 2 in Peer et al. (1980), are included. Median sediment particle diameter from Swift et al. (1973) and maximum current speed from Greenberg (1979).

Station	Range of median particle diameter mm	Maximum current speed $cm \cdot s^{-1}$	Mean tidal stress dynes cm^2	Production suspension feeders $g \cdot m^{-2} \cdot yr^{-1}$
7	0.062−0.0156	80	9.89	0.39
8	4 −1	40	2.47	0
18	0.25 −0.062	94	13.65	0
70	0.062−0.0156	75	8.69	0.36
82	1 −0.25	56	4.85	0
85	0.25 −0.062	86	11.43	0
67	4 −1	109	18.36	0.33
68	4 −1	99	15.14	0.29
33	1 −0.25	135	28.16	0
39	4 −1	140	30.28	133.73
40	1 −0.25	?	?	0
41	1 −0.25	143	31.59	26.60
42	4 −1	110	18.69	70.26
48	1 −0.25	115	20.43	1529.42
49	0.25 −0.062	125	24.14	2.95
51	0.25 −0.062	132	26.92	0
53	1 −0.25	150	34.76	0
56	1 −0.25	138	29.42	0
59	32 −4	70	7.57	0

(Wildish 1983). The total, expressed as the average annual production throughout the lower bay, was 193.4 g $wet \cdot m^{-2} \cdot yr^{-1}$, approximately equivalent to 58 g $dry \cdot m^{-2} \cdot yr^{-1}$ or the same value in $kcal \cdot m^{-2} \cdot yr^{-1}$. Conversion from wet to dry weight was based on ~30% of wet weight, to units of energy (kcal) by multiplying wet weight by 1 and as grams carbon by dividing the energy density (kcal) by 10 as in Steele (1974). A comparable value for standing crop biomass is 339.62 g $wet \cdot m^{-2}$, yielding an overall average annual turnover ratio for the lower Bay of 0.57.

The faunal composition of the bay in relation to the three major surficial sediment types described by Fader et al. (1977) may be interpreted in terms of the trophic group mutual exclusion hypothesis (Wildish 1977; Wildish 1983). The hypothesis states that species composition and productivity are limited directly or indirectly by tidal current velocity. Mutual exclusivity arises because each of the trophic groups can tolerate a different range of tidal velocities. Thus, deposit feeders (Fig. 8) are favored at low current velocities in net depositional areas, and suspension feeders in higher current velocities where deposition and erosion are low or absent. Autecological studies of the deposit-feeding sea star *Ctenodiscus crispatus* in the Gulf of Maine (Shick et al. 1981) showed that is is only present in areas receiving an exceptionally high level of organic carbon sedimentation. The description of Scotian Shelf drift and Sambro sand by Fader et al. (1977) agrees well with the conditions outlined in Fig. 8B and C. Where tidal dynamics cause the sediment to undergo significant erosion-deposition cycles, suspension feeders are absent and only a few hardy deposit feeders may be found (Fig. 8C). Characteristic species present in such habitats include a few polychaetes that live deep in the sediment or are especially adapted for an erosional sediment such as the large and heavy sand dollar, *E. parma* and rapid burrowing amphipod, *P. nobilis*.

Other examples of macroinfaunal impoverishment caused either directly or indirectly by high tidal current energy and sediment scour are given by Wildish (1977), Wildish and Kristmanson (1979), and Warwick and Uncles (1980). Experimental evidence that feeding rates of suspension feeders are inhibited by high concentrations of inorganic sediment particles in suspension is available for some species (Loosanoff and Tommers 1948; Gerrodette and Flechsig 1979 and references therein). Other possibilities are that high current speeds directly inhibit feeding above a threshold speed (see Wildish and Kristmanson 1979), or that high concentrations of food particles themselves inhibit feeding (Winter 1973).

Areas of the bay which can be defined by geology-benthic distribution features are compatible with Mills' (1975) concept of two distinct kinds of benthic macrofauna communities: predominantly epifaunal suspension feeders and soft-tissue infauna. Mills suggested that the latter group, largely made up of deposit feeders, would contribute a much larger proportion of their total energy flow directly to groundfish production. Most species of suspension feeders are hard shelled and difficult for groundfish to eat. In fact, Tyler (1972) has already provided evidence that groundfish prefer to ingest deposit-feeding species. In Passamaquoddy Bay, 13 species of groundfish preyed primarily on between three and nine principal benthic species, most of which were soft-bodied deposit feeders. Only the ocean pout, 20−65 cm long, is specialized for feeding on hard-shelled suspension feeders such as *Arctica*, *Musculus*, and *Venericardia*. Presumably, much of the accumulated energy of suspension feeders is recycled at the sediment interface directly by the decomposer cycle. One

TABLE 6. Secondary benthic production in units of wet biomass for the lower Bay of Fundy. Estimate based on geographic distribution of production in Fig. 3–5 and area of 8620 km^2 within the limits given in the Methods section.

Trophic group	Location	Production unit g wet·m^{-2}·yr^{-1}	Observed mean production for unit t·km^{-2}·yr^{-1}	Area of production unit km^2	Annual production t × 10^4	Percentage of total production	Totals t × 10^4
Suspension feeders	Upper Bay	100–1000	898.19	364	32.69		
		25–100	46.46	240	1.12		
		>1000	1129.75	684	77.27		
	Middle Bay	100–1000	331.18	504	16.69		
		25–100	67.12	2524	16.94		
		<25	6.76	3724	2.52	88.3	147.23
Deposit feeders		>10	32.29	2388	7.71		
		1–10	5.40	5204	2.81	6.3	
		<1	0.57	448	0.03		10.55
Carnivores		>10	(24–50)	940	2.53		
		5–10	(7.37–7.87)	1160	0.86	2.6	
		1–5	(1.5–7.1)	2784	0.83		
		<1	0.25	3156	0.08		4.30
Mixed	Coastal strip	High	100[a]	344	3.44	2.8	
		Low	50[a]	236	1.18		4.62
						100.0	= 166.70

[a]Estimated.

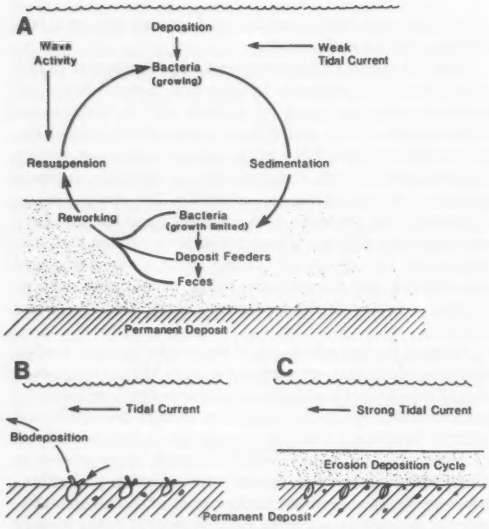

FIG. 8. Concepts of sublittoral macroinfauna in soft sediments — A) deposit feeding, B) primarily suspension feeding, C) impoverished.

other source of energy loss from suspension feeders is the annual spawning by adults which produces planktonic eggs and larvae utilized in the pelagic food web. Because of the large production by suspension feeders in the bay, this potential link between benthic and pelagic systems warrants further quantitative investigation.

Yield data for the Bay of Fundy fisheries are available as follows: for herring, which is the predominant pelagic fishery, an annual average wet biomass yield of 11.06 × 10^4 t for the period 1972–79 (Iles 1979); for over 13 species of groundfish, an annual average wet biomass yield of 2.12 × 10^4 t for the period 1968–78 (Kohler 1979). Major species in the groundfish catch are cod, haddock and pollock. By correcting these values to total yields as in Steele (1974) and dividing by the area of the lower Bay (8620 km^2) values of 25.7 for pelagic and 3.1 g wet·m^{-2}·yr^{-1} for groundfish yields were obtained. These values are larger for pelagic and similar to those for groundfish given by Steele (1974) for the fishable area of the North Sea. If only deposit feeders, carnivores, and the mixed coastal strip production of Table 6 are considered suitable as grounfish food, that is 11.7% of total lower bay production or 21.27 g wet·m^{-2}·yr^{-1}, then there is sufficient benthic production to supply groundfishery energy requirements at a transfer exchange between the two trophic levels of 14%. Mills and Fournier (1979) found that groundfish production on the Scotian Shelf amounted to 4.1 kcal·m^{-2}·yr^{-1}, giving a transfer exchange ratio of 13%, similar to that in the present study. The migratory nature of some groundfish (Hare 1977) indicates that not all groundfish feeding takes place in the lower bay. Other factors affecting the transfer exchange calculations and not accounted for by us include the presence of a hyperbenthos (Brunel 1979) which was not sampled by our grab, and the possibility of cannibalism among larger individual groundfish.

Acknowledgments

We thank A. Wilson and Captain and crew of RV *J. L. Hart* for assistance in field sampling, L. Linkletter, J. Hines and M. Dadswell

for their identifications of benthic animals, and B. Hargrave, D. J. Scarratt, and R. Garnett for constructive criticisms of the manuscript.

AKAGI, H., AND D. J. WILDISH. 1975. Determination of the sorting characteristics and organic carbon content of estuarine sediments. Fish. Res. Board Can. MS Rep. 1370: 15 p.

BANSE, K., AND S. MOSHER. 1980. Adult body mass and annual production/biomass relationships of field populations. Ecol. Monogr. 50: 355–379.

BIERNBAUM, C. K. 1979. Influence of sedimentary factors on the distribution of benthic amphipods of Fisher's Island, Connecticut. J. Exp. Mar. Biol. Ecol. 38: 201–223.

BOUSFIELD, E. L. 1973. Shallow-Water Gammaridean Amphipoda of New England. Cornell University Press, Ithaca, NY. 312 p.

BRUNEL, P. 1979. Seasonal changes of daily vertical migrations in a supra-benthic cold-layer shelf community over mud in the Gulf of St. Lawrence, p. 383–390. *In* E. Naylor and R. A. Hartnoll [ed.] Cyclic phenomena in marine plants and animals. Pergamon Press, Oxford.

BUHR, K.-J., AND J. E. WINTER. 1977. Distribution and maintenance of a *Laonice conchilega* association in the Weser estuary (FRG), with special reference to the suspension-feeding behaviour of *Laonice conchilega*, p. 101–113. *In* B. F. Keegan, P. Ó. Céidigh and P. J. S. Boaden [ed.] Biology of benthic organisms. Pergamon Press, Oxford.

FADER, G. B., L. H. KING, AND B. MACLEAN. 1977. Surficial geology of the eastern Gulf of Maine and Bay of Fundy. Mar. Sci. Pap. 19, Geol. Surv. Can. Pap. 76-17: 23 p. + chart.

FAUCHALD, K., AND P. A. JUMARS. 1979. The diet of worms: A study of polychaete feeding guilds. Oceanogr. Mar. Biol. Ann. Rev. 17: 193–284.

GERRODETTE, T., AND A. O. FLECHSIG. 1979. Sediment-induced reduction in the pumping rate of the tropical sponge *Verongia lacunosa*. Mar. Biol. 55: 103–110.

GODIN, G. 1968. The 1965 current survey of the Bay of Fundy; a new analysis of the data and an interpretation of the results. Dep. Energy, Mines, Resources Mar. Sci. Branch MS Rep. Ser. 8: 97 p.

GRANT, D. R. 1970. Recent coastal submergence of the Maritime Provinces, Canada. Can. J. Earth Sci. 7: 676.

GREENBERG, D. A. 1979. A numerical model investigation of tidal phenomena in the Bay of Fundy and Gulf of Maine. Geodesy 2, No. 2.

HARE, G. M. 1977. Atlas of the major Atlantic coast fish and invertebrate resources adjacent to the Canada–United States boundary areas. Fish. Mar. Serv. Res. Dev. Tech. Rep. 681: 97 p.

HOLM-HANSEN, O., O. J. LORENZEN, R. W. HOLMES, AND J. D. H. STRICKLAND. 1965. Fluorometric determination of chlorophyll. J. Con. Int. Explor. Mer. 30: 3–15.

HUNTER, B., AND A. E. SIMPSON. 1976. A benthic grab designed for easy operation and durability. J. Mar. Biol. Assoc. U.K. 56: 951–957.

ILES, T. D. 1979. The ecology of the herring fisheries of the Bay of Fundy., p. 27–52. *In* D. J. Scarratt [ed.] Evaluation of recent data relative to potential oil spills in the Passamaquoddy area. Fish. Mar. Serv. Tech. Rep. 901.

KOHLER, A. C. 1979. Annual groundfish landings and values data for Charlotte County and Bay of Fundy ports for 1968-78, p. 53–56. *In* D. J. Scarratt [ed.] Evaluation of recent data relative to potential oil spills in the Passamaquoddy area. Fish. Mar. Serv. Tech. Rep. 901.

LOOSANOFF, V. L., AND F. D. TOMMERS. 1948. Effects of suspended silt and other substances on the rate of feeding of oysters. Science 107: 69–70.

MILLS, E. L. 1967. The biology of an ampeliscid amphipod crustacean sibling pair. J. Fish. Res. Board Can. 24: 305.

1975. Benthic organisms and the structure of marine ecosystems. J. Fish. Res. Board Can. 32: 1657–1663.

MILLS, E. L., AND R. O. FOURNIER. 1979. Fish production and the marine ecosystems of the Scotian Shelf, eastern Canada. Mar. Biol. 54: 101–108.

MILLS, E. L., K. PITTMAN, AND B. MUNROE. 1981. Effect of preservation on the weight of marine benthic invertebrates. Can. J. Fish. Aquat. Sci. 39: 221–224.

PARSONS, T. R., M. TAKAHASHI, AND B. HARGRAVE. 1977. Biological oceanographic processes. 2nd ed. Pergamon Press, NY. p. 332.

PEER, D., D. J. WILDISH, A. J. WILSON, J. HINES, AND M. DADSWELL. 1980. Sublittoral macro-infauna of the lower Bay of Fundy. Can. Tech. Rep. Fish. Aquat. Sci. 981: 74 p.

ROBERTSON, A. I. 1979. The relationship between annual production:biomass ratios and lifespans for marine macrobenthos. Oecologia (Berl.) 38: 193–202.

SHICK, J. M., K. C. EDWARDS, AND J. H. DEARBORN. 1981. Physiological ecology of the deposit-feeding sea star *Ctenodiscus crispatus*: ciliated surfaces and animal-sediment interactions. Mar. Ecol. 5: 165–184.

STEELE, J. H. 1974. The Structure of Marine Ecosystems. Harvard University Press, Cambridge, MA. 128 p.

SWIFT, D. J. P., B. R. PELLETIER, A. K. LYALL, AND J. A. MILLER. 1973. Quaternary sedimentation in the Bay of Fundy. Geol. Surv. Can. Pap. 71-23: 113–151.

TAGHON, G. L., A. R. M. NOWELL, AND P. A. JUMARS. 1980. Induction of suspension feeding in spinoid polychaetes by high particulate fluxes. Science 210: 562–564.

TYLER, A. V. 1972. Food resource division among northern, marine demersal fishes. J. Fish. Res. Board Can. 29: 997–1003.

WARWICK, R. M. 1980. Population dynamics and secondary production of benthos. *In* K. R. Tenore and B. C. Coull [ed.] Marine benthic dynamics. Belle W. Baruch Library in Marine Science No. 11: 1–24.

WARWICK, R. M., AND R. J. UNCLES. 1980. Distribution of benthic macrofauna associations in the Bristol Channel in relation to tidal stress. Mar. Ecol. Prog. Ser. 3: 97–103.

WILDISH, D. J. 1977. Factors controlling marine and estuarine sublittoral macrofauna. Helgoländer Wiss. Meeresunters. 30: 445–454.

1983. Sublittoral sedimentary substrates, Chap. 9. *In* M. L. H. Thomas [ed.] Marine and coastal systems of the Quoddy Region, New Brunswick. Can. Spec. Publ. Fish. Aquat. Sci. 64.

WILDISH, D. J., AND D. D. KRISTMANSON. 1979. Tidal energy and sublittoral macrobenthic animals in estuaries. J. Fish. Res. Board Can. 36: 1197–1206.

WINTER, J. E. 1973. The filtration rate of *Mytilus edulis* and its dependence on algal concentration, measured by a continuous, automatic recording apparatus. Mar. Biol. 22: 317–329.

ZAIKA, V. E. 1973. Specific production of aquatic invertebrates. Translated from Russian by A. Mercado, p. 154. John Wiley & Sons, New York and Toronto.

Effect of Turbidity on the Temporal and Spatial Utilization of the Inner Bay of Fundy by American Shad (*Alosa sapidissima*) (Pisces: Clupeidae) and its Relationship to Local Fisheries[1]

M. J. DADSWELL

Department of Fisheries and Oceans, Fisheries and Environmental Sciences, Biological Station, St. Andrews, N.B. E0G 2X0

G. D. MELVIN

Department of Biology, University of New Brunswick, Fredericton, N.B.

AND P. J. WILLIAMS

Department of Biology, Acadia University, Wolfville, N.S.

DADSWELL, M. J., G. D. MELVIN, AND P. J. WILLIAMS. 1983. Effect of turbidity on the temporal and spatial utilization of the inner Bay of Fundy by American shad (*Alosa sapidissima*) (Pisces: Clupeidae) and its relationship to local fisheries. Can. J. Fish. Aquat. Sci. 40(Suppl. 1): 322–330.

Since 1750, a unique, directed fishery for American shad (*Alosa sapidissima*) has existed in shallow, turbid, mega-tidal embayments of the inner Bay of Fundy during summer and fall. Tagging experiments indicated that migrating shad consisting of intermixed, river populations from the entire Atlantic coast of North America occur there between June and October. Shad migration was counterclockwise around the Bay following the residual current structure. Presence and duration of the shad run in Cumberland Basin was a result of interaction between migration timing, turbidity, and temperature. Mean daytime swimming depth was related to tidal phase and turbidity. High turbidity (Secchi $\bar{X}$ = 0.30 m) of the mega-tidal embayments apparently extends the preference zone for light intensity of ocean-feeding shad into surface waters (2–10 m), making them accessible to the local fishery.

Key words: drift gillnets, shad migration, light intensity preference, swimming depth, mega-tidal, eastern Canada

DADSWELL, M. J., G. D. MELVIN, AND P. J. WILLIAMS. 1983. Effect of turbidity on the temporal and spatial utilization of the inner Bay of Fundy by American shad (*Alosa sapidissima*) (Pisces: Clupeidae) and its relationship to local fisheries. Can. J. Fish. Aquat. Sci. 40(Suppl. 1): 322–330.

Il se pratique depuis 1750 une pêche unique d'alose savoureuse (*Alosa sapidissima*) en été et en automne dans les baies peu profondes, turbides et à forte amplitude de marée à la tête de la baie de Fundy. Des expériences de marquage indiquent que les aloses migratrices comprennent des populations fluviatiles mixtes de toute la côte atlantique de l'Amérique du Nord, qui se trouvent dans cette région entre juin et octobre. La migration est liée à la structure du courant résiduaire et se fait dans le sens contraire des aiguilles d'une montre autour de la baie. La présence et la durée de la remonte de cette espèce dans le bassin de Cumberland dépendent de l'interaction entre le moment de la migration, la turbidité et la température. La profondeur moyenne à laquelle les poissons nagent le jour est liée à la phase de la marée et à la turbidité. Une turbidité élevée ($\bar{X}$ = 0,30 m au disque de Secchi) dans les baies à forte amplitude de marée étend, semble-t-il, la zone de préférence d'une intensité lumineuse particulière des aloses se nourrissant en mer en direction des eaux de surface (2–10 m), ce qui les rend accessibles à une pêche locale.

Received October 30, 1981
Accepted August 10, 1982

Reçu le 30 octobre 1981
Accepté le 10 août 1982

[1]This paper forms part of the Proceedings of the Dynamics of Turbid Coastal Environments Symposium convened at the Bedford Institute of Oceanography, Dartmouth, N.S., Canada, September 29–October 1, 1981.

Printed in Canada (J6704)
Imprimé au Canada (J6704)

THE American shad, *Alosa sapidissima* (Wilson, 1811), a large, anadromous clupeid, ranges from Florida to Labrador. Shad are highly migratory, moving north to south and back again annually, following an ocean isotherm envelope of 7–17°C (McDonald 1884; Leggett and Whitney 1972; Neves

and Depres 1979) and homing to their natal rivers for reproduction (Hollis 1948; Dodson and Leggett 1973). Ocean migration rate of reproductive adults during northward movement in spring averages 21 km/d (Leggett 1977) and occurs in shallow coastal waters. Ocean-feeding, nonreproductive shad, however, are mostly found offshore over depths of 50–200 m (Talbot and Sykes 1958; Neves and Depres 1979). Since the tagging studies of Talbot and Sykes (1958), the principal summer congregation of ocean-feeding shad was believed to be based in the Gulf of Maine and adjacent outer Bay of Fundy (Gabriel et al. 1976; Neves and Depres 1979). Older studies by Perley (1852), Prince (1912), and Leim (1924), however, report an extended run and large individual commercial catches of nonspawning, feeding shad in the shallow turbid waters of the inner Bay of Fundy.

The inner Bay of Fundy has tides among the largest in the world and is proposed as a site for future tidal power development (Gordon and Longhurst 1979). Tidal power development will affect the shad and its fishery to some degree in this region and may have widespread impact on shad populations along the entire Atlantic coast. For these reasons and since the presence of juvenile and nonreproductive adult shad in large numbers in oceanic waters seldom exceeding 30 m deep seemed to contradict other findings, this study was initiated to examine temporal and spatial occurrence of shad in the shallow, mega-tidal embayments and to determine which shad populations utilize the Bay of Fundy.

The Study Site

The study was conducted in Cumberland Basin, a 30 × 4 km embayment of Chignecto Bay, the inner northern arm of the Bay of Fundy (Fig. 1). Mean tidal range is 10.5 m with spring tides to 15 m (Anon. 1981). Tide flats are mud and range from 500 to 1000 m wide at low water. The extreme tides cause currents in excess of 3 m/s and in combination with the local sediment regime create very turbid conditions. Surface suspended sediment concentrations reach 1000 mg/L and average 100 mg/L (Munday et al. 1980). The suspended particulate matter is siliciclastic and has a unimodal distribution of size (volume) peaking in the 8- to 16-μm range (Munday et al. 1980). Water temperatures are uniform from surface to bottom and gradually decrease seaward 1–2°C during summer; salinities increase seaward with a range of 28–30 ‰ at high tide (M. J. Dadswell, unpublished data).

The Fishery

The shad fishery of the inner Bay of Fundy has existed since the earliest arrival of Europeans in the region. Perley (1852) identified the start of a weir fishery on the tide flats by 1750. Prince (1912), writing for the Dominion Shad Commission (1908–1910), described the abundance of shad in this region during the 1800s and the relative ease with which primitive and/or simple capture methods (stake seines, brush weirs) could capture 50 000–100 000 shad on a single tide. The shad fishery was so important to the economy of the inner Bay of Fundy that a Special Act of the Nova Scotia Legislature was passed in 1840 for its regulation, one of the first in Canada (Perley 1852). After 1840 driftnets became the major means of capturing shad and at the same time a large export trade in salt shad began with the eastern United States (Perley 1852). In the 1870s collection of fisheries statistics commenced and the course of the fishery could be followed.

Between 1870 and 1900, annual shad landings for the inner Bay of Fundy were $1.0–2.0 \times 10^5$ kg/yr (Fig. 2) and constituted two-thirds of total Canadian shad landings. After 1900, landings declined drastically as a result of markedly decreased shad abundance (Prince 1912) and have remained at low levels up to the present, although abundance now appears to be

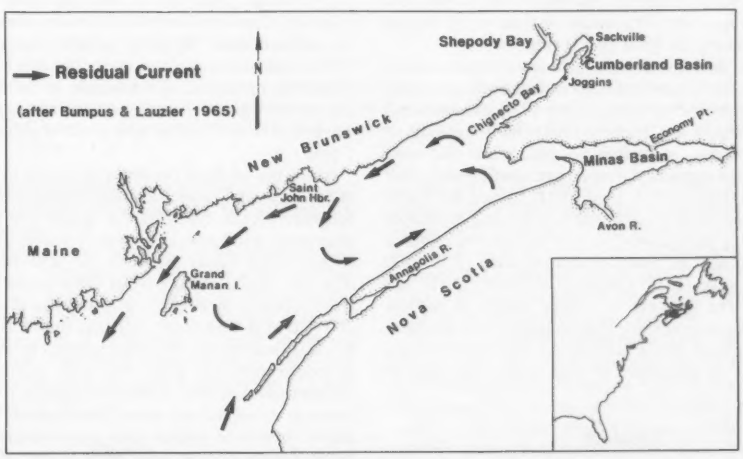

FIG. 1. The Bay of Fundy showing localities mentioned in the text. Residual current structure shown is after Bumpus and Lauzier (1965).

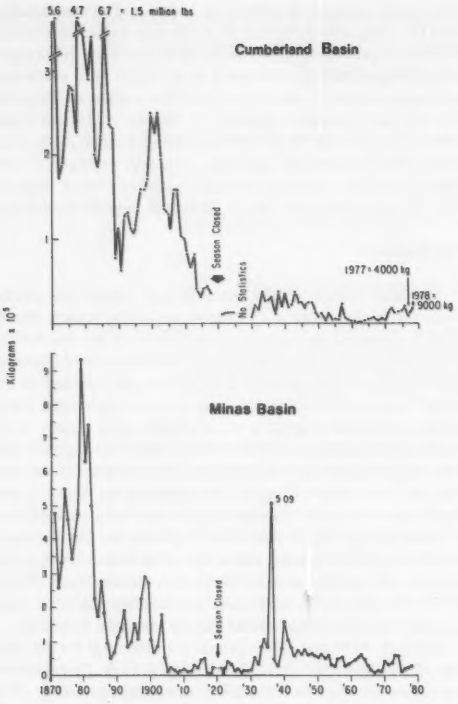

FIG. 2. Annual commercial landings of shad for Cumberland and Minas basins from 1870–1978.

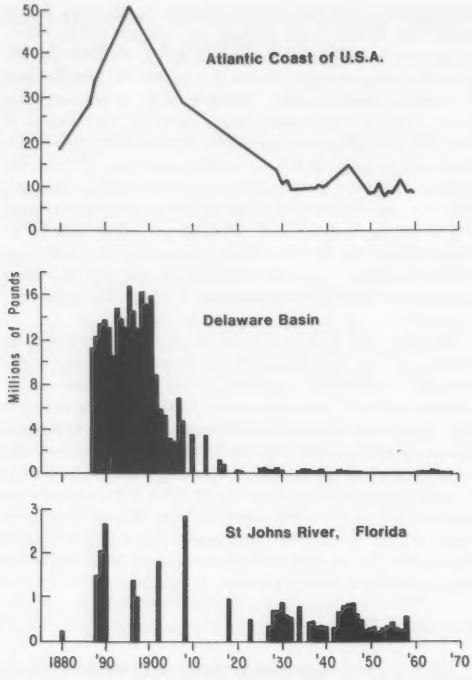

FIG. 3. Annual commercial landings for various river systems and the eastern United States as a whole during 1880–1970.

somewhat restored and landings reflect low effort (Fisheries and Oceans Canada, Fisheries Statistics). The course and decline of landings were very similar to those of the eastern United States during the same period (Fig. 3).

Unlike other shad fisheries, which are concentrated on spawning rivers or their estuaries and exploit adult, spawning shad during a short spring season (Leim 1924; Mansueti and Kolb 1953; Walburg and Nichols 1967), the inner Bay of Fundy fishery occurs in shallow, oceanic water and nonspawning shad are captured during an extended summer–fall season of 5 mo (Perley 1852; Leim 1924). Along the rest of the Atlantic coast, shad are available to fishermen in shallow water only during the spawning season and are not captured afterward unless nets are fished offshore in water of 50–200 m (Talbot and Sykes 1958; Gabriel et al. 1976; Neves and Depres 1979). The presence of a large fishery in shallow oceanic water for nonspawning shad suggests some combination of factors, absent during summer and fall in other coastal regions, creates an abundance of shad in the inner Bay of Fundy.

Methods

Drift gillnets, each 100 m long, in gangs of mixed mesh sizes, were used to capture shad. Mesh sizes were 2.5, 5.5, 8.0, 10.0, 11.2, 12.0, 12.7, and 13.7 cm stretched, of 210/6 multifilament, white nylon tied on the half. Nets were 6 and 12.5 m deep. Two 12.5-m deep nets were dyed different colors in 2.5-m depth intervals to obtain swimming depth data for captured shad. Net gangs usually consisted of five nets (500 m) but were sometimes one or two nets longer or shorter, depending on period of tidal cycle or weather conditions. During the turbidity–catch experiment (Aug. 3–7, 1980), two 6 × 100 m, 12.5-cm monofilament gillnets were used in a gang.

Nets were set from 7-m research vessels in the tidal stream in or near frontal zones (Bowman and Iverson 1978) at points delegated by tide type (neap or spring) and phase (rising or falling) but drifts generally began in mid-Basin and proceeded 10 km to the inland (Sackville) or seaward (Joggins) ends (Fig. 1). Inland or high-water drifts occurred largely over areas occupied by tide flats at low tide and had mean depths of 7–10 m at high water. Net soak time was usually 2 h but this was shortened to 1 h during summer temperature maxima to reduce mortality. Sets were made during all periods of daylight and darkness. A local commercial fisherman, whose methods we copied and whose catch records we were able to utilize, employed similar gear and methods except that he fished during daytime only, used 12 nets (1200 m) of 6-m depth, and usually set for 4 h or more before hauling.

Captured live shad were tagged with FTI dart tags, inserted

FIG. 4. Locality map for recaptures of shad tagged in Cumberland Basin from spawning (natal) rivers in eastern United States and Canada. Numbers in circles indicate total tags recaptured in river system out of 6128 tags applied. Arrows indicate general migration of shad along the east coast (after Leggett and Whitney 1972).

immediately under the posterior portion of the dorsal fin. Tags were numbered and had a return address to facilitate recovery of distant recaptures.

A mercury thermometer was used to determine surface water temperature. Turbidity was measured with a standard 30-cm Secchi disc. Temperature and Secchi disc visibilities (D_s) were measured immediately after setting the net and further D_s's were taken at timed intervals until the net was completely hauled. Subsurface light intensities were measured with a Photomatic underwater photometer with a spectral response peak at 580 μm.

Results

Field work was conducted between May 15 and October 30 for the 3-yr period 1979–81. We completed 276 drifts or approximately 550 h of fishing and captured 6580 shad, of which 4828 were tagged and released. An additional 1200 shad from nets of commercial fishermen were tagged and released in Cumberland Basin, and in May 1981 we tagged 3159 shad from the spawning run of the Annapolis River, a tributary to the Bay of Fundy (Fig. 1).

Of tags applied in Cumberland Basin, there were 264 returns to date from rivers or from outside the Bay of Fundy and 61 from Cumberland Basin and adjacent marine embayments. Tag returns from rivers and from outside the Bay of Fundy are: 16 (6%) from other Canadian marine locations, 55 (20.5%) from coastal United States, 20. (7.5%) from Canadian rivers, and 176 (66%) from United States rivers. Tag returns from spawning shad in rivers on the Atlantic seaboard

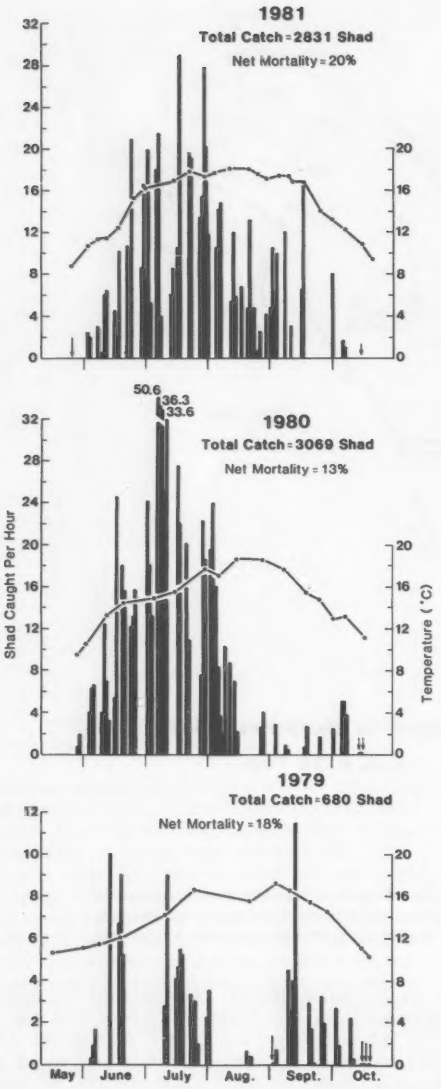

FIG. 5. Capture rate of shad during May to October from experimental gillnets in Cumberland Basin, 1979, 1980, and 1981. Arrows indicate fishing days when few or no shad were captured.

were from virtually every large, extant population from Florida to Quebec (Fig. 4) and indicate the mixed population structure of the shad utilizing Cumberland Basin.

Historical records, experimental fishing, and commercial catches indicate few shad arrived in Cumberland Basin before June 1 (Perley 1852) (Fig. 5, 6). Shad present during May were mostly returning to local rivers for spawning since up to 30% of the small catches at this time were ripe adults. Spawning runs in rivers tributary to the Bay of Fundy usually commenced the first week of May (G. D. Melvin and M. J. Dadswell, unpublished data) and spawning activity peaked during the last week of May (Leim 1924) or during June (Carscadden and Leggett 1975). Large catches of juvenile, resting, and spent adult shad began during the first week of June when the temperature rose above 10°C (Fig. 5). Peak catches and catch rates occurred yearly during the period June 15 to July 30 coincident with a rise in temperature from about 12 to 16°C (Fig. 6). Catch rate declined during August and a second, minor peak occurred in September as water temperatures declined. Shad were not caught after mid-October when water temperatures fell below 10°C (Fig. 5).

Same-year returns from within the Bay of Fundy indicated counterclockwise movement of shad from Cumberland Basin to Shepody Bay and then to the Gulf of Maine (Table 1). In no instance was a tagged shad from Cumberland Basin recaptured that had moved in the opposite direction. The counterclockwise movement around the Bay was also demonstrated by recaptured Annapolis River shad (Table 2). All recaptures occurred in chronological order from Minas Basin, around Chignecto Bay, and out to the Gulf of Maine via the northern Bay of Fundy shore. In addition, fishermen's catch reports indicate that the peak of the shad run occurred in Minas Basin during the last week of June, in Cumberland Basin during the first to second weeks of July, and in Shepody Bay during mid-July, but "fall-run" shad (Gabriel et al. 1976) were not encountered off Saint John Harbor until the last week of July and the peak of the run occurred off Grand Manan during the last 2 wk of September (Fisheries and Oceans, Statistics Branch; M. J. Dadswell, unpublished data).

Mean time of recapture within Cumberland Basin during the 3-yr study period ranged from 1.0 to 8.4 d at large in individual years with an overall mean of 5.1 d (Table 1). Shad recaptures in Shepody Bay usually occurred 2 wk after tagging in Cumberland Basin and some shad remained in Chignecto Bay for up to 2 mo. Mean minimum daily rate of movement was 6.0 ± 2.7 and 6.3 ± 1.5 km/d for Cumberland feeding and Annapolis postspawning shad, respectively (Tables 1, 2).

Stepwise-multiple regression analysis indicated that of environmental parameters measured, tide height, temperature, and turbidity (D_s; Fig. 6) significantly affected the commercial gillnet catch rate during the June 10–September 14 period of the main shad run.

Variable	df	Multiple r	F
Tide height	55	0.2342	7.912**
Temperature	54	0.3129	5.281**
D_s	53	0.4106	4.462**
Air pressure	52	0.4221	1.154
Wind speed	51	0.4370	0.786
Wind direction	50	0.4376	0.035

*Significant at $P > 0.01$.

Since tide height directly influences turbidity ($R = -0.73$, Fig. 7), it is probably the major factor controlling abundance

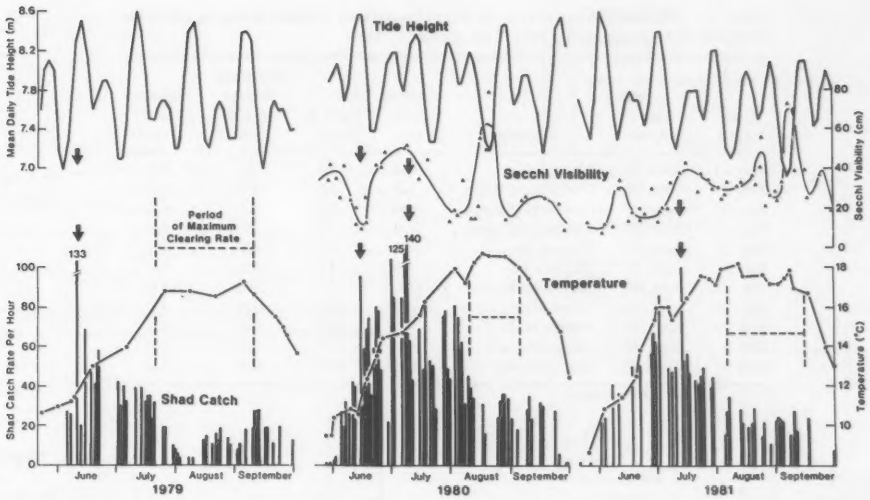

FIG. 6. Daily shad catch/hour of one commercial fisherman in relation to tide height, Secchi-visibility, and temperature during the commercial shad seasons of 1979, 1980, and 1981. Tide height is chart datum, Saint John, N.B. Actual tide height in Cumberland Basin varies between 10 and 15 m.

TABLE 1. Recaptures during the same year in the Bay of Fundy/Gulf of Maine of shad tagged in Cumberland Basin.

Place recaptured	Year tagged[a]			Mean days at large			3-yr mean	Minimum migration (km)	Migration rate (km/d)
	1979	1980	1981	1979	1980	1981			
Cumberland	6	10	16	1.0	6.0	8.4	5.1	60[b]	11.8
Shepody	1	11	6	12.0	15.6	14.2	13.9	120	8.6
Chignecto	5	5	—	78.0	39.6	—	58.8	260	3.4
Gulf of Maine	1	1	1	129.0	139.0	125.0	131.0	400	3.0

[a]Shad tagged/year: 1979, 512; 1980, 2416; 1981, 3200.
[b]Distance for shad to move into and out of Cumberland Basin once.

and/or catchability of shad in Cumberland Basin during the run. In general, but not excessively, maximum catch rates in daytime occurred during or just following spring tides when turbidity was at its maximum (Fig. 6, arrows).

During the week of August 3–7, 1980, an experiment was conducted in which sets were made along the axis of Cumberland Basin and Chignecto Bay according to local turbidity (Fig. 8). Catch/net was highest in Cumberland Basin where turbidity was greatest, and least in outer Chignecto Bay where turbidity was lowest. Catch rates of monofilament nets, which are invisible to fish (Leggett and Jones 1971), were the same as the multifilament nets, indicating swimming depth, not net avoidance, was more important in determining catch rate.

Catch rates for shad in Cumberland Basin declined each year during the summer temperature maxima and neap tide periods or, as defined here, the period of maximum clearing rate (PMCR) (Fig. 5, 6). In this period, reduced tidal energy and an increased sedimentation rate because of higher temperatures caused marked turbidity decrease during slack tide. Timed D_s measurements indicated the water cleared when tidal currents declined during slack tide from just before to 1.75 h after high water (Fig. 9). The lowest commercial catch rates of the study during the main period of the run (June 15–September 15) were recorded in August 1979 (Fig. 6) coincidentally with two 20-d neap-tide periods. These were the longest neap periods during the study and although D_s measurements were not taken, turbidity probably reached its lowest levels.

Photometer measurements of underwater irradiance showed subsurface light increased at slack tide during temperature maxima by 1–2 orders of magnitude at all depths (Fig. 10). The solar attenuation coefficient (K) for Cumberland Basin as determined from D_s, using the Poole-Atkins relationship, $K = 1.7/D_s$ (Weinberg 1976), varied from 2.12 to 17.0. The main difference at higher D_s was the increase in irradiance between 3 and 6 m where light levels increased by $10^1 - 10^2$ $\mu W/cm^2$. Catch rate decrease during PMCR was probably due to this increase in irradiance, causing shad to swim deeper and/or increase their gear avoidance (Leggett and Jones 1971).

TABLE 2. Recaptures during 1981 in the Bay of Fundy/Gulf of Maine of shad tagged in the Annapolis River during spring 1981. Tags applied — 3159.

Date tagged	Date recaptured	Locality	Capture depth (m)	Days at large	Minimum distance traveled (km)	Migration rate (km/d)
May 11	June 30	Minas Basin	<6	50	200	4.0
May 3	June 29	Cumberland Basin	<6	58	360	6.2
May 9	July 6	Cumberland Basin	<6	58	360	6.2
May 11	July 25	Cumberland Basin	<6	75	360	4.8
May 3	June 25	Shepody Bay	<6	54	420	7.7
May 8	June 25	Shepody Bay	<6	49	420	8.6
Apr. 30	July 10	Saint John Harbour	<10	71	560	8.0
Apr. 30	Sept. 14	Grand Manan	60	136	620	4.6
Apr. 28	Sept. 15	Yankee Bank	40	140	600	4.3
May 8	Sept. 17	Grand Manan	60	127	620	4.9
May 11	Sept. 16	Gulf of Maine	100	125	680	5.0

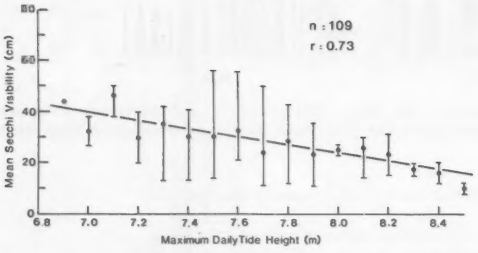

FIG. 7. Mean Secchi-visibility (D_s) for Cumberland Basin in relation to maximum daily tide height.

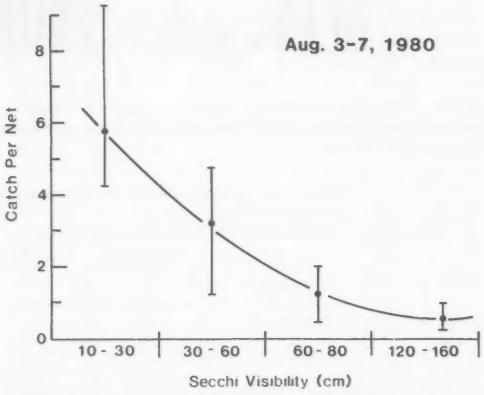

FIG. 8. Capture rate of shad in relation to mean prevailing turbidity during net soak period on a turbidity gradient along the axis of Cumberland Basin and Chignecto Bay.

Tidal phase also determined swimming depth of shad (Fig. 11). Mean swimming depths during rising and ebbing tide were 5.4 and 9.15 m, significantly different (t-test, $P < 0.01$), even though turbidity was similar during each phase (Fig. 9). Mean swimming depth of shad for all tidal phases as determined by depth of capture in 12.5-m nets was 7.22 m or in the irradiance range of 0.05 $\mu W/cm^2$.

Discussion

Long-term existence of a directed shad fishery and the occurrence of large numbers of shad from all east coast populations in the turbid waters of the inner Bay of Fundy during summer and fall indicates their presence there is a normal part of the annual life cycle and migration pattern of this species. Utilization of the area possibly began as these turbid habitats evolved about 6000 yr ago (Amos 1978). Our evidence suggests that, rather than a feeding population based in the Gulf of Maine–Scotian Shelf region with some penetrating the Bay of Fundy, the large mass of shad migrates around the Bay of Fundy which, because of increasing turbidity at its inner end, causes shad to occupy progressively shallower water. The abundance of shad observed in the Gulf of Maine during August and September by Talbot and Sykes (1958) was possibly the same group of yearly migrating fish just then moving out of the Bay of Fundy southward. It is interesting to note that the counterclockwise migration pattern follows the residual current pattern of the Bay of Fundy, suggesting shad employ some form of tidal stream transport to migrate similar to that known for other fishes (Weihs 1973).

Underwater light intensity plays an extremely important role in aquatic biology and most aquatic animals, whose photobiology is known, select a preferred light intensity (Jerlov 1968; Weinburg 1976). Light is known to be important to clupeids, including shad, particularly with respect to schooling behavior and vertical migration (Brawn 1960; Blaxter and Parrish 1965; Katz 1978; Loesch et al. 1982). Previously, the occurrence of shad in clear coastal waters over depths of 50–200 m was thought to be due to a temperature preference (Neves and Depres 1979); however, this depth range in water, with a solar attenuation coefficient of approximately 0.15 (Jerlov 1968), is where light intensity falls between 10^1 and 10^{-4} μWCm^2 during daylight. Mean swimming depth of shad in turbid Cumberland Basin is much shallower than in clear water but within the same light intensity range. Shad possibly

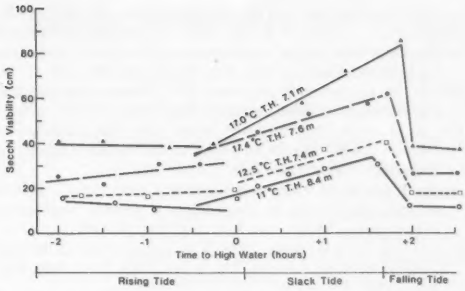

FIG. 9. Secchi-visibility in Cumberland Basin in relation to high-water slack at various tidal amptitudes and water temperatures.

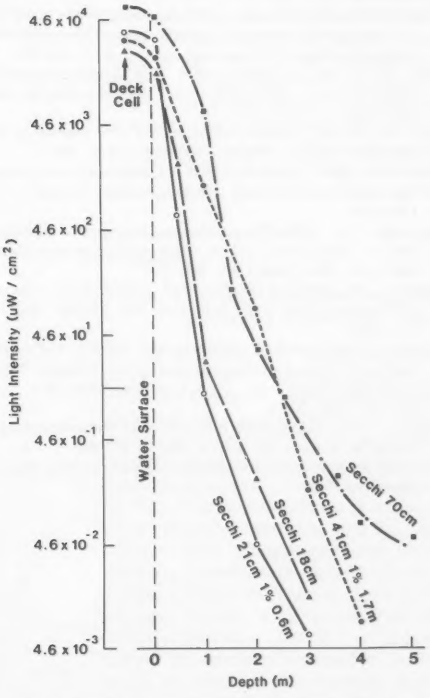

FIG. 10. Subsurface light intensities in Cumberland Basin at various levels of turbidity as determined by photometer.

select greater depths during daylight in clear coastal water because of this preferred light intensity range. Turbidity, by restricting light penetration, may play an important role in the utilization of the shallow, inner Bay of Fundy by shad.

Recent studies indicate these turbid waters are highly productive for zooplankton (G. R. Daborn et al., unpublished data). A filter-feeding planktivore such as shad could prey on this food source while sight-oriented planktivores would be less able. Our studies indicate virtually no other large, pelagic fish utilize Cumberland Basin (M. J. Dadswell, unpublished data), suggesting that turbidity may provide shad with a competitive advantage in such habitats.

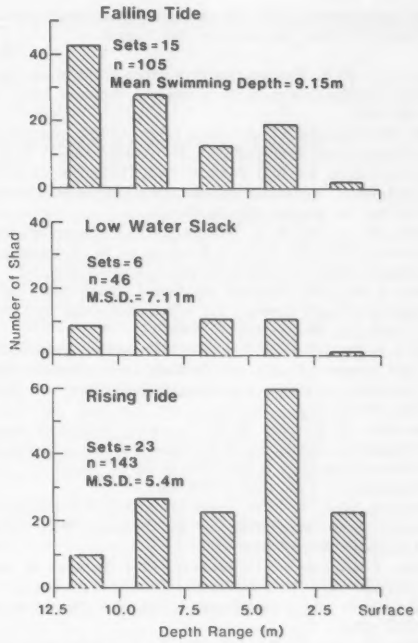

FIG. 11. Mean swimming depth of shad captured in a 12.5-m driftnet during various tidal phases.

Man's exploitation of shad in the inner Bay of Fundy region has occurred because the fish are available to many means of capture and catch rates are high due to turbidity. The impact of distant habitat alterations on the abundance of a fish, and therefore the viability of its fishery are clearly demonstrated in this case. Damming and pollution of natal rivers have been cited as the major causes in the decline of shad abundance on the east coast of North America (Stevenson 1898; Chittenden 1974), and these distant factors are implicated for the past decline of the shad fishery in the inner Bay of Fundy.

Acknowledgments

We express our appreciation to our friend and drift-fishing teacher, Marven Snowden, for his guidance, help, and tolerance and Paula Van Eeckhaute for her combined role of field assistant and housemother, as well as developing most of the methods for operating driftnets from small boats in big waves. We thank Jim Martin, Leslie Linkletter, Carl Jarvis, Gillian Motyer, Mike Kellock, and Jay Parsons for their field and laboratory assistance, and an uncountable number of volunteers who kept us on the water on many days on which fishing was otherwise impossible. D. J. Scarratt encouraged the study and kept administrative burdens at a tolerable level. Frank Cunningham prepared the figures. Brenda McCullough and Jeanine

Hurley typed the manuscript. The manuscript was reviewed by D. J. Scarratt and R. Elner, and edited by Ruth Garnett.

AMOS, C. L. 1978. The post-glacial evolution of the Minas Basin, N.S.: a sedimentological interpretation. J. Sediment. Petrol. 48: 965–982.

ANON. 1981. Canadian tide and current tables. Atlantic coast and Bay of Fundy. Dep. Fish. Oceans, Can. Hydrogr. Serv. 1: 53 p.

BLAXTER, J. H. S., AND B. B. PARRISH. 1965. The importance of light in shoaling, avoidance of nets and vertical migration of herring. J. Cons. Int. Explor. Mer 30: 40–57.

BOWMAN, M. J., AND R. L. IVERSON. 1978. Estuarine and plume fronts, p. 87–104. *In* M. J. Bowman and W. E. Esaias [ed.] Oceanic fronts in coastal processes. Springer-Verlag, NY.

BRAWN, V. M. 1960. Seasonal and diurnal vertical migrations of herring (*Clupea harengus* L.) in Passamaquoddy Bay, N.B. J. Fish. Res. Board Can. 17: 699–711.

BUMPUS, D. F., AND L. M. LAUZIER. 1965. Surface circulation on the Continental Shelf of eastern North America between Newfoundland and Florida. Ser. Atlas. Mar. Environ. Am. Geogr. Soc. Folio 7: 4 p.

CARSCADDEN, J. E., AND W. C. LEGGETT. 1975. Life history variations in populations of American shad, *Alosa sapidissima* (Wilson), spawning in tributaries of the St. John River, New Brunswick. J. Fish. Biol. 7: 595–609.

CHITTENDEN, M. E., JR. 1974. Trends in the abundance of American shad, *Alosa sapidissima*, in the Delaware River basin. Chesapeake Sci. 15: 96–103.

DODSON, J. J., AND W. C. LEGGETT. 1974. Behavior of adult American shad (*Alosa sapidissima*) homing to the Connecticut River from Long Island Sound. J. Fish. Res. Board Can. 30: 1847–1860.

GABRIEL, W. L., C. W. LEGGETT, J. E. CARSCADDEN, AND B. D. GLEBE. 1976. Origin and characteristics of "fall-run" American shad (*Alosa sapidissima*) from the Saint John River, New Brunswick. J. Fish. Res. Board Can. 33: 1764–1770.

GORDON, D. C., AND A. R. LONGHURST. 1979. The environmental aspects of a tidal power project in the upper reaches of the Bay of Fundy. Mar. Pollut. Bull. 10: 38–45.

HOLLIS, E. H. 1948. The homing tendency of shad. Science 108: 332–333.

JERLOV, N. G. 1968. Optical oceanography. Elsevier, NY. 194 p.

KATZ, H. M. 1978. Circadian rhythms in juvenile shad, *Alosa sapidissima*. J. Fish. Biol. 12: 609–614.

LEGGETT, W. C. 1977. Ocean migration rates of American shad (*Alosa sapidissima*). J. Fish. Res. Board Can. 34: 1422–1426.

LEGGETT, W. C., AND R. A. JONES. 1971. Net avoidance behavior in American shad (*Alosa sapidissima*) as observed by ultrasonic tracking techniques. J. Fish. Res. Board Can. 28: 1167–1171.

LEGGETT, W. C., AND R. R. WHITNEY. 1972. Water temperature and the migrations of American shad. Fish. Bull. 70: 659–670.

LEIM, A. H. 1924. The life history of the shad (*Alosa sapidissima* (Wilson)) with special reference to the factors limiting its abundance. Contr. Can. Biol. 2: 163–284.

LOESCH, J. G., W. H. KRIETE, JR., AND E. J. FOELL. 1982. Effects of light intensity on the catchability of juvenile anadromous *Alosa* species. Trans. Am. Fish. Soc. 111: 41–44.

MANSUETI, R., AND H. KOLB. 1953. A historical review of the shad fisheries of North America. Md. Board Natur. Res., Dep. Res. Educ. Pub. 97: 293 p.

MCDONALD, M. 1884. The shad-*Clupea sapidissima*, p. 594–607. *In* The fisheries and fishery industries of the United States. G. B. Goode and Associates. U.S. 47th Congr. 1st. Sess. Senate Misc. Doc. 124

MUNDAY, J. C., T. T. AFOLDI, AND C. L. AMOS. 1980. Application of a system for automated multidate Landsat measurement of suspended sediment. Water Qual. Bull. 5: 6–11 and 24.

NEVES, R. J., AND L. DEPRES. 1979. The oceanic migration of American shad, *Alosa sapidissima*, along the Atlantic coast. Fish. Bull. 77: 199–212.

PERLEY, M. H. 1852. Reports on the sea and river fisheries of New Brunswick. Queen's Printer, Fredericton, N.B. 294 p.

PRINCE, E. E. 1912. The shad fishery of Canada and its restoration. Sea fisheries of eastern Canada. Comm. Conserv. Can. 120–136.

STEVENSON, C. H. 1898. The restricted inland range of shad due to artificial obstructions and its effect on natural reproduction. Bull. U.S. Fish. Comm. 17: 265–271.

TALBOT, G. B., AND J. E. SYKES. 1958. Atlantic coast migrations of American shad. Fish. Bull. U.S. Fish. Wildlf. Serv. 58: 473–490.

WALBURG, C. H., AND P. R. NICHOLS. 1967. Biology and management of the American shad and status of the fisheries, Atlantic coast of the United States, 1960. U.S. Fish. Wildl. Serv., Spec. Sci. Rep. 550: 105 p.

WEIHS, D. 1973. Tidal stream transport as an efficient method for migration. J. Cons. Int. Explor Mer 38: 92–99.

WEINBERG, S. 1976. Submarine daylight and ecology. Mar. Biol. 37: 291–304.

Sediment Mobility in the Severn Estuary and its Influence upon the Distribution of Shorebirds[1]

PETER N. FERNS

Department of Zoology, University College, Cathays Park, Cardiff, CF1 1XL, U.K.

FERNS, P. N. 1983. Sediment mobility in the Severn Estuary and its influence upon the distribution of shorebirds. Can. J. Fish. Aquat. Sci. 40(Suppl. 1): 331–340.

In December 1979, superficial muddy sediments were eroded from considerable areas of the intertidal zone of the southern shores of the Severn Estuary during a period of prolonged westerly gales. Shorebird numbers at the affected sites showed an immediate decline as a result of the depletion of their mud-dwelling invertebrate food resources, and there was a corresponding increase in the numbers of birds along the northern shores of the estuary where no such erosion had occurred. Detailed monthly counts of 14 species of shorebirds in the Severn Estuary during 1971/72 to 1975/76 were therefore examined to determine if any of the previously unexplained anomalies in their distribution coincided with weather conditions likely to have given rise to similar losses of intertidal sediment. Although the 5 yr in question were relatively calm compared with the 1960s, there were five individual months during which the mean hourly windspeeds exceeded 13 $m \cdot s^{-1}$ on more than 25 occasions. During these periods, the average deviations in the numbers of Shelduck, Grey Plover, Dunlin, Curlew, and Redshank from those predicted by a log-linear model taking seasonal, annual, and regional trends into account, were particularly large. Furthermore, the sites which were involved in each case were those that were directly exposed to the prevailing winds during the windiest periods of the month in question. High winds, by propagating waves that mobilize fine sediments in the intertidal zone, are thus implicated as a significant factor influencing the distribution of some shorebirds.

Key words: Severn Estuary, sediment mobility, shorebird distribution, wading birds, local migration

FERNS, P. N. 1983. Sediment mobility in the Severn Estuary and its influence upon the distribution of shorebirds. Can. J. Fish. Aquat. Sci. 40(Suppl. 1): 331–340.

En décembre 1979, pendant une période prolongée de tempêtes de vent d'ouest, il y eut érosion des sédiments vaseux superficiels sur une grande étendue de la zone intertidale des rives méridionales de l'estuaire de la Severn. Le nombre d'oiseaux de rivage diminua immédiatement aux endroits affectés, par suite de l'épuisement des invertébrés limicoles qui leur servent de nourriture. Il y eut augmentation correspondante des oiseaux le long des rives septentrionales de l'estuaire, exemptes d'érosion. Nous avons alors examiné les comptages mensuels détaillés de 14 espèces d'oiseaux de rivage de l'estuaire de la Severn entre 1971/72 et 1975/76 afin de déterminer si des anomalies, demeurées inexpliquées, dans la répartition de ces oiseaux coïncidaient avec des conditions météorologiques susceptibles de causer de telles pertes du sédiment intertidale. Bien que les cinq années étudiées aient été relativement calmes comparativement aux années 1960, on a relevé cinq mois particuliers pendant lesquels la vitesse horaire moyenne du vent a dépassé 13 $m \cdot s^{-1}$ en plus de 25 occasions. Pendant ces périodes, les déviations moyennes du nombre de harles, pluviers gris, bécasseaux cincles, courlis et chevaliers gambettes par rapport au nombre prédit par un modèle log-linéaire tenant compte des tendances saisonnières, annuelles et régionales, ont été particulièrement importantes. De plus, les sites impliqués dans chaque cas étaient ceux directement exposés aux vents dominants pendant les périodes les plus venteuses du mois en question. Les grands vents, en propageant des vagues qui déplacent le fin sédiment de la zone intertidale, influent donc sur la distribution de certains oiseaux de rivage.

Received October 30, 1981
Accepted August 13, 1982

Reçu le 30 octobre 1981
Accepté le 13 août 1982

[1]This paper forms part of the Proceedings of the Dynamics of Turbid Coastal Environments Symposium convened at the Bedford Institute of Oceanography, Dartmouth, N.S., Canada, September 29–October 1, 1981.

Printed in Canada (J6705)
Imprimé au Canada (J6705)

THE Severn Estuary carries the highest suspended sediment load of any estuary in the British Isles. The amount of this sediment varies during the course of the tidal cycle and reaches a peak during the maximum flood and ebb flows of spring tides. The concentration of suspended solids in the

region upstream of the islands of Steep Holm and Flat Holm frequently reaches 10 000 $mg \cdot L^{-1}$ throughout the water column, and there is a denser layer of fluid mud (about 50 000 $mg \cdot L^{-1}$ of suspended solids), 3 m or more in thickness, at the sea bed (Kirby and Parker 1980). During slack water of spring tides, and during neap tides, these sediments are temporarily deposited as dense suspensions of liquid mud in the deeper channels of the estuary. During spring tides there is about 1×10^7 Mg of mobile fine sediment carried in suspension (Kirby and Parker 1980). Not surprisingly, this large capacity for the mobilisation and redeposition of sediment exerts an important influence on the distribution and abundance of living organisms in both the subtidal and intertidal zones (e.g. Warwick and Davies 1977; Mettam 1978).

The Severn Estuary supports internationally important concentrations of shorebirds (Ferns 1980a), and the majority of these feed on mud-dwelling invertebrate animals which inhabit the intertidal zone. The most extensive feeding areas of these birds are situated on the soft, sticky muds which occur mainly at the top of the shore where current velocities are reduced (Fig. 1). As a result of their instability, the extensive sandbanks in the centre of the estuary have a relatively impoverished invertebrate fauna and consequently support rather few waders and wildfowl. New layers of fine sediment are continually being added to and removed from the top of the shore during spring tides, but the amounts are usually so small that they are of little importance to invertebrates or the birds which feed on them. Occasionally, larger amounts of sediment are temporarily removed, and a more significant disruption to invertebrates and their avian predators is then possible. Most of the mud in the Severn Estuary forms a layer between 10 cm and 2 m thick, often overlying a stiff blue clay. If all of the superficial fine sediment is eroded then almost the whole of the invertebrate fauna disappears along with it. Just such an incident happened late in 1979 and this had important consequences for shorebirds which are described below. This incident provided the first indication that sediment erosion could influence shorebird distribution within the estuary. Earlier analyses of the distribution and abundance of these birds at different sites (Ferns 1980b, 1982) showed several unexplained features, with some species exhibiting either temporary declines in abundance or shifts in distribution. These counts were therefore reexamined to see if any of these features were associated with weather conditions similar to those which gave rise to the sediment erosion of 1979.

Methods

The unusual weather leading up to the sediment erosion of 1979 was first noted when surveys of the low tide feeding areas exploited by shorebirds (for the Department of Energy's Severn Barrage Prefeasibility Study) were hampered by strong westerly winds in early December. When field work commenced in the Severn Bridge–Portishead section (see Fig. 1) on December 13, it was immediately apparent that large areas of muddy sediment had been completely swept away from the foreshore. Only about 1000 shorebirds were present, whereas the site normally supports about 5000 at this time of year. Subsequent visits to sites further down the English shores of the estuary (Sand Bay, Berrow Flats, and Stert Flats) during either December or January, as part of the same survey, revealed a similar picture. Studies of the feeding behavior of Dunlin were also being made throughout this period by D. H. Worrall on the Welsh shore and by N. A. Clark on the southern shore. Invertebrate sampling was being carried out at several sites by J. I. Anderson. Information from all these sources has been used to establish the extent of sediment losses at each site (Fig. 1). Weather conditions during the above period were taken from the records of the meteorological station at Rhoose Airport.

The velocity of tidal streams is normally the most important factor determining the suspended sediment burden in the water column and these velocities are lower in most of the peripheral intertidal zone. Wave action, on the other hand, has its greatest effect in this zone. Breaking waves exert a direct scouring action on shore sediments and, because water velocities are locally increased, they enable more sediment to be carried back down the shore on the ebbing tide without being redeposited. Larger waves clearly exert a greater influence in this respect. The wave climate within the Severn Estuary has recently been investigated by means of moored waveriders stationed in the channel transmitting information on wave heights and frequencies to a shore-based receiving station (Hydraulics Research Station 1980b). Two of the three waveriders employed had parted from their moorings during December 1979, but the third, moored about 2 km NW of Steep Holm remained functional. No wave data are available for the period prior to 1978, and the direction and frequency of strong winds has therefore had to be used as an indicator of probable wave action (Hydraulics Research Station 1980a). These windspeeds were taken directly from the records at Rhoose Airport, from Hydraulics Research Station data or from the British Meteorological Office's Daily Weather Reports.

The primary source for all the shorebird counts in the Severn Estuary is the Birds of Estuaries Enquiry, jointly sponsored by the British Trust for Ornithology, the Royal Society for the Protection of Birds and the Wildfowl Trust. During the main years of this Enquiry (1969/70–1975/76) counts were conducted at monthly intervals, mostly by amateur observers, throughout Britain. Only the summer months (June and July) were excluded, because relatively few birds were present at this time. In the Severn, as in most other British estuaries, coverage was not as comprehensive during the first 2 yr and thus the results for 1969/70 and 1970/71 have been excluded. After 1975/76 the counts were also incomplete. During the years of good coverage (1971/72–1975/76) an average of 25 sites was counted at high spring tides, but these sites have been combined into the ten distinct regions shown in Fig. 1. The monthly counts within each year have been similarly lumped to give averages for each of four seasons — fall (August, September, October), early winter (November, December), late winter (January, February), and spring (March, April, May). Counts for the 13 most abundant species of wading birds in the area were examined — Oystercatcher (*Haematopus ostralegus*), Ringed Plover (*Charadrius hiaticula*), Golden Plover (*Pluvialis apricaria*), Grey Plover (*Pluvialis squatarola*), Lapwing (*Vanellus vanellus*), Knot (*Calidris canutus*), Dunlin (*Calidris alpina*), Common Snipe (*Gallinago gallinago*), Black-tailed Godwit (*Limosa limosa*),

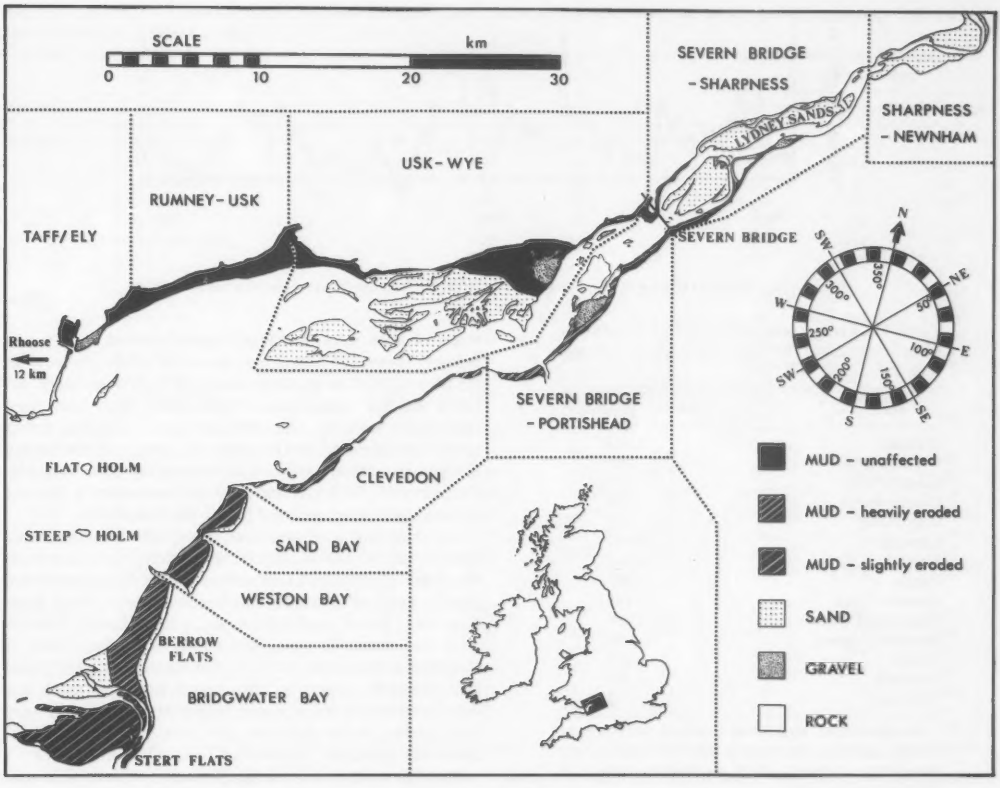

FIG. 1. Intertidal sediments of the Severn Estuary, showing the areas affected by erosion in 1979.

Bar-tailed Godwit (*Limosa lapponica*), Curlew (*Numenius arquata*), Redshank (*Tringa totanus*), and Turnstone (*Arenaria interpres*); together with the most abundant intertidally feeding duck, the Shelduck (*Tadorna tadorna*).

To identify significant deviations from the normal yearly, seasonal and site specific trends in abundance (Ferns 1980b, 1982) in the 1971/72–1975/76 counts, such as those which might be caused by sediment erosion, it was necessary to employ a model which was capable of taking all such factors into account. This was achieved by fitting a hierarchical log-linear model to the three-way frequency table represented by the raw counts, with 0.5 added to each count to avoid zeros. The three "ways" or factors in the table were years, sites, and seasons. Program P3F (revised 1979) of the BMDP package developed at the Health Sciences Computing Facility, UCLA was employed. In this program, the logarithms of the expected cell frequencies are computed as an additive linear function of the main effects and interactions.

It is the deviations from the expected trends which are of interest in the present context and two types of deviations are available with Program P3F — standardized residuals and Freeman–Tukey residuals (Bishop et al. 1975). The latter were found to approach normality more closely and were therefore used. The counts for each of the 14 species were analyzed separately and the Freeman–Tukey residuals were sigma-scaled to normal standard form to aid interpretation and to facilitate comparisons between species. The resultant deviations were subjected to a cluster analysis (P1M) using the absolute value of the correlation and single linkage. The largest deviations were finally examined in relation to the meteorological data.

Results

The sites affected by sediment erosion in December 1979 were all in the southern half of the estuary (Fig. 1). The most severely affected site was Clevedon where the whole of the lower part of the shore was reduced to a hard clay platform with only a little residual mud in gulleys and depressions (N. A. Clark, personal communication). The northern part of the Severn Bridge to Portishead section, and the lower shore at Berrow were also affected. Sand Bay, Weston Bay, and Stert Flats were less seriously eroded with complete losses of muddy sediment being confined to localised patches. No

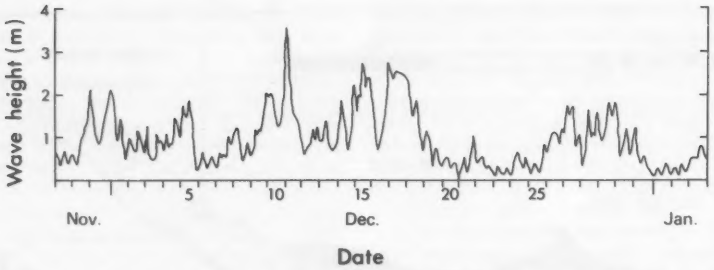

FIG. 2. Significant wave heights near Steep Holm in 1979/80 (from Hydraulics Research Station 1980b).

TABLE 1. Average wintering shorebird populations of the Severn Estuary between November and February from 1971/72 to 1975/76*.

Species	Average population
Shelduck	1 693
Oystercatcher	287
Ringed Plover	330
Golden Plover	778
Grey Plover	412
Lapwing	8 955
Knot	4 261
Dunlin	43 582
Common Snipe	148
Black-tailed Godwit	50
Bar-tailed Godwit	36
Curlew	1 853
Redshank	1 858
Turnstone	211

*Because these figures are averages over several months during several years, they are much lower than the peak counts which are used as criteria of International Importance.

noticeable losses occurred along the Welsh shores of the estuary (Worrall 1981), or in the area above the Severn Bridge, though information from the latter area was limited to the vicinity of Lydney Sands.

There were three periods in December 1979 when the significant wave height (the mean height in metres of the highest third waves) near Steep Holm exceeded 2.5 m (Fig. 2). These were on December 11, 15, and 16/17. During the period when this waverider was in position (April 1979–March 1980), there was only one other occasion (March 7, 1980) when the significant wave height exceeded 2.5 m. The maximum hourly windspeeds recorded at Rhoose Airport during the storms which gave rise to these exceptional wave heights were 19, 14, and 15 $m \cdot s^{-1}$, respectively (36, 27, and 30 knots); and the duration of each storm was 48, 18, and 20 h. On all three occasions the windspeed at Rhoose Airport, taken at hourly intervals and averaged over a period of about 10 min, exceeded 13 $m \cdot s^{-1}$ (25 knots) throughout most of the day.

Clearly, wave action in the intertidal zone must have been particularly intense in December 1979. The peak wave heights on all of the above dates were reached at or near low water of neap tides, but high waves occurred over a sufficiently prolonged period that the whole of the shore, with the exception of the portions above the high water mark and below the low water mark of neap tides, must have been subjected to scouring. The strongest winds and highest waves (over 3 m) occurred on December 11, and since the Severn Bridge–Portishead section of the estuary had been eroded by December 13, we know that most of the erosion, at this site at least, must have occurred during the first storm.

The dominant wind directions during the three December storms were W, WNW, and W, respectively. It is clear from Fig. 1 that all the sites which suffered losses of sediment were directly exposed to winds, and therefore waves, from these directions. For an enclosed estuary, winds blowing towards these sites from the west have a moderately long fetch. It should be emphasized, however, that the wave heights generated within the estuary by quite severe winds are much less than those which are produced by winds blowing over very long fetches in the open sea, and they also decrease progressively upchannel (Hydraulics Research Station 1980b).

Average winter counts of the 14 species of shorebirds considered in this paper are shown in Table 1. Following the losses of sediment in 1979, there was a considerable reduction in the number of shorebirds in the southern half of the estuary (Table 2). No comprehensive counts were made in the Rumney–Usk section, above the Severn Bridge or in Weston Bay. No unusual features were apparent in the counts of Oystercatchers, Ringed Plovers, Golden Plovers, Knots, Common Snipes, Godwits, or Turnstones. Except for the Knot, which is largely restricted to the northern shores of the estuary, and the Godwits which are uncommon in the middle of winter, these species do not feed predominantly on muddy shores. Oystercatchers and Turnstones feed mainly on rocky and sandy areas, Golden Plovers and Lapwings on inland fields, and Common Snipes on saltmarshes. Ringed Plovers feed partly on mud and partly on gravel, but because they are well adapted to feeding on prey at the surface, they may have been able to exploit residual areas of sediment in runnels and gulleys better than the other species.

Counts for the Birds of Estuaries were mostly conducted on December 2 in 1979 (the official count date), before the losses of sediment occurred, and so the December counts were not in any way abnormal. The Taff/Ely was an exception in that it was counted after December 11. At all sites except the latter, changes in numbers were not therefore reflected in the

TABLE 2. Summary of available Birds of Estuaries Enquiry counts during the 1979/80 winter for those species of shorebirds which were clearly affected by sediment erosion.

Species	Site	Nov.	Dec.	Jan.	Feb.	Jan./Feb. average		
						1980	1972–76	% difference
Shelduck	Taff/Ely	28	40	210	320	265	217	+22
	Usk–Wye	1	0	54	203	129	131	−2
	Severn Bridge–Portishead	30	25	30	20	25	64	−61
	Clevedon	0	40	85	55	70	113	−38
	Sand Bay	30	140	70	55	63	68	−7
	Bridgwater Bay	1 250	320	92	93	93	794	−88
	Total					645	1 387	−54
Dunlin	Taff/Ely	5 000	6 000	8 000	7 000	7 500	4 159	+80
	Usk–Wye	6 240	14 000	18 700	23 100	20 900	10 376	+101
	Severn Bridge–Portishead	495	1 000	750	850	800	5 367	−85
	Clevedon	2 500	1 800	2 000	1 200	1 600	2 952	−46
	Sand Bay	1 100	400	200	100	150	1 610	−91
	Bridgwater Bay	12 000	12 000	6 000	4 000	5 000	11 986	−58
	Total					35 950	36 450	−1
Curlew	Taff/Ely	112	100	80	110	95	106	−10
	Usk–Wye	191	208	266	471	369	266	+39
	Severn Bridge–Portishead	100	75	100	70	85	81	+5
	Clevedon	20	24	20	60	40	81	−51
	Sand Bay	111	130	125	85	105	62	+69
	Bridgwater Bay	1 100	400	400	383	392	907	−57
	Total					1 086	1 503	−28
Redshank	Taff/Ely	500	1 200	1 000	500	750	500	+50
	Usk–Wye	306	230	465	360	413	257	+61
	Severn Bridge–Portishead	280	430	350	81	216	344	−37
	Clevedon	80	45	50	60	55	94	−41
	Sand Bay	80	35	45	13	34	42	−19
	Bridgwater Bay	600	720	500	604	552	355	+55
	Total					2 020	1 592	+27

counts until January. The reductions in numbers at sites in the south of the estuary in January and February reflect quite closely the amount of sediment lost at each. Thus Clevedon and the Severn Bridge–Portishead section showed an average reduction compared with previous years of about 45%, Bridgwater Bay about 37%, and Sand Bay about 12%. It is also apparent that many of the displaced birds simply moved across to sites in the north, since there was an average increase in these four species of about 50% in the Usk–Wye section and 36% in the Taff/Ely.

The January/February 1980 totals for each species at the six sites in Table 2 are interesting since they suggest that all of the 14 000 or so Dunlins displaced from the south were accommodated at the two sites in the north. On the other hand there was a net increase in the number of Redshanks compared with 1972–76; in particular the numbers in Bridgwater Bay were above average (the other three species declined at this site). Feeding surveys at the latter site in January and February showed that over 80% of these birds fed on Stert Flats which lost far less sediment than Berrow Flats. It is quite likely that the number of Redshanks in the estuary as a whole was above average in 1979/80 (though the counts are too incomplete to test this), and it is also apparent that feeding conditions for this species were not adversely affected on Stert Flats. Curlew numbers showed a net decline at the six sites in Table 2, but there is good evidence that at least some birds moved into the upper estuary. During the feeding surveys already referred to, 300 Curlews were present on Lydney Sands in the first week of December (before the first storm), while 550 were present in the following February. The Severn Bridge–Sharpness section is an important one for Curlew but nevertheless the average population for the whole section (of which Lydney Sand is only a part) in 1971/72–1975/76 was only 440 in November/December and 456 in January/February. No other species showed above (or below) average numbers on Lydney Sands early in 1980. Shelduck numbers overall showed a net decrease of quite considerable proportions. This may be because birds moved into parts of the estuary which were not counted, but the decrease is so large that the possibility cannot be ruled out that some Shelduck left the Severn altogether.

Counts of Grey Plovers (not shown in Table 2) are curious since they were above average in both the Usk–Wye section and Bridgwater Bay (where they were feeding on Stert Flats). These are the only two sites in the estuary which support large numbers of this species. The peak count in the Usk–Wye section was 1830 in January 1980, compared with a winter average of 412 for the whole of the estuary (Table 1). This suggests that there was an unusually large movement of Grey Plovers into the estuary in the first part of 1980.

The fact that numbers declined shortly after December 11

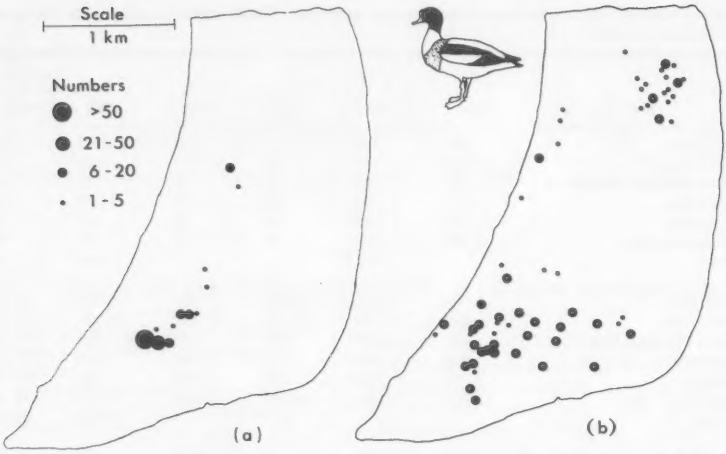

FIG. 3. Distribution of feeding Shelducks in Sand Bay on (a) December 28–30, 1979, and (b) February 17–20, 1980. Both sets of observations were based on approximately the same number of visits and the same flocks were plotted on more than one occasion (from Ferns 1980c).

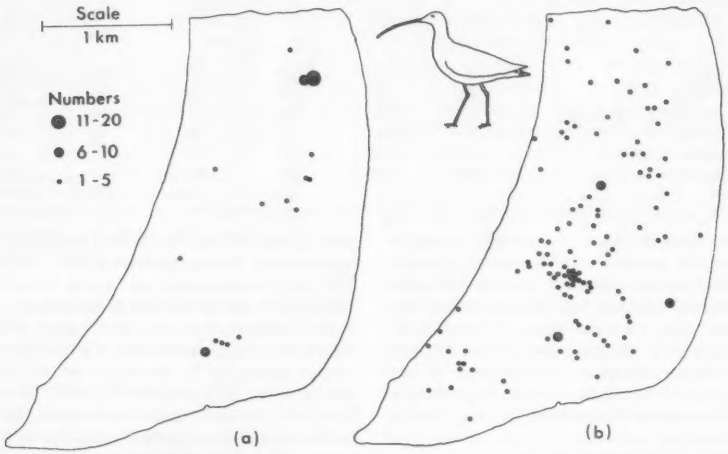

FIG. 4. Distribution of feeding Curlews in Sand Bay on (a) December 28–30, 1979, and (b) February 17–20, 1980. Other details as in Fig. 3.

in the Severn Bridge–Portishead section and increased (especially Redshank) in the Taff/Ely, suggests that birds deserted the affected sites very quickly. There was also a marked change in the feeding dispersion of those birds which remained at the affected sites. Immediately after the sediment losses had occurred, birds concentrated into the remaining suitable feeding areas. Thus at Sand Bay, Shelducks in the middle of December all fed in a few localized dense flocks (Fig. 3a). Curlews (Fig. 4a) behaved similarly, though the flocks were slightly smaller and more spaced out. By the end of February the surviving populations of invertebrates (which were quite large at this site) had readjusted and consequently the birds fed in more typical fashion in well-dispersed flocks (Fig. 3b and 4b).

Throughout January and February, fine sediments were gradually redeposited in the eroded areas. These consisted of liquid muds at first, but they gradually settled and consolidated. The speed with which these areas of fresh sediment became recolonised by invertebrates varied considerably. In places where the losses had been extensive, such as Berrow Flats, recolonization was slow. For example, significant numbers of *Nephthys hombergi* did not appear in the sediment

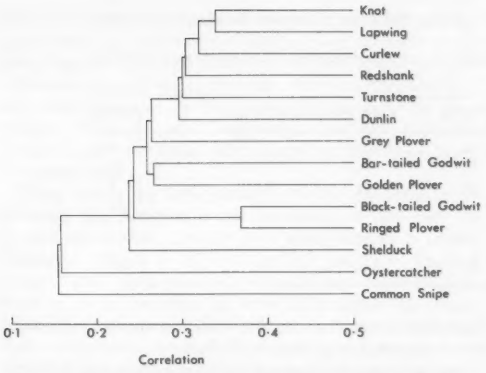

FIG. 5. Dendrogram of the Freeman–Tukey residuals of the log-linear model fitted to the counts for each species.

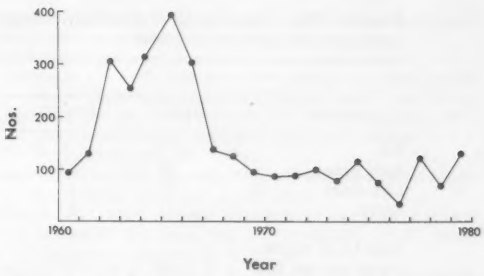

FIG. 6. Annual number of mean hourly windspeeds in excess of 13 $m \cdot s^{-1}$ at Rhoose Airport.

until May 1980 (Anderson 1982). In the less badly affected areas, such as Sand Bay, good numbers of invertebrates were present in February (Lovell and Mettam 1980).

A previously observed more localized incident shows that invertebrates are capable of undertaking movement into areas of fresh sediment. On March 31, 1977 about a hectare of mud near the mouth of the River Rumney was completely swept away. In this area mud forms a layer 5–35 cm thick overlying clay. All that was present in the eroded area was a few dead *Macoma balthica* shells embedded in the clay. When the same area was visited on April 18, 1977 about 3 cm of mud had been redeposited and it contained good numbers of a wide size range of both *Nereis diversicolor* and *Hydrobia ulvae*. This recolonization happened so quickly that it must have occurred by localized migration. *Nereis diversicolor* can swim actively, and *Hydrobia ulvae* is known to be capable of floating at the water surface to aid dispersal (Newell 1962; Little and Nix 1976). Presumably the less badly eroded areas in 1980 became recolonized by processes of this sort, whereas there were no large reservoirs of potential colonizers (in uneroded patches or subtidally) at the badly affected sites, and so these did not become recolonized until spat settlement occurred during the next breeding season.

The detailed monthly counts for 1971/72–1975/76 which were analyzed to identify atypical patterns of shorebird abundance are given in Ferns (1980b). Tests of marginal and partial association (Brown 1976) for each set of factors (year, site, season, and their interactions) in the log-linear model showed that they all exerted a significant influence on the numbers of all 14 species of shorebirds. In fact, taking all these sources of variation into account, numbers still differed significantly from expectation. This unexplained variation could be due to many factors, including changes in the abundance or availability of food, differences in the amount of disturbance, and variations in the efficiency of locating and counting roosts due to changing weather conditions or observers. The 2 yr of lowest numbers (1971/72 and 1974/75) were also years when the numbers of these species in Britain as a whole were lowest. 1974/75 followed an unusually poor breeding season in the arctic (Prater 1977).

TABLE 3. Average Freeman–Tukey residuals (scaled to the standard normal distribution) for Shelduck, Dunlin, Curlew, Redshank and Grey Plover, in three regions of the Severn Estuary.

Region	Season	Year				
		1971/72	1972/73	1973/74	1974/75	1975/76
North shore	Fall	−0.75	1.59	0.69	−0.95	−0.13
	Early winter	0.99	0.09	−1.11	1.88[a]	0.76
	Late winter	−0.26	−0.68	0.29	−0.21	−1.78[a]
	Spring	−0.10	0.35	0.78	−1.68[a]	0.42
Upper estuary	Fall	−0.70	−0.76	0.17	0.98	0.23
	Early winter	−1.90[a]	−0.50	1.47	0.30	0.59
	Late winter	0.96	1.00	−1.74[a]	0.08	−0.57
	Spring	1.69[a]	0.25	−0.55	−1.35	0.33
South shore	Fall	0.01	0.60	0.70	−1.00	−0.25
	Early winter	−1.35	−1.12	−0.47	−1.26	−0.25
	Late winter	0.36	1.11	−0.53	0.18	2.08[b]
	Spring	0.15	−0.60	1.11	1.74[a]	−1.22

[a] 1.65–1.96 (see text).
[b] > 1.96.

TABLE 4. Peak monthly number of mean hourly windspeeds in excess of 13 $m \cdot s^{-1}$ at Rhoose Airport. Based on data in Hydraulics Research Station (1980b).

Season	Year					
	1971/72	1972/73	1973/74	1974/75	1975/76	1979/80
Fall	9	1	4	23	8	9
Early winter	26	17	14	56	2	63
Late winter	12	12	30	11	61	8
Spring	37	12	0	0	0	21
Total for all months except June and July	142	59	67	116	74	137

Four species known to have been affected by sediment erosion in 1979/80 (Curlew, Redshank, Dunlin, and Grey Plover) were closely grouped in the cluster analysis of the correlations of the deviations from expected numbers (Fig. 5). Shelduck, the other affected species, was separated from these by a group of four passage migrants (Bar-tailed Godwit, Golden Plover, Black-tailed Godwit, and Ringed Plover). Because of their scarcity in winter, the latter species are not suitable for detecting changes in numbers resulting from sediment erosion. Average scaled Freeman–Tukey residuals were therefore calculated for the five species known to have been affected in 1979/80 (Curlew, Redshank, Dunlin, Grey Plover, and Shelduck). These figures were then further averaged for three major regions within the estuary — the north shore (Taff/Ely, Rumney–Usk, and Usk–Wye), the upper estuary (Severn Bridge–Sharpness, Sharpness–Newnham) and the south shore (Severn Bridge–Portishead, Clevedon, Sand Bay, Weston Bay, and Bridgwater Bay).

Since the results (Table 3) have been scaled to standard normal form, deviations greater than 1.96 should occur on average in 5% of cases, and deviations greater than 1.65 in 10%. These percentages have no particular biological significance in this context — they merely serve to indicate when the numbers of these five species of shorebird differed most markedly from the average trends predicted by the log-linear model. In early winter 1971/72 numbers were low in the upper estuary and along the south shore, but they were high along the north shore. There were no large deviations in 1972/73. In spring 1974/75 numbers were low along the north shore and in the upper estuary, but high along the south shore. There was a similar trend in late winter 1975/76. Overall, there were no significant correlations between the residuals in any one section of the estuary and those in any other (northshore with upper estuary, $r = -0.12$, $P > 0.10$; north shore with south shore, $r = -0.47$, $P = 0.05-0.10$; upper estuary with south shore, $r = -0.08$, $P > 0.10$; $df = 19$ in all cases).

The number of mean hourly windspeeds each year in excess of 13 $m \cdot s^{-1}$ (25 knots) at Rhoose Airport (Fig. 6) show evidence of a significant long term, perhaps cyclic, trend (Hydraulics Research Station 1980a). The mid-1960s represent a period of more frequent high winds than the 1970s. The storms of December 1979 occurred in a year which did not exhibit an unduly high frequency of strong winds. Therefore, although the shorebird counts analysed above were made in a comparatively quiet period, the wind frequencies clearly need to be examined in greater detail (Table 4).

The peak monthly frequency of 63 in early winter 1979/80 occurred, not surprisingly, in December 1979. The next greatest number occurred in late winter 1975/76. This was precisely a period when larger than expected numbers of birds were present along the south shore of the estuary and less than expected along the north. The month in question was January 1976. There were periods of particularly high winds from both the SW and SE during this month. All three sites in the north had negative Freeman–Tukey residuals in late winter 1975/76, but the largest occurred in the Usk–Wye section which was most exposed to winds from these directions.

Other periods when frequent high winds appear to have been associated with large Freeman–Tukey residuals were as follows — November 1971 (winds W to WSW, shorebird numbers down in upper estuary and along the south shore, especially Sand Bay and Bridgwater Bay), March 1972 (winds NE, SE, and W, numbers up in the upper estuary), January 1974 (winds SW, numbers down in the upper estuary) and December 1974 (winds W and WNW, numbers up along the north shore, especially the Rumney–Usk section, and down along the south shore, especially Bridgwater Bay). In all these cases, mean hourly windspeeds exceeded 13 $m \cdot s^{-1}$ on more than 25 occasions. The year with the lowest frequency of high winds (1972/73) also had the smallest Freeman–Tukey residuals.

Although it would be unwise to rely solely on general correlations of this sort, they do at least provide circumstantial evidence that periods of high winds are associated with deviations from the normal trends of distribution and abundance of these five species of shorebirds in the Severn estuary. Fortunately the events of 1979/80 demonstrate the existence of a causal link between high winds and bird numbers, namely, sediment erosion. However, deviations from the predicted patterns of abundance are clearly associated with other, as yet unknown, factors. For example, in spring 1974/75, numbers were lower than expected along the north shore and in the upper estuary, and higher than expected in the south. Yet this was a period when no mean hourly windspeeds at Rhoose Airport exceeded 13 $m \cdot s^{-1}$.

Discussion

High winds can exert a direct influence on the feeding behavior of shorebirds. For example, wind chill may increase

their rate of energy expenditure (Dugan et al. 1981). Strong winds may also cause them to feed in more sheltered areas, either because they find it difficult to walk across the substratum in exposed areas, or because the wind interferes with the visual clues which they normally use to locate prey (Dugan 1981). However, such effects are short-lived and cannot explain the longer term changes in distribution being considered here.

Wave action has been shown to be an important factor affecting the distribution and abundance of the prey of Sanderlings *Calidris alba* on open beach habitats in central California (Myers et al. 1979, 1981) and N.E. England (Evans 1981). Such beaches are directly exposed to breakers from the open sea when the wind is in certain directions. Although wave action is much less intense in the comparative shelter afforded by most estuaries, there is evidence that some inter-estuarine movements may be caused by losses of invertebrate food resources as a result of sediment changes (Evans 1981). High winds in the Severn Estuary are clearly capable of generating waves of sufficient magnitude to mobilize fine sediments and hence influence the distribution of shorebirds.

Although there have been very few similar studies of annual and seasonal changes in shorebird numbers within large estuaries, the available evidence suggests that movements of the sort that apparently occur in the Severn Estuary are not all that common. For example, the extensive ringing program carried out in the Wash, on the eastern coast of England, by the Wash Wader Ringing Group for more than 10 yr, shows only a negligible number of movements of Dunlins, Redshanks, and Grey Plovers between four major regions of this estuary (Minton 1975). Dunlins seldom moved more than 2 km from the site at which they were ringed. Studies of the movement of colour marked Dunlins in the Firth of Forth also show a relatively small number of long distance movements (Pienkowski and Clark 1979). Knots, on the other hand, are much more mobile both within and between estuaries (Minton 1975; Pienkowski and Clark 1979; Dugan 1981).

Two main factors contribute to the lack of stability of soft sediments in the intertidal zone of the Severn Estuary. Firstly, many of the mudbanks are relatively shallow. Secondly, the large tidal range and associated high water flows ensure that any sediments which are mobilised by wave action are likely to be transported for a considerable distance from their point of origin, and consequently it may take some time for the normal sediment balance to become reestablished. The geographical position of the Severn also means that it is particulary exposed to gales from the south west. Wintering shorebird population densities are somewhat lower in the Severn than they are in many other British estuaries — but whether this is a response to the decreased level of predictability of their food supplies is by no means clear.

Acknowledgments

This work was supported in part by the Energy Technology Support Unit, Harwell (Department of Energy) and the Royal Society. I would like to thank the British Trust for Ornithology for making available the Birds of Estuaries Enquiry counts, and J. I. Anderson, N. A. Clark, F. R. Gomm, C. Johnson, and D. H. Worrall for their help in the preparation of this paper.

ANDERSON, J. I. 1982. Some heavy metal studies in an estuarine food chain. Ph.D. thesis, University College, Cardiff, U.K. 313 p.

BISHOP, Y. M. M., S. E. FIENBERG, AND P. W. HOLLAND. 1975. Discrete multivariate analysis : theory and practice. M.I.T. Press, Cambridge, MA. 557 p.

BROWN, M. B. 1976. Screening effects in multidimensional contingency tables. Appl. Stat. 25: 37–46.

DUGAN, P. J. 1981. Seasonal movements of shorebirds in relation to spacing behaviour and prey availability. Ph.D. thesis, University of Durham, U. K. 212 p.

DUGAN, P. J., P. R. EVANS, L. R. GOODYER, AND N. C. DAVIDSON. 1981. Winter fat reserves in shorebirds : disturbance of regulated levels by severe weather conditions. Ibis 123: 359–363.

EVANS, P. R. 1981. Migration and dispersal of shorebirds as a survival strategy, p. 275–290. *In* N. V. Jones and W. J. Wolff [ed.] Feeding and survival strategies of estuarine organisms, Plenum Publishing, London.

FERNS, P. N. 1980a. Distribution of wading birds and wildfowl in the Severn Estuary and the Coastal Levels, p. 144–169. *In* T. L. Shaw [ed.] An environmental appraisal of tidal power stations, Pitman Advanced Publishing Program, London.

1980b. Annual and seasonal changes in the distribution of shorebirds in the Severn Estuary. Report to the Department of Energy, Cardiff, U.K. 73 p.

1980c. Intertidal feeding areas of seven species of shorebirds at seven sites in the Severn Estuary. Report to the Department of Energy, Cardiff, U.K. 181 p.

1982. Seasonal and annual changes in the distribution of shorebirds in the Severn Estuary. Cormorant. (In press)

HYDRAULICS RESEARCH STATION. 1980a. The Severn Estuary — wave climate study — wind wave correlation. Report to the Department of Energy (No. EX 914), Wallingford, U.K. 12 p.

1980b. The Severn Estuary — wave climate study. Report to the Department of Energy (No. EX933), Wallingford, U.K. 11 p.

KIRBY, R., AND W. R. PARKER. 1980. Sediment dynamics in the Severn Estuary, p. 47–62. *In* T. L. Shaw [ed.] An environmental appraisal of tidal power stations, Pitman Advanced Publishing Program, London.

LITTLE, C., AND W. NIX. 1976. The burrowing and floating behaviour of the gastropod *Hydrobia ulvae*. Estuarine Coastal Mar. Sci. 4: 555–566.

LOVELL, M. A., AND C. J. METTAM. 1980. Intertidal sediments and fauna: distribution of shore birds and their invertebrate prey. Report to the Department of Energy (No. STP52(a)), Cardiff, U.K. 14 p.

METTAM, C. J. 1978. Environmental effects of tidal power generating schemes. Hydrobiol. Bull. 12: 307–321.

MINTON, C. D. T. 1975. The waders of the Wash — ringing and biometric studies. Report to the Central Water Planning Unit, Lichfield, U.K. 21 p.

MYERS, J. P., P. G. CONNORS, AND F. A. PITELKA. 1979. Territory size in wintering sanderlings : the effects of prey abundance and intruder density. Auk 96: 551–561.

1981. Optimal territory and the sanderling : compromises in a variable environment, p. 135–158. *In* A. C. Kamil and T. D. Sargent [ed.] Foraging behavior : ecological, ethological and psychological approaches. Garland STPM Press, New York, NY.

NEWELL, R. C. 1962. Behavioural aspects of the ecology of *Peringia* (= *Hydrobia*) *ulvae* (Pennant) (Gastropoda, Prosobranchia). Proc. Zool. Soc. Lond. 138: 49–75.

PIENKOWSKI, M. W., AND H. CLARK. 1979. Preliminary results of winter dye-marking on the Firth of Forth, Scotland. Wader Study Group Bull. 27: 16–18.

PRATER, A. J. 1977. Birds of Estuaries Enquiry 1974/75. British Trust for Ornithology, Tring, U.K. 32 p.

WARWICK, R. M., AND J. R. DAVIES. 1977. The distribution of sublittoral macrofauna communities in the Bristol Channel in relation to the substrate. Estuarine Coastal Mar. Sci. 5: 267–288.

WORRALL, D. H. 1981. .The feeding behaviour of Dunlin *Calidris alpina* (L.). Ph.D. thesis, University College, Cardiff, U.K. 144 p.

Development of an Ecosystem Model of a Turbid Estuary[1]

I. R. JOINT

U.K. Natural Environment Research Council, Institute for Marine Environmental Research, Prospect Place, The Hoe, Plymouth, PL1 3DH U.K.

JOINT, I. R. 1983. Development of an ecosystem model of a turbid estuary. Can. J. Fish. Aquat. Sci. 40(Suppl. 1): 341–348.

This paper describes the development of those aspects of the whole ecosystem model, GEMBASE, which are most influenced by water turbidity. Mean values of surface turbidity, determined for a coarse grid of the Bristol Channel, were found to be highly correlated with tidal range and $\log_{10}$ 14-d mean river flow. Parameters derived from multiple regressions of these variables were used to obtain realistic simulations of surface turbidity for an 8-yr period from 1972 to 1980; simulated extinction depths derived from turbidity simulations were also realistic. Results of GEMBASE are discussed for phytoplankton and suspension feeding benthos, the two components of the ecosystem most affected by suspended solids concentrations. Simulations of phytoplankton biomass were obtained which compared well with field data. However, results for suspension feeding benthos were less good and showed slight increases in biomass from year to year which have not been found in the Bristol Channel; possible reasons for this are discussed.

Key words: Bristol Channel, ecosystem modeling, turbidity, extinction depth, phytoplankton, suspension feeding macrofauna

JOINT, I. R. 1983. Development of an ecosystem model of a turbid estuary. Can. J. Fish. Aquat. Sci. 40(Suppl. 1): 341–348.

Les aspects du modèle d'un écosystème entier, GEMBASE, les plus influencés par la turbidité de l'eau sont décrits dans le présent article. On a constaté que les valeurs moyennes de la turbidité de surface, déterminées dans un quadrillage grossier du chenal de Bristol, sont en étroite corrélation avec l'amplitude de la marée et le $\log_{10}$ du débit moyen, par période de 14 jours, de la rivière. Nous avons utilisé des paramètres dérivés des régressions multiples de ces variables afin d'obtenir des simulations réalistes de la turbidité de surface pendant une période de 8 ans, de 1972 à 1980; les profondeurs d'extinction simulées découlant des simulations de turbidité sont également réalistes. Nous examinons les résultats de GEMBASE en relation avec le phytoplancton et le benthos se nourrissant de matière en suspension, les deux composantes de l'écosystème les plus influencées par les concentrations de solides en suspension. Nous obtenons des simulations de biomasse phytoplanctonique qui s'accordent bien avec les données recueillies sur le terrain. Cependant, les résultats relatifs au benthos se nourrissant de matière en suspension sont moins bons et montrent de faibles augmentations de biomasse d'une année à l'autre, qui n'avaient pas été observées dans le chenal de Bristol; nous analysons les raisons possibles de ce phénomène.

Received October 14, 1981
Accepted June 21, 1982

Reçu le 14 octobre 1981
Accepté le 21 juin 1982

ECOSYSTEM models of estuaries are driven by a variety of environmental forcing functions; some physical processes which determine biological activity are predictable but others have a high degree of randomness. In attempting to model the previous behavior of an ecosystem, environmental data can be included either in digital form, derived from field data, or as a submodel which simulates the environmental variable concerned. Some forcing functions, such as river runoff or solar radiation are so variable that their impact on an ecosystem can only be modeled by including historic data. However, other forcing functions are more predictable: Radford and Joint (1980) described how the seasonal cycle of water temperature in the Bristol Channel could be adequately described by a sinusoidal curve, fitted to field data obtained over 4 years; this was used as a forcing function in the estuarine ecosystem model, GEMBASE (General Ecosystem Model of the Bristol Channel and Severn Estuary).

Variables dominated by random fluctuations such as solar radiation and river flow are included in GEMBASE as tables

[1]This paper forms part of the Proceedings of the Dynamics of Turbid Coastal Environments Symposium convened at the Bedford Institute of Oceanography, Dartmouth, N.S., Canada, September 29–October 1, 1981.

Printed in Canada (J6671)
Imprimé au Canada (J6671)

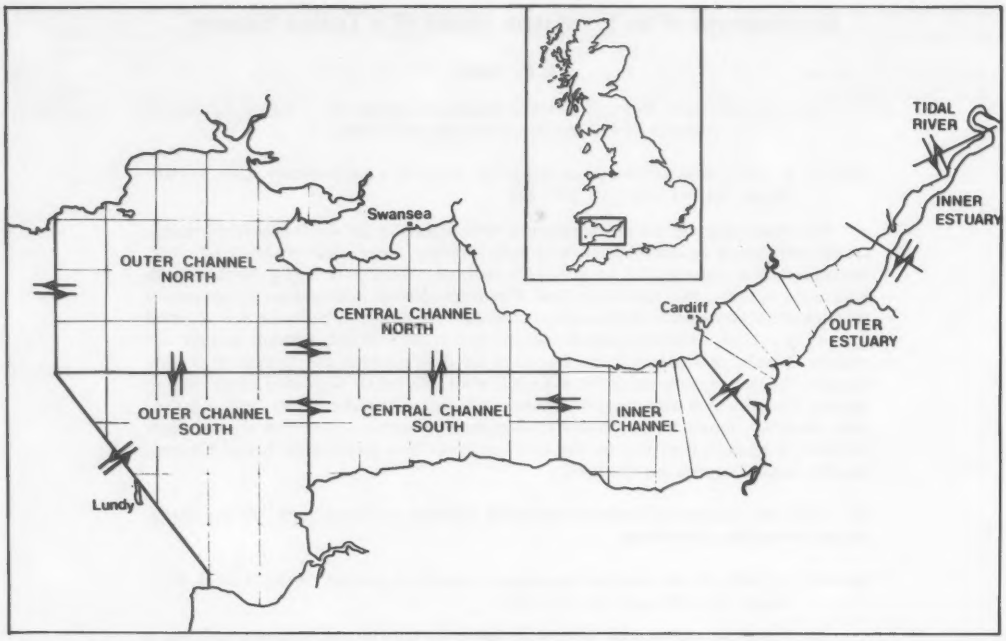

FIG. 1. Bristol Channel showing the seven regions modeled in GEMBASE. The small 5 nautical mile squares are used in calculating mean values of each variable for the large regions.

of digital data derived from field observations (Radford 1979). However, large tables of data tend to make working with a computer simulation model cumbersome and submodels, if they are not so complicated that they use a lot of computer core and computing time, are easier to use. Submodels, once verified, also have the advantage that it is no longer necessary to collect field data for that environmental variable at the same intensity of sampling.

Turbidity is one environmental variable which has been successfully included in GEMBASE as a submodel. The Bristol Channel has considerable quantities of particulate matter in suspension in certain regions of the estuary. Turbidity is a crucial forcing function because it affects light penetration into the water column, and hence photosynthesis, as well as affecting the feeding responses of filter feeding animals. The purpose of this paper is to describe the methods which have been used to model turbidity changes in the estuary, within the context of a whole ecosystem model, and to report the results of the model for phytoplankton and suspension feeding benthos.

Methods and Data Treatment

The Bristol Channel (Fig. 1) is one of the major estuaries of the United Kingdom with seven large river systems draining into the upper 100 km. It is a highly dynamic estuary with a tidal range of up to 14 m in the Outer Estuary and a tidal excursion of up to 25 km. Mean depth ranges from 41 m at the seaward end to 9.5 m in the Outer Estuary.

As part of a multidisciplinary study of the Bristol Channel, the Institute for Marine Environmental Research has been sampling in the estuary since 1971, collecting data on zoobenthos (Warwick and Davies 1977; Warwick et al. 1978), zooplankton (Collins and Williams 1981), phytoplankton and bacterial biomass and production (Joint and Pomroy 1981, 1982) and on physical variables and hydrodynamics (Uncles 1979; Uncles and Jordan 1980; Uncles and Radford 1980). These data form the base initially used to formulate GEMBASE and subsequently to validate and verify the model.

Turbidity was measured on each cruise with a Partech Suspended Solids Monitor which was calibrated by comparison with gravimetric determinations of suspended solids concentrations. From 1972 until 1975 samples were taken on a grid of stations 5 nautical miles apart; after 1977, turbidity measurements were made continuously on water sampled with a submersible pump as the ship steamed round the sampling grid. Before 1975, estimates of extinction depth were also made with a Secchi disc.

Contour charts were prepared for every variable measured on each cruise; the position of each sampling station was corrected to the computed locations at high and low water and the data were contoured using the Surface Approximations and Contour Mapping System (SACM) developed by Appli-

cations Consultants Inc., Texas to give separate charts for the positions the stations would occupy at high water and low water. For the purposes of ecosystem modeling, the Bristol Channel was divided into the coarse grid of seven regions (Radford 1979) shown in Fig. 1 and the mean for each variable was computed for each region. Values for each square of 5 nautical miles (Fig. 1) were read from the contour charts for high and low water, and averaged. A mean for each of the seven large regions was determined from these small square means by weighting the data according to the volume of water in the 5 nautical mile squares. These average values for the large regions were used in GEMBASE development and validation (Radford and Joint 1980).

Results and Discussion

Modeling Turbidity

The concentrations of suspended solids vary considerably in the Bristol Channel from the highly turbid Inner Estuary to the Outer Channel which has low particulate loads typical of British coastal waters. In addition to the vertical distribution of suspended particles which is controlled by tidal resuspension, there is a distinct seasonal variation in surface turbidity in the Bristol Channel; Fig. 2 shows typical contour charts for turbidity of surface water in March and August. The very turbid regions show little variation with season but the turbidity of the Inner and Central Channel regions is significantly reduced in summer. It is this seasonal change in turbidity which was modelled in GEMBASE and no attempt was made to model turbidity changes due to the semidiurnal tide.

During model development, various attempts were made to find a simple expression which would successfully simulate seasonal changes in turbidity. An initial correlation of turbidity and daily values of river flow gave a reasonable approximation to observed turbidities. However, the simulated turbidity was highly variable with unreasonable daily fluctuations resulting from the changing river flow. These rapid oscillations were damped by relating turbidity to the logarithm of river runoff, averaged over the previous 14 d. The simulations were based on a regression of mean surface particulate concentration for each region, derived from 14 cruises in 1973 and 1974, and $\log_{10}$ 14-d mean river flow ($r = 0.71$, $P \leq 0.01$). Although this expression gave reasonable seasonal simulations of turbidity, there were still unrealistic daily fluctuations and the simulation was particularly susceptible to short-term increases in river flow. It was also difficult to envisage how river flow could affect turbidity of the whole Bristol Channel, although it might be a crude indication of weather conditions in the region. Attempts were, therefore, made to relate turbidity to those other environmental variables which were intuitively thought more likely to control resuspension in the estuary, such as wind speed and tidal range (as indicators of wind and tidal stress).

Regressions were done between the mean values of turbidity for each of the seven regions and the following variables: (a) mean tidal range on mid-date of cruise, (b) mean tidal range over whole cruise period, (c) range of last Spring tide before cruise, (d) river flow, (e) $\log_{10}$ 14-d mean river flow, (f) mean wind speed over cruise, (g) mean wind speed

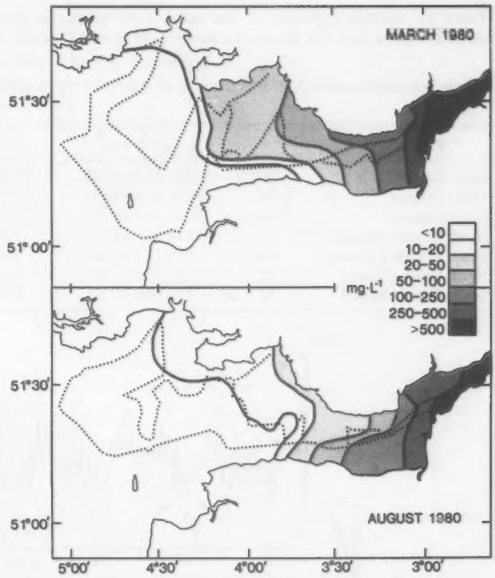

FIG. 2. Contour charts of surface turbidity in the Bristol Channel in March and August 1980: station positions were corrected to the position they would occupy at low water before contouring. The dotted line shows the tidally correct position of the sampling track.

for 7 and 14 d before cruise, (h) westerly component of wind speed for 7 and 14 d before cruise. Significant correlations were obtained between turbidity and $\log_{10}$ 14-d mean river flow and tidal range of the Spring tide prior to data collection. Multiple regression of these two variables together against turbidity resulted in a significantly better correlation coefficient than was obtained against the individual variables; the correlation could not be significantly improved by including any measurement of wind as a third variable. The results of the multiple regressions for the seven regions of the Bristol Channel are given in Table 1; the F ratio is significant at $P \leq 0.05$ for the Inner Channel and South Outer Channel, at $P \leq 0.001$ for the South Central Channel and at $P \leq 0.01$ for the other four regions.

These regression equations form the basis of turbidity simulation in GEMBASE. The results of the simulation for 8 years are shown in Fig. 3 for two contrasting regions, the turbid Inner Channel and the least turbid region, the South Outer Channel. Data points prior to 1975 were used in the formulation of the model and were based on gravimetric determinations of particle load; the data after 1976 were Partech readings and, since these were not used in model formulation, they provide verification of the goodness-of-fit of the simulated and observed turbidities.

The problem of how to validate the output from a model is a very difficult one. Platt and Radach (1981) state that, for complex models that generate time series of many state variables, there is no objective criterion for goodness-of-fit and

TABLE 1. Multiple regression of tidal range of the Spring tide prior to data collection (1st variable) and $\log_{10}$ 14-d mean river flow (2nd variable) against turbidity for seven regions of the Bristol Channel. The equation is

$$\text{Turbidity} = a + (b \times \text{tidal range}) + (c \times \log_{10} \text{river flow})$$

r is the correlation coefficient, F is the ratio of regression mean squared over residual mean squared, and P is the level of significant of the F-ratio.

Region	n	a (SE)	b (SE)	c (SE)	r	F	P
Inner Estuary	24	−565.61±243.46	70.27±19.42	1.16±1.17	0.63	6.67	≤0.01
Outer Estuary	24	−763.54±273.16	75.98±19.10	55.51±32.79	0.66	8.15	≤0.01
Inner Channel	14	−98.39±56.50	9.90±5.76	6.17±8.73	0.68	4.74	≤0.05
North Central Channel	14	−44.81±18.70	3.37±1.91	5.98±2.89	0.82	11.51	≤0.01
South Central Channel	14	−38.14±10.54	3.44±1.08	2.71±1.63	0.88	18.76	≤0.001
North Outer Channel	13	−27.57±14.63	1.79±1.51	4.02±2.10	0.79	8.14	≤0.01
South Outer Channel	12	−13.08±10.07	0.97±1.05	2.01±1.44	0.72	4.75	≤0.05

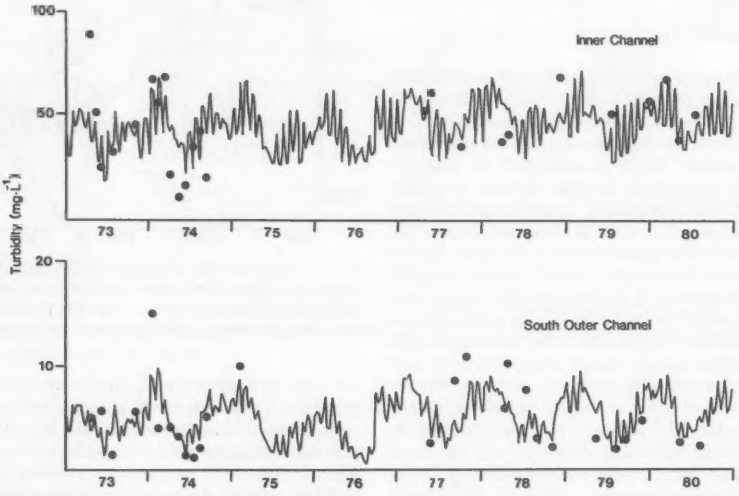

FIG. 3. Simulated values for surface turbidity from 1973 until 1980 for the Inner Channel and South Outer Channel. The data points are mean values of turbidity calculated for each region from field observations.

that most model fits are judged subjectively. Statistical validation of the output from GEMBASE has not been attempted and the results shown on this paper are based on subjective assessments of goodness-of-fit.

Weekly variations in simulated turbidity, which were often considerable, are the result of the spring–neap tidal cycle. The field data also indicate large changes in turbidity over short time periods but our sampling program was too infrequent to determine whether or not the fine detail of the simulation is realistic. It would be naïve to think that such a simple model could be used to simulate short-term changes in turbidity in a finer grid in the Bristol Channel; but, for the purposes of GEMBASE, with the assumed homogeneity over large regions, the results are acceptable. The complexity of many of the biological processes in an estuarine ecosystem are so great that a simulation model is much more likely to break down as a result of poor modeling of the biology than of a poor approximation of water turbidity.

MODELING EXTINCTION DEPTH

Estimates of extinction depth are needed to model the response of phytoplankton to light. A correlation was found between turbidity and Secchi disc depth for the 14 cruises in the Bristol Channel in 1973 and 1974 and formed the basis of simulation of extinction depth in GEMBASE. A regression of reciprocal Secchi disc depth against surface particulate load of the form $1/\text{SD} = 0.034$ turbidity $+ 0.134$ gave a correlation coefficient of 0.892 ($P \leq 0.001$); extinction depth was, therefore, modeled in GEMBASE by correlating with simulated daily values of turbidity. Figure 4 shows the agreement between simulated and observed Secchi disc depths for the Inner and South Outer Channels from 1973, plotted as $\log_{10}$ Secchi disc depth. Unfortunately, too few Secchi disc measurements were made after 1974 for a meaningful test of the long-term simulation of extinction depth. However, in view of the close fit of simulated and observed turbidities for 1973 until 1980,

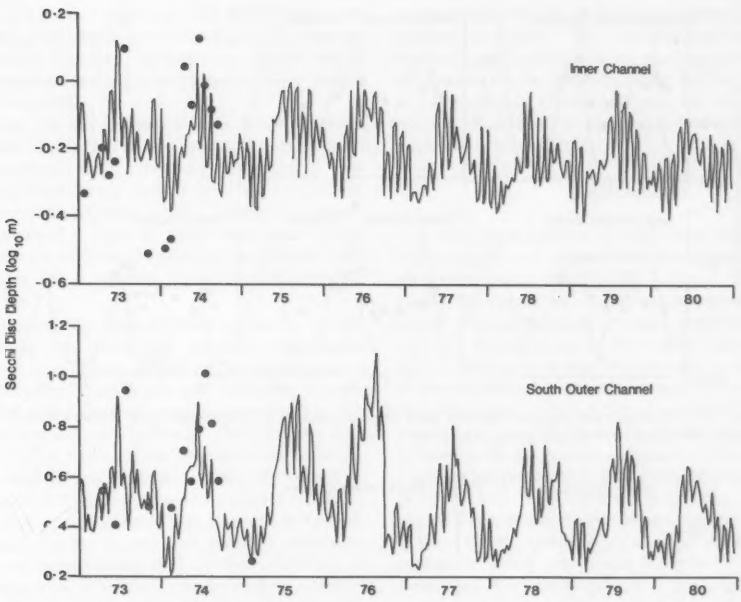

FIG. 4. Log_{10} Secchi disc depth simulated for 1973 until 1980 for the Inner Channel and South Outer Channel: the data points are mean values of Secchi disc calculated for each region from field data.

it seems reasonable to assume that Fig. 4 is a reasonable representation of mean extinction depth in each of the seven regions of the Bristol Channel. Daily values of extinction depth computed in GEMBASE are modified for self-shading by a term which responds to changing phytoplankton density (Kremer and Nixon 1975, 1978) and represents the sum of light attenuation by inorganic particles and phytoplankton cells.

Modeling Phytoplankton Biomass

To model the Bristol Channel in just seven regions, a large degree of spatial homogeneity in the distribution of plankton was assumed. Moreover, it was decided that too fine a temporal scale would also not be appropriate for GEMBASE and that it would not be feasible to model processes with a relaxation time of less than 1 d. With one exception, all ecological processes simulated in GEMBASE are assumed to occur at a constant rate for a time period of 1 d; this is justifiable in modeling processes such as filter feeding because the average food concentration (phytoplankton) is not likely to change dramatically over 24 h and a mean daily feeding rate is a close approximation to reality. However, a similar coarse approach to modeling photosynthesis could not be justified because photosynthesis is influenced more by the instantaneous light intensity than by the daily integrated value. Photosynthesis increases with increasing light intensity until a saturating light level, then the rate decreases due to photoinhibition. It was felt that it would be inappropriate to drive GEMBASE with an idealized daily value for solar radiation (such as Kremer and Nixon (1978) used in their model of Narragansett Bay) because it would not be possible to adequately model the response of phytoplankton to natural fluctuations in light intensity. The GEMBASE primary production subroutine uses hourly values of solar radiation to model primary production and the hourly rates are summed to give a precise integral for daily primary production; Radford (1979) has described the procedure in detail.

Photosynthesis, integrated down the water column, was modeled using the equation of Steele (1962), assuming a constant value for extinction coefficient over each 24-h period. The estimates of primary production obtained by this model compare well with measurements made in the Bristol Channel (Radford and Joint 1980). All other processes involving primary producers, i.e. respiration, excretion of dissolved organic matter, mortality, grazing by zooplankton and zoobenthos and physical transfer from one region to another, were calculated on a daily basis.

Simulated phytoplankton biomass in five regions is shown in Fig. 5 and compared with mean values of observed biomass for each region; the data and simulations are plotted on a $\log_{10}$ scale to allow better visual comparison of the agreement at both high and low biomass values. There is a tendency for simulated values in the Outer and Central Channels to be too low in winter and too high in summer, and the simulation for the Inner Channel does not agree well with observed data.

Although chlorophyll *a* concentrations in the Inner Channel are similar to those in the Central and Outer Channels, annual

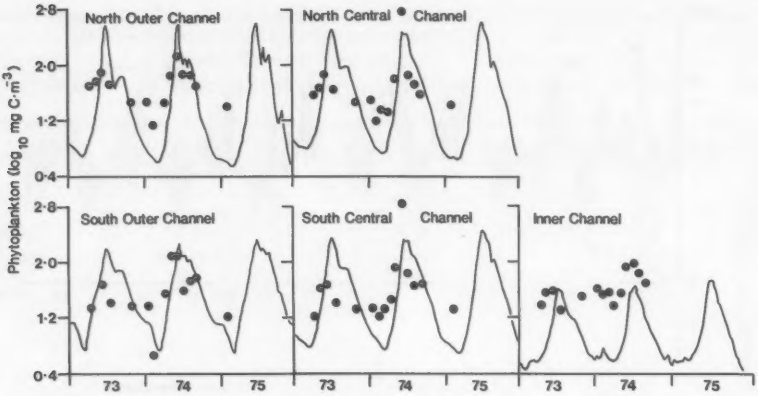

FIG. 5. Simulated and observed standing stock of phytoplankton in five regions of the Bristol Channel from 1973 until 1975 plotted as $\log_{10}$ mg C·m^{-3}.

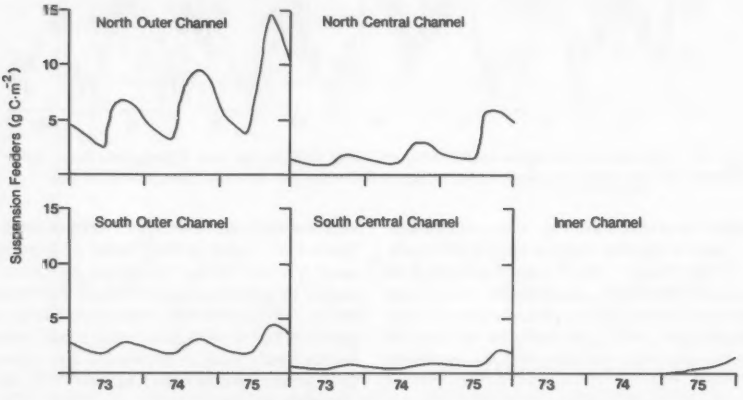

FIG. 6. Simulated biomass of suspension feeding benthos in five regions of the Bristol Channel from 1973 until 1975.

primary production in the Inner Channel is only 4% of that in the Outer Channel (Joint and Pomroy 1981). Radford (1981) has shown that the rate of primary production simulated in GEMBASE compares well with the estimates made by Joint and Pomroy (1981) using the ^{14}C technique. The low simulated biomass must result because a process other than photosynthesis is inadequately modeled by GEMBASE. In the Inner Channel, the impact of grazing is very small because of the low biomass of herbivores in the region (Collins and Williams 1981); therefore, the equations either for mortality, respiration or inter-region transfers are inadequate for the Inner Channel, although they result in realistic simulations for the less turbid regions. Transfers of material from one region to another are unlikely to be at fault because of the good simulation of salinity in GEMBASE (Uncles 1983). If either mortality or respiration of phytoplankton in winter in the Inner Channel is less than assumed then the simulated results would be closer to the observed high constant standing stock of phytoplankton. However, very little research has been done on phytoplankton physiology in turbid environments. Smayda and Mitchell-Innes (1974) and Antia (1976) have reported that laboratory cultures of algae can retain viability in the dark for many months without forming resting stages. Under conditions of continuous darkness, similar to those experienced by phytoplankton in turbid waters, these authors reported a considerable reduction in respiration rate. However, no field data are available to confirm this observation with natural phytoplankton populations. The behavior of phytoplankton in the darkness of a turbid water column is one example of several where GEMBASE output has highlighted important lacunae in our understanding of estuarine ecology.

MODELING THE BIOMASS OF SUSPENSION FEEDING BENTHOS

Other components of the pelagic ecosystem have been modeled with similar success to phytoplankton; Radford and

Joint (1980) reported realistic results for the simulation of omnivorous and carnivorous zooplankton which compared well with field data. However, the benthic ecosystem, and in particular suspension feeding macrobenthos have proved more difficult to model.

Macrofauna are patchily distributed in the Bristol Channel; this was modeled in GEMBASE by assuming a homogeneous distribution of animals over a notional proportion of each region, the proportion being derived from the field observations of Warwick and Davies (1977). Biomass, expressed as g C, was simulated for each m^2 where suspension feeders occurred. Changes in simulated biomass are the integral of the feeding processes and respiration, excretion, feces production, and grazing.

The model simulates the effect of changing particle concentration on feeding rate; using data obtained with *Mytilus edulis*, Bayne et al. (1976a) derived an expression which resulted in decreasing filtering rate and increasing pseudofeces production with increasing particle concentration; this expression has been used in GEMBASE. Daily feeding rates were computed using results of the simulation for turbidity, phytoplankton, and particulate organic carbon; phytoplankton carbon was ingested by macrofauna with a greater efficiency than detrital carbon and the latter was assumed to be 90% refractory. Equations for routine and standard respiration were based on the data of Bayne et al. (1976b). Predation on benthic macrofauna in GEMBASE was by birds in intertidal regions and by demersal fish and carnivorous invertebrates in those sublittoral regions where macrofauna occurred.

Simulation results, expressed as g C for each m^2 where suspension feeders exist, are shown in Fig. 6 for five regions from 1973 until 1975. Seasonal data for all zoobenthos in the Bristol Channel were not obtained during our sampling program so it is not possible to compare the simulation results with field data. No year-to-year variations in biomass have been found in the zoobenthos of the North Outer Channel (R. M. Warwick, personal communication) so the criterion adopted for judging the success of the simulation is that the output should show a reasonable seasonal cycle with similar biomass in successive years. It is clear from Fig. 6 that this criterion is not satisfied because there is an increase in biomass in successive years, particularly in the North Outer and North Central Channels.

The increases occur in a short period of 30–60 d in late spring when GEMBASE simulates low turbidity (Fig. 3) and rapid increases in standing stock of phytoplankton. Food intake by suspension feeders in GEMBASE is related to food concentration and to water turbidity which modulates filtering efficiency, so the conditions which occur in the model each spring favour ingestion of food at high efficiency by suspension feeding benthos.

There are several explanations for the poor simulation of suspension feeding macrofauna. The relationships used to define feeding rate, ingestion, and pseudofeces production were derived for *Mytilus edulis* and may not be appropriate for other suspension feeding fauna, such as *Sabellaria*, which are abundant in the turbid regions of the Inner Channel. Alternatively, the increase in gross simulated biomass may be reasonable; GEMBASE does not attempt to model processes such as gamete production and a significant proportion of production which would normally be lost to the particulate organic matter pool may be retained within the simulated suspension feeder biomass resulting in unrealistic net production. If this is the explanation for the poor simulation results, the present level of complexity of GEMBASE may be too simple to allow realistic simulations of suspension feeding benthos and the model must be modified.

Conclusions

A multiple regression of tidal range, river flow and turbidity was the basis of a realistic simulation of turbidity in the ecosystem model GEMBASE. Although this expression is clearly too simple for simulating short-term changes in turbidity, it was adequate to simulate changes in mean turbidity over the large regions of the Bristol Channel modeled in GEMBASE and was used successfully as a forcing function of the model. Another expression derived from a regression of extinction depth with turbidity also resulted in realistic simulation of extinction depth and contributed towards a successful simulation of the pelagic ecosystem. These simple expressions are adequate within the coarse geographic grid adopted in GEMBASE but the success or failure of large ecosystem models depends much more on our understanding and ability to simplify into mathematical expressions the complex interactions occurring within and between the biological components of the ecosystem.

Acknowledgments

I am grateful to P. J. Radford, the system analyst for the group which developed GEMBASE, for his advice and help. This work forms part of the estuarine program of the Institute for Marine Environmental Research, a component of the U.K. Natural Environment Research Council.

ANTIA, N. J. 1976. Effects of temperature on the darkness survival of marine microplanktonic algae. Microbiol. Ecol. 3: 41–54.

BAYNE, B. L., J. WIDDOWS, AND R. J. THOMPSON. 1976a. Physiological integrations, p. 261–291. *In* B. L. Bayne [ed.] Marine mussels: their ecology and physiology, IBP 10, Cambridge University Press, U.K.

BAYNE, B. L., C. J. BAYNE, T. C. CAREFOOT, AND R. J. THOMPSON. 1976b. The physiological ecology of *Mytilus californianis* Conrad: metabolism and energy balance. Oecologia (Berl.) 22: 211–228.

COLLINS, N. R., AND R. WILLIAMS. 1981. Zooplankton of the Bristol Channel and Severn Estuary. The distribution of four copepods in relation to salinity. Mar. Biol. 64: 273–283.

JOINT, I. R., AND A. J. POMROY. 1981. Primary production in a turbid estuary. Estuarine Coastal Shelf. Sci. 13: 303–316.

1982. Aspects of microbial heterotrophic production in a highly turbid estuary. J. Exp. Mar. Biol. Ecol. 58: 33–46.

KREMER, J. N., AND S. W. NIXON. 1975. An ecological simulation model of Narragansett Bay in the plankton community, p. 672–690. *In* L. E. Cronin [ed.] Estuarine research, Vol. 1, Academic Press Inc., New York, NY.

1978. A coastal marine ecosystem, Springer-Verlag, Berlin.

PLATT, T., AND G. RADACH. 1981. Validation, p. 46–48. *In* T. Platt, K. H. Mann, and R. E. Ulanowicz [ed.] Mathematical models in biological oceanography. UNESCO Press, Paris.

RADFORD, P. J. 1979. Some aspects of an estuarine ecosystem model — GEMBASE, p. 301–322. *In* S. E. Jørgensen [ed.] State-of-

the-art in ecological modelling, Vol. 7, International Society for Ecological Modelling, Copenhagen.

1981. Modelling the impact of a tidal power scheme on the Severn estuary ecosystem, p. 235–247. *In* W. J. Mitsch, R. W. Bosserman, and J. M. Klopatek [ed.] Energy and ecological modelling, Elsevier Scientific Publishing Co., Amsterdam.

RADFORD, P. J., AND I. R. JOINT. 1980. The application of an ecosystem model to the Bristol Channel and Severn Estuary. Water Pollut. Control 79: 244–254.

SMAYDA, T. J., AND B. MITCHELL-INNES. 1974. Dark survival of autotrophic planktonic marine diatoms. Mar. Biol. 25: 195–202.

STEELE, J. H. 1962. Environmental control of photosynthesis in the sea. Limnol. Oceanogr. 7: 137–150.

UNCLES, R. J. 1979. A comparison of the axial distribution of salt and ^{137}Cs in the Severn Estuary — during August 1974. Estuarine Coastal Mar. Sci. 9: 585–594.

1983. Modeling physical processes in the Bristol Channel as a prerequisite for ecosystem studies. Can. J. Fish. Aquat. Sci. Suppl. 40. (This issue)

UNCLES, R. J., AND M. B. JORDAN. 1980. A one dimensional representation of residual currents in the Severn Estuary and associated observations. Estuarine Coastal Mar. Sci. 10: 39–60.

UNCLES, R. J., AND P. J. RADFORD. 1980. Seasonal and spring neap dependance of axial dispersion coefficients in the Severn Estuary. J. Fluid. Mech. 98: 703–726.

WARWICK, R. M., AND J. R. DAVIES. 1977. The distribution of sublittoral macrofauna communities in the Bristol Channel in relation to the substrate. Estuarine Coastal Mar. Sci. 5: 267–288.

WARWICK, R. M., C. L. GEORGE, AND J. R. DAVIES. 1978. Annual macrofauna production in a *Venus* community. Estuarine Coastal Mar. Sci. 7: 215–241.

Concluding Remarks of Session Chairmen at the Dynamics of Turbid Coastal Environments Symposium, I

A. J. Bowen

Department of Oceanography, Dalhousie University, Halifax, N.S. B3H 4J1

A notable feature of the symposium was the range of scale of the processes considered; events discussed ranged from the micro-turbidity current generated by a single shrimp to the 100-year flood in the Yangtse River. This tremendous scope provided an opportunity to observe the interplay of two important themes, sediment transport and sediment mobility, over a wide range of phenomenology. It is clear that the concepts of transport and mobility are closely related, mobility as expressed as erosion or deposition is mathematically the divergence of the sediment transport vector. However, the practical problems of identifying changes in the transport are formidable and discussion of this and related problems led to a third theme, that of sampling strategy in a complex turbid environment.

In a number of papers, transport of sediment or of water and sediment provided the focal point of the study. The transport in a river, an estuary or along the shore provided a strong, measurable signal which could be reasonably well sampled despite the real complexity of the system. A single ship could be used to investigate the outflow from the Yangtse by integrating data taken in different channels at different times with general information of the freshwater discharge upstream (Milliman). A general picture of the transport paths, the sources including rice field management and possible sinks could be obtained. The fluctuations in transport with the spring/neap tidal cycle and the changes in freshwater flow were also observed. In this large system, with the fourth highest annual sediment load in the world, the sediment transport is clearly the focus of interest. A similar situation was revealed in the estimate of the sediment transport in the Miramachi (Winters). An interesting measure of the author's interest in mobility of the sediments is whether any serious attempt is made to discover the size of material in suspension, particularly the floc sizes. To calculate the sediment transport rates such discrimination is unnecessary; to consider the possible disposition of material in the system such analysis is essential (Dobereiner and McManus; Smith and Williams).

The sediment transport is also well observed whenever it is efficiently trapped. Where artificial traps such as harbors require dredging, particularly detailed records of the sediment movement may be available which provide substantial insight into the important processes. This is particularly interesting in relatively undeveloped areas of the world where scientific observation of coastal processes is virtually absent (Kendrick and Darbyshire). Again, field data only provide very general ideas as to the details of the transport processes. However, bringing the sediment back to the laboratory for flume studies provides an insight into the sediment mobility which is difficult to obtain in the field.

Further observations of fine sediment on an open coast (Wells) showed the transition from known transport rates to known transport directions in Surinam and Louisiana to unobserved, possibly unobservable, but inferred directions of transport off western Korea. The final step was the general discussion of mobility per se close to the shoreline (Anderson). It is interesting to observe the change of scale considered as one moves from the transport of several million cubic metres of mud per year, to the question as to whether, and if so how, a particle is moved at all.

In the absence of a strong transport, the phenomenology may be fascinating but the science is less clearly defined. The need for further understanding of sediment mobility arises explicitly in the attempts to develop numerical models describing sediment transport and deposition in turbid environments (Greenberg and Amos). In the strong tidal currents typical of turbid regions, the net transport over a tidal cycle is likely to be small compared to the instantaneous transport at maximum ebb or flood. The response of the bed or near bed layers to the changing stress is likely to be critical in determining the net sedimentary pathways.

The question of the pattern of deposition as a function of the sediment characteristics and the hydrodynamic environment illustrates the difficulties created by the flocculation of small sediment particles. The distribution of sand size can be reasonably correlated with the strength of the tidal current but the muds are less tractable (Kranck and Bezanson).

To adequately investigate the whole system, a sampling strategy is needed which resolves all the processes of interest in a particular problem. In this context it was interesting to see the range of sophistication in the presentation. For chemical studies of the Tamar, a straightforward water sampling with no particular attention to time and space scales was considered appropriate (Loring et al.).

In the Tay, considerable care was taken to sample the estuary under different conditions, one technique was to follow the tide up the estuary staying with the high tide (Dobereiner and McManus). For this area, the long-term nature of the investigation showed that the particle size in suspension, the floc size, was smaller on stormy days, presumably due to the break up of preexisting flocs.

The floc problem was carefully examined in the Severn Estuary with detailed measurements of the concentrated sediment load close to the bed showing high viscosity suspensions with concentrations as great as 8% by volume of solids (Smith and Williams). Analysis of these samples (Bryant and Williams) showed that the flocs themselves are 91% water by volume — the suspension observed is solid flocs! Final settling requires a shearing of the flocs but the local energy levels are apparently too low. The turbulent levels are obviously suppressed by the increase in both viscosity and density close to the bed, making a distinct interface between the general flow above and the settled sediment beneath. This layer may play an important role, the question as to what determines its existence and thickness needs to be addressed. If very thin

Printed in Canada (J6983)
Imprimé au Canada (J6983)

layers of this type can physically exist, they could play an important role and yet be extremely difficult to sample.

The impact of biological processes on sediment mobility was both of interest and concern for many of the speakers. Detailed measurements of the boundary layer as a function of season (Rhoads and Boyer) provide ambivalent results on the role of such organisms. Concern was expressed that creatures such as flatfish play an important role which is difficult to investigate with fixed instruments. However the possible role of biological processes is well illustrated by the organisms that control the benthic environment to their own advantage (Cary).

Concluding Remarks of Session Chairmen at the Dynamics of Turbid Coastal Environments Symposium, II

D. C. RHOADS

Department of Geology and Geophysics, Yale University, New Haven, CT 06520, USA

IF the sum of the papers in this symposium represent a definition of turbid coastal waters, one is lead to conclude that all coastal environments are, at one time or another, turbid. Turbidities reported for coastal environments range from 10 $mg \cdot L^{-1}$ to gram quantities of particulates per litre. Some environments are occasionally turbid related, for example, to aperiodic turbidity currents (fjords) or more-or-less perpetually turbid in the case of estuaries which lie at the mouths of major river systems.

Each investigator has chosen a time and space scale that defines an observational window on the turbidity phenomenon being studied. Most observations range from fractions of a tidal cycle to an annual period. Some studies extend to a few years and fewer to geological time. All of these time perspectives are valid and important depending on the questions being addressed. Nevertheless, it is often instructive to ask the question, how are the processes I measure in real time related to processes that operate in geological time? This latter question is seldom asked.

Space scales for coastal turbidity studies also cover a wide geographic range. One may approach the turbidity problem on a worldwide scale looking at the major inputs of sediment to the world's oceans (e.g. Milliman). From this exercise we learn that the major inputs are from S.E. Asia, major river systems, and surprisingly, the islands of Oceania. Studies of small dimensional scale also contribute to our understanding of processes which generate turbid water, for example, the point source injection of grains into the water column by wake turbulence behind biological roughness elements (Carey). Such a study may not contribute much to understanding regional sediment transport but such an approach is crucial for understanding how fluid–sediment–organism interactions can influence benthic secondary productivity (Wildish and Peer).

Sources of suspended loads are diverse, including lateral inputs from glacial melt water, shore-face erosion, and rivers. In the latter case, man may be responsible for as much as 25–50% of the suspended load (Milliman; Biggs et al.). Most coastal turbidity, not directly associated with river or glacial discharge, appears to be related to resuspension and remobilization of sediment already present within coastal systems by tidal currents or wave-generated turbulence. Resuspension events may be periodical related to tidal scour or seasonal climatic factors. Spring tides, high runoff periods, and storm waves may purge or otherwise flush-out sediment that accumulates during periods of low kinetic energy (e.g. Kendrick and Derbyshire). The importance of catastrophic events in structuring both the geology and biology of near shore environments cannot be overemphasized. The geological record of nearshore facies is repleat with storm-produced stratigraphic units.

Printed in Canada (J6986)
Imprimé au Canada (J6986)

Resuspension of the seafloor also releases pore water into the overlying water (Guillaud; Helder and Rutgers van der Loeff). This can be described as a kind of local "upwelling" and may explain why some estuaries rival many oceanic upwelling regions in chemical reactivity (Loring and Rantala) and biological production. However, the full potential of this production may be compromised by the turbidity associated with bottom erosion or by rapid dilution of released pore water nutrients in the mixing zone. Resuspension of the seafloor places not only sediment into the water column but also some benthic meiofauna and microfauna (Palmer and Coull). Passive transport of organisms in the water column may be necessary for completion of life cycles and successful dispersion of these species.

The contribution of autochthonously produced particulates to coastal turbidity remains poorly studied. The status of this research remains near that of some 20 years ago when the in situ production of particulates was first described by adsorption of organic molecules to bubble surfaces ("micelles"). The size distribution and composition of suspended particles appears to be different for each system studied and apparently depends on sources, mechanisms, and intensities of flocculation or bioaggregation. The bioaggregation mechanism for producing organic-mineral aggregates is rather poorly understood relative to zeta-potential flocculation.

The turbidity maximum (or maxima) described for many estuaries is (are) associated with a region of particle "growth." Such turbidity maxima may migrate up and down the axis of an estuary with a tidal period. A seasonal component to the migration may also exist. Suspended sediment fronts may be manifested on the surface of the water as foam lines or convergence lineations (Koske). High water turbulence may counteract particle aggregation resulting in disaggregation and dispersion.

Sediment transport modeling of cohesive sediment is a difficult problem, especially when applied to natural sediments containing living organisms. No predictive equations exist which will allow one to state how a particular mud will respond to a given boundary shear stress. The critical shear stress depends on dynamically changing geotechnical properties and biological factors which can destabilize or stabilize muds relative to an "azoic" sediment. Future flume studies on this difficult problem will no doubt define a wide range of $\bar{U}^*_{crit}$ for muds depending on a comparably wide range of physical and biological variables. My own opinion is that we may have to be satisfied with understanding the possible seasonal range in $\bar{U}^*_{crit}$ rather than being able to accurately predict $\bar{U}^*_{crit}$ from any subset of physical–biological parameters. A major problem for those of us who work on organism–sediment–fluid interactions is to convince sedimentologists and geochemists that organisms can be of first-order importance in sediment transport equations or chemical flux calculations (Anderson; Risk and Yeo). Dense mud

suspensions may behave as non-Newtonian materials and have unusual rheological properties. Many fluid muds move as a coherent bottom layer with the tide or as solitary waves (Wells; Smith and Williams). The physics of this sediment transport problem are of first-order importance yet are poorly known.

The biological influence of turbidity may be positive or negative, depending on the concentration of particulates and frequency of encounter. Turbidity has been demonstrated to effect specie's adaptive strategies and both primary and secondary production. A major ecological problem is relating how different levels of seafloor turbidity and stability affect faunal or floral succession and hence primary and secondary production (e.g. Hargrave et al.; Schwinghamer et al.; Daborn et al.; Dadswell; Ferns).

If any theme results from my overview it should be that an understanding of the complex coastal environment demands interdisciplinary cooperation between physical, chemical, and biological oceanographers. Attempts at system modeling are one manifestation of such cooperation. One major value of this modeling exercise is that it can help to identify inputs and potential interactions which require future cooperative research.

Concluding Remarks of Session Chairmen at the Dynamics of Turbid Coastal Environments Symposium, III

G. EVANS

Department of Geology, Imperial College of Science and Technology, Prince Consort Road, London, SW7 2BP U.K.

THE meeting has been concerned with the freshwater–marine interface in coastal environments. However, if a true understanding of the supply and distribution of fine-grained sediment in this zone is to be achieved it is necessary to consider a rather larger system which includes at least the areas of supply of this material.

Studies of suspended sediment load of rivers have shown that in some areas small specific parts of the river basin may be the major producers of the suspended load. For instance, Gibbs (1967) has claimed that 82% of the suspended load of the Amazon comes from 12% of the drainage basin. If such patterns are widespread, it is obviously critical to establish the dominant areas of supply, as human interference even on a small scale could have very significant effects in estuarine areas from which they appear to be very remote.

Man's activities in land clearance since the Neolithic and particularly in modern times have generally increased runoff and with it the supply of fine-grained sediment to fluvial systems. However, as pointed out by Biggs at the symposium, economic considerations may reverse this trend in areas where arable land becomes less profitable. Also, in other areas such as in eastern England, the widespread deepening of natural channels for drainage purposes may sometimes lead to these channels' acting as sediment traps.

A point that needs to be constantly kept in mind, in consideration of coastal environments, is that fine-grained sediment, and indeed coarser-grained sediment, is not supplied equally to the whole coastal perimeter. Instead, it is injected at relatively few, often widely spaced points. These point-sources supply fine-grained material which is transported along the coastline and driven into estuaries and lagoons or plastered against the shore for many kilometres, from the point of injection. As with the transport of sand and coarser-grained sediment, fine-grained sediment seems to be transported largely parallel to the shoreline. It escapes seawards onto the outer shelves and ultimately the deep sea only in places where river flow is very strong, as off large deltas or elsewhere where oceanographical processes are favorable for such seaward advection, or spasmodically during periods of storms. Even when it reaches the continental slope and rise, it is again transported parallel to the continental margins by contour currents. Such lateral transport was a recurrent theme during the meeting and was illustrated by Wells in his studies of the coasts of Louisiana, Surinam, and South Korea.

This phenomenon introduces an important problem for those engaged in coastal studies. Local investigations may often reveal variations in availability of fine-grained sediment which are not easily related to local processes but instead may be due to changes that have occurred hundreds of kilometres from the study site. Such processes may be not only geographically remote but, and this produces a more intractable problem, may be relatively remote in time. The lag-effect may often be very great where an enhanced river input or a coincidence of stormy weather with high tides on an easily erodable coast or on the adjacent submarine areas, may introduce large volumes of fine-grained sediment into the nearshore system. This may take months to reach a particular coastal location. Unless such lag-effects are considered, poor correlation and a poor understanding of local variations will be all that are achieved in spite of the most careful work at the site under investigation.

If we are not to leave ourselves open to the criticism of being concerned only with the immediate problems, the effects of land/sea level changes must be taken into account. It must not be forgotten that we are in a transient period when the sea is slowly stabilizing itself at a new level after rising rather rapidly from the low levels of the last glaciation. Areas of the seafloor that have been drowned in the last few thousand years have been sources of supply of sediment to the nearshore zone — but perhaps they will become depleted! Workers in the Netherlands and elsewhere have suggested that the erosion of some barrier-coastlines is due to the exhaustion of offshore sand supplies because of the erosion of the source area down to bedrock. Surely the same could be argued, particularly in tidal seas, for fine-grained sediment. The characteristic pattern of landward transport of fine-grained sediment into estuaries, so common in areas such as the North Sea and elsewhere, may not be a process that will continue indefinitely. This of course would be greeted with relief by coastal engineers plagued by siltation in estuaries but with dismay by land-hungry reclaimers of marginal intertidal areas.

Attention has been drawn by some speakers to the erosional effects of storms, both as agents of removal of sediment (Anderson) and then subsequent effect on the fauna of estuaries. However, although such events may lead to the export of sediment from estuaries and lagoons, it seems very important to stress that estuaries and their adjacent coastal plains have accumulated vast volumes of fine-grained sediment, certainly since and during the latest rise of sea level. To the geologist, these deposits are very impressive. In the Severn Estuary U.K., tens of metres of fine-grained sediment, covering hundreds of square kilometres, have accumulated during this period. Similar large deposits border the flanks of the Thames U.K., and the Carse Clays of the Tay Scotland U.K. are very extensive. In these estuaries, the estuarine channels seem to have been trapped in their own marginal fine-grained deposits. Elsewhere, the channel systems seem to have been able to migrate laterally and have managed to build up sand accumulations with much less impressive accumulation of fine-grained material. The differences between such estuaries is perhaps worthy of more attention.

Throughout the discussion, frequent mention has been made of the seemingly fairly well understood turbidity-maxima in estuaries, which sometimes show more complex

Printed in Canada (J6980)
Imprimé au Canada (J6980)

features due to late-ebb runoff (Dobereiner and McManus). These sometimes appear to have led to extraordinary accumulations of "fluid mud" which, as so strikingly demonstrated by Kirby and Parker, often settle to form semiplastic layers and ultimately relatively consolidated deposits (Bryant and Williams; Smith and Williams). However, a point on which a great deal of ignorance still appears to exist is how old are these plugs of muddy water and their semiconsolidated deposits. What is the residence time of such turbid bodies of water in an estuarine system? Do they build up over tens of hundreds of years and then either become entrapped on the adjacent marginal areas, due to man-made changes, or are they periodically flushed out into the nearby marine environment? Even then are they lost or do they return to the estuary? This must be a point that needs investigation in view of the heavy metal pollution in many coastal estuaries. Surely some tagging could be done to see what is the ultimate fate of such fine-grained sediment.

The problem of data collection has arisen many times during the discussions. The siting of stations from which the data are to be collected is difficult. It was clearly demonstrated by Koske's reiteration of the presence of separate water bodies that behave distinctly in estuarine systems. With the advent of large-scale air-photographs, remote sensing, and an appreciation of such phenomena, these sites will be easier to select.

A very timely warning was given by Caspers on the interpretation of variations and the need of caution in interpreting them as being due to man's interference. The rapidity and frequency of natural changes which are not yet readily explainable show what a ready trap awaits the provider of any quick glib answer to such questions. The difficulty of interpreting why particular changes occur even when the degree of man's interference was quite well-known was amply demonstrated by de Jonge's paper on the effects of dredging on the Ems Estuary. Is the increased turbidity due merely to the scale of the dredging? Is it temporary, or is it due to deepening of the tidal channels and the subsequent increased intertidal erosion at low water stages? Or is it due merely to the notorious leaky vessels of the dredgers?

The effects of organic agencies on the deposition of fine-grained sediment was a topic touched upon by many speakers. Although the increased erosion produced by turbulence caused by the tubes of *Lanice conchilega* was discussed (Cary), little mention was made of the incredible ability of some suspension feeders such as *Mytilus edulis* to fix large volumes of fine-grained sediment in areas where velocities are high and deposition of this material would otherwise not occur. The work of Verwey (1952) in the Dutch Wadden Sea among others has shown the efficiency of such creatures.

Similarly, the blue-green algae surprisingly were hardly mentioned. These most effective binders and stabilizers of sediment merit further attention, particularly their role as inducers of intertidal accretion.

Physiochemical flocculation and the production of aggregates by organic processes (the products of both processes leading to more rapid deposition) were commonly reported phenomena. However, there still seems to be a great need for much more detailed studies on the organic aspects of the production of flocs. What is the relative importance of inorganic produced aggregates on the one hand and the production of fecal clots on the other hand? There appears to be a field of study which needs the cooperation of the sedimentologist and the microbiologist. As estuaries are areas of such high organic productivity the organic effects must be very considerable.

The great problem of prediction remains perhaps the most difficult one that faces estuarine scientists. However, the application of numerical modeling to this problem as exemplified by Uncles' work on the Severn Estuary U.K. and Greenberg and Amos on the Bay of Fundy seems very encouraging. The ensuing discussion showed how necessary it is, if these models are to be realistic and useful, to determine all the parameters that are used locally and not to glean them from the literature. If they are based on good and reasonably abundant, locally derived field data, they provide, as their proponents so persuasively argued, a most valuable tool to deal with large natural systems and to predict what variations of particular factors are likely to result from man's interference. But what music to the ears of those that have been drawn into the study of nearshore systems because of their love of the open air to hear that more and more good field data are required!

I, like my co-chairman Peter Wangersky, would like to close with a plea for the establishment of long-term continuous programs of scientific research based in government institutes. It is impossible for university staff with their multiple commitments to devote the money and more importantly, the continuous attention to long-term programs. Measurements often have to be made day after day and perhaps, following a large storm, a large number of personnel have to be marshalled into service for a critical few days at very short notice. This is not to say that universities have no role to play in such studies. They can provide an invaluable source of good quality, low cost, and often very ingenious scientific personnel in the form of research students. These, with the guidance of their supervisors, should be coordinated into such programs. The institutes, however, remain the only establishments which can give continuity to such programs. They should not — as has happened too often in the past — just go into an area and do a short-term study when economic considerations demand it. Long-term planning by them and cooperation with the universities seem the only sensible way to proceed. There seem to be great opportunities in a country such as Canada which is not yet so beset with economic problems as the old world and where man still has barely had a chance to influence the natural scene.

GIBBS, R. J. 1967. The geochemistry of the Amazon River system, Part 1. Bull. Geol. Soc. Am. 60: 561–590.

VERWEY, J. 1952. On the ecology of distribution of cockle and mussel in the Dutch Wadden Sea, their role in sedimentation and the source of food supply, with a short review of the feeding behaviour of bivalve molluscs. Arch. Neerl. Zool. 10: 171–239.

Concluding Remarks of Session Chairmen at the Dynamics of Turbid Coastal Environments Symposium, IV

PETER J. WANGERSKY

Department of Oceanography, Dalhousie University, Halifax, N.S. B3H 4J1

THIS symposium gathered together scientists working in those unusual environments marked by high turbidity, and usually by high energy, in an attempt to compare problems, exchange solutions, and seek common factors in their diverse working areas. One of the first impressions I have gained from these presentations, however, is the uniqueness of each environment. For example, we can look at the Seine, where the high particulate phosphorus seems to be primarily in the form of phosphate, instead of the expected organic compounds. There are also the deeper parts of the Severn Estuary, with their bands of pseudo-plastic suspended matter which neither disperse nor settle, like Mahomet hovering forever between Heaven and Earth. Then there are the thin muds, or thick soups, of the west coast of Korea, aerobic to depths far below those of any sensible mud. We must not forget our own Minas Basin, carrying a sediment load which is uniform from top to bottom, kept that way by the high tidal velocities. It would seem that each of these environments is special enough so that insights gained in one area could hardly be transferred to any other.

Yet there are recurrent themes in these presentations. One such theme is the control of primary productivity through light limitation. In the paper presented by de Jonge, the deleterious effect of high suspended loads on the production of phytoplankton is clearly shown, and in many of the other papers, including that of Biggs et al., primary production has clearly stopped long before the available inorganic nutrients have been consumed. One might be justified in concluding that these estuaries could be improved markedly as fish nurseries and feeding grounds by curbing those of man's activities which add to the particulate load of the rivers.

However, we must not get carried away by our enthusiasm for salmon, shad, lobster, and other end products of the estuarine food chain. In many of these estuaries the particle load is almost entirely inorganic, and the sources of the nutrients are uncoupled from the sources of the suspended matter. Thus, a decrease in particle load would result in an increase in light penetration, but no concommitant decrease in nutrient load. This way lies anoxia, noxious blooms of blue-green algae, and all the other horrors of extreme eutrophication. Perhaps what we should be seeking in our computer models is an optimum balance between particle load and nutrient regeneration, one which will permit a high level of secondary and tertiary productivity and yet leave the estuary a pleasant site for man's recreational activities.

This leads directly into the topic of computer modeling of the estuaries. To this point, we have been satisfied — nay, overjoyed — if our computer models could approximate the present or the recent past in our systems. Obviously, if we wish to control, we must predict, and prediction, at least so far, has escaped us. It may be that true prediction will always escape us. We could look to the lack of success of contemporary economic models in predicting the curious doldrums in which we now wallow, and in prescribing any useful remedies. Economic models are excellent at telling us how we got into our present mess, but could not allow ahead of time for the creation of OPEC; similarly, our environmental model of an estuary may predict the results of the continuance of trends already evident, but may not be able to handle the restructuring of a river bed brought about by a major flood.

The presentations also point out the importance of the unique event. Much of our sampling is done on some predetermined schedule, with the frequency of sampling being a compromise between the amount of time available for working up the samples, the amount of ship time we can scrounge from other programs, and the amount of overtime and weekend pay we can squeeze from our already suffering budgets. If some unique event occurs between scheduled sampling periods, we may miss it altogether, or we may be presented with a change in regime for which we have no cause. I have been told of a river in Vermont which normally discharges 90% of its annual sediment load in 3 days. If the hydrographers had not been stranded in the area by the flood, they would have miscalculated the contribution of that river rather badly. We have estuaries with sand beaches in Nova Scotia where the very form of the beach changes with each easterly gale. Our sampling schedules are usually very good at showing us long-term and seasonal changes, giving us the background upon which the unique event acts. If we are to understand the effects of extraordinary events, we must be in a position to sample before, during, and after these events.

Another recurrent theme in the presentations is the high variability in both space and time. Milliman's discussion of the sediment load in the Yangtse River, Anderson's comments on sources of variability in muddy intertidals, de Jonge on the Ems, and particularly Koske on the Elbe and the Weser, all point out how badly one could be led astray by a sampling program which is either too sparse or badly chosen. I would enter a plea here for the development of instruments which furnish continuous records of the variables being measured. In blue-water oceanography we have traditionally relied upon the principle of continuity; we have assumed that the quantity we have measured varied smoothly between sampling points. This would not seem to be a risky assumption in what appears to be a featureless expanse of open sea. Yet every new instrument capable of measuring some variable continuously in either space or time has shown us discontinuities in that variable. Furthermore, when we have measured several variables at the same time, we have found that the discontinuities in the several variables are not necessarily coincident. How much more must this be the case in rivers and estuaries, where bottom topography and shape of the channel and coastline play so large a role in determining the distributions of water currents and velocities?

Printed in Canada (J6984)
Imprimé au Canada (J6984)

Our studies of changes in the environment are complicated by our only too evident desire to understand the workings of the environment, so that we seek causes for every noticeable effect. Correlations are only too easy to find, particularly with the newer computer statistics packages which permit multiple correlations and factor analyses at the pointing of a finger. Perhaps there was some virtue to the old mechanical calculators; in those days, we attempted no correlations unless we had some reason to believe we had isolated a cause and an effect, and not simply a co-occurrence.

Our belief in a deterministic universe is so great that we are more than willing to look at population change, either of number or of kind, as certain evidence of the efficacy of our latest manipulation. Yet Caspers has shown that even with no discernable change in environmental conditions, populations wax and wane, succeed and are replaced by other populations. We can always speak in terms of subtle changes, of unknown requirements, and if we search long enough we will certainly find such changes. If we now try to recreate the conditions, we will find we have not recreated the populations, and we will speak again of subtler changes.

There is certainly no need to look upon all population changes as reflections of environmental changes. If we accept the condition that nutrients need not be distributed homogeneously in time and space, but may instead occur in packets, large or small, arriving here and there, we can then furnish a strong theoretical basis for the occurrence of population changes in an otherwise unvarying universe. Before we assign all unwelcome population changes to the effects of man's interference with Nature, and all welcome ones to our efforts to undo this interference, we must know the variability to be expected in a given ecosystem in the absence of obvious change. Someone at this symposium has already used the quotation that "one man's noise is another man's signal"; this is true enough, but unless we understand the nature of the signal and its associated noise, we will be forever mistaking normal noise for purposeful signal, interpreting and reacting to a variability we cannot reduce, and wondering why our remedies do not seem to work.

Finally, I would note that in some of the investigations reported here there are too many pieces missing. Where the engineering approach has been taken, perhaps the geochemistry or the specialized knowledge of the taxonomist is lacking. When the geologist has managed to combine forces with the physical oceanographer, they have still missed the contribution which might have come from a chemical oceanographer. This kind of applied research requires the team approach to be truly successful. Such teams can only be organized within or between government laboratories. While in principle a team could be assembled by a university or a consortium of universities, no university department has the support staff necessary to gather and process the data going into an estuarine model. Furthermore, no university staff or faculty has the stability of a government laboratory, the stability needed to undertake a project which may run for 10 or more years, possibly with little in the way of publishable results for the first 3 or 4 years.

While the scientific direction of such a project may rest in the hands of a committee of senior scientists, ultimately one person must have the authority to decide between alternative research strategies. Although I may have the utmost respect for my fellow academics as research scientists, I cannot imagine that they would accept, either meekly or otherwise, the decisions of some single authority on the direction of their research efforts. University scientists may be very usefully employed within the larger framework of an area project, and should perhaps be used as consultants called in to ensure that no important area of research has been overlooked. The research team, particularly the large team aimed at the investigation of the physical and ecological regime of a relatively large system, should have the permanence, completeness, and direction available only in government laboratories.

Concluding Remarks of Session Chairmen at the Dynamics of Turbid Coastal Environments Symposium, V

H. POSTMA

Netherlands Institute for Sea Research, P.O. Box 59, Den Burg, Texel, The Netherlands

THE symposium demonstrated, once again, that coastal environments, and even the special class of turbid environments discussed, exhibit a wide range of conditions. To arrive at generalizing concepts it is necessary to ask a number of fundamental questions, of which the answers make such environments mutually comparable and which, at the same time, define the size of the basic processes taking place. Such questions should concentrate on the budgets and cycles of water, sediment, and organic matter and their mutual relations.

The first fundamental question concerns the residence time of water masses. An answer to this question is essential to understand the degree of autonomy of a coastal system and the influence exerted on the system from outside. Depending on the state of the art it has to be answered in smaller or greater detail. The most straightforward answer is obtained if the flushing time of a tracer can be measured, for example a well-defined inflow of river water. If such a tracer is not available, as in the case of the Bay of Fundy, it is imperative to describe water movements in great detail. Such a description should include a study of the residual circulation, which because of the complicated topography will be both tidal and wind driven, and a study of tidal turbulence and diffusion. A large tidal range does in itself not necessarily cause a fast water exchange, since the shape of a basin, wide or elongated, is also of great importance.

The second question is about the processes causing dispersion or accumulation of the mobile sediments. These processes act in a different manner on different grainsize fractions, but in the Bay of Fundy the fine-grained fraction is obviously the most important one. To answer the question it is often quite useful to consider also geological development. The Bay has a particularly interesting history, since the large vertical tides now found in the inner bay have developed gradually since 5000−6000 BC and are still increasing with about 15 cm per century. The mud seems originally to have been dispersed over a large area of the Bay, but has subsequently become concentrated in its inner parts as shown by the burial of entire saltmarsh communities in Minas Basin about 4000 BC.

Several concepts have been developed on tidal accumulation mechanisms for finegrained materials, ranging from the simple "bathtub" trapping mechanism, first assumed to act in the French macrotidal systems, to more elaborate mechanisms based on ebb and flood current asymmetries. A start of studies on this subject has been made in the Bay of Fundy. For the Minas basin it has been assumed that the mud enters the area from outside. This is quite probable, but one should be aware of the fact that it is almost impossible to derive residual transport of mud from budget measurements at tidal stations. Shore erosion seems to supply chiefly sandy materials and the addition of mud by rivers is extremely small; therefore, it is almost certain that the turbidity of the inner Bay is caused by constant recycling of old mud, including reworking of old deposits.

The third central question concerns the degree of autonomy in a given area of the various cycles of biologically important elements or, inversely, the relative importance of export towards and import from adjacent areas. Most important in this respect is the cycle of organic carbon. Regarding the autonomous cycle, it has been shown in the inner parts of the Bay of Fundy that phytoplankton productivity is very low. In this respect the bay is quite comparable to other very turbid areas. Most probably, primary productivity in the much clearer central area is considerably larger, even on a volumetric basis. This opens the possibility of input of organic matter from the outer to the inner parts of the bay by water exchange. This process may be supported by the fact that particulate organic matter behaves like fine-grained sediment and, therefore, may be trapped in the inner basins.

As in the case of mud, residual transport of organic carbon might be difficult to measure directly at fixed tidal stations. Indirectly, however, it might be measured by looking at the cycle of another element, for example a nutrient. In this respect dissolved mutrient concentrations show a decrease seaward so that there should be an export of dissolved nutrients from the inner basins to the open Bay of Fundy. Assuming, again, that river supply of nutrients, except perhaps silica, is negligible, this export can only be compensated for by import of particulate organic matter.

The magnitude of this exchange process, and its quantitative relation to local production of organic matter, can only be estimated if rates of water exchange, i.e. residence times, are known. Also, it would be very important to find out what part of particulate organic matter indeed behaves like very fine-grained sediment. This exposition shows how the three main questions, in three different disciplines, are interconnected.

Compared to phytoplankton production, primary production of micro-algal on high sandflats in the Bay of Fundy is very high and indeed not lower than on intertidal sandflats in less turbid areas. This, of course, is due to the condition that the high sandflats are covered with turbid water only during a small part of the tidal period; just above the low water line productivity is most probably much smaller. In fact, tidal flats in a turbid environment may be better off than in a clear environment, since in the former, nutrients are not easily depleted in the water column so that their supply is more firmly assured all year round.

In addition to micro-algal production there is a large production of organic matter by Spartina and other plants in the marshes surrounding the Bay of Fundy, the remains of which might contribute to the fertility of the area as a whole by export from their growing sites into deeper water. No study

Printed in Canada (J6985)
Imprimé au Canada (J6985)

has yet been made on the size of this contribution, which might be substantial.

Because of lack of data, one can at present only guess that the autonomous carbon cycle is less important than the import–export cycle. Pieces of information on the production side are missing but even less is known on mineralization rates. It should be mentioned that although organic carbon percentages in the mud and in the mud suspensions are low (less than 1%), the organic load is still significant because of the high mud concentrations. A study of mineralization might reveal, however, that a considerable part of the organic matter is refractory.

The study of present physico-chemical, sedimentological, and biological processes in the Bay will facilitate predictions of the new equilibria that will be established during and after the building of a tidal barrage. Probably it is too early to speculate about equilibrium shifts. It is quite obvious, however, that key factors will be the changes in tidal strengths and shapes on both sides of the barrage and the accompanying changes in turbidity. This feature is accessible to quantitative prediction. The subsequent ecological consequences might be more difficult to predict but an increase in water transparency behind the barrage, for example, would almost certainly lead to a higher productivity and, therefore, to an ecological system of which comparable examples can be found elsewhere in the world. Whether import of organic matter into the newly formed basin would decrease or increase would require a separate study, but since it is related to mud transport it might also be predicted. Changes in tidal range would further have a profound effect on the ecology of the surrounding marshes or cause losses of marsh areas. Modification of marshes by civil engineering occurs on a worldwide scale so that several examples useful for a comparison may be indicated.

Concluding Remarks of Session Chairmen at the Dynamics of Turbid Coastal Environments Symposium, VI

A. R. LONGHURST

Department of Fisheries and Oceans, Ocean Science and Surveys, Bedford Institute of Oceanography, P.O. Box 1006, Dartmouth, N.S. B2Y 4A2

SUCH a symposium as this one gives everyone who attends it something new to take away with them — not only new facts, but also new concepts — as well as reinforces some of their opinions concerning the subject of the symposium. I want to point to some things which have been new to me, and some old ideas that have been reinforced, rather than to try to summarize the salient points of the whole symposium, or of the session with which I have been mostly concerned.

In fact, I do not think that such a summary would be very useful, and indeed there is a sense in which it would be misleading: several speakers have referred to the results presented in this symposium as a kind of statement of where we are in research in turbid waters, and of what we know about how they work. I think this is actually not correct, for what we have heard in the last few days is only the tip of the iceberg as far as the sheer volume of such research is concerned. Those who have been connected with the research itself are well aware of how much has been left undiscussed; for myself, I know that what has been said of the GEMBASE model, and the research associated with it, was calculated neither to expose the full scope of the work, nor to evaluate its usefulness in understanding turbid estuaries — to have done so would require a symposium devoted solely to that topic. This is a perennial problem, and one for which I know no solution: how to marshal a very large, complex, and evolving corpus of work within a small compass, either of a report or of a symposium. Especially when we come to use our ecology for practical purposes it is so easy to ignore the main body of what has been done in the past, and to hope to answer our new questions with some new research which adds but relatively little to our whole understanding of a subject, or even of a region.

So what will I take away from this symposium that is quite new to me? I think two principal things. Firstly, the simple fact that a turbid coastal environment is not necessarily macrotidal, or even mesotidal. The descriptions of the glutinous mud banks along the Louisiana coast were a revelation to me, and the manner in which they damp the energy of swell arriving at the coast was very striking. The coastwise migration of fluid mud banks here and elsewhere was also a revelation, and was connected with the second topic which I had not thought much about before, but was forced to do so by this symposium. Thus, I shall also carry away a new understanding of the extent to which the turbidity one studies may have originated very distantly; particularly striking, I thought, were the data on the mud-drowned estuaries of southwestern Korea where no local source appears to exist, yet where the stupendous output of silt from the rivers of China, across the Yellow Sea, must be looked at as a candidate source. The photographs of endless mud-flats on the coast of China in one of the poster exhibits were a related revelation. Thirdly, and I think in common with many others with whom I talked, I was struck by a new understanding of the complexities of the mud–water interface; the biological complexities I had expected, but not the physics of fluidification and cohesion which were introduced by so many speakers.

And now, in what did the symposium reinforce my prejudices and opinions? Firstly, and most strongly, that we have not by any means all of us understood the multidisciplinary nature of what makes for a successful study of sedimentation and the ecology of turbid areas; there are still too many papers in which the author fails to convince me that their physical — or chemical, or biological — approach to their subject, and their explanation for the mechanism of their study, adequately reflects nature. Too many people do not yet work in comprehensive teams, and appear to consider that a unitary approach (both in the discipline and the regional sense) will be successful; it seemed to me that we saw some examples of this in our symposium. Secondly, I have always wondered how far one could generalize about estuaries and other inshore environments, and this symposium reinforced my conviction of the dangers of extrapolation between such regions where the accidents of topography and of tidal regimes — both acting as independent and unique forcing functions — differ in every single area studied. Consequently, I am by no means surprised that the ranks of coastal oceanographers have thrown up no Stommel's or Swallow's; even such generalizations as can be dragged out — that the Coriolis phenomenon acts similarly in all estuaries, tending to put more water seawards along one bank than the other — are commonly ignored, and such a pattern of circulation often reported as if unique.

Finally, though the symposium did not address the matter, I am now even more perplexed to understand the nature of the advice that ecologists — defining the field broadly — will be capable of giving to administrators in the environmental assessment of the consequences of coastal engineering projects. On the one hand, from analytical studies of single phenomena or single groups of organisms it is relatively easy to draw out nonquantitative advice which will be understood and appreciated by others in the same field of study, but with which an engineer may have trouble because of its nonquantitative nature, and because the individual pieces of advice cannot be made formally to interact. On the other hand, from synthetic, model-building simulation studies one can readily draw quantitative advice welcomed by the engineer for its interactive abilities; but it may be very difficult to get agreement with nonmodeling colleagues that the output, and hence the advice, bears any relation to ecological reality. In both kinds of research for advice, the difficulties become greater as one

Printed in Canada (J6982)
Imprimé au Canada (J6982)

proceeds down the messy road from physics to biology. I am convinced we haven't got it right yet, I can see very little evidence in this symposium that we are getting smarter at how to formulate advice — especially ecological advice — and I worry about it because we shall all be on the firing line in the next few years if tidal energy barrages of great size go ahead in Fundy and Severn — and that, after all, was the origin of this symposium even if we didn't talk about it very much.

Papers Presented at the Symposium

Authors and titles of papers presented verbally in sequence given at the symposium. Speakers are underlined.

M. P. Kendrick and B. V. Derbyshire (UNITED KINGDOM)
Factors affecting the supply and distribution of sediment in the turbid coastal environment

J. Milliman (USA)
The transfer of suspended sediment load from the Yangtse River to the East China Sea

J. T. Wells (USA)
Dynamics of coastal fluid muds: low-, moderate- and high-tide range environments

R. B. Biggs, J. H. Sharp, T. M. Church, and C. H. Culberson (USA)
Optical properties and chemistry associated with the turbidity maxima of the Delaware Estuary

D. C. Rhoads and L. F. Boyer (USA)
Estuarine turbidity: biogenic processes controlling changes in seafloor erodibility in Central Long Island Sound

G. V. Winters (CANADA)
Suspended sediment dynamics of the inner Miramichi Estuary, New Brunswick, Canada

K. Kranck and D. S. Bezanson (CANADA)
Current control of bottom sediment grain size modes

L. J. Albright (CANADA)
Heterotrophic bacterial biomasses, activities and productivities within the Fraser River plume

G. E. Farrow, J. P. M. Syvitski, and V. Tunnicliffe (UNITED KINGDOM AND CANADA)
Suspended particulate loading on the macro-benthos in a highly turbid fjord; Knight Inlet, British Columbia

F. E. Anderson (USA)
The northern muddy intertidal: a seasonally changing source of suspended sediments to estuarine waters — a review

J.-F. Guillaud (FRANCE)
Nutrient fluxes in the Seine Estuary (France); the role and significance of the turbidity maximum during estuarine mixing

W. Helder and M. M. Rutgers van der Loeff (NETHERLANDS)
Observations on the regeneration of nitrogen nutrients and silica in the Ems–Dollard Estuary

V. N. deJonge (NETHERLANDS)
Reasonable increase in suspended matter concentrations of the Ems Estuary between 1954–1980 due to dredging operations and its significance for the ecosystem

P. H. Koske (WEST GERMANY)
Observations on quasi-permanent convergences in highly turbid mixing regions of tidal-influenced river estuaries

H. Caspers (WEST GERMANY)
The characteristics of turbid environments: effects of sedimentation on the benthos in the outer part of the Elbe Estuary

D. H. Loring, R. T. T. Rantala, A. W. Morris, A. J. Bale, and R. J. M. Howland (CANADA AND UNITED KINGDOM)
The chemical composition of suspended particles in an estuarine turbidity maximum zone

D. A. Carey (UNITED KINGDOM)
Particle resuspension in the benthic boundary layer by a tube-building polychaete

C. Dobereiner and J. McManus (UNITED KINGDOM)
Turbidity maximum migration and harbour siltation in the Tay Estuary

R. J. Uncles (UNITED KINGDOM)
Modelling of physical processes in the Bristol Channel as a prerequisite for ecosystem studies

D. A. Greenberg and C. L. Amos (CANADA)
Suspended sediment transport and deposition modelling in the Bay of Fundy, Nova Scotia — a region of potential tidal power development

R. Bryant and D. J. A. Williams (UNITED KINGDOM)
(Presented by R. Kirby)
Characteristics of suspended cohesive sediment in the Severn Estuary

R. Kirby and W. R. Parker (UNITED KINGDOM)
The distribution and structure of fine sediment phenomena in the Severn Estuary

T. J. Smith and D. J. A. Williams (UNITED KINGDOM)
Evidence for the existence of a new mechanism for fine sediment deposition in estuaries

M. F. C. Thorn and T. N. Burt (UNITED KINGDOM)
Sediments and metal pollutants in a turbid tidal estuary

P. D. Keizer and D. C. Gordon (CANADA)
Nutrient dynamics in the turbid waters of Chignecto Bay, Bay of Fundy

I. R. Joint (UNITED KINGDOM)
The development of an ecosystem model of a turbid estuary

D. J. Wildish and D. L. Peer (CANADA)
Tidal current speed and production of benthic macrofauna in the lower Bay of Fundy

B. T. Hargrave, N. J. Prouse, G. A. Phillips, and P. A. Neame (CANADA)
Primary production and respiration in pelagic and benthic communities at two intertidal sites in the upper Bay of Fundy

P. Schwinghamer, F. C. Tan, and D. C. Gordon (CANADA)
Stable carbon isotope studies on the Pecks Cove mudflat ecosystem in the Cumberland Basin, Bay of Fundy

M. J. Risk and R. K. Yeo (CANADA)
Organism-sediment interdynamics in a turbid macrotidal environment, Minas Basin, Bay of Fundy

G. R. Daborn, M. Brylinsky, C. M. Gilmurray, K. W. Strong, G. S. Brown, and C. Pennachetti (CANADA)

Occurrence, movements and role of zooplankton in the upper regions of the Bay of Fundy system

M. J. Dadswell (CANADA)
Effect of turbidity on the temporal and spatial utilization of the Bay of Fundy by shad (*Alosa sapadissima*) and its relationship to local fisheries

P. N. Ferns (UNITED KINGDOM)
Sediment mobility in the Severn Estuary and its influence upon the distribution of shorebirds

Poster Papers Presented at the Symposium

D. Baird and H. Milne (UNITED KINGDOM)
Energy flow in the Ythan Estuary, Aberdeenshire, Scotland

B. Balch, P. C. Reid, and S. C. Surey-Gent (UNITED KINGDOM)
Spatial and temporal variability of dinoflagellate cyst abundance in a tidal estuary

J. S. Bleakney (CANADA)
Entombment of Minas Basin flora and fauna (4470–3750 BP) and erosional exposure of same (60–40 BP)

M. B. Collins (UNITED KINGDOM)
Suspended sediment transport in the Bristol Channel based on Landsat imagery and survey data

G. R. Daborn and P. Smith (CANADA)
Corophium, fish and shorebird interactions in the Bay of Fundy

B. d'Anglejan, J. P. Savard, and R. G. Ingram (CANADA)
Time series observations in the turbid boundary layer of the St. Lawrence Estuary

J. H. B. W. Elgershuizen and P. M. B. Stortelder (NETHERLANDS)
A direct measurement of the transport of organic matter in the eastern Scheldt (southwest Netherlands): application of a trend surface method

D. V. Ellis, T. Kessler, G. C. Geen, and C. Pelletier (CANADA)
Statistical reconnaissance of monitoring data from a decade of mine-driven turbidity

R. W. Faas (USA)
Viscous behavior patterns of fluid mud suspensions

H. Farke, S. A. Gerlach, and M. Schulz-Baldes (WEST GERMANY)
The caisson as a new tool in intertidal field experiments

R. J. Gibbs (USA)
Flocculation processes in the Delaware Estuary/Bay

M. Nichols (USA)
Response and recovery of sediment to Kepone contamination

M. A. Palmer and B. Coull (USA)
Saltmarsh sediment transport and the resuspension of meiobenthos

J. W. Pierce, D. L. Correll, M. A. Faust, W. H. Klein, and B. Goldberg (USA)
Attenuation of underwater light, Rhode River, Maryland

M. Pommepuy, M. Cornier, and A. Aminot (FRANCE)
Behavior of bacterial populations from sewage outfalls discharged into the Bay of Brest (France): relations with particulate suspended matter

C. Vale and B. Sundby (PORTUGAL)
The relationship between the turbidity maximum and the tidal amplitude in a coastal plain estuary

L. A. van Geldermalsen (NETHERLANDS)
Import-export measurements of nutrients in a tidal area in the eastern Scheldt

I. L. van Heerden and J. T. Wells (USA)
River-dominated suspended sediment deposition in a new Mississippi subdelta

Y. Wang (CHINA)
The mudflat coast of China

List of Participants

ALBRIGHT, L. T. Department of Biological Sciences, Simon Fraser University, Burnaby, B.C., Canada V5A 1S6

AMOS, C. L. Woodward Clyde Consultants, 29 O'Leary Avenue, St. John's, Nfld., Canada A1C 5P5

ANDERSON, F. E. Department of Earth Sciences, University of New Hampshire, Durham, NH 03824, USA

BAIRD, D. Department of Zoology, University of Port Elizabeth, P.O. Box 1600, Port Elizabeth 6000, Republic of South Africa

BALCH, W. M. Institute of Marine Resources — A018, Scripps Institute of Oceanography, La Jolla, CA 92093, USA

BARRIE, J. V. C-Core, Memorial University of Newfoundland, St. John's, Nfld., Canada A1B 3X5

BEUNDERS, J. P.O. Water Resources Branch, New Brunswick Environment, Box 6000, Fredericton, N.B., Canada E3B 5H1

BIGGS, R. B. College of Marine Studies, University of Delaware, Newark, DE 19711, USA

BLEAKNEY, J. S. Department of Biology, Acadia University, Wolfville, N.S., Canada B0P 1X0

BOWEN, A. J. Department of Oceanography, Dalhousie University, Halifax, N.S., Canada B3H 4J1

BOYER, L. F. Department of Geology and Geophysics, Yale University, P.O. Box 6666, New Haven, CT 06511, USA

BRADFORD, J. D. Department of Fisheries and Oceans, 7th Floor, 240 Sparks Street, Ottawa, Ont., Canada K1A 0E6

CAMMEN, L. M. Bigelow Laboratory, West Booth Bay Harbour, ME 04575, USA

CAREY, D. A. Gatty Marine Laboratory, The University, St. Andrews, Fife, Scotland KY16 8LB

CASPERS, H. Institute für Hydrobiologie und Fischereiwissenschaft, Zeiseweg 9, 2000 Hamburg 50, F.R.G.

CATALOTTI-VALDINA, D. Université du Québec, Institut National de la Recherche Scientifique, 310, avenue des Ursulines, Rimouski, Qué., Canada G5L 3A1

CHARRON, R. L. Brunswick Mining and Smelting Company, Smelting Division, Belledune, N.B., Canada E0B 1G0

COLLINS, M. B. Department of Oceanography, University College, Singleton Park, Swansea, South Wales, U.K.

DABORN, G. R. Department of Biology, Acadia University, Wolfville, N.S., Canada B0P 1X0

DADSWELL, M. J. Department of Fisheries and Oceans, St. Andrews Biological Stn., St. Andrews, N.B., Canada E0G 2X0

DALE, J. Marine Ecology Laboratory, Bedford Institute of Oceanography, P.O. Box 1006, Dartmouth, N.S., Canada B2Y 4A2

DALRYMPLE, R. W. Department of Geological Sciences, Queens University, Kingston, Ont., Canada K7L 3N6

D'ANGLEJAN, B. Institute of Oceanography, McGill University, 3620 University Street, Montreal, Qué., Canada H3A 2B2

DESPLANQUE, C. Maritime Resource Management Service, P.O. Box 310, Amherst, N.S., Canada B4H 3Z5

DURVASULA, S. R. V. Marine Ecology Laboratory, Bedford Institute of Oceanography, P.O. Box 1006, Dartmouth, N.S., Canada B2Y 4A2

ELGERSHUIZEN, J. H. B. W. Delta Service of the State Department of Public Works, Postbus 439, Grenadierweg 31, 4330 AK Middelburg, The Netherlands

ELLIS, D. V. Biology Department, University of Victoria, Victoria, B.C., Canada V8W 2Y2

ESSINK, K. Government Institute for Sewage and Waste Water Treatment, Hereweg 99A, 9721 AA Groningen, The Netherlands

EVANS, G. Imperial College, Department of Geology, Prince Consort Road, London SW7 2BP United Kingdom

FAAS, R. W. Department of Geology, Lafayette College, Easton, PA, U.S.A. 18042

FARKE, H. Institut für Meeresforschung, Am Handelshafen 12, 2850 Bremerhaven, W. Germany

FARROW, G. E. Department of Geology, University of Glasgow, Glasgow, G12 8QQ Scotland

FERNS, P. N. Zoology Department, University College, P.O. Box 78, Cathays Park, Cardiff, CF1 1X1, United Kingdom

GELDERMALSEN, L. A. VAN. Delta Institute for Hydrobiological Research, Vierstraat 28, 4401 EA Yerseke, The Netherlands

GIBBS, R. J. College of Marine Studies, University of Delaware, Newark, DE 19711, USA

GORDON, D. C., JR. Marine Ecology Laboratory, Bedford Institute of Oceanography, P.O. Box 1006, Dartmouth, N.S., Canada B2Y 4A2

GRANT, J. Institute of Oceanography, Dalhousie University, Halifax, N.S., Canada B3H 4J1

GREENBERG, D. A. Atlantic Oceanographic Laboratory, Bedford Institute of Oceanography, P.O. Box 1006, Dartmouth, N.S., Canada B2Y 4A2

GUILLAUD, J. F. Centre Océanologique de Bretagne, B.P. 337, 29273 Brest Cedex France

HALL, H. A. Environment Canada, 5th Floor, Queen's Square, 45 Alderney Drive, Dartmouth, N.S., Canada B2Y 2N6

HARGRAVE, B. T. Marine Ecology Laboratory, Bedford Institute of Oceanography, P.O. Box 1006, Dartmouth, N.S., Canada B2Y 4A2

HAWKINS, C. Marine Ecology Laboratory, Bedford Institute of Oceanography, P.O. Box 1006, Dartmouth, N.S., Canada B2Y 4A2

HEERDEN, I. VAN. Coastal Studies Institute, Louisiana State University, Baton Rouge, LA 70803, USA

HELDER, W. NIOZ, Postbus 59, Den Burg, Texel, The Netherlands

HICKLIN, P. W. c/o Canadian Wildlife Service, P.O. Box 1590, Sackville, N.B., Canada E0A 3C0

HILL, S. Geomarine Associates Ltd., 5112 Prince Street, Halifax, N.S., Canada B3J 1L3

JAMIESON, W. D. Atlantic Research Laboratory, National Research Council, 1411 Oxford Street. Halifax, N.S., Canada B3H 3Z1

JOINT, I. R. Institute of Marine Environmental Research, Prospect Place, The Hoe, Plymouth, Devon, PL1 3DH, United Kingdom

JONGE, V. N. DE. Biological Research Ems–Dollard Estuary, c/o Biological Centre State University, Groningen Kerklaan 30, 9751 NN Haren, The Netherlands

KEIZER, P. D. Marine Ecology Laboratory, Bedford Institute of Oceanography, P.O. Box 1006, Dartmouth, N.S., Canada B2Y 4A2

KELLEY, J. T. Earth Science Department, University of New Orleans, New Orleans, LA 70122, USA

KENDRICK, M. P. Hydraulics Research Station, Wallingford, Oxon, England 35381

KIRBY, R. Institute of Oceanographic Sciences, Crossway, Taunton, Somerset, TA1 2DW, England

KNAUTH, H. Institut für Chemie, GKSS-Forschungszentrum, 2054 Geesthacht, F.R.G.

KOPPER, L. Geomarine Associates Ltd., P.O. Box 41, Station M, Halifax, N.S. Canada

KOSKE, P. Institut für Chemie, GKSS-Forschungszentrum, 2054 Geesthacht, F.R.G.

KRANCK, K. Atlantic Oceanographic Laboratory, Bedford Institute of Oceanography, P.O. Box 1006, Dartmouth, N.S., Canada B2Y 4A2

KULLENBERG, G. Inst. Phys. Oceanography, Haraldsgade 6, 2200 Copenhagen N, Denmark

LABAN, C. Rijks Geologische Dienst, P.O. Box 157, 2000 AD Haarlem, The Netherlands

LAKSHMINARAYANA, J. S. S. Department of Biology, University of Moncton, Moncton, N.B., Canada

LONGHURST, A. R. Ocean Science and Surveys Atlantic, Bedford Institute of Oceanography, P.O. Box 1006, Dartmouth, N.S., Canada B2Y 4A2

LORING, D. H. Atlantic Oceanographic Laboratory, Bedford Institute of Oceanography, P.O. Box 1006, Dartmouth, N.S., Canada B2Y 4A2

MACKNIGHT, S. MacLaren Plansearch Ltd., 1000 Windmill Road, Dartmouth, N.S., Canada B3B 1L7

MANN, K. H. Marine Ecology Laboratory, Bedford Institute of Oceanography, P.O. Box 1006, Dartmouth, N.S., Canada B2Y 4A2

MCMANUS, J. Tay Estuary Research Centre, University of Dundee, Dundee DDL 4HN Scotland

MIDDLETON, G. V. Department of Geology, McMaster University, Hamilton, Ont., Canada L8S 4M1

MILLIMAN, J. Woods Hole Oceanographic Institution, Woods Hole, MA 02543, USA

MITCHELL, M. Marine Sciences Research Center, State University of New York, Stony Brook, NY 11794, USA

MORRIS, A. W. Institute for Marine Environmental Research, Prospect Place, The Hoe, Plymouth, Devon, PL1 3DH, United Kingdom

NELSON, D. Coastal Carolina College, Conway, SC 29526, USA

NICHOLS, M. Virginia Institute of Marine Science, Gloucester Pt., VA 23062, USA

PALMER, M. A. Belle W. Baruch Institute for Marine Biology and Coastal Research, University of South Carolina, Columbia, SC 29208, USA

PEER, D. L. Marine Ecology Laboratory, Bedford Institute of Oceanography, P.O. Box 1006, Dartmouth, N.S., Canada B2Y 4A2

PHILLIPS, G. Marine Ecology Laboratory, Bedford Institute of Oceanography, P.O. Box 1006, Dartmouth, N.S., Canada B2Y 4A2

PIERCE, S. W. NHB MX 125, Smithsonian Institute, Washington, D.C., U.S.A. 20560

POMMEPUY, M. Centre Océanologique de Bretagne, B.P. 337, 29273 Brest Cedex France

POSTMA, H. Netherlands Institute for Sea Research, P.O. Box 59, Texel, The Netherlands

PROUSE, N. Marine Ecology Laboratory, Bedford Institute of Oceanography, P.O. Box 1006, Dartmouth, N.S., Canada B2Y 4A2

RHOADS, D. C. Department of Geology and Geophysics, Yale University, New Haven, CN 06520, USA

RISK, M. J. Department of Geology, McMaster University, Hamilton, Ont., Canada

ROWSELL, K. A. Public Works of Canada, Marine Directorate, Room E-519, Sir Charles Tupper Bldg., Riverside Dr., Ottawa, Ont., Canada K1A 0M2

RUXTON, T. D. Binnie and Partners, Artillery House, Artillery Row, Westminster, London SW1P 1RX United Kingdom

SAVARD, J. P. Institute of Oceanography, McGill University, 3620 University Street, Montréal, Qué., Canada H3A 2B2

SCARRATT, D. J. St. Andrews Biological Station, St. Andrews, N.B., Canada E0G 2X0

SCHROEDER, F. Institut für Chemie, GKSS-Forschungszentrum, 2054 Geesthacht, F.G.R.

SCHULZ-BALDES, M. Institut für Meeresforschung, 2850 Bremerhaven, W. Germany

SCHWINGHAMER, P. Marine Ecology Laboratory, Bedford Institute of Oceanography, P.O. Box 1006, Dartmouth, N.S., Canada B2Y 4A2

SERODES, J. Dept. Génie Civil, Université Laval, Ste-Foy, Qué., Canada G1K 7P4

SHARP, J. College of Marine Studies, University of Delaware, Lewes, DE 19958, USA

SMITH, T. J. Dept. of Civil Engineering, University College of Swansea, Singleton Park, Swansea, SA2 8PP, West Glamorgan, Wales

STERNBERG, R. W. Department of Oceanography, WB-10, University of Washington, Seattle, WA 98195, USA

SYVITSKI, J. P. M. Atlantic Geoscience Centre, Bedford Institute of Oceanography, P.O. Box 1006, Dartmouth, N.S., Canada B2Y 4A2

TAN, F. C. Atlantic Oceanographic Laboratory, Bedford Institute of Oceanography, P.O. Box 1006, Dartmouth, N.S., Canada B2Y 4A2

THORN, M. F. C. Hydraulics Research Station, Wallingford, Oxfordshire, OX10 8BA England

TOPINKA, J. Bigelow Laboratory for Ocean Sciences, West Boothbay Harbor, ME 04575, USA

TUNNICLIFFE, V. Institute of Ocean Sciences, P.O. Box 6000, 9860 West Saanich Road, Sidney, B.C., Canada V8L 4B2

UNCLES, R. J. Institute for Marine Environmental Research, Prospect Place, The Hoe, Plymouth, PL1 3DH, United Kingdom

VALE, C. Département de Océanologie, Université du Québec à Rimouski, Rimouski, Qué., Canada

WANG, Y. Atlantic Geoscience Centre, Bedford Institute of Oceanography, P.O. Box 1006, Dartmouth, N.S., Canada B2Y 4A2

WANGERSKY, P. J. Department of Oceanography, Dalhousie University, Halifax, N.S. Canada B3H 4J1

WARD, L. University of Maryland, Horn Point Environmental Laboratories, Box 775, Cambridge, MD 21613, USA

WARWICK, R. M. Institute for Marine Environmental Research, Prospect Place, The Hoe, Plymouth, PL1 3DH, United Kingdom

WELLS, J. T. Coastal Studies Institute, Louisiana State University, Baton Rouge, LA 70803, USA

WILDISH, D. J. St. Andrews Biological Station, St. Andrews, N.B., Canada E0G 2X0

WINTERS, G. Atlantic Geoscience Centre, Bedford Institute of Oceanography, P.O. Box 1006, Dartmouth, N.S., Canada B2Y 4A2

ZUILSTRA, J. J. Netherlands Institute for Sea Research, P.O. Box 59, 1190 AB Texel, The Netherlands

Behavior of nitrogen nutrients and silica in the Ems-Dollard Estuary
W. Helder, R. T. P. de Vries, and M. M. Rutgers van der Loeff 188–200
Chemical composition of suspended particles in an estuarine turbidity maximum zone
D. H. Loring, R. T. T. Rantala, A. W. Morris, A. J. Blake, and R. J. M. Howland 201–206
Sediments and metal pollutants in a turbid estuary **M. F. C. Thorn and T. N. Burt** 207–215
Heterotrophic bacterial biomasses, activities, and productivities within the Fraser River plume **L. J. Albright** 216–220
Vertical mixing and its effects on phytoplankton growth in a turbid estuary
R. J. Uncles and I. R. Joint 221–228
Primary production and respiration in pelagic and benthic communities at two intertidal sites in the upper Bay of Fundy
B. T. Hargrave, N. J. Prouse, G. A. Phillips, and P. A. Neame 229–243
Spatial and temporal variability of dinoflagellate cyst abundance in a tidal estuary
W. M. Balch, P. C. Reid, and S. C. Surrey-Gent 244–261
Stable carbon isotope studies on the Pecks Cove mudflat ecosystem in the Cumberland Basin, Bay of Fundy **P. Schwinghamer, F. C. Tan, and D. C. Gordon Jr.** 262–272
Suspended particulate loading on the macrobenthos in a highly turbid fjord: Knight Inlet, British Columbia **G. E. Farrow, J. P. M. Syvitski, and V. Tunnicliffe** 273–288
Relations between annual dredging activities, suspended matter concentrations, and the development of the tidal regime in the Ems Estuary **V. N. de Jonge** 289–300
Particle resuspension in the benthic boundary layer induced by flow around polychaete tubes
D. A. Carey 301–308
Tidal current speed and production of benthic macrofauna in the lower Bay of Fundy
D. J. Wildish and D. Peer 309–321
Effect of turbidity on the temporal and spatial utilization of the inner Bay of Fundy by American shad (*Alosa sapidissima*) (Pisces: Clupeidae) and its relationship to local fisheries
M. J. Dadswell, G. D. Melvin, and P. J. Williams 322–330
Sediment mobility in the Severn Estuary and its influence upon the distribution of shorebirds
P. N. Ferns 331–340
Development of an ecosystem model of a turbid estuary **I. R. Joint** 341–348
Concluding remarks of session chairmen at the Dynamics of Turbid Coastal Environments Symposium, I **A. J. Bowen** 349–350
Concluding remarks of session chairmen at the Dynamics of Turbid Coastal Environments Symposium, II **D. C. Rhoads** 351–352
Concluding remarks of session chairmen at the Dynamics of Turbid Coastal Environments Symposium, III **G. Evans** 353–354
Concluding remarks of session chairmen at the Dynamics of Turbid Coastal Environments Symposium, IV **P. J. Wangersky** 355–356
Concluding remarks of session chairmen at the Dynamics of Turbid Coastal Environments Symposium, V **H. Postma** 357–358
Concluding remarks of session chairmen at the Dynamics of Turbid Coastal Environments Symposium, VI **A. R. Longhurst** 359–360
Papers presented at the Symposium 361–362
Poster papers presented at the Symposium 363
List of participants 364–365

Canadian Journal of Fisheries and Aquatic Sciences (Supplement)

Journal canadien des sciences halieutiques et aquatiques (Supplément)

CJFSDX40(SUPPL. 1) 1–365 (1983)
ISSN 0714-7937

Volume 40, Supplement No. 1, 1983 Volume 40, Supplément n° 1, 1983

Correct citation for this publication:

GORDON, D. C., JR., AND A. S. HOURSTON [ED.]. 1983. Proceedings of the Symposium on the Dynamics of Turbid Coastal Environments. Can. J. Fish. Aquat. Sci. 40(Suppl. 1): 1–365.

Contents 1–2

Introduction to the Symposium on the Dynamics of Turbid Coastal Environments
D. C. Gordon Jr. 3–7

Modeling tidal stress, circulation, and mixing in the Bristol Channel as a prerequisite for ecosystem studies **R. J. Uncles** 8–19

Suspended sediment transport and deposition modeling in the Bay of Fundy, Nova Scotia — a region of potential tidal power development **D. A. Greenberg and C. L. Amos** 20–34

Factors affecting the supply and distribution of sediment in the turbid coastal environment
M. P. Kendrick and B. V. Derbyshire 35–43

Supply, distribution, and transport of suspended sediment in a macrotidal environment: Bristol Channel, U.K. **M. Collins** 44–59

River-dominated suspended-sediment deposition in a new Mississippi delta
I. Ll. van Heerden, J. T. Wells, and H. H. Roberts 60–71

Transfer of water and sediment from the Yangtze River to the East China Sea, June 1980
Z.-S. Yang, J. D. Milliman, and M. G. Fitzgerald 72–82

Distribution and behavior of fine sediment in the Severn Estuary and Inner Bristol Channel, U.K. **R. Kirby and W. R. Parker** 83–95

Characteristics of suspended cohesive sediment of the Severn Estuary, U.K.
R. Bryant and D. J. A. Williams 96–101

Size of flocs suspended in Delaware Bay **R. J. Gibbs, L. Konwar, and A. Terchunian** 102–104

Modeling suspended sediment dynamics of the Miramichi Estuary, New Brunswick, Canada
G. V. Winters 105–116

Turbidity maximum migration and harbor siltation in the Tay Estuary
C. Dobereiner and J. McManus 117–129

Dynamics of coastal fluid muds in low-, moderate-, and high-tide-range environments
J. T. Wells 130–142

The northern muddy intertidal: a seasonally changing source of suspended sediments to estuarine waters — a review **F. E. Anderson** 143–159

The mudflat coast of China **Y. Wang** 160–171

Optical properties, suspended sediments, and chemistry associated with the turbidity maxima of the Delaware Estuary
R. B. Biggs, J. H. Sharp, T. M. Church, and J. M. Tramontano 172–179

Les flux de sels nutritifs dans l'estuaire de la Seine (France); rôle et importance du bouchon vaseux au cours du mélange estuarien **J.-F. Guillaud** 180–187

(*continued inside back*)

Canada $12.00
Other countries/Autres pays $14.40

©Minister of Supply and Services Canada 1983
Ministre des Approvisionnements et Services Canada 1983